DEVELOPMENT OF A FLYWHEEL ENERGY STORAGE SYSTEM - UNINTERRUPTED POWER SUPPLY (FLY-UPS)

Dissertation submitted in fulfilment of the requirements for the degree *Magister Ingeneriae* **at the Potchefstroom campus of the North-West University**

J.J. Janse van Rensburg

Supervisors: Mr. J.G. Roberts, Prof G. van Schoor, Mr. E.O. Ranft

December 2007

Declaration

I hereby declare that all the material incorporated in this dissertation is my own original unaided work except where specific reference is made by name or in the form of a numbered reference. The word herein has not been submitted for a degree at another university.

Signed: . . . . . .
Jan Janse van Rensburg

Abstract

The School of Electrical, Electronic and Computer Engineering is in the process of establishing an active magnetic bearing (AMB) and high speed permanent magnet synchronous machine (PMSM) laboratory. This is done to gain knowledge on AMB, flywheel and high speed PMSM technologies. Some of the advantages of using AMBs are: no mechanical wear or friction, no need for lubrication, active vibration control and unbalance compensation.

This project's purpose is the development of an AMB suspended flywheel energy storage system. This system should be able to store energy for a certain period with minimal losses. Energy stored should then be readily available for use by a load such as a personal computer. This system will be similar to a conventional uninterrupted power supply (UPS). Instead of using a lead-acid cell to store the energy, a flywheel is used. The acronym for the system is FLY-UPS (FLYwheel Uninterrupted Power Supply).

Charging the system should not take longer than 5 minutes using 2000 W of power. One of the system's main function is to protect sensitive equipment from mains power spikes and short power interruptions. This system should be able to supply 2000 W for at least 3 minutes, allowing enough time to switch sensitive equipment off in a controlled manner.

Two heteropolar radial AMBs, one axial AMB, a high speed permanent magnet synchronous machine (PMSM) for propulsion and generating purposes, and a disc that will serve as the flywheel is the main components of this system.

This system should be operated at a rotational speed of 30000 rpm. Development of this system facilitates testing of control algorithms and establishes knowledge on AMBs and flywheels. An important outcome of this project is delivering a working FLY-UPS system. Future research on advanced control techniques, low loss AMB's and flywheel design optimising is made possible with the development of the FLY-UPS system.

An in depth investigation into rotor-dynamics and flywheels has been conducted. Research into flywheels is relevant because recently there has been a growing focus on renewable energy. A modular approach was used in the design of the FLY-UPS system. A rotor-dynamic analysis has been done on the rotor/flywheel assembly, resulting in predicted displacements and the critical frequencies of the rotor/flywheel assembly. Analytical and computer aided strength analysis has been done on the rotor/flywheel assembly. Both the analytical and computer aided strength analysis concludes that the rotor/flywheel achieves the minimum factor of safety of 1.5.

Measured critical frequencies correlate to the predicted critical frequencies. Predicted displacement does not correlate to the measured displacement. This is attributed to insufficient balancing of the rotor/flywheel. Rotational speed of the rotor/flywheel is currently limited to 7000 rpm, in stead of the required 30000 rpm, due to the greater displacements.

Further investigation into the reasons for the greater displacement is still required. A possible solution to this problem is re-balancing the rotor/flywheel assembly. Further research is required on the dynamic stiffness of the AMBs. A delevitation system needs to be developed. Research has to be done on the accurate prediction of the behaviour of a rotor during delevitation. An investigation into the development of a carbon-fibre composite flywheel needs to be conducted. Measured against the outcomes, the project has been a success.

Contents

List of figures 17

List of tables 19

Acknowledgements 21

1 Introduction **23**

1.1 Background 23

1.2 Objective 24

1.3 Problem statement 24

1.4 Issues to be addressed and methodology 25

1.4.1 Conceptual analysis 25

1.4.2 FLY-UPS system engineering 26

1.4.3 Rotor/flywheel assembly 26

1.4.4 Rotor/flywheel enclosure 27

1.4.5 Component development and procurement 27

1.4.6 System integration 27

1.4.7 System evaluation 28

1.4.8 Chapter breakdown of dissertation 28

2 Literature study **31**

2.1 Flywheel design 31

2.1.1 The concept of flywheels 32

2.2 Magnetic bearings . . . 35
2.2.1 AMB basics . . . 36
2.3 Rotor dynamics . . . 37

3 Mechanical system design **41**
3.1 Design process . . . 41
3.2 FLY-UPS specification and calculations . . . 43
3.2.1 Material selection . . . 43
3.2.2 Rotational speed . . . 43
3.2.3 Energy requirements . . . 45
3.2.4 Rotor length . . . 45
3.2.5 System size . . . 47
3.2.6 Load capacity . . . 47
3.3 FLY-UPS design decisions . . . 48
3.3.1 Rotor/flywheel design . . . 48
3.3.2 Enclosure design . . . 49
3.4 System evaluation . . . 50

4 Rotor detail design **51**
4.1 Energy storage . . . 51
4.2 Strength analysis . . . 53
4.2.1 Magnet adhesive . . . 53
4.2.2 Flywheel disc strength . . . 59
4.3 Rotor dynamics . . . 61
4.3.1 Unbalance . . . 61
4.3.2 Detail design of the rotor . . . 68
4.4 Example of API 612 design verification process . . . 72

5 Rotor/flywheel enclosure detail design **79**

5.1 Enclosure operational functions . . . 79

5.2 Enclosure concept . . . 80

5.3 Interfacing . . . 81

5.3.1 Sensors . . . 81

5.3.2 Pressure feedthroughs . . . 86

5.3.3 Vacuum pump . . . 88

5.3.4 Base-plate securing . . . 89

5.4 Sub-components . . . 90

5.4.1 Axial AMBs . . . 90

5.4.2 Radial AMBs . . . 90

5.4.3 PMSM . . . 91

5.4.4 Auxiliary bearings . . . 92

5.5 Heat dissipation of the enclosure . . . 92

5.6 Modular design . . . 94

5.6.1 Module 1 . . . 94

5.6.2 Module 2 . . . 96

5.6.3 Module 3 . . . 97

5.6.4 Module 4 . . . 98

5.6.5 Module 5 . . . 99

5.6.6 Module 6 . . . 100

5.6.7 Module 7 . . . 101

5.7 Aerodynamic losses . . . 102

5.8 Integration . . . 103

6 System characterisation, evaluation and verification **105**

6.1 Stationary critical frequency test results . . . 105
6.2 Rotating displacements . . . 108
6.3 Vacuum . . . 110
6.4 Aerodynamic losses . . . 111

7 Conclusions and recommendations 113

7.1 Conclusions . . . 113
7.1.1 Stationary critical frequencies . . . 113
7.1.2 Rotating displacements . . . 113
7.1.3 Vacuum . . . 114
7.1.4 Aerodynamic losses . . . 114
7.1.5 Modular design . . . 114
7.1.6 Securing the PMSM magnets . . . 115
7.1.7 Energy storage . . . 115
7.2 Recommendations . . . 115
7.2.1 Stationary critical frequencies . . . 115
7.2.2 Rotating displacements . . . 115
7.2.3 Aerodynamic losses . . . 116
7.2.4 Modular design . . . 116
7.2.5 Securing the PMSM magnets . . . 116
7.2.6 Auxiliary bearings . . . 116
7.2.7 Energy storage . . . 116
7.3 Closure . . . 117
Bibliography . . . 119

Appendices

A Type A specification **121**

B Type B specification **129**

C Photos **139**

D Appendix and data DVD **149**

D.1 Shaft layout design . . . 150

D.2 PMSM specification . . . 176

D.3 PMSM unbalance magnetic pull . . . 187

D.4 Eddy probe and gland selection . . . 198

D.5 EES Program Results . . . 205

D.6 DyRoBeS rotor-dynamic analysis . . . 212

D.7 CosmosWorks strength analysis . . . 246

D.8 Drawing numbering conventions . . . 256

D.9 Manufacturing drawings . . . 258

D.10 Photos . . . 288

D.11 Data sheets . . . 301

D.11.1 Adhesive . . . 301

D.11.2 Rotational speed sensor and display . . . 307

D.11.3 Vacuum pump . . . 313

D.11.4 Pressure transducer . . . 316

D.11.5 Wire gauge . . . 321

D.11.6 SKF eddy current sensors . . . 323

D.11.7 Feedthroughs and glands . . . 327

D.11.8 NPT pipe . . . 340

D.11.9 PT100 resistive table . . . 342

D.11.1017-4PH stainless . . . 345
D.11.11Valves . . . 350
D.11.12Auxiliary bearings . . . 353
D.12 Adhesive technologies . . . 355
D.12.1 Acrylics, Two-Step . . . 355
D.12.2 Acrylics, Two-Part . . . 356
D.12.3 Anaerobics . . . 358
D.12.4 Cyanoacrylates . . . 360
D.12.5 Epoxies . . . 362
D.12.6 Hot Melts . . . 363
D.12.7 Light Cure . . . 364
D.12.8 Polyurethanes . . . 366
D.12.9 Silicones . . . 367

List of Figures

1.1 Simplified FLY-UPS layout 25

1.2 Simplified FLY-UPS system diagram 26

2.1 Comparison of different energy storage systems [1] 32

2.2 Representation of radial and tangential stresses in a uniform disc 34

2.3 Four different flywheel shapes and the corresponding form factor 34

2.4 Schematic diagram of a single-axis AMB system 36

2.5 Effect of bearing support stiffness K on lateral vibration modes of a uniform shaft 37

2.6 Rigid-rotor modes of whirling for a symmetrical rotor 38

2.7 Synchronous response to unbalance through both rigid-body modes 38

2.8 Critical speed map for three modes 39

2.9 First two rigid-support modes of whirling for a symmetric elastic two-disk rotor 39

3.1 Design process 41

3.2 FLY-UPS design process 42

3.3 The effect of elevated temperatures on the yield strength of 17-4PH(H1025) . . . 44

3.4 Calculation of the axial length of the rotor 46

3.5 The relationship between the power available and the period that it is available . 48

3.6 The layout of the rotor/flywheel assembly 49

3.7 The layout of the enclosure assembly 49

4.1 Solid cylinder . . . 51
4.2 Thick cylinder . . . 52
4.3 Completed rotor assembly . . . 52
4.4 Magnet sector . . . 54
4.5 Combination of adhesive and carbon fibre layout . . . 57
4.6 Tangential stress in the flywheel disc . . . 60
4.7 Radial stress in the flywheel disc . . . 60
4.8 Von Misses stress in the flywheel disc . . . 60
4.9 FOS of the rotor/flywheel . . . 62
4.10 ISO standard balancing application for a centred rotor . . . 63
4.11 ISO standard balancing application for a dumbbell rotor setup . . . 64
4.12 API standard for an operating range lower than the critical frequency . . . 65
4.13 API standard for an operating range higher than the critical frequency . . . 65
4.14 Clearance of the rotor . . . 66
4.15 Flowchart of API 612 procedure . . . 67
4.16 Rotor design process diagram . . . 68
4.17 First rigid mode of the rotor simulated, using the dynamic stiffness of the radial AMBs. . . . 69
4.18 First rigid mode of the rotor simulated, using the static stiffness of the radial AMBs. 69
4.19 Second rigid mode of the rotor, simulated using the dynamic stiffness of the radial AMBs. . . . 70
4.20 Second rigid mode of the rotor, simulated using the static stiffness of the radial AMBs. . . . 70
4.21 Unbalance placement for second rigid mode of the rotor . . . 71
4.22 First bending mode of the rotor simulated, using the dynamic stiffness of the radial AMBs. . . . 71
4.23 First bending mode of the rotor simulated, using the static stiffness of the radial AMBs. . . . 72

4.24 Critical speed map of the system, showing the dynamic and static stiffness of the AMBs. . . . 72

4.25 Multiple response plot at 5 different locations for mode 1 unbalance . . . 73

4.26 Multiple response plot at 5 different locations for mode 2 unbalance . . . 73

4.27 Transmitted bearing forces for lower and upper radial AMBs . . . 74

4.28 Response peak at 33280 RPM . . . 74

4.29 Corresponding rotational speeds . . . 75

4.30 Response peak 2 . . . 75

4.31 Corresponding rotational speeds . . . 76

5.1 The final enclosure layout. . . . 80

5.2 The sensor signal distribution of the FLY-UPS system. . . . 81

5.3 Principal of an eddy current sensor. . . . 82

5.4 Photograph of an eddy current sensor. . . . 82

5.5 Photograph of the chosen inductive proximity switch. . . . 83

5.6 Photograph of the chosen speed sensor display. . . . 83

5.7 Photograph of the chosen infra-red temperature sensor. . . . 84

5.8 Required target area for the infra-red temperature sensor. . . . 84

5.9 Drawing of a Pt100 resistive temperature device . . . 85

5.10 A photo of the chosen pressure transducer . . . 85

5.11 A photo of the in-house developed PMSM and pickup coils. . . . 86

5.12 The layout of the CONAX high current feedthrough. . . . 87

5.13 An illustration of the low current feedthroughs. . . . 87

5.14 An illustration of a pressure gland. . . . 88

5.15 A photograph of the vacuum pump. . . . 88

5.16 A diagram of the interfacing of the vacuum pump and the enclosure. . . . 89

5.17 Schematic of the securing of the rotor/flywheel enclosure to the ground. . . . 89

5.18 Drawing of the bottom of the baseplate. 90

5.19 Schematic representation of the two axial AMB units. 91

5.20 Photograph of a radial AMB unit, showing the pole pairs and the radial movement directions. 91

5.21 Photograph of the PMSM's flared end-windings. 92

5.22 An illustration of the backup bearings. 93

5.23 A sectioned illustration of the backup bearing locations. 93

5.24 A few of the designed heat conducting modules. 94

5.25 Schematic representation of module 1. 95

5.26 Schematic representation of module 2. 96

5.27 Schematic representation of module 3. 97

5.28 Schematic representation of module 4. 98

5.29 Schematic representation of module 5. 99

5.30 Schematic representation of module 6. 101

5.31 Schematic representation of module 7. 102

5.32 The assembled FLY-UPS system. 104

6.1 The amplification of the disturbance force on the lower AMB's x-axis, showing the predicted and measured critical frequencies. 106

6.2 The amplification of the disturbance force on the lower AMB's y-axis, showing the predicted and measured critical frequencies. 106

6.3 The amplification of the disturbance force on the upper AMB's x-axis, showing the predicted and measured critical frequencies. 107

6.4 The amplification of the disturbance force on the upper AMB's y-axis, showing the predicted and measured critical frequencies. 107

6.5 The amplification of the disturbance force on the axial AMB's z-axis. 108

6.6 The major displacement of the rotor/flywheel assembly measured at the eddy current sensor locations. 109

6.7 The predicted major displacement of the rotor/flywheel assembly. 109

6.8 The vacuum leakage for 30 minutes. 110

6.9 The vacuum leakage with automatic vacuum pump control enabled. 110

6.10 A comparison of the losses with the rotor in a vacuum and open to atmosphere. . 111

7.1 A comparison of the expected aerodynamic losses. 114

List of Tables

1.1 Procured and developed components 28

3.1 Material decision matrix 43

3.2 Chosen axial length values 47

4.1 Comparison of adhesive and carbon fibre performance 59

6.1 Predicted and measured critical frequencies 105

6.2 Predicted and measured first critical frequency of the rotating rotor/flywheel assembly 108

Acknowledgements

I would like to firstly thank and acknowledge the following people and institutions, in no particular order, for their contributions during the course of this project:

- Fika & Sunette Janse van Rensburg
- Stefan Myburgh
- Belinda Strydom
- Eugén Ranft
- George van Schoor
- Jacques Jansen van Rensburg
- Sarel Janse van Rensburg
- Andries de Klerk
- M-Tech Industrial
- THRIP

TODAY'S NECESSITIES WERE YESTERDAY'S LUXURIES!

ALLES HET DEUR HOM ONTSTAAN, EN SONDER HOM HET NIE EEN DING WAT BESTAAN, ONTSTAAN NIE. DIE LIG VERLIG DIE DUISTERNIS EN DIE DUISTERNIS KAN DIT NIE UITDOOF NIE.
Johannes 1:3, 5

Chapter 1

Introduction

This chapter discusses the background to the FLY-UPS project. The problem statement is given, whereafter the objective is stated. Issues to be addressed and the methodology to be followed are discussed.

1.1 Background

Flywheels have been used since ancient times. Only in recent years has the possibility to store large amounts of energy in relatively small flywheels become a reality. The development of new composite materials and super-alloys has made it possible to increase the speed and lower the weight of flywheels. This has enabled the development of flywheels with a higher specific energy $\left[\frac{\text{Wh}}{\text{kg}}\right]$ making the flywheel a viable alternative to other energy storage technologies.

With flywheels energy is stored in the form of kinetic energy. One of the main applications for flywheels is the provision of backup power. This is done by using an electric motor to spin the flywheel up, and when there is a power failure the same motor is then used in generator mode to extract the kinetic energy from the flywheel. To optimise the efficiency, this setup uses active magnetic bearings (AMBs) to fully suspend the flywheel so that there is no mechanical contact or friction. To further enhance the efficiency, the flywheel is operated in a vacuum to minimise the aerodynamic losses. To improve the specific energy $\left[\frac{\text{Wh}}{\text{kg}}\right]$ of the flywheel the flywheel should be operated at high rotational speed. With the recent development of new alloys and control techniques the flywheel has become more viable as a replacement for super-capacitors and other chemical energy storage units such as lead-acid batteries.

With the use of AMBs the advantages of using flywheels to store energy become clear. Firstly, an AMB provides an actively controlled, near-frictionless bearing that can be used to damp out vibrations in an active manner. Secondly a flywheel with no chemical memory or weakening of storage capacity over time or duty cycles is realised.

A flywheel energy storage system - uninterrupted power supply was identified as a suitable application. This application was chosen because it places stringent requirements on the AMBs.

Another reason is that AMBs is a driving technology behind high speed flywheels. This project takes an in depth look at the systems engineering and mechanical design involved in developing a flywheel energy storage system - uninterrupted power supply.

Flywheels are an important enabling technology for renewable energy. A flywheel has the ability of infinite ride through cycles unlike conventional lead-acid cells. Conventional lead-acid cells have a limited amount of charge-discharge cycles. The infinite ride through capabilities makes flywheels a viable alternative to lead-acid cells. The efficiency of flywheels is also greater than the conventional lead-acid cells currently in use. With a lifetime of 20 years or more the use of flywheels for energy storage is certainly worth investigating.

The FLY-UPS system will enable the School of Electrical, Electronic and Computer Engineering and the McTronX Research Group to become acquainted with flywheel and AMB technology. This system could also be used to test the effectiveness of AMBs in specific applications, including renewable energy storage. The system enables research on low loss AMBs, high speed AMBs and vacuum applications for AMBs.

1.2 Objective

This project's objective is to develop an active magnetic bearing suspended system for uninterrupted power supply (UPS) delivering 2000 *W* for 3 minutes.

1.3 Problem statement

The purpose of this project is the development of an AMB suspended flywheel system. The system should be able to store energy for a certain period with minimal losses. This stored energy should then be readily available for use by a load such as a personal computer. The system will be similar to a conventional uninterrupted power supply (UPS). Instead of using a lead-acid cell to store the energy, a flywheel is used. The acronym for the system is FLY-UPS (FLYwheel Uninterrupted Power Supply).

The system needs to be fully charged after 5 minutes using 2000 W of power. The system's main function is to protect sensitive equipment from mains power spikes and short power interruptions. The FLY-UPS should be able to supply 2000 W for at least 3 minutes; allowing enough time to switch sensitive equipment off in a controlled manner.

The FLY-UPS comprises two heteropolar radial AMBs, one axial AMB, a high speed permanent magnet synchronous machine (PMSM) for propulsion and generating purposes and a disc that will serve as the flywheel. An illustration of the envisaged system is given in figure 1.1. This figure displays the top AMB (axial), used to suspend the system vertically. The radial AMBs are used to suspend the system laterally.

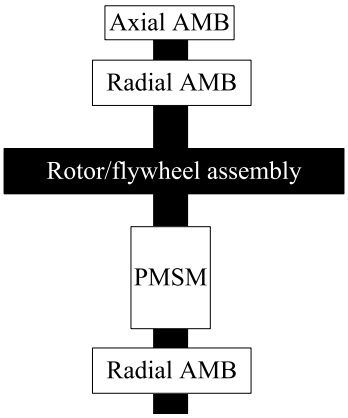

Figure 1.1: Simplified FLY-UPS layout

1.4 Issues to be addressed and methodology

The issues to be addressed includes the conceptual analysis, the system engineering, the rotor/flywheel assembly, the enclosure, component development, component procurement, system integration and system evaluation.

1.4.1 Conceptual analysis

The high speed AMB suspended flywheel system can be divided into six main sub-systems. Figure 1.2 shows the interfacing of the different sub-systems. This dissertation takes an in-depth look at the rotor/flywheel assembly, the rotor/flywheel enclosure and the overall system integration.

The system functions as follows: The rotor/flywheel assembly is firstly suspended by AMBs. The AMBs use sensors to measure the displacement from a certain reference point. The position information is sent to the controllers that generate current reference signals. Power amplifiers convert the reference signals into currents flowing through the electromagnets. The currents realise appropriate forces acting upon the rotor, resulting in the suspension of the system. After the system is suspended, the PMSM operates in motor mode. While the motor is powered, the motor will be controlled so that it does not exceed the maximum allowable speed. The rotor/flywheel enclosure houses the subcomponents and sensors. The rotor/flywheel enclosure is vacuumed in order to run the FLY-UPS system in a low pressure environment. When there is an interruption in the mains power the PMSM will switch to generator mode and the flywheel will supply the generator with the angular force needed to power the generator. The layout of the system is based on systems already in use, as well as design decisions made specifically for this system.

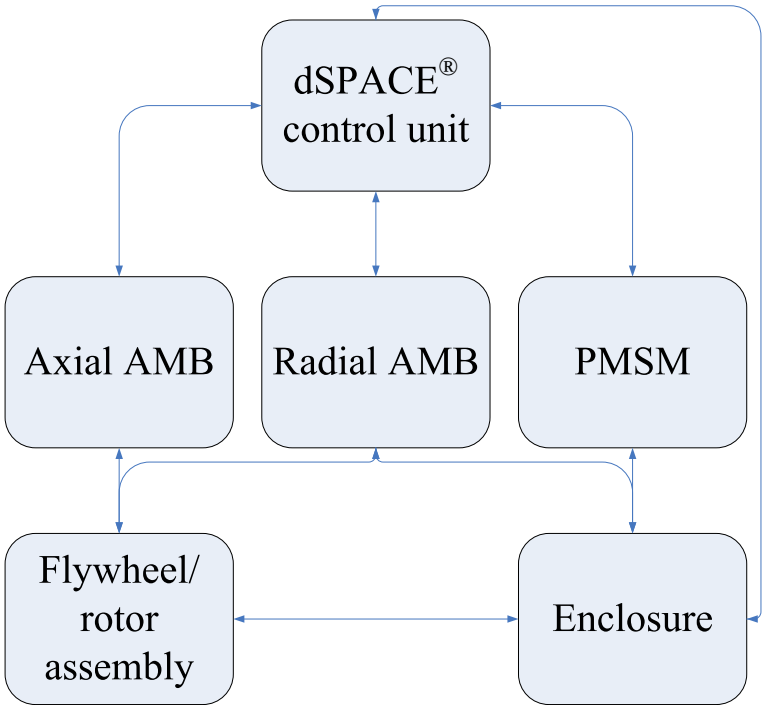

Figure 1.2: Simplified FLY-UPS system diagram

1.4.2 FLY-UPS system engineering

The FLY-UPS system and sub-systems have been designed according to specifications for the system and each individual sub-system. The drawn up specifications for the system is in the form of a Type A specification document, see appendix A. The Type A document will also be used to evaluate the system upon completion.

FLY-UPS system specifications have been compiled from firstly the user requirements as stated in the problem statement. Secondly from information gathered from literature [2, 3, 4, 5, 6, 7, 8, 9, 10, 11, 12, 13, 14], current setups in the industry, discussions with experts in the field and research groups. The maximum model size and cost are also specified.

1.4.3 Rotor/flywheel assembly

The flywheel has to be able to store a specified amount of energy. A decision was taken to operate the system at a relatively high speed of 30000 rpm. The rotor must be able to handle the centrifugal forces acting upon it. The rotor should be able to traverse the critical frequencies without an adverse effect on the rotor.

The rotor/flywheel assembly has been designed according to the energy storage requirements. The energy design has been verified using *SolidWorks*® to verify the moment of inertia of the rotor/flywheel assembly. The strength design of the rotor is done by using analytical methods

[15]. This has been verified using the strength analysis software *CosmosWorks*®. The rotor-dynamic rotor design takes into account the maximum model size, the maximum operating speed and the basic rotor shape as determined by the analytical strength analysis. The rotor-dynamic analysis is done using the rotor-dynamic software *DyRoBeS*®. The rotor design is adapted until it displays the desired characteristics. The bearing forces, mode shapes, critical frequencies and displacements are obtained from the rotor-dynamic analysis. The aerodynamic losses caused by the flywheel have also been taken into account.

1.4.4 Rotor/flywheel enclosure

The enclosure should be able to safely handle a delevitation of the FLY-UPS, operate in a vacuum and dissipate heat effectively. The enclosure is the main interface between the *dSPACE*® control unit and the FLY-UPS.

The CAD software used to create the manufacturing drawings is *SolidWorks*®. The enclosure has been designed using a modular approach. A vacuum within the enclosure has been achieved by using a vacuum pump connected to the enclosure. The heat generated will be dissipated using materials that conduct the heat toward the outer part of the enclosure where natural convection dissipates the heat. The interfaces needed for the control of the system have been connected to their individual sub-systems using pressure feedthroughs.

1.4.5 Component development and procurement

The FLY-UPS system is a complicated system using both off-the-shelf products and in-house developed products. The system should be built using the maximum amount of procured components to enhance the system's reliability.

Detailed mechanical drawings of the system were prepared using *SolidWorks*®. These drawings have been submitted for quotations and used to manufacture the developed components. The procured components are specified from parameters obtained from the design and simulation of the system. The components of the FLY-UPS system can be grouped into two categories namely procured and developed, as shown in table 1.1.

1.4.6 System integration

All the procured and developed components are integrated into a functional FLY-UPS.

After the development and procurement of the items listed in table 1.1, the different components were integrated. After the integration of the procured and developed components, the control has been programmed into the *dSPACE*® controller to form a fully functional flywheel energy storage system - uninterrupted power supply.

Developed	Procured
Enclosure	Sensors
Rotor	*dSPACE*® controllers
Flywheel	Cabling
Enclosure	I/O Cards
Radial AMBs	Vacuum pump
Axial AMBs	Power amplifiers
PMSM motor drive	
PMSM	

Table 1.1: Procured and developed components

1.4.7 System evaluation

The system has been evaluated according to the specifications set in the developmental phase of the system. This includes the FLY-UPS system and all sub-systems.

The evaluation of the system has been done by using the available sensors to verify that the system meets the specifications. This is done by repetitive testing and interpretation of the results obtained.

1.4.8 Chapter breakdown of dissertation

Chapter 2 gives a overview on the literature applicable to the main technologies of high speed flywheels, namely flywheels, strength analysis, magnetic bearings and rotor dynamics. This is done to enlighten the reader on the theory of flywheels and the associated technologies.

Chapter 3 discusses the mechanical system design of the FLY-UPS. The chapter includes a few basic system calculations, explanations of some of the design decisions made and how these decisions influence the detail designs discussed in chapters 4 and 5.

Chapter 4 discusses the detail design of the rotor/flywheel assembly. The chapter focuses on the energy storage capabilities of the rotor and the strength analysis of the final designed rotor/flywheel assembly. The strength design includes the adhesion of the magnets on the rotor and the rotor assembly strength.

Chapter 5 discusses the detail design of the rotor/flywheel enclosure. Chapter 5 focuses on FLY-UPS interfacing, heat dissipation, modular design, vacuum and aerodynamic losses. The interaction of all these factors determines the final design of the rotor/flywheel enclosure.

Chapter 6 displays some of the results of tests preformed on the FLY-UPS system. The stationary critical frequencies are determined and the results compared to the simulated results. The displacement of the rotor, while rotating, is compared to the simulated results. A log of the

vacuum leakage is shown and the aerodynamic losses are calculated from acquired data.

Chapter 7 discusses the conclusions made from the results as well as practical experiences. Appropriate recommendations are made from the conclusions.

Chapter 1 discussed the background to the FLY-UPS project. The problem statement was given. The issues to be addressed and the methodology to be followed were stated.

Chapter 2

Literature study

This chapter looks into the literature applicable to the main technologies of high speed flywheels, namely flywheels, strength analysis, magnetic bearings and rotor-dynamics. This is done to enlighten the reader to the theory of flywheels and associated technologies.

2.1 Flywheel design

The design of flywheel energy storage systems requires consideration of the following:

- Energy storage
- Material strength
- Rotor-dynamics
- Energy efficiency
- Spatial constraints

This literature study is an in depth look only into the four main design considerations, namely energy requirements of the system, material strength, background on magnetic bearings and rotor-dynamics.

Flywheels are fully bi-directional. This means that a flywheel can be used to store energy as well as to supply the stored energy without any inherent losses. This and the fact that flywheels have one of the highest specific power capabilities presently available, certainly indicate that flywheels have a future as a burst power source [16]. Figure 2.1 displays a comparison between the different energy storage technologies [1]. The figure shows that advanced flywheels can have the same peak power as super capacitors, while also having higher specific energy. This

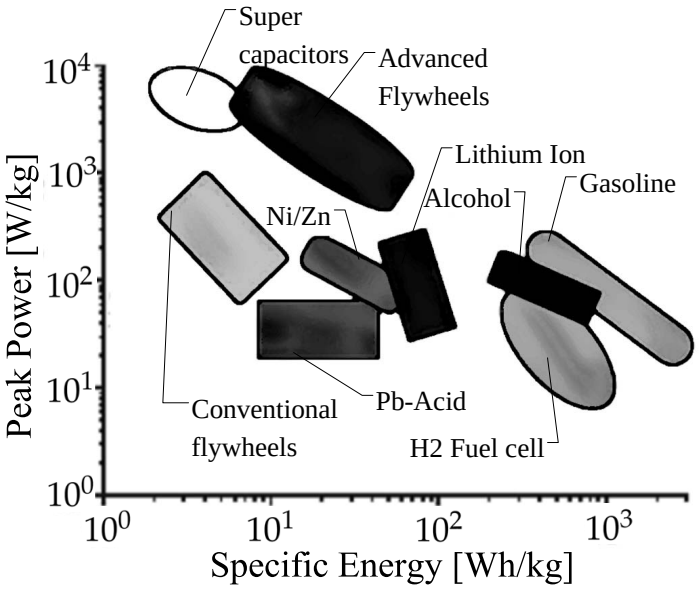

Figure 2.1: Comparison of different energy storage systems [1]

fact enables the use of flywheels instead of using super-capacitors while occupying less physical space.

Flywheels are commonly used in mechanical systems to smoothen the output of the kinetic energy. Flywheels are used less commonly in the storage and smoothing of electrical systems. Some commercial products are available that use flywheels in conjunction with backup generators to facilitate the transition from mains power to the backup generator power without a voltage drop.

2.1.1 The concept of flywheels

A flywheel uses the concept of storing kinetic energy in a rotating mass. Kinetic energy is transferred to the flywheel by using an electrical machine working as a motor and extracted through the machine operated as a generator. This is known as bi-directionality. The kinetic energy stored in a flywheel can be described by (2.1) [16]

$$E_K = \frac{I \cdot \omega^2}{2} \qquad [\,\mathrm{J}\,] \tag{2.1}$$

with I the moment of inertia of the flywheel and ω the angular velocity of the flywheel.

The moment of inertia as given by (2.2) [16] is a function of the geometry and mass of the flywheel

$$I = \int x^2 dm_x \qquad [\mathrm{kg \cdot m^2}] \tag{2.2}$$

with x the distance from the axis of rotation to the differential mass and dm_x the differential mass.

The main considerations when designing a flywheel are therefore the shape of the flywheel and the maximum rotational speed that this specific geometry will allow for a specific material. The range of operable energy levels can be determined from the range of operating speeds. The maximum stresses in a homogenous uniform rotating disc can be determined using (2.3), (2.4) and (2.5) [17]

$$\sigma_{Max} = \frac{(\nu + 3) \cdot \rho \cdot (r \cdot \omega)^2}{8} \qquad [\mathrm{Pa}] \tag{2.3}$$

$$\sigma_{Tangential} = \rho \cdot \omega^2 \cdot \frac{\nu + 3}{8} \cdot (r_i^2 + r_o^2 + \frac{r_i^2 \cdot r_o^2}{r^2} - \frac{1 - 3\nu}{3 + \nu} \cdot r^2) \qquad [\mathrm{Pa}] \tag{2.4}$$

$$\sigma_{Radial} = \rho \cdot \omega^2 \cdot \frac{\nu + 3}{8} \cdot (r_i^2 + r_o^2 - \frac{r_i^2 \cdot r_o^2}{r^2} - r^2) \qquad [\mathrm{Pa}] \tag{2.5}$$

with σ_{Max} the maximum stress in the disc, $\sigma_{Tangential}$ the tangential stress in the disc and σ_{Radial} the radial stress in the disc, ν is Poisons ratio, ρ is the density of the disc material, ω is the rotational speed of the disc, r_i is the inner diameter of the disc, r_o is the outer diameter of the disc and r the radial distance from the disc.

Equations (2.3), (2.4) and (2.5) are for homogenous uniform discs. Equation (2.3) represents the maximum stress experienced by the disc which is a maximum at the centre of the disc. The tangential stress of a disc (2.4) is shown in figure 2.2 represented by the curve with a higher starting value. The radial stress of a disc (2.5) is shown in figure 2.2. This is represented by the curve which is 0 at the extremities of the radius. The maximum for all these equations are the same at the centre of the disc. These equations are only valid in a disc where the thickness of the disc is at least 10 times smaller than the radius of the disc. For first order calculations (2.3) should be sufficient to determine the basic stress on the material. From this result the maximum diameter at a certain speed can be determined.

General expressions for the maximum energy density and maximum specific energy are given in (2.6) and (2.7) respectively [16].

$$\widehat{e}_{Density} = K \cdot \sigma_{min} \qquad \left[\frac{\mathrm{J}}{\mathrm{m^3}}\right] \tag{2.6}$$

$$\widehat{e}_{Specific} = \frac{K \cdot \sigma_{min}}{\rho} \qquad \left[\frac{\mathrm{J}}{\mathrm{kg}}\right] \tag{2.7}$$

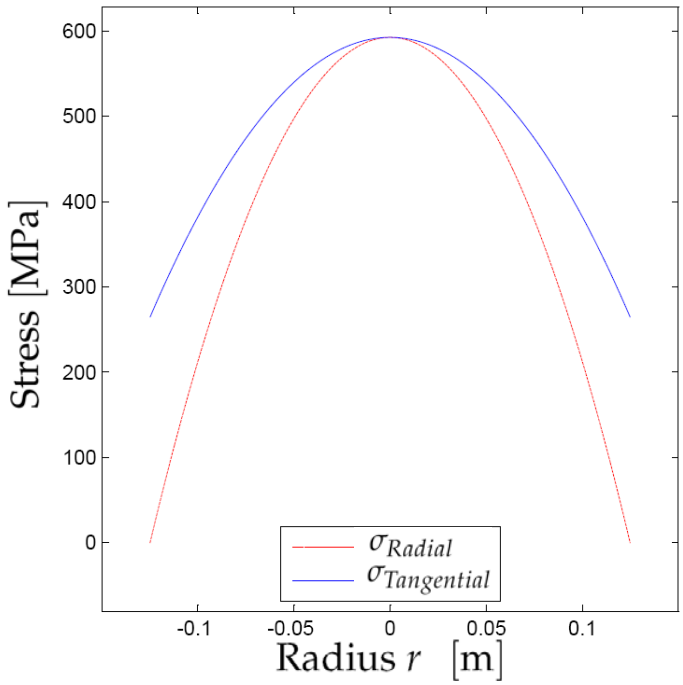

Figure 2.2: Representation of radial and tangential stresses in a uniform disc

K is the form or shape factor (see figure 2.3, ρ the mass density of disc material and σ_{min} the yield strength of the flywheel material.

The use of anisotropic material is only suitable when using the last two shapes seen in figure 2.3. Anisotropic materials have different strengths in different directions. Anisotropic materials include glass and carbon fibre. All of these shapes are suitable when using an isotropic material like metal. Isotropic material has the same strength in all directions [16].

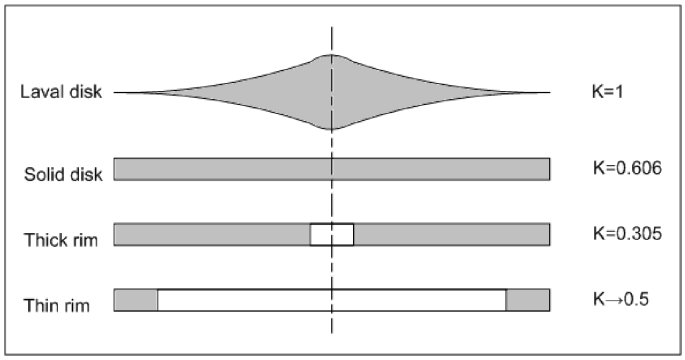

Figure 2.3: Four different flywheel shapes and the corresponding form factor

2.2 Magnetic bearings

A magnetic bearing is a bearing which supports a load using magnetic levitation [18]. Magnetic bearings can be divided into two main categories: Passive magnetic bearings (PMBs) and active magnetic bearings (AMBs) [19]. PMBs make use of permanent magnets to levitate and support a rotor, while AMBs use electromagnets to levitate and support the rotor. Magnetic bearings are used in high speed milling machines and in vacuum applications. A vacuum has very low aerodynamic losses. Conventional bearings usually fail quickly in a vacuum due to poor lubrication [20]. Magnetic bearings are sometimes used to support trains in order to achieve low noise and a smooth ride by eliminating physical contact surfaces [18].

Advantages of magnetic bearings include very low and predictable friction, ability to run without lubrication and in a vacuum. Disadvantages include high cost and relatively large size. In addition, it is difficult to build a magnetic bearing using permanent magnets. Furthermore, techniques using diamagnetic materials are relatively undeveloped [18].

Magnetic Bearings (PMB and AMB) have the following advantages over rolling element bearings [19]:

- no mechanical wear and friction
- low drag torque
- no lubrication
- low energy consumption
- higher circumferential speeds
- operation in severe environments

PMBs utilise pairs of permanent magnets with opposing field directions producing mutual repulsion. This seems like a very simple solution but there are a few major drawbacks. Firstly a complete six degree of freedom support of a rigid body by uncontrolled ferromagnetic forces is impossible. Secondly a PMB's characteristics cannot be changed during operation [19].

AMBs have the following advantages over PMBs [19]

- adjustable bearing characteristics
- vibration control
- on-line balancing and unbalance compensation
- on-line system parameter identification
- on-line system monitoring

AMBs require continuous power input and an active control system to stably suspend the load. Due to this complexity, magnetic bearings (PMBs and AMBs) also typically require some kind of back-up bearing in case of power failure, overloading or control system failure. Since the introduction of AMBs to industry their application has grown extensively. AMBs have a few unique features. These features have enabled a diverse range of applications for AMBs [21].

2.2.1 AMB basics

Non-contact rotor support is achieved by controlling the reluctance forces generated by the electromagnets. It must be controlled as the rotor position changes. The electromagnet is part of a control loop as shown in figure 2.4.

The position of the shaft is monitored by sensors which produce position signals that are fed to a controller. The controller generates an appropriate control signal for the power amplifiers which in turn provides the desired current to the electromagnets. The attractive force generated by the electromagnets then corrects the error [22].

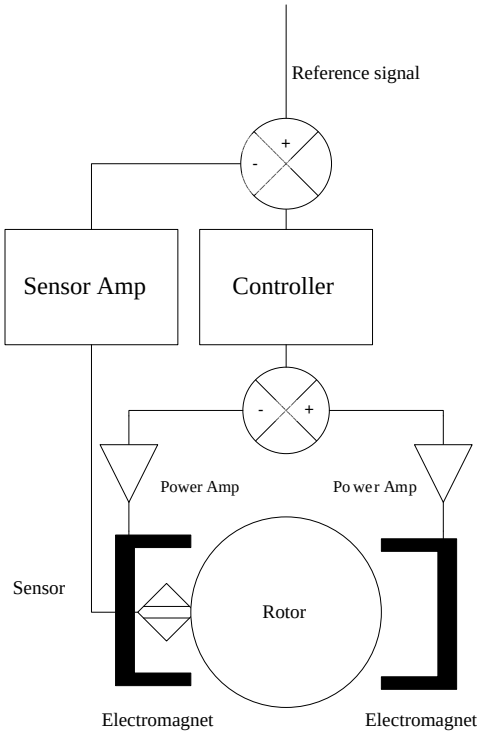

Figure 2.4: Schematic diagram of a single-axis AMB system

The ability to adjust the stiffness and damping of an AMB while in use can be utilised in the FLY-UPS system to dampen out the critical frequencies while the system traverses these frequencies. By using AMBs the system's stiffness can be adjusted for minimal vibrations and power consumption.

2.3 Rotor dynamics

All oscillating matter has natural frequencies. At the natural frequency the oscillations of the mass is exaggerated. In a rotor-bearing system there are a number of discrete natural frequencies. Every individual natural frequency has a specific mode shape. The mode shape is a snapshot of the deflection curve at maximum strain during the vibration [23].

The critical speed of a shaft is defined as the shaft speed that coincides with the natural frequency of the shaft. At this shaft speed the rotor is bowed into the mode shape associated with that particular natural frequency. The different modes can be seen in figure 2.5.

The natural frequencies are represented by Eigen values and the mode shapes are represented by Eigen vectors. In a distributed mass-elastic system there are an infinite number of Eigen values and Eigen vectors. In practice, however, only the lowest three or four critical speeds are traversed in the operating speed range of high speed machines [24].

Mode shapes are functions of the distribution of mass and the stiffness along the rotor, and also the bearing support stiffness. The first three modes of a uniform shaft are shown in figure 2.5 [23].

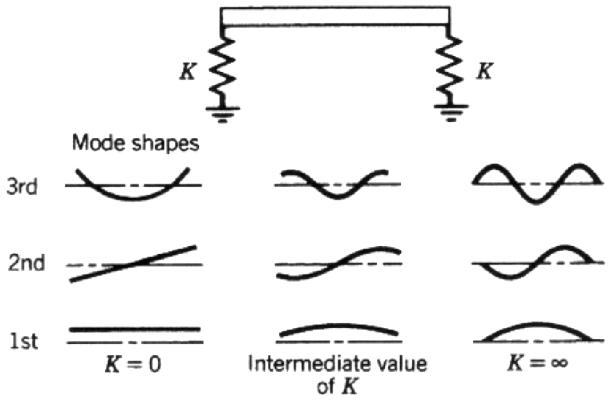

Figure 2.5: Effect of bearing support stiffness K on lateral vibration modes of a uniform shaft

The two rigid-rotor modes for a rotor with two massive disks are shown in figure 2.6. The disks are identical and evenly spaced. If the bearing supports are identical, the first rigid-rotor mode traces a cylinder and the second mode traces two cones with a common apex at the centre of the shaft. If the discs are not evenly spaced or the bearings are not identical the mode shapes will slightly differ in shape [24].

The synchronous response of the rotor-bearing system of figure 2.6 would appear as shown in figure 2.7, if moderate damping is applied. The amplitude of the whirling in the shaft, measured at the bearings, is plotted against the shaft speed in figure 2.7. This whirling is caused by the imbalance of the rotor. The critical speeds of the system can be identified by the shaft speed at the peaks of this graph.

The critical speeds vary with support stiffness, as shown in figure 2.8. This type of plot is

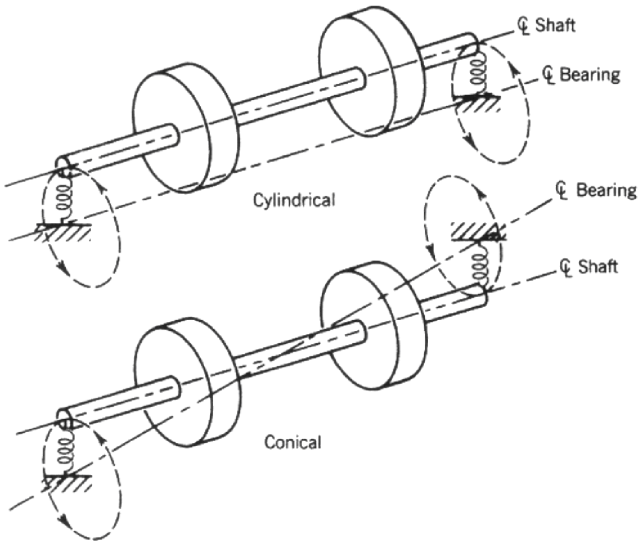

Figure 2.6: Rigid-rotor modes of whirling for a symmetrical rotor

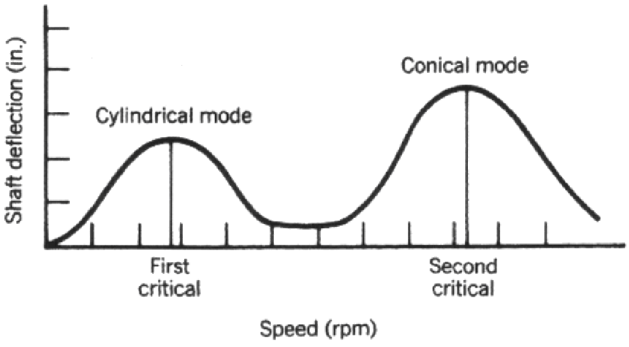

Figure 2.7: Synchronous response to unbalance through both rigid-body modes

known as a critical speed map. The third critical speed is insensitive to the stiffness of the supports. This allows for a range of operating speeds that does not exceed any of the critical speeds. The present trend toward higher speeds makes it difficult not to exceed the third critical speed although it is better practise not to do so [23, 24].

For stiffer bearing supports the modes are more like the modes shown on the right of figure 2.5. The first two modes of operation for a symmetric rotor with two identical discs on an elastic shaft is shown in figure 2.9 [23]. The first operating mode can be approximated by a half sine wave and the second operating mode can be approximated by a full sine wave. Rigid bearing supports cannot dissipate energy and internal damping destabilizes at high speeds. This means that almost all flexing is in the rotor and this creates severe rotor dynamic problems [23].

The dynamic properties of an AMB are electromagnetically controlled, within the physical limits allowed by the system. This characteristic of AMBs enables the active damping of

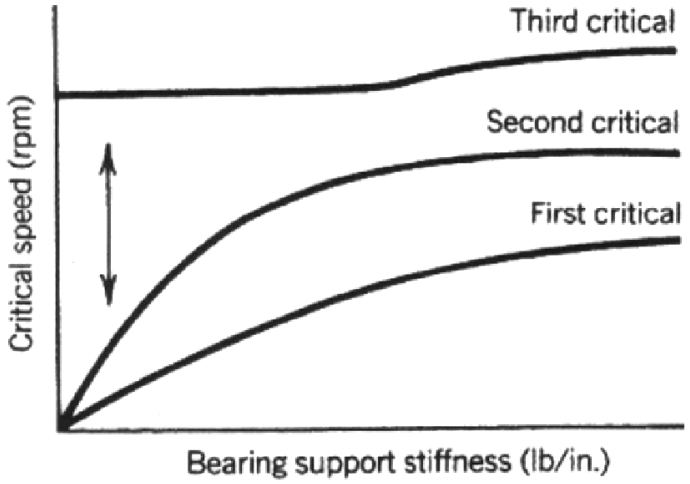

Figure 2.8: Critical speed map for three modes

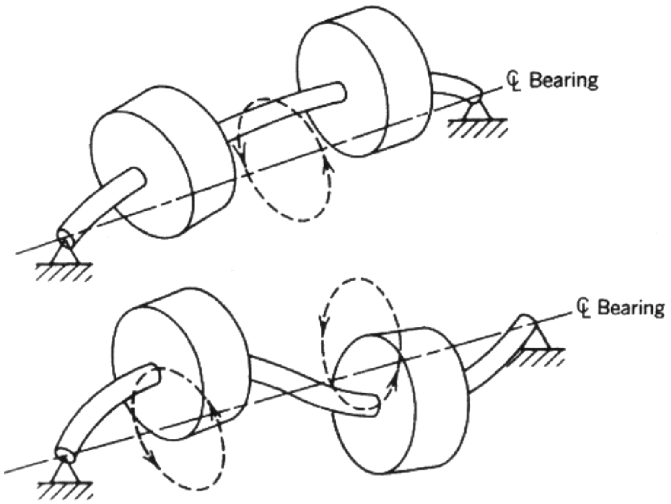

Figure 2.9: First two rigid-support modes of whirling for a symmetric elastic two-disk rotor

vibrations which leads to an increase in the natural frequencies of the system [23].

The rotor dynamics will be a critical design parameter in the final design of the FLY-UPS system. There cannot be any mechanical contact between the stationary and rotating parts of the FLY-UPS system and thus the system should be designed accordingly.

This chapter delved into the research that has already been done in the fields of AMBs, high speed flywheels and rotor-dynamics. It was found that combining this research an efficient way of storing energy in an environmentally safe and friendly way can be developed. The next chapter will discuss the mechanical system design focussing on a system level, and how the different systems involved in the FLY-UPS interconnect.

Chapter 3

Mechanical system design

In this chapter the mechanical system design of the FLY-UPS is discussed. The chapter includes a few basic system calculations, explanations of some of the design decisions made and how these decisions influence the detail designs discussed in chapters 4 and 5.

3.1 Design process

In figure 3.1 the process of designing a system is shown. In the figure the concentric circles represent the process followed when designing a system (working inwards). The output of each activity is shown on the right hand side. Designing of a system starts with research of the relevant fields. The output of this activity can be seen in chapter 2. The research is done to gain knowledge on the system to be designed. Concept identification is done after the literature research is completed. Concept identification is done by comparing the systems already in use, and selecting a workable concept. The output of this activity is a system specification, or Type A specification (refer to appendix A). This is followed by a sub-system specification or a Type B specification (refer to appendix B). This includes concept designs as can be seen in appendix D.1.

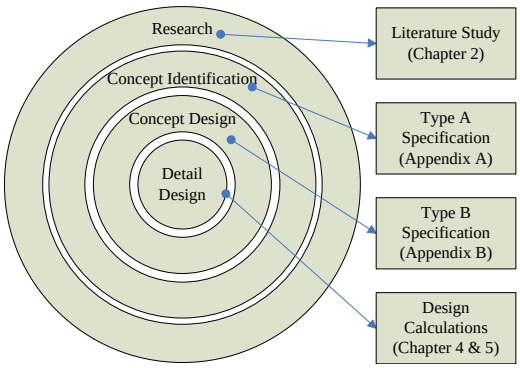

Figure 3.1: Design process

In figure 3.1 a broad overview of the system design was given. In figure 3.2 a more specific look into the design of the FLY-UPS system is shown. The research done with regards to the FLY-UPS system includes AMBs, rotor-dynamics, vacuum seals, current Flywheel systems, flywheels, materials and vibrations. After the completion of the research system specifications are drawn up. From the system specifications a Type A specification is compiled. Next a workable concept is identified. A concept design is drawn up. The concept design is evaluated using the system specifications. If the concept does not meet the requirements a new concept is identified. If the concept meets the requirements a detailed design is done. If the detail design does not meet the requirements, the detail design is redone until the requirements are met. After the detail design, the procurement and manufacturing of components can begin. The manufactured items need to be validated to assess if the items are manufactured to the required tolerances. After the validation of manufactured items and the procurement of items the system can be assembled. After assembly the system is evaluated against the Type A system specifications.

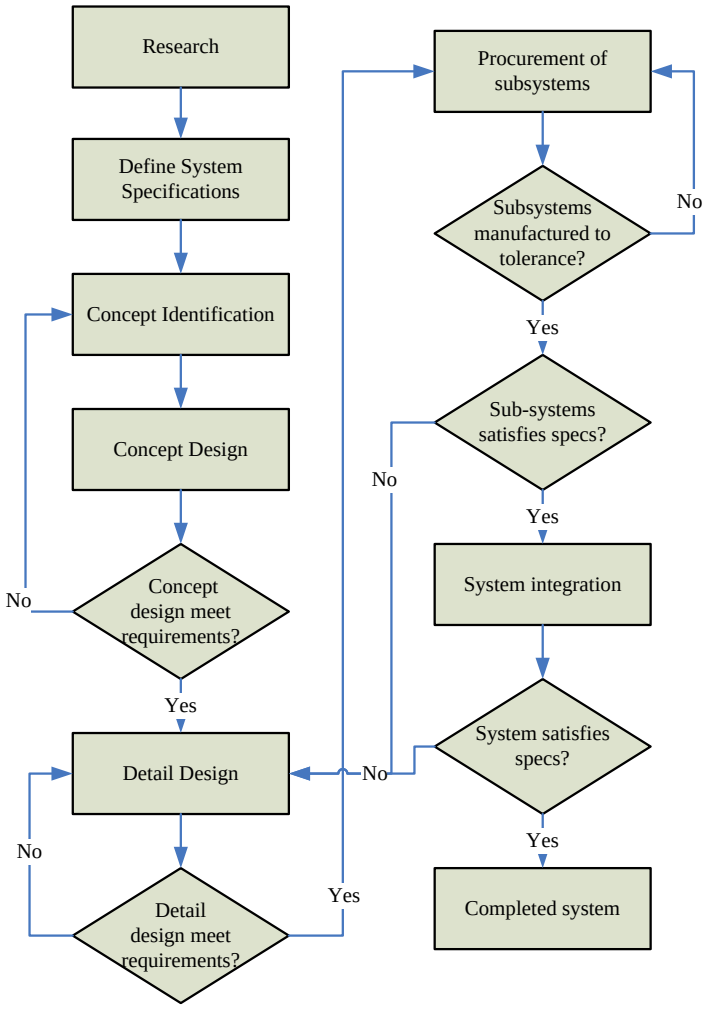

Figure 3.2: FLY-UPS design process

3.2 FLY-UPS specification and calculations

The first step in the development of a FLY-UPS system is to assess what the requirements for the system are. These requirements are used to generate the system specifications. The system specifications include: maximum rotational speed, stored energy requirements, shaft characteristics, physical size, load capacity, and mounting layout. These will be specified and used as a point of departure for the FLY-UPS design.

3.2.1 Material selection

Firstly a material needs to be chosen on which the rest of the calculations will be based. The chosen material has to have a very high yield strength [σ_{yield}]. This material should also be machineable, readily available, and relatively inexpensive. Using these parameters, four materials were chosen, to be narrowed down using a decision matrix (see table 3.1). These materials are:

- Mild steel
- 17-4PH stainless steel
- Titanium alloy
- Carbon fibre

The material chosen is 17-4PH stainless steel. All further calculations on the FLY-UPS system are done using 17-4PH as the material.

Material	Yield strength	Machinability	Availability	Relative price	Total
Weigh factor	0.5	0.1	0.1	0.3	1
Mild steel	6 (350 MPa)	100	100	100	53
17-4PH(H1025)	*23 (1172 MPa)*	*85*	*80*	*85*	***53.5***
Titanium Alloy	15 (830 MPa)	25	10	50	26
Carbon Fibre	100 (5650 MPa)	10	10	1	52.3

Table 3.1: Material decision matrix

An elevated temperature has a negative effect upon the yield strength of 17-4PH stainless steel. Refer to figure 3.3 for a graph of the yield strength at elevated temperatures. The operating temperature of the FLY-UPS system is $\pm$ 60°C. Using this value to determine the yield strength it is found that the yield strength for 17-4PH @ 60°C is 1158 MPa.

3.2.2 Rotational speed

A decision has been made that the maximum operating speed should be in the range of 25000 to 45000 rpm. This decision is based on existing flywheel energy storage systems' operating

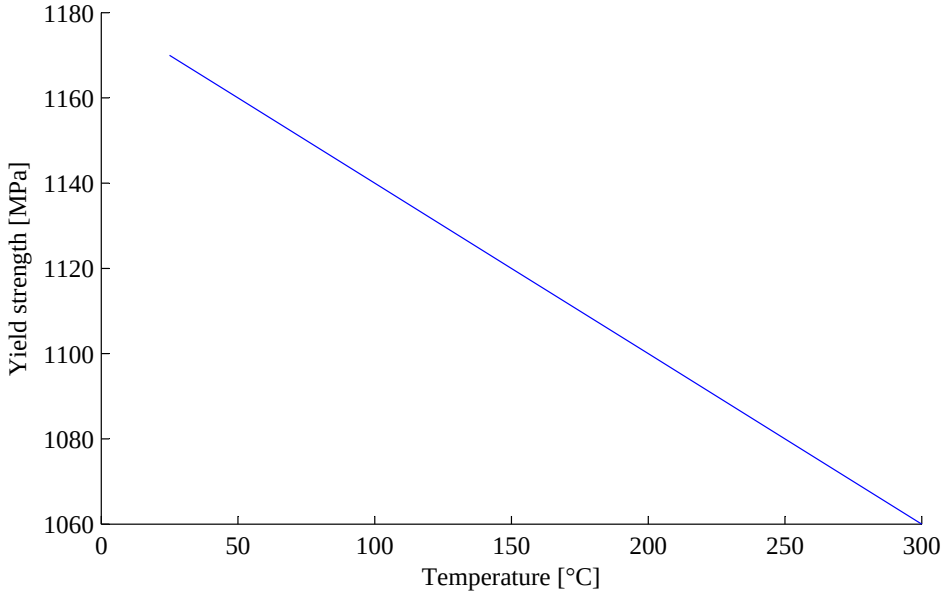

Figure 3.3: The effect of elevated temperatures on the yield strength of 17-4PH(H1025)

speeds. Use (2.3) to calculate the ranges of outer radii for these ranges of speeds. The FLY-UPS system needs to be as small as possible. Thus a factor of safety of 1.5 is used. The use of such a low factor of safety requires that the system needs to be inspected at regular intervals.

For 25000 rpm:

$$\sigma_{Max} = \frac{(\nu + 3) \cdot \rho \cdot (r \cdot \omega)^2}{8} \tag{3.1}$$

$$\frac{1158}{FOS} = \frac{(0.27 + 3) \cdot 7.8 \cdot (r \cdot 2618)^2}{8} \tag{3.2}$$

$$FOS = 1.5 \tag{3.3}$$

$$r = 0.188 \text{ m} \tag{3.4}$$

$$D = 0.3759 \text{ m} \tag{3.5}$$

Similarly for 45000 rpm:

$$D = 0.2088 \text{ m} \tag{3.6}$$

Thus the flywheel should not exceed a diameter of 0.4 m and should not be less than 0.22 m. The chosen dimensions for the flywheel is a diameter of 0.2495 m and a trip speed of 33000 rpm. This yields a factor of safety of 2.

3.2.3 Energy requirements

To calculate the kinetic energy storage potential (2.1) is used. A conservative approach is used by assuming all the energy has to be stored in the flywheel disc. The chosen rotational trip speed is 33000 rpm, although the maximum operating speed is 30000 rpm.

The output of the FLY-UPS should be able to deliver 2000 Watt for 3 minutes, spinning from full speed to half-speed. This value is chosen so the FLY-UPS can be used to power a personal computer system for at least 3 minutes. This equates to a value of 360 kJ. To determine the total energy to be stored in the flywheel, the energy used from full speed to half speed represents 75 % of the total energy.

$$E_K = \frac{E_{Required}}{0.75} = \frac{360}{0.75} = 480 \text{ kJ} \tag{3.7}$$

$$E_K = \frac{I \cdot \omega^2}{2} \tag{3.8}$$

$$480000 = \frac{I \cdot 3142^2}{2} \tag{3.9}$$

$$I = 0.09727 \text{ kg} \cdot \text{m}^2 \tag{3.10}$$

with

$$I = \frac{m \cdot r^2}{2} \tag{3.11}$$

$$0.09727 = \frac{m \cdot 0.125^2}{2} \tag{3.12}$$

$$m = 12.45 \text{ kg} \tag{3.13}$$

with

$$m = \rho \cdot \frac{\pi \cdot r^2}{2} \cdot H \tag{3.14}$$

$$\rho = 7800 \frac{\text{kg}}{\text{m}^3} \tag{3.15}$$

$$H = 65 \text{ mm} \tag{3.16}$$

Now all the dimensions of the disc are known: $D = 0.25$ m and $H = 65$ mm. The final flywheel needs to be thinner than this because the rotor adds to the moment of inertia, but the size extremities are now known.

3.2.4 Rotor length

The rotor/flywheel assembly is manufactured from one solid piece of material. The rotor needs to be as short as possible to make sure that the rotor does not traverse unnecessary bending modes (section 2.3). The rotor needs enough axial space for two radial AMBs, an axial AMB a PMSM and sensing area for the eddy probes. The rotor also needs to be fitted with laminations;

these improve the performance of the PMSM, and the AMBs. Finally the rotor has to be fitted with auxiliary bearings.

From figure 3.4 it is clear that the total axial length is:

$$L_{axial} = (A + B + C + D + E + F + G + H + I) \cdot 1.50 \tag{3.17}$$

With A the axial length of the auxiliary bearing, B and G the sensing area needed by the eddy probes, C and F the axial length needed by the radial AMBs, D the axial length needed by the PMSM, E the thickness of the flywheel, H the axial space needed for the axial AMB's lower coil and I the axial AMB's disc thickness. The total is multiplied with a factor of 1.5 to leave room for the enclosure that will hold each of these sub-components.

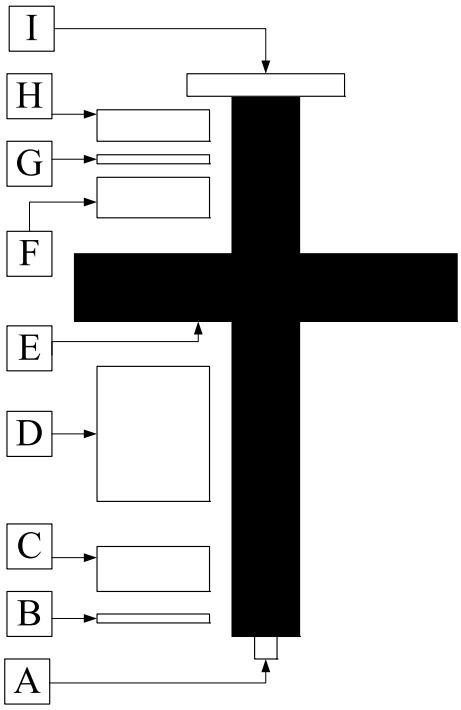

Figure 3.4: Calculation of the axial length of the rotor

The choice of the values for A through I is made by checking the relevant documentation on the procured components, and checking the preliminary designs of the developed items as well as referring to systems already developed. The goal of this calculation is to estimate the axial length needed for the rotor to be able to order the correct amount of material before the final design is done in order to be able to complete the project in the minimum time. This also provides an estimation of the physical size of the rotor flywheel assembly. As can be seen in table 3.2 the length of material required is 505.5 mm.

Item	Description	Axial length	Reference	Total
A	Auxiliary bearing	15 mm	Glacier catalogue	
B	Eddy probe	10 mm	SKF catalogue	
C	Radial AMB	50 mm	Contractor SM	
D	PMSM	110 mm	Contractor SRH	
E	Flywheel	30 mm	Section 3.2.3	
F	Radial AMB	50 mm	Contractor SM	
G	Eddy probe	10 mm	SKF catalogue	
H	Axial AMB coil	50 mm	Contractor SM	
I	Axial AMB disc	12 mm	Contractor SM	$337 \cdot 1.5 = 505.5[\text{mm}]$

Table 3.2: Chosen axial length values

3.2.5 System size

The overall size of the system is necessary to be known before final designs are completed. The reason is that the safety room which will house the FLY-UPS system can be prepared in advance. This is done in order to complete the project in the minimum time. Calculate the estimated size of the system using the rotor length and diameter to determine the estimated enclosure height and diameter. Using table 3.2 the minimum height of the system is known (505.5 mm). Refer to section 3.2.3 to establish the minimum diameter of the rotor/flywheel. The enclosure needs to fit around these measurements, thus the system will have a diameter larger than 250 mm and a height greater than 505.5 mm. Thus the limit for the system height (including the enclosure) is set at 550 mm and the diameter is set at 350 mm.

3.2.6 Load capacity

The load of the system is specified at 2000 W for 3 minutes (see appendices A and B). The specified load is equivalent to 360 kJ of energy (3.18). This energy can be extracted from the system at a greater or lower tempo. The time the energy is extracted will influence the power able to be supplied by the system. However, the system has certain limitations: the copper wires used in the PMSM can only handle a maximum of 25 Amperes. The relationship between the power extracted versus the time it is available, is shown in figure 3.5. The PMSM is designed to extract 2000 W from maximum operating speed (30000 rpm) until the rotational speed is 15000 rpm.

$$P = \frac{E}{t} \qquad [\text{W}] \tag{3.18}$$

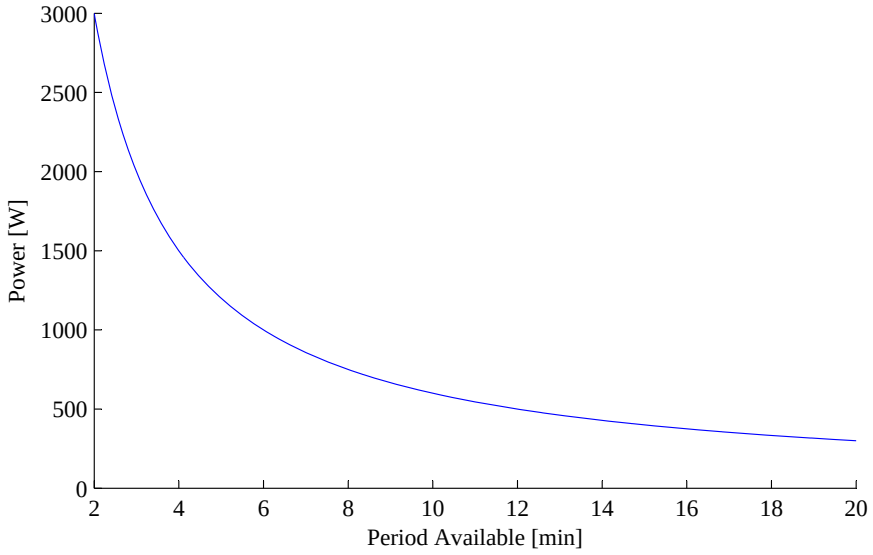

Figure 3.5: The relationship between the power available and the period that it is available

3.3 FLY-UPS design decisions

The design of the FLY-UPS is done according to the system specifications. As a starting point for the detail design of the FLY-UPS a few preliminary design decisions have to be taken. The following two subsystem design issues are addressed.

- Rotor/flywheel design
- Enclosure design

3.3.1 Rotor/flywheel design

The flywheel design must ensure that the amount of stored energy meets the specifications. An appropriate shape for the flywheel needs to be determined. The rotor/flywheel assembly must be able to handle the forces acting upon it. The maximum electromagnetic carrying force, stiffness, damping and position of the bearings must be determined.

The flywheel is to be an internal type flywheel, with the PMSM magnets on the rotor. The magnets are placed on the rotor to keep the design of the PMSM as simple as possible. The rotor/flywheel will be manufactured from a solid piece of metal, to increase the maximum rotational speed achievable by the rotor without having to resort to composite materials. The flywheel is in a simple disc shape so that the rotor can be easily manufactured. A diagram of the rotor/flywheel assembly is shown in figure 3.6.

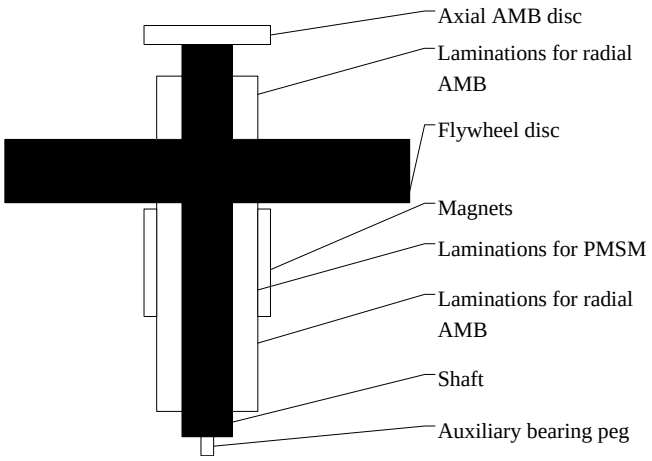

Figure 3.6: The layout of the rotor/flywheel assembly

3.3.2 Enclosure design

The enclosure must be able to safely withstand a failure of the rotor/flywheel assembly. To reduce losses the enclosure should be designed so that the FLY-UPS system operates in a vacuum.

The enclosure is designed using a modular concept. A modular concept means that each of the main components of the system will have its own enclosure with all the separate enclosures fitting onto each other to produce the final completed system. A modular approach is used to facilitate the replacement of a single component. The replacement of a component will either be done because of failure of the component or if another component needs to be tested or even if the system needs an upgrade. It can be done without having to completely redevelop a new system. The FLY-UPS's enclosure will be designed to seal relatively airtight. This will be achieved by using o-rings. The system is connected to a vacuum pump to pump the air out. A diagram of the rotor/flywheel assembly is shown in figure 3.7.

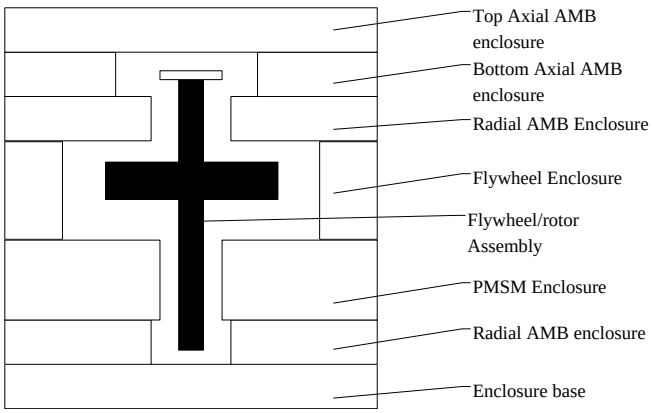

Figure 3.7: The layout of the enclosure assembly

3.4 System evaluation

An evaluation process is to be established and included in the system specification. This evaluation specification will then be used to benchmark the system's performance according to predicted performance values.

This chapter has explained the reasons behind some of the decisions made regarding the FLY-UPS system. The most suitable material for this application is 17-4PH stainless steel, the operating speed of 30000 rpm was chosen, the trip speed is chosen at 33000 rpm. The flywheel needs to be able to supply 2000 W of energy for 3 minutes, which equates to 360 kJ. The energy required translated into a disc with a mass of 12.45 kg and an axial height of 65 mm. The maximum axial length of the rotor is 505.5 mm. The maximum enclosure height is 550 mm and the diameter is 350 mm. To keep the rotor assembly relatively simple an internal PMSM setup is chosen. The flywheel enclosure is designed using a modular design approach.

Chapter 4

Rotor detail design

In this chapter the detail design of the rotor/flywheel assembly is discussed. Chapter 4 focuses on the energy storage capabilities of the rotor and verifying the strength analysis of the final designed rotor/flywheel assembly. The verification includes the adhesion of the magnets on the rotor and the rotor assembly strength.

4.1 Energy storage

A similar process to that followed in section 3.2.3 is now followed to include the rotor and flywheel assembly into the calculations of the kinetic energy stored. From the results in section 3.2.3 it is known that the flywheel needs to have a total moment of inertia of no less than 0.09727 $\text{kg} \cdot \text{m}^2$. To calculate the total moment of inertia, the moments of inertia of all the sub-components of the rotor/flywheel assembly are added. The first step is to determine all the formulas for the moments of inertia that are important to determine the total moment of inertia of the rotor assembly. The moments of inertia are determined by dividing the rotor into smaller basic pieces i.e. solid cylinders (see figure 4.1 and (4.1)) and thick cylinders (see figure 4.2 and (4.2))

$$I_z = \frac{\pi \cdot r_1^4 \cdot h \cdot \rho}{2} \qquad [\text{m}^2 \cdot \text{kg}] \tag{4.1}$$

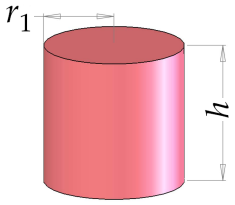

Figure 4.1: Solid cylinder

$$I_z = \frac{1}{2} \cdot \pi \cdot h \cdot \rho \cdot (r_2^2 - r_1^2)^2) \qquad [\mathrm{m}^2 \cdot \mathrm{kg}] \tag{4.2}$$

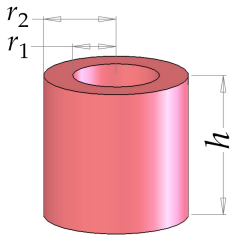

Figure 4.2: Thick cylinder

with ρ the density of the material.

These equations are used to determine the total moment of inertia. The values obtained through (4.1) and (4.2) are simply added until the complete rotor's moment of inertia is obtained. Refer to the completed rotor assembly in figure 4.3.

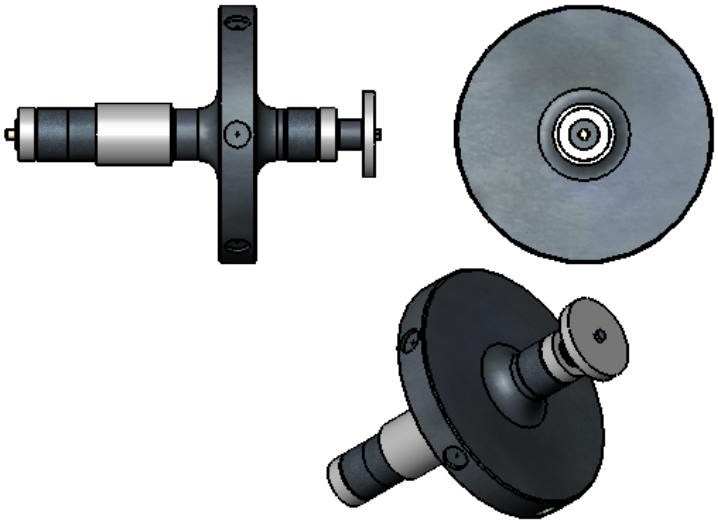

Figure 4.3: Completed rotor assembly

The moment of inertia obtained analytically is $I_{z,analytical} = 0.10669\ \mathrm{m}^2 \cdot \mathrm{kg}$. The value obtained analytically corresponds to the value obtained with the software package *SolidWorks*® $I_z = 0.10668621\ \mathrm{m}^2 \cdot \mathrm{kg}$. The difference in the values can be attributed to rounding errors and simplifications made when determining the analytical value. The value obtained using the software package is verified and is the value to be used in determining the energy storage capabilities of the rotor.

To verify the energy storage capabilities use (4.3) to determine the energy storage of the completed rotor assembly

$$E_K = \frac{I \cdot \omega^2}{2} = \frac{0.10668621 \cdot 3142^2}{2} = 526475.344 \text{ J} \tag{4.3}$$

ω is taken as 3142 $\frac{\text{rad}}{\text{s}}$ corresponding to 30000 rpm. This result is used to determine the period of time that the flywheel can provide 2000 W of power from full speed to half speed. The period of time that the flywheel provides 2000 W of power is determined with (4.4).

$$t = \frac{E}{P} = \frac{0.75 \cdot 526475.344}{2000} = 197.4 \text{ s} = 3.29 \text{ min} \tag{4.4}$$

This value is more than the required value of 3 minutes. The flywheel's energy storage design has therefore been verified.

4.2 Strength analysis

The design of the FLY-UPS is based on a factor of safety (FOS) of 1.5 or greater according to the type A specification (Appendix A). This section discusses the magnet adhesive design as well as a FEM strength analysis of the rotor.

4.2.1 Magnet adhesive

4.2.1.1 Performance requirements of the magnet adhesive

To determine the minimum shear strength required for the adhesive used to secure the magnets on the rotor, an equation is now derived referring to figure 4.4:

Firstly divide the rotor into infinitesimal pieces as shown in figure 4.4. Determine the infinitesimal circumference (ds) of the infinitesimal piece.

$$d\phi = \tan\frac{ds}{r} \approx \frac{ds}{r}$$

$$\therefore ds = r \cdot d\phi \tag{4.5}$$

Determine the equation for the infinitesimal mass (dm) on a radius (r).

$$dm = \rho \cdot l \cdot (r \cdot d\phi) \cdot dr \tag{4.6}$$

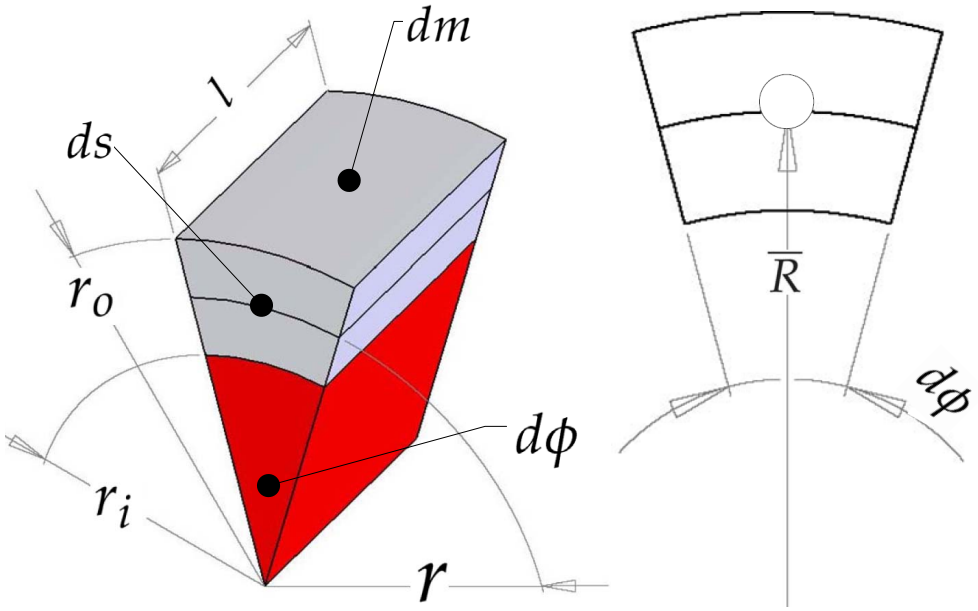

Figure 4.4: Magnet sector

Integrate from the inner radius (r_i) to the outer radius (r_o) to determine the mass (m) of a piece with an angle of $d\phi$. *Note: this is still only the mass of an infinitesimal piece of the rotor.*

$$\begin{aligned} \therefore m &= \rho \cdot l \cdot d\phi \cdot \int_{r_i}^{r_o} \cdot r \cdot dr \\ &= \rho \cdot l \cdot d\phi \cdot \frac{(r_o^2 - r_i^2)}{2} \end{aligned} \tag{4.7}$$

Determine the radius to the centre of mass ($\overline{R}$) with (4.8).

$$\overline{R} = \frac{\int r \cdot dm}{\int dm} \tag{4.8}$$

Substituting (4.6) into (4.8) and simplifying results in (4.10).

$$\therefore \overline{R} = \frac{\rho \cdot l \cdot d\phi \int_{r_i}^{r_o} r^2 \cdot dr}{\rho \cdot l \cdot d\phi \int_{r_i}^{r_o} r \cdot dr}$$

$$= \frac{2 \cdot r^3 \big|_{r_i}^{r_o}}{3 \cdot r^2 \big|_{r_i}^{r_o}} \tag{4.9}$$

$$= \frac{2}{3} \cdot \frac{(r_o^3 - r_i^3)}{(r_o^2 - r_i^2)} \tag{4.10}$$

The centrifugal force (F_c) is given by (4.11).

$$F_c = m \cdot \overline{R} \cdot \omega^2 \tag{4.11}$$

The magnitude of the force trying to pull the magnets from the rotor is given by (4.12) with A_i the inner surface area.

$$F_b = \sigma_r \cdot A_i = \sigma_r \cdot l \cdot r_i \cdot d\phi \tag{4.12}$$

Equation (4.11) is now set equal to (4.12).

$$\begin{aligned} F_c &= F_b \\ \therefore m \cdot \omega^2 \cdot \overline{R} &= \sigma_r \cdot l \cdot r_i \cdot d\phi \\ \therefore \sigma_r &= \frac{m \cdot \omega^2 \cdot \overline{R}}{l \cdot r_i \cdot d\phi} \end{aligned} \tag{4.13}$$

Substituting (4.10) and (4.7) into (4.13) and simplifying it, results in (4.14).

$$\therefore \sigma_r = \frac{(\rho \cdot l \cdot d\phi \cdot \int_{r_i}^{r_o} \cdot r \cdot dr) \cdot \omega^2 \cdot (\frac{\int r \cdot dm}{\int dm})}{l \cdot r_i \cdot d\phi}$$

$$\therefore \sigma_r = \frac{(\rho \cdot l \cdot d\phi \cdot \frac{(r_o^2 - r_i^2)}{2}) \cdot \omega^2 \cdot (\frac{2}{3} \cdot \frac{(r_o^3 - r_i^3)}{(r_o^2 - r_i^2)})}{l \cdot r_i \cdot d\phi}$$

$$\therefore \sigma_r = \frac{\rho \cdot \omega^2 \cdot (r_o^3 - r_i^3)}{3 \cdot r_i} \qquad [\text{Pa}] \tag{4.14}$$

Equation (4.14) is used to determine the tension in the adhesive used to secure the magnets to the rotor. Substitute $\rho = 7400\ \frac{\text{kg}}{\text{m}^3}$, $\omega = 3456\ \frac{\text{rad}}{\text{s}}$, $r_i = 0.025$ m and $r_o = 0.03$ m.

The minimum tension required on the adhesive to prevent the magnets from being dislodged by the centrifugal force is determined to be $\sigma_r = 13.4$ MPa. With a factor of safety of 1.5 included the required tension increases to 20.1 MPa.

Thus an adhesive with at least a performance value of 20.1 MPa should be selected, keeping in mind that the adhesive should be effective up to a temperature of 60 °C.

4.2.1.2 Adhesive vs. carbon fibre sleeve

Adhesive

The yield strength σ_{Ady} of the adhesive (Loctite 324) is 15 MPa, which is less than the required 20.1 MPa. Securing the magnets with adhesive only is not a suitable solution. If the magnets were to be secured with adhesive only, the maximum rotational speed will have to be reduced in order to maintain the factor of safety.

Carbon fibre sleeve

A suitable adhesive could not be found. Thus the magnets needs to be held in place by mechanical means, namely a wound carbon-fibre filament. The requirements of the carbon fibre is calculated using the hoop-strength equation given by (4.15) [17]

$$\sigma_{t,max} = \frac{p \cdot (d_i + t)}{2t} \qquad \text{[Pa]} \tag{4.15}$$

with the stress on the inside $p = \sigma_r \cdot \left(\frac{A_o}{A_i}\right)$, A_i and A_o the inner and outer contact areas on the magnets, $\sigma_{t,max}$ the maximum hoop-strength approximation, d_i the inner diameter of the sleeve, or the outer diameter of the magnets and t the thickness of the carbon fibre sleeve.

Substituting the values $p = 24.13$ MPa, $d_i = 60$ mm, $t = 0.5$ mm and $\left(\frac{A_o}{A_i}\right) = 1.2$ into (4.15) determines the required yield strength as 1460 MPa. The yield strength of carbon fibre is 800 MPa, which is less than the required value of 1460 MPa. The wound carbon fibre is thus also not a suitable solution to secure the magnets to the rotor. The maximum rotational speed will have to be reduced in order to maintain the factor of safety for this particular setup.

Combination of carbon fibre and adhesive

To optimise the properties of the sleeve as well as the adhesive, a combination of adhesive and a carbon fibre sleeve is used. This improves the mechanical properties of the assembly. Refer to

figure 4.5 for the layout of the combination approach. The 2 magnet sectors are secured to the rotor/flywheel assembly using an adhesive. After the adhesive has fully cured a carbon-fibre filament is wound around the magnet sectors. After the carbon-fibre filament has cured, the carbon fibre sleeve is machined to the required thickness.

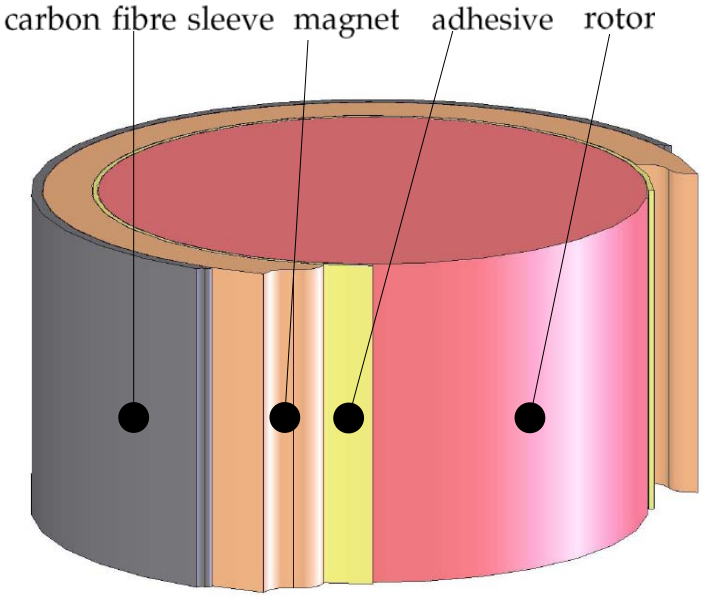

Figure 4.5: Combination of adhesive and carbon fibre layout

The adhesive is firstly transformed into an equivalent amount of carbon fibre, using the transformation factor [25] of the adhesive and carbon fibre's Young's modula. The transformation factor is given by (4.16).

$$n = \left(\frac{E_{Ad}}{E_{CF}}\right) \qquad [\text{-}] \tag{4.16}$$

Substituting $E_{Ad} = 614$ MPa and $E_{CF} = 110$ GPa into (4.16), results in a transformation factor value of 0.00558.

The transformation factor (n) is used to transform the area on which the *adhesive is applied* (A_{Ah}) to a *cross-sectional area* of carbon-fibre (A_{CFt}) using (4.17).

$$A_{CFt} = A_{Ah} \cdot n \qquad [\text{mm}^2] \tag{4.17}$$

Substituting $A_{Ah} = 9047.79$ mm^2 and $n = 0.00558$ into (4.17) results in a transformed value of the adhesive's equivalent cross sectional area of $A_{CFt} = 50.503$ mm^2.

Determine the cross sectional area of the carbon fibre using (4.18).

$$A_{CF} = \left(\pi \cdot \left(\frac{d_o}{2}\right)^2\right) - \left(\pi \cdot \left(\frac{d_i}{2}\right)^2\right) \qquad [\text{mm}^2] \tag{4.18}$$

Substituting $d_o = 61$ mm, and $d_i = 60$ mm into (4.18) determines the cross sectional area of the carbon fibre as $A_{CF} = 95.03$ mm^2.

The total equivalent carbon fibre cross sectional area is determined by adding the cross sectional area of the carbon fibre and the equivalent carbon fibre cross sectional area of the adhesive.

$$A_{tot} = A_{CF} + A_{CFt} = 145.53 \text{ mm}^2 \tag{4.19}$$

The total area is used to find an equivalent thickness (t) for the carbon sleeve, using (4.20).

$$A_T = \left(\pi \cdot \left(\frac{d_{oT}}{2}\right)^2\right) - \left(\pi \cdot \left(\frac{d_i}{2}\right)^2\right) \qquad [\text{mm}^2] \tag{4.20}$$

Substituting $d_i = 60$ mm, and $A_T = 145.533$ mm^2 into (4.20) results in an equivalent diameter of $d_{oT} = 61.52$ mm. The wall thickness is calculated by subtracting the inner radius from the outer radius:

$t = \frac{d_{oT} - d_i}{2} = 0.76$ mm

The result of the addition of the adhesive is that the equivalent thickness of the carbon-fibre sleeve has increased by 0.26 mm.

The hoop strength equation is used (4.21) to determine the tension on the transformed adhesive and carbon fibre combination.

$$\sigma_{t,maxC} = \frac{p \cdot (d_i + t)}{2t} \qquad [\text{Pa}] \tag{4.21}$$

Substituting $p = 24.1254$ MPa, $d_i = 60$ mm, and $t = 0.76$ mm into (4.21) results in $\sigma_{t,max} = 964.4$ MPa. This is for a carbon fibre sleeve with a thickness of 0.5 mm, adhesive on the inner diameter of the magnets and a rotational speed of 33000 rpm. The stress in the combined material is more than the allowable value of 800 MPa. The maximum allowable rotational speed of the rotor will have to be adjusted to a lower value in order to keep the factor of safety higher than 1.5. The option of increasing the thickness of the carbon fibre sleeve is unavailable; there is not enough radial space available. The stress on the adhesive is verified by multiplying $\sigma_{t,max}$ with the transformation factor (n). The value for the stress on the adhesive is 5.3813 MPa. The stress on the adhesive is lower than the yield strength of the adhesive. Thus the adhesive will not fail.

The maximum allowable rotational speed is determined by using (4.21) and substituting $\sigma_{t,maxC} =$ 800 MPa and $t = 0.76$ mm. The pressure p is determined as 20.01 MPa with a factor of safety of 1.5 included. Using (4.22) and substituting $p = 20.01$ MPa and $\rho = 7400$ $\frac{\text{kg}}{\text{m}^3}$, the maximum allowable rotational speed is determined as $\omega = 3147$ $\frac{\text{rad}}{\text{s}}$ or 30056 rpm.

$$p = \frac{\rho \cdot \omega^2 \cdot (r_o^3 - r_i^3)}{3 \cdot r_i} \cdot FOS \cdot \frac{A_o}{A_i} \qquad [\text{Pa}] \tag{4.22}$$

The stress on the carbon fibre sleeve and adhesive combination is $\sigma_{t,max} = 800$ MPa. The stress calculated is for a carbon fibre sleeve with a thickness of 0.5 mm, adhesive on the inner diameter of the magnets and a rotational speed of 30056 rpm.

Table 4.1: Comparison of adhesive and carbon fibre performance

Parameter	Adhesive	Carbon fibre	Combination
Max Speed [rpm]	28504	24431	30056
FOS_{min}	1.5	1.5	1.5

Table 4.1 is a summary of the results of the analytical calculations done.

4.2.2 Flywheel disc strength

The flywheel disc needs to be able to withstand the centrifugal forces acting upon the disc due to the rotation of the rotor/flywheel assembly. A simplistic analytical calculation is done to verify the design and determine the factor of safety. The result of the analytical calculations is verified using the software package *CosmosWorks*® to check the design of the final rotor/flywheel assembly. The life-cycle of the flywheel is also determined using this software package.

4.2.2.1 Analytical calculations

Equation (4.23) is used to determine the tangential stress and (4.24) to determine the radial stress

$$\sigma_{Tangential} = \rho \cdot \omega^2 \cdot \frac{\nu + 3}{8} \cdot (r_i^2 + r_o^2 + \frac{r_i^2 \cdot r_o^2}{r^2} - \frac{1 - 3\nu}{3 + \nu} \cdot r^2) \qquad [\text{Pa}] \tag{4.23}$$

$$\sigma_{Radial} = \rho \cdot \omega^2 \cdot \frac{\nu + 3}{8} \cdot (r_i^2 + r_o^2 - \frac{r_i^2 \cdot r_o^2}{r^2} - r^2) \qquad [\text{Pa}] \tag{4.24}$$

with $\rho = 7800\ \frac{\text{kg}}{\text{m}^3}$, $\omega = 3147\ \frac{\text{rad}}{\text{s}}$ (30056 rpm), $r_i = 0$ m, $r_o = 0.125$ m and $r = 1 \times 10^{-50} \mapsto 0.125$ m. The maximum result is $\sigma_{Tangential} = 491.53$ MPa. The tangential stress in the disc is shown in figure 4.6. The radial stress in the disc is shown in figure 4.7.

Equation (4.25) is used to determine the von Misses stress in the disc. Refer to figure 4.8.

$$\sigma_{vM} = \frac{1}{\sqrt{2}} \cdot \sqrt{\sigma_{Radial}^2 + \sigma_{Tangential}^2 + (\sigma_{Radial} - \sigma_{Tangential})^2} \qquad [\text{Pa}] \tag{4.25}$$

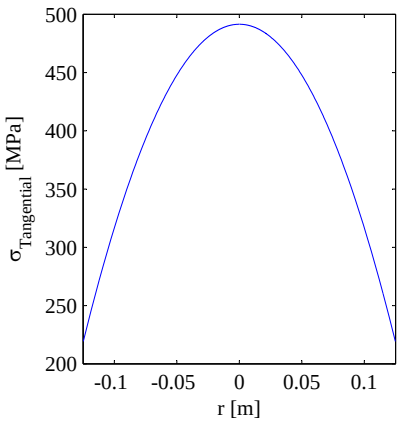

Figure 4.6: Tangential stress in the flywheel disc

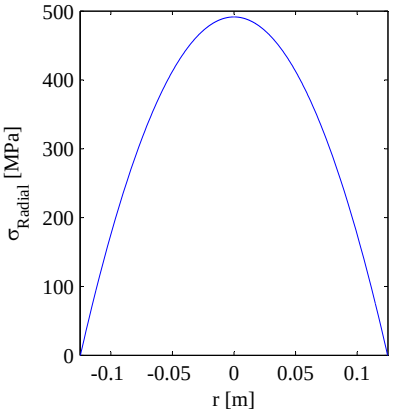

Figure 4.7: Radial stress in the flywheel disc

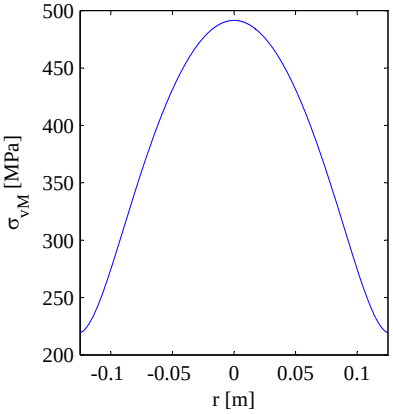

Figure 4.8: Von Misses stress in the flywheel disc

In figure 4.6, figure 4.7 and figure 4.8 the maximum stress in the flywheel disc is shown to be $\sigma_{MAX} = 491.53$ MPa. Use $\sigma_{MAX} = 491.53$ MPa to determine the factor of safety of the flywheel disc, using (4.26).

$$FOS_{disc} = \frac{\sigma_y}{\sigma_{MAX}} \qquad [\text{-}] \tag{4.26}$$

With $\sigma_y = 1158$ MPa (the yield strength of 17-4PH [condition H1025]) it is found that the factor of safety in the flywheel disc is 2.36. The factor of safety satisfies the design parameter of a minimum factor of safety of 1.5.

4.2.2.2 Software verification

CosmosWorks® was used to verify the analytical calculations done in section 4.2.2.1. The analytical calculations gave a result of a minimum factor of safety of 2.36. The software package's result is a minimum factor of safety of 1.7. The FEM package's value is a better representation of the true factor of safety. The reason for this statement is that the analytical calculations have certain limitations. The analytical calculations are a purely two dimensional analysis on a simple disc shape. The software package on the other hand is a totally three dimensional analysis and takes into account all of the features on the final rotor design. Refer to figure 4.9.

The fatigue life of the flywheel is 812600 cycles. The flywheel does not have an infinite life. Regular tests should be performed in order to ensure that the flywheel is safe to operate. These tests shall include tests to verify that the natural frequencies have not changed, as well as tests to measure the moment of inertia. The results of the Software package *CosmosWorks*® can be found in appendix D.7.

4.3 Rotor dynamics

4.3.1 Unbalance

The unbalance of a rotor determines the forces acting upon the bearings. In this case the AMBs' forces need to be kept at a minimum. It is important to define these forces in order to accurately simulate the rotor-dynamic effects of the rotor.

4.3.1.1 ISO 1940/1 unbalance designation

The ISO 1940/1 standard utilises a ″G″ designation. This indicates the level of balance that the rotor is balanced to. A lower ″G″ indicates a better balanced rotor. The equation for the calculation of the unbalance is shown in (4.27). The ″G″ designation is used when the rotor is balanced by a contractor to determine the permissible unbalance

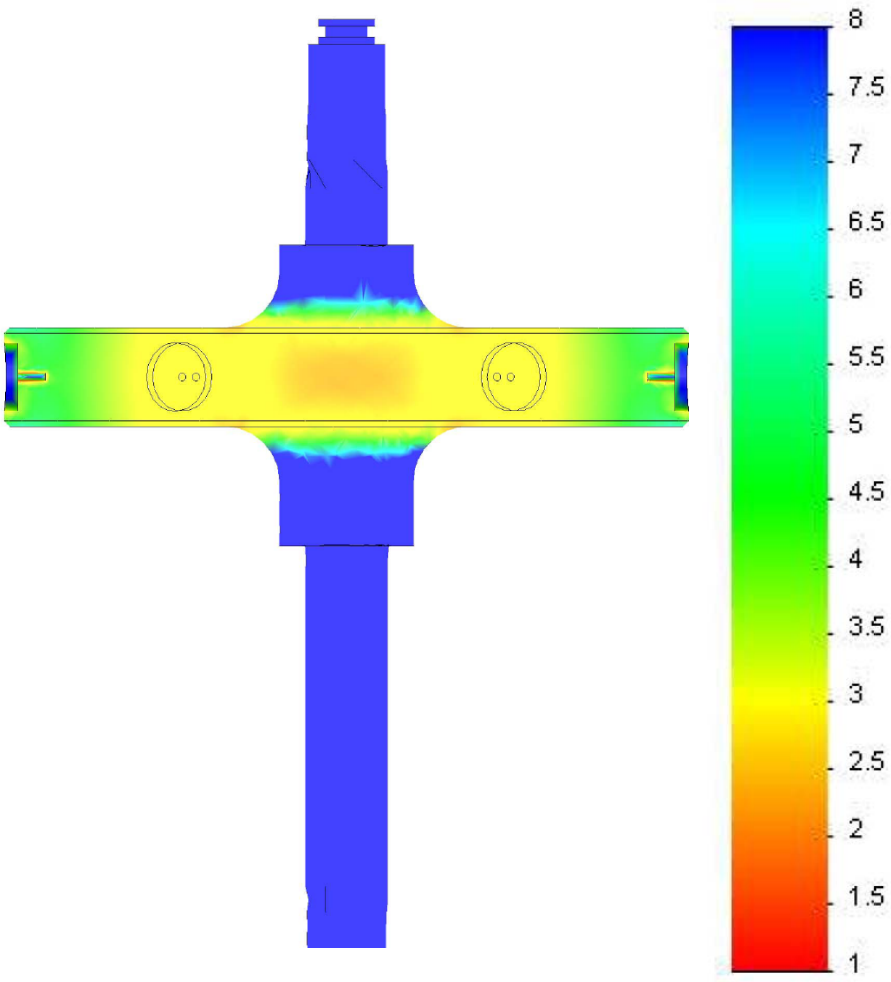

Figure 4.9: FOS of the rotor/flywheel

$$U_{per} = \frac{9.549 \cdot (G \cdot W)}{N} \qquad [\mathrm{kg \cdot m}] \tag{4.27}$$

with W the weight of the rotor, U_{per} the permissible unbalance and N the speed of the rotor in revolutions per minute.

4.3.1.1.1 For overhung and narrow rotors: According to the API 612 [26] standard the ISO 1940/1 [27] standard is adjusted for overhung and narrow rotors according to these parameters. The results of (4.28) and (4.29) are used to determine the rotor-dynamic simulation unbalance

$$U_{per,static} = \frac{U_{per}}{2} \cdot \frac{d}{2c} \qquad [\mathrm{kg \cdot m}] \tag{4.28}$$

$$U_{per,couple} = \frac{U_{per}}{2} \cdot \frac{3d}{4c} \qquad [\mathrm{kg \cdot m}] \tag{4.29}$$

with c the distance between the centre of the rotor and the furthest bearing support, and d the distance between the bearings. The static and couple unbalance is applied as shown in figure 4.10.

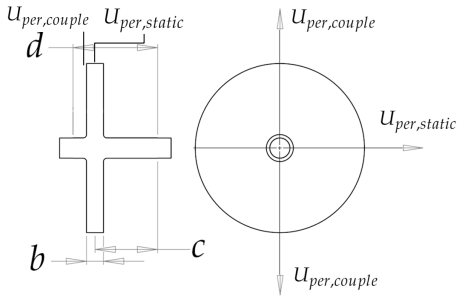

Figure 4.10: ISO standard balancing application for a centred rotor

4.3.1.1.2 For rotors with outboard correction planes: According to the API 612 [26] standard the ISO 1940/1 [27] standard is adjusted for rotors with outboard correction planes according to these parameters. The results of (4.30), (4.31) and (4.32) are used to determine the rotor-dynamic simulation unbalance.

$$U_{per,adjusted} = U_{per} \cdot \frac{d}{b} \qquad [\mathrm{kg \cdot m}] \tag{4.30}$$

$$U_{per,left} = U_{per,adjusted} \cdot \frac{h_r}{b} \qquad [\mathrm{kg \cdot m}] \tag{4.31}$$

$$U_{per,right} = U_{per,adjusted} \cdot \frac{h_l}{b} \qquad [\mathrm{kg \cdot m}] \tag{4.32}$$

The distance between the rotors is defined as b, the distance between the bearings is defined as d, and h_l and h_r are defined as the distances from the centre of gravity to the left and right rotor respectively, as shown in figure 4.11.

4.3.1.2 API 612 standard

According to the API standard the critical frequencies of a system have to be separated by a certain margin from the operating range of the system in order for the system to be considered critically damped [26].

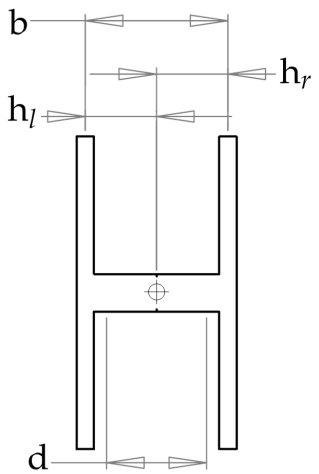

Figure 4.11: ISO standard balancing application for a dumbbell rotor setup

Determine 0.707 of the maximum amplitude and the corresponding rotational speeds ($N_{0.707,lower}$ and $N_{0.707,upper}$) as shown in figure 4.12 and figure 4.13.

Now determine the amplification factor (4.33)

$$F_A = \frac{N_{critical}}{N_{0.707,upper} - N_{0.707,lower}} \qquad [\text{-}] \tag{4.33}$$

If the amplification factor is less than 2.5, the response is considered critically damped [26] and no separation margin is required and no further testing is required. If the amplification factor is greater than 2.5 then the separation margin needs to be determined [26]. Below is an explanation for both possibilities, namely where the operating range is lower than the critical frequency, and where the operating range is higher than the critical frequency. These tests should be done on all the critical frequencies near the operating range of the rotor.

4.3.1.2.1 Operating range lower than critical frequency : If the amplification factor is 2.5 or greater and that particular critical speed is above the maximum continuous speed, the separation margin (4.34) should be larger than (4.35) or 26, whichever is less [26] (see figure 4.12).

$$S_m = 100 \cdot \frac{N_{0.707,lower} - N_{maximum,continuous}}{N_{maximum,continuous}} \qquad [\%] \tag{4.34}$$

$$M_s = 10 + 17 \cdot (1 - \frac{1}{F_A - 1.5}) \tag{4.35}$$

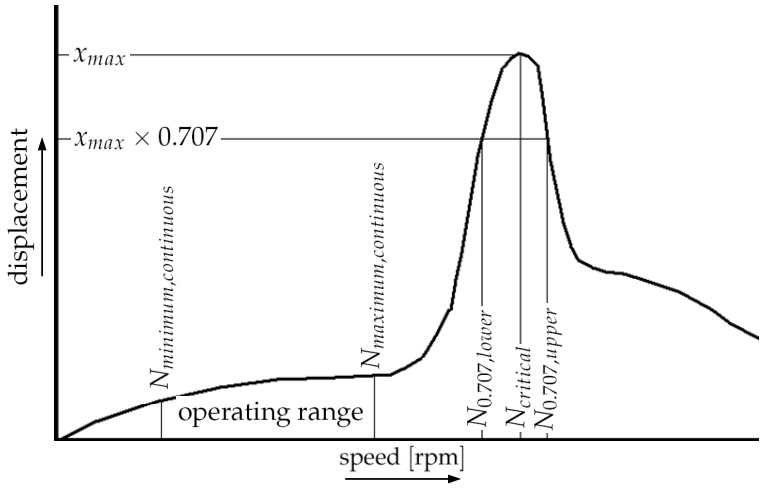

Figure 4.12: API standard for an operating range lower than the critical frequency

4.3.1.2.2 Operating range higher than critical frequency : If the amplification factor is 2.5 or greater and that particular critical speed is below the minimum continuous speed the separation margin (4.36) should be larger than (4.37) or 16 whichever is less [26]. Figure 4.13 shows a typical frequency response plot and the corresponding values used in the API 612 standard.

$$S_m = 100 \cdot \frac{N_{minimum,continuous} - N_{0.707,upper}}{N_{minimum,continuous}} \qquad [\%] \tag{4.36}$$

$$M_s = 17 \cdot (1 - \frac{1}{F_A - 1.5}) \tag{4.37}$$

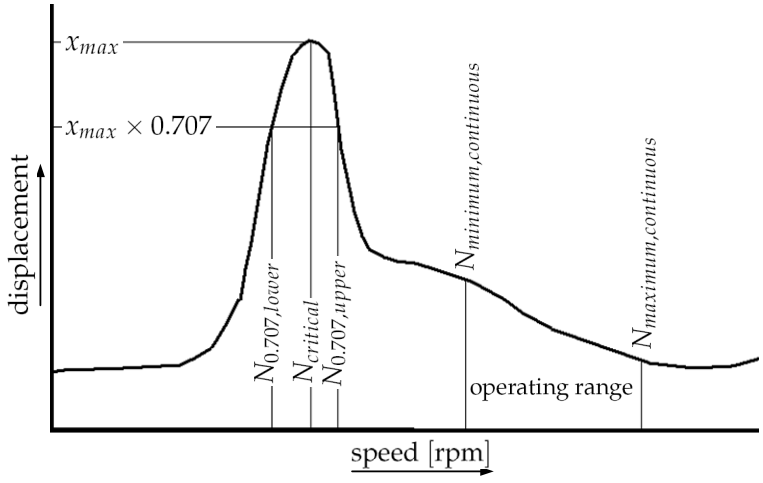

Figure 4.13: API standard for an operating range higher than the critical frequency

If the rotor does not satisfy these requirements, the final test requires a check of all the clearances of the system on all operating speeds. The requirement is that the clearance multiplied with a

correction factor should never exceed 75% of the total clearance [26]. In the FLY-UPS system the clearances of concern are located at the auxiliary bearings, the sensor positions, and the PMSM and AMB positions. The FLY-UPS rotor-dynamic analysis results should be checked at all these locations and at all speeds. Refer to figure 4.14. The value of the clearance at a certain speed needs to be multiplied with a correction factor as seen in (4.38).

$$F_c = \frac{A_1}{A_{4x}} \qquad [-] \tag{4.38}$$

$$A_1 = 25.4 \cdot \sqrt{\frac{12000}{N}} \qquad [\mu\text{m}]$$

where F_c is the correction factor, A_1 is the amplitude limit, A_{4x} is the calculated peak-to-peak amplitude at the probe locations in [μm] and N is the operating speed nearest the relevant critical frequency.

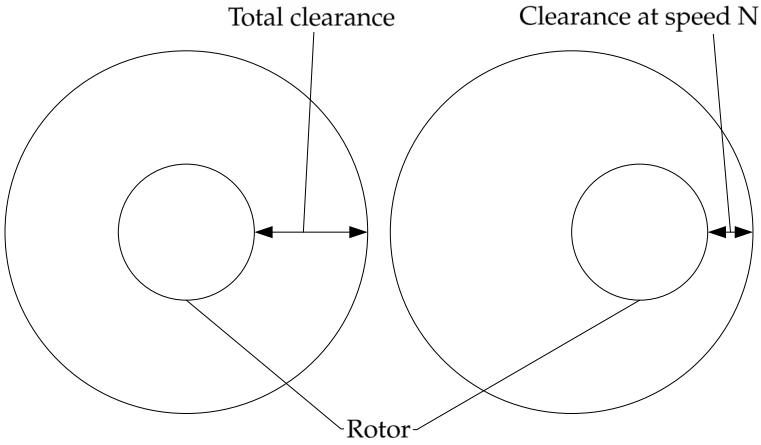

Figure 4.14: Clearance of the rotor

To conclude this section a summary of the API 612 process is shown in figure 4.15.

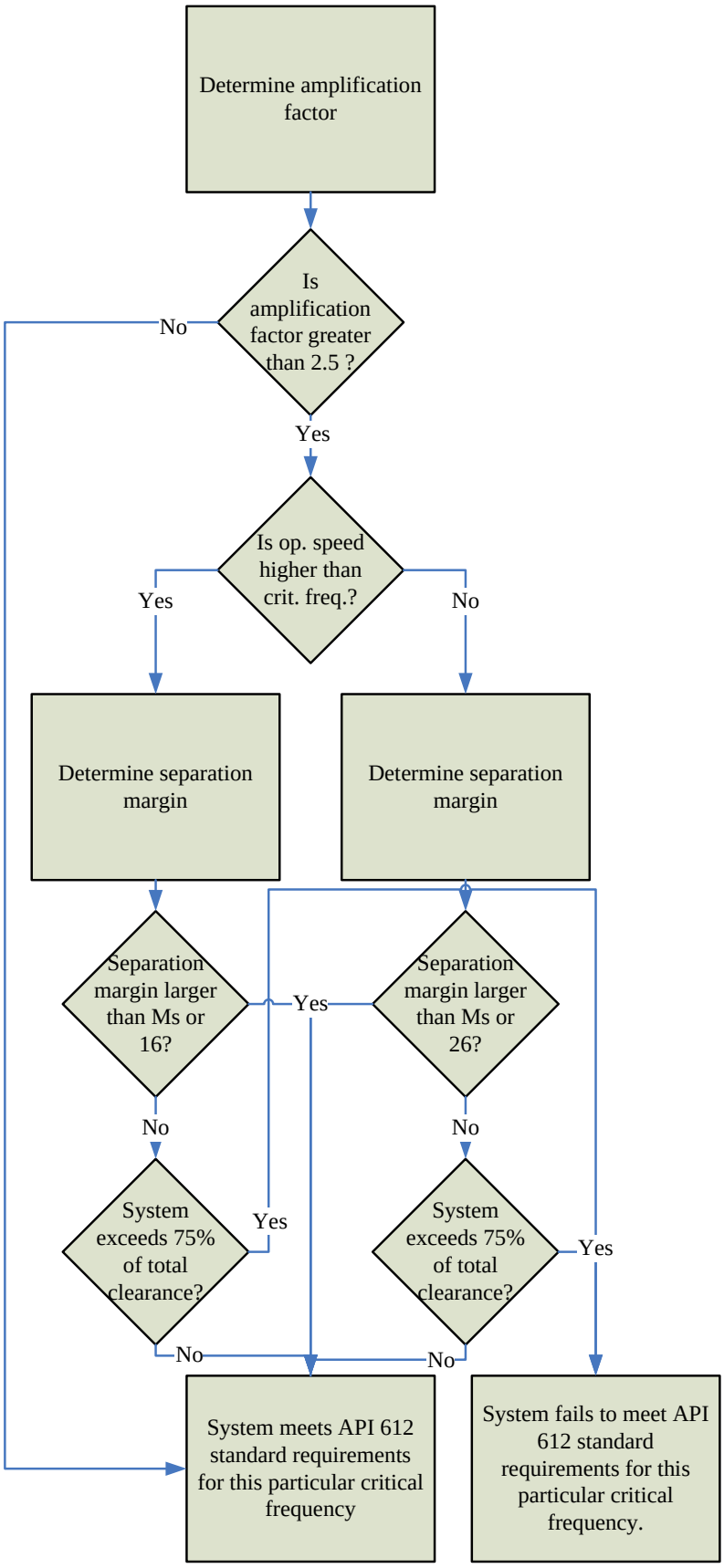

Figure 4.15: Flowchart of API 612 procedure

4.3.2 Detail design of the rotor

4.3.2.1 Rotor design process

The nature of the design of a rotor is an iterative process with many interacting variables. The process of optimising the rotor for rotor-dynamic stability, strength and energy storage is a complicated task. The process followed is shown in figure 4.16. Figure 4.16 does not go into all the detail of the iterative process. It shows the main tasks involved in the design of the rotor. The rotor/flywheel detail design drawings can be seen in appendix D.9

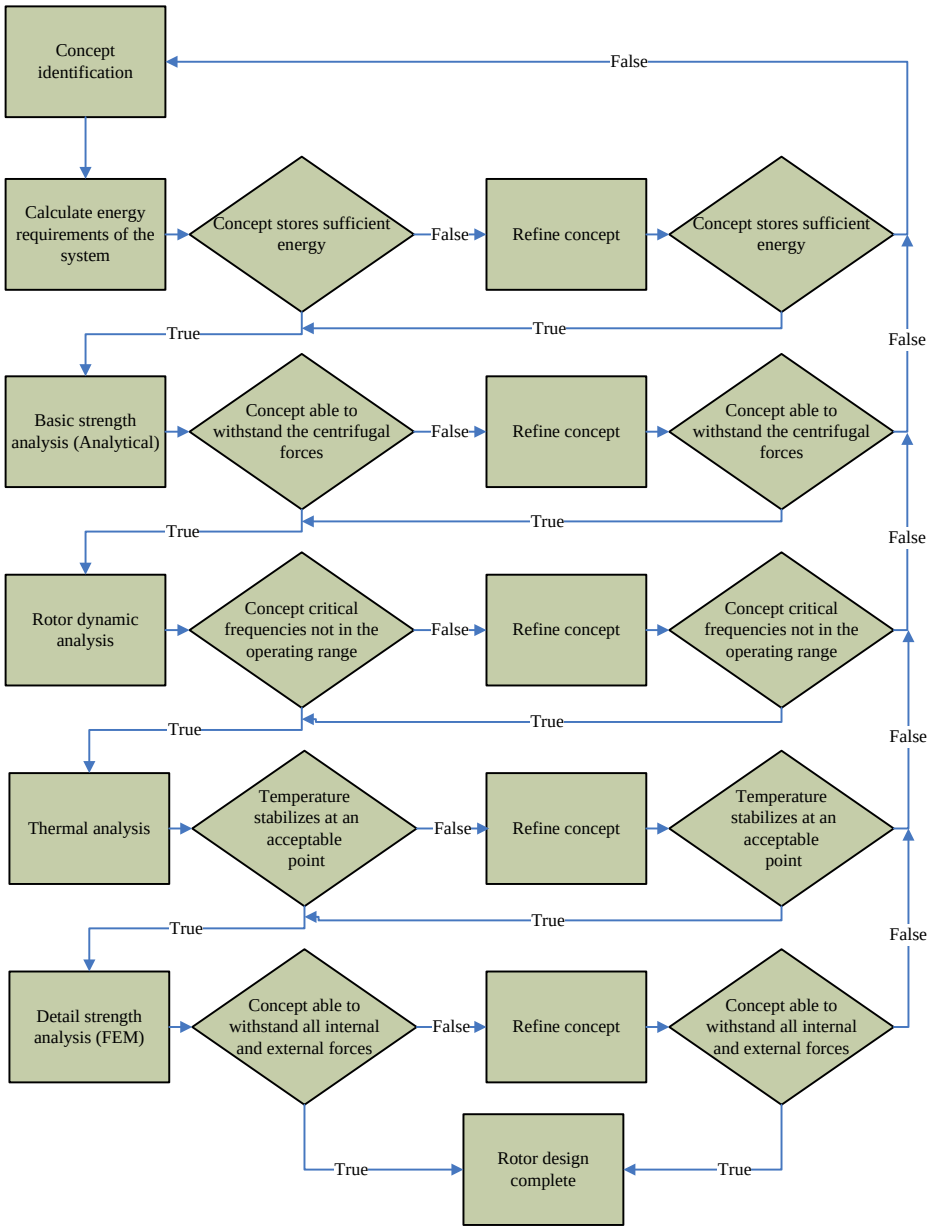

Figure 4.16: Rotor design process diagram

4.3.2.2 Rotor-dynamic analysis and results :

The rotor-dynamic program *DyRoBeS*® is used to determine the rotor-dynamic properties of the system. The unbalance acting upon the rotor has been determined using the ISO standard for balancing rotors; see section 4.3.1.1. The API standard has been used to determine the simulated unbalance on the rotor. The rotor-dynamic simulations are done for 2 possible worst case scenarios. The first of these scenarios is if the residual unbalance directly exaggerates the rotor-dynamic effects of the rotor, as seen in mode 1 (refer to figure 4.17 and figure 4.18). The simulated unbalance is therefore placed on the sides of the flywheel disc. The angle between these unbalances is set at zero. The reason for the angle between the unbalances is simple: the unbalance would most adversely effect the rotor displacement if they are in phase.

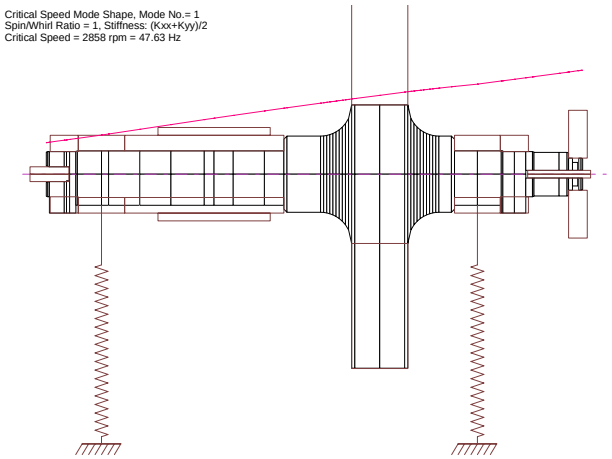

Figure 4.17: First rigid mode of the rotor simulated, using the dynamic stiffness of the radial AMBs.

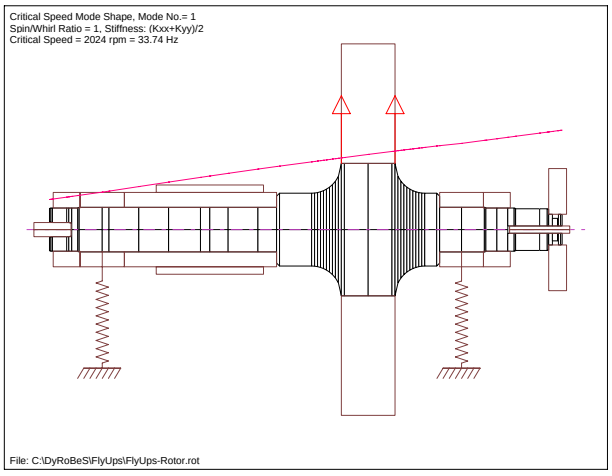

Figure 4.18: First rigid mode of the rotor simulated, using the static stiffness of the radial AMBs.

The second is when the residual unbalance amplifies the rotor-dynamic effects of mode 2 (refer to figure 4.19 and figure 4.20). For this case the unbalances need to be placed on the extremities

of the rotor and the phase needs to be 180 degrees. This is represented in figure 4.21.

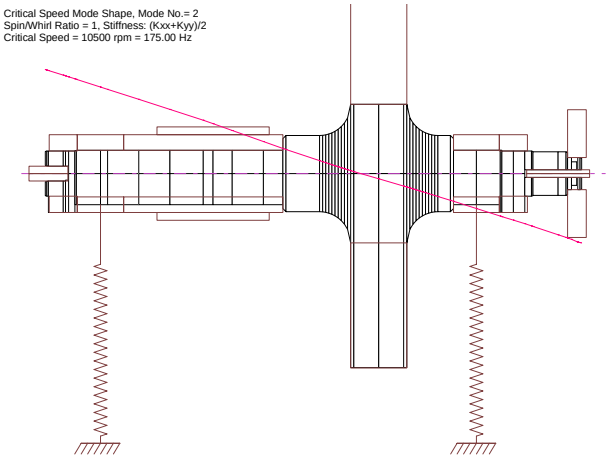

Figure 4.19: Second rigid mode of the rotor, simulated using the dynamic stiffness of the radial AMBs.

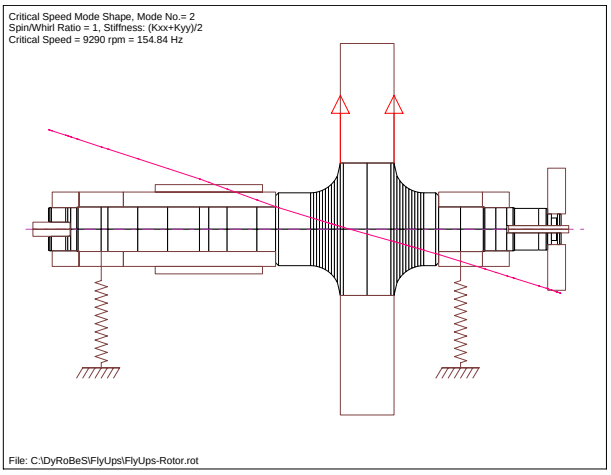

Figure 4.20: Second rigid mode of the rotor, simulated using the static stiffness of the radial AMBs.

The results of the rotor dynamic analysis can be classified into 2 categories. The first category is the results that are independent of the unbalance placement. The independent results include the critical speed analysis and the whirl speed analysis. The critical speed map (figure 4.24) is used to determine the possible range of stiffnesses of the AMBs. The horizontal green lines indicate the operating speed of the system. As the flywheel speeds up it will traverse the first two critical modes. The third critical mode is independent of the selected bearing stiffness. The stiffness is chosen at 500 $\frac{\mathrm{N}}{\mathrm{mm}}$. The complete set of rotor dynamic results can be found in appendix D.6. The first critical frequency is 47.63 Hz or 2858 rpm. The mode shape for the first critical frequency is shown in figure 4.18. The second critical frequency is located at 175Hz or 10500 rpm. The mode shape for the second critical frequency is shown in figure 4.20. The third critical frequency is shown in figure 4.22 and figure 4.23. The third critical frequency is located at 739.22 Hz (44353 rpm). The operating range of the FLY-UPS system is between 15000 rpm

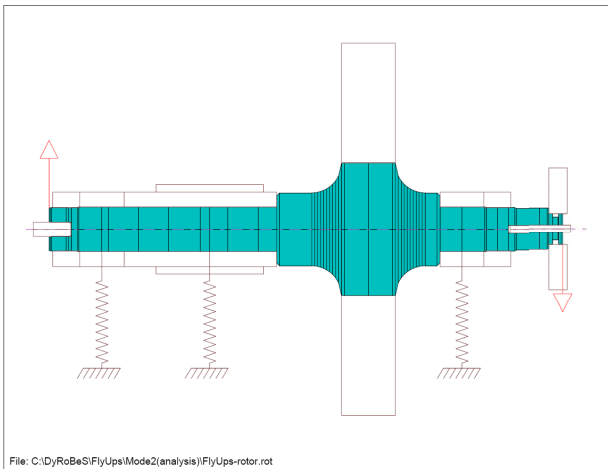

Figure 4.21: Unbalance placement for second rigid mode of the rotor

and 30000 rpm. There are no critical frequencies within the operating range of the FLY-UPS system.

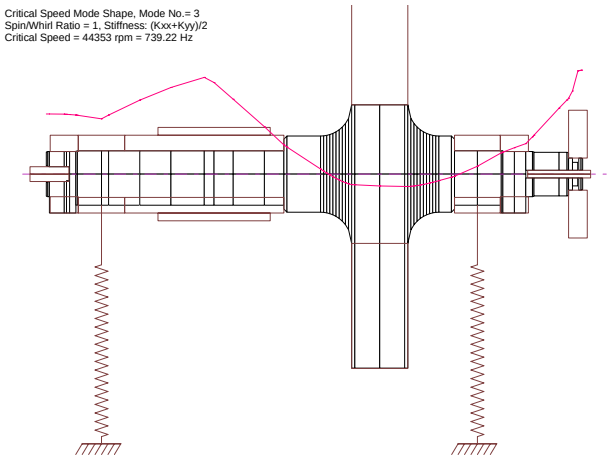

Figure 4.22: First bending mode of the rotor simulated, using the dynamic stiffness of the radial AMBs.

The rotor displacement, for the unbalance as seen in figure 4.18, at five different locations is shown in figure 4.25. The rotor displacement, for the unbalance in figure 4.21 is shown in figure 4.26. The magenta line represents the lower AMB's sensor location. The light red line represents the displacement at the AMB. The dark green line represents the displacement at the PMSM. The purple line represents the displacement at the upper AMB. The pink line represents the displacement at the upper AMB's sensor location. In both of cases the displacement never exceeds 75 % of the total clearance of the system, thus the API 612 standard is achieved with this design.

The forces transmitted to the bearings for the mode 1 unbalances are shown in figure 4.27. The force transmitted to the lower bearing is at a maximum at the upper limit of the operating

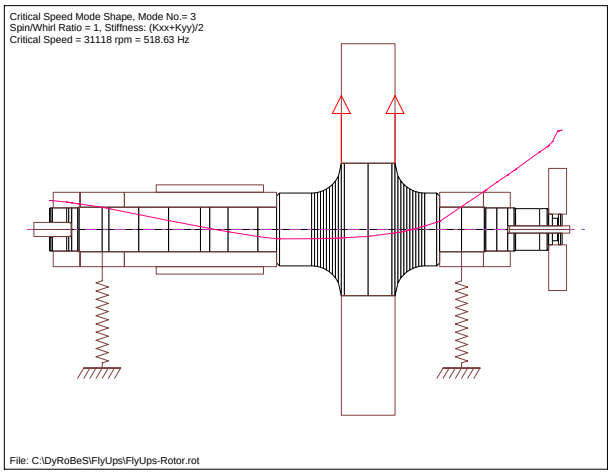

Figure 4.23: First bending mode of the rotor simulated, using the static stiffness of the radial AMBs.

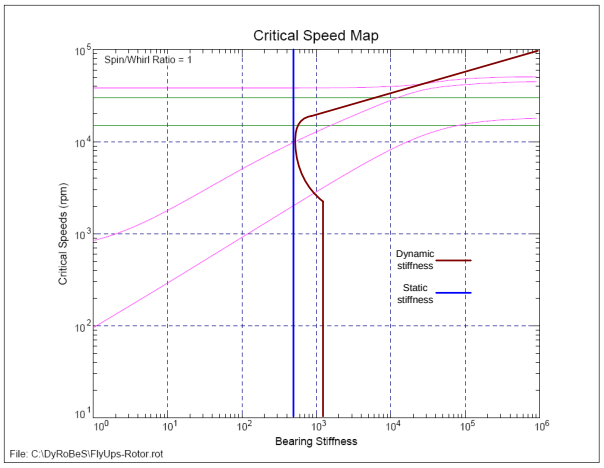

Figure 4.24: Critical speed map of the system, showing the dynamic and static stiffness of the AMBs.

speed and has a value of 17 N. The transmitted force on the upper bearing has a value of 87 N at 29000 rpm. Both of these values are well within the design specifications of 150 N.

4.4 Example of API 612 design verification process

A short example of one peak for one critical frequency follows. The process is outlined in figure 4.15.

Step 1: Identify peak (refer to figure 4.28). The peak value is 0.0061947 mm at 33280 rpm

Step 2: Determine 0.707 of the maximum amplitude

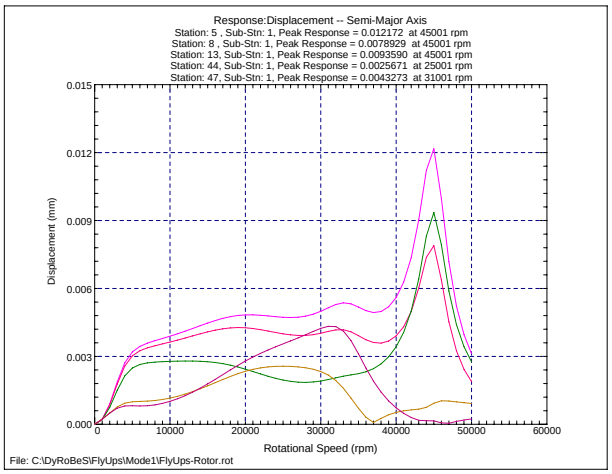

Figure 4.25: Multiple response plot at 5 different locations for mode 1 unbalance

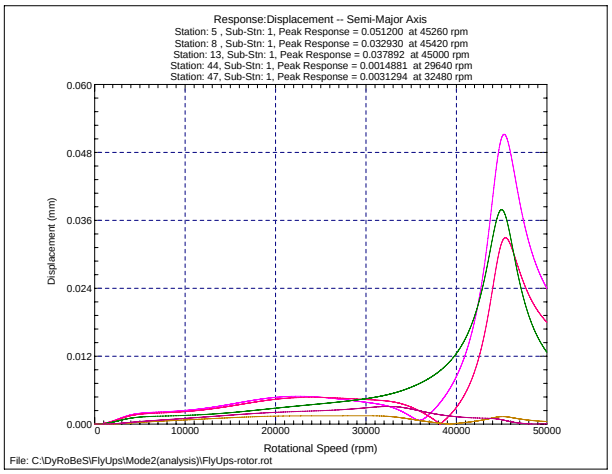

Figure 4.26: Multiple response plot at 5 different locations for mode 2 unbalance

$x_{max} \cdot 0.707 = 0.0061947 \cdot 0.707 = 0.0043797$ mm

Step 3: Determine the corresponding rotational speeds. Refer to figure 4.29. $N_{0.707,lower} = 27500$ rpm and $N_{0.707,upper} = 45500$ rpm.

Step 4: Determine the amplification factor.

$$F_A = \frac{N_{critical}}{N_{0.707,upper} - N_{0.707,lower}} = \frac{33280}{45500 - 27500} = 1.85$$

The amplification factor is less than 2.5 thus the peak is considered critically damped and no further testing is needed on this particular response peak. Consider another peak shown in figure 4.30.

Continue at step 3: Determine the corresponding rotational speeds. Refer to figure 4.31. $N_{0.707,lower} = 43000$ rpm and $N_{0.707,upper} = 46500$ rpm.

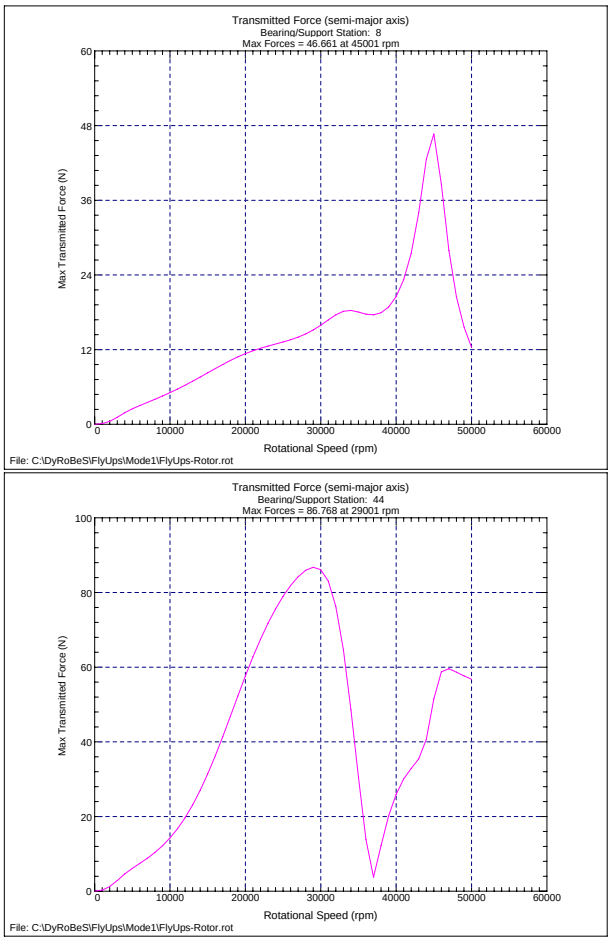

Figure 4.27: Transmitted bearing forces for lower and upper radial AMBs

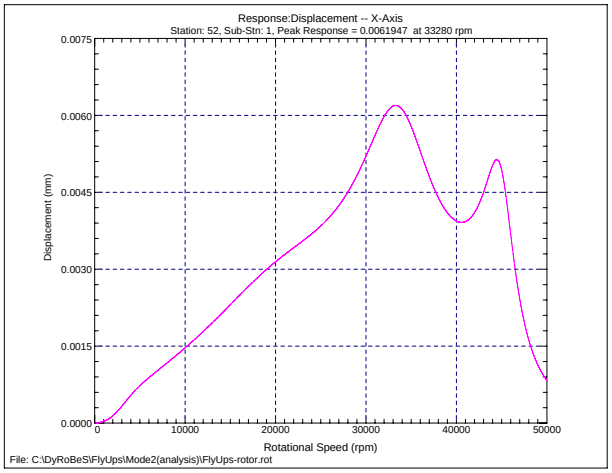

Figure 4.28: Response peak at 33280 RPM

Step 4: Determine the amplification factor.

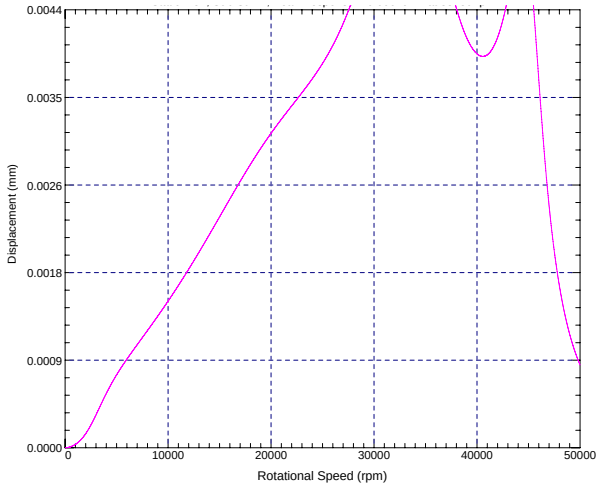

Figure 4.29: Corresponding rotational speeds

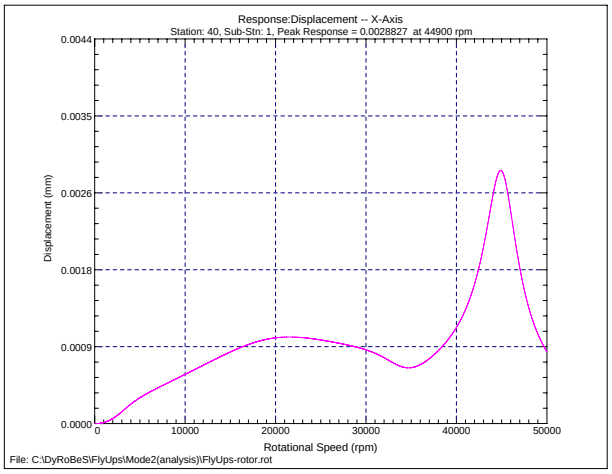

Figure 4.30: Response peak 2

$$F_A = \frac{N_{critical}}{N_{0.707,upper} - N_{0.707,lower}} = \frac{44900}{46500 - 43000} = 12.83$$

The amplification factor is more than 2.5

Step 5: Determine the separation margin.

$$S_m = 100 \cdot \frac{N_{0.707,lower} - N_{maximum,continuous}}{N_{maximum,continuous}} = 100 \cdot \frac{43000 - 30000}{30000} = 43.3\,\%$$

Step 6: Determine the margin of separation

$$M_s = 10 + 17 \cdot (1 - \frac{1}{F_A - 1.5}) = 10 + 17 \cdot (1 - \frac{1}{12.83 - 1.5}) = 25.49$$

Step 7: Evaluate the separation margin

The separation margin should be more than M_s or 26 whichever is less [26]. The separation

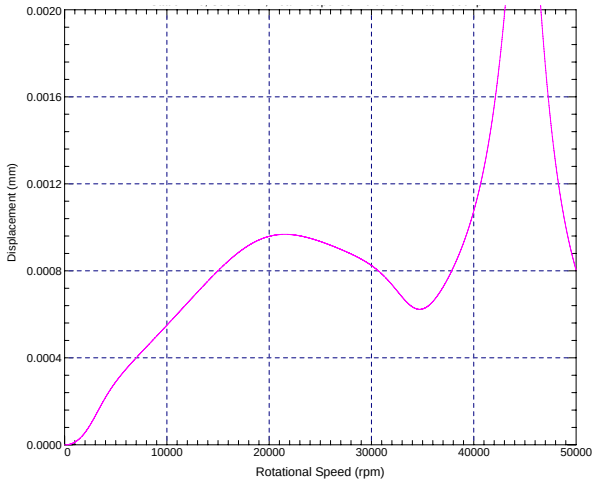

Figure 4.31: Corresponding rotational speeds

margin is greater than M_s ($S_m = 43.3 > M_s = 25.49$). This peak complies with the API 612 standard.

If the separation margin was less than M_s the following steps would have been taken.

Step 8: Determine the minimum clearance. The minimum clearance is at the maximum displacement of the rotor, in this case 0.0028827 mm. This value has to be multiplied with a correction factor shown in (4.39).

$$F_c = \frac{A_1}{A_{4x}} \qquad [-] \tag{4.39}$$

$$A_1 = 25.4 \cdot \sqrt{\frac{12000}{N}} \qquad [\mu\text{m}]$$

where F_c is the correction factor, A_1 is the amplitude limit, A_{4x} is the calculated peak-to-peak amplitude at the probe locations in [μm] and N is the operating speed nearest the relevant critical frequency. Substitute $A_4x = 2.8827$ and $N = 30000$. This results in $A_1 = 16.06$ and $F_c = 5.57$.

$C_{min} = C_{total} - x_{disp} = 0.25 - 0.0028827 = 0.2471$ mm

Step 9: Evaluate the clearance. The peak should not exceed 75 % of the clearance [26].

$PercentClearance = 100 \cdot \left(\frac{F_c \cdot A_{operating}}{C_{total}}\right) = 100 \cdot \left(\frac{5.57 \cdot 0.001}{0.25}\right) = 2.23$ %

(**Note:** $A_{operating}$ is the maximum amplitude within the operating range [15000 rpm $\longleftrightarrow$ 30000 rpm] of the rotor. Refer to figure 4.30 to see that the maximum amplitude within the operating speed is 0.001 mm)

The response satisfies the API 612 standard. The rotor is rotor dynamically sound. If the percentage clearance exceeds 75 % the rotor should be redesigned. In appendix D.6 the full results of the rotor dynamic analysis are shown. The results show that none of the peaks exceeds 75% of the total clearance (0.03375 mm). The rotor is rotor dynamically sound.

This chapter took an in depth look at the detail design behind the rotor, focussing on the energy storage capabilities of the rotor, a strength analysis on the magnet adhesive as well as the flywheel disc itself and lastly a quick overview of the rotor-dynamics of the rotor/flywheel assembly. The rotor was found to be rotor dynamically sound.

Chapter 5

Rotor/flywheel enclosure detail design

In this chapter the detail design of the rotor/flywheel enclosure is discussed. The chapter focuses on FLY-UPS interfacing, heat dissipation, modular design, vacuum, and aerodynamic losses. The interaction of all these factors determines the final design of the rotor/flywheel enclosure.

5.1 Enclosure operational functions

The operational functions of the enclosure determine, to a great extent, the final design of the enclosure. The first step is to determine all of the main functions of the rotor/flywheel enclosure:

Interfacing The main function of the rotor/flywheel enclosure is the interfacing between the control unit and the FLY-UPS hardware unit. This includes all the sensors and all the power connections.

House the sub-components Another important function of the rotor/flywheel enclosure is the ability to house all the sub-components. The sub-components include the sensors, the AMBs, the PMSM and rotor/flywheel assembly itself.

Efficient heat dissipation Another function of the rotor/flywheel enclosure is the dissipation of heat using natural convection and radiation only. The rotor/flywheel assembly is run in a near vacuum so the efficiency of convection from the flywheel is very low. The rotor/flywheel enclosure should dissipate and conduct the maximum amount of heat away from the rotor/flywheel assembly.

Modularity The enclosure should be modular. The modularity of the enclosure ensures that sub-components can be swapped with other test-components. The modularity of the FLY-UPS system ensures that the system can be used in laboratory testing of newly developed components.

Vacuum The enclosure should be able to have a low air-pressure inside in order to keep aerodynamic losses to a minimum.

Aerodynamic losses The enclosure should be designed with aerodynamic losses in mind. This means that components with a high surface speed should have the maximum amount of clearance to the stationary components.

The main operational functions have been identified. The sub-components of these functions also need to be identified. The identification of the sub-components is done to determine the final layout of the FLY-UPS enclosure. The sub-components required to achieve the operational functions of the enclosure is described in sections 5.3 - 5.7. Finally the integration of these sub-components is discussed in section 5.8.

5.2 Enclosure concept

The final design of the rotor/flywheel enclosure is shown in figure 5.1. This figure shows all of the sub-components and the interfacing of these sub-components to each other. In the following sections the details of the design of the enclosure is discussed.

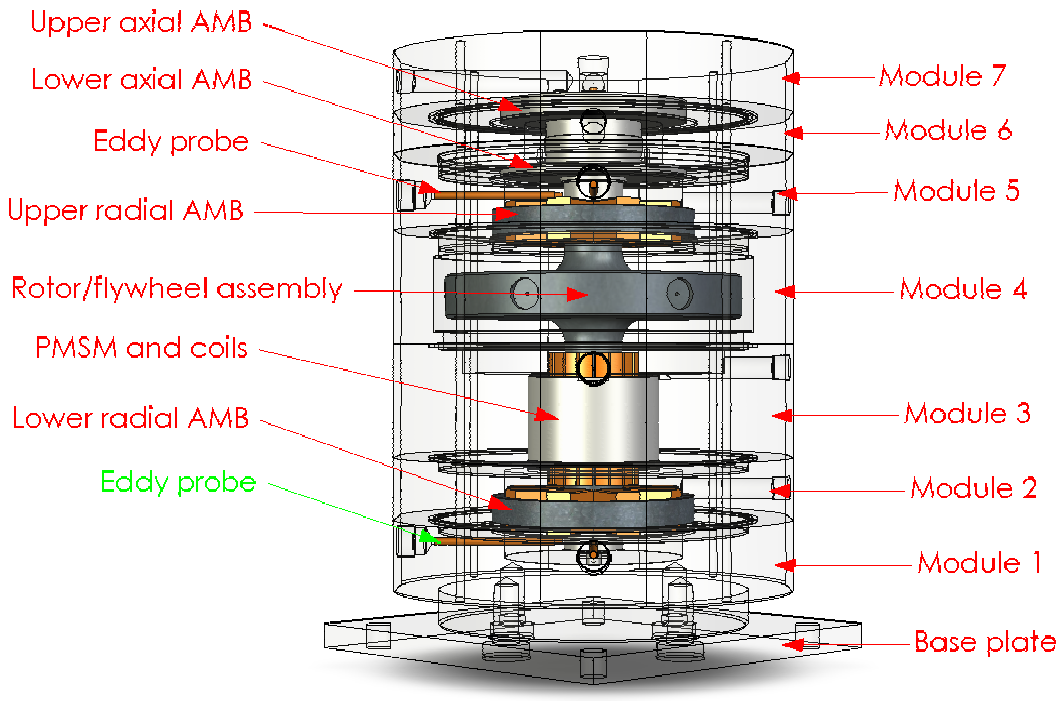

Figure 5.1: The final enclosure layout.

Module 1 houses the lower backup bearing and the lower eddy current sensors. Module 2 houses the lower radial AMB. Module 3 houses the PMSM. Module 4 houses the external sensors and encloses the flywheel disc. Module 5 houses the upper radial AMB and eddy current sensors and module 6 houses the lower axial AMB unit. Module 7 houses the upper axial AMB unit and the axial eddy current sensor.

5.3 Interfacing

As stated in section 5.1 the main function of the FLY-UPS enclosure is the interfacing of the control enclosure, the sub-components of the FLY-UPS and the rotor/flywheel assembly to each other and the environment. The interfacing is broken down into 4 categories, namely sensors, power feedthroughs, vacuum interfacing and the base plate securing.

5.3.1 Sensors

The sensors are the eyes and ears of the system and the control enclosure is the brain. The sensors supply the control enclosure with all the relevant raw information. The raw information is transformed into control signals used to control the FLY-UPS. The sensor signal distribution is illustrated in figure 5.2. The FLY-UPS system consists of the operator interface, a control enclosure and the rotor/flywheel enclosure. The rotor/flywheel enclosure should house all the relevant sensors, the rotor/flywheel assembly and all the relevant actuators. The sensors gather information from both the rotor/flywheel assembly and the rotor/flywheel enclosure. The sensor information is sent to the control enclosure. The control enclosure transforms the sensor information into a control signal. The control signals are sent either to the rotor/flywheel enclosure or to the actuators in the rotor/flywheel enclosure.

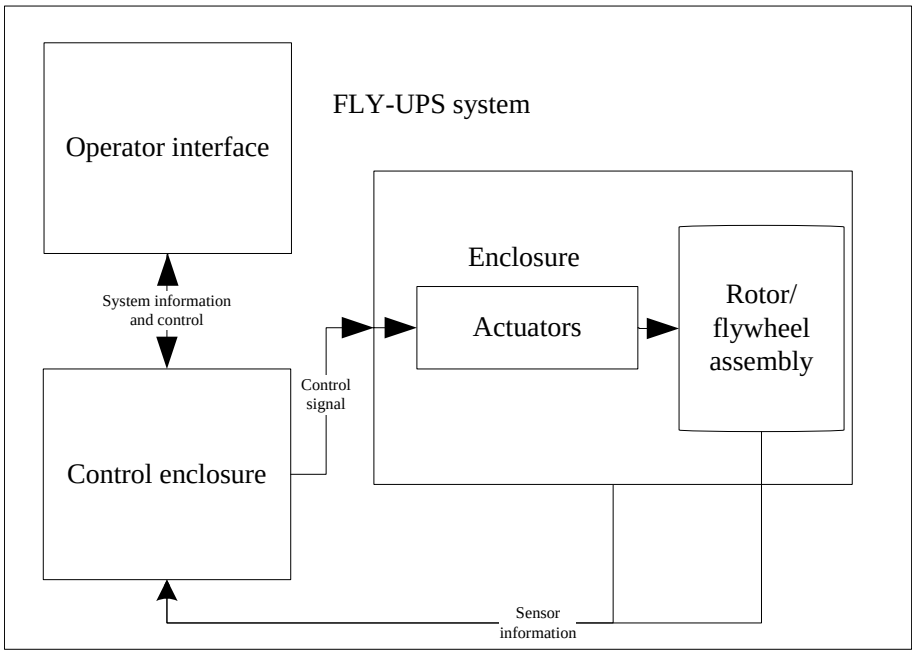

Figure 5.2: The sensor signal distribution of the FLY-UPS system.

The sensors required to achieve the operational functions of the enclosure is described in sections 5.3.1.1 - 5.3.1.5.

5.3.1.1 Rotor position sensors

The position of the rotor needs to be known in order to control the rotor position. The position sensors need to be accurate, and also need to have high resolution. The position sensors also should not make contact with the rotor. The type of sensor identified for this application is the eddy current sensor. An eddy current sensor works by producing an alternating magnetic field. The alternating magnetic field induces eddy currents in the object being measured. The change in impedance is transformed into a distance measurement. Eddy current sensors have resolutions of up to 1μm. A diagram of the eddy current sensor and the induced magnetic field is shown in figure 5.3.

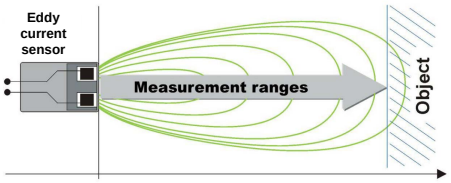

Figure 5.3: Principal of an eddy current sensor.

The FLY-UPS needs a total of 5 eddy current sensors, 2 sensors for each of the radial AMBs and one sensor for the axial AMB. The choice of eddy current sensors influences the design of the rotor/flywheel enclosure. The enclosure should have enough space in the sensing areas for the 5 eddy current sensors. The enclosure's magnetic fields should also not interfere with the magnetic fields of the eddy current sensors. The manufacturer of the eddy current sensors defines the minimum clearance required by the sensors as 2.5 times the diameter of the sensor's tip radius. The sensor manufacturer chosen for this application is *SKF condition monitoring*®. The reasoning behind this choice is given in appendix D.4. The eddy current sensors selected has a tip diameter of 5 mm and 1/4 .28 UNF thread. A photograph of one eddy current sensor is shown in figure 5.4. The eddy probe data-sheet can be found in appendix D.11.6.

Figure 5.4: Photograph of an eddy current sensor.

5.3.1.2 Rotational speed sensor

A rotational speed sensor is needed to activate the emergency shutdown procedure if the rotor exceeds the trip speed. The rotational speed sensor should be able to determine the

rotational speed of the rotor without direct contact with the rotor. The rotational speed should be displayed for visual inspection. The chosen speed sensor is a *SELET*® M12 series. The chosen speed sensor is an inductive proximity switch. An inductive proximity switch detects the presence of metallic objects. The presence of a metallic object in the field modifies the energy of the high frequency magnetic field. The sensor is shown in figure 5.5. The sensor has a M12-fine thread, and has to be within 4 mm of the sensing surface.

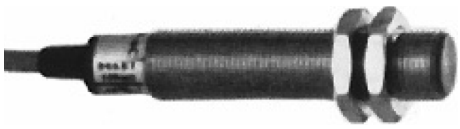

Figure 5.5: Photograph of the chosen inductive proximity switch.

The speed sensor also needs a display and counter to determine the rotational speed in revolutions per minute. The chosen display to accompany the inductive proximity switch is a *Instrotech*® Model 5012-Q. The display is used to display the current rotational speed. The display is also used to trip the system, should the speed exceed the trip speed. A photograph of the speed sensor is shown is figure 5.6. The data sheet for the sensor and the display is given in appendix D.11.2

Figure 5.6: Photograph of the chosen speed sensor display.

5.3.1.3 Temperature sensors

The temperature of the system plays an important role in the operational safety of the system. High temperatures have an adverse effect on the carbon fibre epoxy, the magnets, the material of the rotor/flywheel, the adhesive, the insulation of the electrical wires used in the PMSM and the AMBs. The temperature is therefore measured at a few key locations. Four resistive temperature devices and one infra red temperature sensor are used. The placement of these sensors should be as close as possible to the areas mentioned above. The elevation of temperatures is caused by the alternating magnetic fields in the system. The alternating fields induce eddy currents in the rotor/flywheel assembly. The eddy current losses cause the temperatures of the rotor/flywheel enclosure and the rotor/flywheel assembly to rise.

5.3.1.3.1 Infra red temperature sensor

The infra red temperature sensor is used to determine the temperature of the rotor/flywheel assembly. Once again the sensor should not be in contact with the rotor/flywheel assembly. The budget of this project allows for the procurement of only one infra red sensor thus the placement of this sensor is very crucial. The sensor should be placed as close as possible to the magnets, the carbon fibre sleeve, the rotor/flywheel material and the adhesive. The PMSM is a major source of heat. The infra red temperature sensor should be placed near the PMSM. The chosen infra-red temperature sensor is a *CALEX*® Convir EL series. A photograph of the chosen infrared temperature sensor is shown in figure 5.7. The infra-red temperature sensor has an M16 thread with a 1 mm pitch.

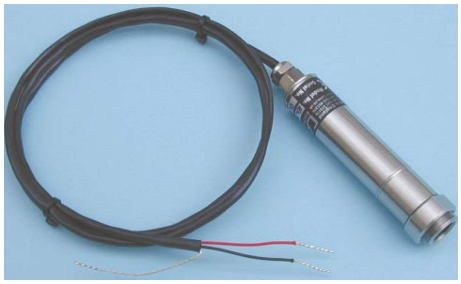

Figure 5.7: Photograph of the chosen infra-red temperature sensor.

The chosen infra-red temperature sensor's required target spot is dependent on the distance from the target. This relation is shown in figure 5.8.

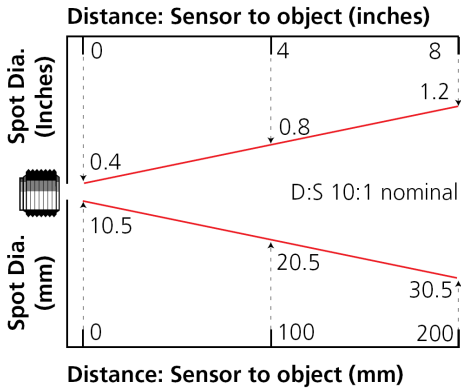

Figure 5.8: Required target area for the infra-red temperature sensor.

5.3.1.3.2 Resistive temperature device

The resistive temperature device is based on the principle that the resistance in a resistor increases with higher temperatures. The resistance of a resistive temperature device is known for a range of temperatures. Refer to appendix D.11.9 for the complete set of resistances for specified temperatures. In contrast to the infra red temperature sensor, the resistive temperature devices should be placed in direct contact with the sensing area. The resistive temperature devices are placed inside the coils of both the radial AMBs and the end-windings of the PMSM.

A resistive temperature device is also placed in the upper axial AMB and not in the lower axial AMB. This is done because the load on the upper axial AMB is greater than the load on the lower axial AMB. The upper axial AMB also supports the entire weight of the rotor/flywheel assembly. Platinum resistive temperature devices result in the most repeatable and linear response to changes in temperature. The resistive temperature device chosen for this application is the Pt100 type. A drawing of the Pt100 resistive temperature device and some basic dimensions is shown in figure 5.9.

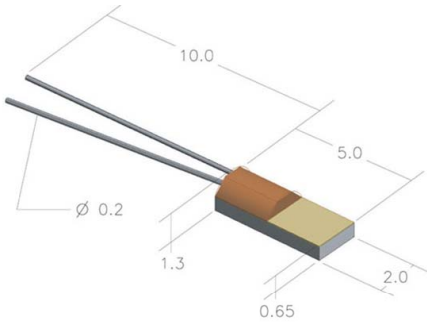

Figure 5.9: Drawing of a Pt100 resistive temperature device

5.3.1.4 Pressure sensor

A pressure sensor is required to measure the level of vacuum inside the rotor/flywheel enclosure. In the process of selecting a pressure sensor there are 2 options; an analogue pressure sensor or a digital pressure sensor. The analogue pressure sensor is less expensive. The decision was taken to opt for an analogue sensor in the form of a pressure transducer. The chosen pressure transducer is shown in figure 5.10. The signal from the transducer is used to control the vacuum pump. The data sheet for the selected pressure transducer can be found in appendix D.11.4.

Figure 5.10: A photo of the chosen pressure transducer

5.3.1.5 Pickup coils

The pickup coils are used to sense the current position of the magnetic field in the PMSM. The frequency at which the field rotates determines the rotational speed of the rotor. The pickup coils can be used for various measurements in the PMSM. The pickup coils are probably the simplest of all the sensors used in the FLY-UPS system. The pickup coils are basically just separate wires wound in with each phase of the PMSM's stator. The pickup coils work on the principle of induction by magnetic fields. The FLY-UPS's PMSM was developed in-house, thus the pickup coils were also developed in-house. A photo of the in-house developed PMSM and pickup coils is shown in figure 5.11.

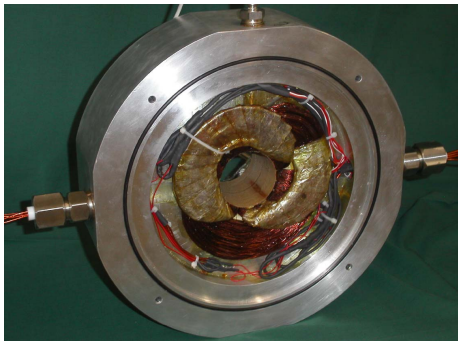

Figure 5.11: A photo of the in-house developed PMSM and pickup coils.

5.3.2 Pressure feedthroughs

Pressure feedthroughs are very important sub-components of the rotor/flywheel enclosure. The feedthroughs ensure that a vacuum is maintained inside the enclosure, facilitates the connection of power to the sub-components and connection of the sensors to the control enclosure. In the rotor/flywheel enclosure a wide variety of feedthroughs are required. The FLY-UPS system requires three types of pressure feedthroughs: a high current type, a low current type and a pressure gland type. The pressure glands are required for the eddy current sensors. The eddy current sensors' cabling is calibrated and thus it is not recommended that the cabling of the eddy current sensors is cut. The low current feedthroughs are used for the resistive temperature devices. The high current feedthroughs are used to supply all the sub-components with power. Because of the widely varying needs on the feedthroughs three different companies were identified to supply the feedthroughs. The companies are *CONAX BAFFALO*® for the high current feedthroughs, *Wika*® for the low current feedthroughs and *SKF*® for the pressure glands. The data sheets for the feedthroughs and pressure glands are given in appendix D.11.7.

5.3.2.1 High current feedthroughs

The high current feedthroughs vary from 5 Ampere maximum current to 25 Ampere maximum current. There are also three different layouts needed, 4-wire, 6-wire and 8-wire. A photograph

of the feedthrough layout can be seen in figure 5.12. The CONAX feedthroughs are available in 1/2″ and 3/4″ NPT threads.

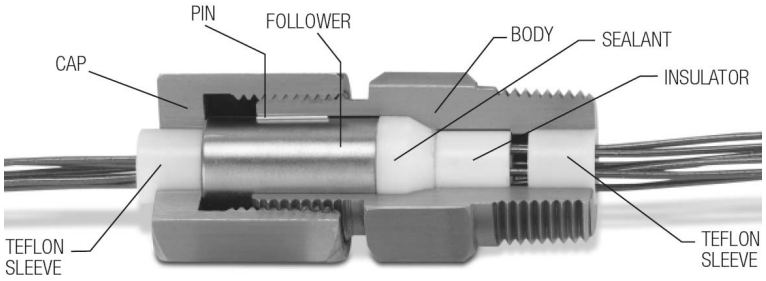

Figure 5.12: The layout of the CONAX high current feedthrough.

5.3.2.2 Low current feedthroughs

The low current feedthroughs are used for the resistive temperature devices. The low current feedthroughs were custom made for this application. These feedthroughs also have a 1/2″ NPT thread. The low current feedthroughs have a 3-wire configuration. An illustration of the low current feedthroughs can be seen in figure 5.13.

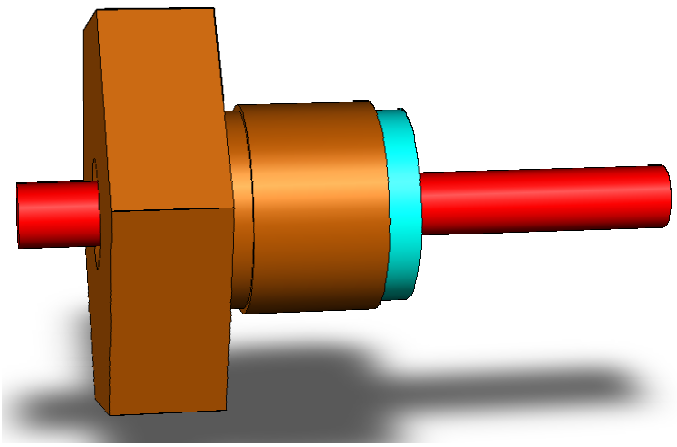

Figure 5.13: An illustration of the low current feedthroughs.

5.3.2.3 Pressure gland

The SKF pressure glands are used to interface the eddy current sensors with the rotor/flywheel enclosure. The pressure gland assembly is shown in figure 5.14. The glands are used because the eddy current sensors' cabling should not be cut. The 3/4″ NPT thread was chosen for this application.

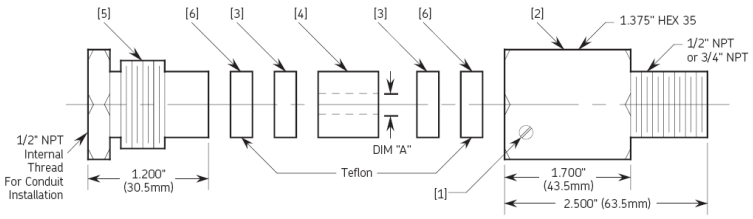

Figure 5.14: An illustration of a pressure gland.

In figure 5.14: 1 is the setscrew, 2 is the body, 3 is the split washers, 4 is the gland, 5 is the compression nut and 6 is the teflon washers.

5.3.3 Vacuum pump

The vacuum pump chosen for this application is a *vacuubrand*® ME 2. The data sheet for this vacuum pump can be found in appendix D.11.3. A photograph of the vacuum pump is shown in figure 5.15. The vacuum pump interfaces with the rotor/flywheel enclosure by means of a NW 10 hose nozzle. The hose nozzle is connected to a hose, and the hose connects to a pipe nozzle connected to the valves.

Figure 5.15: A photograph of the vacuum pump.

5.3.3.1 Vacuum pump interfacing

The hose is connected to a normally closed solenoid valve. The normally closed valve is connected to a tee piece. The other side of the tee piece is connected to a normally open solenoid valve. The normally open solenoid valve's other side is left open to the atmosphere. This is done to ensure that as soon as the power supply of the FLY-UPS system is interrupted the valves will open to the atmosphere. The cool air rushing into the rotor/flywheel enclosure helps to cool the backup bearings. The air also helps to slow the flywheel. The setup is shown in figure 5.16.

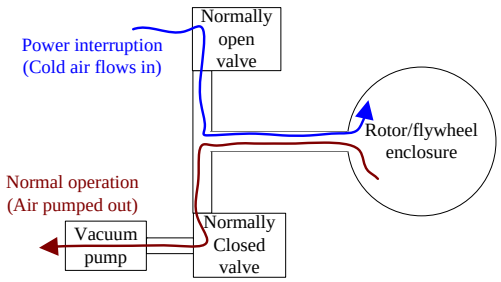

Figure 5.16: A diagram of the interfacing of the vacuum pump and the enclosure.

5.3.4 Base-plate securing

The FLY-UPS system needs to be secured to the ground for safety reasons. The concept of the securing is basically to achieve a rigid connection to a sufficiently large mass. The large mass is in the form of a 600x600x600 mm concrete block. Within the concrete block there is a structure on which the rotor/flywheel assembly is secured with M20 nuts. The assembly is shown in figure 5.17.

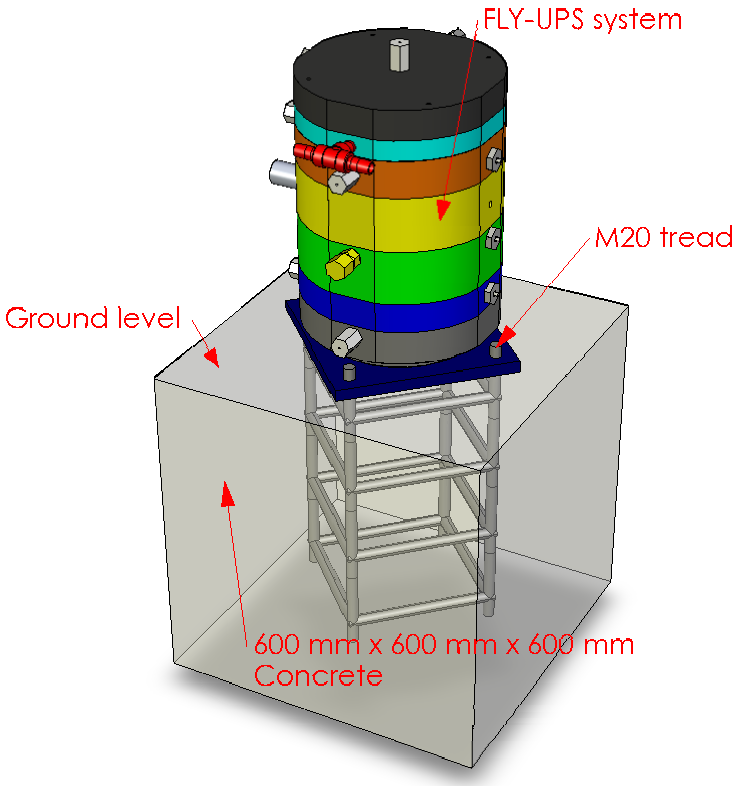

Figure 5.17: Schematic of the securing of the rotor/flywheel enclosure to the ground.

The bottom of the baseplate is shown in figure 5.18. The baseplate is manufactured from mild steel and is nickel plated to prevent rust. Module 1 of the rotor/flywheel enclosure is fastened

to the baseplate by means of 4xM20 bolts. The nuts securing the baseplate to module 1 of the rotor/flywheel enclosure are sunken. This ensures the maximum amount of contact surface of the baseplate with the concrete. This is done to maximise the rigidity of the connection. The rotor/flywheel enclosure is levelled by using a level and shimming the baseplate as necessary.

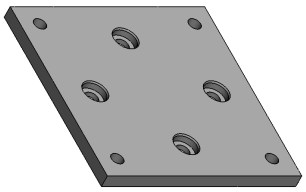

Figure 5.18: Drawing of the bottom of the baseplate.

5.4 Sub-components

Another operational function of the rotor/flywheel enclosure is the housing of the sub-components. These sub-components include the axial AMBs, the radial AMBs, the PMSM and the auxiliary bearings. All of these components need to be secured within the rotor/flywheel enclosure. These components also need to interface with the control enclosure and the rotor/flywheel assembly. The axial position of these components is to be fixed after the final rotor design. The enclosure modules for the sub-components need to be designed to facilitate easy access to the sub-components.

5.4.1 Axial AMBs

The axial AMB is made up of two units. The two units have a mild steel disc between them. The disc is connected to the rotor/flywheel assembly. The disc is suspended between the two units. The air gap between the disc and the axial AMB units on either side is 0.5 mm. The distance between the two units is adjusted by means of shims. The decision was taken to house each of the two units in a separate module. This is done to ease the assembly of the system. A schematic representation of the axial AMB assembly is shown in figure 5.19. The details of the design of the enclosure modules for the axial AMB units are discussed in section 5.6.6 and section 5.6.7.

5.4.2 Radial AMBs

The radial AMBs are made up of four pole pairs. Opposing pole pairs control the rotor/flywheel assembly in one axis of movement. A photograph of the radial AMB is shown in figure 5.20. In the figure the pole pairs and radial movement directions are shown. The radial AMBs need to be securely fitted to the rotor/flywheel enclosure. The radial AMBs should also be removable and replaceable. The AMBs should be able to dissipate heat to the rotor/flywheel enclosure.

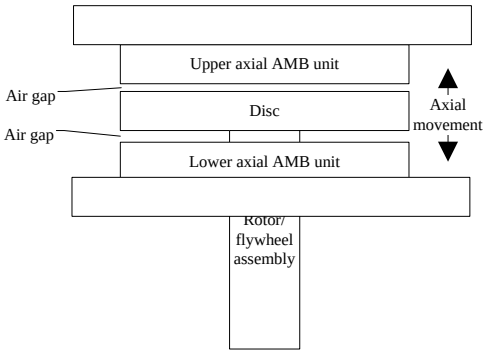

Figure 5.19: Schematic representation of the two axial AMB units.

The details of the modules housing the radial AMBs are discussed in section 5.6.2 and section 5.6.5.

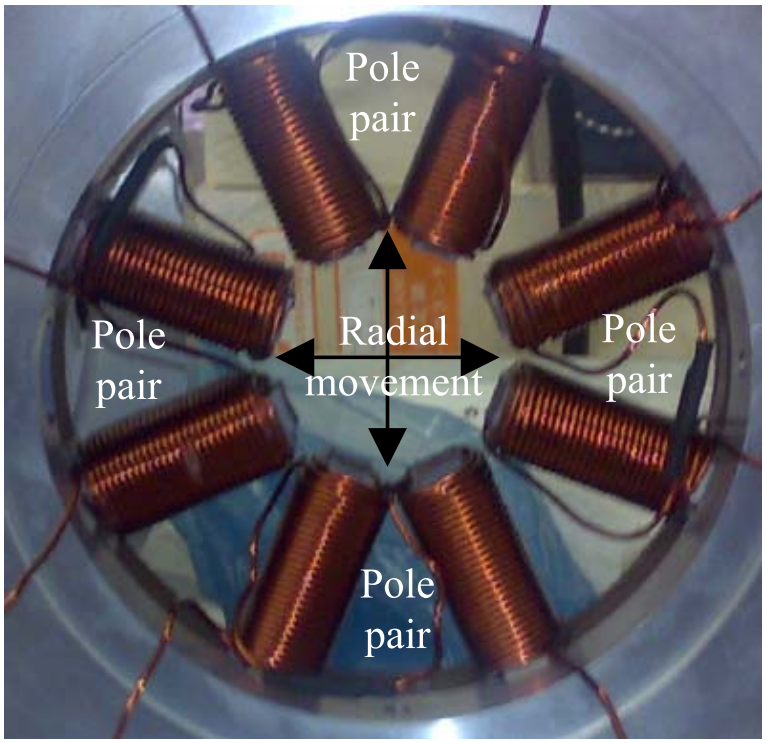

Figure 5.20: Photograph of a radial AMB unit, showing the pole pairs and the radial movement directions.

5.4.3 PMSM

The permanent magnet synchronous machine is made up of back iron laminations, windings and permanent magnets. The PMSM works by inducing a rotating field in the windings. The magnets follow this rotating field. When the PMSM is in generator mode the rotating magnets

induce current in the windings. The PMSM is an untoothed machine. The PMSM should fit into the rotor/flywheel enclosure securely. The end-windings of the PMSM should not intrude on the adjacent enclosure modules. To ensure the PMSM's end-windings do not intrude on the modules next to it, the end windings are flared outwards. The flared end-windings can be seen in figure 5.21. The PMSM module is discussed further in section 5.6.3. The module should also be designed to dissipate the heat caused by the copper and back iron losses of the PMSM.

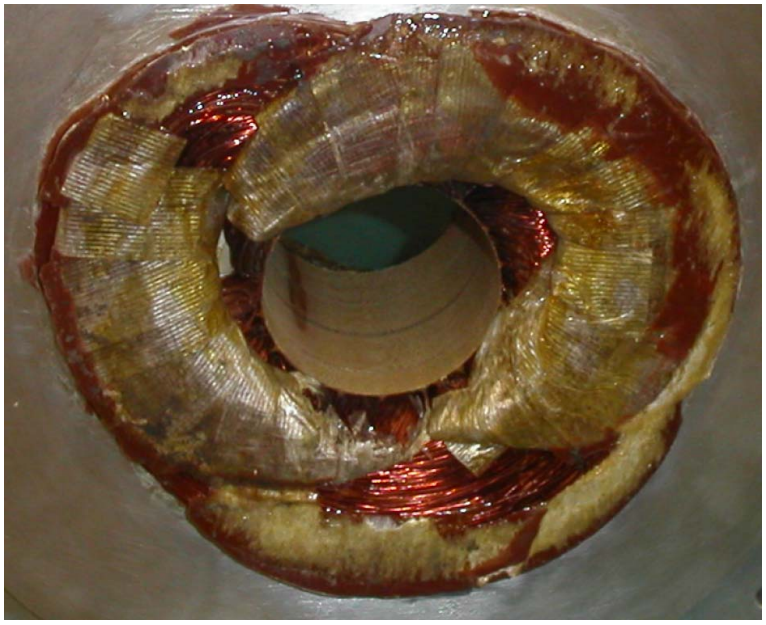

Figure 5.21: Photograph of the PMSM's flared end-windings.

5.4.4 Auxiliary bearings

The auxiliary or backup bearings are used to safely facilitate a failure of the AMBs. The backup bearings also protect the rest of the sub-components inside the rotor/flywheel enclosure. The backup bearing chosen for this application are *Glacier*® DS cylindrical bushes and thrust washers. An illustration of the cylindrical bush and the thrust washer is shown in figure 5.22.

The backup bearings are located in two positions; inside the lower axial AMB unit and on the lower tip of the rotor/flywheel assembly. The locations of the backup bearings are shown in figure 5.23. The figure also shows the details of each of the backup bearings. A backup bearing consists of one axial thrust washer and one radial cylindrical bush. The data sheet for the backup bearings can be found in appendix D.11.12.

5.5 Heat dissipation of the enclosure

The dissipation of heat is a major design issue of the rotor/flywheel enclosure. The heat generated by the actuators inside the rotor/flywheel enclosure should be conducted away

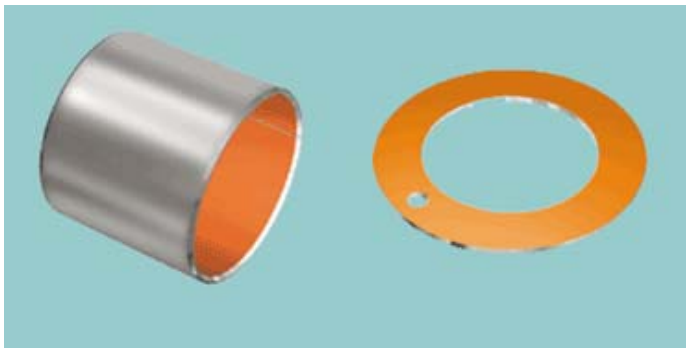

Figure 5.22: An illustration of the backup bearings.

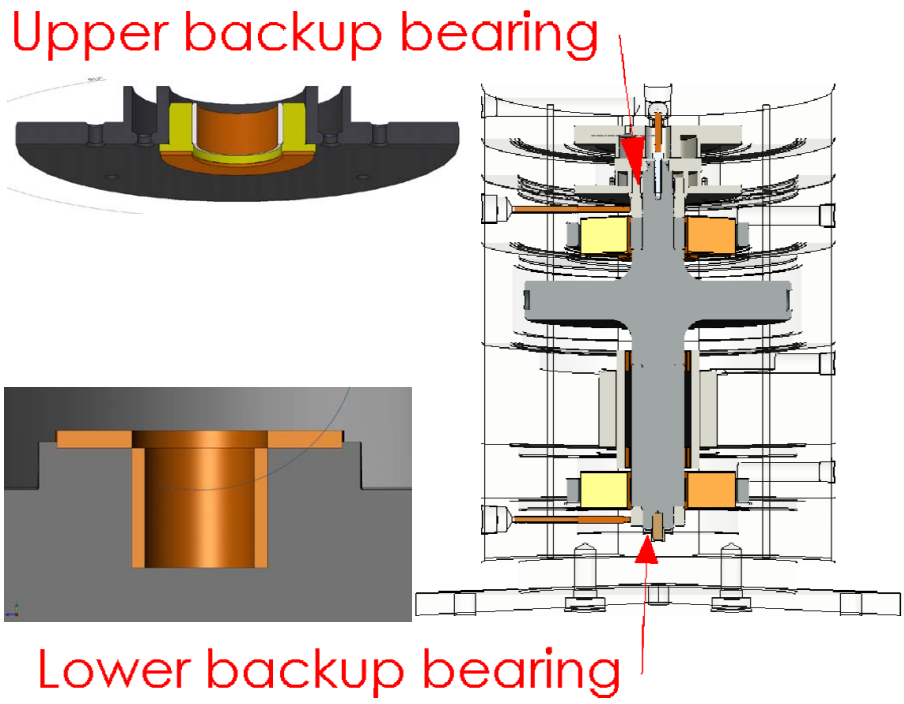

Figure 5.23: A sectioned illustration of the backup bearing locations.

from the rotor/flywheel assembly. The rotor/flywheel assembly only makes use of limited convection and radiation. Due to the low pressure inside the enclosure, the convection is very limited.

The design of the enclosure for heat dissipation is not done in great detail. A basic design rule is followed. The design rule is to have as much heat conductive material near the subcomponents generating the most heat. The subcomponents generating the most heat are the AMBs, the PMSM, and the backup bearings during a failure. The idea is to be able to conduct the heat through the aluminium body of the rotor/flywheel enclosure to the environment. In figure 5.24 the main heat generating components' enclosures are shown. As can be seen in the figure the maximum amount of heat conducting material is left in the enclosure. This is done

to ensure that the heat is conducted away from the relevant component.

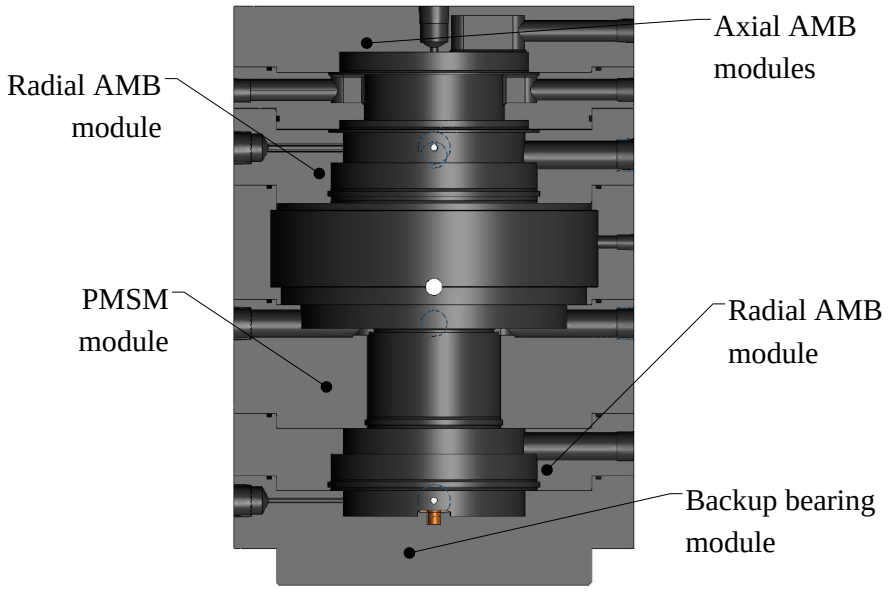

Figure 5.24: A few of the designed heat conducting modules.

5.6 Modular design

The modularity of the rotor/flywheel enclosure ensures that the FLY-UPS system can be upgraded and repaired. The modules are designed to ensure that each module forms a complete sub-component. In sections 5.6.1 - 5.6.7 each of the modules of the rotor/flywheel enclosure is discussed in detail. The manufacturing drawings of each of the modules can be found in appendix D.9. This section discusses the final design of the various modules. Refer to figure 5.1 for the location of the modules.

5.6.1 Module 1

Module 1 is designed to house the lower radial AMB's eddy current sensors and the lower backup bearing. The module interfaces with the baseplate, module 2 and with the environment. The interfacing to the environment is achieved through the SKF pressure glands. A description of the operational functions and how these operational functions were achieved for module 1 follows:

Interface with the baseplate The first operational function of this module is to interface with the baseplate. The baseplate needs to be connected rigidly to module 1. This is achieved by fastening the module to the baseplate with 4xM20 bolts, as shown in figure 5.25.

Housing the lower AMB's eddy current sensors This module houses the eddy current sensors for the lower AMB. This is achieved by tapping two UNF threads as required by the eddy current sensors. The eddy current sensors' cabling is fed through the pressure glands to ensure minimal leakage. The pressure glands and the eddy current sensors are shown in figure 5.25.

Housing the lower backup bearing The lower backup bearing is housed in this module. The backup bearing can potentially generate a lot of heat. The module is therefore designed to have a lot of heat conducting material close to the backup bearing. The backup bearing consists of a thrust washer and a cylindrical bush. The module is designed to house the 2 components of the backup bearing. The backup bearing is shown in figure 5.25.

Vacuum seal with module 2 This module needs to seal with module 2. The seal is achieved by means of an o-ring. The modules are to be held together by 4xM5 threaded rods to ensure the o-ring seals sufficiently. The module is designed with a groove for the o-ring. The holes for the threaded rods as well as the o-ring are shown in figure 5.25.

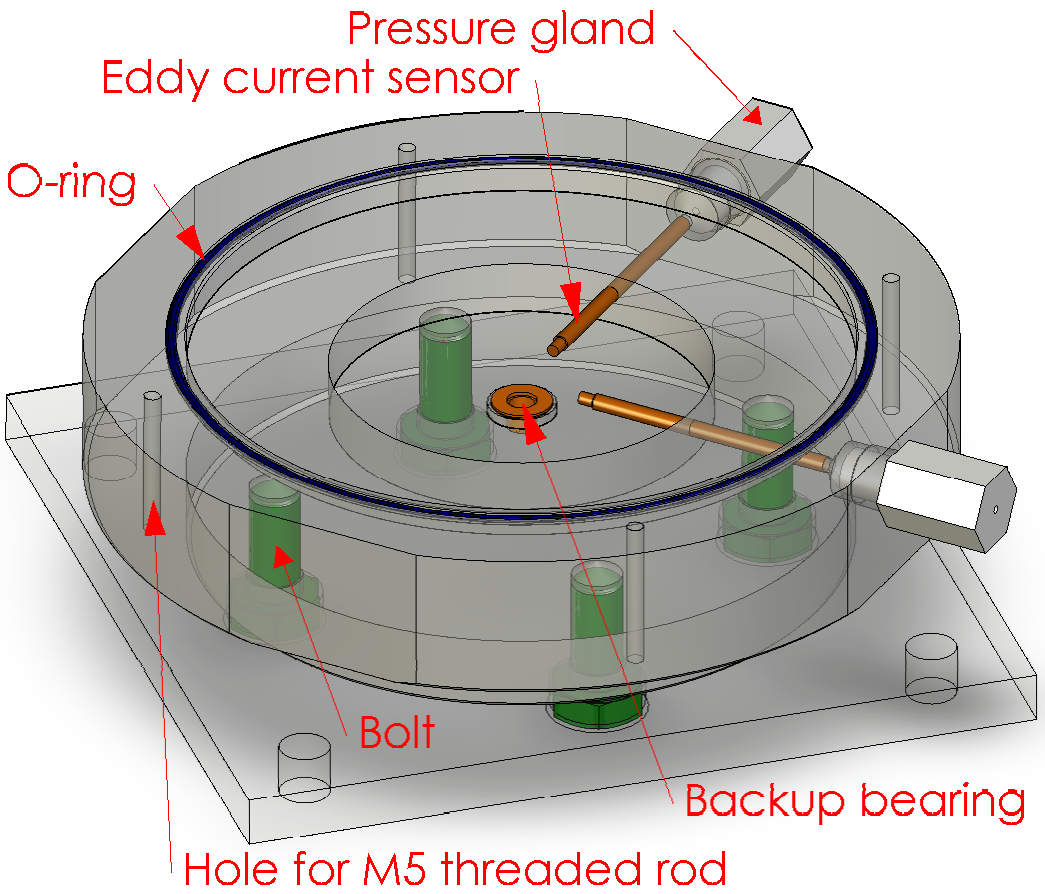

Figure 5.25: Schematic representation of module 1.

5.6.2 Module 2

Module 2 is designed to house the lower radial AMB. The module interfaces with module 1 and module 3. This module fits onto module 1 and seals with the o-ring fitted in module 1. Module 3 fits onto this module and seals with the o-ring fitted to this module. The radial AMB is held in place by means of an internal retaining ring. Module 2 is fitted with feedthroughs: a low current feedthrough for the resistive temperature device and a high current feedthrough for the power supply of the radial AMB. The operational functions of module 2 follow:

Housing the lower Radial AMB The lower radial AMB is housed in this module. The lower radial AMB is held in place by means of an internal retaining ring. A resistive temperature device is placed among the coils of the radial AMB. The resistive temperature device is connected to the control enclosure through the low current feedthrough. The power for the radial AMB is connected to the control enclosure through the high current feedthrough. The feedthroughs, AMB and the internal retaining ring are shown in figure 5.26.

Vacuum seal with module 1 and 3 This module needs to seal with module 1 and 3. The seal is achieved by means of an o-ring fitted to this module and a sealing surface on the other side of the module. The modules are to be held together by four M5 threaded rods to ensure the o-rings seal sufficiently. The holes for the threaded rods as well as the o-ring are shown in figure 5.26.

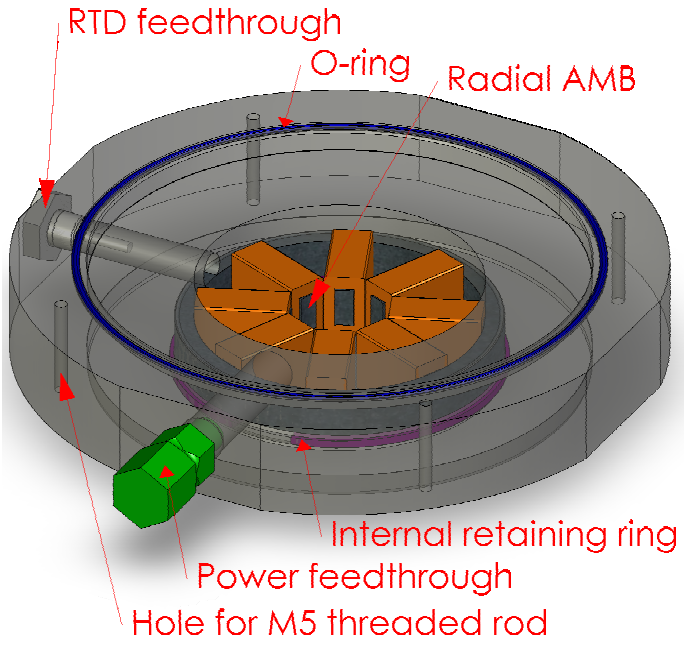

Figure 5.26: Schematic representation of module 2.

5.6.3 Module 3

This module is designed to house the PMSM, and to conduct the heat from the PMSM. This module fits onto module 2 and seals with the o-ring fitted in module 2. Module 4 fits onto this module and seals with the o-ring fitted to this module. The radial PMSM is held in place by an internal retaining ring. Module 3 is fitted with three feedthroughs: a low current feedthrough for the resistive temperature device and two high current feedthroughs for the power supply and pick up coils of the PMSM. The operational functions of module 3 follow:

Housing the PMSM This module houses the PMSM. The PMSM's coil temperature is fed through the low current feedthrough. The pick up coil is used to determine the rotational position of the rotor. The pick up coil's signals are fed through one of the high current feedthroughs. The power supply of the PMSM is fed through the other high current feedthrough. The PMSM is held in place by an internal retaining ring. The feedthroughs, the PMSM and the retaining ring are shown in figure 5.27. The module is designed to have the maximum amount of conducting material adjacent to the PMSM.

Vacuum seal with module 2 and 4 Similar to module 2, module 3 needs to seal with the adjacent modules. This is achieved in the same way as with module 2.

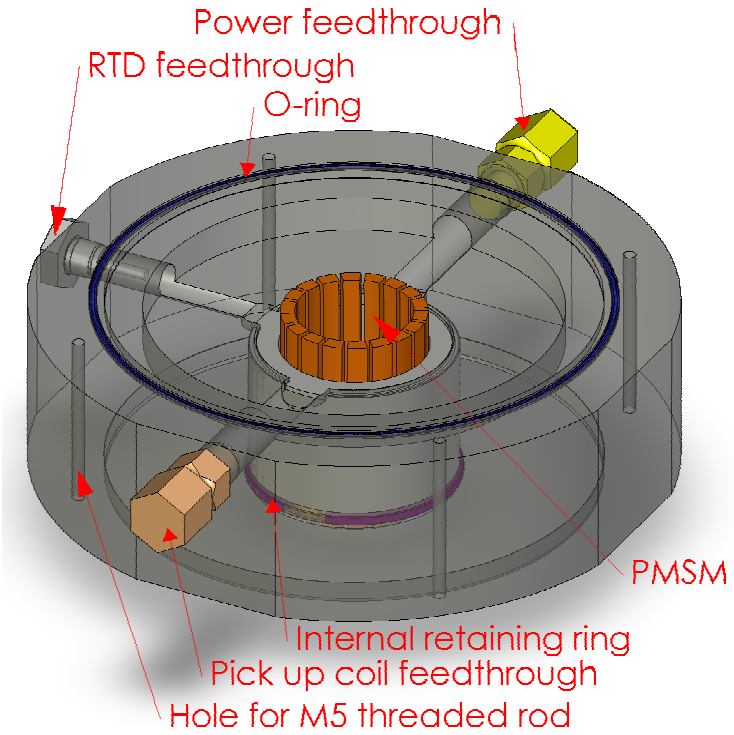

Figure 5.27: Schematic representation of module 3.

5.6.4 Module 4

Module 4 is designed mainly to encapsulate the flywheel and gather information from the flywheel. This module interfaces the speed, pressure and temperature sensors' signals to the control enclosure. This module has to seal with module 3 and module 5. The operational functions of module 4 follow:

Sensor interfacing This enclosure module has no powered sub-components. The module is used to house many of the sensors used in the FLY-UPS system. The internal pressure of the rotor/flywheel enclosure is sensed using a pressure transducer. The pressure transducer's position is shown in figure 5.28. The temperature of the rotor/flywheel assembly is measured using an infrared temperature sensor. The infra red temperature sensor's position is shown in figure 5.28. The rotational speed of the rotor/flywheel assembly is measured using an inductive proximity switch and a digital counter. The location of the proximity switch is shown in figure 5.28.

Vacuum seal with module 3 and 5 The vacuum seal is achieved in the same way as with module 2 and 3.

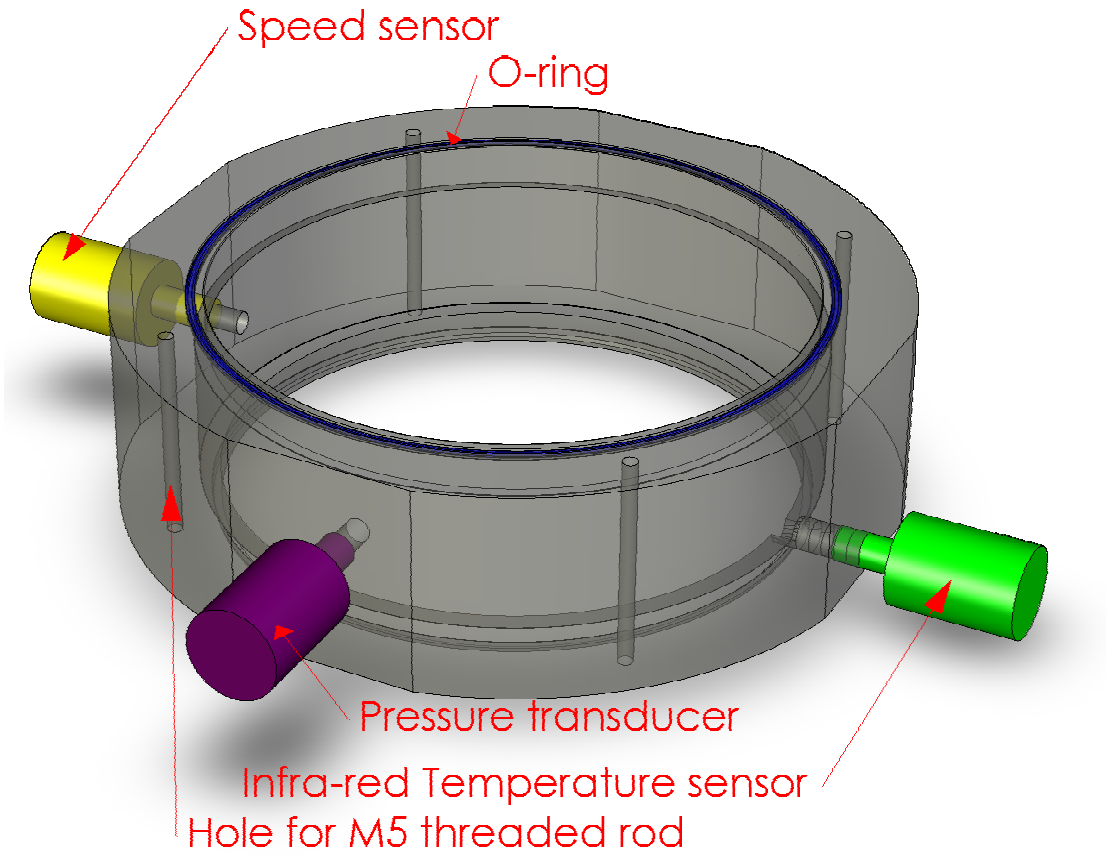

Figure 5.28: Schematic representation of module 4.

5.6.5 Module 5

Module 5 contains the upper radial AMB. This module is a complete enclosed unit containing the AMB itself as well as the power feedthrough and all of the sensors required by the AMB. This module interfaces uniquely with the adjacent modules in the sense that this module has no o-rings. This module has no o-rings because module 6 has two o-rings, used to facilitate axial shimming. The operational functions of module 5 follow:

Housing the upper radial AMB The upper radial AMB is secured to the unit similar to the lower AMB as described in section 5.6.2.

Housing the AMB's sensors The sensors of the upper radial AMB are also housed in module 5. The sensors include the 2 eddy current sensors and the resistive temperature device. The resistive temperature device is embedded in one the AMB's coils. The design of this module ensures that the use of this specific AMB unit can also be used on other systems, with the same rotor diameter. The possibility thus arises to use this module separately from the FLY-UPS system. The sensors and their corresponding feedthroughs are shown in figure 5.29.

Interface with units 4 and 6 Module 5 interfaces uniquely to the adjacent modules. This module contains no o-rings. The need to adjust the overall axial length of the rotor/flywheel enclosure is identified. This requirement arises due to the machining tolerance build-up. The rotor/flywheel enclosure is basically separated just above module 5. The axial distance of module 5 and module 6 is adjustable by means of shims. The rotor/flywheel enclosure is separated at this location to enable the relative axial movement between the rotor/flywheel enclosure and the rotor/flywheel assembly. Module 6 and module 7 contain the axial AMB units.

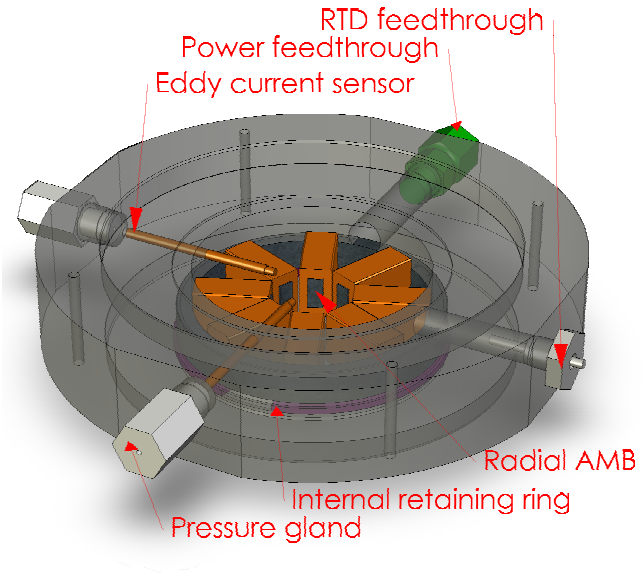

Figure 5.29: Schematic representation of module 5.

5.6.6 Module 6

Module 6 contains the lower axial AMB unit and a backup bearing. This module interfaces with module 5 by means of a radially sealing o-ring. The radially sealing o-ring ensures that the vacuum is maintained inside the rotor/flywheel enclosure. This enables relative adjustment between the rotor/flywheel enclosure and the rotor/flywheel assembly. The operational functions of module 6 follow:

Housing the lower axial AMB unit The lower unit of the axial AMB is housed in this module. The lower axial AMB unit is secured to the module using four M5 bolts. The power for the axial AMB unit is supplied through the high current feedthrough shown in figure 5.30. The ability to adjust the axial position of this axial AMB unit is necessary. The axial adjustment enables the adjustment of the air-gap between the axial AMB's and the axial disc. This adjustment is done by means of shims. The shims are to be placed between the axial AMB unit and the enclosure. This axial AMB unit is not fitted with a resistive temperature device, because this unit has a much lower work rate than the upper axial AMB. The upper axial AMB supports the entire weight of the rotor/flywheel assembly.

Housing the upper backup bearing The upper backup bearing is fitted into the lower axial AMB unit. This backup bearing functions in the same way as the backup bearing unit described in section 5.6.1.

Interface with the vacuum pump Module 6 interfaces with the vacuum pump in the manner depicted in figure 5.16. Figure 5.30 shows the tee-piece placement. The position of the vacuum interface is chosen at this location due to the presence of the upper backup bearing. The upper backup bearing does not have a much heat conducting material surrounding it. Due to this fact the cooling of this backup bearing is done by airflow. The moment the control enclosure detects a problem with the system, the valves open to atmosphere as described in section 5.3.3.1. The air flows over the backup bearing, thus cooling the upper backup bearing unit. The backup bearing location is shown in figure 5.30.

Interface with module 5 and 7 This module is the only unit equipped with both a radially and an axially sealing o-ring. The axially sealing o-ring functions similar to the o-rings described in sections 5.6.1 - 5.6.4. The radially sealing o-ring enables the axial movement of modules 6 and 7 relative to modules 1 - 5.

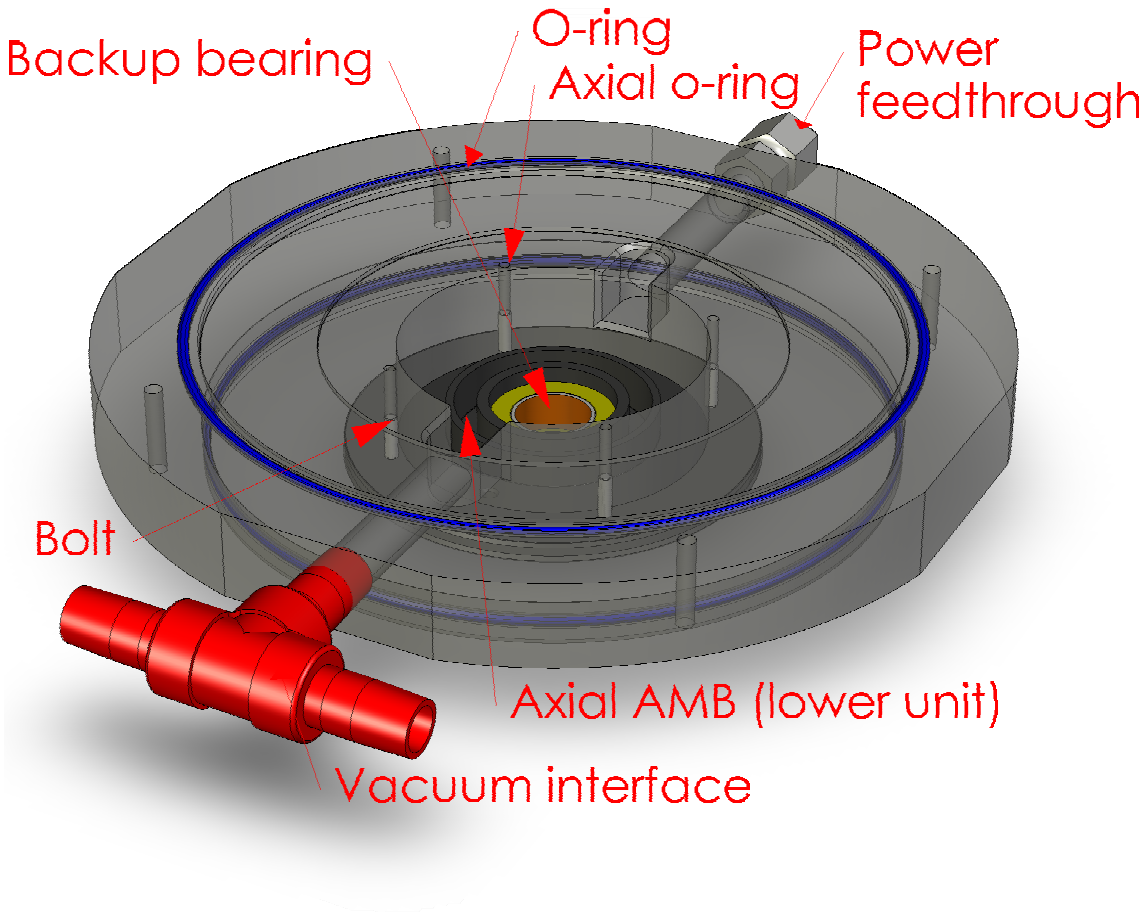

Figure 5.30: Schematic representation of module 6.

5.6.7 Module 7

The last module of the rotor/flywheel enclosure, module 7, houses the upper axial AMB unit and the axial eddy current sensor. The module is shown in figure 5.31. The figure displays the top and bottom of module 7. The operational functions of module 7 follow:

Housing the upper axial AMB unit The upper axial AMB unit is secured in the same way as the lower axial AMB unit. The axial AMB unit can also be shimmed. The shims are placed between the axial AMB unit and the module. To simplify the assembly process of this module, the module has two machined cavities. The cavities are used to store the excessive cabling. The cabling in the cavities enables the removal of the axial AMB unit. The axial AMB unit is fitted with a resistive temperature device inside the coil of the axial AMB unit. The upper axial AMB unit supports the entire weight of the rotor/flywheel assembly. Thus the workload of this unit is greater than the workload of the lower unit. The module is designed to have a lot of heat conductive material near the upper axial AMB. The power of the upper axial AMB unit is fed through the high current feedthrough.

House the axial eddy current sensor The axial eddy current sensor is housed in this module. The axial eddy current sensor is used to determine the axial distance of the axial AMB disc from the two axial AMB units. This reference distance signal is used control the upper and lower axial AMB units. The eddy current sensor's axial position is adjusted by screwing the sensor in the threaded hole and locking the position with a nut on the inside of the rotor/flywheel enclosure. The eddy current sensor's cabling is fed through the pressure gland. The sensing surface of this eddy current sensor is the bolt head used to secure the axial AMB disc to the rotor/flywheel assembly. The bolt's head is machined to the required surface finish.

Interface with module 6 Module 7 is the final module of the rotor/flywheel enclosure. The module interfaces with module 6. The vacuum seal is achieved through the o-ring fitted in module 6. The rotor/flywheel enclosure's modules are secured to each other by means of four threaded rods. The threaded rods are tightened on module 1 and module 7.

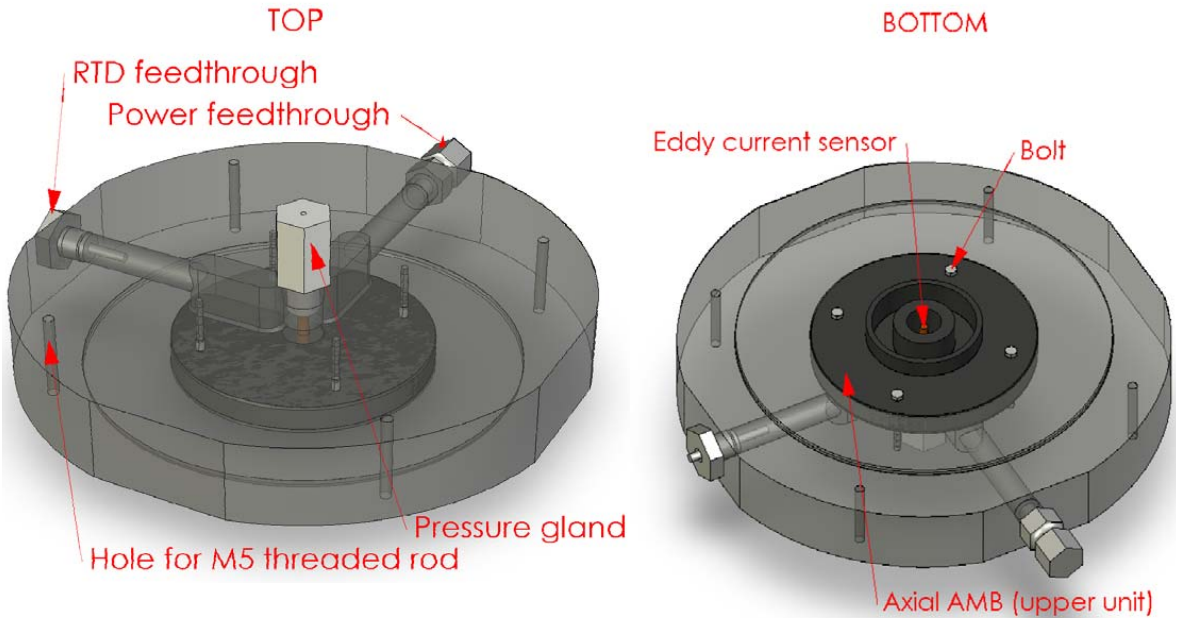

Figure 5.31: Schematic representation of module 7.

5.7 Aerodynamic losses

Aerodynamic losses are defined as the power lost due to the friction between fluid particles and solid surfaces. A similar design approach regarding the aerodynamic losses of the rotor/flywheel enclosure was used as in the design of the enclosure for heat dissipation as discussed in section 5.5. The design guideline for the enclosure aerodynamic loss design is to simply maximize the air gaps between the rotor/flywheel and the enclosure. The aerodynamic loss is dependent on the gap between the rotating and stationary parts of the assembly. The flywheel disc has the greatest surface speed, thus the flywheel disc is the area with the potential for high aerodynamic

losses. The solution is to design the rotor/flywheel enclosure with a relatively large gap between the enclosure and the flywheel disc. The aerodynamic losses are further reduced by operating the FLY-UPS system in a low pressure environment.

5.8 Integration

The final section of this chapter deals with the integration of the modules and the rotor/flywheel assembly. The result of the integration of the modules and rotor/flywheel is the final FLY-UPS system. This section endeavours to explain the process of assembling the FLY-UPS system in a step by step manner. This section will not discuss the assembly of each module.

The first step is to assemble each module separately as shown in figures 5.25 - 5.31. Module 1 is fastened to the baseplate and the assembly of module 1 and the baseplate is fastened to the concrete block as shown in figure 5.17. The threaded rods are placed in module 1. Module 2 is now placed upon module 1 and tightened using the threaded rods and nuts. After the two modules fit together the nuts are loosened and removed. This procedure is repeated until module 4 is fitted. After module 4 is fitted, the rotor/flywheel assembly is inserted into the half completed rotor/flywheel enclosure. The axial AMB disc of the rotor/flywheel is not installed at this time. The process followed to install module 2 to module 4 is now repeated for modules 5 and 6. The axial AMB disc is now installed onto the rotor/flywheel assembly. Finally module 7 is placed upon the semi-completed assembly and is tightened using the threaded rods and the nuts. The sensors and power cabling are connected to the control enclosure. The vacuum pump is connected to the system. The vacuum pump is switched on and the threaded rod nuts are retightened. After assembly the control for the FLY-UPS system is calibrated. The assembled FLY-UPS system is shown in figure 5.32.

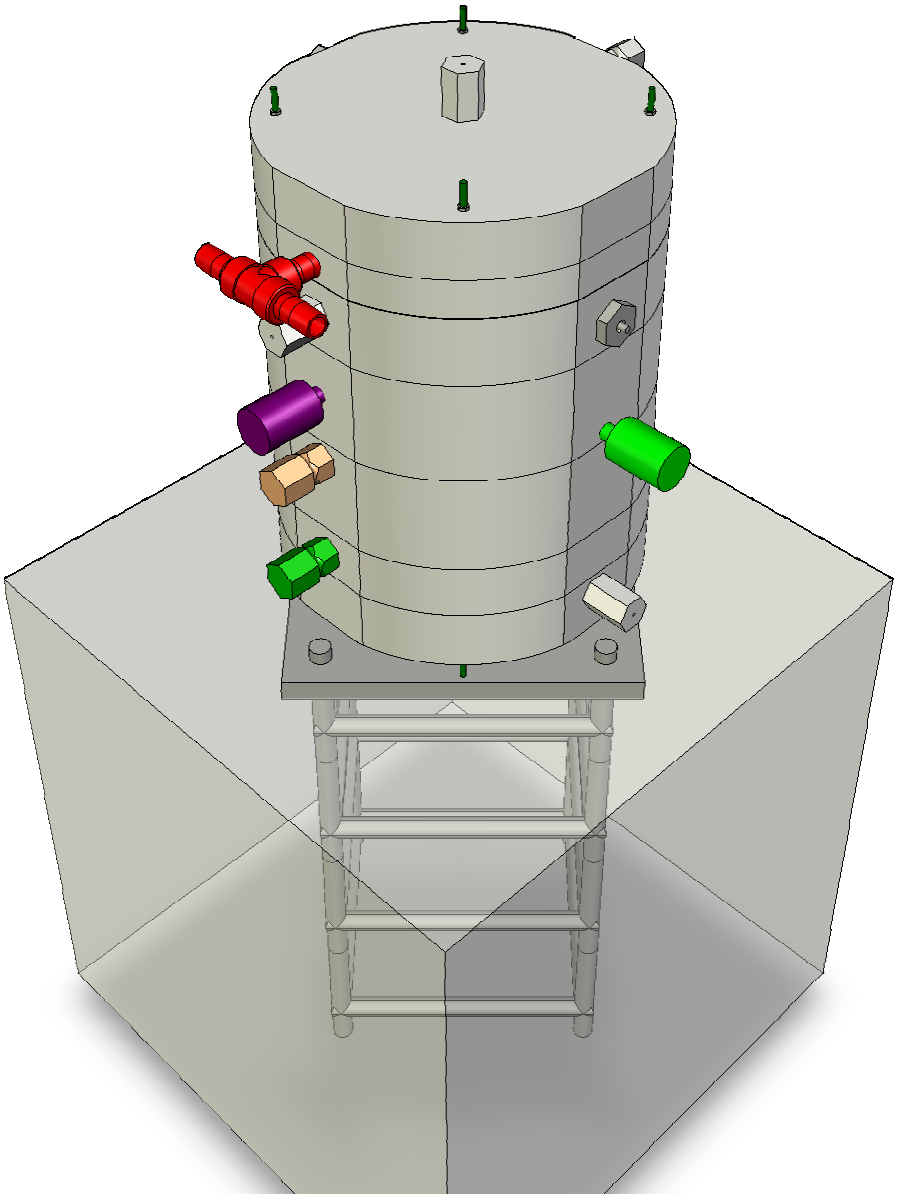

Figure 5.32: The assembled FLY-UPS system.

Chapter 5 dealt with the detail design of the rotor/flywheel enclosure. The operational functions of the enclosure were identified. The interfacing of the rotor/flywheel enclosure was discussed. The sub-components housed in the rotor/flywheel enclosure were identified and the requirements of each sub-component on the rotor/flywheel enclosure were discussed. The heat dissipation design of the rotor/flywheel was briefly discussed. The operational functions of each module were reviewed. An overview of the effect of aerodynamic losses on the final design of the rotor/flywheel enclosure was given. Finally the integration of all of the modules was explained.

Chapter 6

System characterisation, evaluation and verification

In this chapter some of the results of tests performed on the FLY-UPS system are displayed. The stationary critical frequency was determined and the results compared to the simulated results. The displacement of the rotor, while rotating, is compared to the simulated results. A log of the vacuum leakage is shown and the aerodynamic losses are calculated from acquired data.

6.1 Stationary critical frequency test results

The stationary critical frequency test is done by exciting the shaft at different frequencies. The shaft is excited by adding a disturbance signal on the control signal of the relevant AMB. The disturbance signal is added to one axis of one AMB at a time. The results displayed in figures 6.1 - 6.5 were obtained by adding a sinusoidal disturbance with a magnitude of 1μm to the control signal and measuring the displacement of the rotor in that particular axis. The peaks in figures 6.1 - 6.5 represent the critical frequencies of the rotor/flywheel assembly. The predicted critical frequencies were obtained using the predicted dynamic stiffness of the AMBs.

	1st critical [Hz]	2nd critical [Hz]	3rd critical [Hz]
Predicted (static stiffness)	34	155	519
Predicted (dynamic stiffness)	48	175	739
Lower AMB x-axis	48	174	732
Lower AMB y-axis	50	184	732
Upper AMB x-axis	52	176	730
Upper AMB y-axis	48	184	730

Table 6.1: Predicted and measured critical frequencies

In table 6.1 the predicted and measured critical frequencies are given. The predicted critical

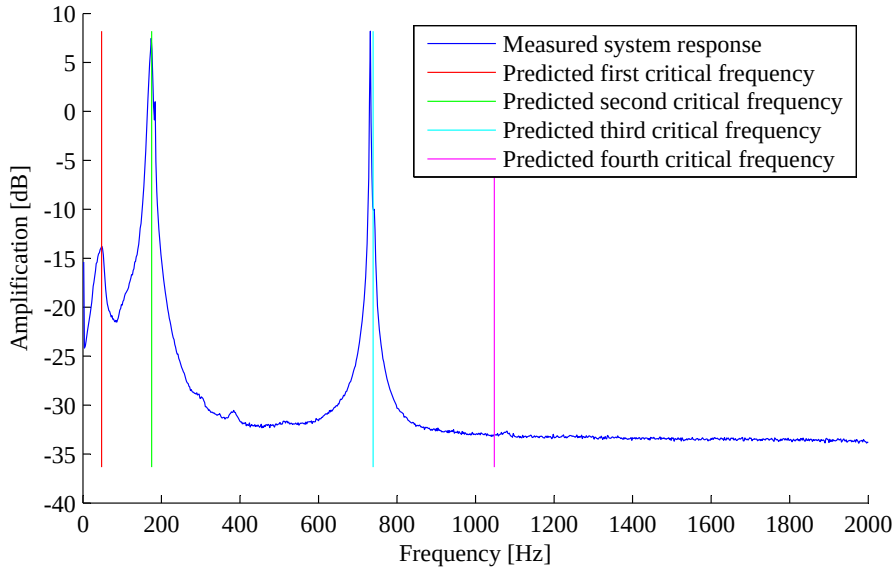

Figure 6.1: The amplification of the disturbance force on the lower AMB's x-axis, showing the predicted and measured critical frequencies.

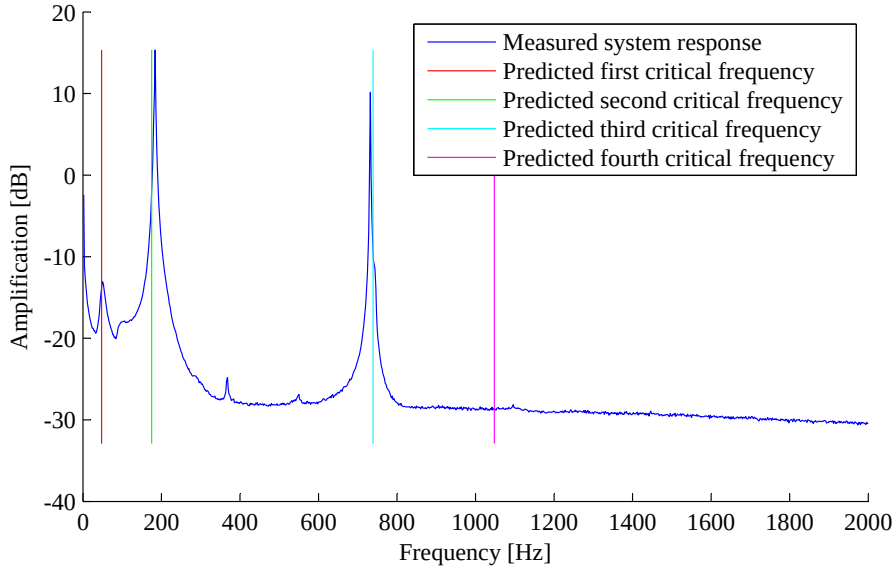

Figure 6.2: The amplification of the disturbance force on the lower AMB's y-axis, showing the predicted and measured critical frequencies.

frequencies obtained using the static stiffness differs significantly from the measured results. The predicted critical frequencies obtained using the dynamic stiffness of the AMBs correlate with the measured results.

The critical frequencies predicted with the software package *DyRoBeS*® correlate well with the

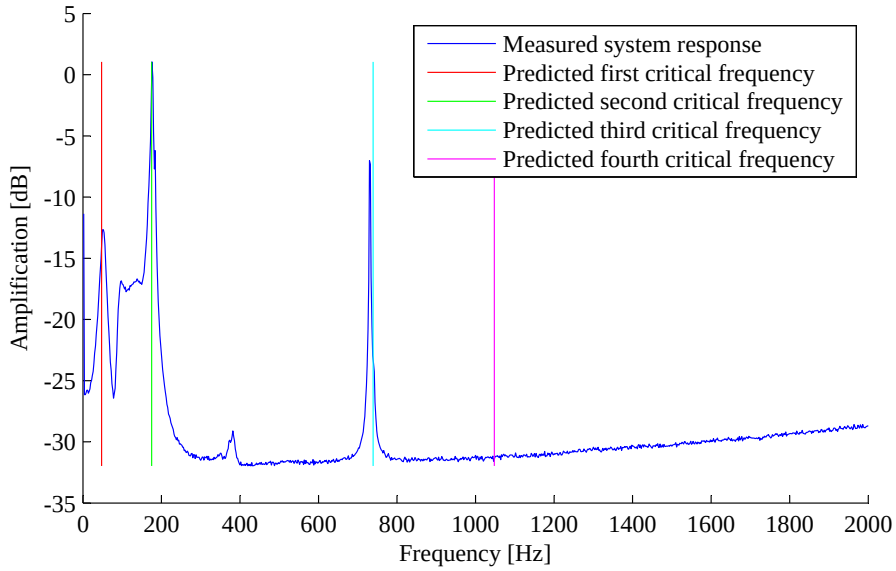

Figure 6.3: The amplification of the disturbance force on the upper AMB's x-axis, showing the predicted and measured critical frequencies.

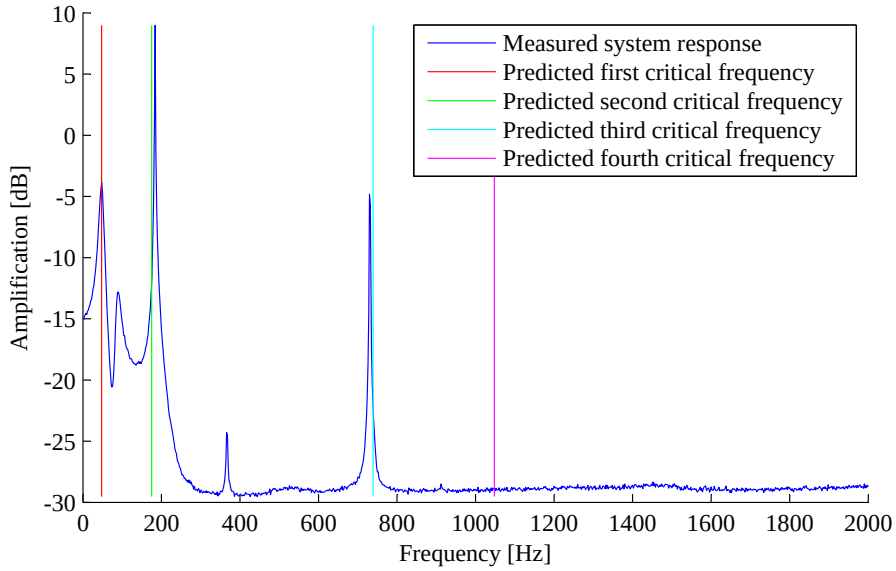

Figure 6.4: The amplification of the disturbance force on the upper AMB's y-axis, showing the predicted and measured critical frequencies.

measured values. The rotor-dynamic model is thus a good representation of the rotor/flywheel assembly. The axial critical frequencies are represented by the peaks in figure 6.5. The first critical frequency is at 20 Hz and the second at 550 Hz.

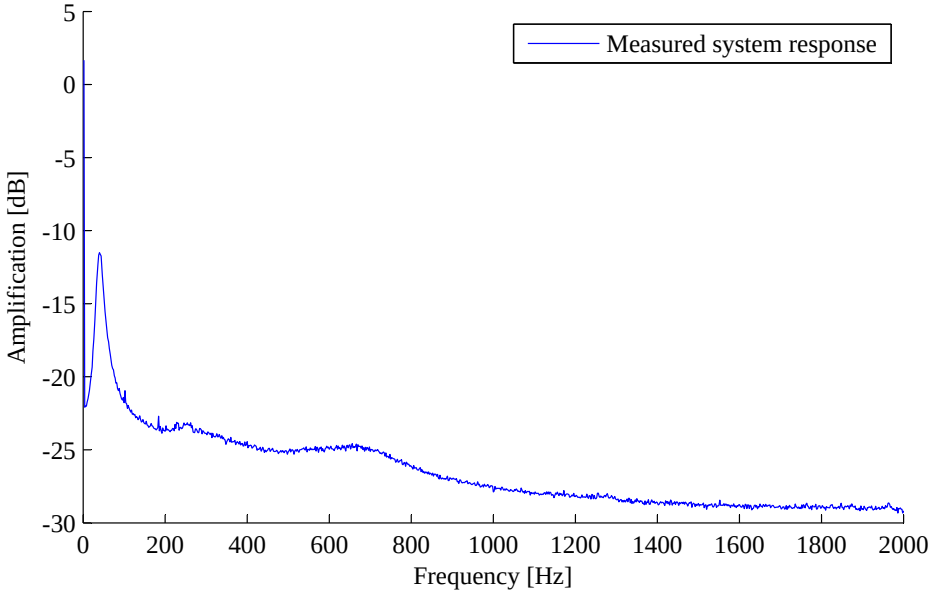

Figure 6.5: The amplification of the disturbance force on the axial AMB's z-axis.

6.2 Rotating displacements

These results were determined by speeding up the FLY-UPS and measuring the displacement of the rotor/flywheel assembly. The major axis displacement was determined from the obtained data. The major axis displacement is the maximum displacement of the rotor from the centre of the AMB. A graph of the displacement and the predicted first critical frequency is given in figure 6.6. As shown in figure 6.6 the displacements are greater than the predicted displacements given in figure 6.7. A probable explanation for this is that the rotor/flywheel assembly is not sufficiently balanced. The measured displacement seems to follow a trend of becoming greater with higher rotational speeds. This trend suggests that the rotor is insufficiently balanced.

	1st critical [Hz]
Predicted (static stiffness)	34
Predicted (dynamic stiffness)	48
Lower AMB	41
Upper AMB	43

Table 6.2: Predicted and measured first critical frequency of the rotating rotor/flywheel assembly

In table 6.2 the predicted and measured first critical frequencies of the rotating rotor/flywheel assembly are given. The dynamic stiffness predicted results correlate with the measured results.

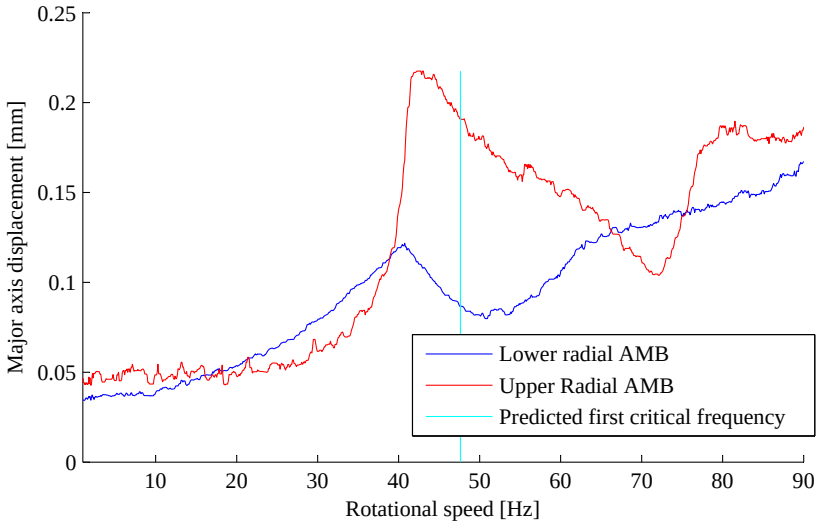

Figure 6.6: The major displacement of the rotor/flywheel assembly measured at the eddy current sensor locations.

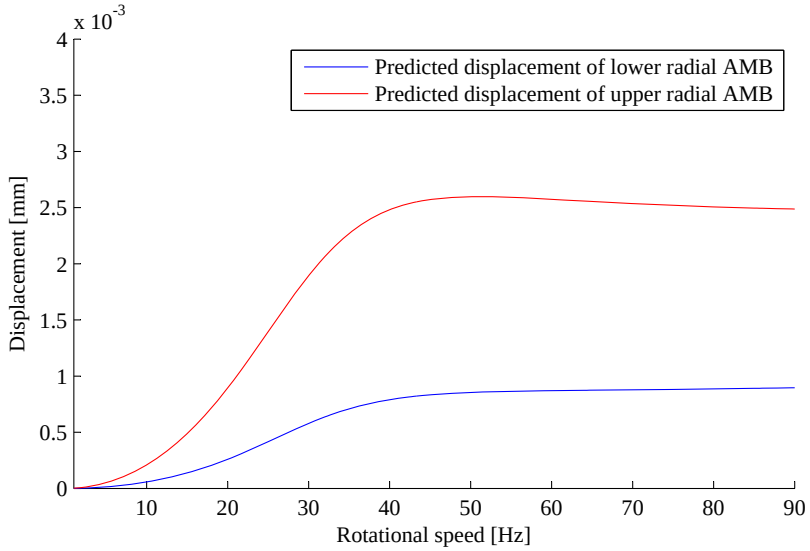

Figure 6.7: The predicted major displacement of the rotor/flywheel assembly.

6.3 Vacuum

The pressure inside the rotor/flywheel enclosure is monitored with a pressure transducer. The leakage of the vacuum is given in figure 6.8. The vacuum pump is controlled, based on the measurement of the pressure transducer. If the pressure inside the rotor/flywheel enclosure increases to a preset value, the vacuum pump automatically switches on. The vacuum pump remains on until the pressure lowers to a set value. The minimum pressure the rotor/flywheel enclosure can be vacuumed to is 23 kPa, shown in figure 6.8. The vacuum inside the rotor/flywheel enclosure with the automatic vacuum pump control enabled is given in figure 6.9. The results shown verifies the rotor/flywheel enclosure vacuum design.

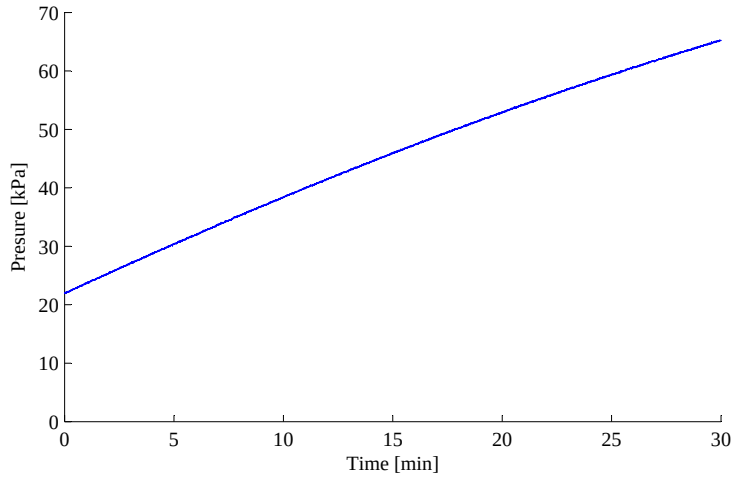

Figure 6.8: The vacuum leakage for 30 minutes.

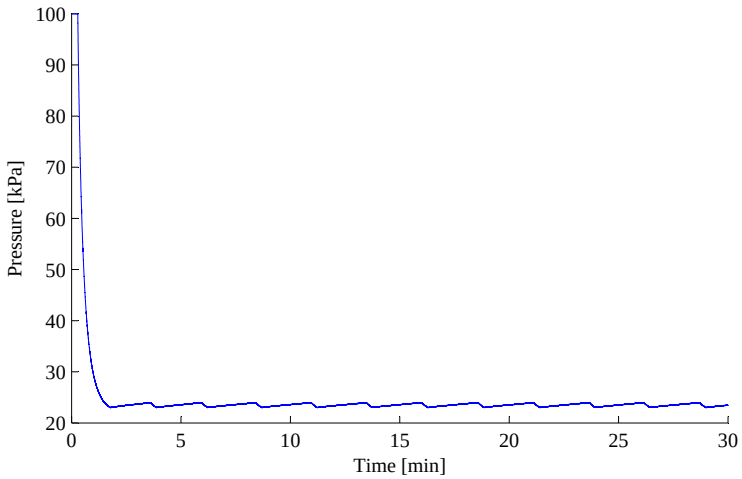

Figure 6.9: The vacuum leakage with automatic vacuum pump control enabled.

6.4 Aerodynamic losses

The losses of the rotor/flywheel assembly are given in figure 6.10. The losses were calculated from data acquired while the rotor/flywheel assembly is running free of loads, with the PMSM switched off. The rotor/flywheel is spun up to a rotational speed of 3000 rpm. When the rotor/flywheel reaches 3000 rpm the PMSM is switched off. The time and rotational speed is logged. With the moment of inertia known, the energy loss can be determined with (6.1). The power losses can be determined with (6.2). Figure 6.10 clearly shows the advantage of running the FLY-UPS system at low pressure.

$$\Delta E = \frac{I \cdot (\omega_{(i-1)} - \omega_i)^2}{2} \qquad [\mathrm{J}] \tag{6.1}$$

$$P = \frac{\Delta E}{\Delta t} \qquad [\mathrm{W}] \tag{6.2}$$

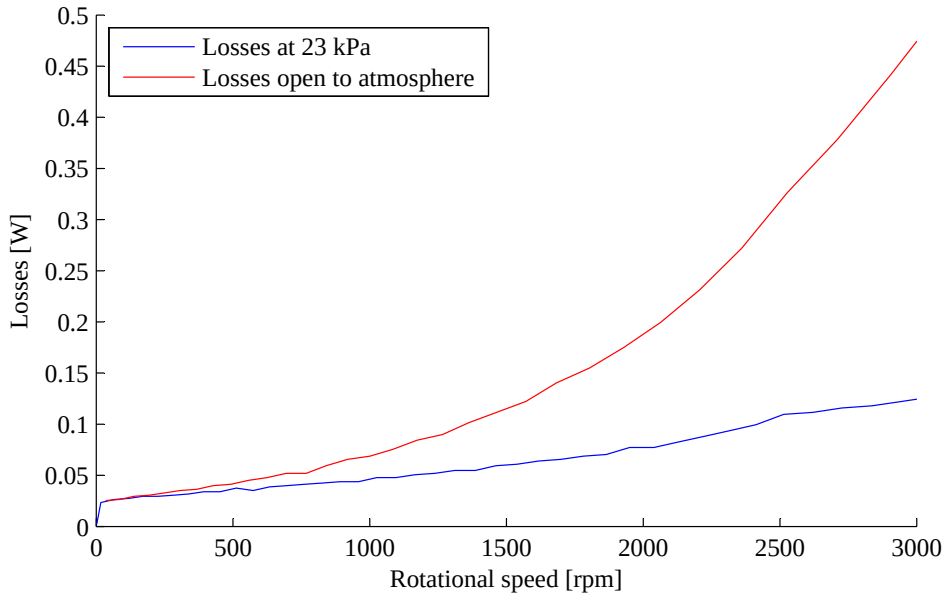

Figure 6.10: A comparison of the losses with the rotor in a vacuum and open to atmosphere.

Chapter 6 has shown comparisons between the simulated results and the measured results for the rotating displacements and the stationary critical frequencies. Results for the vacuum leakage and aerodynamic losses have also been given.

Chapter 7

Conclusions and recommendations

In this chapter the conclusions made from the results as well as practical experiences are discussed in greater detail. Appropriate recommendations for future work are made from the conclusions.

7.1 Conclusions

The conclusions discussed in this section are made from the results discussed in chapter 6 and from practical experiences encountered while developing the FLY-UPS system.

7.1.1 Stationary critical frequencies

The actual stationary critical frequencies correspond well with the predicted critical frequencies determined using the dynamic stiffness of the AMBs. Therefore, to accurately predict the critical frequencies of a rotating system, suspended on AMBs, the dynamic stiffness of the AMBs should be used. An accurate simulation to determine the dynamic stiffness of an AMB is therefore very important.

7.1.2 Rotating displacements

The displacements measured do not correlate with the simulated results. The probable reason for this discrepancy is that the rotor is not sufficiently balanced. The critical frequency traversed in the rotating displacement test correlates accurately with the critical frequency predicted using the dynamic stiffness of the bearing. The correlation of the predicted and measured critical frequencies further explains that the probable cause for the difference in the measured and simulated displacements is the rotor being insufficiently balanced. The displacements of the rotor/flywheel assembly are too great for the system to be safely spun up to the operating speed.

7.1.3 Vacuum

The vacuum inside the rotor/flywheel enclosure is reached within 3 minutes of the pump being switched on. The control for the pump can either be to leave the pump on while the system is running or to switch the pump on and off periodically. The vacuum is leaked to the minimum required level of 50 kPa in 20 minutes. The rotor/flywheel enclosure design for vacuum is therefore achieved.

7.1.4 Aerodynamic losses

The aerodynamic losses of the system are greatly reduced by running the system in a vacuum. A graph of the expected aerodynamic losses from 0 to 30000 rpm is shown in figure 7.1. The expected aerodynamic losses were obtained by fitting curves through the data shown in figure 6.10. The expected aerodynamic efficiency at 30000 rpm with the rotor/flywheel assembly open to atmosphere is 82.5 %. The expected efficiency with the rotor/flywheel assemble in a low pressure environment is 99.6 %. The aerodynamic efficiency design of the system is therefore achieved.

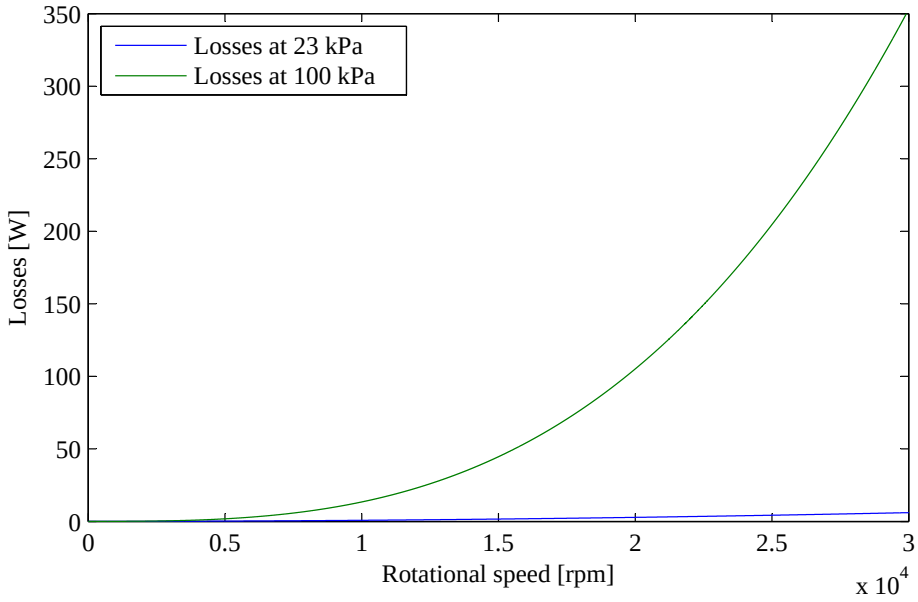

Figure 7.1: A comparison of the expected aerodynamic losses.

7.1.5 Modular design

The modular design of the system was verified by assembling and disassembling the system a few times. The tolerance build-up was within the specified value of 0.2 mm, and shimming

resolved the inconsistencies in the measurements. The modular design is a good concept for laboratory test and development equipment.

7.1.6 Securing the PMSM magnets

Securing the PMSM magnets to the rotor was problematic. The use of a combination of carbon-fibre and adhesive resolves the problem to a certain extent. The rotor/flywheel assembly's maximum speed is limited to 30056 rpm by the strength of this combination. The magnet adhesive is the weakest link in the rotor/flywheel assembly.

7.1.7 Energy storage

The energy storage capabilities of the rotor/flywheel assembly cannot be verified yet. The rotor/flywheel assembly is insufficiently balanced to spin the rotor to the operating speed. The moment of inertia about the axis of rotation was accurately determined using *SolidWorks*®. Thus the energy storage capability is expected to correlate well with the expected value.

7.2 Recommendations

This section states the recommended future work to resolve the problems currently encountered in the FLY-UPS system.

7.2.1 Stationary critical frequencies

Further work should be done in the accurate rotor-dynamic modelling of laminations on a rotating shaft. The complete rotor-dynamic analysis and verification of the system should be redone, using the dynamic stiffnesses of the AMBs. An accurate model for predicting the dynamic stiffnesses of AMBs used in non-symmetric systems should be developed.

7.2.2 Rotating displacements

To resolve the discrepancies of the simulated and measured results, the rotor/flywheel assembly should be re-balanced. Further investigation into the simulation of unbalance forces should be done to accurately predict the displacement of the rotor.

7.2.3 Aerodynamic losses

Investigation into the prediction of aerodynamic losses should be done to accurately predict the losses caused by aerodynamic effects. To improve the current performance a more effective vacuum pump should be procured. The proposed alternative vacuum pump should be able to lower the operating pressure even further.

7.2.4 Modular design

The modular design is optimal for use in a laboratory where sub-components should be replaceable with other components, without having to develop a totally new system. The use of a modular designed flywheel energy storage system for use by an end-user is discouraged. Flywheel energy storage systems designed for mass production should be of a single unit design to minimise the effects of tolerance build-up.

7.2.5 Securing the PMSM magnets

The problem of securing the PMSM magnets to the rotor/flywheel assembly can be overcome by using an external rotor PMSM with the magnets fitted to the inside of the flywheel. A new system should be developed using a hollow carbon-fibre flywheel with the PMSM magnets fitted to the inside of the carbon-fibre flywheel. The use of carbon-fibre is recommended because of the higher specific energy and yield strength of carbon-fibre. Another advantage of carbon-fibre is that the flywheel fails relatively safely, compared to a metal flywheel.

7.2.6 Auxiliary bearings

The auxiliary bearings used in the FLY-UPS system were not investigated in detail. A further investigation into auxiliary bearing design is recommended. The development of an accurate prediction model for the delevitation of an AMB suspended rotor is recommended.

7.2.7 Energy storage

The energy storage capabilities can be improved by using an internal PMSM setup. The use of an external rotor PMSM enables the flywheel disc to be of a greater height without adversely affecting the rotor-dynamic properties of the rotor. The development of an external rotor PMSM and internal radial AMBs should be investigated.

7.3 Closure

The purpose of this project was to develop an AMB suspended flywheel system. The system had to be able to store energy and the stored energy should be readily available for use. The charge time of the system should be no more than 5 minutes and the system should be able to supply 2000 W of power for at least 3 minutes. The main purpose of this project was achieved, namely the development of a fully suspended AMB system. The energy storage capabilities could not be verified due to the rotor being insufficiently balanced. The charge time of the system could also not be verified for the same reason. Another important outcome of the project that was achieved, is the local expertise gained in the field of high speed systems, AMBs and rotor-dynamic simulation and interpretation. The project is viewed as a success. Photos of the completed assembly can be seen in appendix C and appendix D.10.

Chapter 7 consists of the conclusions and recommendations regarding the FLY-UPS system.

Bibliography

[1] F. Werfel, U. Floegel-Delor, and R. R. et al, "Flywheel energy storage system (fess) with hts magnetic bearings," in *Proceedings of the 8th International Symposium on Magnetic Suspension Technology*, Dresden, Germany, September 2005, pp. 256–260.

[2] B. Bolund, H. Bernhoff, and M. Leijon, "Flywheel energy and power storage systems," *Renewable and Sustainable Energy Reviews*, vol. xx, pp. 1–25, 2005.

[3] W. Canders, H. May, and J. Hoffman, "Contactless magnetic bearings for flywheel energy storage systems," in *8th International Symposium On Magnetic Suspension Technology (ISMST)*, Dresden, Germany, September 2005, pp. 246–255.

[4] M. Chen, T. Walter, S. Wheeler, and E. Al, "Development and application of a passive magnetic bearing system to an energy storage flywheel," in *8th International Symposium On Magnetic Suspension Technology (ISMST)*, Dresden, Germany, September 2005, pp. 266–270.

[5] R. de Andrade Jr., A. Ferreira, and G. Sotelo, "A superconducting high-speed flywheel energy storage system," *Physica C*, vol. 930, pp. 408–410, 2004.

[6] Y. Fan, J. Fang, and G. Liu, "Analysis and design of magnetic bearings controller for a high speed momentum wheel." in *8th International Symposium On Magnetic Suspension Technology (ISMST)*, Dresden, Germany, September 2005, pp. 276–280.

[7] L. Hawkins, B. Murphy, and J. Kajs, "Analysis and testing of a magnetic bearing energy storage flywheel with gain-scheduled, mimo control." in *Asme Turboexpo*. Munich Germany: ASME, May 2000, pp. 1–8.

[8] T. Ichihara, K. Matsunaga, M. Kita, and et al, "Fabrication and evaluation of superconducting magnetic bearing for 10 kw h-class flywheel energy storage system," *Physica C*, vol. 426-431, pp. 752–758, 2005.

[9] M. K. Y. N. e. a. Koshizuka, N., "Construction of the stator installed in the superconducting magnetic bearing for a 10 kwh flywheel," *Physica C*, vol. 412-414, pp. 756–760, 2002.

[10] B. Murphy, H. Ouroua, M. Caprio, and et al, "Permanent magnet bias, homopolar magnetic bearings for a 130 kw-hr composite flywheel," in *The Ninth International Symposium on Magnetic Bearings*, August 2004.

[11] H. Nakai, A. Matsuda, and M. Suzuki, "Development and testing of the suspension system for a flywheel battery," *Control Engineering Practice*, vol. 9, pp. 1039–1046, 2001.

[12] T. Sung, J. Lee, Y. Han, and et al, "300 w-h class superconductor flywheel energy storage system with a horizontal axle," *Physica C*, vol. 372-376, pp. 1451–1456, 2002.

[13] R. Takahata, A. Kubo, F. Thoolen, and et al, "Compact flywheel energy storage system," Koyo Seiko Co., Tech. Rep., 2001.

[14] R. Viznichenko, A. Plyushchay, and A. Kordyuk, "Superconducting flywheel model for energy storage applications." in *8th International Symposium On Magnetic Suspension Technology (ISMST)*, Dresden, Germany, September 2005, pp. 236–239.

[15] J. Akpobi and I. Lawani, "Computer-aided-design of flywheels," *Advances in Engineering Software*, vol. 37, pp. 222–235, 2006.

[16] S. Holm, "Modelling and optimization of a permanent-magnet machine in a flywheel," PH.D Thesis, Technishe Universiteit Delft, 2003.

[17] J. Shingley and C. Mischke, *Mechanical Engineering Design*, 6th ed. Singapore: Mc Graw Hill, 2001, ch. 8, pp. 1034–1038.

[18] Wikipedia, "Magnetic bearings," Online, Febuary 2006. [Online]. Available: http://en.wikipedia.org/wiki/Magnetic_bearing

[19] R. Larsonneur, "Design and control of active magnetic bearing systems for high speed rotation," PH.D Thesis, Swiss Federal Institute of Technology, Zürich, March 1990.

[20] Z. Kohari and I. Vajda, "Losses of flywheel energy storages and joint operation with solar cells," *Materials Processing Technology*, vol. 161, pp. 62–65, 2005.

[21] SKF, "Magnetic bearings," Online, April 2006. [Online]. Available: http://www.skf.com/portal/skf_rev/home

[22] H. Chang and S. Chung, "Integrated design of radial active magnetic bearing system using genetic algorithms," *Mechatronics*, vol. 12, pp. 19–36, 2002.

[23] J. Vance, *Rotordynamics of Turbomachinery*. New York: Wiley, 1988, ch. 3, pp. 116–170.

[24] E. Ranft, "The development of a flexible rotor active magnetic bearing system," Master's thesis, North West University, Potchefstroom South Africa, 2005.

[25] R. Hibbeler, *Mechanics of materials*, 6th ed. Pearson Prentice Hall, 2005, ch. 6, pp. 324–331.

[26] API, "Steam turbines - special-purpose applications," Petroleum, Petrochemical and Natural Gas Industries, Standard API 612, 2005.

[27] ISO, "Mechanical vibration - balance quality requirements for rotors in a constant (rigid) state - part 1: Specification and verification of balance tolerances," International Standards Organisation, Standard ISO 1940-1:2003, 2003.

[28] Loctite, "Adhesives for electric motors and generators," Online, June 2007. [Online]. Available: http://www.motors.loctite.com/int_henkel/loctite_us/index.cfm

Appendix A

Type A specification

APPENDIX

Appendix A: Type-A specification

TITLE: SYSTEM SPECIFICATION FOR THE HIGH SPEED AMB FLYWHEEL ENERGY STORAGE SYSTEM (FLY-UPS)

DOCUMENT NUMBER: TYPE-A

VERSION: A

APPROVAL:

NWU PUKKE	
Signature:	Signature:
Name: JJ Janse van Rensburg	Name: Eugen Ranft

Table of Contents

Page

1 SCOPE 124

1.1 IDENTIFICATION 124

1.2 DESCRIPTION OF TYPE OF SYSTEM 124

2 REQUIREMENTS 124

2.1 SYSTEM DEFINITION 124

2.1.1 General Description 124

2.1.2 Operational Requirements 124

2.1.3 Maintenance Concept 125

2.1.4 Functional Analysis and System Definition 125

2.1.5 Allocation of Requirements 125

2.2 SYSTEM CHARACTERISTICS 126

2.2.1 Performance Characteristics 126

2.2.2 Physical Characteristics 126

2.2.3 Effectiveness Requirements 126

2.2.4 Reliability 126

2.2.5 Maintainability 126

2.2.6 Usability (human factors) 126

3 NOTES 127

3.1 PROPOSED USES OF FLY-UPS 127

SYSTEM SPECIFICATIONS FOR THE HIGH-SPEED ACTIVE MAGNETIC BEARING (AMB) FLYWHEEL ENERGY STORAGE SYSTEM

SCOPE

This document defines the system requirements for the high speed AMB flywheel energy storage system (FLY-UPS).

IDENTIFICATION

HSAFESS01, high speed AMB flywheel energy storage system, FLY-UPS

DESCRIPTION OF TYPE OF SYSTEM

The FLY-UPS is a vertical flywheel system and consists of:

- 1 Mounting
- 1 Flywheel
- 2 Radial AMBs
- 1 Axial AMB
- 1 Motor
- Electrical control enclosure

REQUIREMENTS

SYSTEM DEFINITION

General description

The FLY-UPS supplies uninterrupted power to a load of at least 300 W for at least 15 minutes. The system uses a magnetically suspended flywheel to store energy gained from a high-speed motor/generator, the energy gained from the motor is then used to power a load of 300 W for 15 minutes or more.

Operational requirements

Need

The need for such an energy storage system has become apparent in the use of emergency backup power systems. The backup generators needs time to start up, this system will be the

"in-between" system for equipment that is sensitive to such power outages or dips in mains power.

Mission
The mission of this first phase development is to be able to study the uses of flywheel energy storage thus enabling the production of larger scale flywheel systems, in areas such as renewable energy

Use profile
The usage of such a system is of such a nature that it will always be running in the a mode of energy input, but energy will only be extracted from the system during a power dip or a power failure.

Distribution
The FLY-UPS will be installed in the AMB laboratory of the North-West University.

Life cycle
The system will be designed for a life cycle of 8 years.

Maintenance concept

A modular approach to maintenance will be used where the system will be divided into smaller system which can be replaced if failure occurs. Thus a Corrective Maintenance policy will be used in this system with the possibility of investigating preventative maintenance on later systems.

Functional analysis and system definition

The functions of the system are:

- To enable further research into Flywheels and AMBs as well as to enhance the collaboration between the mechanical and electrical departments on the North-West University.
- To enhance the knowledge on systems engineering in the electrical engineering department.
- To establish a knowledge base in the field of mechatronics within the faculty.

Allocation of Requirements

FLY-UPS:

Time power level can be maintained

300 W (NET) mode:	15 minutes
1100 W (NET) mode	5 minutes

A_o=	0.9835	(Operational availability)
A_i=	0.9997	(inherent availability)
MTBM=	10 000 hr	(Mean Time Between Maintenance)
MTBF=	20 000 hr	(Mean Time Between Failure)
MDT=	168 hr (1week)	(Maintenance downtime)
Mct=	6hr	(Mean corrective maintenance time)
MLH/OH=	0.0006	(Maintenance labour hours per operating hour)
Cost	R300 000	
Skill level needed:	High (For Maintenance) - Low (for Operation)	

SYSTEM CHARACTERISTICS

Performance Characteristics

The FLY-UPS's rotational speed needs to be at least 28 000 RPM.

The FLY-UPS has to be able to supply 300W of uninterrupted power after mains power is shut off.

Physical Characteristics

The FLY-UPS should not exceed 1.2m X 1.2m X 1.5m (L X B X H)

Should not weigh more than 200 kg

Effectiveness Requirements

The FLY-UPS needs to be at least 85% efficient when operating in a near vacuum

Reliability

The FLY-UPS should be able to run continuously for 10 000 hours with at least 25 full-rundown cycles.

Maintainability

The FLY-UPS will use a modular maintenance policy. The different components should be able to be replaced by another module within 3 hours

Usability (human factors)

The FLY-UPS has to be able to be used by unschooled labour, but the maintenance requires schooled labour. Modular replacement of components should be able to be done by unschooled labour.

NOTES

PROPOSED USES OF FLY-UPS

The use of the FLY-UPS will primarily be for researching and developing other Flywheel and AMB systems. The FLY-UPS may also be used for testing advanced control algorithms. The FLY-UPS is one of the first steps for developing a flywheel based renewable energy system.

Appendix B

Type B specification

Appendix B: Type-B specification

TITLE: SUB-SYSTEM SPECIFICATION FOR THE HIGH SPEED AMB FLYWHEEL ENERGY STORAGE SYSTEM (FLY-UPS)

DOCUMENT NO: TYPE B

VERSION: D

APPROVAL:

NWU PUKKE	
Signature:	Signature:
Name: S. Myburgh	Name: Eugen Ranft

TABLE OF CONTENTS

Page

1 SCOPE 132

2 APPROPRIATE DOCUMENTS 132

2.1 STANDARDS 132

3 REQUIREMENTS 132

3.1 ITEM DEFINITION 132

3.1.1 ITEM DIAGRAM 133

3.1.2 INTERFACE DEFINITION 133

3.1.3 MAIN COMPONENT LIST 133

3.2 CHARACTERISTICS 134

3.2.1 PERFORMANCE 134

3.2.2 PHYSICAL CHARACTERISTICS 134

3.2.3 SERVICEABILITY 134

3.2.4 ENVIRONMENTAL FACTORS 135

3.3 DEVELOPMENT 135

3.3.1 COMPONENTS 135

3.3.2 ELECTROMAGNETIC RADIATION 135

3.3.3 SAFETY 135

3.3.4 ERGONOMIC FACTORS 135

3.4 DOCUMENTATION 135

3.5 LOGISTICS 135

3.5.1 MAINTENANCE 135

3.5.2 FACILITIES AND EQUIPMENT 136

3.6 PERSONNEL AND TRAINING 136

3.6.1 PERSONNEL 136

3.6.2 TRAINING 136

3.7 MAIN COMPONENT CHARACTERISTICS 136

3.7.1 Radial AMB 136

3.7.2 Axial AMB 136

3.7.3 PERMANENT MAGNET MACHINE 137

3.7.4 FLYWHEEL/ROTOR 137

3.7.5 FLYWHEEL/ROTOR ENCLOSURE 138

3.8 IMPORTANCE 138

TYPE B SPECIFICATION OF THE FLY-UPS SYSTEM

SCOPE

This document specifies the requirements on the sub-systems of the FLY-UPS system.

APPROPRIATE DOCUMENTS

STANDARDS

API 612	Petroleum, petrochemical and natural gas industries - -steam turbines – special-purpose applications
ISO/CD 14839-3	mechanical vibration – vibration of rotating machinery equipped with active magnetic bearings – Part 3: Evaluation of stability margin
ISO/FDIS 14839-2	mechanical vibration – vibration of rotating machinery equipped with active magnetic bearings – Part 2: Evaluation of vibration
ISO 1940/1	Balance quality Requirements of rigid rotors
MIL-STD-1472	Department of defence design criteria – Human engineering

REQUIREMENTS

ITEM DEFINITION

The FLY-UPS system's main purpose is to serve an uninterrupted power supply system. Secondly the system will be used for future research in self-sensing and motor drive development.

ITEM DIAGRAM

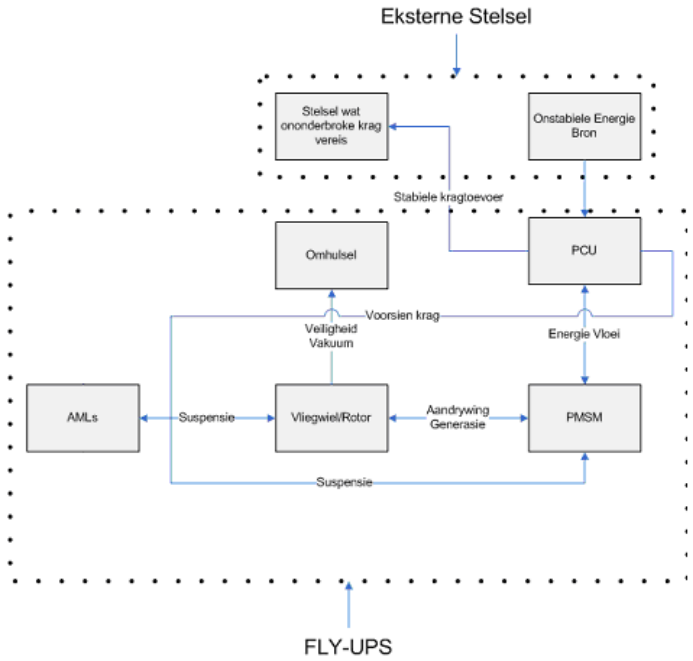

Note: AMB active magnetic bearing

PCU power conversion unit

The FLU-UPS consists of 5 basic components namely:

- PCU
- Enclosure
- PMSM
- Rotor
- AMBs

INTERFACE DEFINITION

The system interfaces with the following conditions:

The air pressure of the surroundings: 1 atm.

The physical surroundings the FLY-UPS should fit through a standard door (780 x 2100mm).

MAIN COMPONENT LIST

Radial AMBs (x2)
Axial AMB (x1)
Permanent magnet machine (x1)
Flywheel/rotor assembly (x1)
Flywheel/rotor enclosure (x1)

CHARACTERISTICS

PERFORMANCE

3.2.1.1	Minimum gross power:	2000	W
3.2.1.2	Minimum net power:	1300	W
3.2.1.3	Unbalance	ISO G6.3	ISO1940/ 1
3.2.1.4	Minimum time of power output	3	Min
3.2.1.5	Life cycle:	10	year
3.2.1.6	Maximum rotational speed for trip	30000	RPM

PHYSICAL CHARACTERISTICS

3.2.2.1	Maximum mass of each module	25.4	kg
3.2.2.2	Maximum sizes:		
	Flywheel diameter	300	mm
3.2.2.2.1	FLY-UPS diameter	500	mm
	Rotor-length	500	mm
3.2.2.2.2	FLY-UPS height	700	mm

SERVICEABILITY

3.2.4.1	Mean time to repair (MTTR):	1,0	h
3.2.4.2	Skill level of maintenance personnel:	high	

ENVIRONMENTAL FACTORS

3.2.5.1	Maximum temperature:	30,0	°C
3.2.5.2	Minimum temperature:	0	°C
3.2.5.3	Maximum relative humidity:	80,0	%
3.2.5.4	Minimum relative humidity:	5,0	%

DEVELOPMENT

COMPONENTS

Standard items will be used as much as possible.

ELECTROMAGNETIC RADIATION

(To be determined at a later stage).

SAFETY

A minimum factor of safety of 1.5 (based on the von Misses stress) will be used throughout the design phase.

ERGONOMIC FACTORS

The noise that the FLY-UPS produces should be less than 80dB.
For the handling of modules the standard MIL-STD-1472 is applicable.

DOCUMENTATION

The minimum required documentation is a design report.

LOGISTICS

MAINTENANCE

The maintenance philosophy is a modular replacement of failed or near failed components.

FACILITIES AND EQUIPMENT

A safety room will be built for the testing purposes of the FLY-UPS system

PERSONNEL AND TRAINING

PERSONNEL

Item design personnel

Item	No. of personnel	Training level	
FLY-UPS	6	High	

Operational personnel: 1

Service personnel: 1

TRAINING

Training takes place at North-West University within the McTronX research group.

MAIN COMPONENT CHARACTERISTICS

Radial AMB

PERFORMANCE

3.7.1.1.1	Maximum power used per radial AMB:	100	W
3.7.1.1.2	Minimum force applied to rotor by AMB	150	N
3.7.1.1.3	Maximum allowable displacement of rotor	0.35	mm

Axial AMB

PERFORMANCE

3.7.2.1.1	Minimum force applied to the rotor by the upper axial AMB unit	517	N

3.7.2.1.2	Minimum force applied to the rotor by the lower axial AMB unit	100	N
3.7.2.1.3	Maximum allowable displacement of rotor	0.35	mm
3.7.2.1.4	Maximum power usage	40	W

PERMANENT MAGNET SYNCHRONOUS MACHINE

PERFORMANCE

3.7.3.1.1	Minimum power output at 15000 rpm:	2000	W
3.7.3.1.2	Trip speed	33,000	rpm
3.7.3.1.3	Operating speed	30,000	rpm

FLYWHEEL/ROTOR

PERFORMANCE

3.7.4.1.1	Minimum energy storage potential	550	kJ
3.7.4.1.2	Maximum losses	100	W
3.7.4.1.3	Maximum unbalance	ISO 6.3G	ISO 1940/1
3.7.4.1.4	Design rotational speed	30,000	rpm

FLYWHEEL/ROTOR ENCLOSURE

PERFORMANCE

3.7.5.1.1	Maximum absolute pressure inside enclosure	50	kPa

PHYSICAL CHARACTERISTICS

3.7.5.2.1	Maximum sizes:		
	Enclosure diameter	500	mm
	Enclosure height	700	mm

IMPORTANCE

The relative importance of the characteristics of the FLY-UPS is shown in table 3.8.1, a scale of 1 (min) to 9 (max) is used to define the relative importance.

TABLE 3.8.1: IMPORTANCE TABLE

No	Ref. No.	PARAMETER	IMPORTANCE
3.8.1	3.1 & 3.7.4.1.1	Energy storing capabilities	9
3.8.2	3.2.1.5	Life-cycle	5
3.8.3	3.2.3	Reliability	7
3.8.4		Cost	2
3.8.5	3.2.2.1	Mass	4
3.8.6	3.3.4	Human factors	4
3.8.8	3.2.4 3.5.1	Serviceability	5
3.8.9	3.2.5	Operational environment conditions	8

Appendix C

Photos

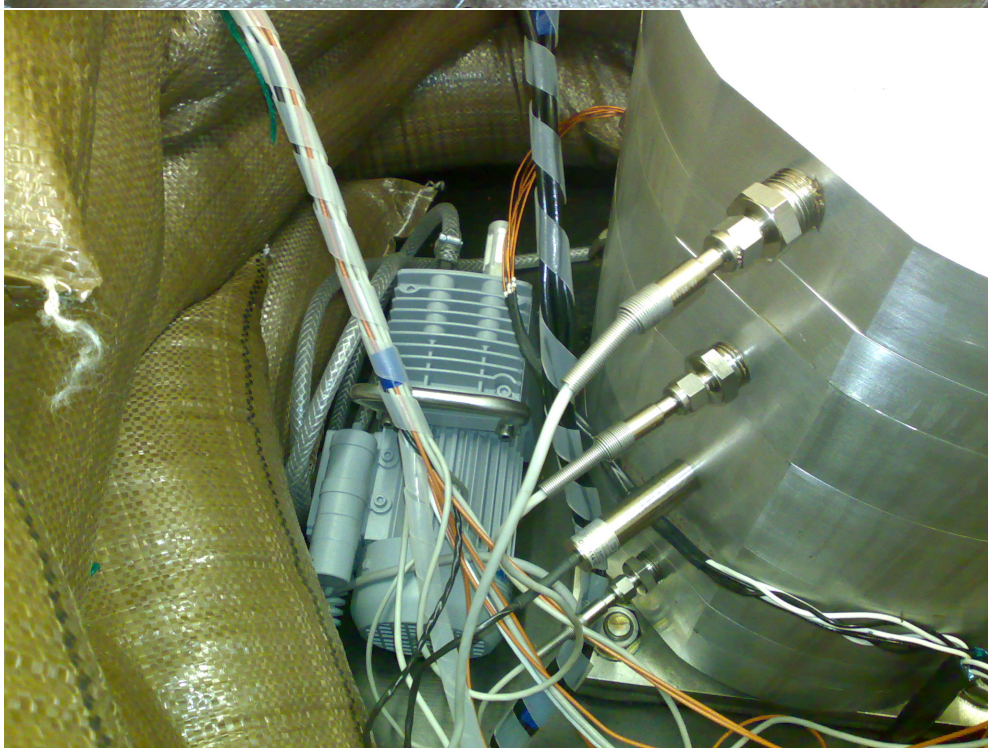

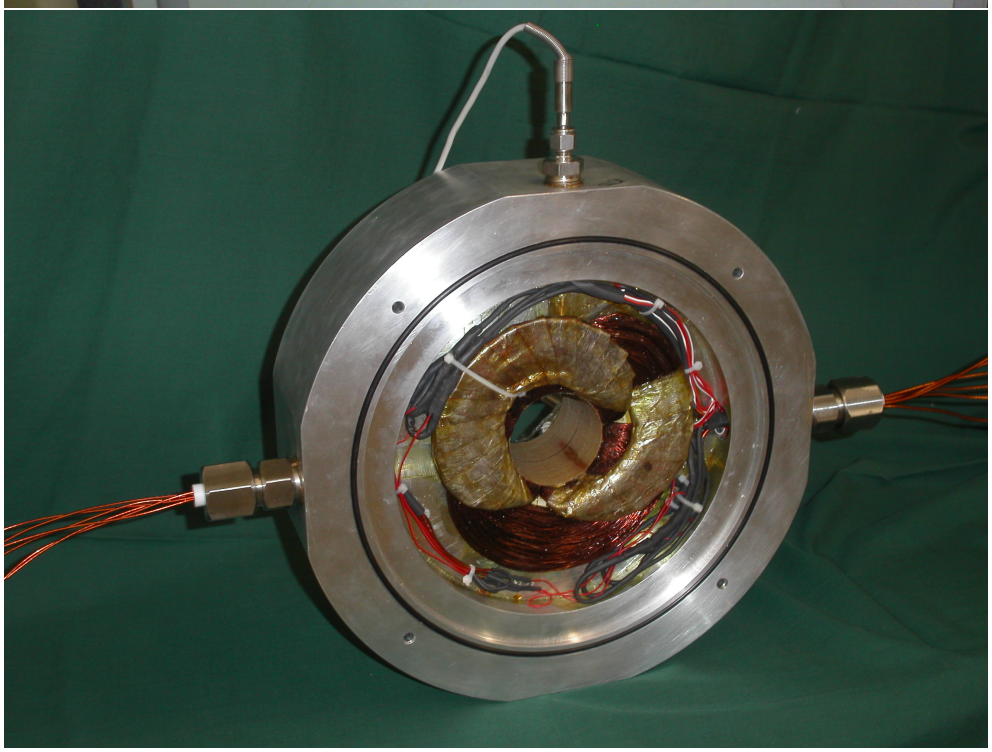

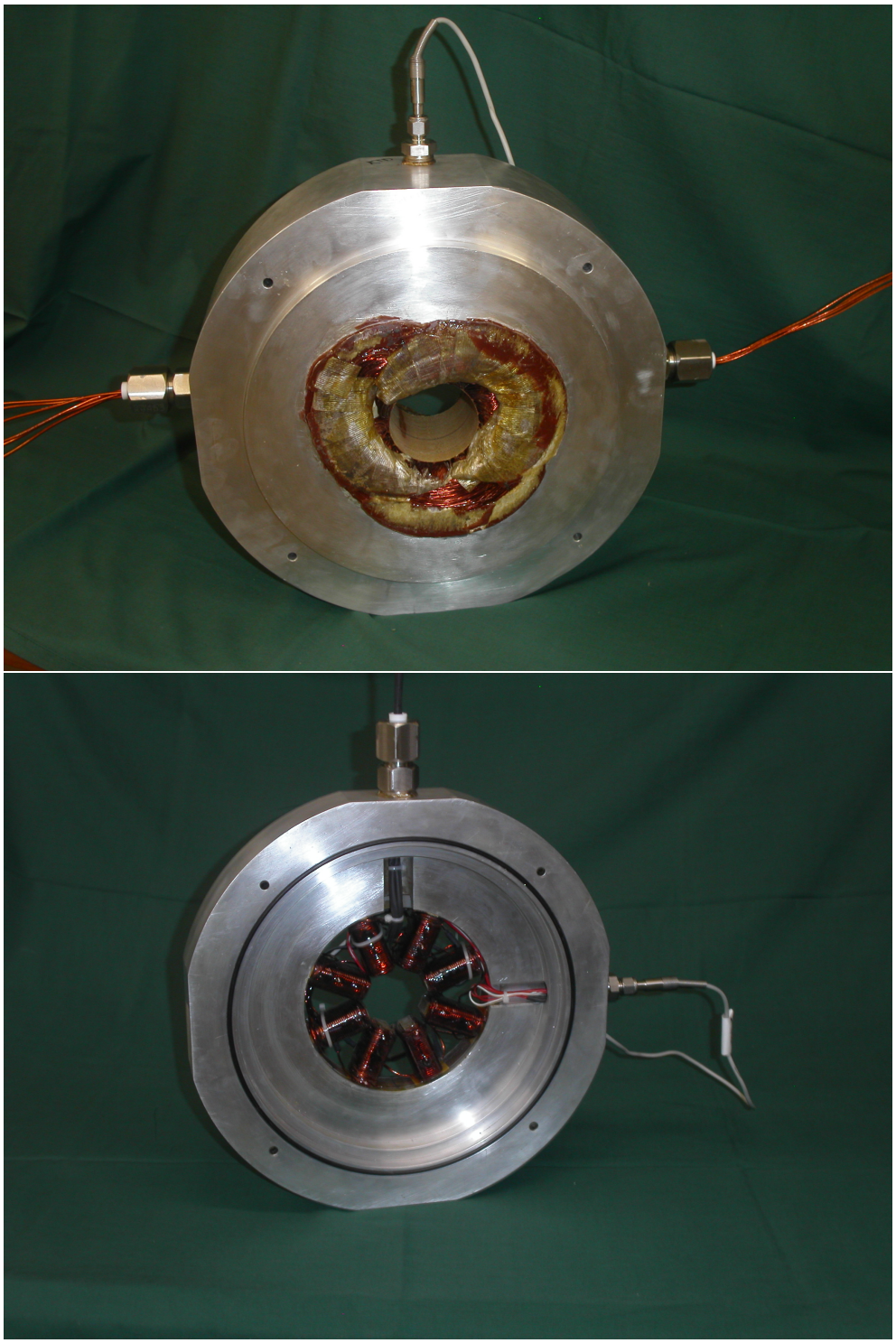

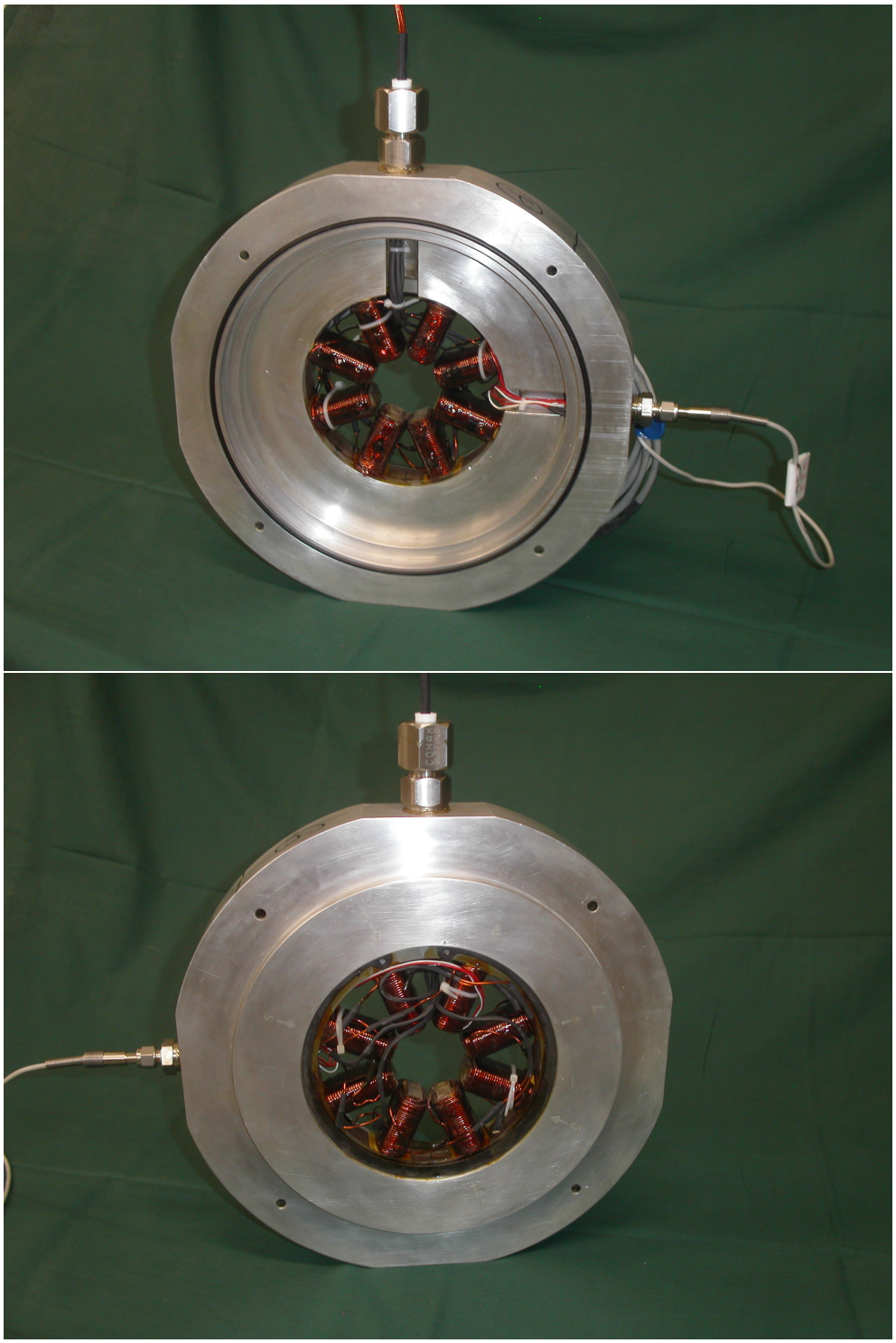

2
1
4
5
3
6
7
8

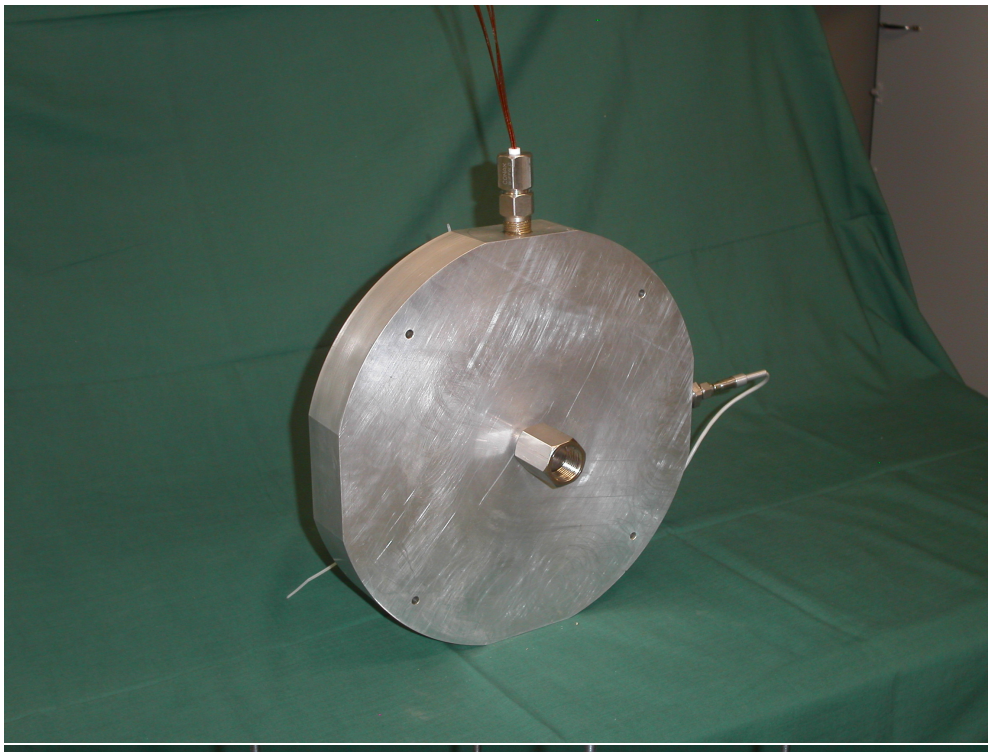

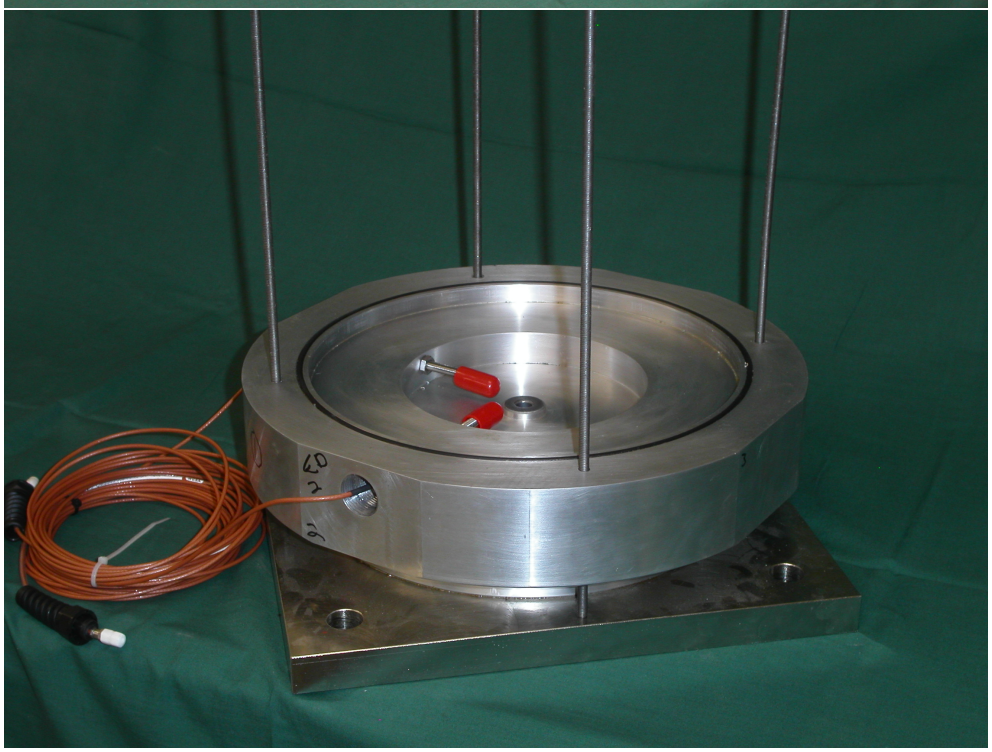

Appendix D

Appendix and data DVD

The appendix and data DVD contains pages 150-368. The complete document including all appendices is located on the root of the DVD. The data, *SolidWorks®*, *CosmosWorks®*, *MATLAB®*, *DyRoBeS®* and *ees®* files is in the FLY-UPS sub-directory.

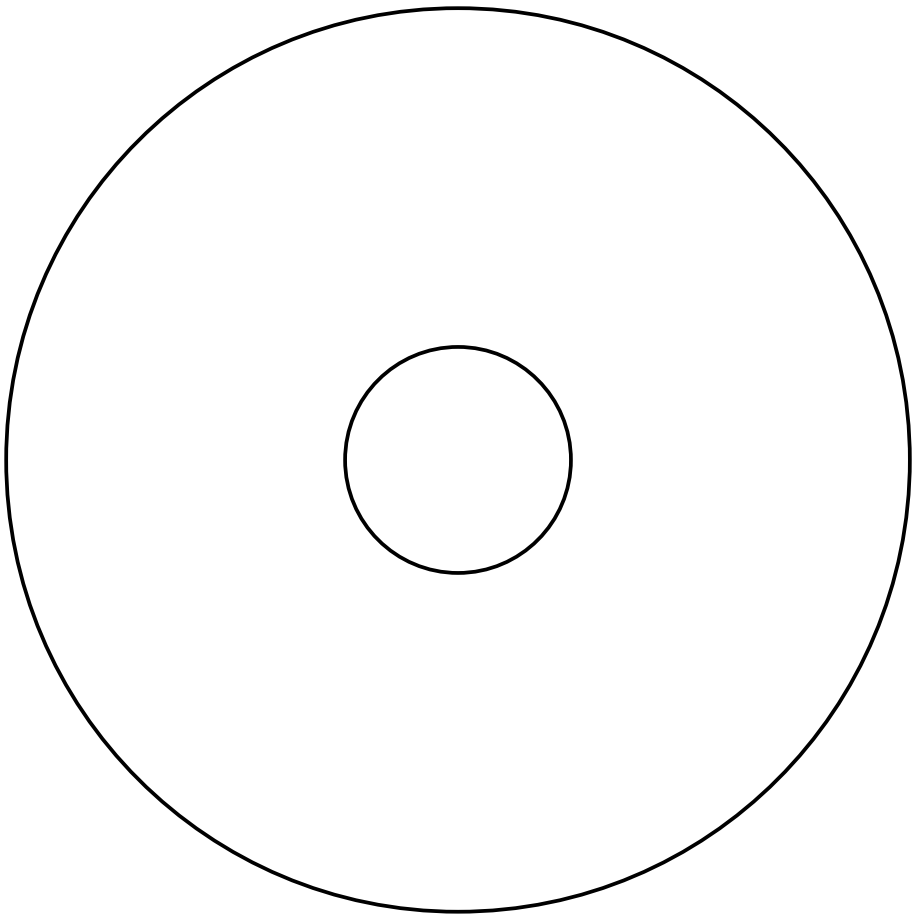

D.1 Shaft layout design

Design Report:

FLY-UPS Shaft Layout

Prepared by: Jan Janse van Rensburg

For the NWU MBMC Research group

Version 4

Revision 2

Table of Contents

1 BACKGROUND 4

1.1 Energy Storage Capabilities 4

1.2 Determining the unbalance 5
1.2.1 ISO 1940/1 unbalance standard for Overhung and Narrow Rotors: 5
1.2.2 API 612 Unbalance Standard: 6

1.3 API 612 Rotordynamic Standard 7
1.3.1 Operating Range Lower than Critical Frequency 8
1.3.2 Operating Range Higher than Critical Frequency 9

2 DESIGN 10

2.1 Rotor Design Process 10

2.2 Design Concept 11
2.2.1 Model Summary 11
2.2.2 Strength Analysis Results 11
2.2.3 Rotor-Dynamic Results 14

3 SUMMARY OF RESULTS 25

4 CONCLUSION 25

List Of Figures

Figure 1: The centred flywheel layout 4
Figure 2: ISO standard balancing application for a centred rotor 6
Figure 3: Translatory first rigid mode 6
Figure 4: Conical, rocking second rigid mode 7
Figure 5: API standard for a operating range lower than the critical frequency 8
Figure 6: API standard for a operating range higher than the critical frequency 9
Figure 7: Rotor Design Process Diagram 10
Figure 8: The model layout 11
Figure 9: The Factor of Safety distribution 30 000RPM side view 12
Figure 10: The Factor of Safety distribution 30 000RPM top view 12
Figure 11: The Factor of Safety distribution 33 000RPM side view 13
Figure 12: The Factor of Safety distribution 33 000RPM top view 13
Figure 13: The critical speed map of the system 14
Figure 14: Mode shape 1 of the system (2 046 RPM) 15
Figure 15: Mode shape 2 of the system (36 674 RPM) 15
Figure 16: Bode plot: sensor position 1 16
Figure 17: Bode plot: sensor position 2 17
Figure 18: The transmitted force [N] at bearing 1 (70.144 N) 17
Figure 19: The transmitted force [N] at bearing 2 (14.651 N) 18
Figure 20: The Shaft shape at 15000RPM 18
Figure 21: The shaft shape at 33000RPM 19
Figure 22: The stability map 19
Figure 23:The whirl speed map 20
Figure 24: Bode plot: sensor position 1 20
Figure 25: Bode plot: sensor position 2 21
Figure 26: The transmitted force [N] at bearing 1 (104.16 N) 22
Figure 27:The transmitted force [N] at bearing 2 (21.348 N) 22
Figure 28: The Shaft shape at 15000RPM 22
Figure 29: The Shaft shape at 33000RPM 23
Figure 30: The stability map 23
Figure 31:The whirl speed map 24

1 Background

This report deals with the layout of the FLY-UPS. The layout is determined by four factors namely:

- The energy storage capability of the flywheel
- The strength and type of material used
- The rotor-dynamic properties of the system
- The Thermal properties of the system

The layout that will be used is a centred flywheel (Figure 1)

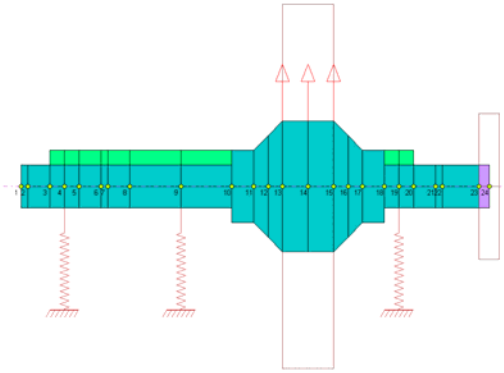

Figure 1: The centred flywheel layout

1.1 Energy Storage Capabilities

The energy storage capabilities were calculated using the formula for the energy stored in a rotating disc. (1)

$$E = J\omega^2 / 2 \qquad [\text{J}] \qquad (1)$$

with the required energy and the rotational speeds known a value can be calculated for the moment of inertia.
Using (2) calculate the minimum thickness required for a specific radius.

$$t = \frac{\pi\rho}{JR^4} \qquad [\text{m}] \qquad (2)$$

The maximum radius will be determined by the strength of the material used in the disc (3)

$$\sigma_{Yield} = \frac{(3+\nu)\rho(R\omega)^2}{8} \qquad \text{[Pa]} \qquad (3)$$

1.2 Determining the unbalance

Two standards were identified for determining the unbalance on the rotor for the rotordynamic analysis. Since the API standard 612 is more comprehensive, the API 612 will be used for the rotordynamic analysis.

1.2.1 ISO 1940/1 unbalance standard for Overhung and Narrow Rotors:

The ISO standard makes use of a "G" designation this indicates the level of balance that the rotor is balanced to. With a lower "G" indicating a better balanced rotor. See (4)

$$U_{Per} = \frac{(9.549)(GW)}{N} \qquad \text{[kg*mm]} \qquad (4)$$

W is the weight of the rotor

N is the maximum operating speed of the rotor

For overhung and narrow rotors the ISO 1940/1 standard is adjusted according to these parameters.

$$U_{Per,Static} = \left(\frac{U_{Per}}{2}\right)\left(\frac{d}{2c}\right) \qquad \text{[kg*mm]} \qquad (5)$$

$$U_{Per,Couple} = \left(\frac{U_{Per}}{2}\right)\left(\frac{3d}{4b}\right) \qquad \text{[kg*mm]} \qquad (6)$$

b is the axial length of the rotor, *c* is the distance between the centre of the rotor and the furthest bearing support, *d* is the distance between the bearings. The static and couple unbalance is applied as seen in Figure 2

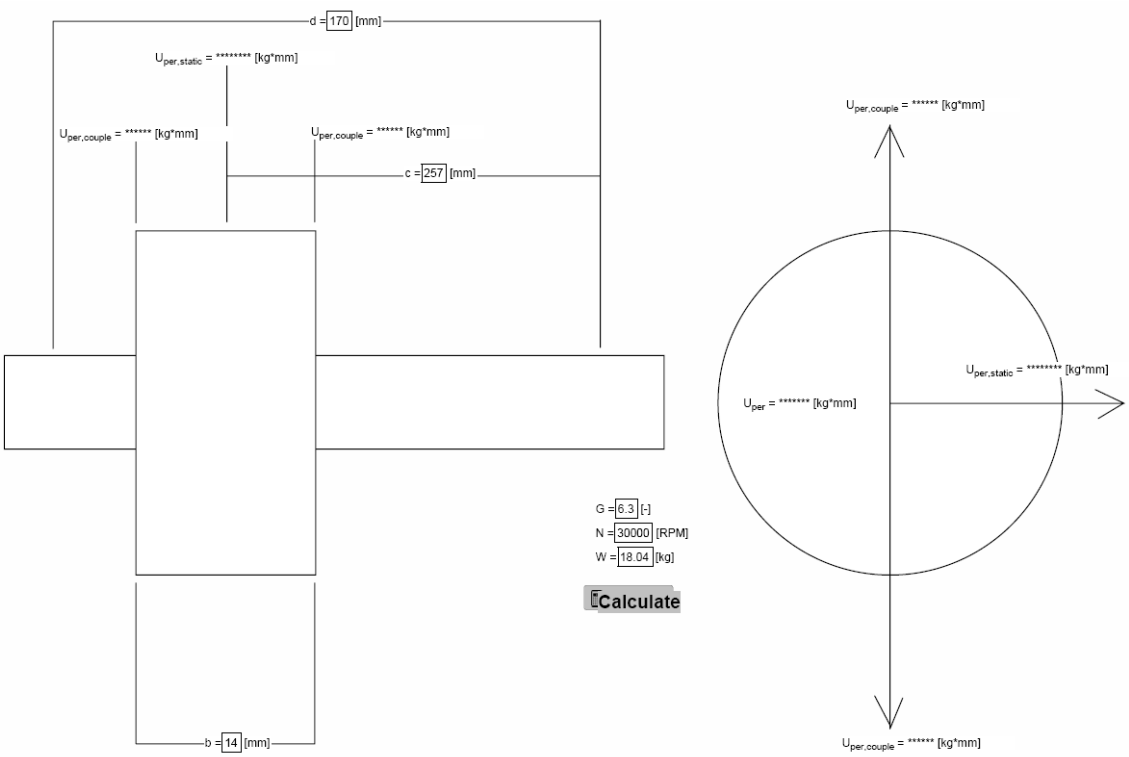

Figure 2: ISO standard balancing application for a centred rotor

1.2.2 API 612 Unbalance Standard:

A separate damped unbalanced response analysis shall be conducted for each critical speed within the range of 0%-125% of trip speed, in this case from 0RPM-41250RPM. Unbalance shall be placed at the locations that most adversely affect that particular mode. The first two modes are shown in Figure 3 and Figure 4.

$$U = (4)\frac{(6.35)(W)}{N} \qquad \text{[kg*mm]} \qquad (7)$$

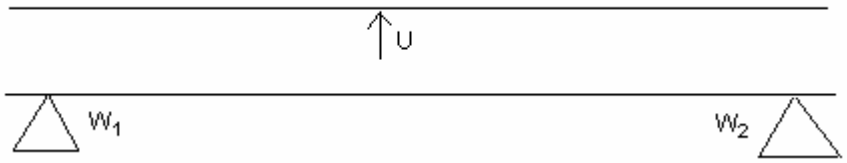

Figure 3: Translatory first rigid mode

For the Translatory first rigid mode use Eq (7) and apply at the node with the greatest displacement

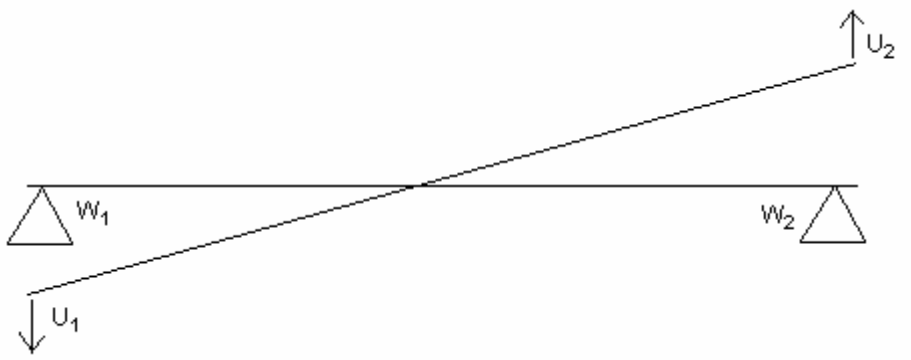

Figure 4: Conical, rocking second rigid mode

$$W_1 = \frac{L_{Right_{Com}}}{L_{Total}} \mathrm{W} \qquad \text{[kg]} \qquad (8)$$

$$W_2 = \frac{L_{Left_{Com}}}{L_{Total}} \mathrm{W} \qquad \text{[kg]} \qquad (9)$$

For the Conical, rocking second rigid mode use Eq 8 & 9 in conjunction with:

$$U_1 = 4\frac{(6.35)(W_1)}{N} \qquad \text{[kg*mm]} \qquad (10)$$

$$U_2 = 4\frac{(6.35)(W_2)}{N} \qquad \text{[kg*mm]} \qquad (11)$$

1.3 API 612 Rotordynamic Standard

According to the API standard the critical frequencies of a system has to be separated by a certain margin form the operating range of the system in order for the system to be considered critically damped.

Firstly determine 0.707 of the maximum amplitude and determine the corresponding rotational speeds ($N_{0.707,Lower}$ and $N_{0.707,Upper}$) see Figure 5 and Figure 6

Now determine the amplification factor (12)

$$F_A = \frac{N_{Critical}}{N_{0.707,Upper} - N_{0.707,Lower}} \qquad \text{[-]} \qquad (12)$$

If the amplification factor is less than 2.5, the response is considered critically damped and no separation margin is required and no further testing is required.

1.3.1 Operating Range Lower than Critical Frequency

If the amplification factor is 2.5 or greater and that particular critical speed is above the maximum continuous speed the separation margin (13) should be larger than M_s (14) or 26 whichever is less, see Figure 5.

$$SM = 100\left(\frac{N_{0.707,Lower} - N_{Maximum,Continuous}}{N_{Maximum,Continuous}}\right) \quad [-] \qquad (13)$$

$$M_s = 10 + 17\left(1 - \frac{1}{F_A - 1.5}\right) \quad [-] \qquad (14)$$

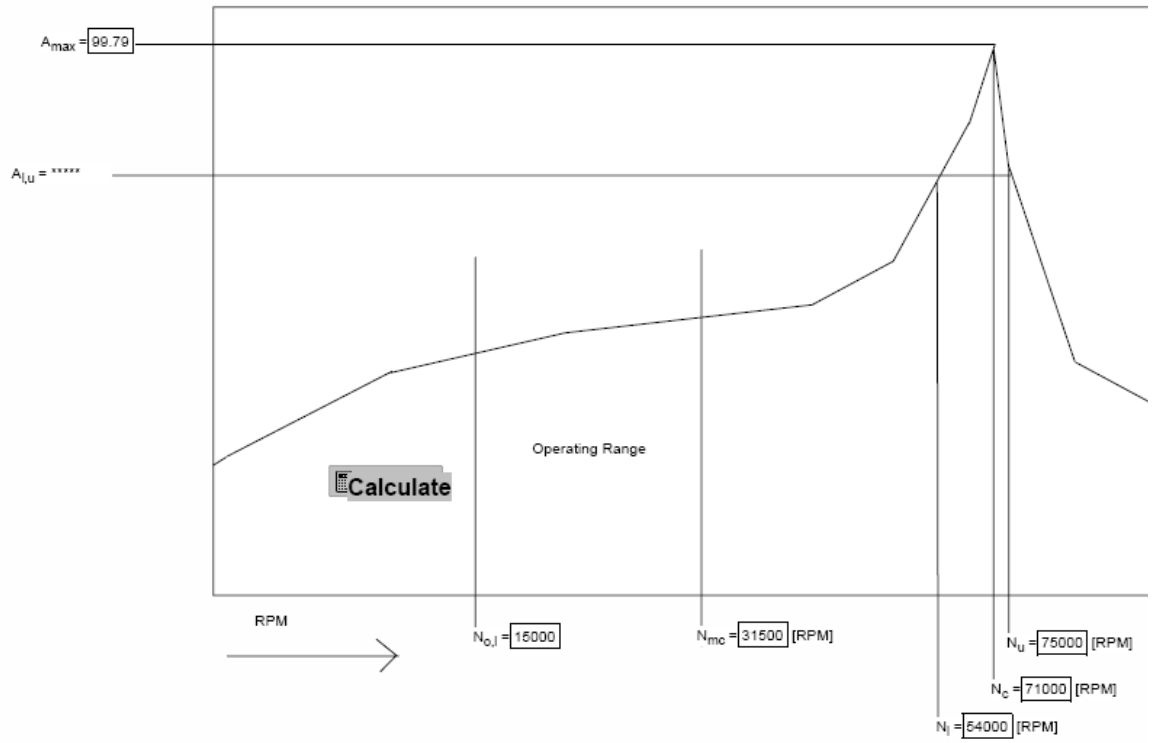

Figure 5: API standard for a operating range lower than the critical frequency

1.3.2 Operating Range Higher than Critical Frequency

If the amplification factor is 2.5 or greater and that particular critical speed is below the minimum continuous speed the separation margin (15) should be larger than M_s (16) or 16 whichever is less, see Figure 6.

$$SM = 100\left(\frac{N_{Minimum,Continuous} - N_{0.707,Upper}}{N_{Minimum,Continuous}}\right) \quad [-] \quad (15)$$

$$M_s = 17\left(1 - \frac{1}{F_A - 1.5}\right) \quad [-] \quad (16)$$

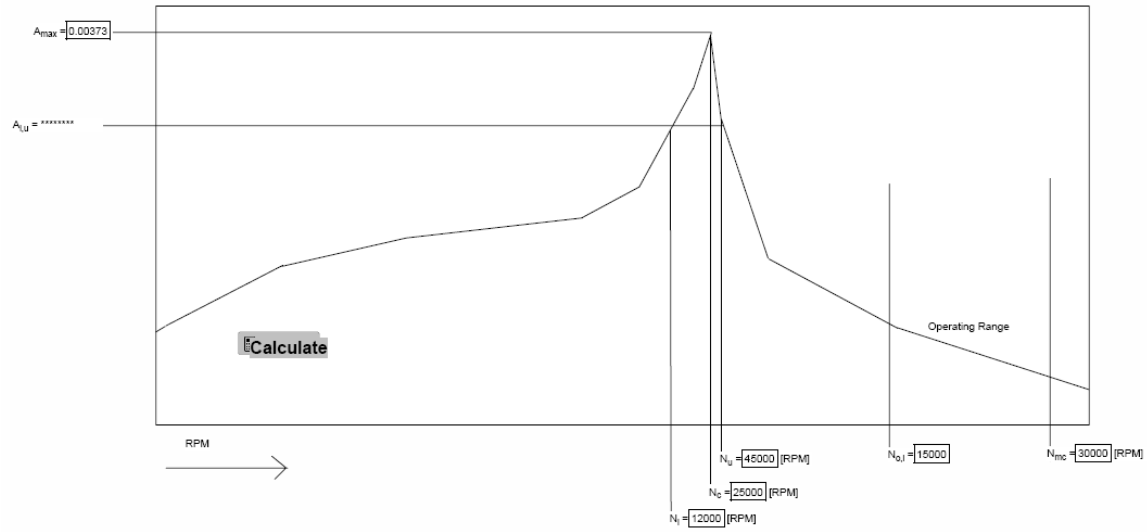

Figure 6: API standard for a operating range higher than the critical frequency

2 Design

2.1 Rotor Design Process

Figure 7: Rotor Design Process Diagram

2.2 Design Concept

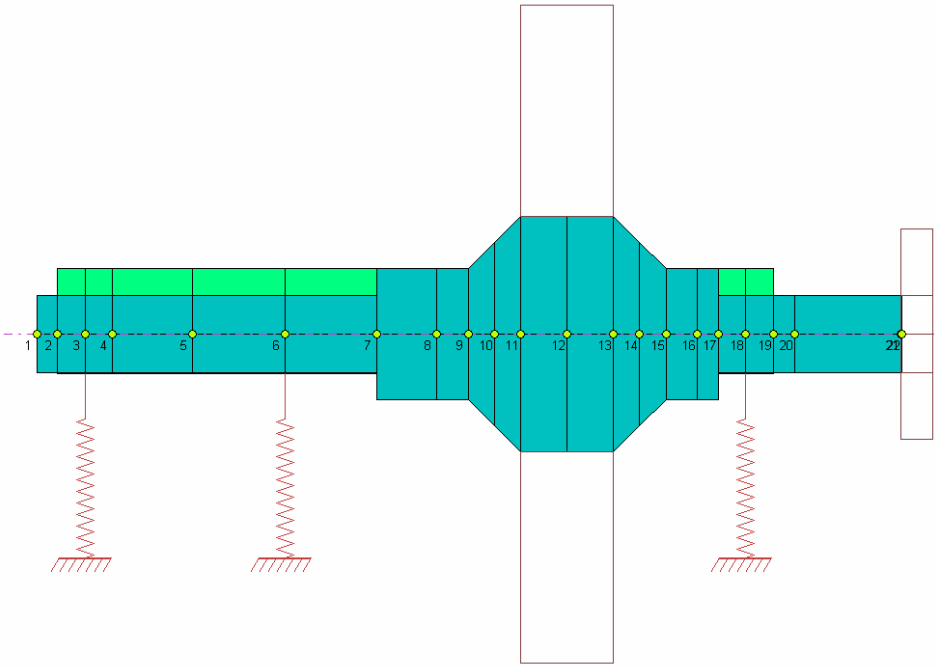

Figure 8: The model layout

2.2.1 Model Summary

Total Mass: 18.374 [kg]

Total Length: 327 [mm]

the geometry for the flywheel disc is:

$t = 35$

$R = 125$ [mm]

2.2.2 Strength Analysis Results

COSMOS works was used for the strength analysis. The minimum factor of safety on the rotor, for maximum operating speed (30 000RPM), is 1.49 as can be seen in Figure 9 and Figure 10. The figures also display the distribution of the factor of safety.

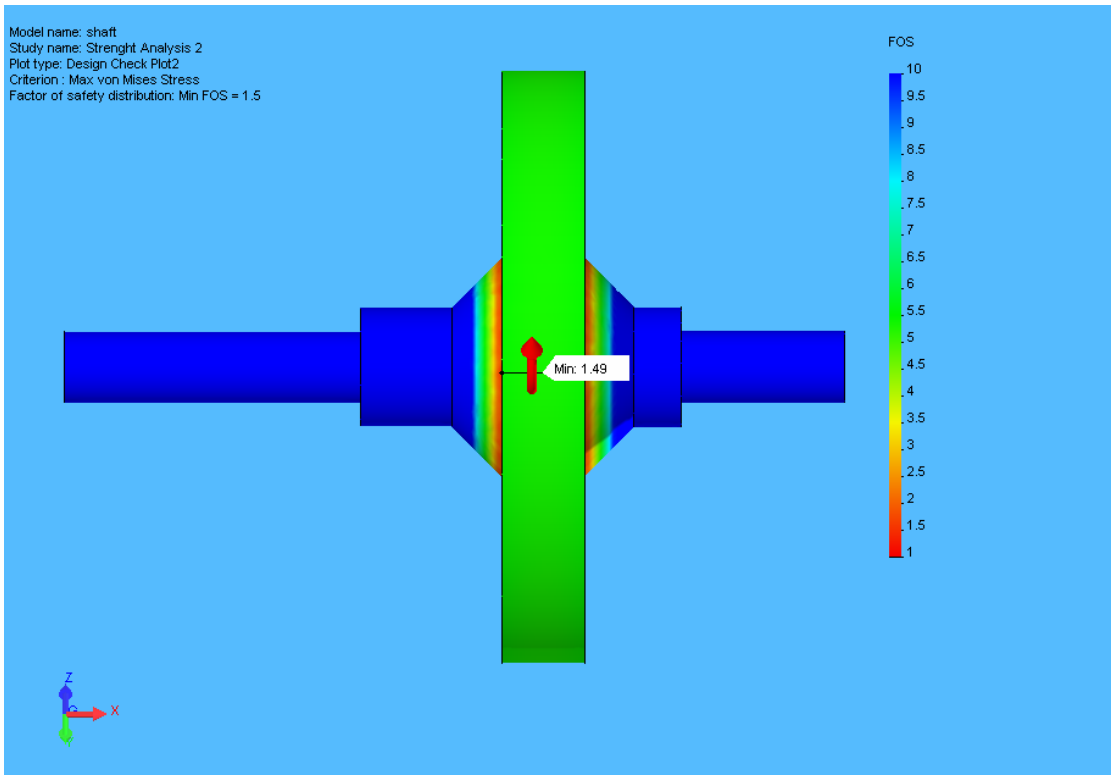

Figure 9: The Factor of Safety distribution 30 000RPM side view

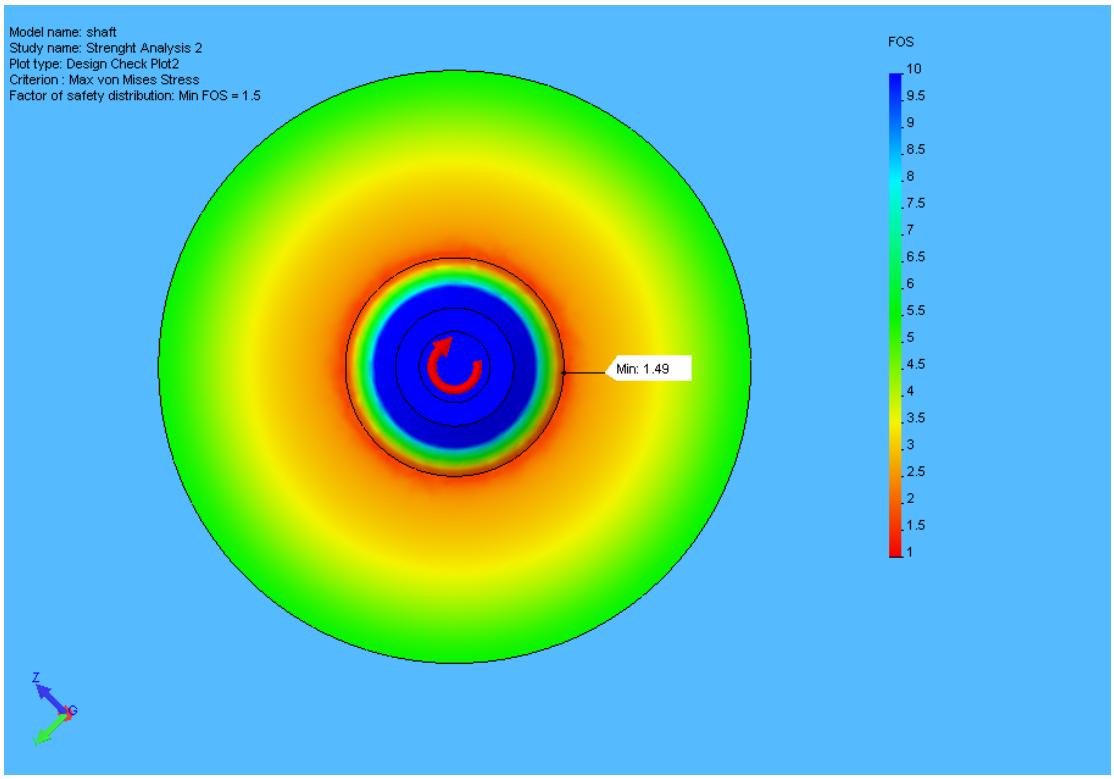

Figure 10: The Factor of Safety distribution 30 000RPM top view

The minimum factor of safety on the rotor, for trip speed (33 000RPM), is 1.23 as can be seen in Figure 11 and Figure 12

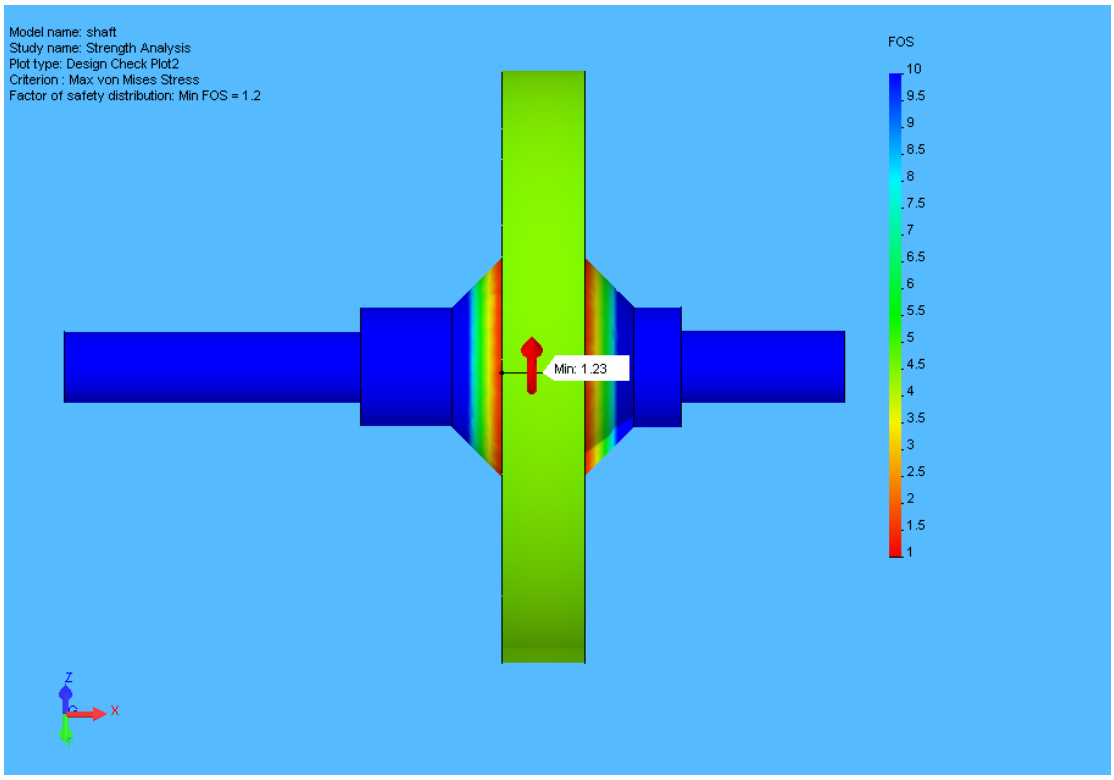

Figure 11: The Factor of Safety distribution 33 000RPM side view

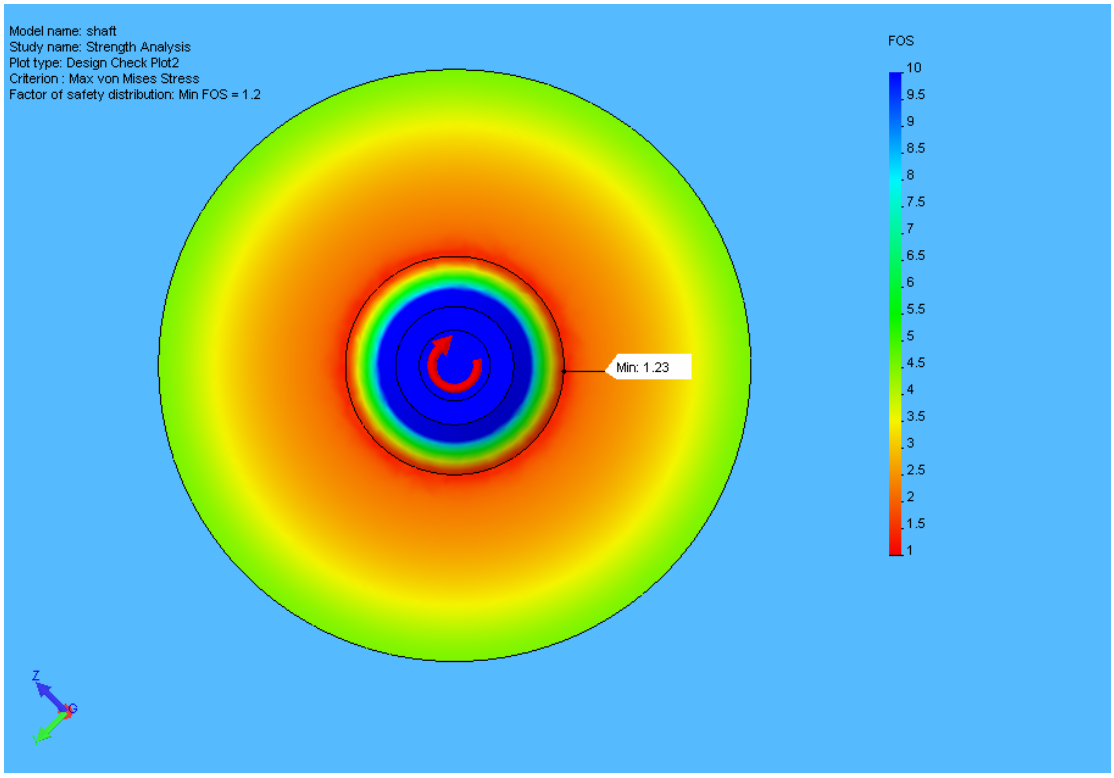

Figure 12: The Factor of Safety distribution 33 000RPM top view

2.2.3 Rotor-Dynamic Results

The Rotor-dynamic program, DyRoBeS was used to determine the Rotor-Dynamic properties of the system. To determine the unbalance acting upon the rotor the API standard for balancing rotors was used (see 1.2.2). Two separate rotordynamic analysis were done in accordance with the API standard. DyRoBeS was used to create a critical speed map, seen in Figure 13, this was used to determine the possible range of stiffnesses of the AMBs.

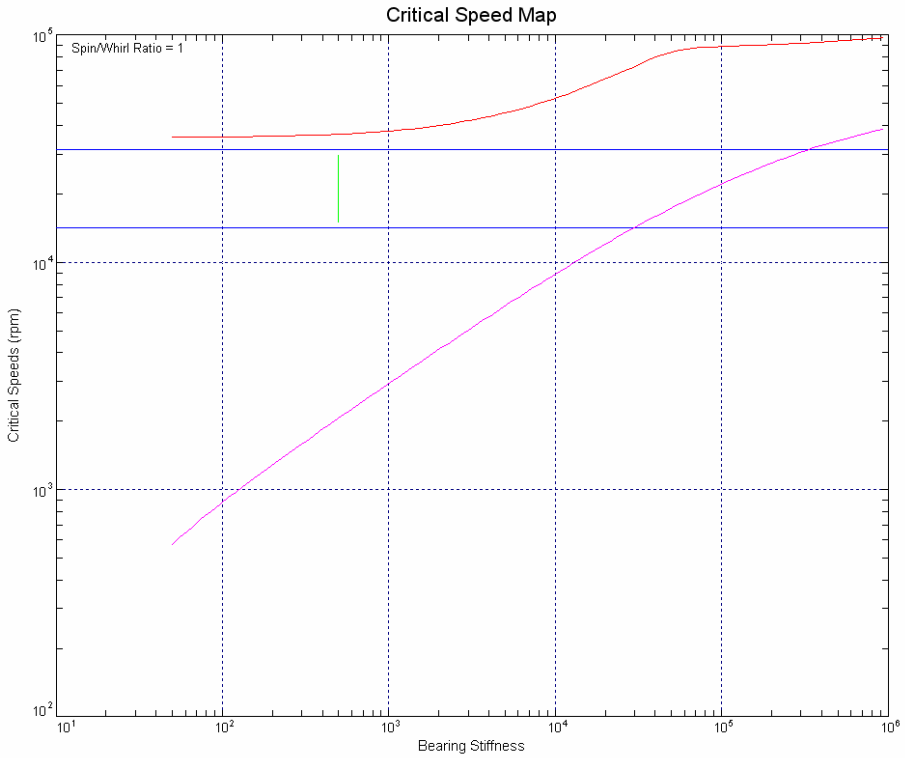

Figure 13: The critical speed map of the system

None of the critical frequencies (2064RPM, 36674RPM) fall within the operating range (15000-30000RPM) of the FLY-UPS as can be seen in Figure 14 and Figure 15

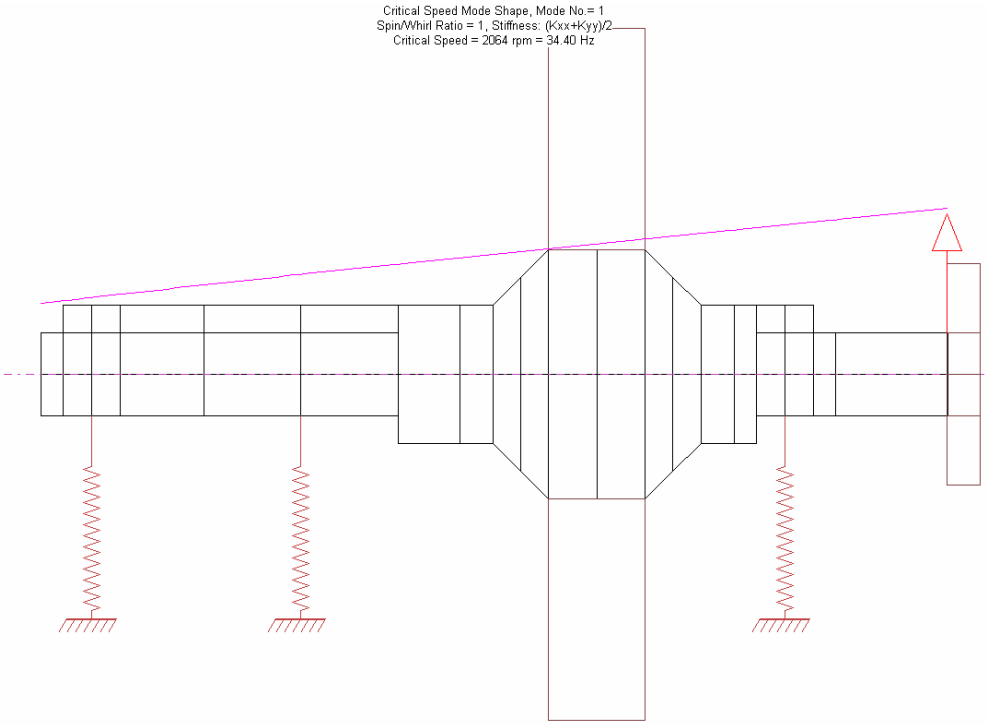

Figure 14: Mode shape 1 of the system (2 046 RPM)

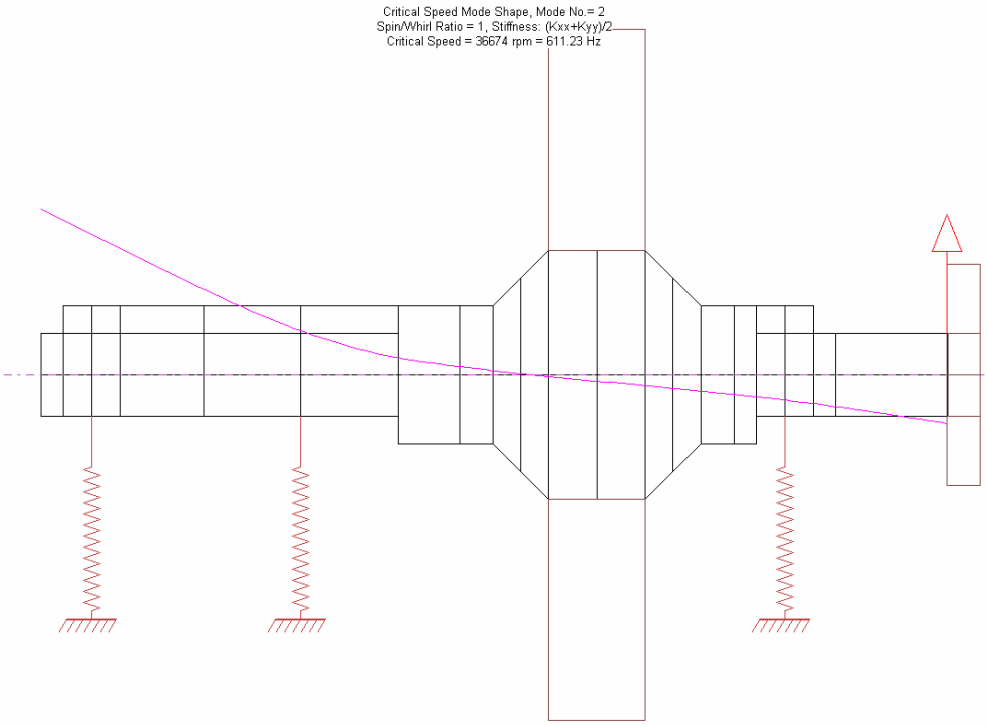

Figure 15: Mode shape 2 of the system (36 674 RPM)

2.2.3.1 Critical frequency 1

In Figure 16 and Figure 17 the displacements within the operating range of the FLY-UPS can be seen the displacements are measured in millimetres. The damped critical frequency of the FLY-UPS has shifted towards higher frequencies, the first 2 critical frequencies are sufficiently damped, thus no separation margin is required.

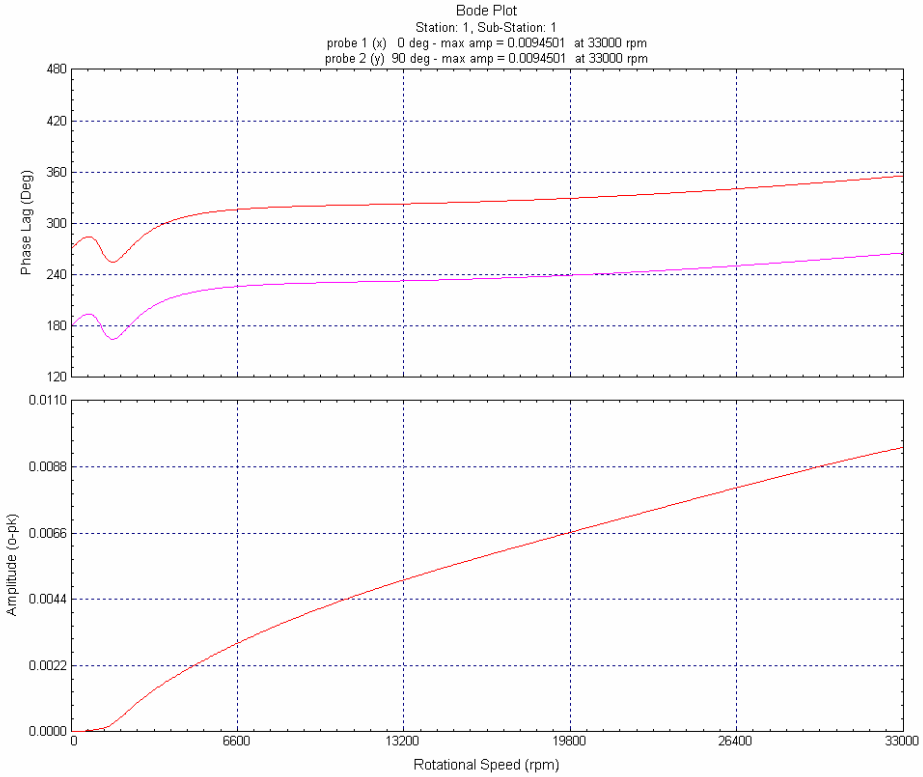

Figure 16: Bode plot: sensor position 1

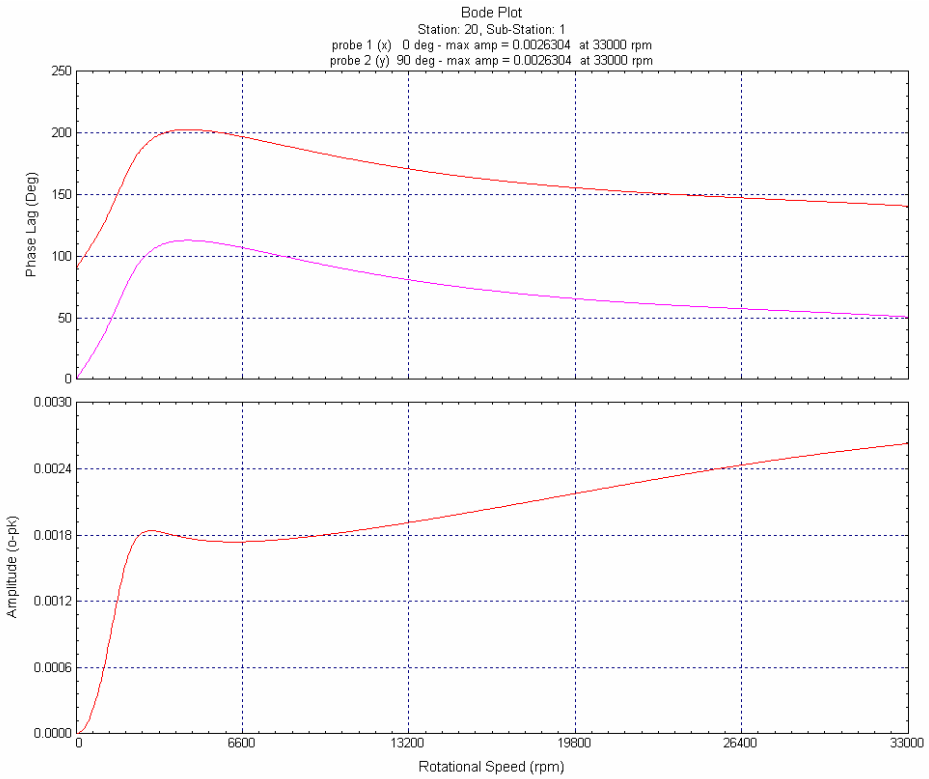

Figure 17: Bode plot: sensor position 2

In Figure 18 and Figure 19 the maximum force acting upon the bearings can be seen thus the AMBs will be designed according to these parameters.

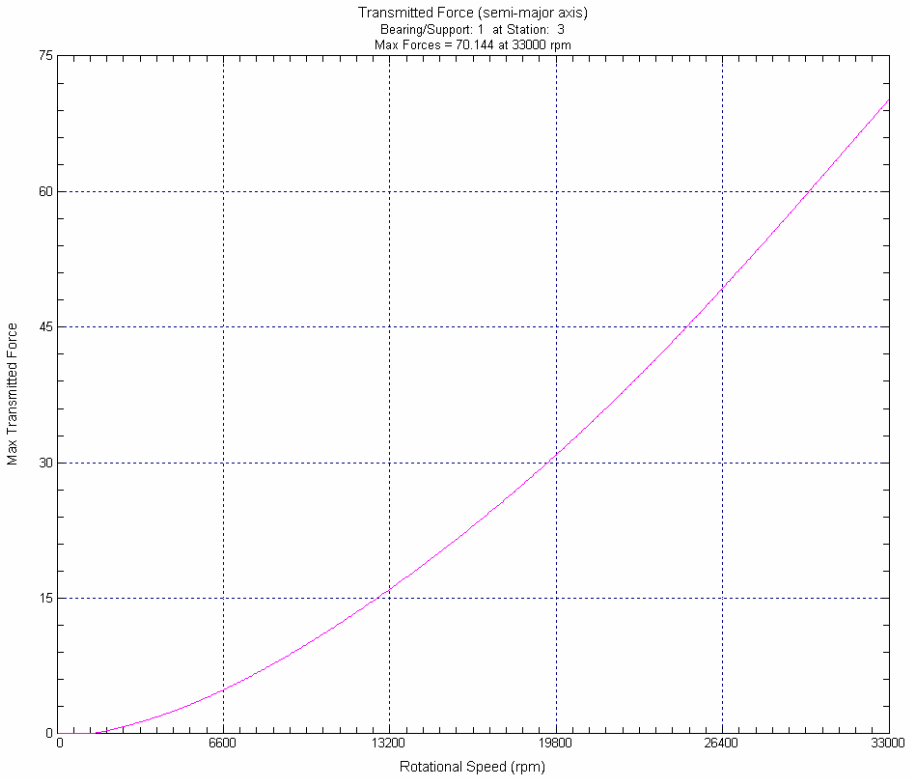

Figure 18: The transmitted force [N] at bearing 1 (70.144 N)

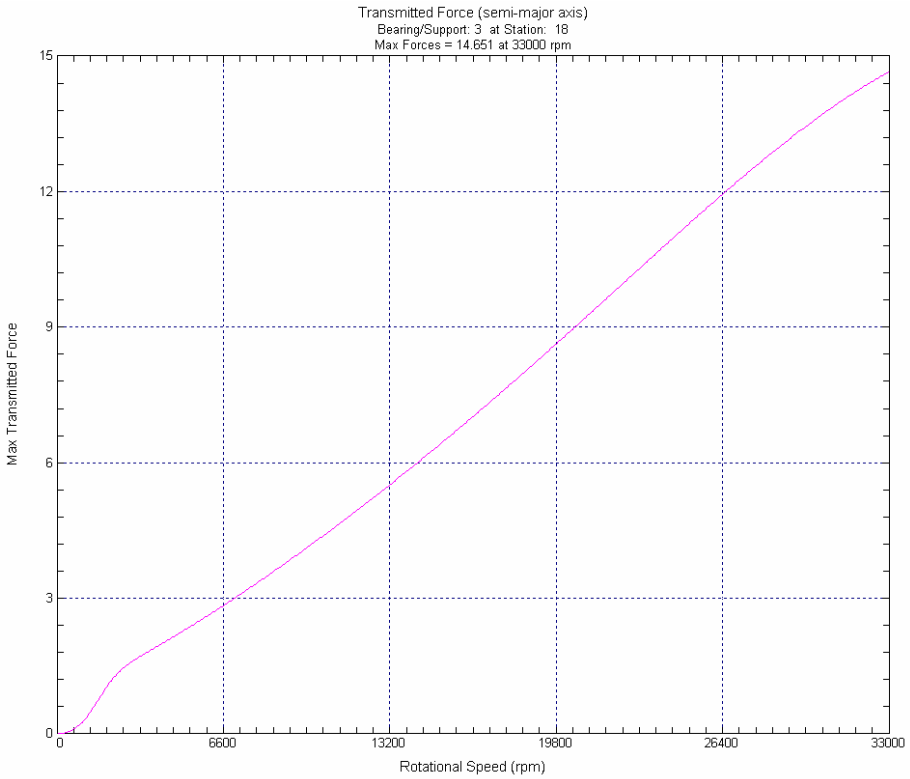

Figure 19: The transmitted force [N] at bearing 2 (14.651 N)

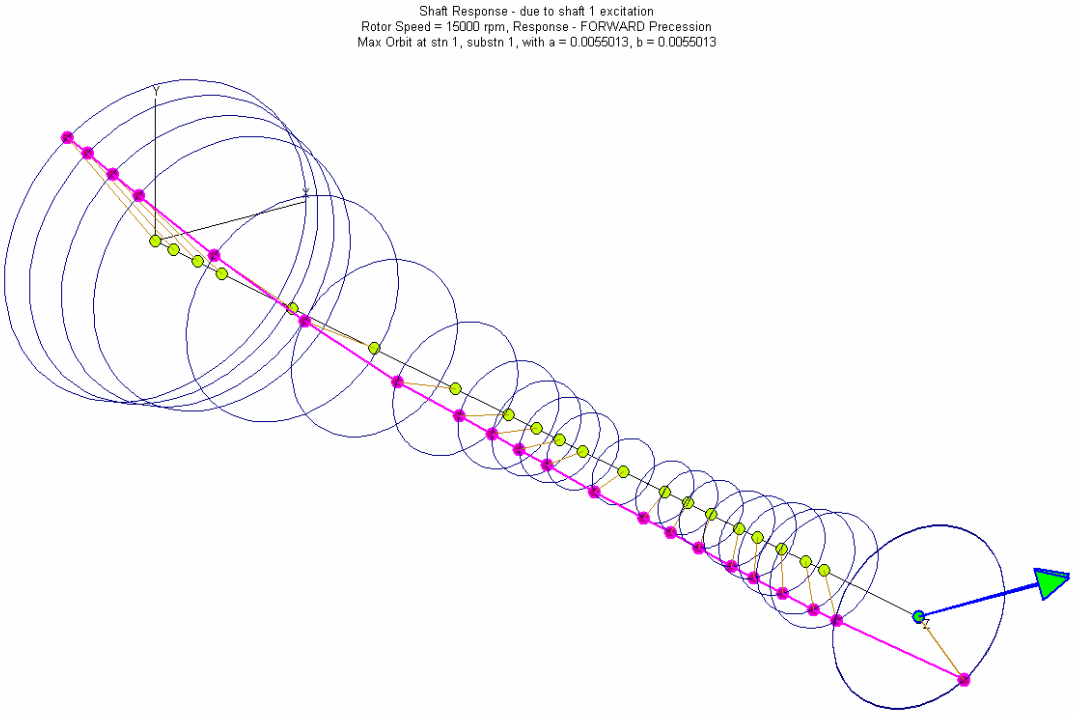

Figure 20: The Shaft shape at 15000RPM

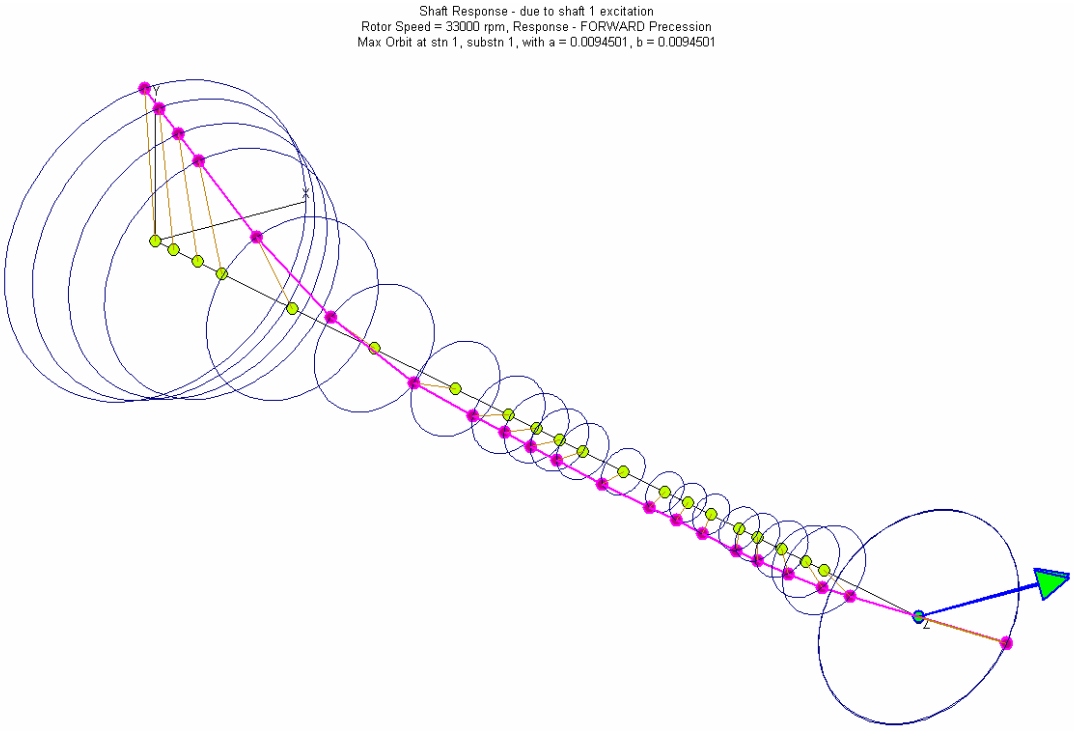

Figure 21: The shaft shape at 33000RPM

Figure 22 displays the stability map for the first three forward and backward modes, because the value of the log decrements never drop below nil the system can be considered stable from starting speed up to maximum operating speed.

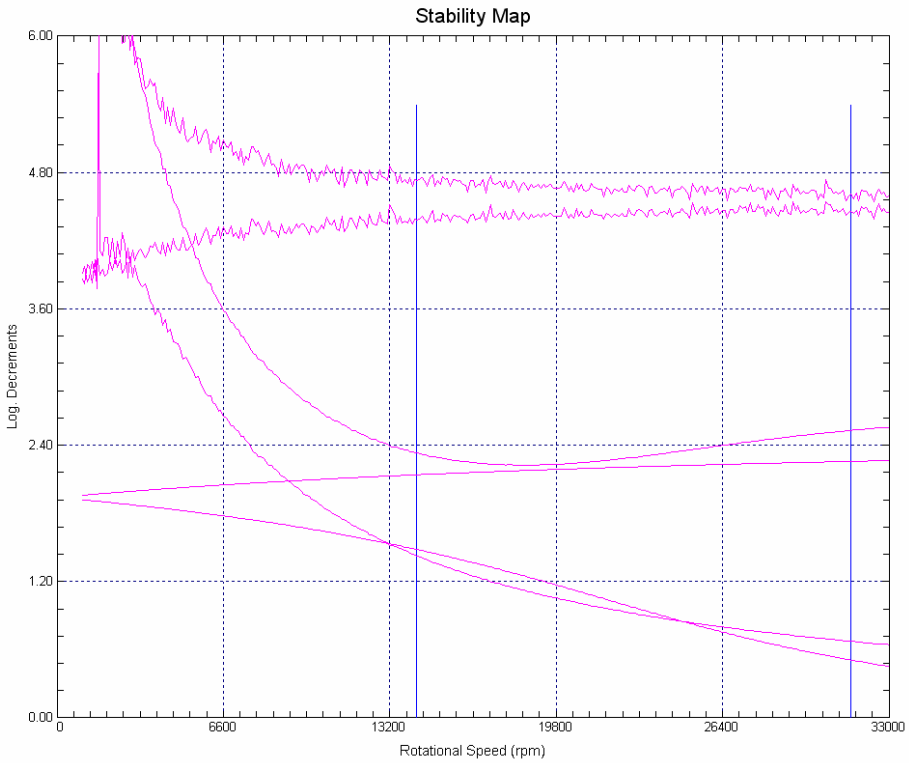

Figure 22: The stability map

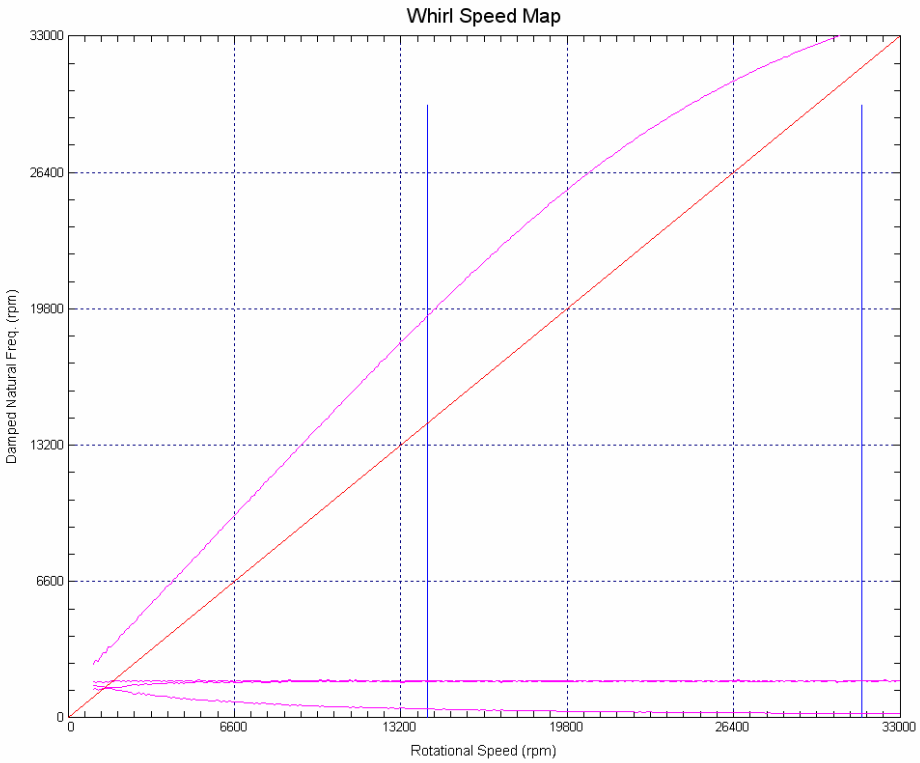

Figure 23:The whirl speed map

2.2.3.2 Critical frequency 2

In Figure 24 and Figure 25the displacements within the operating range of the FLY-UPS can be seen the displacements are measured in [mm]

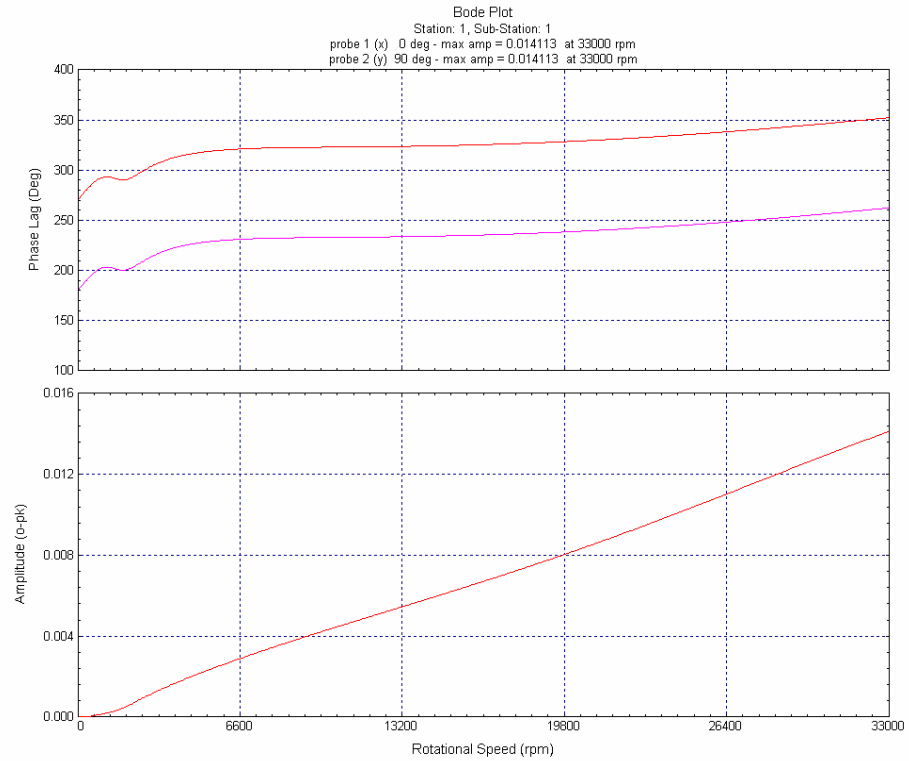

Figure 24: Bode plot: sensor position 1

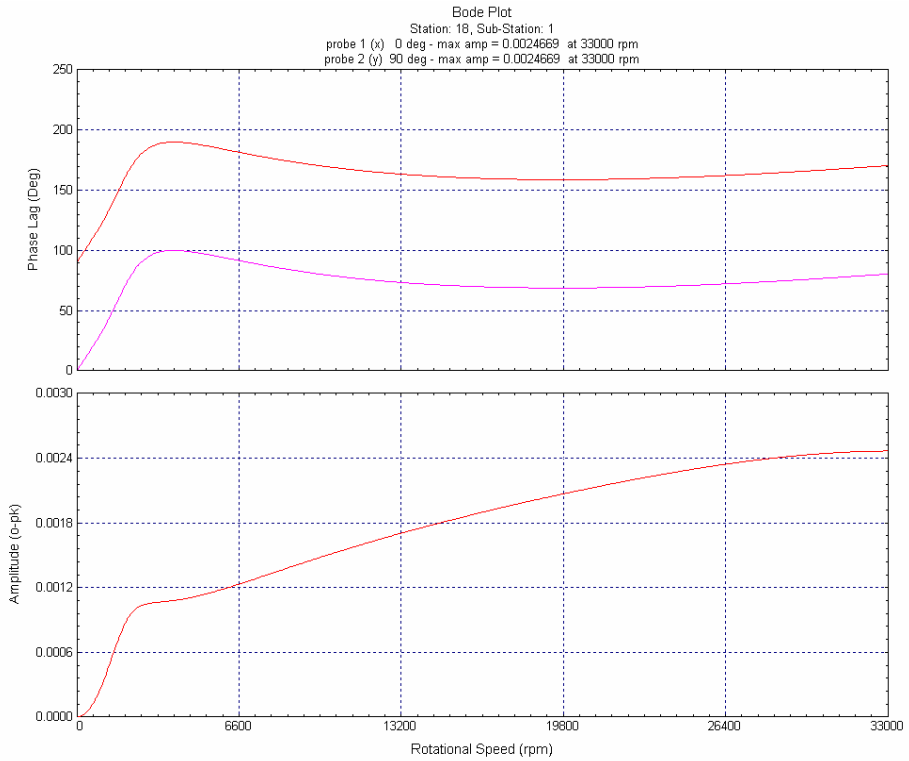

Figure 25: Bode plot: sensor position 2

In Figure 26 and Figure 27 the maximum force acting upon the bearings can be seen thus the AMBs will be designed according to these parameters. Figure 26 displays the highest transmitted force thus all of the bearings will be designed according to this specification (Max force: 104.16 N AMB Designed for: 200N)

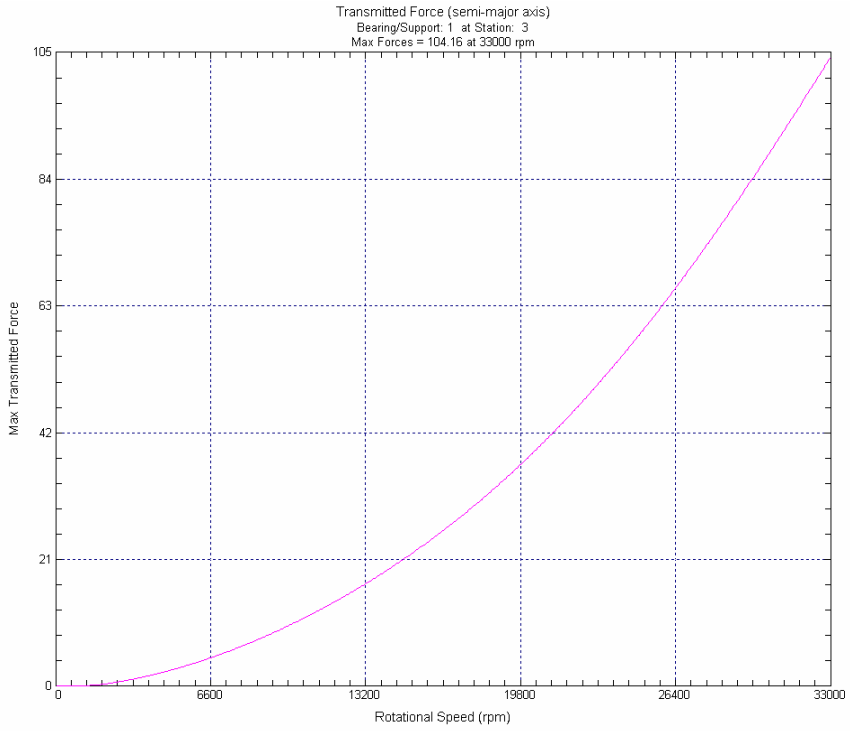

Figure 26: The transmitted force [N] at bearing 1 (104.16 N)

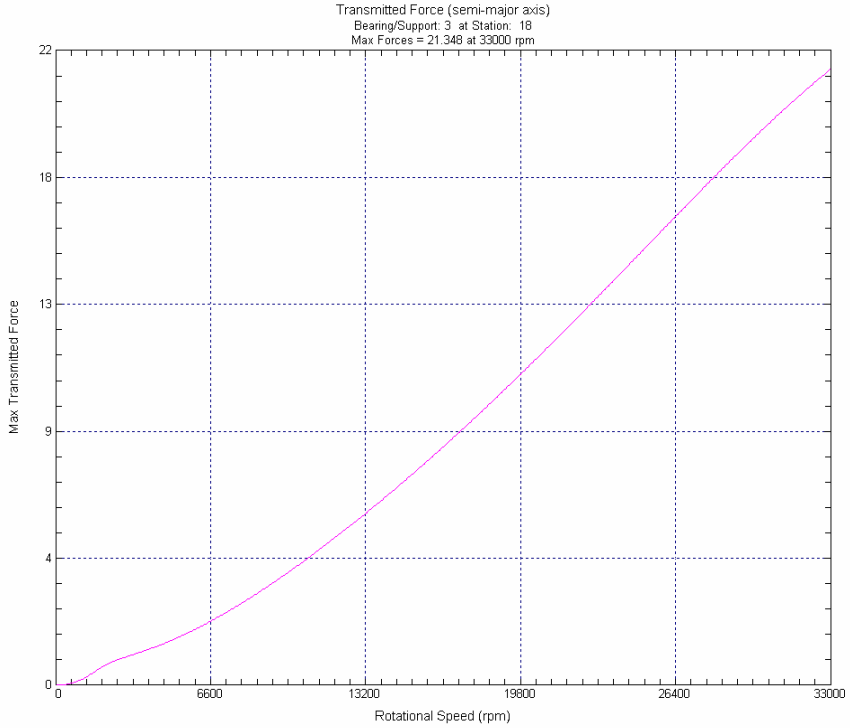

Figure 27:The transmitted force [N] at bearing 2 (21.348 N)

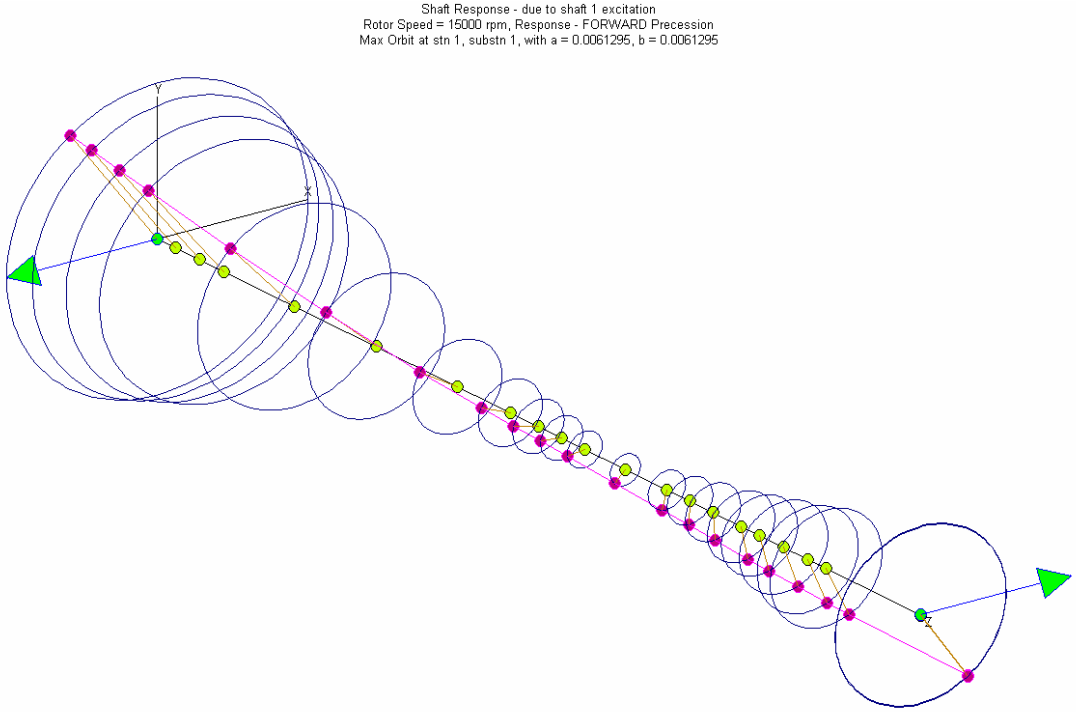

Figure 28: The Shaft shape at 15000RPM

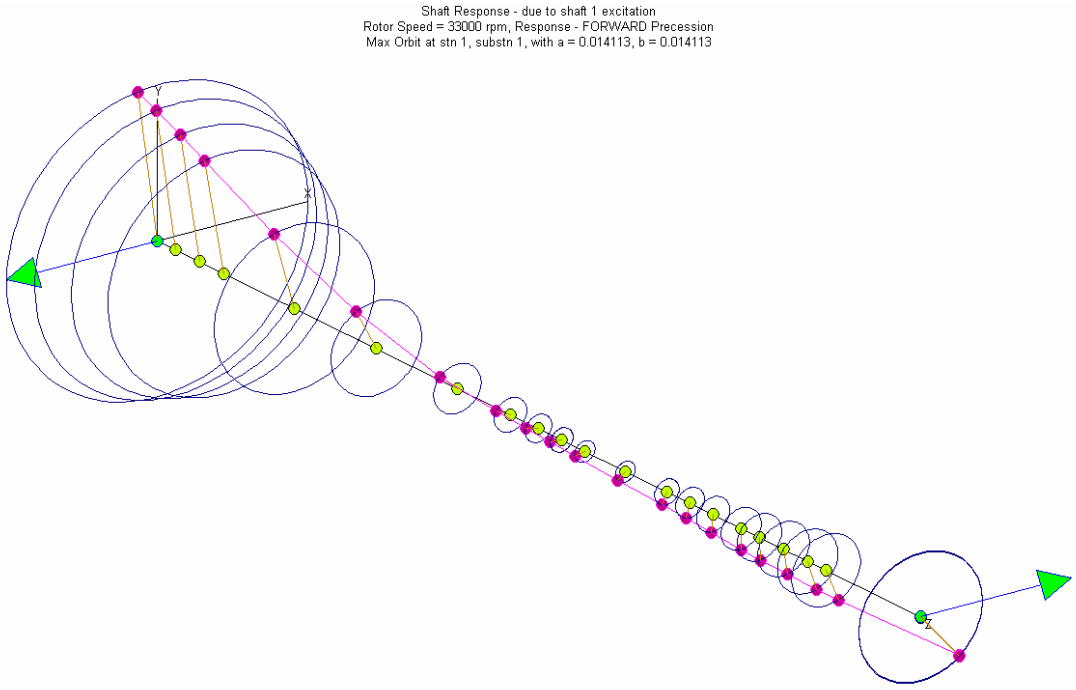

Figure 29: The Shaft shape at 33000RPM

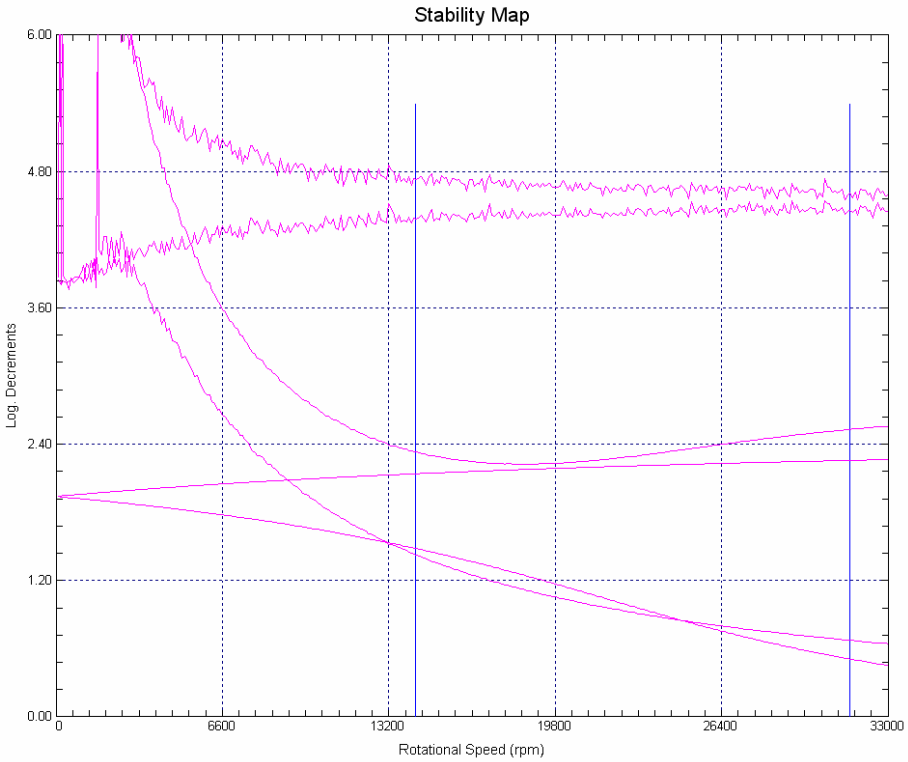

Figure 30: The stability map

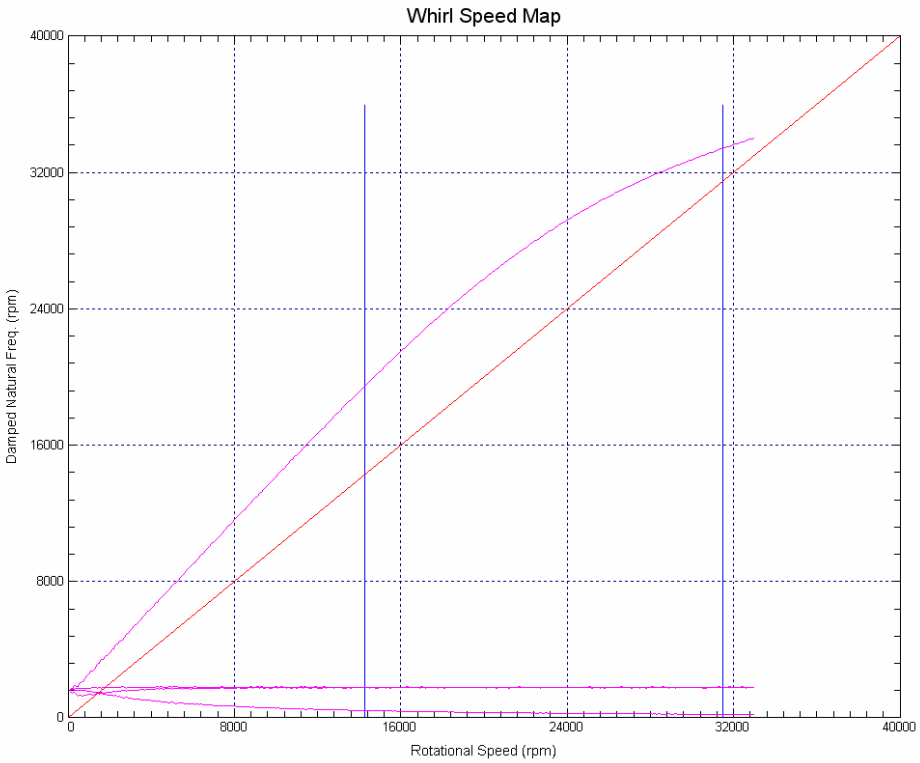

Figure 31:The whirl speed map

2.2.3.3 Axial natural frequency

The axial natural frequency is determined by using Eq (17) and (18)

$$\omega = \sqrt{\frac{K_{eq}}{M_{Total}}} \quad \text{[rad/s]} \quad (17)$$

$$f = \frac{\omega}{2\pi} \quad \text{[Hz]} \quad (18)$$

Using:

$M_{Total} = 18.374$ [kg]

$K_{eq} = 500000$ [N/m]

Yields:

$\omega = 165$ [rad/s]

$f = 26.25$ [Hz]

3 Summary of results

Table 1: Summary of results

	Critical frequency 1	Units	Critical frequency 2
Length	327	[mm]	-
Weight	18.374	[kg]	-
Minimum Factor of Safety @ 30 000RPM	1.49	[-]	-
Minimum Factor of Safety @ 33 000RPM	1.23	[-]	-
Mode Shape 1 (RPM)	2046	[RPM]	-
Mode Shape 2 (RPM)	36674	[RPM]	-
Maximum Displacement @ sensor 1	0.0094501	[mm]	0.014113
Maximum Displacement @ sensor 2	0.0026304	[mm]	0.0024669
Maximum Transmitted Force on bearing 1 (33000RPM)	70.144	[N]	104.16
Maximum Transmitted Force on bearing 2 (33000RPM)	14.651	[N]	21.348
Axial Natural Frequency	26.25	[Hz]	-

4 Conclusion

The factor of safety on the strength analysis is sufficient. This Design for the FLY-UPS rotor is rotor dynamically sound. All of the critical frequencies within 0%-125% of trip speed are damped so that no separation margin is required. Taking these results into account this design is approved.

D.2 PMSM specification

Permanente Magneet Masjien Ontwerp Spesifikasies

(3 Augustus 2006)

1 Permanente Magneet Masjien 2
1.1 WERKVERRIGTING 2
1.2 FISIESE KARAKTERISTIEKE 2
1.3 OMGEWINGSTOESTANDE 2
1.4 Materiale (Sien bylae vir data velle) 2
1.5 Sketse 3
2 Bylaag 1 (17-4PH datavel) 5
3 Bylaag 2 (Laminasie datavel) 7

1 Permanente Magneet Masjien

1.1 WERKVERRIGTING

Minimum Drywing van PMSM by 15000 RPM:	2000	W
Bedryf omwenteling snelheid	30000	RPM
Maksimum omwenteling snelheid	35000	RPM

1.2 FISIESE KARAKTERISTIEKE

Maksimum PMM Stator Buite Diameter	250	mm
Maksimum PMM Aksiale lengte	115	mm
Vliegwiel Buite Diameter	250	mm
As Diameter	30	mm
As lengte	400	mm
Laminasie Buite Diameter	50	mm

1.3 OMGEWINGSTOESTANDE

Maksimum temperatuur:	80,0	`C
Minimum temperatuur:	-5	`C
Maksimum relatiewe humiditeit:	95	%
Minimum relatiewe humiditeit:	5,0	%
Maksimum Absolute druk binne omhulsel	50	kPa

1.4 Materiale (Sien bylae vir data velle)

As:	17-4PH	Nie-magneties
Laminasies (sien skets):	M270-35A	Magneties
Huls:	Aluminium	Nie-magneties

1.5 Sketse

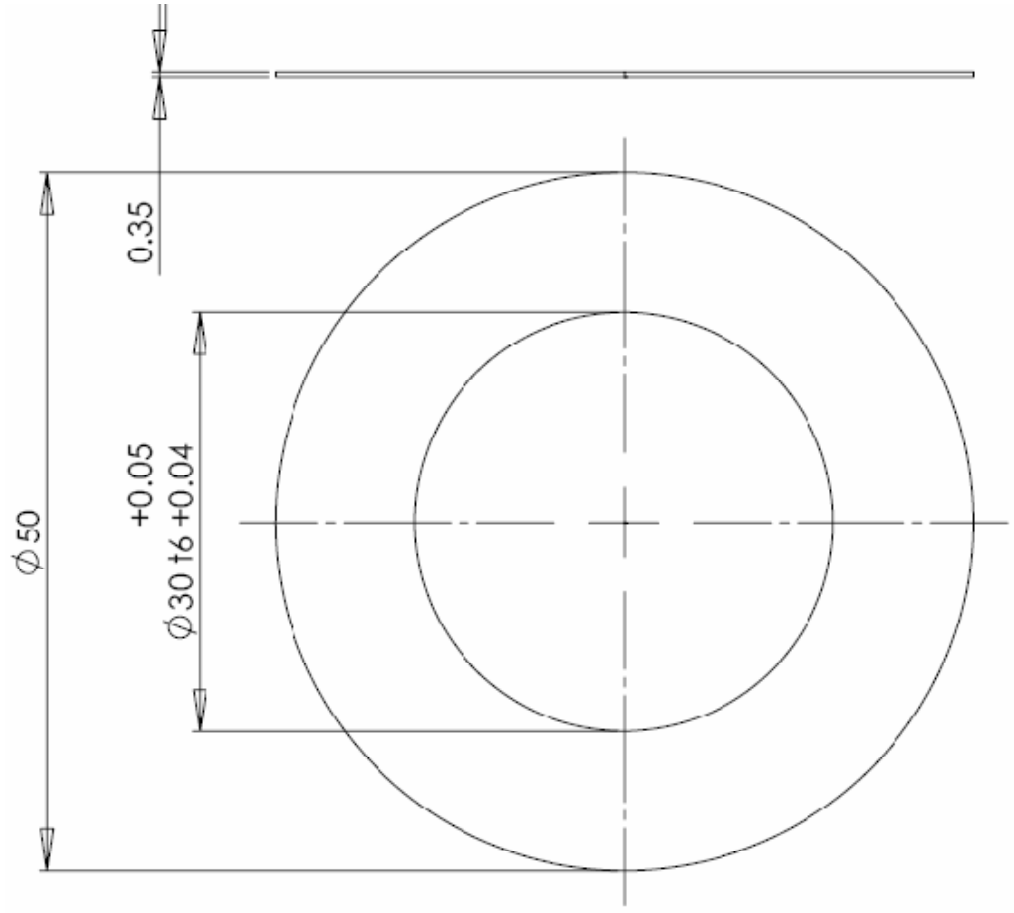

Laminasie

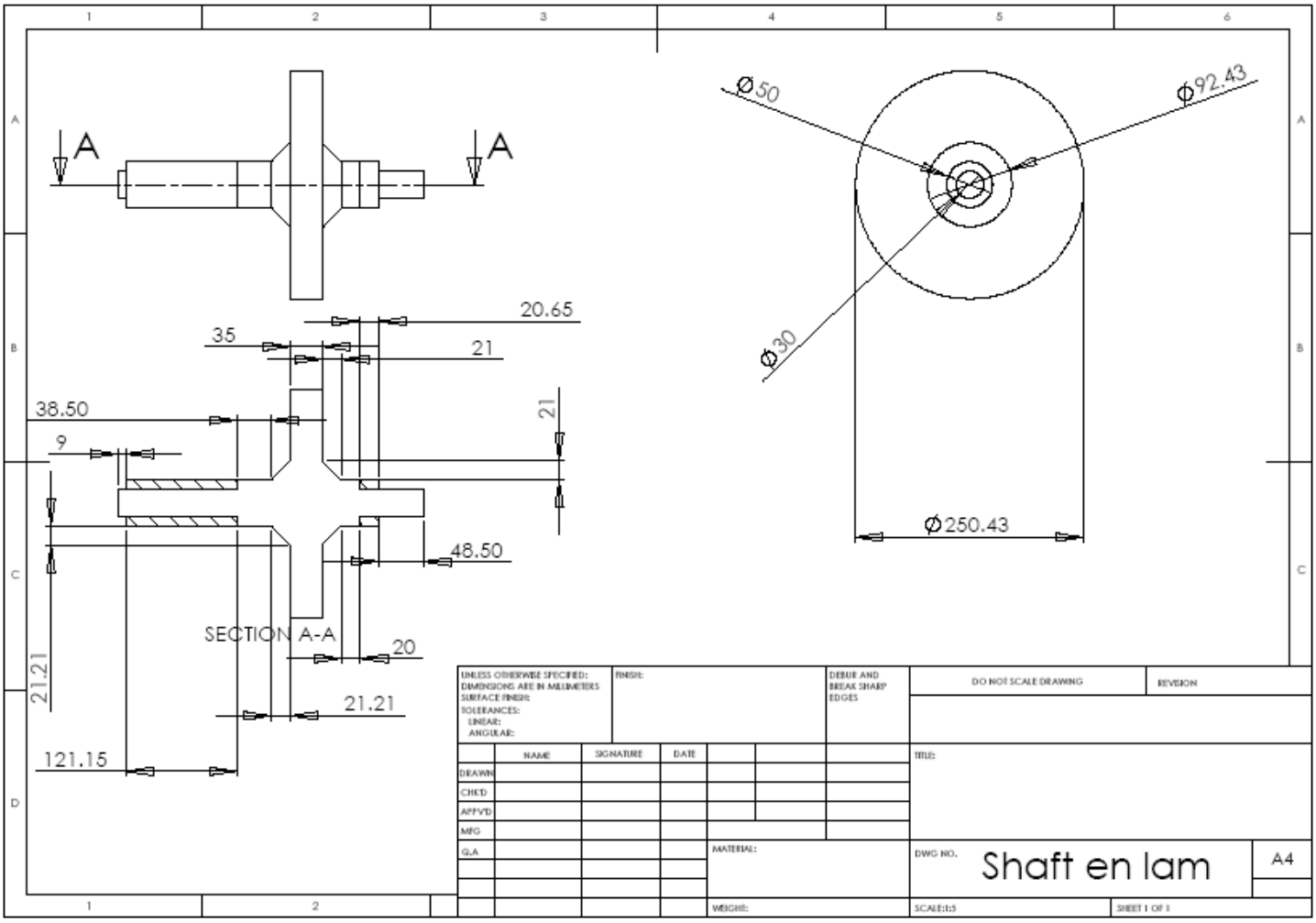

UNLESS OTHERWISE SPECIFIED: DIMENSIONS ARE IN MILLIMETERS SURFACE FINISH: TOLERANCES: LINEAR: ANGULAR:		FINISH:		DEBUR AND BREAK SHARP EDGES	DO NOT SCALE DRAWING	REVISION
	NAME	SIGNATURE	DATE		TITLE:	
DRAWN						
CHK'D						
APP'VD						
MFG						
Q.A				MATERIAL:	DWG NO. Shaft en lam	A4
				WEIGHT:	SCALE:1:5	SHEET 1 OF 1

2 Bylaag 1 (17-4PH datavel)

AK Steel

AK Steel 17-4 PH® is a martensitic precipitation-hardening stainless steel that provides an outstanding combination of high strength, good corrosion resistance, good mechanical properties at temperatures up to 600°F (316°C), good toughness in both base metal and welds, and short-time, low-temperature heat treatments that minimize warpage and scaling. This versatile material is widely used in the aerospace, chemical, petrochemical, food processing, paper and general metalworking industries.

COMPOSITION

	%
Carbon	0.07 max.
Manganese	1.00 max.
Phosphorus	0.040 max.
Sulfur	0.030 max.
Silicon	1.00 max.
Chromium	15.00 - 17.50
Nickel	3.00 - 5.00
Copper	3.00 - 5.00
Columbium plus Tantalum	0.15 - 0.45

AVAILABLE FORMS

AK Steel produces 17-4 PH Stainless Steel sheet and strip in thicknesses from 0.015" to 0.125" (0.38 to 3.18 mm) in Condition A.

STANDARD HEAT TREATMENTS

As supplied from the mill in Condition A, AK Steel 17-4 PH Stainless Steel can be heat treated at a variety of temperatures to develop a wide range of properties. Eight standard heat treatments have been developed.

	Condition	Heat To ± 15°F (8.4°C)	Time at Temperature, hour	Type of Cooling
Condition A Solution Treated 1900°F ± 25°F (1038°C ± 14°C) Air cool below 90°F (32°C)	H 900	900°F (482°C)	1	Air
	H 925	925°F (496°C)	4	Air
	H 1025	1025°F (551°C)	4	Air
	H 1075	1075°F (580°C)	4	Air
	H 1100	1100°F (593°C)	4	Air
	H 1150	1150°F (621°C)	4	Air
	H 1150+1150	1150°F (621°C)	4	Air
			followed by	
		1150°F (621°C)	4	Air
	H 1150-M	1400°F (760°C)	2	Air
			followed by	
		1150°F (621°C)	4	Air

FORMABILITY

Because this alloy in Condition A is hard, forming normally should be limited to mild operations. However, formability can be greatly improved by heat treating before cold working or by use of hot-forming methods.

CORROSION RESISTANCE

AK Steel 17-4 PH Stainless Steel withstands corrosive attack better than any of the standard hardenable stainless steels and is comparable to Type 304 in most media.

MECHANICAL PROPERTIES

Typical Mechanical Properties*

Property	Condition A	H 900	H 925	H 1025	H 1075	H 1150	H 1150-M
UTS, ksi (MPa)	160 (1103)	210 (1448)	200 (1379)	185 (1276)	175 (1207)	160 (1103)	150 (1034)
0.2% YS, ksi (MPa)	145 (1000)	200 (1379)	195 (1345)	170 (1172)	165 (1148)	150 (1034)	130 (896)
Elongation, % in 2" (50.8 mm)	5.0	7.0	8.0	8.0	8.0	11.0	12.0
Hardness, Rockwell	C35	C45	C43	C38	C37	C35	C33

*Cold-flattened sheets and strip.

PHYSICAL PROPERTIES

	Condition A (Magnetic)	Condition H 900 (Magnetic)	Condition H 1075 (Magnetic)	Condition H 1150 (Magnetic)
Density, lbs/in³ (g/cm³)	0.28 (7.78)	0.282 (7.80)	0.283 (7.81)	0.284 (7.82)
Electrical Resistivity, microhm-cm	98	77	–	–
Specific Heat BTU/lb/°F (32 - 212°F) kJ/kg•K (0 - 100°C)	0.11 (0.46)	0.11 (0.46)		
Thermal Conductivity BTU/hr/ft²/in/°F (W/m•K)				
300°F (149°C)		124 (17.9)		
500°F (260°C)		135 (19.5)		
900°F (482°C)		157 (22.6)		
Mean Coefficient of Thermal Expansion in/in/°F (µm/m•K)				
–100 - 70°F (-73 - 21°C)	–	5.8 x 10^{-6} (10.4)	–	6.1 x 10^{-6} (11.0)
70 - 200°F (21 - 93°C)	6.0 x 10^{-6} (10.8)	6.0 x 10^{-6} (10.8)	6.3 x 10^{-6} (11.3)	6.6 x 10^{-6} (11.9)
70 - 600°F (21 - 316°C)	6.2 x 10^{-6} (11.2)	6.3 x 10^{-6} (11.3)	6.6 x 10^{-6} (11.9)	7.1 x 10^{-6} (12.8)
70 - 800°F (21 - 427°C)	6.3 x 10^{-6} (11.3)	6.5 x 10^{-6} (11.7)	6.8 x 10^{-6} (12.2)	7.2 x 10^{-6} (13.0)

WELDABILITY

The precipitation hardening class of stainless steels is generally considered to be weldable by the common fusion and resistance techniques. Special consideration is required to achieve optimum mechanical properties by considering the best heat-treated conditions in which to weld and which heat treatments should follow welding. This particular alloy is the most common member of the class and is generally considered to have the best weldability. When a weld filler is needed, AWS E/ER 630 is most often specified. AK Steel 17-4 PH Stainless Steel is well known in reference literature and more information can be obtained in this way.

SPECIFICATIONS

Specifications are listed without revision indications. Contact ASTM Headquarters for latest ASTM revision. For AMS revision, contact AMS Division of SAE.

AMS 5604 Sheet, Strip and Plate

ASTM A 693 Plate, Sheet and Strip (Listed as Grade 630-UNS S17400)

METRIC CONVERSION

Data in this publication are presented in U.S. customary units. Approximate metric equivalents may be obtained by performing the following calculations:

Length (inches to millimeters) – Multiply by 25.4

Strength (ksi to megapascals or meganewtons per square meter) – Multiply by 6.8948

Temperature (Fahrenheit to Celsius) – (°Fahrenheit - 32) – Multiply by 0.5556

Density (pounds per cubic inch to kilograms per cubic meter) – Multiply by 27,670

The information and data in this product data sheet are accurate to the best of our knowledge and belief, but are intended for general information only. Applications suggested for the materials are described only to help readers make their own evaluations and decisions, and are neither guarantees nor to be construed as express or implied warranties of suitability for these or other applications.

Data referring to mechanical properties and chemical analyses are the result of tests performed on specimens obtained from specific locations with prescribed sampling procedures; any warranty thereof is limited to the values obtained at such locations and by such procedures. There is no warranty with respect to values of the materials at other locations.

AK Steel and the AK Steel logo, 17-4 PH, 17-7 PH and PH 15-7 Mo are registered trademarks of AK Steel Corporation.

SPECIALTY AND STAINLESS STEEL FIELD SALES OFFICES

AK Steel Corporation
703 Curtis Street
Middletown, OH 45043-0001
Customer Service 800-331-5050

Butler Works
P.O. Box 1609
Butler, PA 16003-1609
Customer Service 800-381-5663

Coshocton Works
17400 State Route 16
Coshocton, OH 43812
Customer Service 800-422-4422

AK Steel Sales Offices
Atlanta, GA-Southeast Region 770-514-0023
Baltimore, MD 410-612-1338
Charlotte, NC 704-662-0786
Chicago, IL-West Central Region 630-368-0001
Cincinnati, OH- Mideast Region 513-683-5300
Detroit, MI-North Central Region 248-641-7595
Grand Rapids, MI 616-949-5278
Nashville, TN-Southwest Region 615-771-3134
New England 401-658-3468
Pittsburgh, PA 412-635-9835
Tulsa, OK 918-298-2272
International Sales-Houston, TX ... 281-872-8741
Specialty Stainless and Electrical Commercial-Butler, PA 800-381-5663

© 2000 AK Steel Corporation

www.aksteel.com

7100-0096 7/00

3 Bylaag 2 (Laminasie datavel)

Grade EN 10106	Thickness	Maximum specific total loss at 50 Hz		Minimum magnetic polarization at 50 Hz			
		$\hat{J}$ = 1,5 T	1,0 T**	$\hat{H}$= 2500	5000	10000	A/m
	mm	W/kg	W/kg	T	T	T	
M235-35A	0,35	2,35	0,95	1,49	1,60	1,70	
M250-35A	0,35	2,50	1,00	1,49	1,60	1,70	
M270-35A	0,35	2,70	1,10	1,49	1,60	1,70	
M300-35A	0,35	3,00	1,20	1,49	1,60	1,70	
M330-35A	0,35	3,30	1,30	1,49	1,60	1,70	
M700-35A*	0,35	7,00	3,00	1,60	1,69	1,77	

Typical magnetic properties at 50 Hz

This data relates to products manufactured by Cogent at Surahammars Bruks AB

Grade EN 10106	Specific total loss at 50 Hz		Anisotropy of loss	Magnetic polarization at 50 Hz			Coercivity (DC)	Relative permeability at 1,5 T
	$\hat{J}$= 1,5 T	1,0 T		$\hat{H}$ = 2500	5000	10000 A/m		
	W/kg	W/kg	%	T	T	T	A/m	
M235-35A	2,25	0,92	10	1,53	1,64	1,76	35	610
M250-35A	2,35	0,98	10	1,53	1,64	1,76	40	660
M270-35A	2,47	1,01	10	1,54	1,65	1,77	40	700
M300-35A	2,62	1,10	10	1,55	1,65	1,78	45	830
M330-35A	2,93	1,19	10	1,56	1,66	1,78	45	860
M700-35A*	5,50	2,53	7	1,63	1,71	1,83	100	1750

Typical specific total loss at 60 Hz, W/kg and W/lb at $\hat{J}$ = 1,5 T

This data relates to products manufactured by Cogent at Surahammars Bruks AB

Grade EN 10106	Thickness	Maximum**		Typical	
	mm	W/kg	W/lb	W/kg	W/lb
M235-35A	0,35	2,97	1,35	2,78	1,26
M250-35A	0,35	3,14	1,42	2,91	1,32
M270-35A	0,35	3,36	1,52	3,06	1,39
M300-35A	0,35	3,74	1,70	3,26	1,48
M330-35A	0,35	4,12	1,87	3,66	1,66
M700-35A*	0,35	8,66	3,93	6,81	3,09

Typical physical and mechanical properties

Grade EN 10106	Conventional density kg/dm³	Resistivity µΩcm	Yield strength N/mm²	Tensile strength N/mm²	Young's Modulus (E) RD N/mm²	TD N/mm²	Hardness HV5 (VPN) –
M235-35A	7,60	59	460	580	185 000	200 000	220
M250-35A	7,60	55	455	575	185 000	200 000	215
M270-35A	7,65	52	450	565	185 000	200 000	215
M300-35A	7,65	50	370	490	185 000	200 000	185
M330-35A	7,65	44	300	430	200 000	220 000	150
M700-35A*	7,80	30	290	405	210 000	220 000	125

Comparison of grades and standards

Core loss 1,5 T 50 Hz W/kg	Cogent grade EN 10106 (1995)	Previous grade (1987)	IEC 60404-8-4 (1998)	JIS C2552 (2000)	GOST 21427.2 (1983)	Old AISI grade	ASTM A677 (1999)	Core loss 1,5 T 60 Hz W/lb	Core loss 1,5T 50 Hz W/kg
2,35	M235-35A	(CK-27)	M235-35A5	(35A230)					
2,50	M250-35A	CK-30	M250-35A5	35A250	2413	(M-15)	(36F145)	1,45	2,58
2,70	M270-35A	CK-33	M270-35A5	35A270	2412	(M-19)	(36F155)	1,55	2,76
3,00	M300-35A	CK-37	M300-35A5	35A300	2411	(M-22)	(36F175)	1,75	3,10
3,30	M330-35A	CK-40	M330-35A5			M-36	(36F185)	1,85	3,26
7,00	M700-35A*								

Typical specific total loss data, W/kg at 50 Hz

Grade EN 10106	Thickness mm	Specific total loss, W/kg at 50 Hz and peak magnetic polarization $\hat{J}$ (T) of									
		0,10	0,20	0,30	0,40	0,50	0,60	0,70	0,80	0,90	1,00
M235-35A	0,35	0,02	0,06	0,11	0,20	0,29	0,38	0,50	0,62	0,77	0,92
M250-35A	0,35	0,02	0,06	0,13	0,21	0,31	0,41	0,52	0,66	0,81	0,98
M270-35A	0,35	0,03	0,07	0,13	0,22	0,31	0,43	0,54	0,68	0,83	1,01
M300-35A	0,35	0,03	0,08	0,15	0,24	0,35	0,48	0,61	0,76	0,92	1,10
M330-35A	0,35	0,03	0,08	0,16	0,27	0,39	0,52	0,66	0,82	1,00	1,19
M700-35A*	0,35	0,06	0,17	0,35	0,57	0,82	1,09	1,40	1,74	2,12	2,53

Specific total loss, W/kg at 50 Hz and peak magnetic polarization $\hat{J}$ (T) of								Grade EN 10106
1,10	1,20	1,30	1,40	1,50	1,60	1,70	1,80	
1,10	1,31	1,56	1,92	2,25	2,53	2,75	2,94	M235-35A
1,15	1,37	1,65	2,00	2,35	2,65	2,87	3,06	M250-35A
1,20	1,42	1,70	2,12	2,47	2,80	3,05	3,25	M270-35A
1,30	1,54	1,82	2,20	2,62	2,98	3,25	3,41	M300-35A
1,42	1,67	1,99	2,42	2,93	3,47	3,90	4,23	M330-35A
2,93	3,38	3,93	4,66	5,50	6,51	7,31	7,94	M700-35A*

Typical specific apparent power, VA/kg at 50 Hz

Grade EN 10106	Thickness mm	Specific apparent power, VA/kg at 50 Hz and peak magnetic polarization $\hat{J}$ (T) of									
		0,10	0,20	0,30	0,40	0,50	0,60	0,70	0,80	0,90	1,00
M235-35A	0,35	0,05	0,14	0,24	0,37	0,51	0,67	0,87	1,09	1,36	1,71
M250-35A	0,35	0,06	0,15	0,27	0,40	0,56	0,74	0,95	1,21	1,52	1,92
M270-35A	0,35	0,06	0,17	0,29	0,44	0,61	0,81	1,04	1,31	1,63	2,04
M300-35A	0,35	0,07	0,17	0,30	0,45	0,62	0,82	1,05	1,31	1,63	2,03
M330 35A	0,35	0,08	0,19	0,32	0,47	0,64	0,85	1,08	1,35	1,68	2,08
M700-35A*	0,35	0,14	0,37	0,62	0,90	1,20	1,53	1,88	2,26	2,67	3,13

Specific apparent power, VA/kg at 50 Hz and peak magnetic polarization $\hat{J}$ (T) of								Grade EN 10106
1,10	1,20	1,30	1,40	1,50	1,60	1,70	1,80	
2,17	2,89	4,45	10,3	32,4	84,6	162	274	M235-35A
2,46	3,30	4,97	10,3	30,0	75,7	153	267	M250-35A
2,58	3,38	4,90	9,64	28,0	72,3	149	264	M270-35A
2,55	3,32	4,71	8,61	23,7	64,1	138	255	M300-35A
2,62	3,41	4,85	8,69	22,7	61,8	135	252	M330-35A
3,66	4,32	5,25	6,93	11,8	31,8	86,0	182	M700-35A*

Typical peak magnetic field strength, A/m at 50 Hz

Grade EN 10106	Thickness mm	Peak magnetic field strength, A/m at 50 Hz and peak magnetic polarization $\hat{J}$ (T) of									
		0,10	0,20	0,30	0,40	0,50	0,60	0,70	0,80	0,90	1,00
M235-35A	0,35	24,7	32,6	38,1	43,1	48,2	53,9	60,7	68,8	79,3	93,7
M250-35A	0,35	26,8	35,7	41,8	47,5	53,4	60,0	67,9	77,5	90,0	107
M270-35A	0,35	30,0	39,6	46,0	52,0	58,2	65,2	73,3	83,1	95,5	112
M300-35A	0,35	30,9	40,2	46,4	52,1	57,9	64,4	72,0	81,1	92,6	108
M330-35A	0,35	31,4	41,4	48,2	54,3	60,4	67,1	74,9	84,2	96,3	113
M700-35A*	0,35	70,2	89,1	98,8	106	113	120	127	135	144	155

Peak magnetic field strength, A/m at 50 Hz and peak magnetic polarization $\hat{J}$ (T) of								Grade EN 10106
1,10	1,20	1,30	1,40	1,50	1,60	1,70	1,80	
115	156	260	690	1950	4410	7630	12000	M235-35A
133	179	284	642	1810	4030	7290	11700	M250-35A
136	178	272	596	1700	3880	7160	11600	M270-35A
130	168	250	510	1440	3490	6700	11300	M300-35A
137	179	266	521	1380	3400	6610	11100	M330-35A
169	192	237	342	681	1890	4570	8580	M700-35A*

Typical specific total loss data, W/kg at 100 Hz - 2500 Hz

Measurements are carried out in the 25 cm Epstein frame according to IEC 60404-2 at 100 Hz and 200 Hz, according to IEC 60404-10 at 400 Hz to 2500 Hz. Half of the sample strips are taken in the rolling direction and half in the transverse direction. Samples are tested as sheared and are not aged or stress relief annealed.

100 Hz

Grade EN 10106	Specific total loss, W/kg at 100 Hz and peak magnetic polarization $\hat{J}$ (T) of														
	0,10	0,20	0,30	0,40	0,50	0,60	0,70	0,80	0,90	1,00	1,10	1,20	1,30	1,40	1,50
M235-35A	0,04	0,14	0,30	0,49	0,71	0,97	1,25	1,57	1,92	2,31	2,75	3,26	3,88	4,67	5,54
M250-35A	0,04	0,14	0,31	0,51	0,75	1,01	1,31	1,64	2,00	2,41	2,87	3,40	4,03	4,83	5,72
M270-35A	0,04	0,16	0,34	0,55	0,80	1,08	1,38	1,73	2,10	2,51	2,98	3,51	4,15	4,97	5,92
M300-35A	0,04	0,17	0,35	0,58	0,84	1,14	1,46	1,83	2,23	2,66	3,16	3,72	4,39	5,23	6,22
M330-35A	0,04	0,18	0,38	0,63	0,92	1,24	1,61	2,01	2,46	2,96	3,52	4,17	4,95	5,93	7,13

200 Hz

Grade EN 10106	Specific total loss, W/kg at 200 Hz and a peak magnetic polarization $\hat{J}$ (T) of														
	0,10	0,20	0,30	0,40	0,50	0,60	0,70	0,80	0,90	1,00	1,10	1,20	1,30	1,40	1,50
M235-35A	0,08	0,32	0,73	1,21	1,78	2,44	3,19	4,03	4,97	6,01	7,19	8,54	10,1	12,2	14,4
M250-35A	0,08	0,33	0,73	1,23	1,82	2,49	3,26	4,12	5,07	6,14	7,33	8,69	10,3	12,4	14,7
M270-35A	0,09	0,37	0,79	1,31	1,91	2,61	3,39	4,26	5,23	6,30	7,51	8,88	10,5	12,5	14,9
M300-35A	0,09	0,40	0,85	1,41	2,06	2,81	3,66	4,61	5,65	6,80	8,09	9,54	11,2	13,4	15,7
M330-35A	0.10	0.43	0.92	1.55	2.30	3.16	4.13	5.23	6.45	7.83	9.37	11.1	13.2	15.7	18.6

400 Hz

Grade EN 10106	Specific total loss, W/kg at 400 Hz and peak magnetic polarization $\hat{J}$ (T) of														
	0,10	0,20	0,30	0,40	0,50	0,60	0,70	0,80	0,90	1,00	1,10	1,20	1,30	1,40	1,50
M235-35A	0,19	0,87	1,88	3,17	4,73	6,56	8,67	11,0	13,8	16,9	20,3	24,3	28,9	34,8	41,2
M250-35A	0,21	0,90	1,93	3,24	4,81	6,69	8,82	11,2	14,0	17,1	20,6	24,6	29,2	35,1	41,6
M270-35A	0,21	0,92	1,99	3,33	4,94	6,84	9,00	11,4	14,2	17,3	20,9	24,9	29,5	35,4	41,8
M300-35A	0,23	1,00	2,15	3,61	5,36	7,42	9,75	12,4	15,4	18,8	22,5	26,8	31,6	37,7	44,3
M330-35A	0,27	1,15	2,45	4,13	6,16	8,58	11,4	14,5	18,2	22,3	27,0	32,4	38,7	46,2	54,7

1000 Hz

Grade EN 10106	Specific total loss, W/kg at 1000 Hz and peak magnetic polarization $\hat{J}$ (T) of										
	0,10	0,20	0,30	0,40	0,50	0,60	0,70	0,80	0,90	1,00	1,10
M235-35A	0,93	3,55	7,45	12,3	18,5	25,8	34,6	45,0	57,2	71,5	88,3
M250-35A	0,98	3,65	7,58	12,7	18,8	26,3	35,2	45,7	58,1	72,6	89,6
M270-35A	0,99	3,67	7,63	12,7	18,9	26,4	35,4	46,0	58,4	73,0	90,1
M300-35A	1,07	4,08	8,48	14,0	20,9	29,2	39,0	50,6	64,1	79,8	98,0
M330 35A	1,30	4,84	10,0	16,7	24,9	34,9	46,9	61,3	78,3	98,4	122

2500 Hz

Grade EN10106	Specific total loss, W/kg at 2500 Hz and peak magnetic polarization $\hat{J}$ (T) of									
	0,10	0,20	0,30	0,40	0,50	0,60	0,70	0,80	0,90	1,00
M235-35A	3,89	14,3	29,6	50,2	76,7	110	153	205	270	349
M250-35A	4,09	14,8	30,6	51,7	78,8	113	155	208	273	352
M270-35A	4,10	14,9	30,7	52,0	79,1	113	156	209	274	353
M300-35A	4,45	16,1	33,6	56,9	86,6	124	170	227	297	382
M330-35A	5,44	19,5	40,9	69,5	107	154	213	287	373	476

D.3 PMSM unbalance magnetic pull

University of Johannesburg

Faculty of Engineering and the Built Environment

Department of Electrical and Electronic Engineering Science

Design of a permanent-magnet synchronous machine (PMSM) for the FLY-UPS project of Northwest University: Report 1 (rev. 1) — The unbalanced magnetic pull

by

Robert Holm

B4 Lab 212

Tel.: (011) 489-2594

email: robertholm@ieee.org

19 June 2006

Contents

1 Introduction **2**

2 The unbalanced magnetic pull **2**

2.1 Machine cross section 2

2.2 Assumptions 2

2.3 Derivation 3

2.3.1 The air gap flux density 3

2.3.2 Modeling of an unbalanced rotor position 4

2.3.3 Magnetic field coenergy and force for an unbalanced rotor position 6

2.4 Preliminary machine dimensions 7

2.5 Numerical results 7

3 Summary and conclusion **8**

1 Introduction

The author is in the design process of a PMSM for a flywheel energy storage system for a Northwest University research project. The design decisions up to date are as follows:

- rotor yoke inner diameter: 30 mm
- rotor yoke outer diameter: 50 mm
- the stator is slotless (report 2 will revisit this decision)
- there is no shielding cylinder on the rotor
- the machine has two magnetic poles and three phases

Based on the decisions above, this report addresses the unbalanced magnetic pull (UMP) of the machine. The UMP reported here is a very crude calculation and meant for initial orientation only. If required, a more detailed (FEM) calculation may be done after the machine design has been completed and the dimensions of the machine components are therefore more accurately known.

2 The unbalanced magnetic pull

2.1 Machine cross section

Figure 1 shows a radial cross section of the machine based on the decisions of Section 1. The different radii in the machine are also labelled for later reference. Only the inner and outer rotor yoke radii are drawn to scale (since the other machine dimensions are not yet known, they are not).

2.2 Assumptions

In addition to the list of decisions made in Section 1, the following assumptions are made in this report:

- the unbalance is in the radial direction only (i.e., no axial movement);
- the unbalance is uniform along the axis of the machine; and

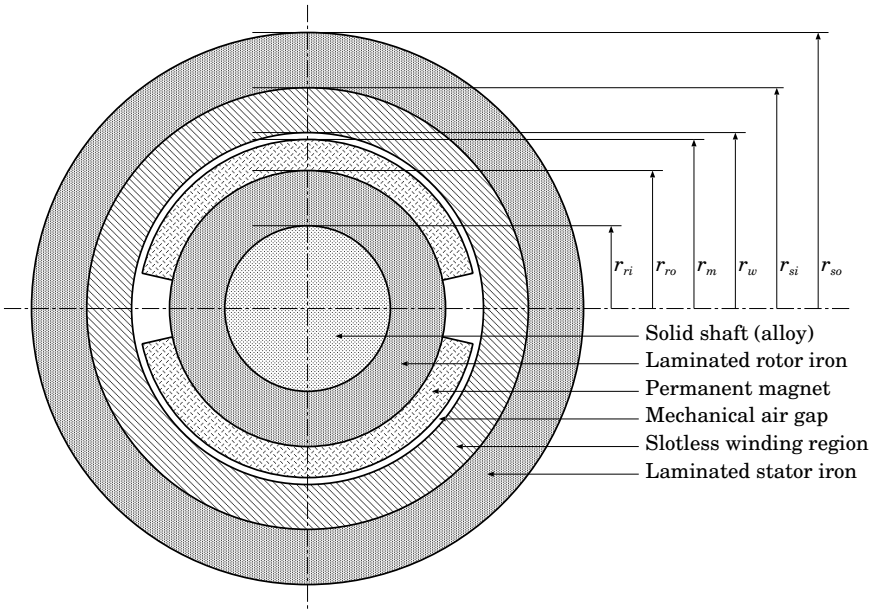

Figure 1: Radial cross section of the PMSM based on the decisions of Section 1.

- the radial unbalance is in a direction parallel to the magnetic axes of the permanent magnets.

2.3 Derivation

2.3.1 The air gap flux density

The derivation of the electromagnetic force due to an unbalance in the rotor position is based upon a linear magnetic circuit model of the machine. Consider Figure 2, where the machine cross section is shown with the winding removed since the field of the winding currents is much smaller than that of the permanent magnets (on the order of 10%).

In Figure 2, ϕ_r is the permanent-magnet flux, R_m is the magnet reluctance, R_l the leakage reluctance, R_s the stator yoke reluctance, R_r the rotor yoke reluctance and R_{g1} and R_{g2} the reluctances of the two air gaps. These latter two quantities will change when the rotor is in an unbalanced position.

The magnetic circuit model of the machine with only the permanent-magnet flux sources are also shown in Figure 2. This circuit can be simplified by removing R_l; this is done by modifying the flux in the air gap such that $\phi_g = K_l\phi$, where K_l is a *leakage factor*, $0.9 \leq K_l \leq 1.0$. Also, the air-gap reluctances can be slightly increased to account for the iron reluctances of the stator and rotor yokes by multiplying them with a *reluctance*

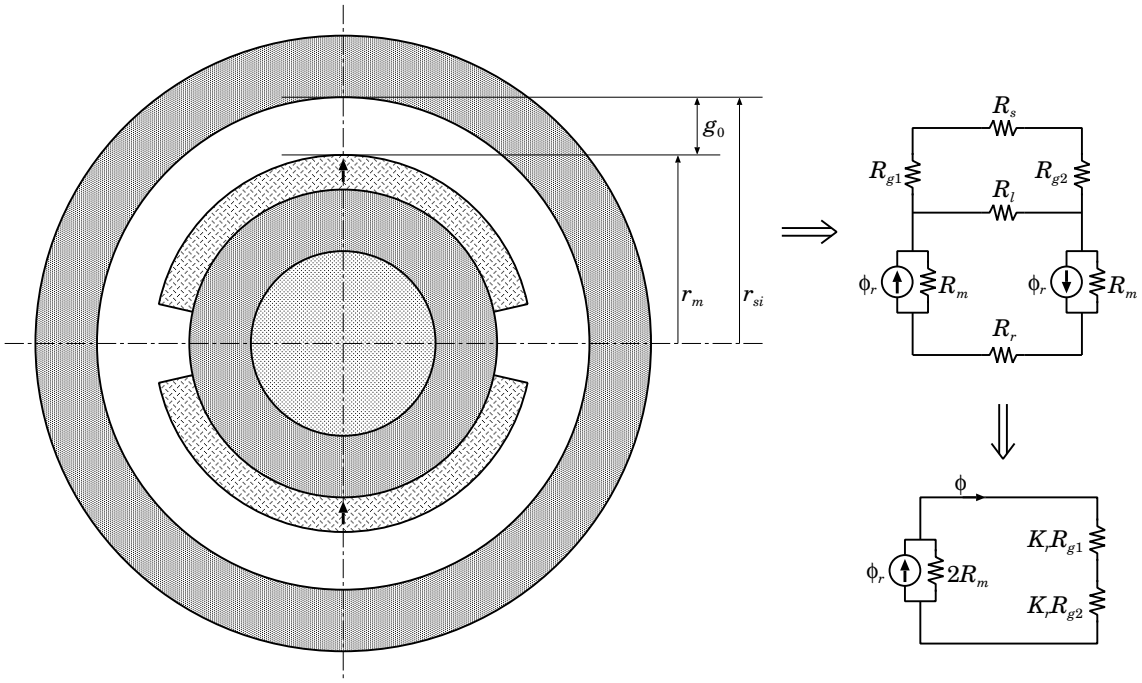

Figure 2: Derivation of the magnetic circuit for the UMP calculation.

factor K_r, $1.0 \leq K_r \leq 1.2$. (Both the ranges of magnitude for K_l and K_r are valid for surface-mounted PMSMs.)

From Figure 2, the flux in the magnetic circuit is

$$\phi = \frac{2R_m}{2R_m + K_r(R_{g1} + R_{g2})}\,\phi_r = \frac{1}{1 + \frac{K_r}{2R_m}(R_{g1} + R_{g2})}\,\phi_r$$

The flux in the air gap is

$$\phi_g = \frac{K_l}{1 + \frac{K_r}{2R_m}(R_{g1} + R_{g2})}\,\phi_r, \tag{1}$$

from which the flux density in the air gap can be written as

$$B_g = \frac{K_l}{1 + \frac{K_r}{2R_m}(R_{g1} + R_{g2})}\,\frac{\phi_r}{A_g}, \tag{2}$$

where A_g is the magnetic flux area in the air gap.

2.3.2 Modeling of an unbalanced rotor position

In (1) and (2), the reluctances are given by

$$R_{g1} = \frac{g_1}{\mu_0 A_m}, \tag{3}$$

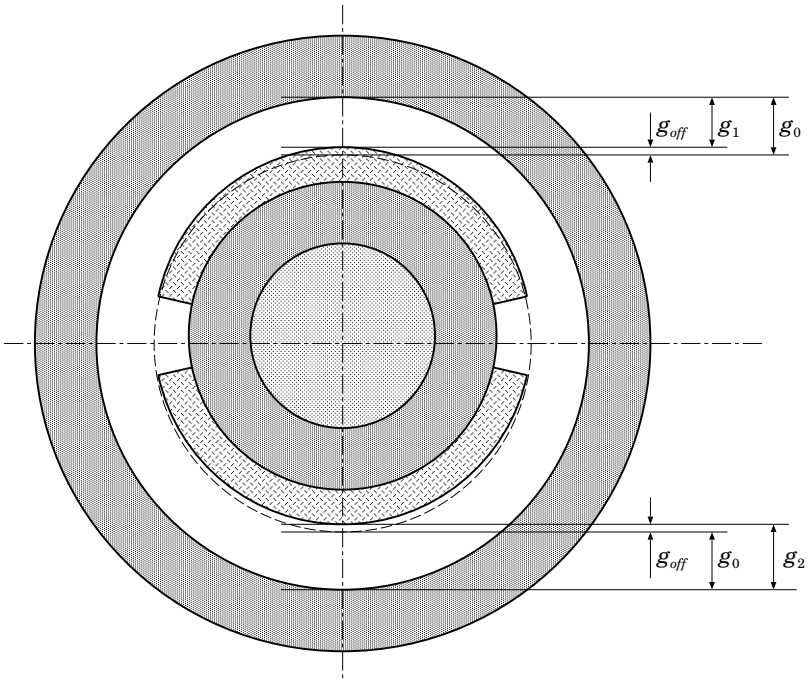

Figure 3: The rotor in an unbalanced position; the dashed line shows its balanced position.

$$R_{g2} = \frac{g_2}{\mu_0 A_m}, \tag{4}$$

and

$$R_m = \frac{l_m}{\mu_0 \mu_{rm} A_m}, \tag{5}$$

where g_1 and g_2 are the air gap lengths of the top and bottom magnets, respectively, A_m the magnetic flux area in the magnets, l_m the length of the magnets and μ_{rm} the relative permeability of the magnets. Also, in a surface-mounted machine, $A_m = A_g$.

The air gap lengths g_1 and g_2 are given by

$$g_1 = g_0 - g_{off}, \tag{6}$$

and

$$g_2 = g_0 + g_{off}, \tag{7}$$

where g_{off} is the offset of the rotor from its balanced position, defined in Figure 3.

In Figure 2, the sum of the two air-gap reluctances is present. This is given by

$$R_{g1} + R_{g2} = \frac{g_0 - g_{off} + g_0 + g_{off}}{\mu_0 A_m}, \tag{8}$$

where it can be seen that g_{off} dissapears. The nett air gap is therefore the same whether the rotor is in either the balanced or an unbalanced position. The modeling therefore

has to consider the air gaps separately. This is done for air gap 1 by making its length equal to (6) while keeping air gap length 2 equal to g_0. The opposite is done when air gap 2 is considered: its length is made equal to (7) while air gap length 1 is kept at g_0.

2.3.3 Magnetic field coenergy and force for an unbalanced rotor position

The modeling described above[1] when the imbalance is considered to be only in air gap 1 leads to the magnetic field coenergy

$$W'_{fld1} = \frac{1}{2}\left(2R_m + R_{g1} + R_0\right)\phi_1^2, \tag{9}$$

where

$$\phi_1 = \frac{2R_m\phi_r}{2R_m + R_{g1} + R_0}\,. \tag{10}$$

In (10), R_0 is the reluctance of one air gap when the rotor position is balanced. After substitution of (3) and (5) and simplification, the coenergy is

$$W'_{fld1}(g_{off}) = \frac{2\phi_r^2 l_m}{\mu_0\mu_{rm}A_m\left[2l_m + \mu_{rm}\left(2g_0 - g_{off}\right)\right]}\,. \tag{11}$$

The magnetic force is given by $f_{fld1} = \partial W'_{fld1}/\partial g_{off}$, which is

$$f_{fld1}(g_{off}) = \frac{2B_r^2 A_m l_m^2}{\mu_0\left[2l_m + \mu_{rm}\left(2g_0 - g_{off}\right)\right]^2} \tag{12}$$

from (11) and making use of the fact that $\phi_r = B_r A_m$, where B_r is the remanent flux density of the magnets.

The magnetic force f_{fld2} when the imbalance is considered to be only in air gap 2 is

$$f_{fld2}(g_{off}) = -\frac{2B_r^2 A_m l_m^2}{\mu_0\left[2l_m + \mu_{rm}\left(2g_0 + g_{off}\right)\right]^2} \tag{13}$$

The total force due to an unbalanced rotor position is

$$f_u(g_{off}) = f_{fld1} + f_{fld2} \tag{14}$$

in the upward direction where the unbalance is as shown in Figure 3. The force f_u is zero when $g_{off} = 0$, which agrees with the expectation.

[1] The constants K_l and K_r are both made equal to 1.0 in the rest of this report since their influence on the result is not substantial. (The UMP calculation accuracy is also deliberately not maximised to keep the expressions as simple and transparent as possible.)

2.4 Preliminary machine dimensions

In this section, preliminary machine dimensions are listed. These dimensions will lead to a working machine, but it will not necessarily meet the specifications. It will certainly not be the optimised machine. After the machine design has been completed, these dimensions will be changed and f_u recalculated for a more representative result.

The preliminary machine dimensions are in [mm]:

r_{ri}	r_{ro}	r_m	r_w	r_{si}	r_{so}
30	50	65	68	88	115

The above dimensions lead to the following: rotor yoke thickness $=$ 20 mm, $l_m =$ 15 mm, mechanical air gap $=$ 3 mm, winding thickness $=$ 20 mm and rotor yoke thickness $=$ 27 mm. In addition to the above, the polar magnet span is assumed to be 80% of the available angle to limit the magnet leakage flux. The active stator length is assumed to be $l_s = 70$ mm.

As a check of the above values, the air-gap flux density is calculated for $B_r = 1.0$ T and $\mu_{rm} = 1.05$ (typical values for NdFeB magnets), $K_l = 0.9$, $K_r = 1.1$ and $C_\phi = 1.0$ (flux concentration factor). For these values, the air gap flux density evaluates to $B_g = 0.73$ T by means of (2). This is quite high for a machine with an air-gap winding, but not impossible. (A large B_g is actually desireable since it leads to an increase of machine performance.) The permeance coefficient for the above dimensions is $P_c = 5$, which is in the normal range[2] for PMSMs (to keep the magnets in a safe operating region of their *B-H* characteristic).

2.5 Numerical results

The dimensions of the previous section are substituted into (12) and (13) using MATLAB®. This leads to the graph of f_u as a function of g_{off} shown in Figure 4. The limit of g_{off} was chosen as 3 mm since then the rotor is already in physical contact with the stator. It can be seen that the relationship looks linear, an indeed for this small range of g_{off}, it may weel be approximated as linear. This should simplify modeling for the rest of the system. (To show that the relationship is not linear, as is evident from (12) and (13), Figure 5 shows a graph of f_{fld1}, f_{fld2} and f_u as a function of g_{off} up to the (unrealistic) value of 30 mm.) The figure shows that the UMP is quite small; for example, $f_u = 31.4$ N at $g_{off} = 0.99$ mm. The reason for this is the fact that an air-gap winding is used (the effective electromagnetic air gap is very large). The force is expected to be much larger in the case of a slotted machine.

[2] $4 \leq P_c \leq 6$

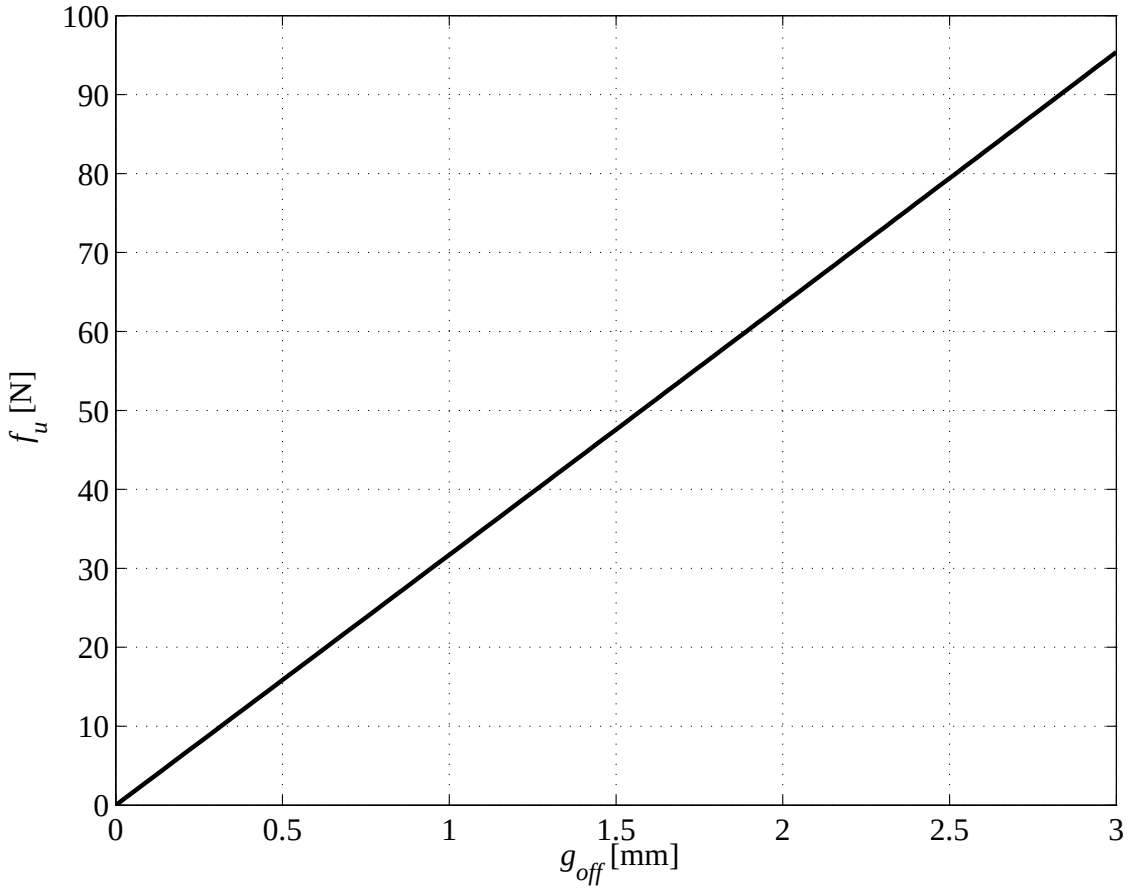

Figure 4: The unbalanced magnetic force (UMP) as a function of the offset g_{off}.

3 Summary and conclusion

This report focused on the calculation of the unbalanced magnetic pull of a PMSM for use in the FLY-UPS system of Northwest University. The calculation model was derived from first principles based on magnetic circuit theory. The work presented followed from the design decisions of Section 1 and the assumptions of Section 2.2. Preliminary machine dimensions where chosen in Section 2.4 to provide a numerical result. These dimensions will be updated after the completion of the machine design, thereby obtaining a more representative numerical result for f_u. The numerical calculations showed that the UMP is quite small and may be approximated as a linear function of g_{off} for the small values that are physically possible. The small values of the UMP is a consequence of the air-gap winding. The report is accompanied by the MATLAB® file used to generate Figures 4 and 5.

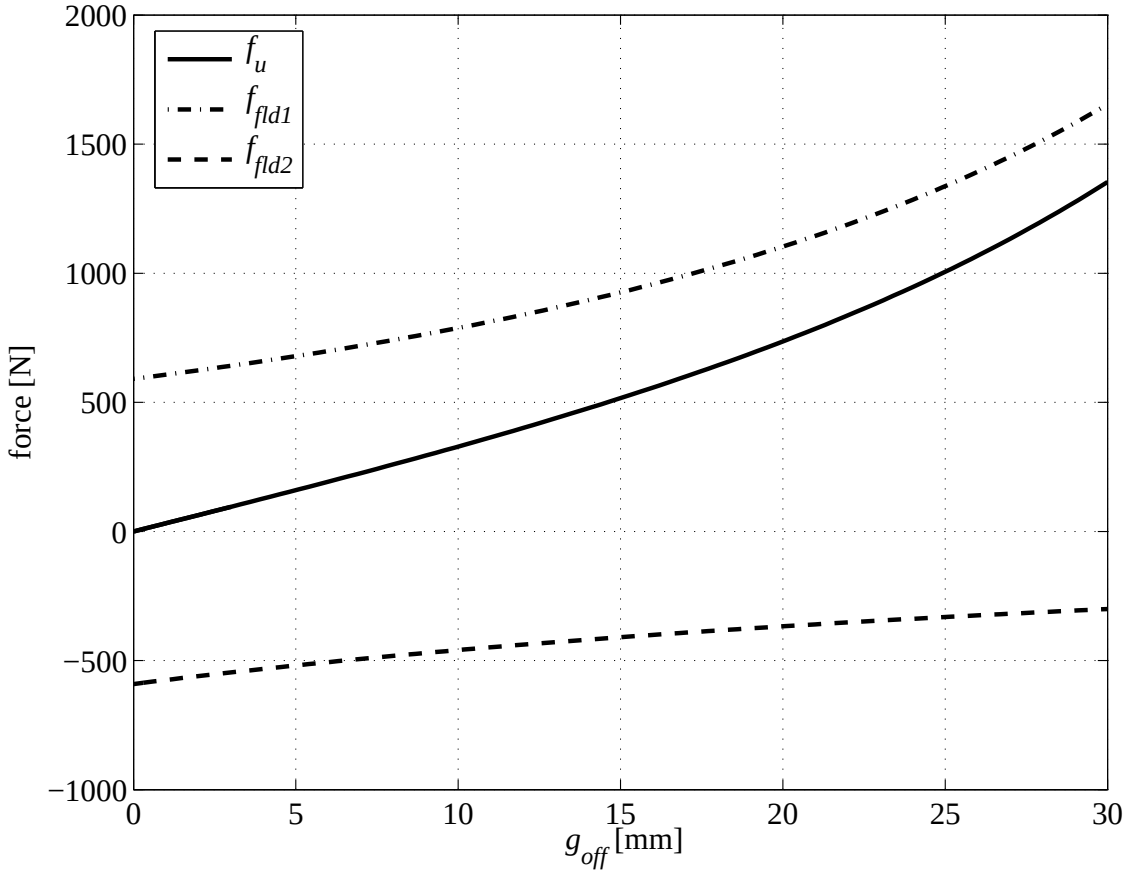

Figure 5: The unbalanced magnetic force (UMP) as a function of the offset g_{off} up to 30 mm (unrealistic).

D.4 Eddy probe and gland selection

Design Report:

FLY-UPS Probe and Gland Selection

Prepared by: Jan Janse van Rensburg

For the NWU MBMC Research group

Version 1

Revision 1

Table of Contents

1 BACKGROUND....4

2 EDDY-CURRENT PROBES....4

2.1 Costs....5

3 GLANDS AND FEED-TROUGHS....5

3.1 Costs....5

4 CONCLUSION....6

List Of Figures

Error! No table of figures entries found.

1 Background

This report deals with the selection of the required eddy probes and the glands/feed-troughs for use with the FLY-UPS. The basic requirements for the probes are:

- Should be relative inexpensive
- Should be relatively accurate
- Should be standard sizes

The basic requirements for glands and feed-troughs are

- Should seal off the vacuum sufficiently
- Should preferably be replaceable with standard sizes
- Easy installation

2 Eddy-current probes

The two options considered was a SKF system and a micro-epsilon system, both of these systems had their merits, see the decision-matrix below.

	Requirement	Replaceablity	Accuracy	Price	Complete system?	Service	Support	
	Weigt-factor	0.05	0.2	0.35	0.2	0.1	0.1	
SKF	(1-10)	10	7	8	10	5	10	**Total**
SCORE		0.5	1.4	2.8	2	0.5	1	**8.2**
Micro-epsilon	(1-10)	10	4	4	8	10	10	**Total**
SCORE		0.5	0.8	1.4	1.6	1	1	**6.3**

Using this Decision making matrix It was decided to opt for the SKF system.

2.1 Costs

Part Number	Description	Qty	Total
CMSS 65-002-00-40-5A	PROBE, 5mm, 1/4-28 Thread, 4.0" Case Length, 5m Integral Cable.	4	R 11,571.10
CMSS 65-002-00-12-5A	PROBE, 5mm, 1/4-28 Thread, 1.2" Case Length, 5m Integral Cable.	1	R 2,892.78
CMSS 665	DRIVER, Standard, 200mV/mil, +/- 5%, 4140 Steel, 80mil Range, 5m System.	5	R 20,696.58
CMSS 30112003	CABLE PACKING GLAND ASSY, 1 Cable, 3/4" NPT Fitting.	5	R 8,005.84
CMSS 31123300	Power Supply, +/- 24 VDC, DIN Rail Mount	1	R 5,106.03
		Total Excl. VAT.	**R 48,272.33**

3 Glands and Feed-troughs

Glands will be sourced from 3 manufactures namely: SKF (for the probes price included in the Eddy-probe quote), WIKA (for all the power supplies except for the motor) and CONAX (Power supply to the motor). The reasoning behind the choice for three manufactures is that SKF's glands are designed for SKF's probes, WIKA is made in Johannesburg with distributors in klerksdorp so is easily replaceable, and meets din standards, CONAX is supplied by the same company distributing the WIKA glands, and is able to handle the high Ampere rating of the motor.

3.1 Costs

Item		Description	Part Number	Qty	Each Price	Discount	Line Total
1	*R*	Wika 4-wire feedthrough c/w 1/2" BSP swiwel connection 6mm MI-Cable & Extension cable as per specification Conductor size:: 0,8mm diam L= +/- 100mm; X1= +/-250mm; X2= 250mm	T4-Special/4C	4	R 1,561.80	20.00%	R 4,997.76
2	*R*	Wika 2-wire feedthrough c/w 1/2" BSP swiwel connection 6mm MI-Cable & Extension cable as per specification Conductor size:: 0,8mm diam L= +/- 100mm; X1= +/-250mm; X2= 250mm	T4-Special/2C	2	R 1,470.60	20.00%	R 2,352.96
3	*R*	Wika 2-wire feedthrough c/w 1/2" BSP swiwel connection 6mm MI-Cable & Extension cable as per specification Conductor size:: 0,8mm diam L= +/- 100mm; X1= +/-250mm; X2= 250mm	T4-Special/2C	5	R 1,470.60	20.00%	R 5,882.40
						QUOTE TOTAL	R 13,233.12

NOTE: (Old quote waiting for new quote final price will be in that region)

4 Conclusion

The SKF System can be ordered, the whole system uses standard sizes, and the representative at SKF, South-Africa (Mr. Andre Du Bruyn) and I have a agreement that if I get a ‘green light’ he will order the System immediately, to hasten the process (Purchase requests)

The WIKA and CONAX Glands will be ready to be ordered on 2006-09-18. The WIKA representative (Mr. Henk Venter) is in potchefstroom regularly, and we have already had a quick meeting, he has done work for the PBMR, Johan Roberts, Chemical dept, Mechanical Dept. and Physics Dept.

D.5 EES Program Results

EES Ver. 7.173: #0753: Mechanical & Materials Engineering, North-West University, Potchefstroom, South Africa

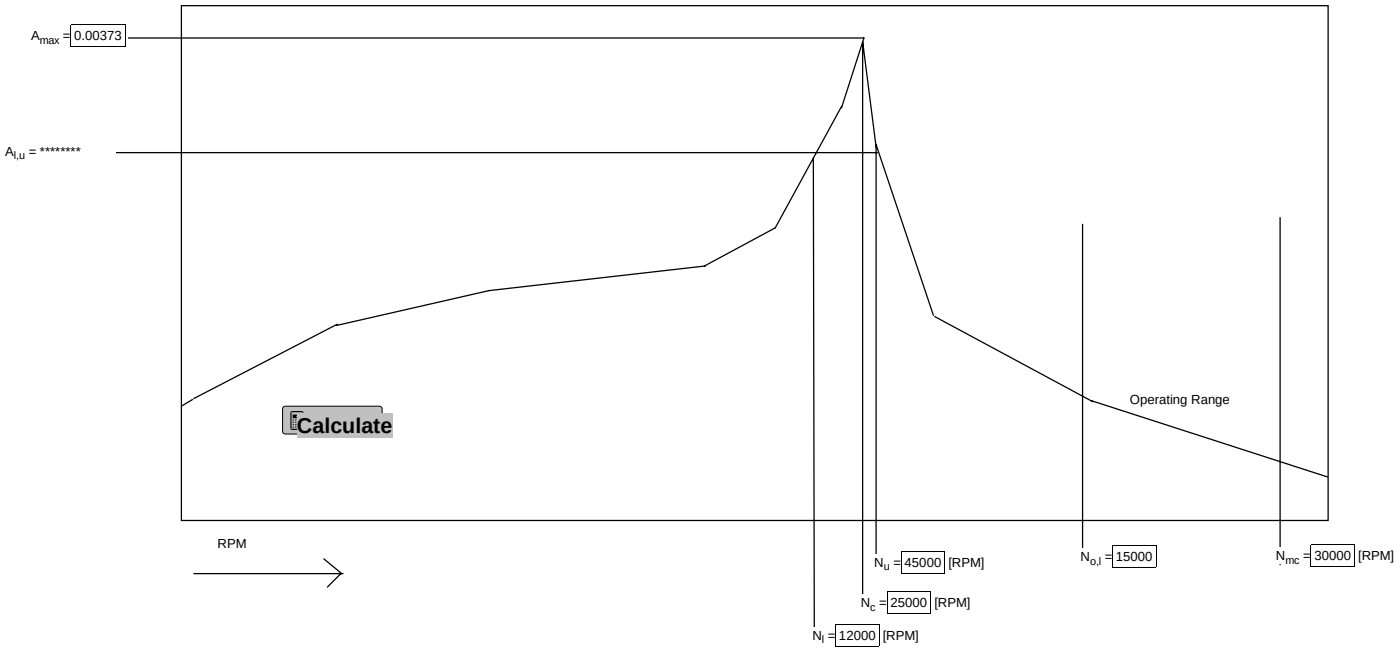

F_a = ****** If F_a is less than 2.5 no Separation Margin is neccesary (The response is considered critically damped)

M_s = ** [%]

$M_{s,verrify}$ = ** [%]** $M_{s,verify}$ has to be larger than M_s for the system to be considered critically damped

SeperationMargin = ****** [RPM]

Result$ = **

API 612 - Critical Frequency Seperation Factor (Lower)

Procedure **TEST** ($M_{s,1}$: M_s)

If [$M_{s,1}$ > 16] Then M_s := 16 Else M_s := $M_{s,1}$ EndIf

End **TEST**

Procedure **TEST2** ($M_{s,verrify}$, F_a, M_s : Result$)

If [(M_s < $M_{s,verrify}$) or (F_a < 2.5)] Then Result$:= 'PASSED' Else Result$:= 'FAILED'

EndIf

End **TEST2**

$$A_{l,u} = A_{max} \cdot 0.707$$

$$F_a = \frac{N_c}{N_u - N_l}$$

$$M_{s,1} = 17 \cdot \left[1 - \left(\frac{1}{F_a - 1.5} \right) \right]$$ *Or $M_{s,1}$=16 witchever is smallest*

$$SeperationMargin = N_{o,l} - N_u$$

$$M_{s,verrify} = \frac{SeperationMargin}{N_{o,l}} \cdot 100$$

Call **TEST** [$M_{s,1}$: M_s]

Call **TEST2** [$M_{s,verrify}$, F_a , M_s : Result$]

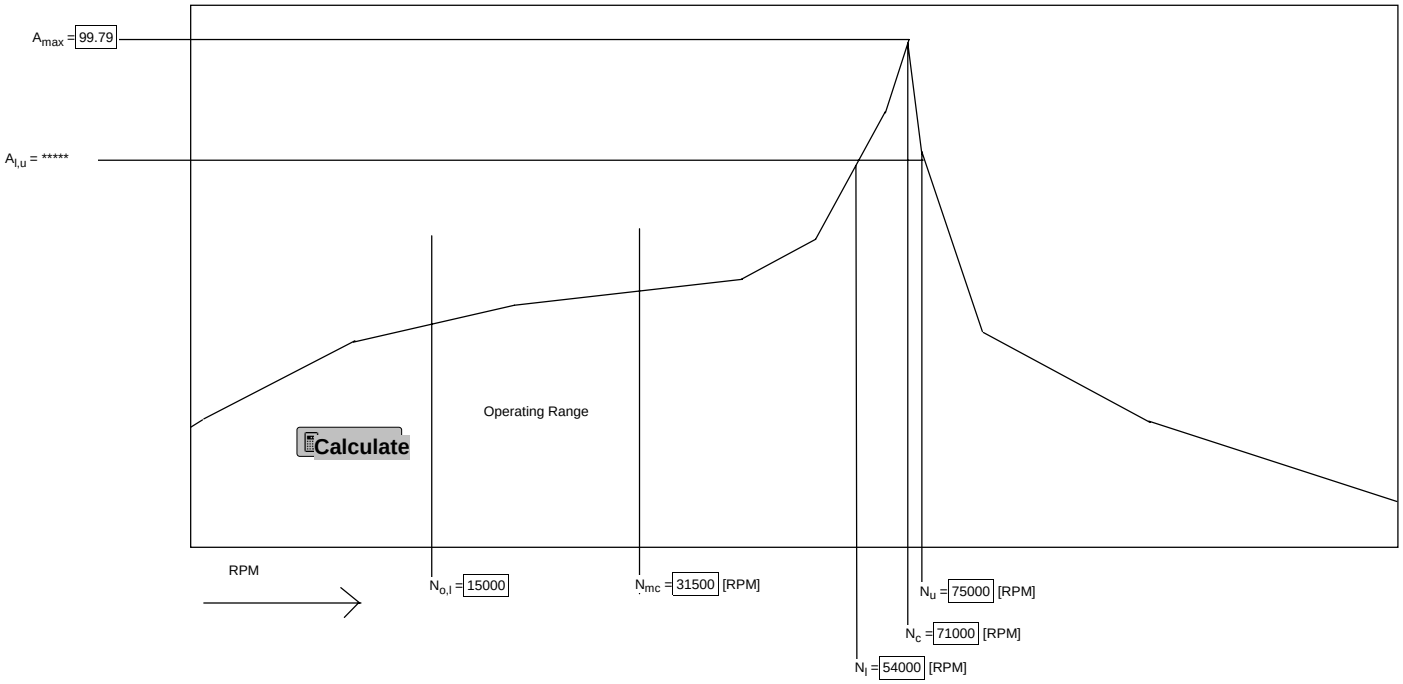

F_a = ***** If F_a is less than 2.5 no Separation Margin is neccesary (The response is considered critically damped)

M_s = *** [%]**

$M_{s,verrify}$ = *** [%]** $M_{s,verify}$ has to be larger than M_s for the system to be considered critically damped

SeperationMargin = ***** [RPM]

Result$ = **

API 612 - Critical Frequency Seperation Factor (Lower)

Procedure **TEST** ($M_{s,1}$: M_s)

If [$M_{s,1}$ > 26] Then M_s := 26 Else M_s := $M_{s,1}$ EndIf

End **TEST**

Procedure **TEST2** ($M_{s,verrify}$, F_a, M_s : Result$)

If [(M_s < $M_{s,verrify}$) or (F_a < 2.5)] Then Result$:= 'PASSED' Else Result$:= 'FAILED'

EndIf

End **TEST2**

$$A_{l,u} = A_{max} \cdot 0.707$$

$$F_a = \frac{N_c}{N_u - N_l}$$

$$M_{s,1} = 10 + 17 \cdot \left[1 - \left(\frac{1}{F_a - 1.5}\right)\right]$$ *Or M_s = 26, witchever is smallest*

$$SeperationMargin = N_l - N_{mc}$$

$$M_{s,verrify} = \frac{SeperationMargin}{N_{mc}} \cdot 100$$

Call **TEST** [$M_{s,1}$: M_s]

Call **TEST2** [$M_{s,verrify}$, F_a , M_s : Result$]

EES Ver. 7.173: #0753: Mechanical & Materials Engineering, North-West University, Potchefstroom, South Africa

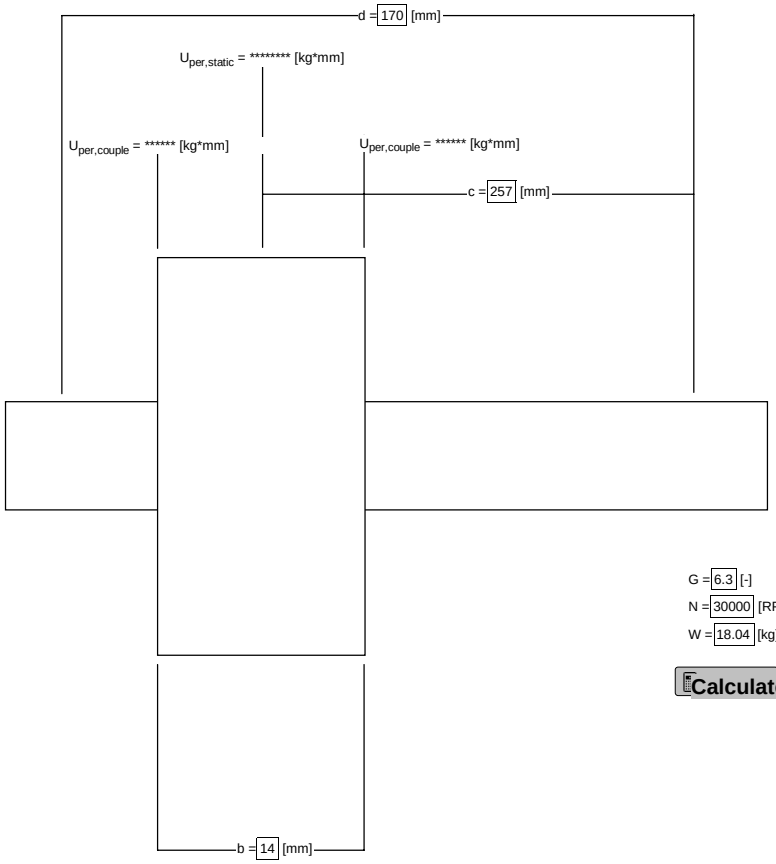

G = 6.3 [-]
N = 30000 [RPM]
W = 18.04 [kg]

Calculate

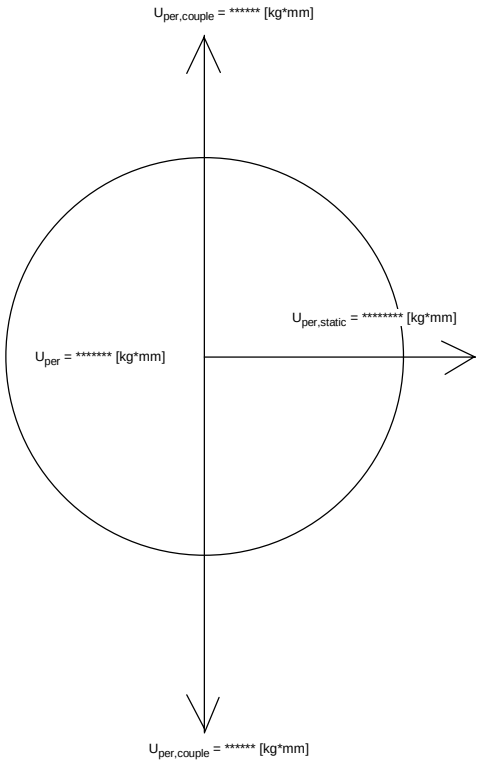

ISO 1940/1 Standard Balance Quality Requirements

$$U_{per} = 9.549 \cdot G \cdot \frac{W}{N}$$

For overhung and narrow rotors

$$U_{per,static} = \frac{U_{per}}{2} \cdot \frac{d}{2 \cdot c}$$

$$U_{per,couple} = \frac{U_{per}}{2} \cdot 3 \cdot \frac{d}{4 \cdot b}$$

$$U_{per} = 9.549 \cdot G \cdot \frac{Weight}{RPM}$$

$G = 6.3$ [-]

$Weight = 19.4 \cdot 1000$ [g]

$RPM = 33000$ [RPM]

$D_{rotor} = 250$ [mm]

$$L_{Mmidpunt,stud} = \frac{D_{rotor}}{2} - \frac{L_{stud}}{2}$$

$$\omega = RPM \cdot 2 \cdot \frac{\pi}{60}$$

$$F_{API} = \frac{U_{per} \cdot \omega^2}{1000000}$$

$$F_{bout} = \frac{M_{stud}}{1000} \cdot \omega^2 \cdot \frac{L_{Mmidpunt,stud}}{1000}$$

$$M_{stud} = \rho \cdot \pi \cdot \left[\frac{R_{stud}}{1000}\right]^2 \cdot \frac{L_{stud}}{1000} \cdot 1000$$

$\rho = 7800$ [kg/m^3]

$$R_{stud} = \frac{2.5}{2}$$

$L_{stud} = 8$ [mm]

$F=F_2$

SOLUTION
Unit Settings: [kJ]/[C]/[kPa]/[kg]/[degrees]

D_{rotor} = 250 [mm]	F_{API} = 422.3	F_{bout} = 442.6
G = 6.3 [-]	$L_{Mmidpunt,stud}$ = 121 [mm]	L_{stud} = 8 [mm]
M_{stud} = 0.3063 [g]	ω = 3456 [rad/s]	ρ = 7800 [kg/m^3]
RPM = 33000 [RPM]	R_{stud} = 1.25 [mm]	U_{per} = 35.37 [g*mm]
Weight = 19400 [g]		

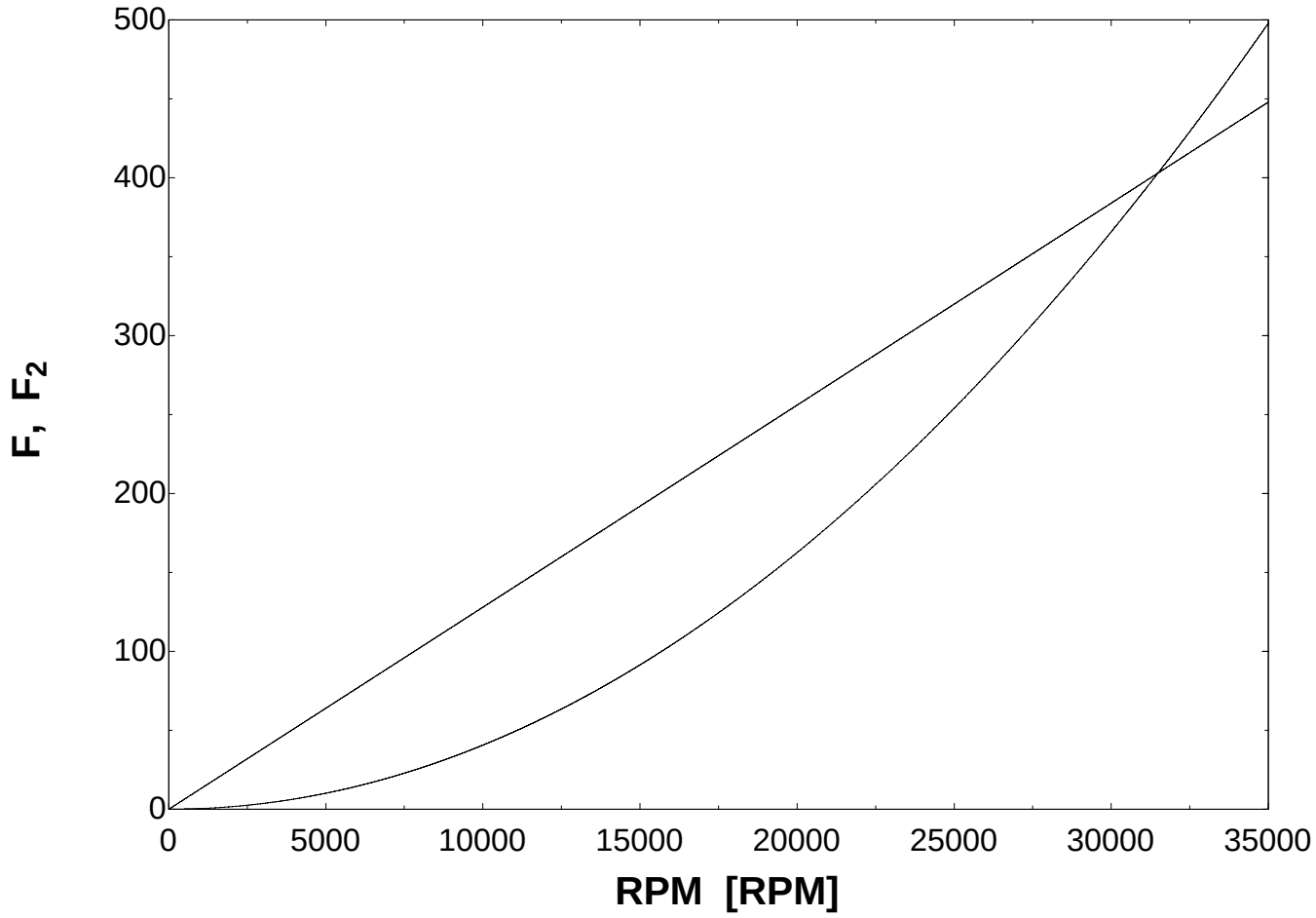
500
400
300
200
100
0
F, F2
0
5000
10000
15000
20000
25000
30000
35000
RPM [RPM]

D.6 DyRoBeS rotor-dynamic analysis

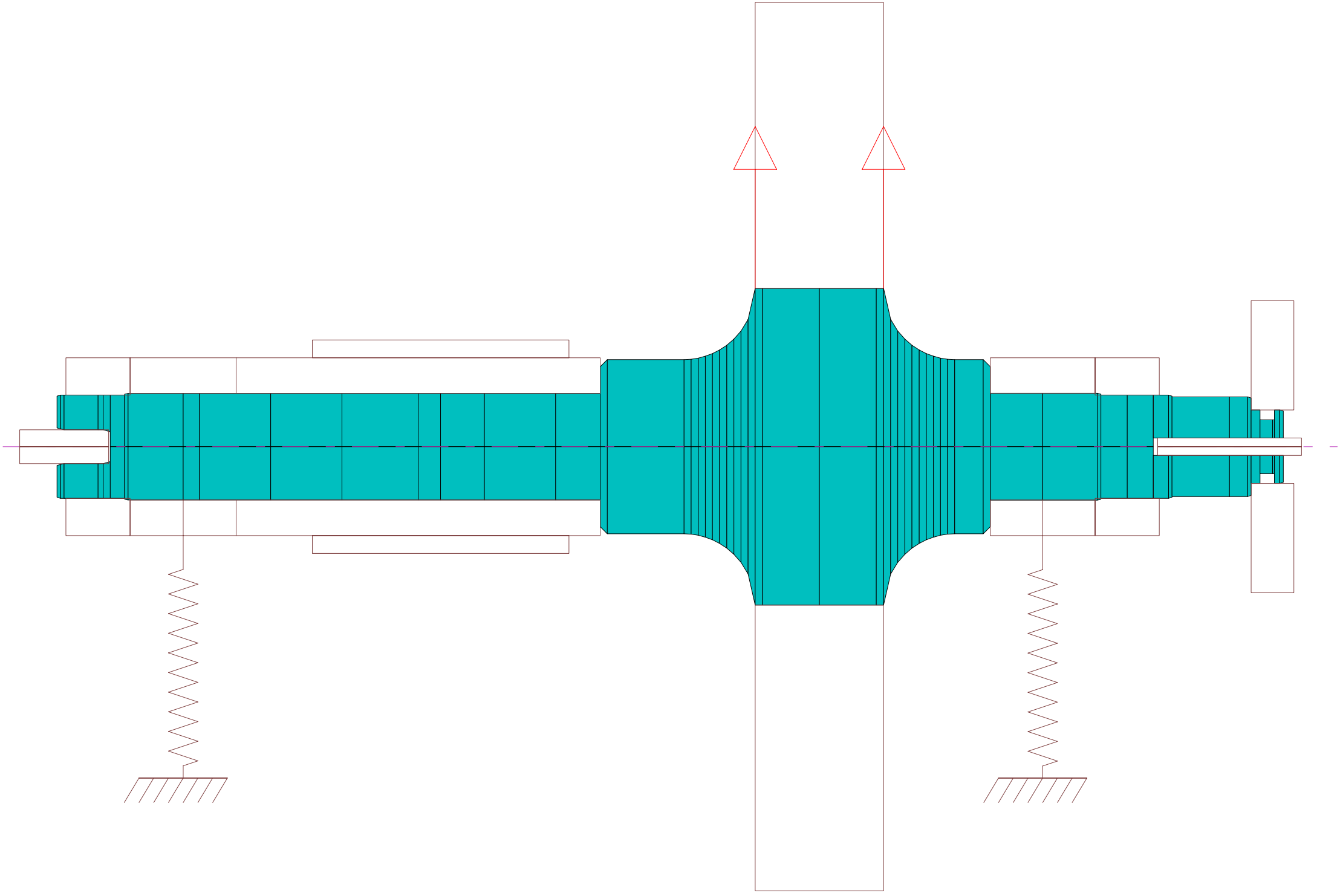

Critical Speed Map

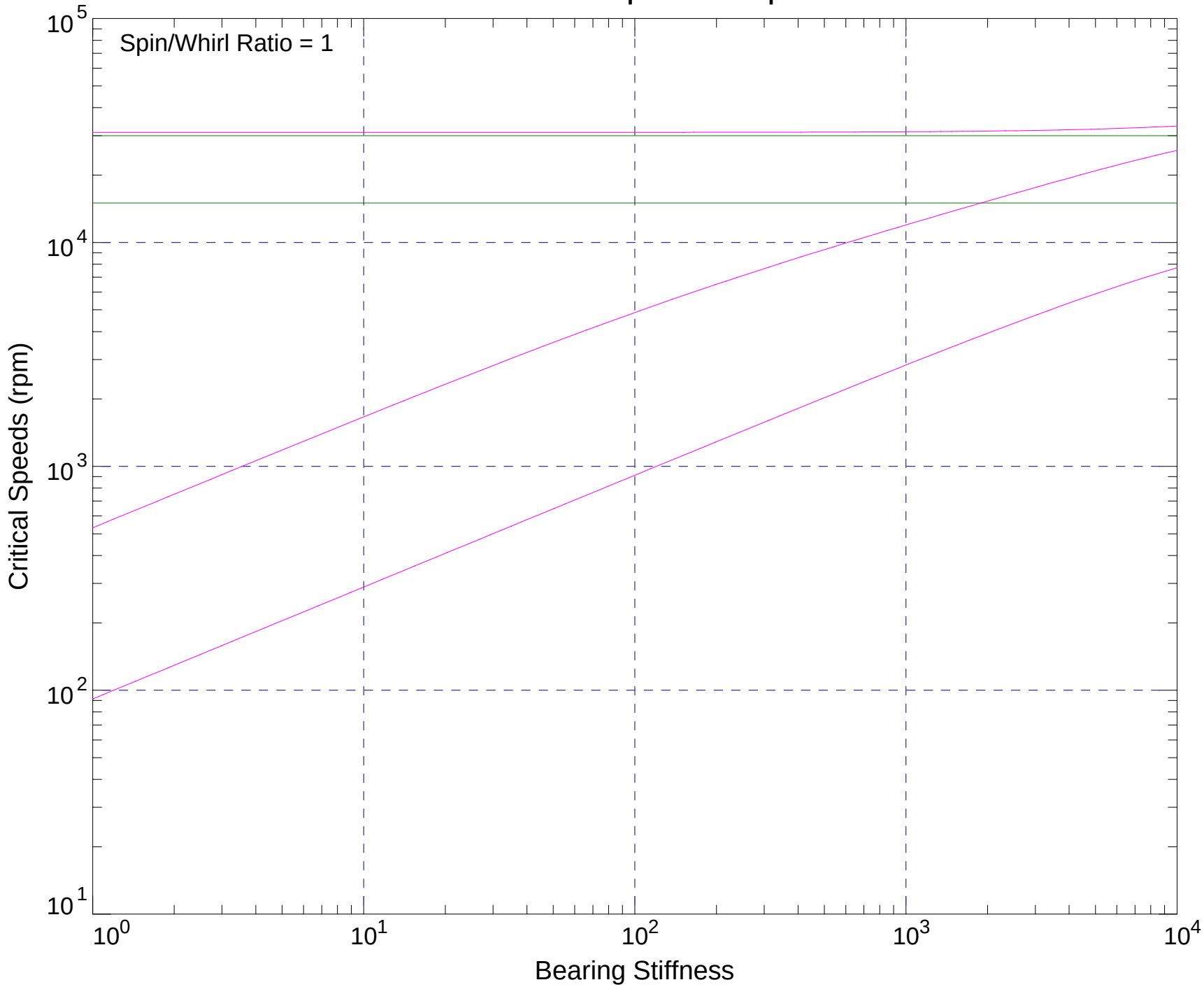

File: C:\DyRoBeS\FlyUps\FlyUps-Rotor.rot

Critical Speed Mode Shape, Mode No.= 1
Spin/Whirl Ratio = 1, Stiffness: (Kxx+Kyy)/2
Critical Speed = 2024 rpm = 33.74 Hz

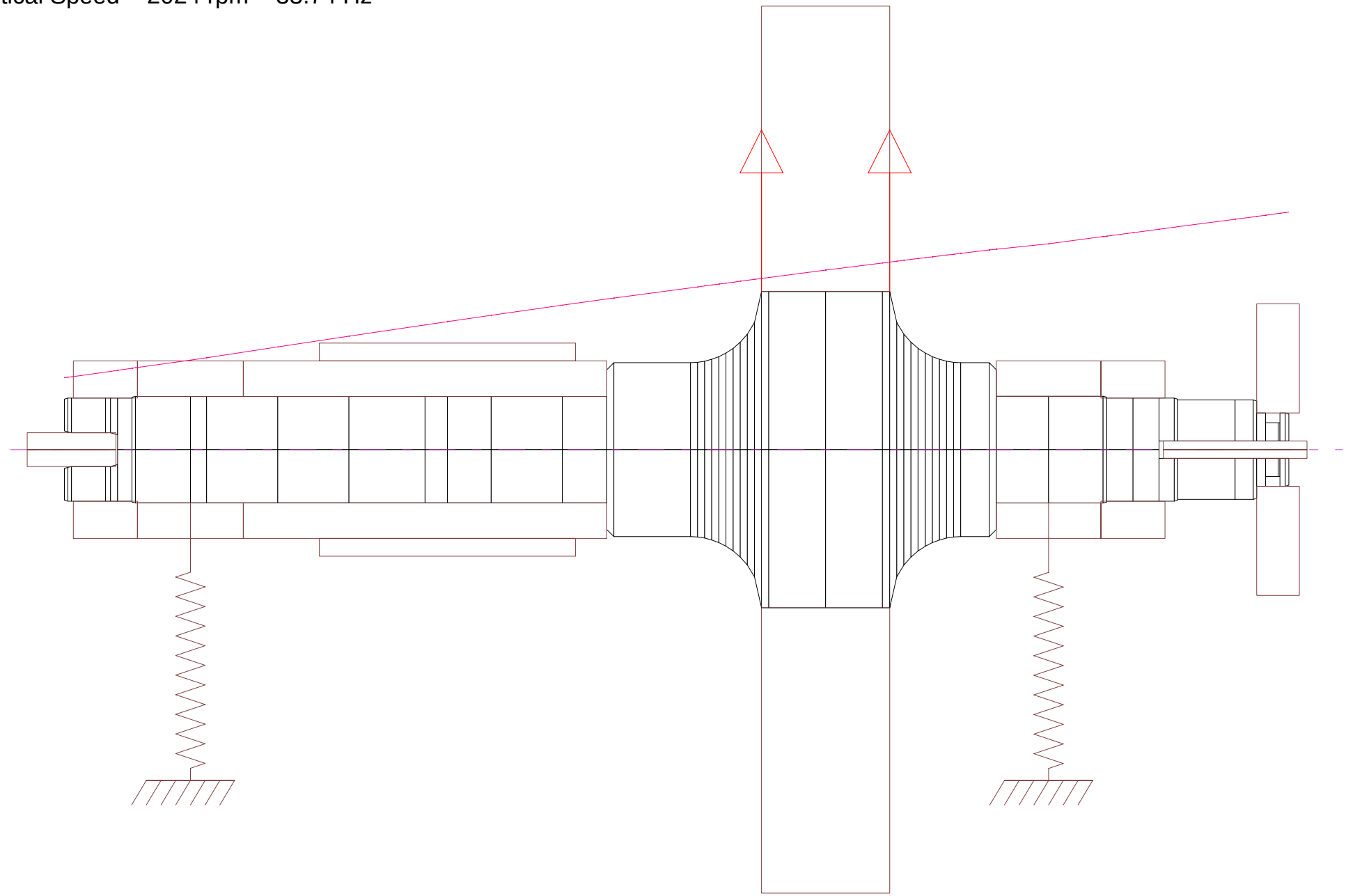

File: C:\DyRoBeS\FlyUps\FlyUps-Rotor.rot

Critical Speed Mode Shape, Mode No.= 2
Spin/Whirl Ratio = 1, Stiffness: (Kxx+Kyy)/2
Critical Speed = 9290 rpm = 154.84 Hz

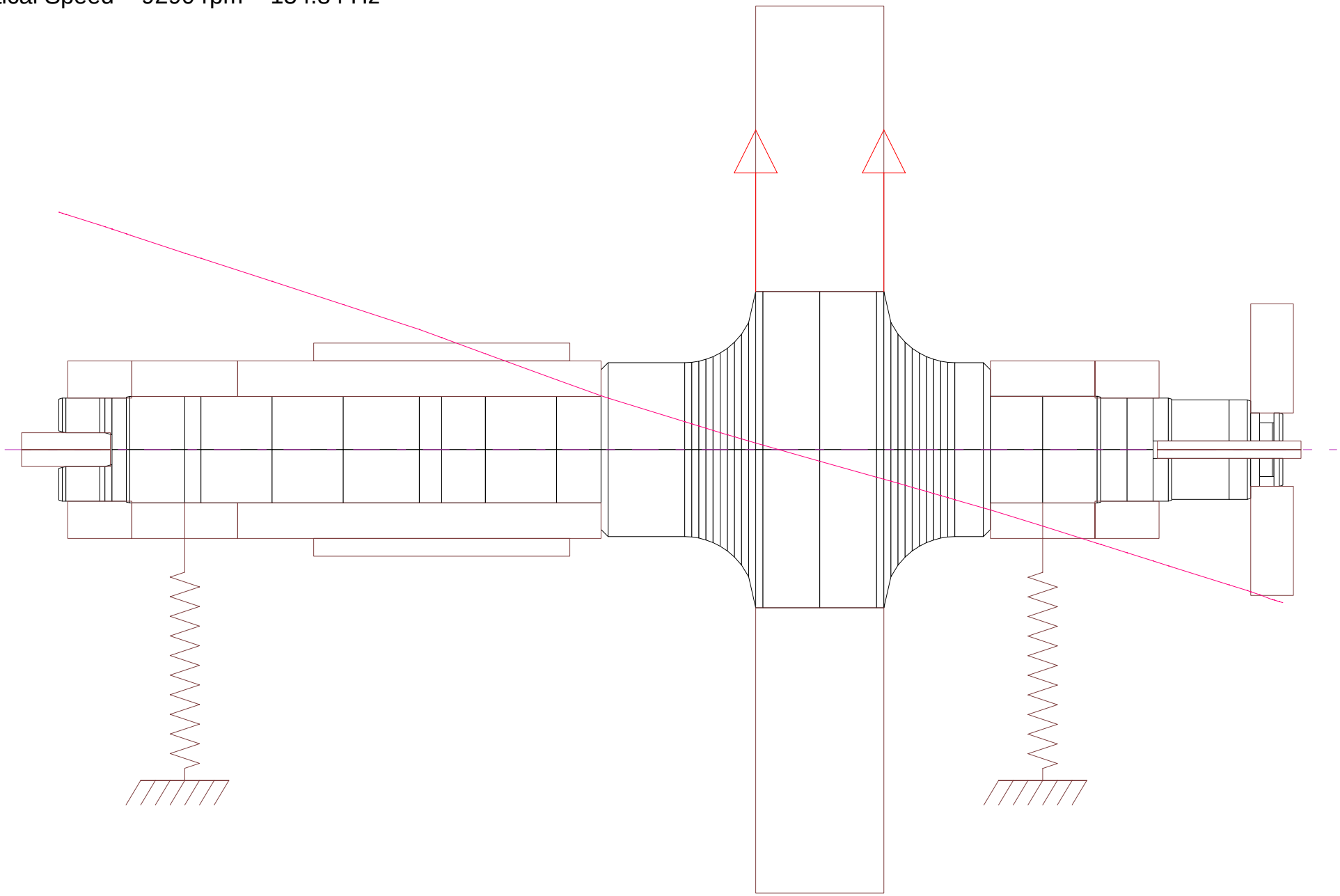

File: C:\DyRoBeS\FlyUps\FlyUps-Rotor.rot

Critical Speed Mode Shape, Mode No.= 3
Spin/Whirl Ratio = 1, Stiffness: (Kxx+Kyy)/2
Critical Speed = 31118 rpm = 518.63 Hz

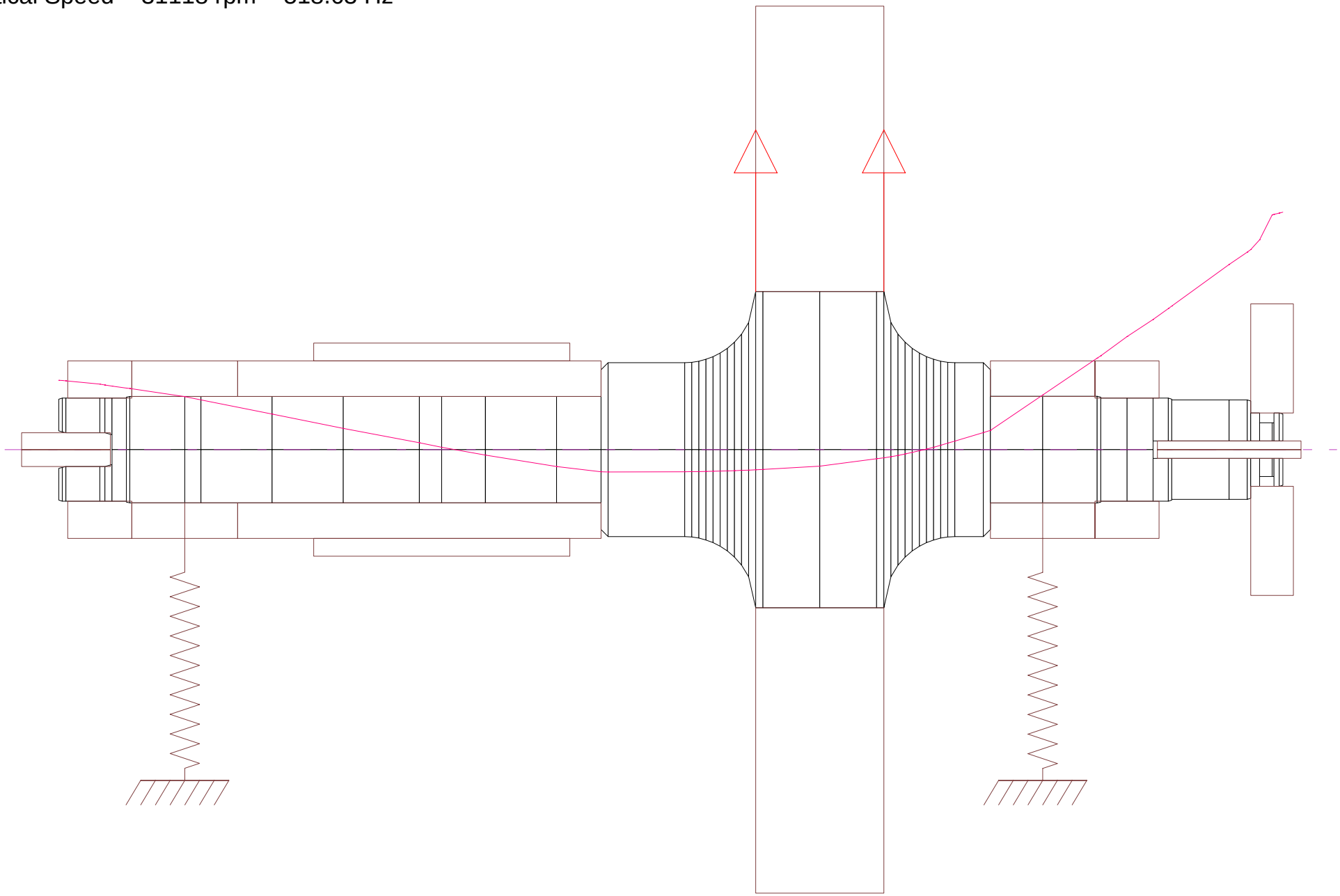

File: C:\DyRoBeS\FlyUps\FlyUps-Rotor.rot

Critical Speed Mode Shape, Mode No.= 4
Spin/Whirl Ratio = 1, Stiffness: (Kxx+Kyy)/2
Critical Speed = 45363 rpm = 756.05 Hz

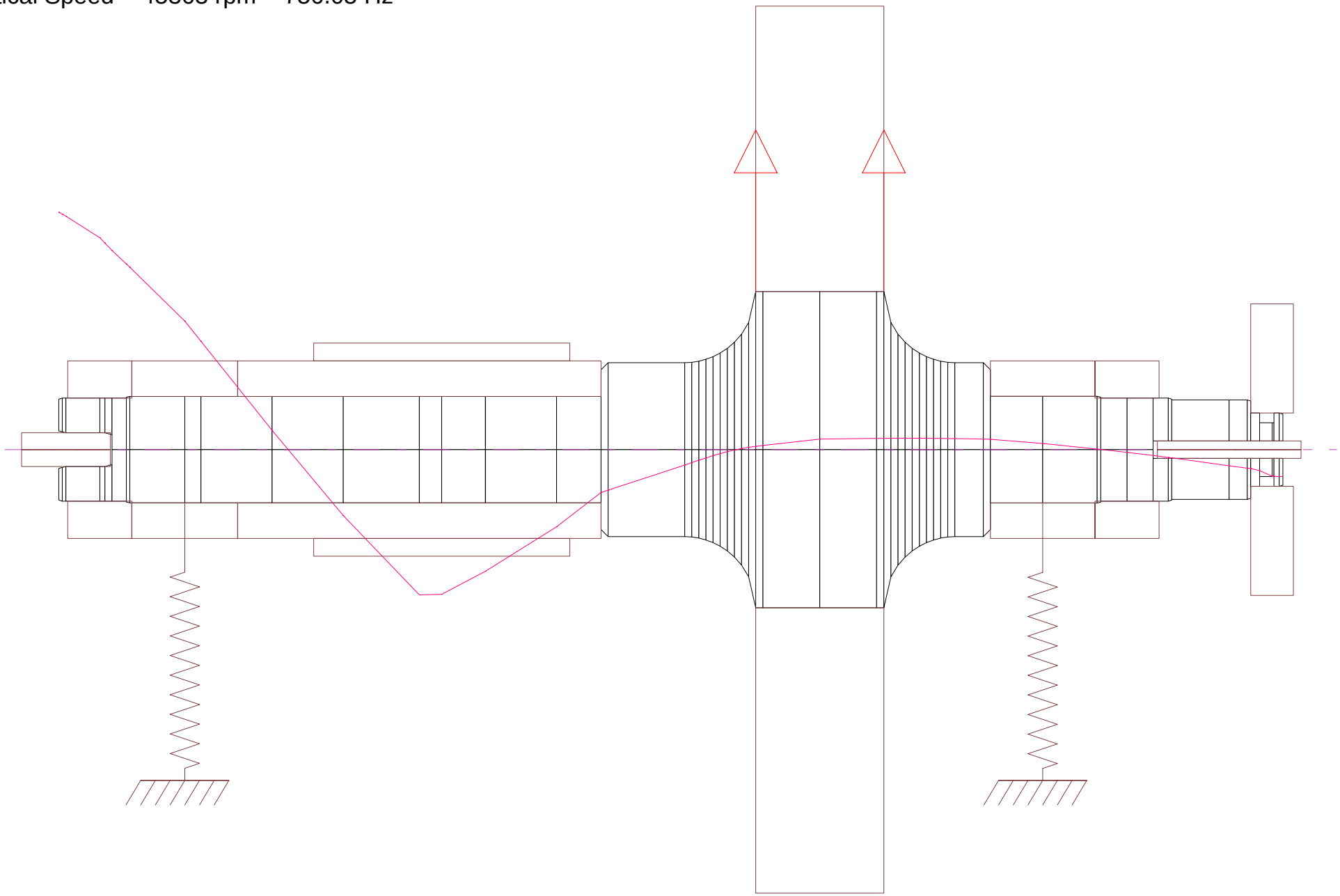

File: C:\DyRoBeS\FlyUps\FlyUps-Rotor.rot

Critical Speed Mode Shape, Mode No.= 5
Spin/Whirl Ratio = 1, Stiffness: (Kxx+Kyy)/2
Critical Speed = 85291 rpm = 1421.52 Hz

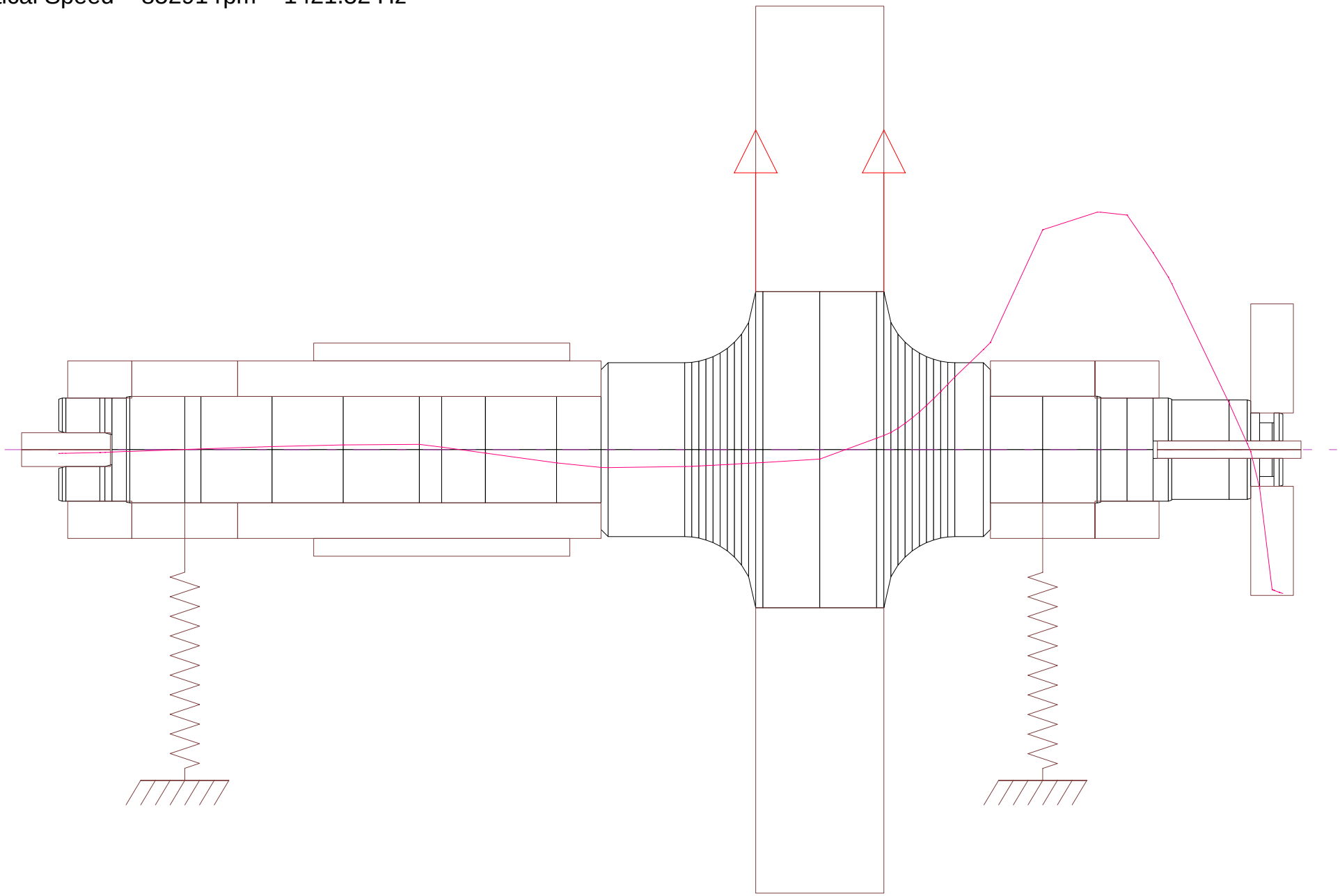

File: C:\DyRoBeS\FlyUps\FlyUps-Rotor.rot

Critical Speed Mode Shape, Mode No.= 6
Spin/Whirl Ratio = 1, Stiffness: (Kxx+Kyy)/2
Critical Speed = 135465 rpm = 2257.76 Hz

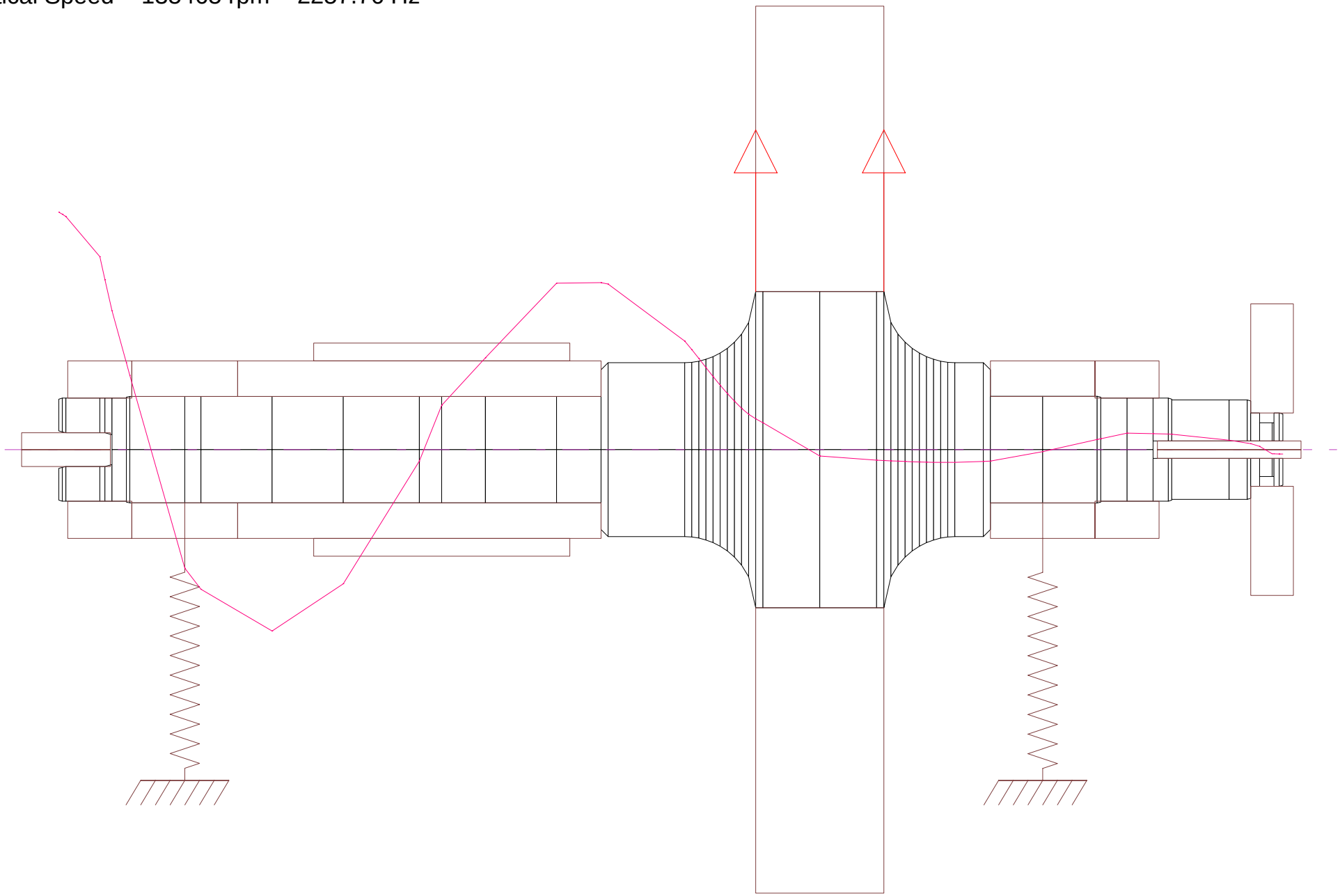

File: C:\DyRoBeS\FlyUps\FlyUps-Rotor.rot

Critical Speed Mode Shape, Mode No.= 7
Spin/Whirl Ratio = 1, Stiffness: (Kxx+Kyy)/2
Critical Speed = 140759 rpm = 2345.99 Hz

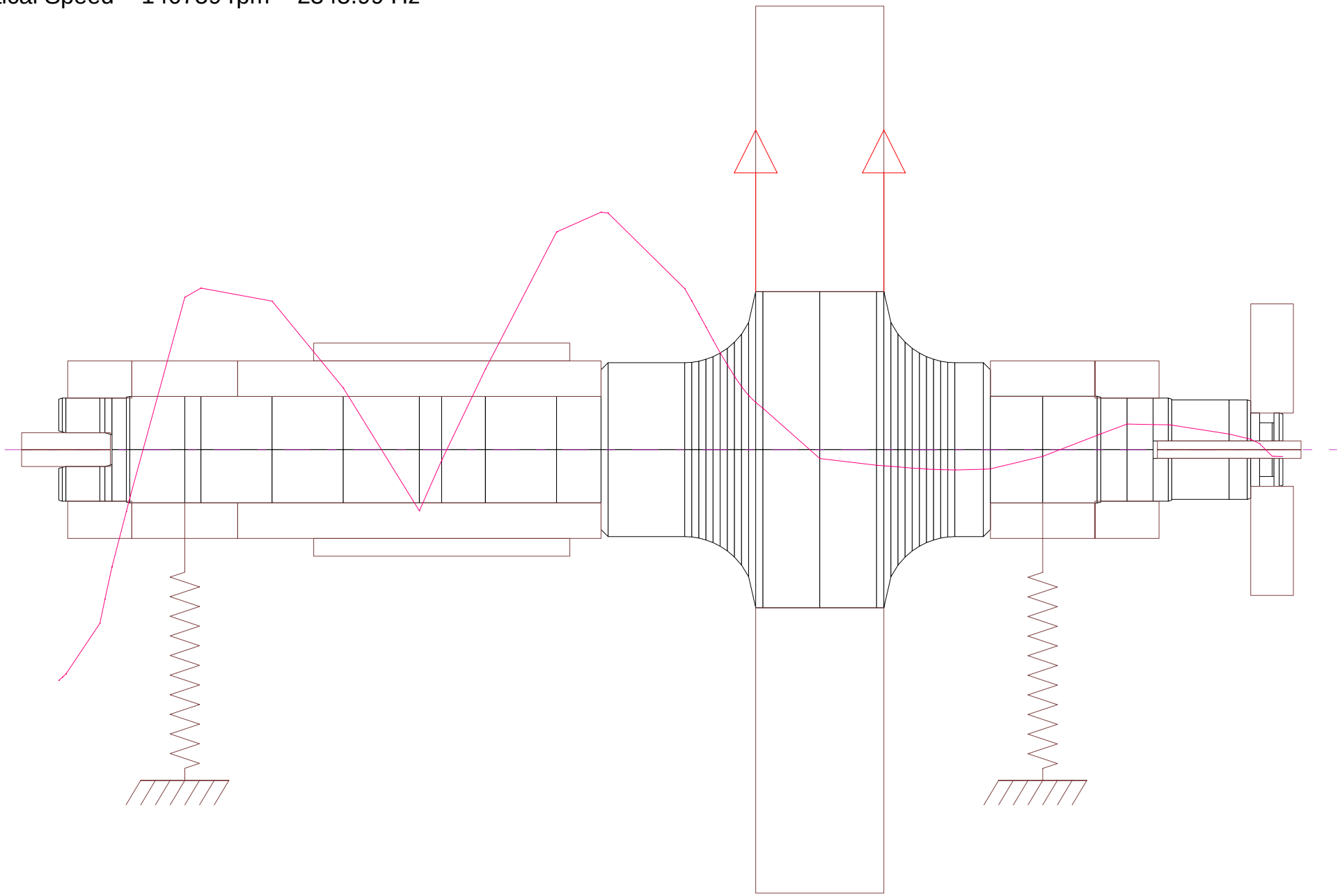

File: C:\DyRoBeS\FlyUps\FlyUps-Rotor.rot

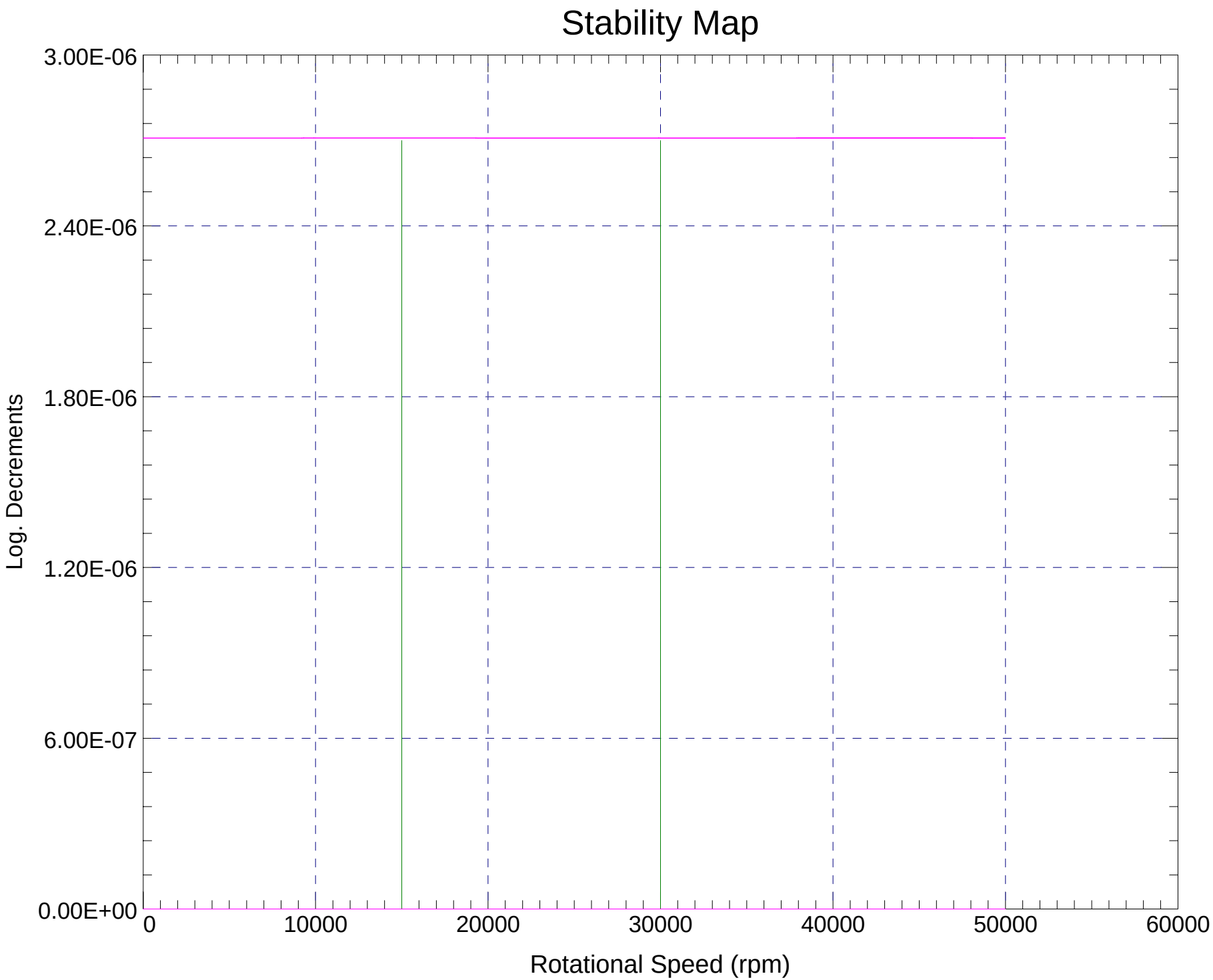

File: C:\DyRoBeS\FlyUps\Mode1\FlyUps-Rotor.rot

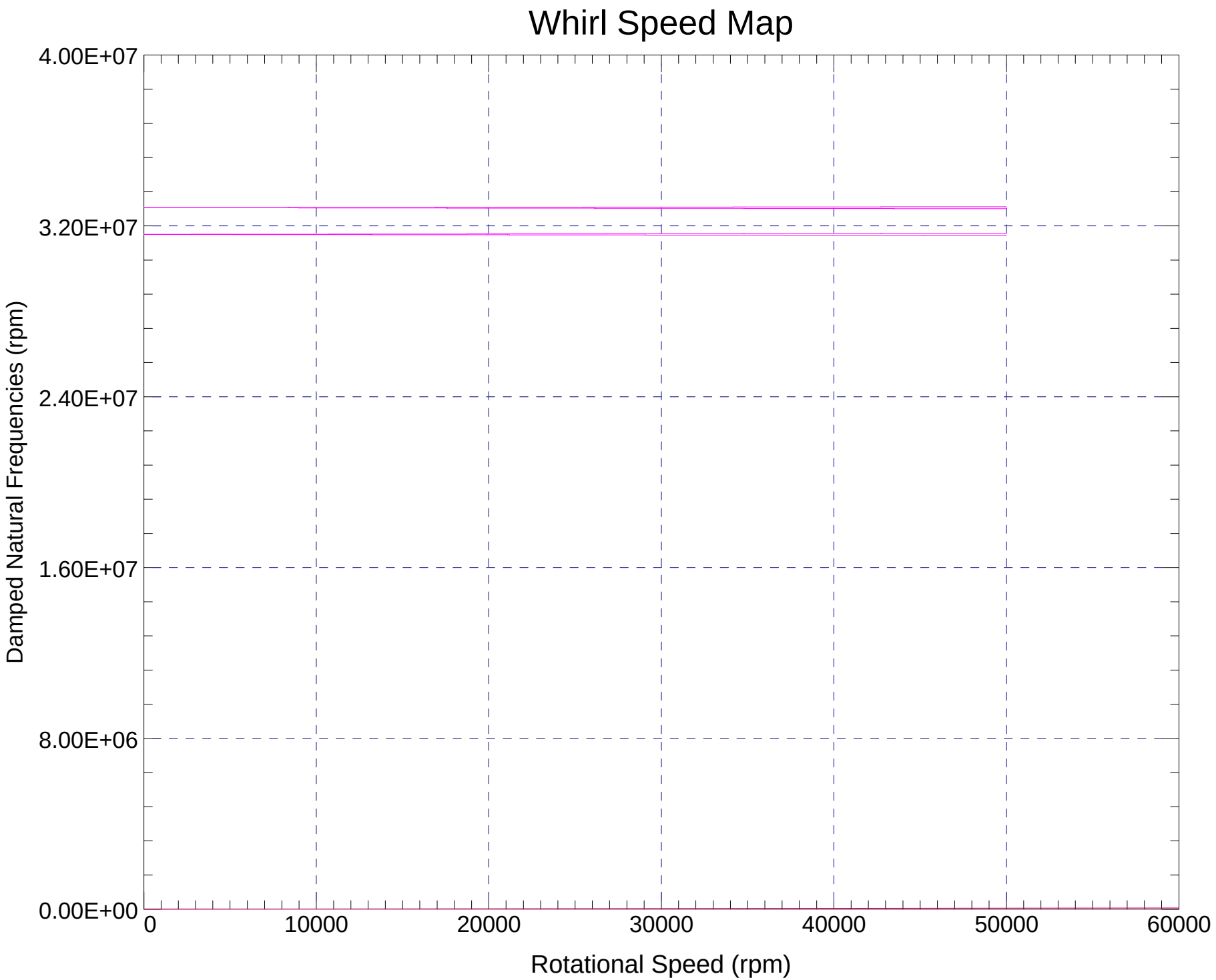

File: C:\DyRoBeS\FlyUps\Mode1\FlyUps-Rotor.rot

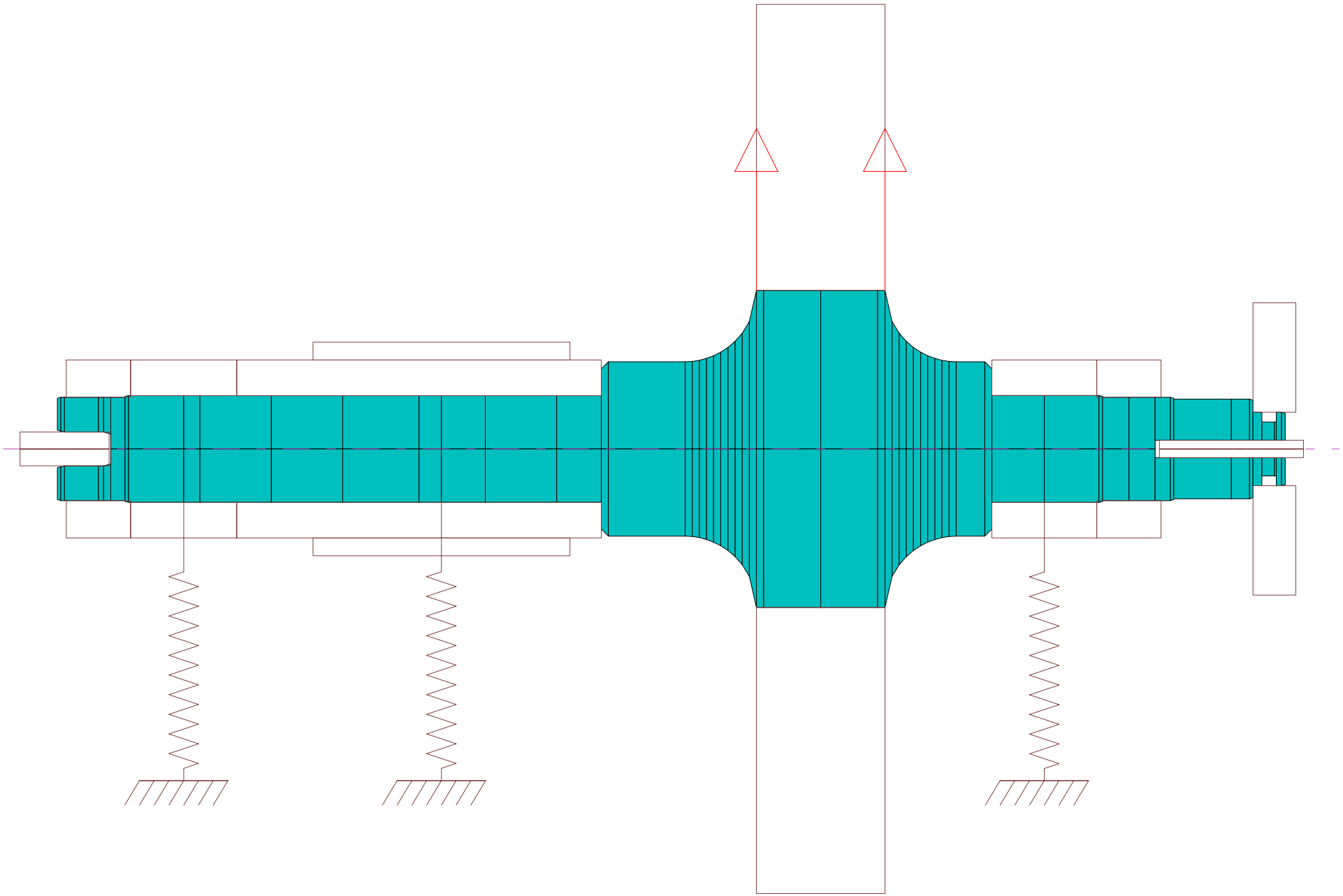

File: C:\DyRoBeS\FlyUps\Mode1\FlyUps-Rotor.rot

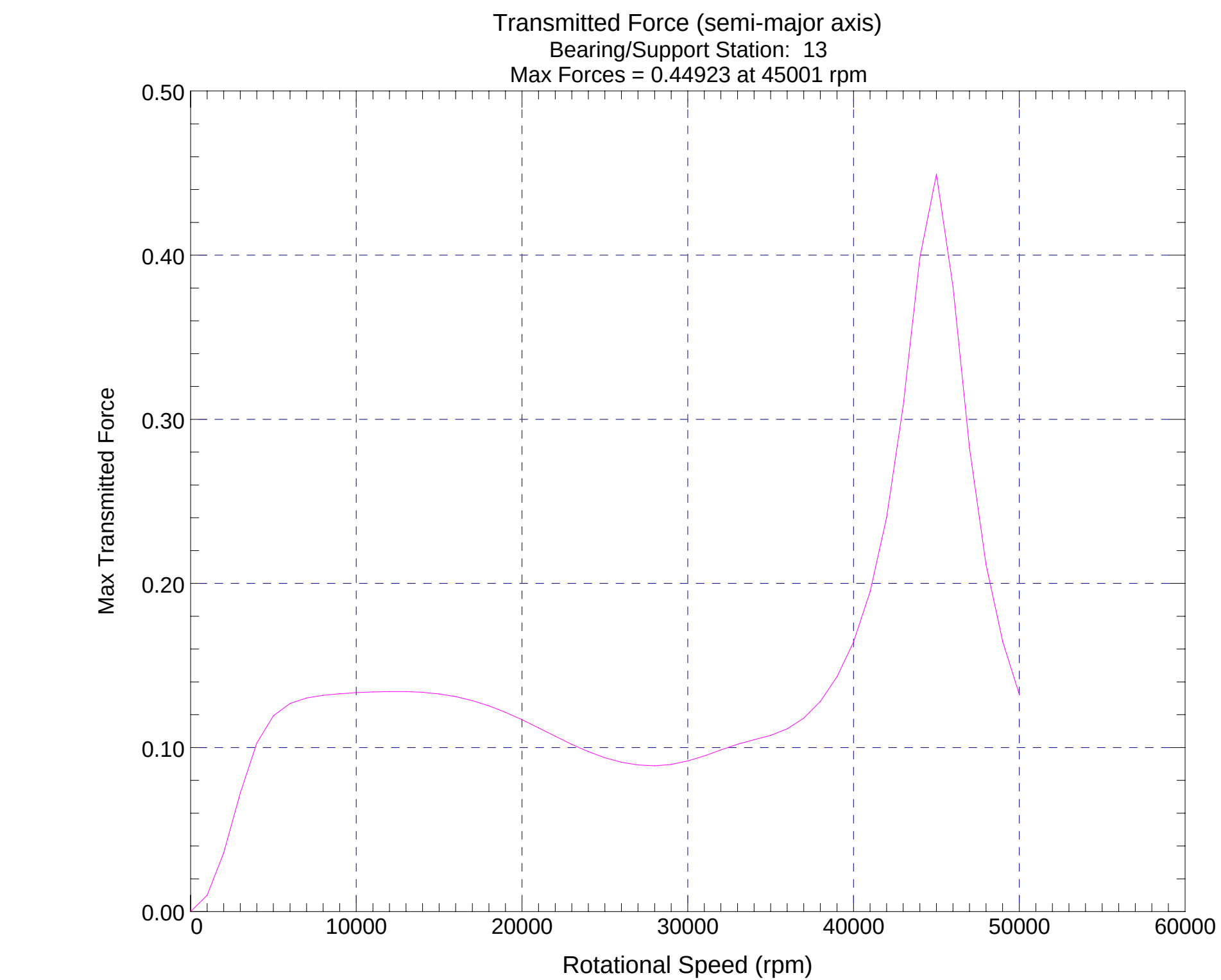

File: C:\DyRoBeS\FlyUps\Mode1\FlyUps-Rotor.rot

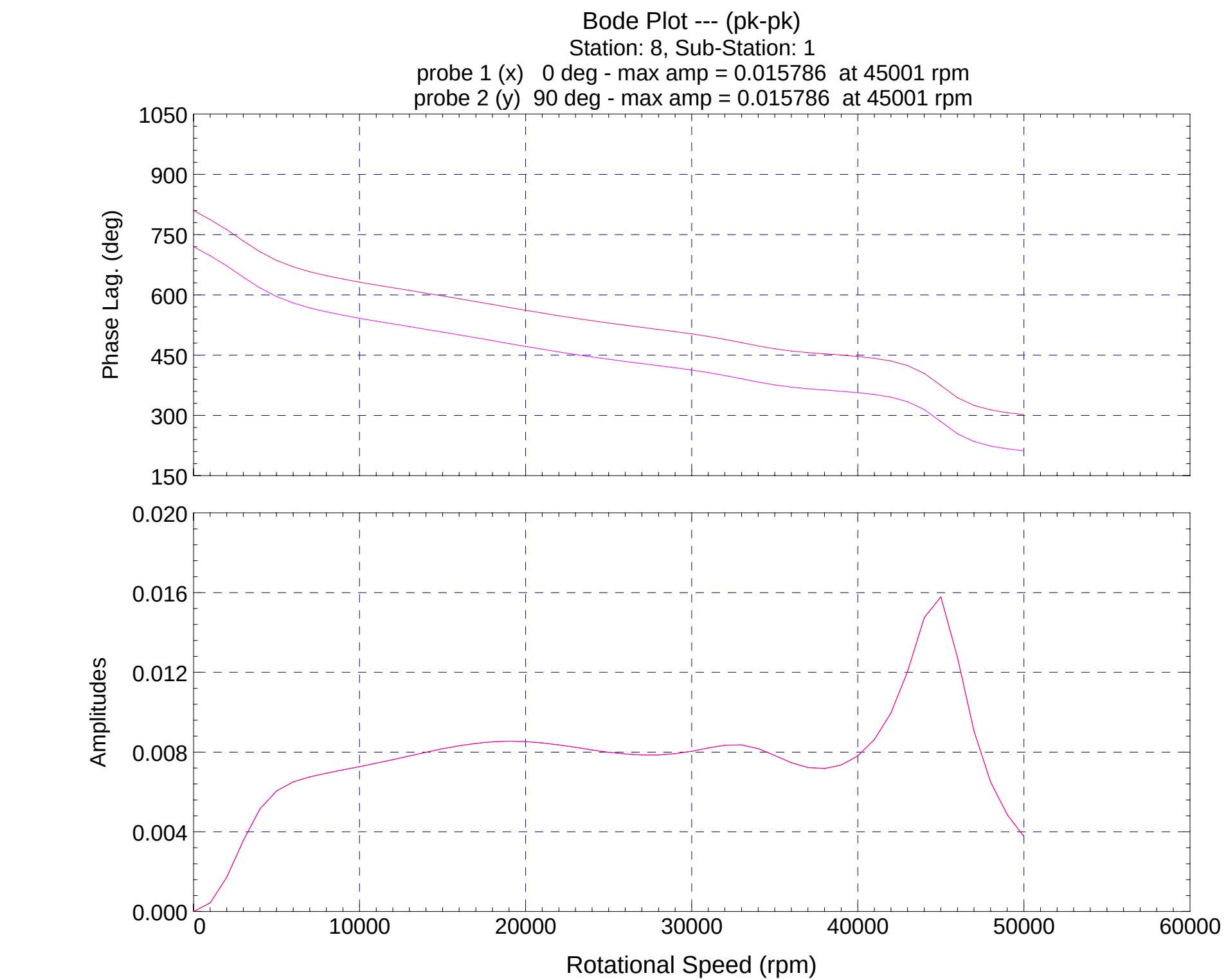

File: C:\DyRoBeS\FlyUps\Mode1\FlyUps-Rotor.rot

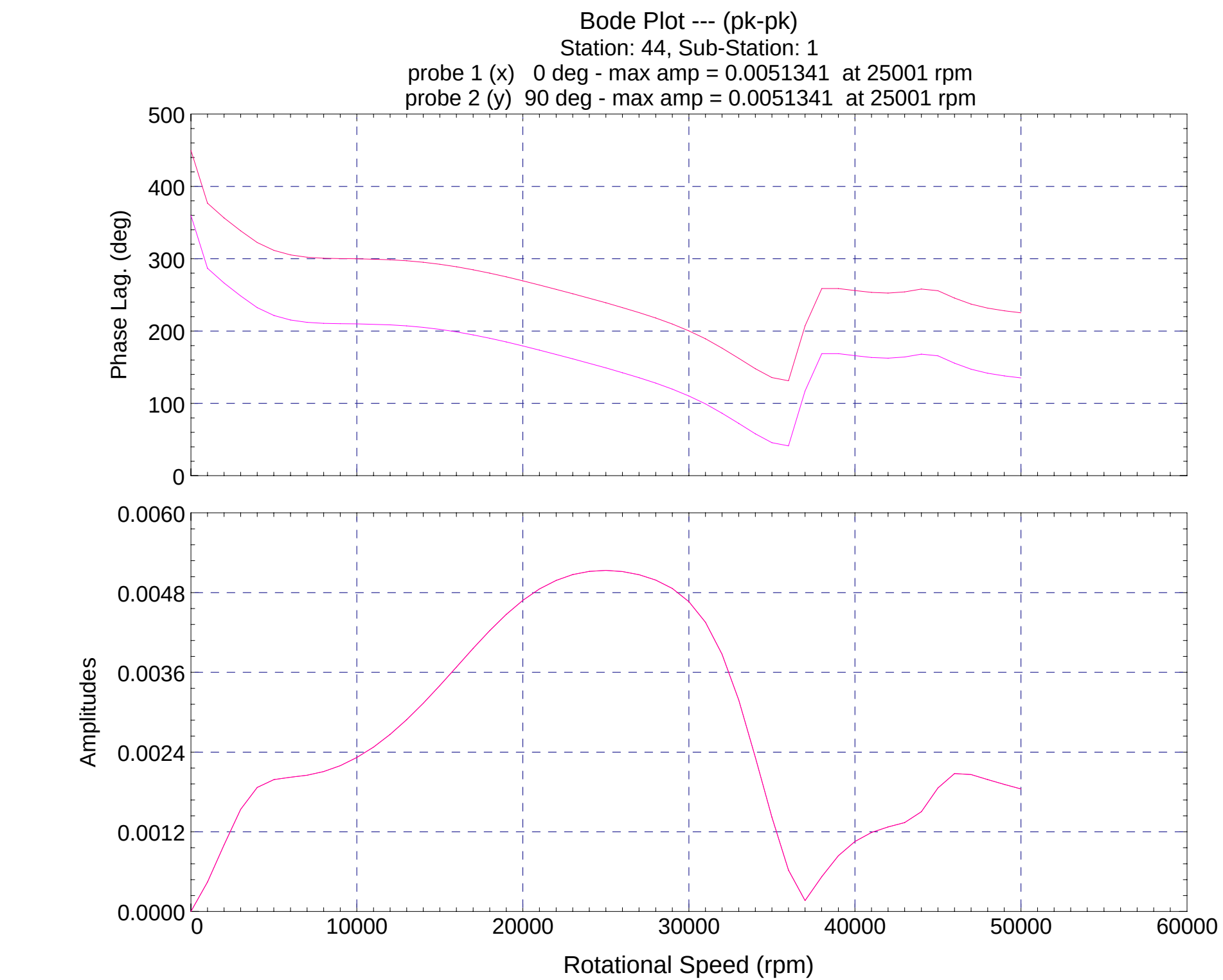

File: C:\DyRoBeS\FlyUps\Mode1\FlyUps-Rotor.rot

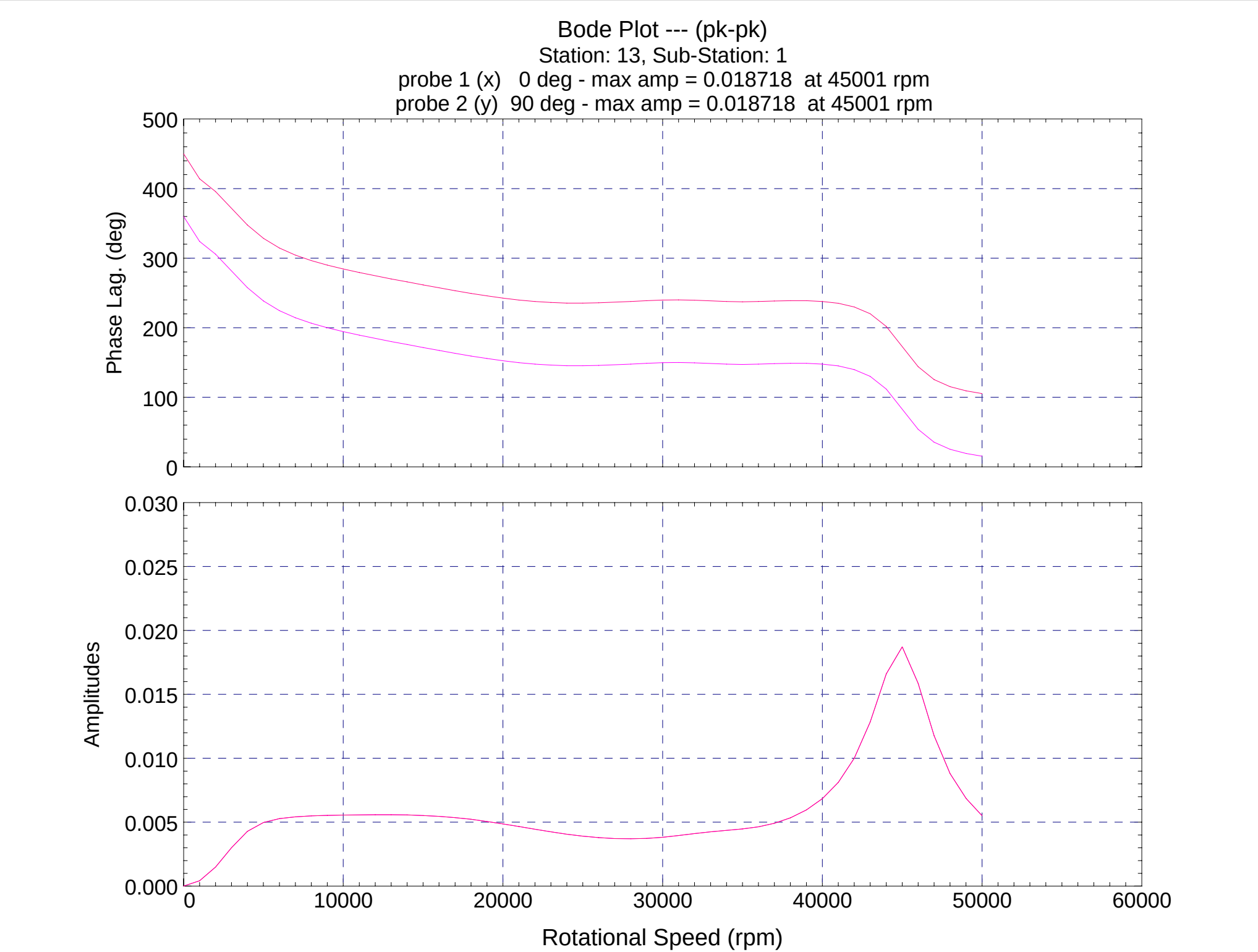

File: C:\DyRoBeS\FlyUps\Mode1\FlyUps-Rotor.rot

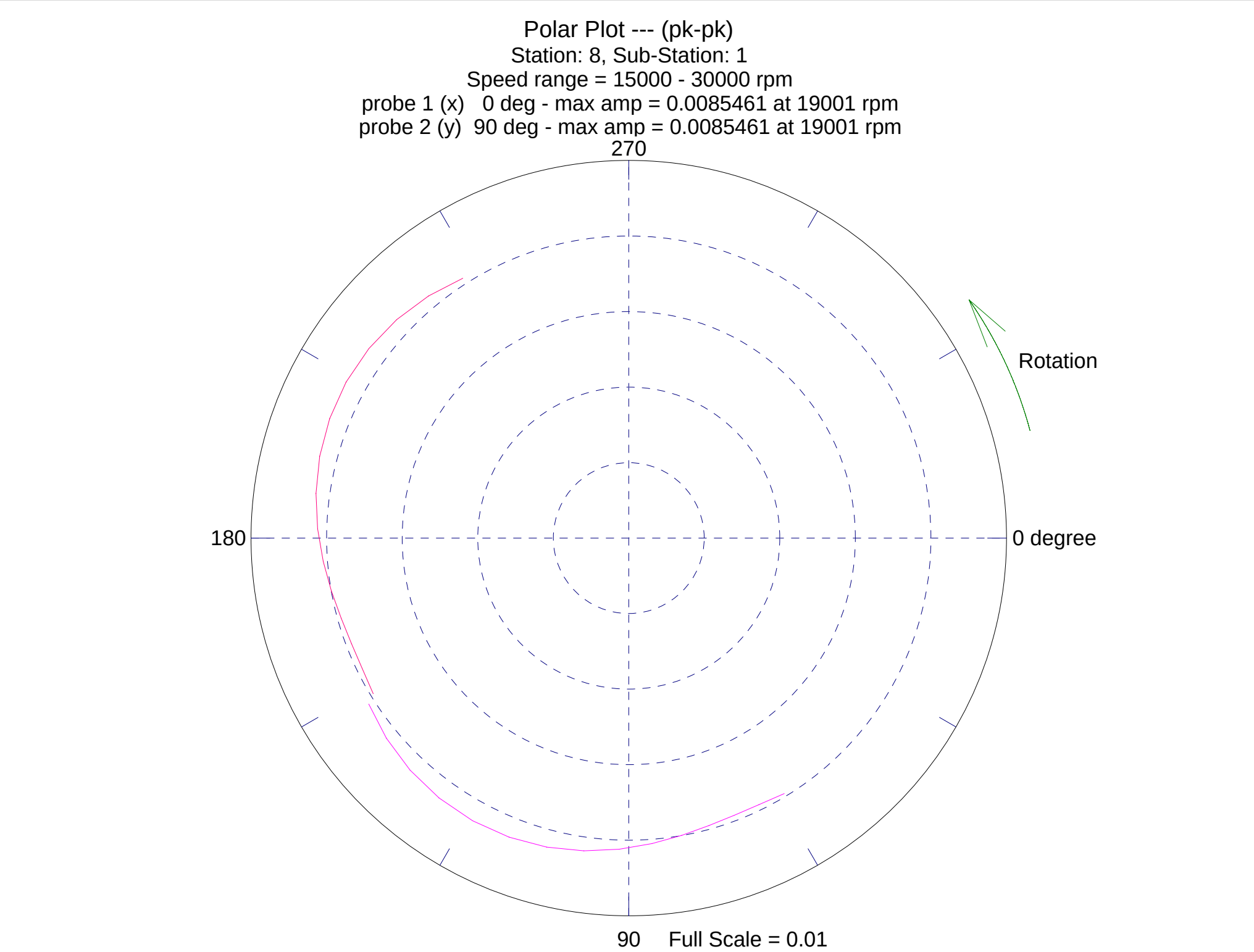
Polar Plot --- (pk-pk)
Station: 8, Sub-Station: 1
Speed range = 15000 - 30000 rpm
probe 1 (x) 0 deg - max amp = 0.0085461 at 19001 rpm
probe 2 (y) 90 deg - max amp = 0.0085461 at 19001 rpm
270
180
0 degree
90
Full Scale = 0.01
Rotation
File: C:\DyRoBeS\FlyUps\Mode1\FlyUps-Rotor.rot

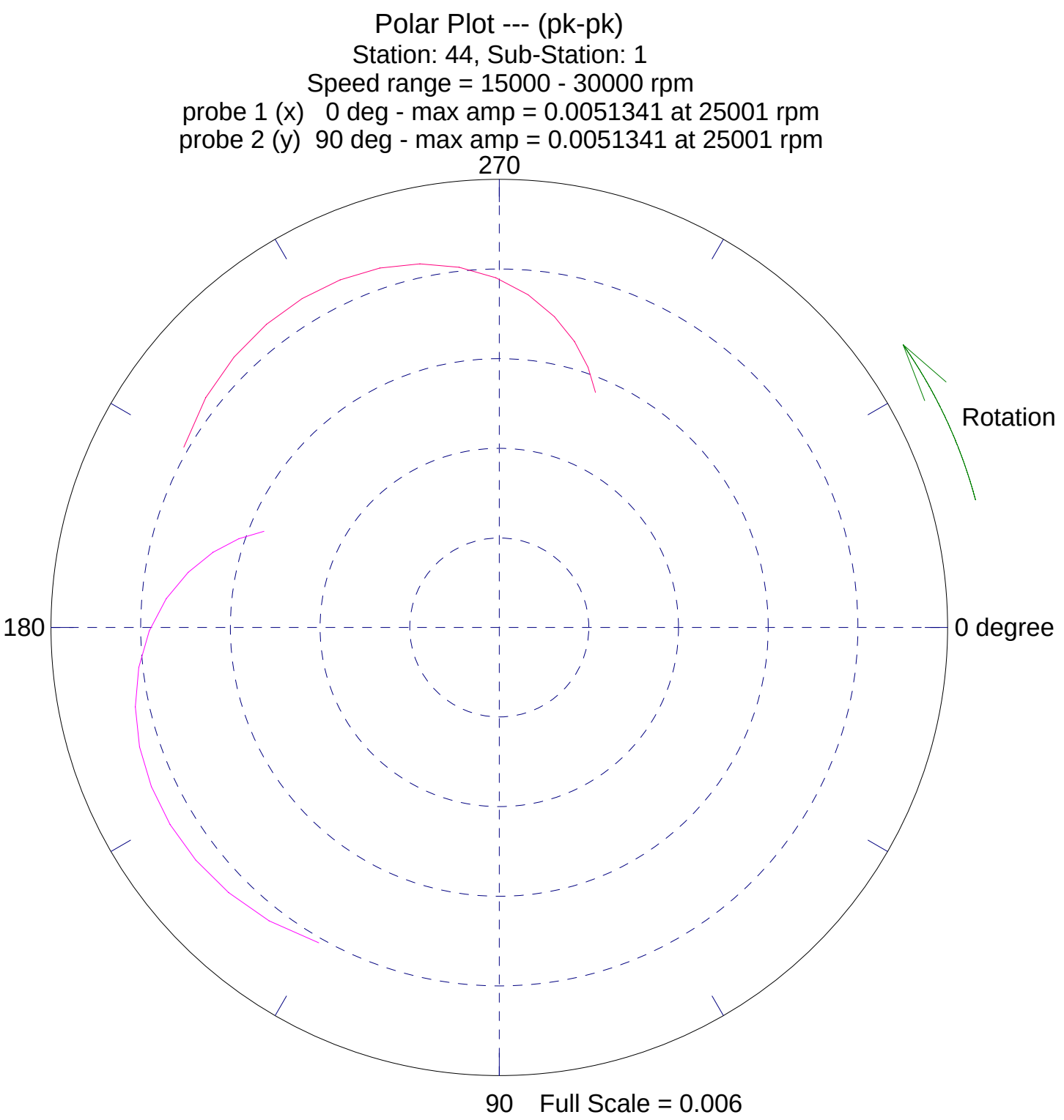

File: C:\DyRoBeS\FlyUps\Mode1\FlyUps-Rotor.rot

Polar Plot --- (pk-pk)
Station: 13, Sub-Station: 1
Speed range = 15000 - 30000 rpm
probe 1 (x) 0 deg - max amp = 0.0055271 at 15001 rpm
probe 2 (y) 90 deg - max amp = 0.0055271 at 15001 rpm

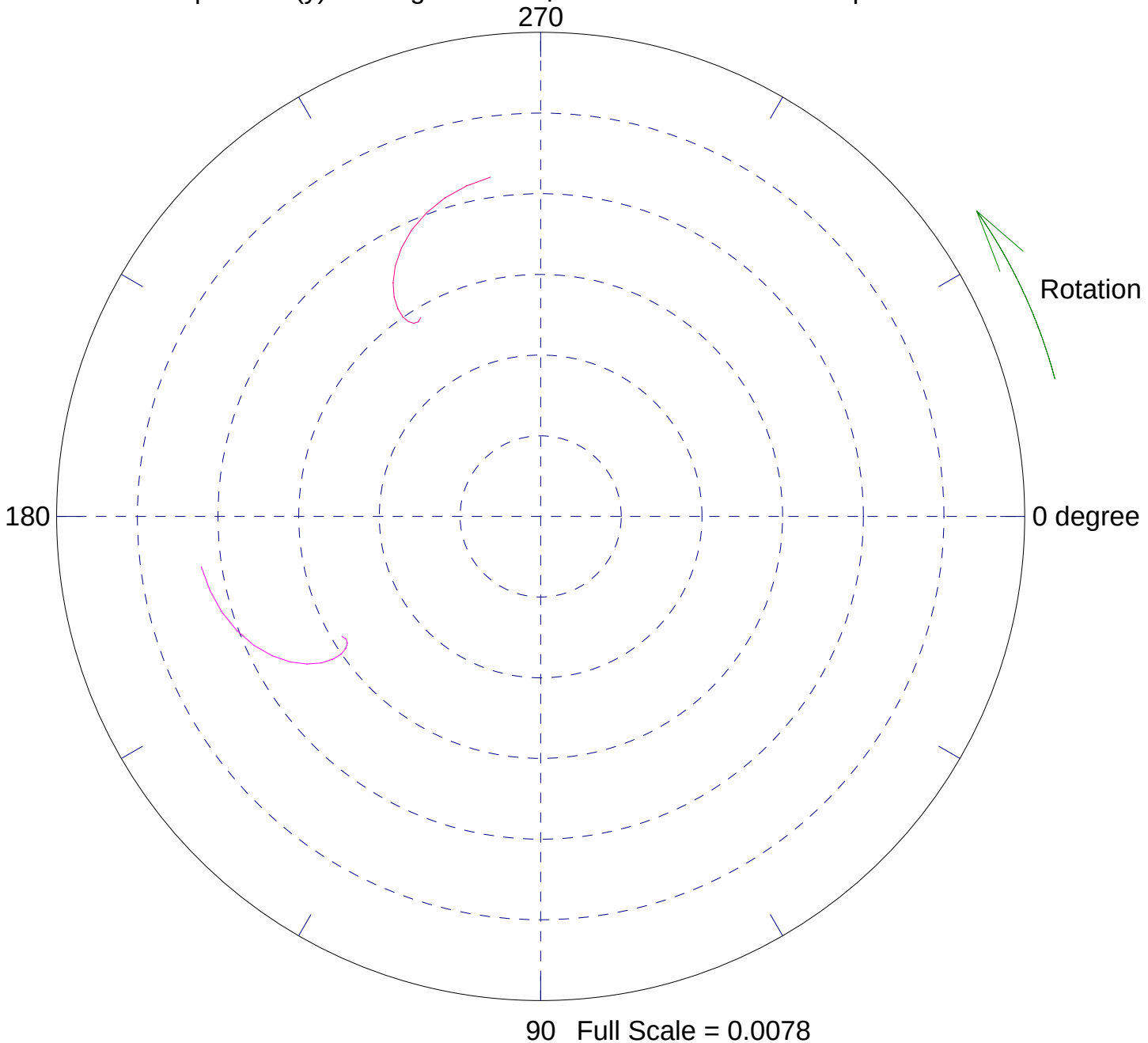

File: C:\DyRoBeS\FlyUps\Mode1\FlyUps-Rotor.rot

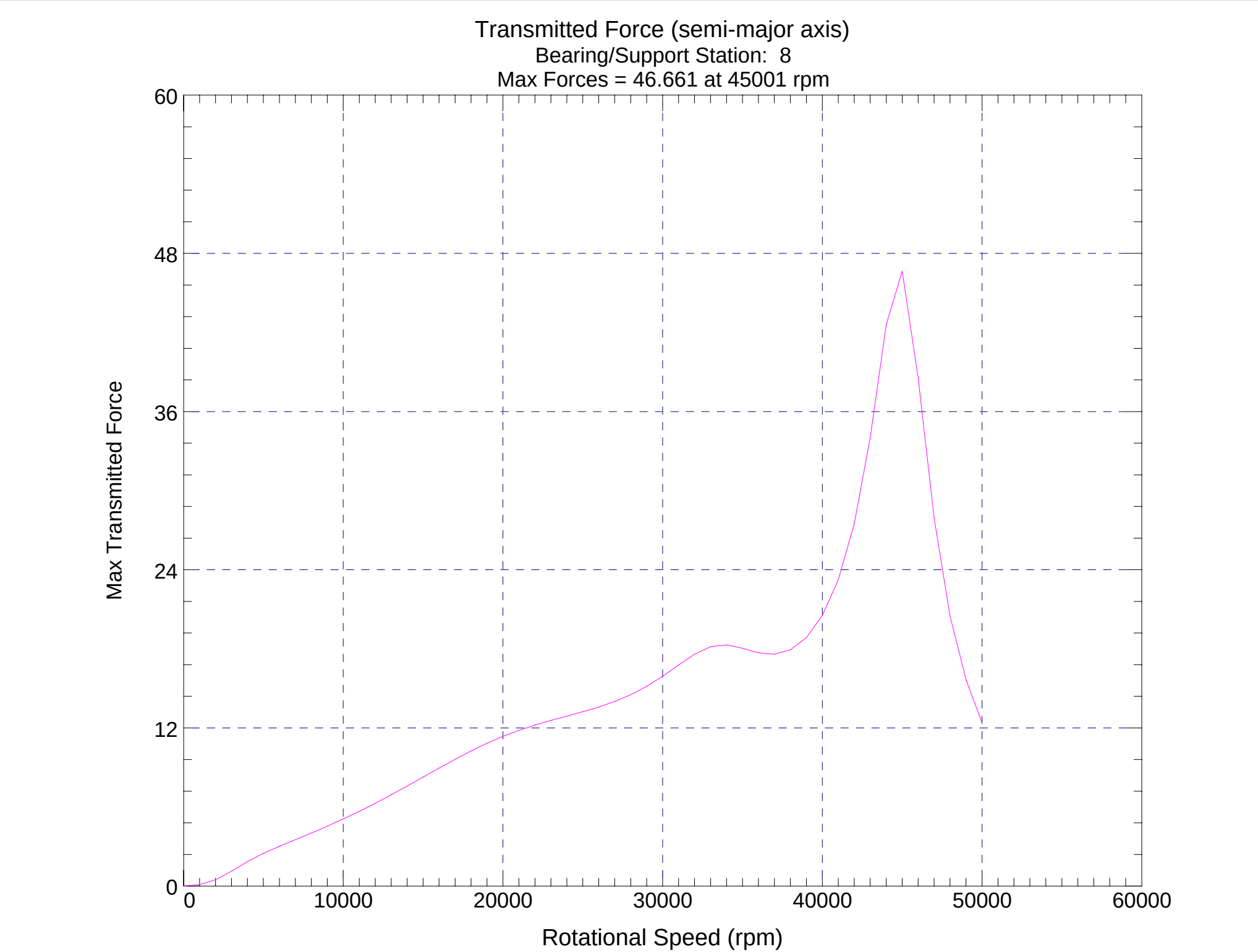

File: C:\DyRoBeS\FlyUps\Mode1\FlyUps-Rotor.rot

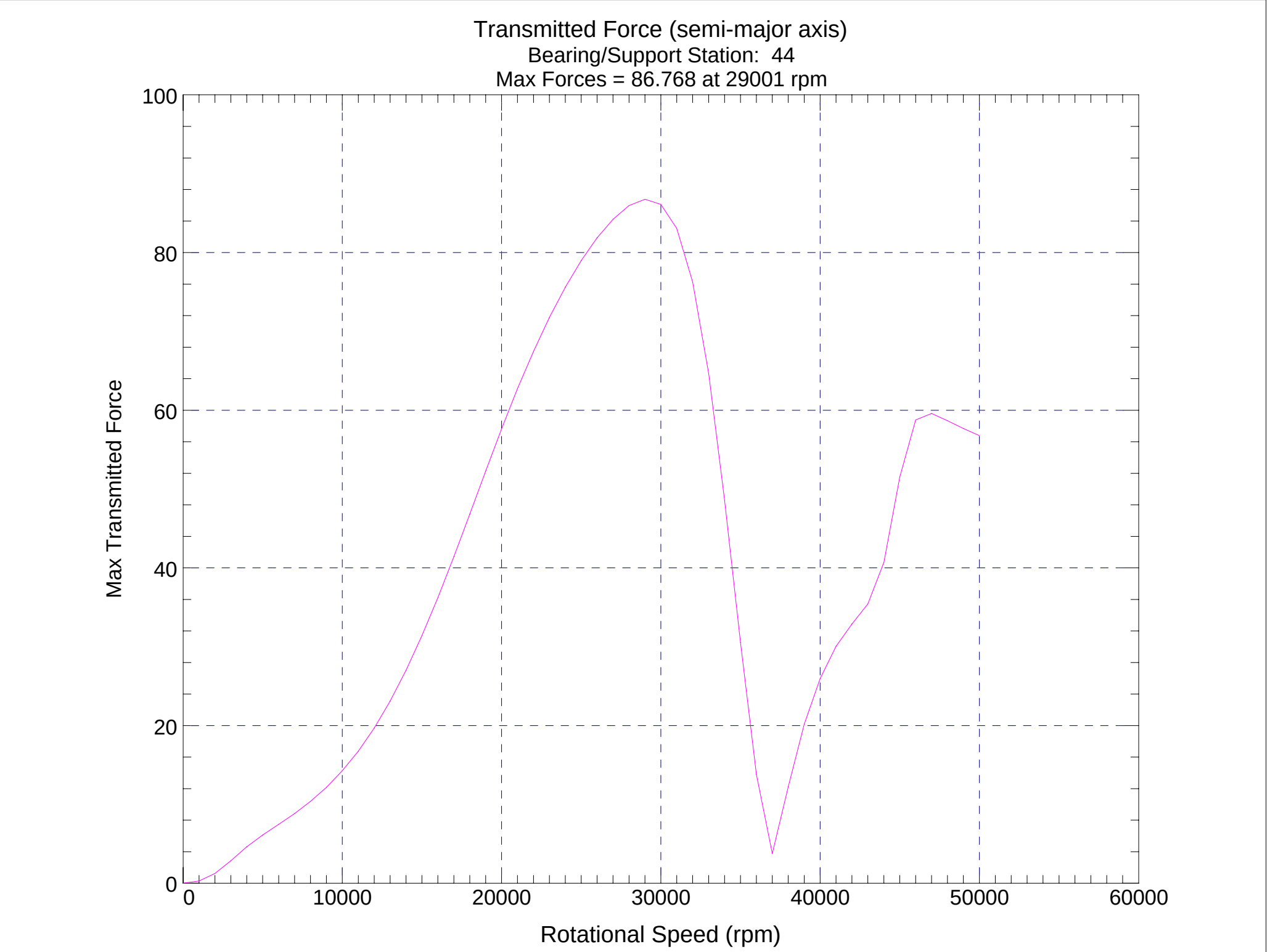

File: C:\DyRoBeS\FlyUps\Mode1\FlyUps-Rotor.rot

Response:Displacement -- Semi-Major Axis

Station: 5 , Sub-Stn: 1, Peak Response = 0.012172 at 45001 rpm

Station: 8 , Sub-Stn: 1, Peak Response = 0.0078929 at 45001 rpm

Station: 13, Sub-Stn: 1, Peak Response = 0.0093590 at 45001 rpm

Station: 44, Sub-Stn: 1, Peak Response = 0.0025671 at 25001 rpm

Station: 47, Sub-Stn: 1, Peak Response = 0.0043273 at 31001 rpm

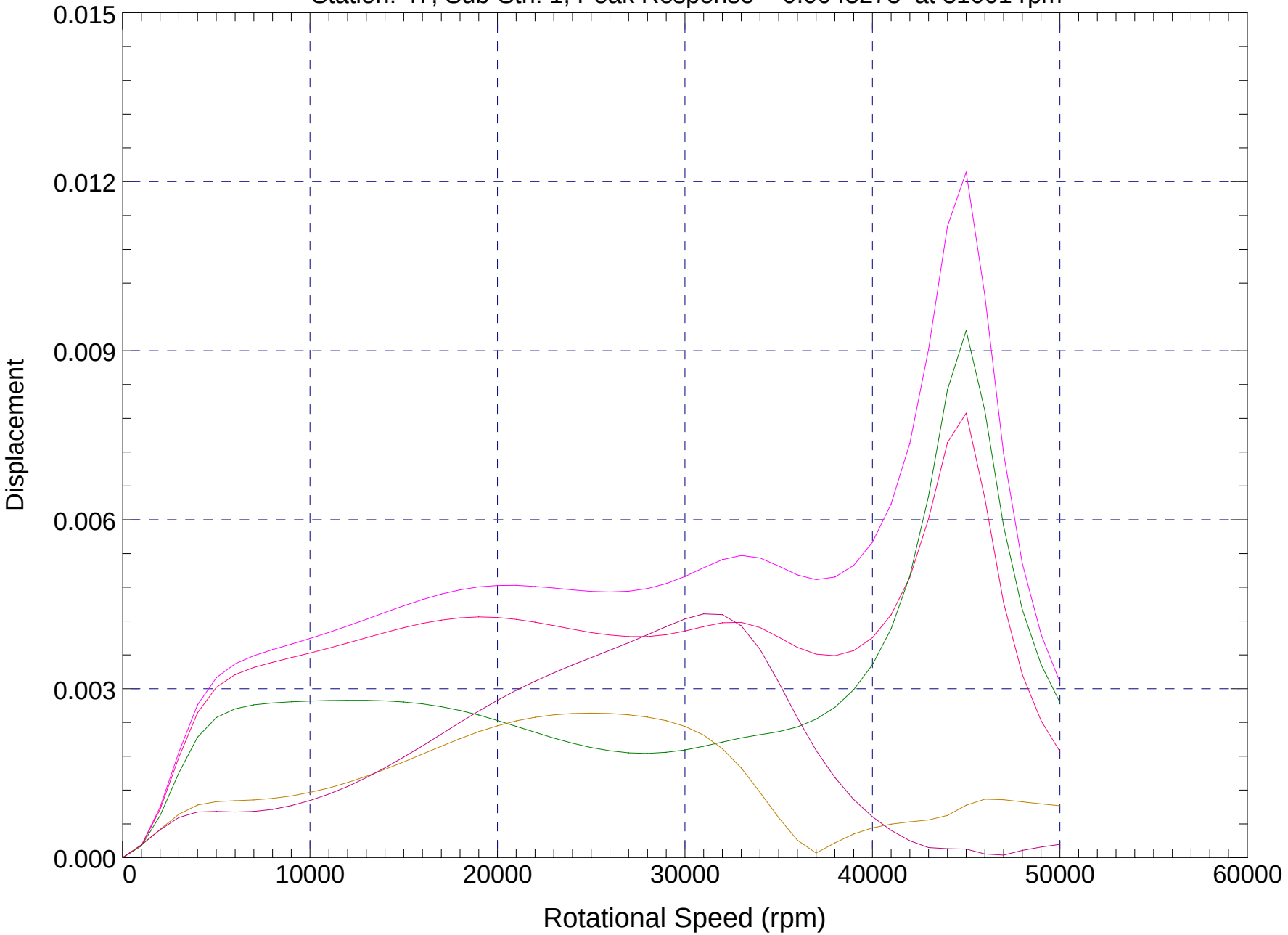

File: C:\DyRoBeS\FlyUps\Mode1\FlyUps-Rotor.rot

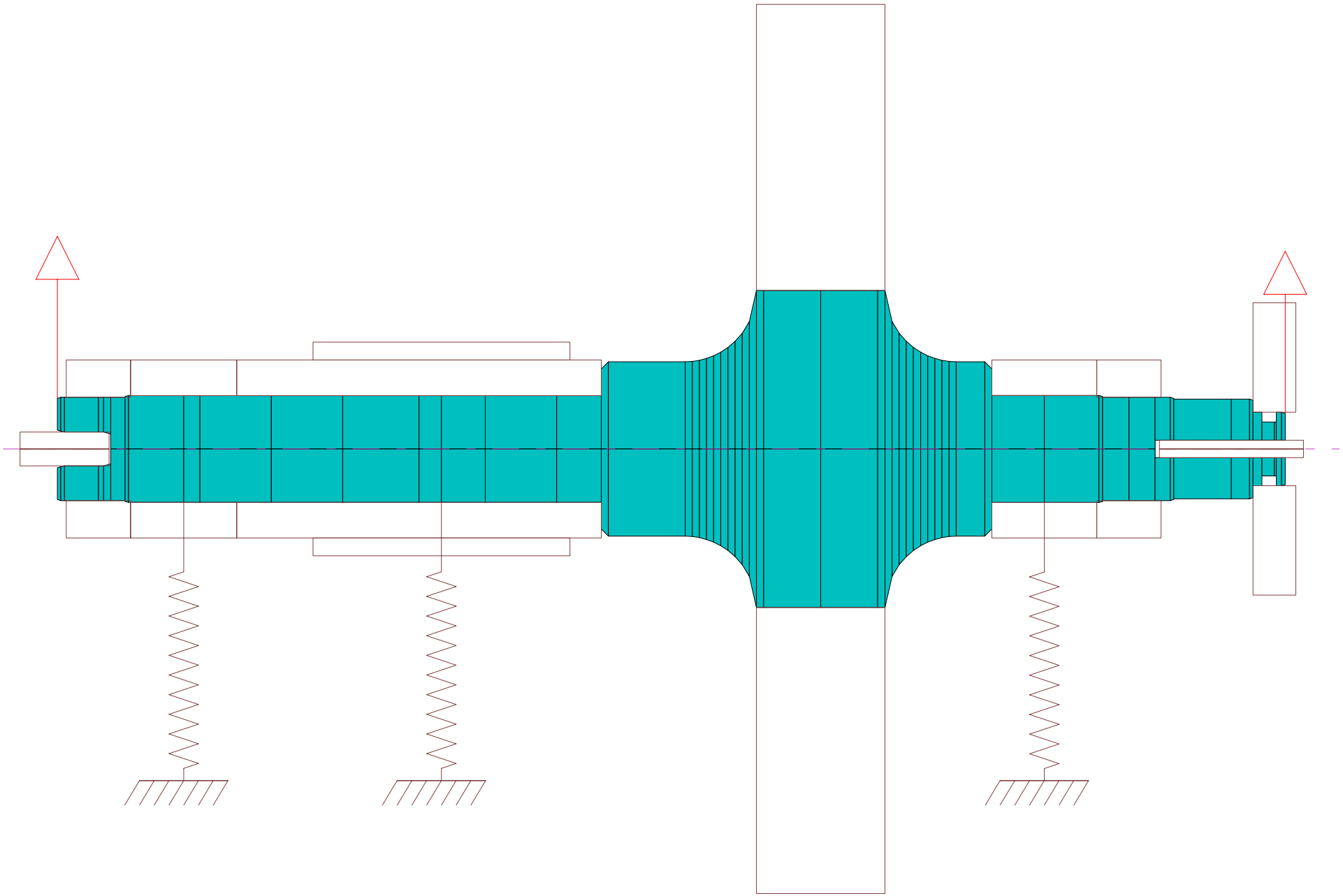

File: C:\DyRoBeS\FlyUps\Mode2(analysis)\FlyUps-rotor.rot

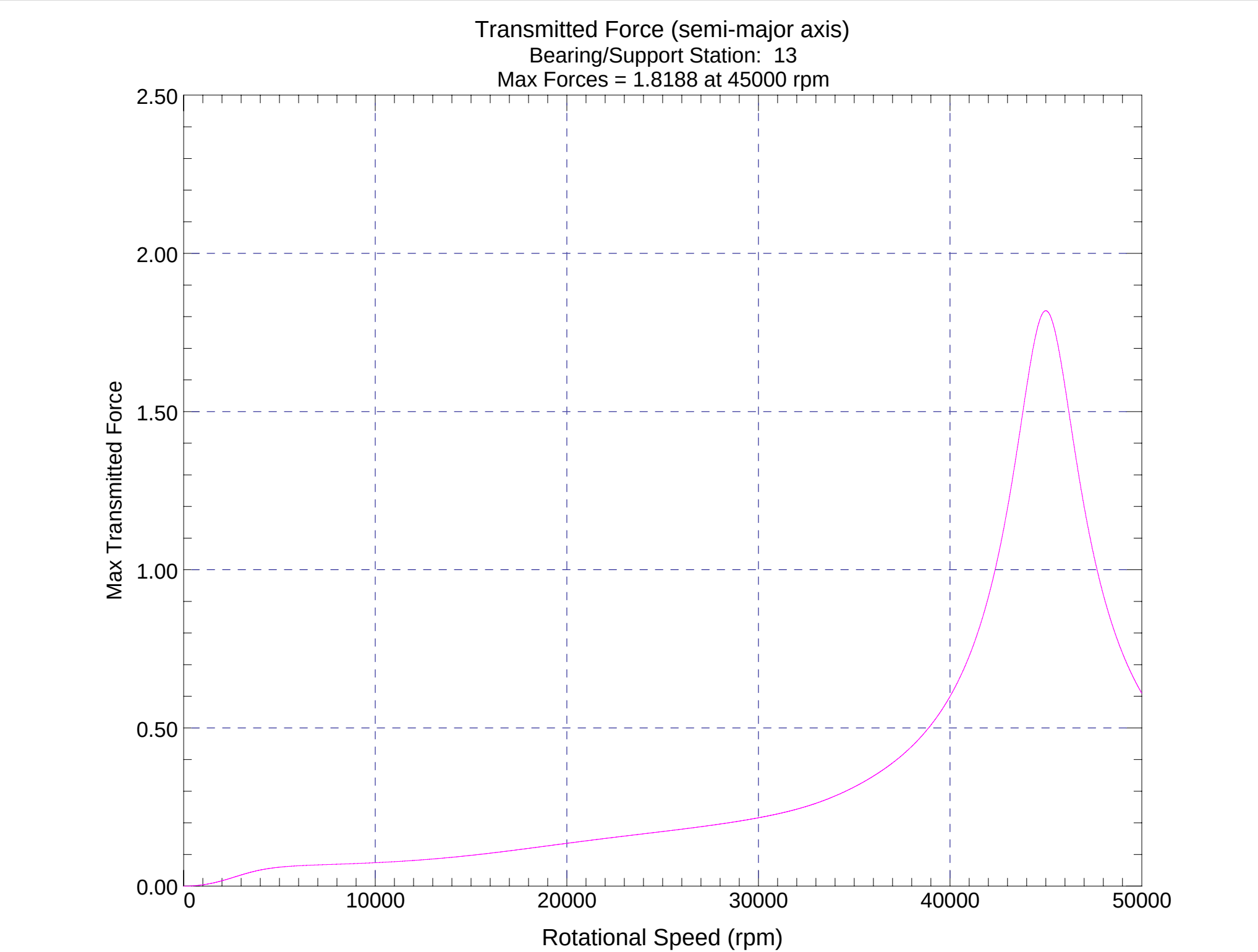

File: C:\DyRoBeS\FlyUps\Mode2(analysis)\FlyUps-rotor.rot

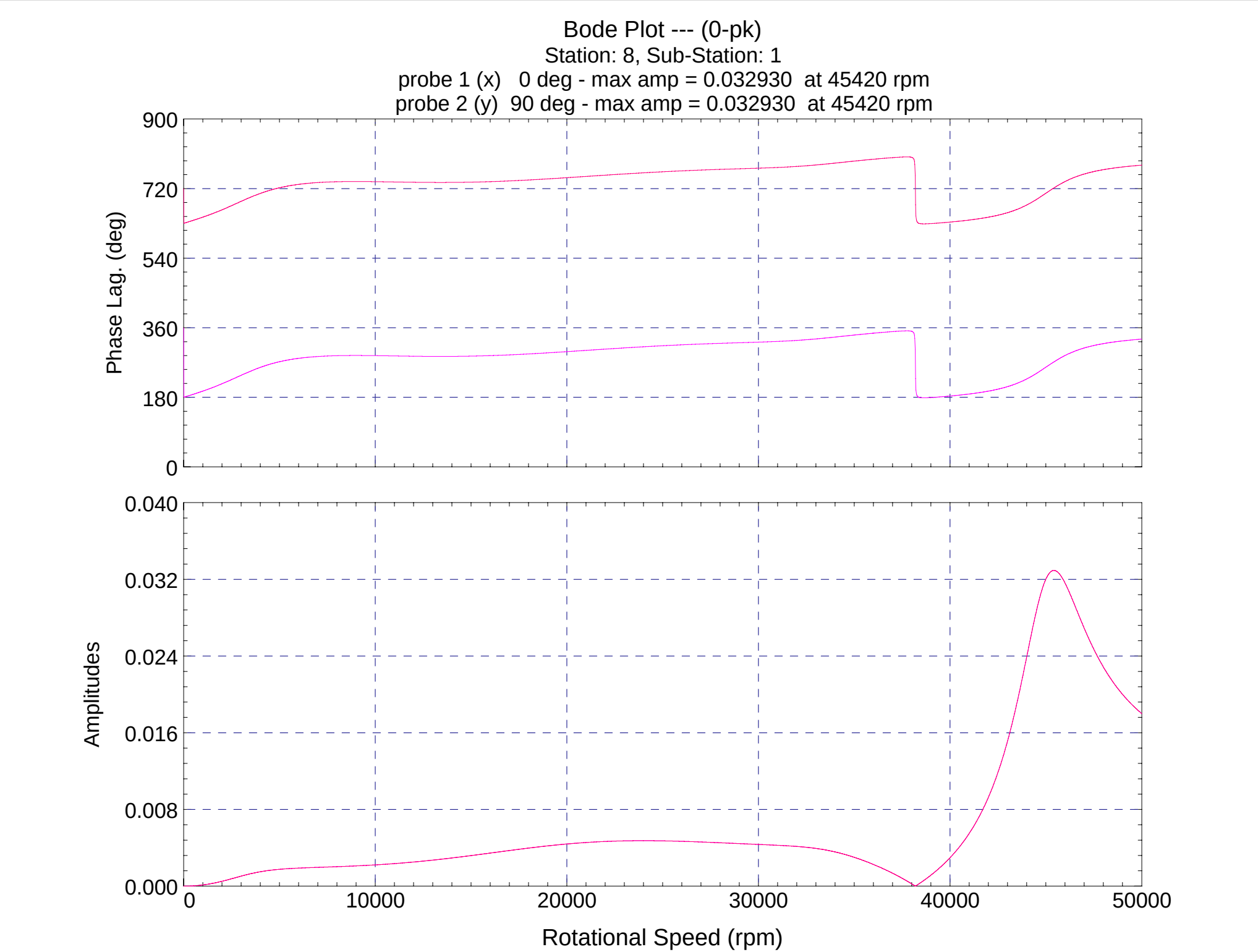

File: C:\DyRoBeS\FlyUps\Mode2(analysis)\FlyUps-rotor.rot

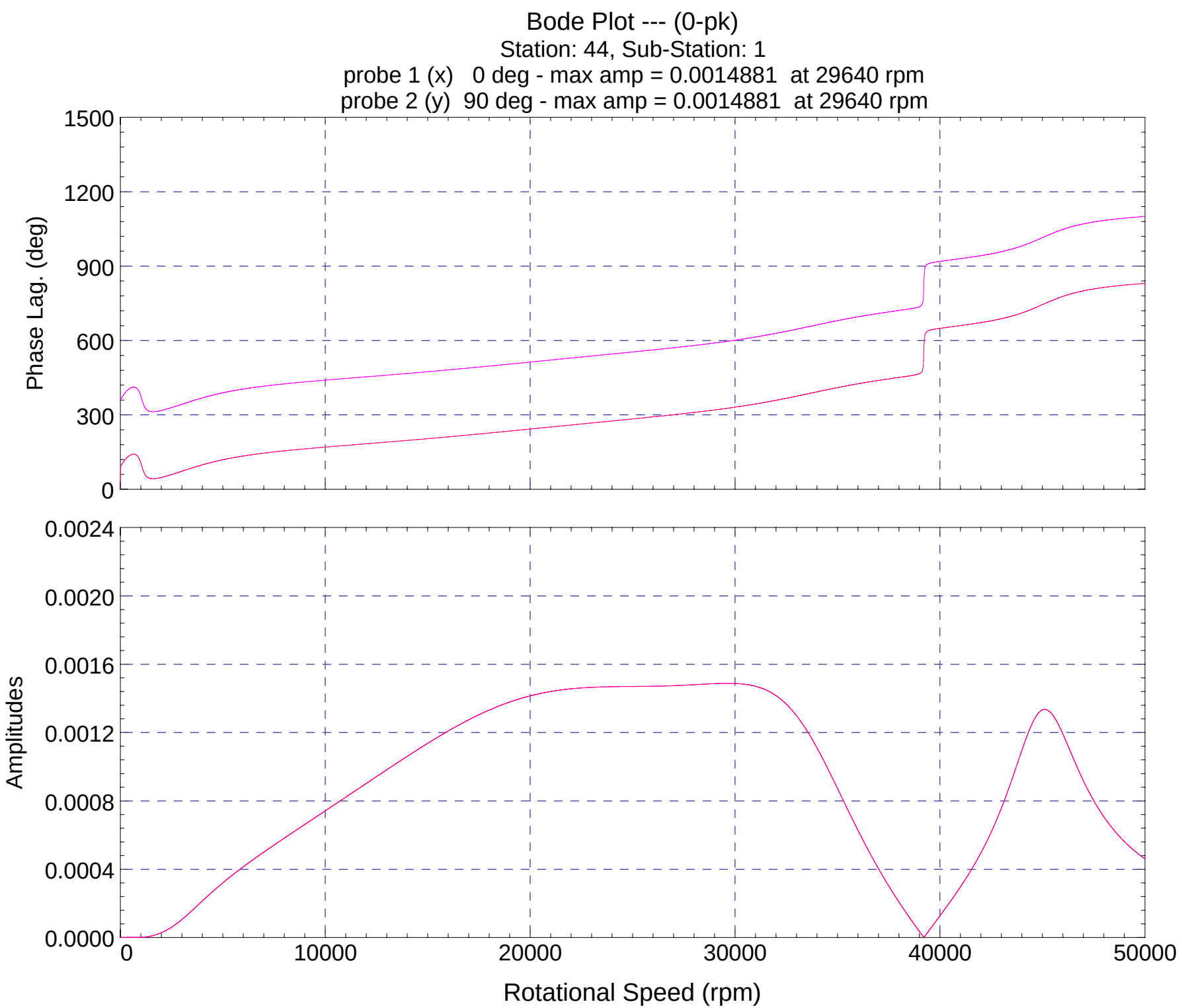

File: C:\DyRoBeS\FlyUps\Mode2(analysis)\FlyUps-rotor.rot

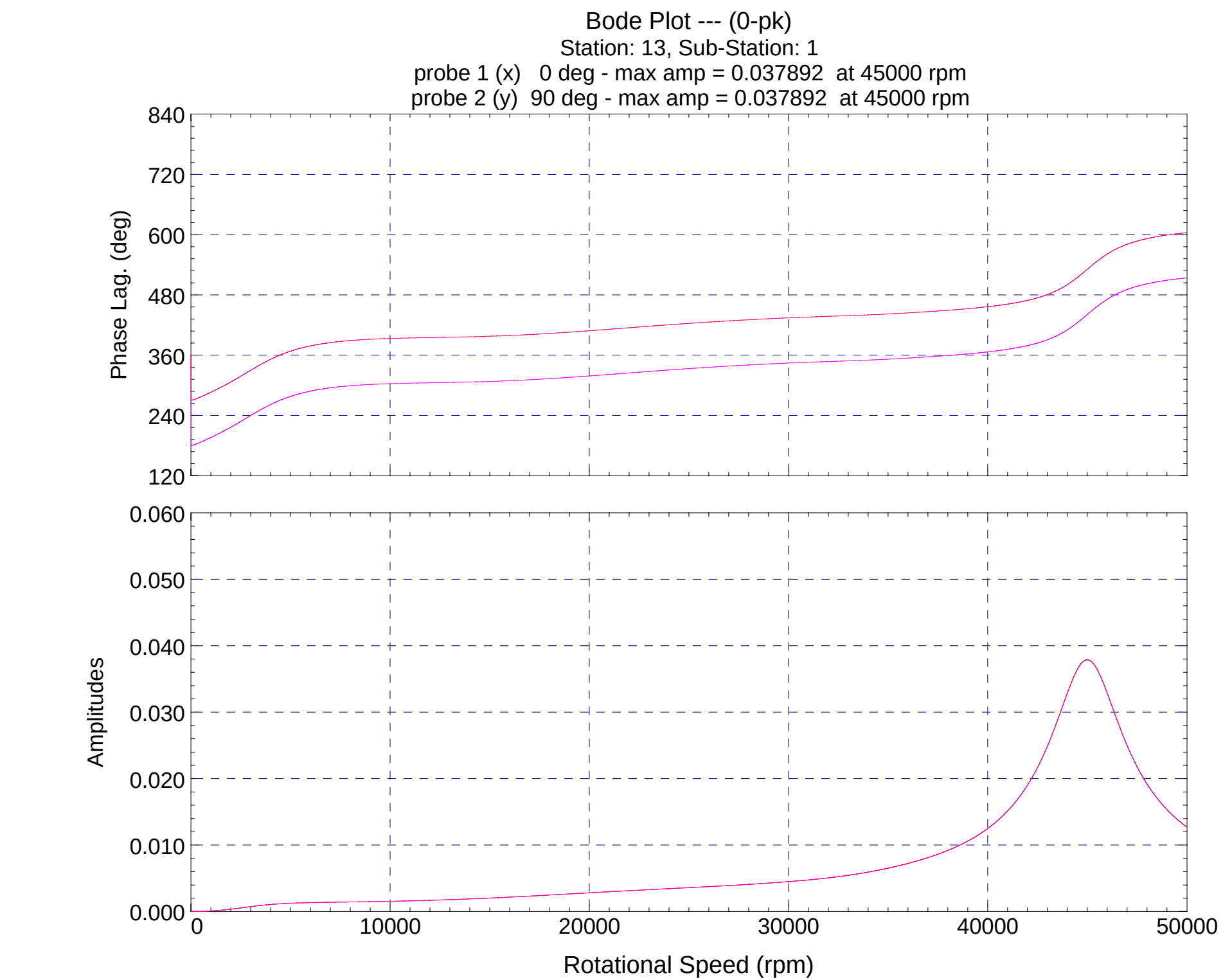

File: C:\DyRoBeS\FlyUps\Mode2(analysis)\FlyUps-rotor.rot

Polar Plot --- (pk-pk)
Station: 8, Sub-Station: 1
Speed range = 15000 - 30000 rpm
probe 1 (x) 0 deg - max amp = 0.0094825 at 24000 rpm
probe 2 (y) 90 deg - max amp = 0.0094825 at 24000 rpm

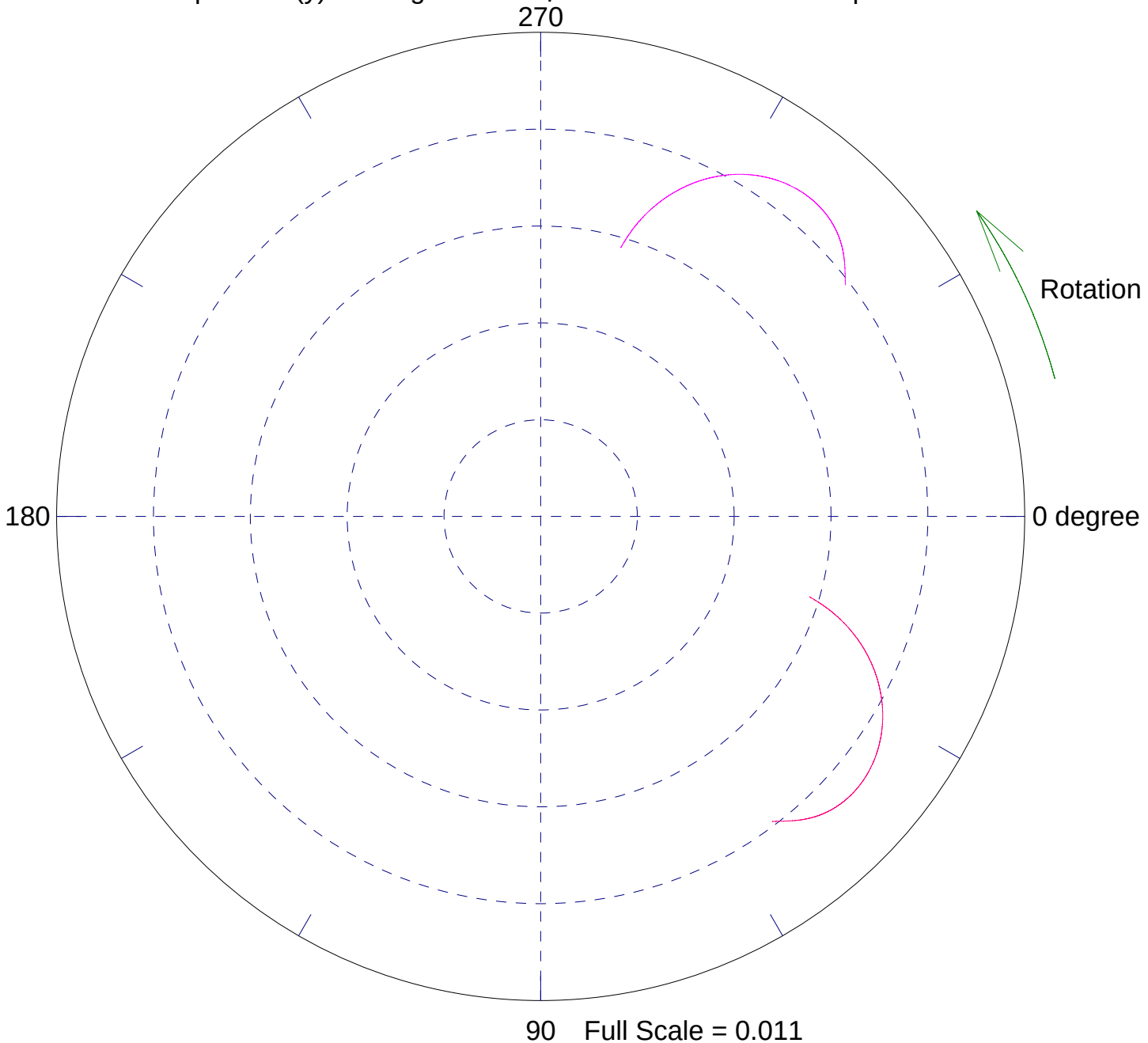

File: C:\DyRoBeS\FlyUps\Mode2(analysis)\FlyUps-rotor.rot

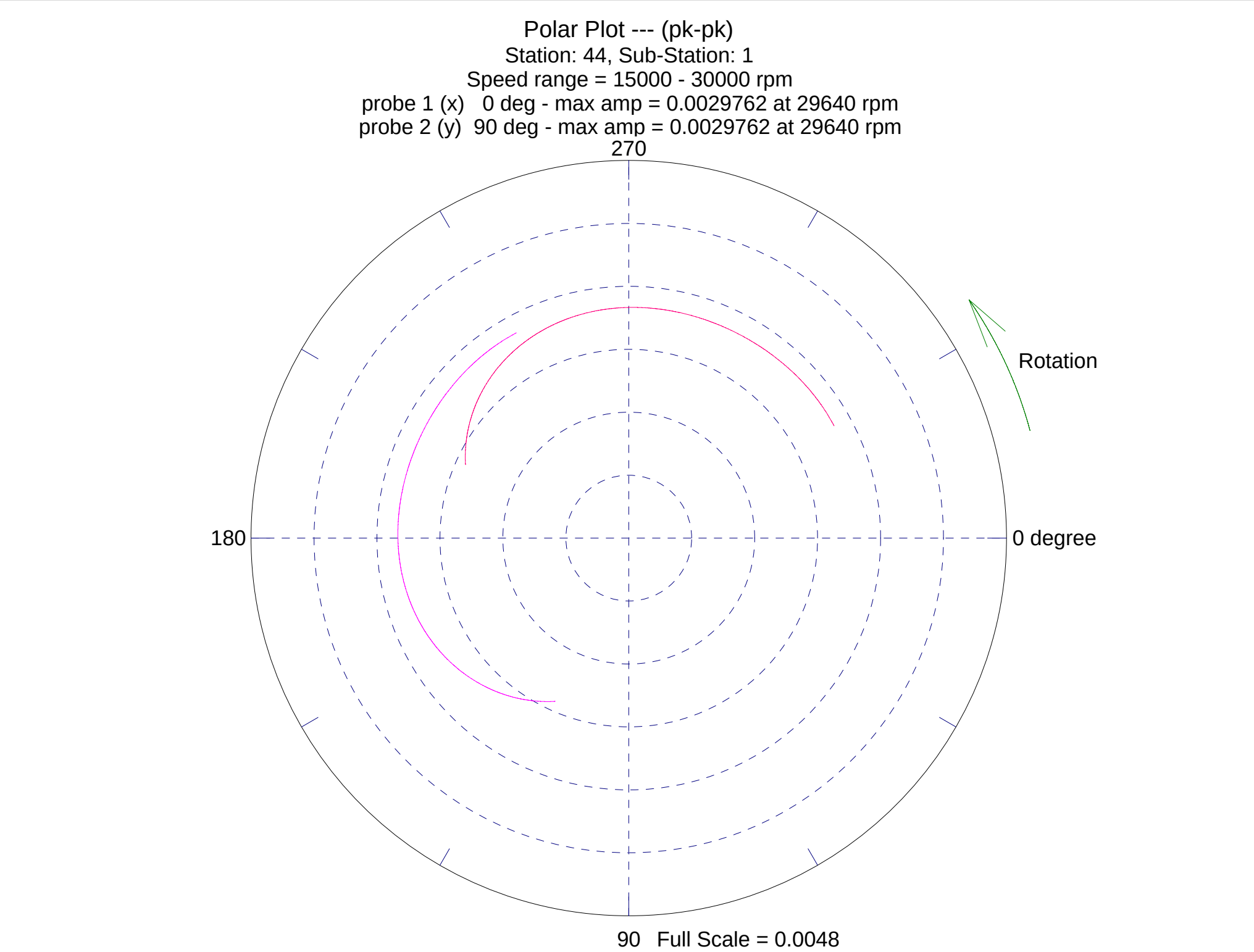
Polar Plot --- (pk-pk)
Station: 44, Sub-Station: 1
Speed range = 15000 - 30000 rpm
probe 1 (x) 0 deg - max amp = 0.0029762 at 29640 rpm
probe 2 (y) 90 deg - max amp = 0.0029762 at 29640 rpm
270
180
0 degree
90
Full Scale = 0.0048
Rotation
File: C:\DyRoBeS\FlyUps\Mode2(analysis)\FlyUps-rotor.rot

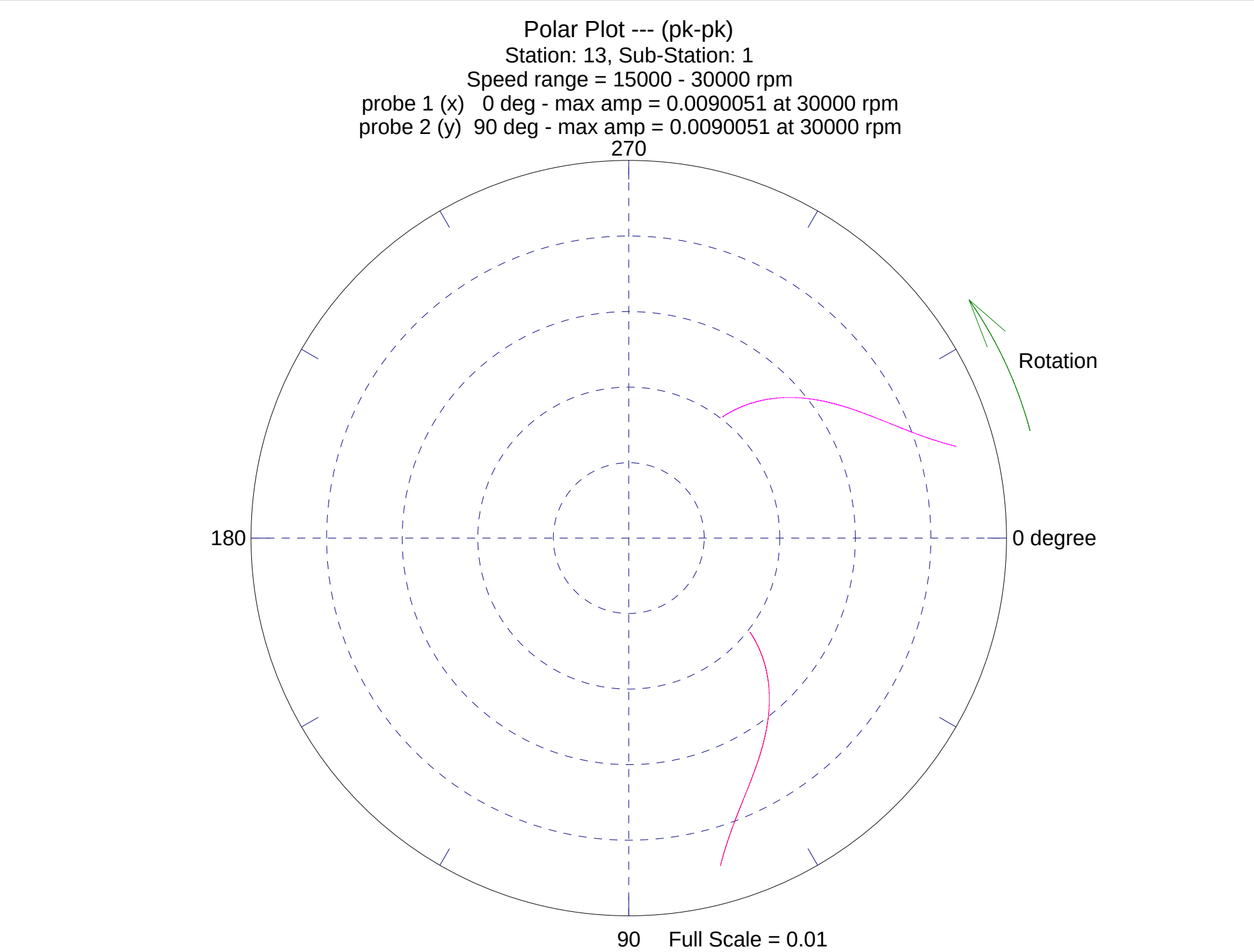
Polar Plot --- (pk-pk)
Station: 13, Sub-Station: 1
Speed range = 15000 - 30000 rpm
probe 1 (x) 0 deg - max amp = 0.0090051 at 30000 rpm
probe 2 (y) 90 deg - max amp = 0.0090051 at 30000 rpm
270
180
0 degree
90
Full Scale = 0.01
Rotation
File: C:\DyRoBeS\FlyUps\Mode2(analysis)\FlyUps-rotor.rot

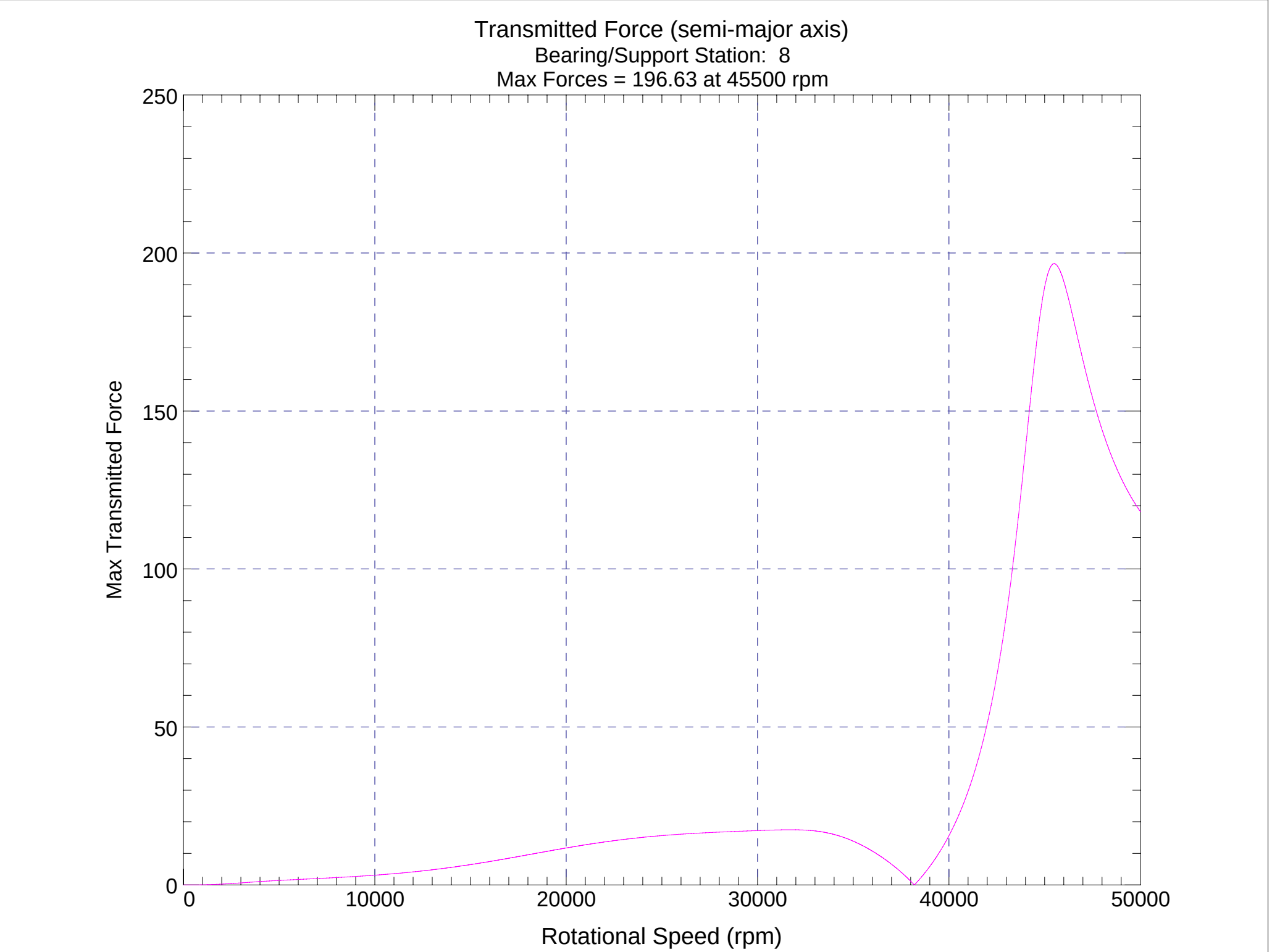

File: C:\DyRoBeS\FlyUps\Mode2(analysis)\FlyUps-rotor.rot

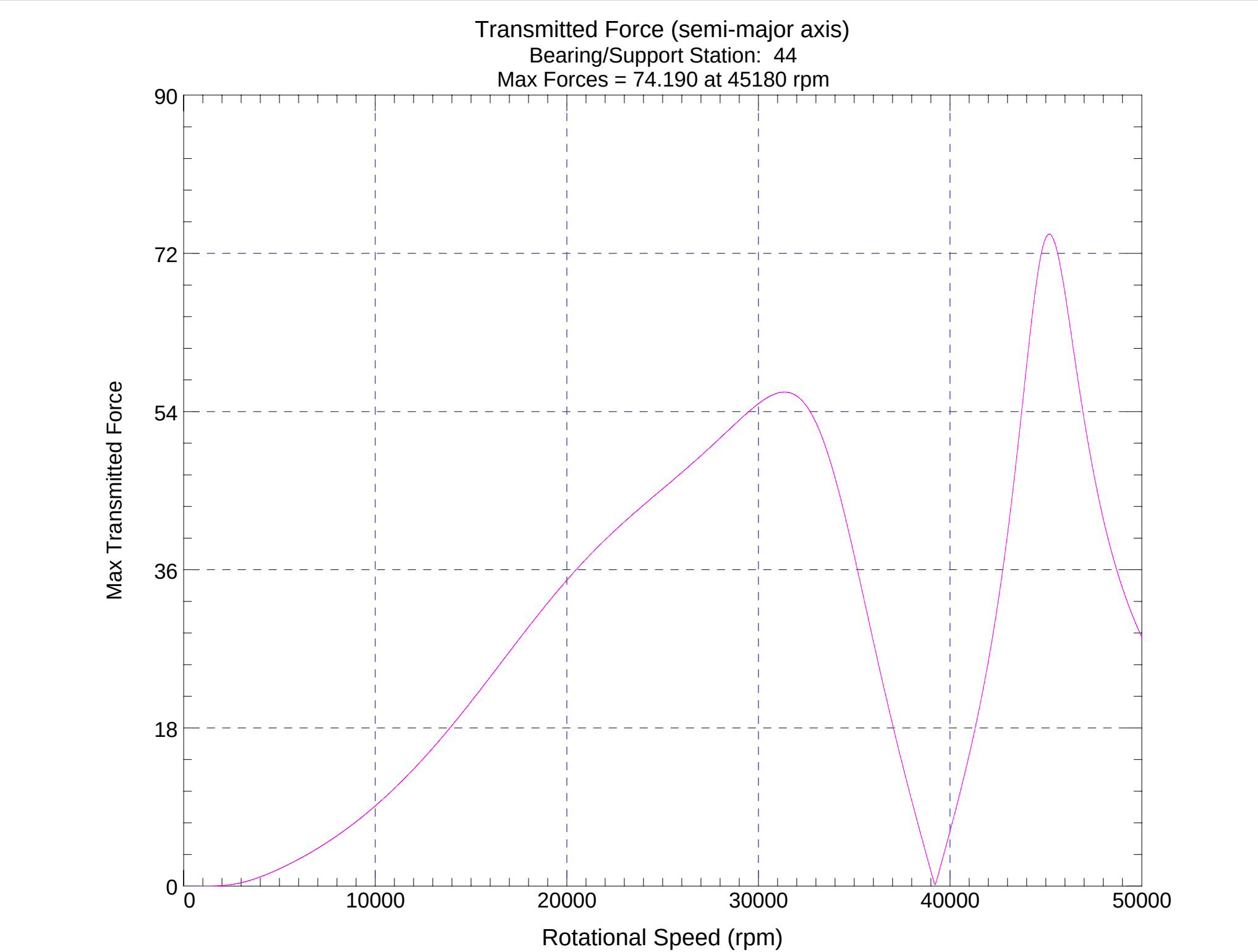

File: C:\DyRoBeS\FlyUps\Mode2(analysis)\FlyUps-rotor.rot

Response:Displacement -- Semi-Major Axis

Station: 5 , Sub-Stn: 1, Peak Response = 0.051200 at 45260 rpm

Station: 8 , Sub-Stn: 1, Peak Response = 0.032930 at 45420 rpm

Station: 13, Sub-Stn: 1, Peak Response = 0.037892 at 45000 rpm

Station: 44, Sub-Stn: 1, Peak Response = 0.0014881 at 29640 rpm

Station: 47, Sub-Stn: 1, Peak Response = 0.0031294 at 32480 rpm

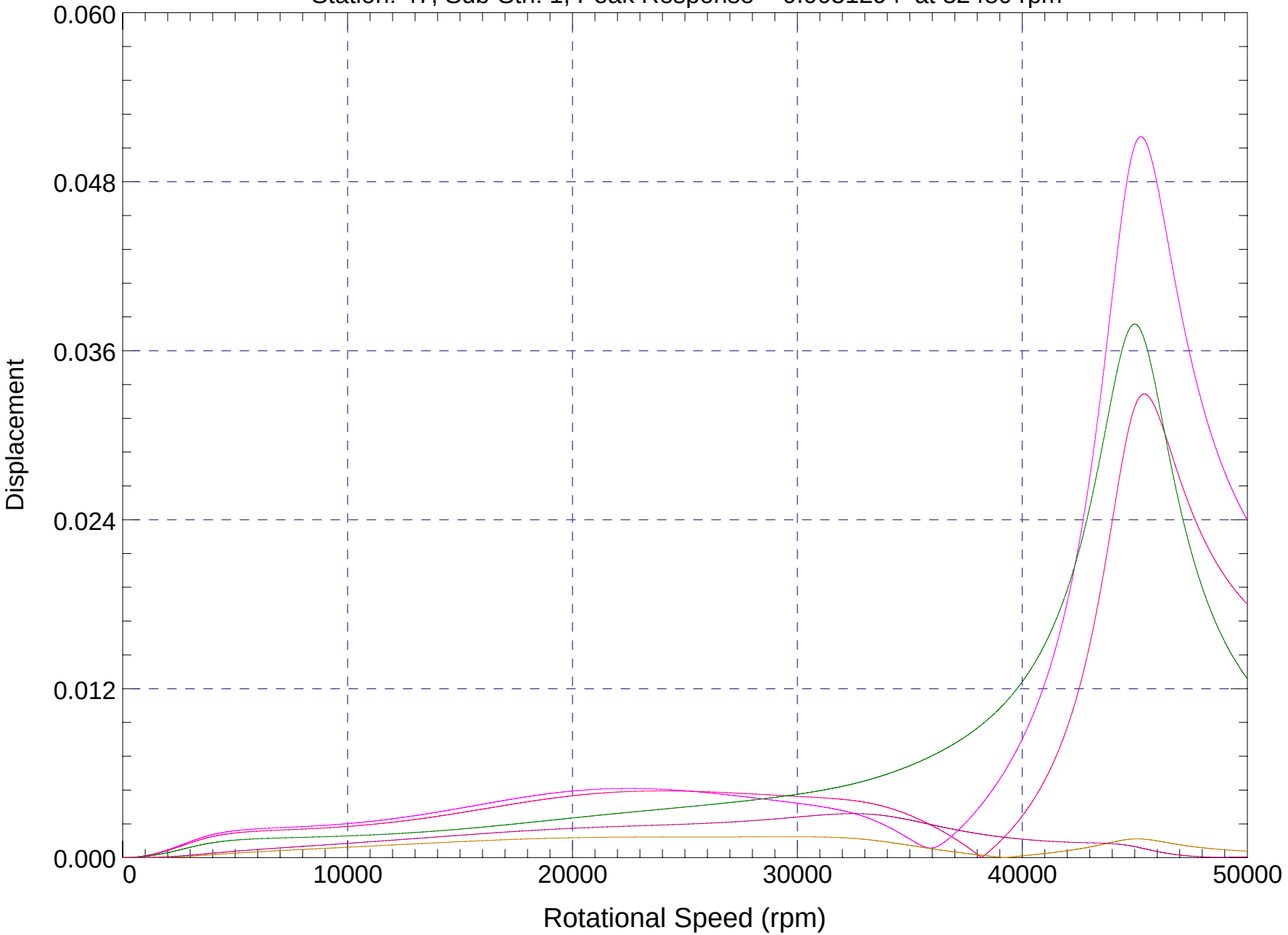

File: C:\DyRoBeS\FlyUps\Mode2(analysis)\FlyUps-rotor.rot

D.7 CosmosWorks strength analysis

Stress analysis of RF-SC-008-D

1. Introduction
2. File Information
3. Materials
4. Load & Restraint Information
5. Study Property
6. Contact
7. Results
    a. Mesh Quality Plots
    b. Default Results
8. Appendix

---

1. Introduction

Summarize the FEM analysis on RF-SC-008-D

Note:

Do not base your design decisions solely on the data presented in this report. Use this information in conjunction with experimental data and practical experience. Field testing is mandatory to validate your final design. COSMOSWorks helps you reduce your time-to-market by reducing but not eliminating field tests.

---

2. File Information

Model name:	RF-SC-008-D
Model location:	C:\Documents and Settings\Jan\Desktop\Thesis\25 JULY 2007\FLY-UPS\RF-FA-A\RF-SC-008-D.SLDPRT
Results location:	C:\Program Files\SolidWorks\COSMOS\work
Study name:	Study 1 (-Default-)

---

3. Materials

No.	Part Name	Material	Mass	Volume
1	RF-SC-008-D	User Defined	16.1352 kg	0.00206861 m^3

---

4. Load & Restraint Information

Load		
Centrifugal-1	CentriFugal with respect to **Face< 1 >** with angular velocity **31500 rpm** and angular acceleration **0 rpm^2**	Sequential Loading
Description:		

---

5. Study Property

Mesh Information	
Mesh Type:	Solid mesh
Mesher Used:	Standard
Automatic Transition:	Off
Smooth Surface:	On
Jacobian Check:	4 Points
Element Size:	6.3721 mm
Tolerance:	0.31861 mm
Quality:	High
Number of elements:	65297
Number of nodes:	96379
Time to complete mesh(hh;mm;ss):	00:00:14
Computer name:	JAN-PC

Solver Information	
Quality:	High
Solver Type:	FFEPlus
Option:	Include Thermal Effects
Thermal Option:	Input Temperature
Thermal Option:	Reference Temperature at zero strain: 298 Kelvin

---

6. Contact

Contact state: Touching faces - Bonded

7. Results

7a. Mesh Quality Plots

7b. Default Results

Name	Type	Min	Location	Max	Location
Stress1	VON: von Mises stress	519390 N/m^2 Node: 32633	(310.397 mm, -0.124221 mm, -0.590293 mm)	7.68951e+008 N/m^2 Node: 95075	(251.827 mm, 101.411 mm, -58.8506 mm)
Displacement1	URES: Resultant displacement	0 m Node: 4719	(237.231 mm, -0.394196 mm, -1.24887 mm)	0.00051574 m Node: 90142	(36.35 mm, 14.2321 mm, 8.71462e-016 mm)
Strain1	ESTRN: Equivalent	3.50341e-006	(182.735 mm,	0.00260971 Element:	(248.711 mm,

	strain	Element: 62832	-1.17671 mm, 0.59705 mm)	14449	101.181 mm, -59.2543 mm)

RF-SC-008-D-Study 1-Stress-Stress1

JPEG

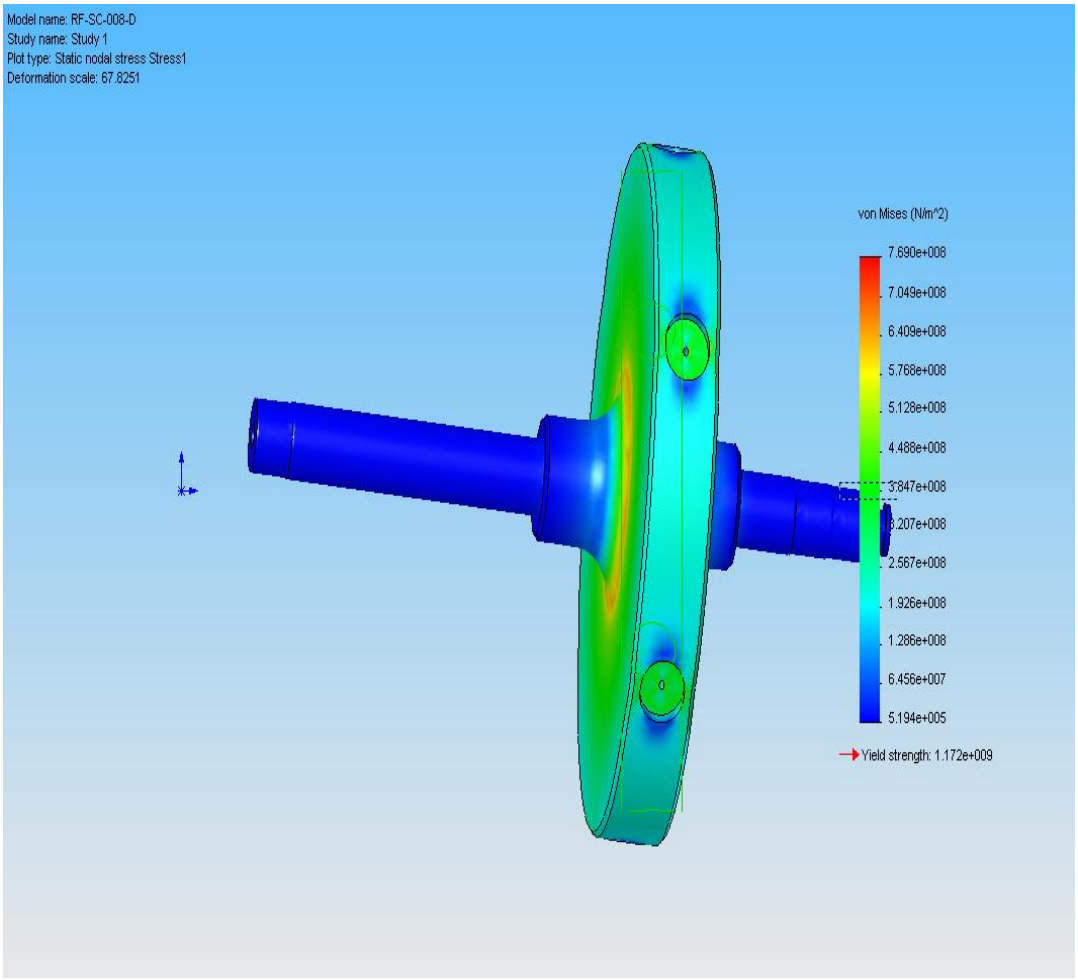

RF-SC-008-D-Study 1-Displacement-Displacement1

JPEG

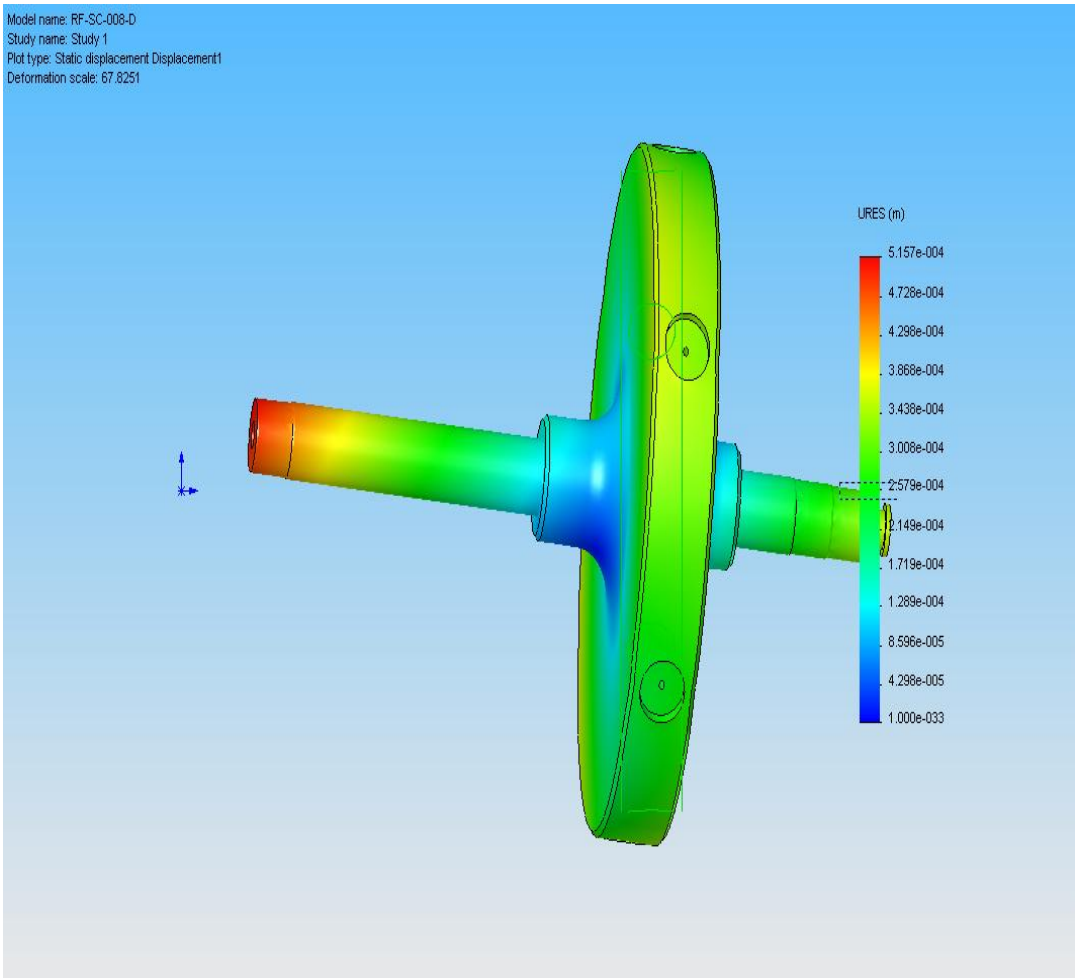

RF-SC-008-D-Study 1-Strain-Strain1

JPEG

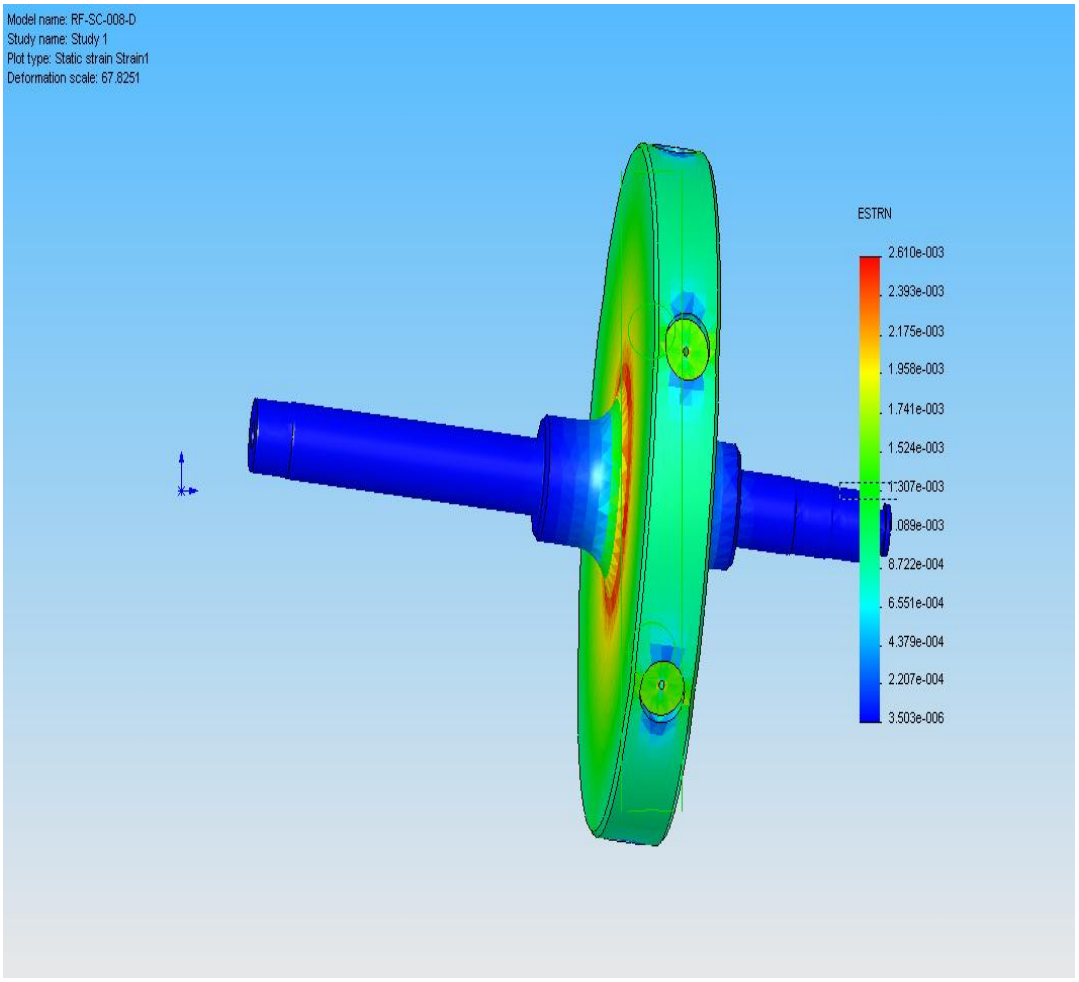

RF-SC-008-D-Study 1-Design Check-Design Check1

JPEG

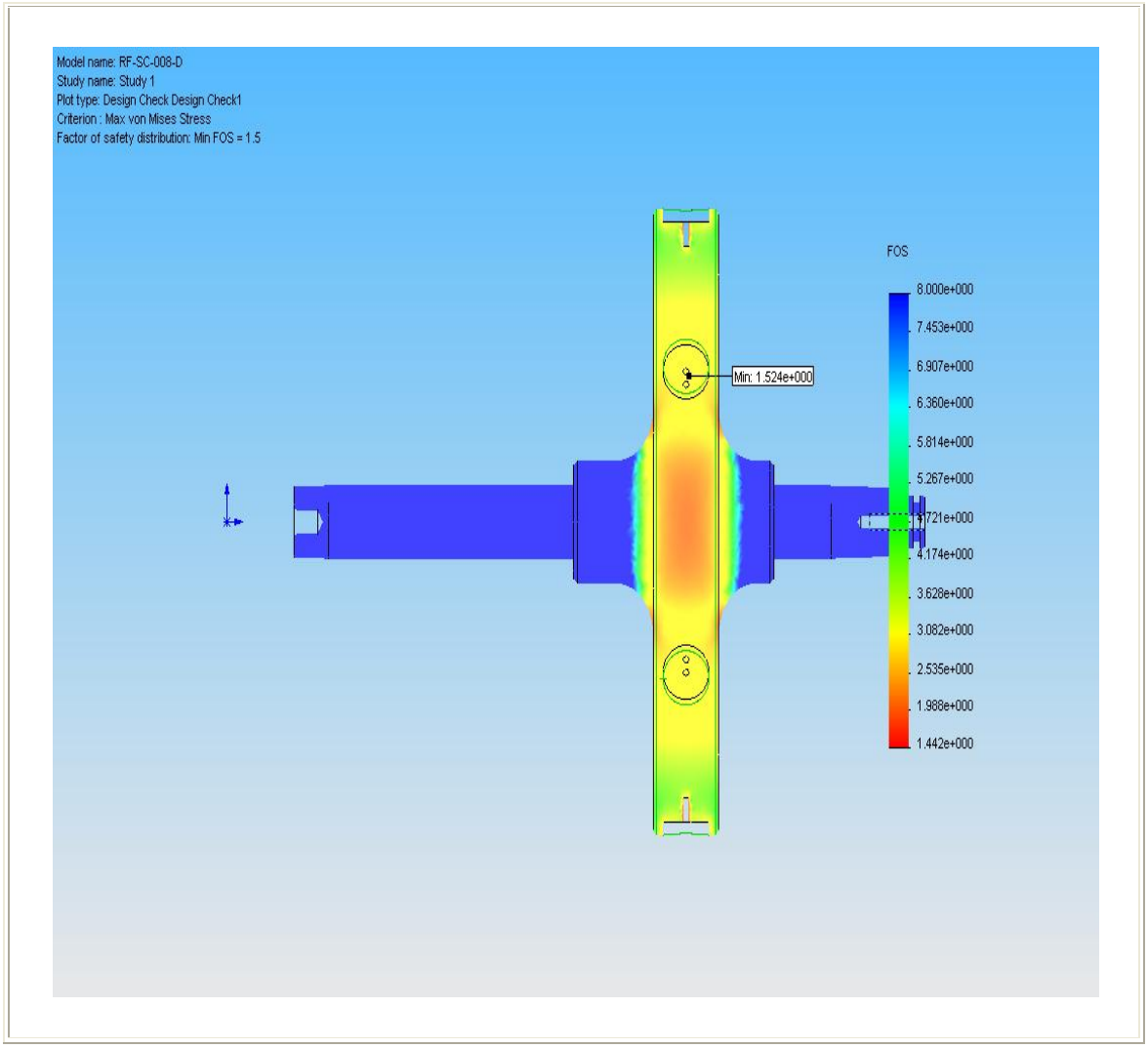

8. Appendix

Material name: User Defined

Description:

Material Source: Input

Material Model Type: Linear Elastic Isotropic

Property Name	Value	Units	Value Type
Elastic modulus	1.97e+011	N/m^2	Constant
Poisson's ratio	0.27	NA	Constant
Mass density	7800	kg/m^3	Constant
Tensile strength	1.276e+009	N/m^2	Constant
Compressive strength	1e+009	N/m^2	Constant
Yield strength	1.172e+009	N/m^2	Constant

D.8 Drawing numbering conventions

Component	Main component serial number		Main component or sub-component	Sub-component Number	Revision Number
Radiale AMB	RAMB		SC of FA (Sub-Comp of Final Assembly)	001-999	A tot Z
Aksiale AMB	AAMB		SC of FA	001-999	A tot Z
Rotor/Vliegwiel	RF		SC of FA	001-999	A tot Z
Huls	ENCL		SC of FA	001-999	A tot Z
Motor	PMM		SC of FA	001-999	A tot Z
Totale thing	FLYUPS		FA	-	A tot Z

D.9 Manufacturing drawings

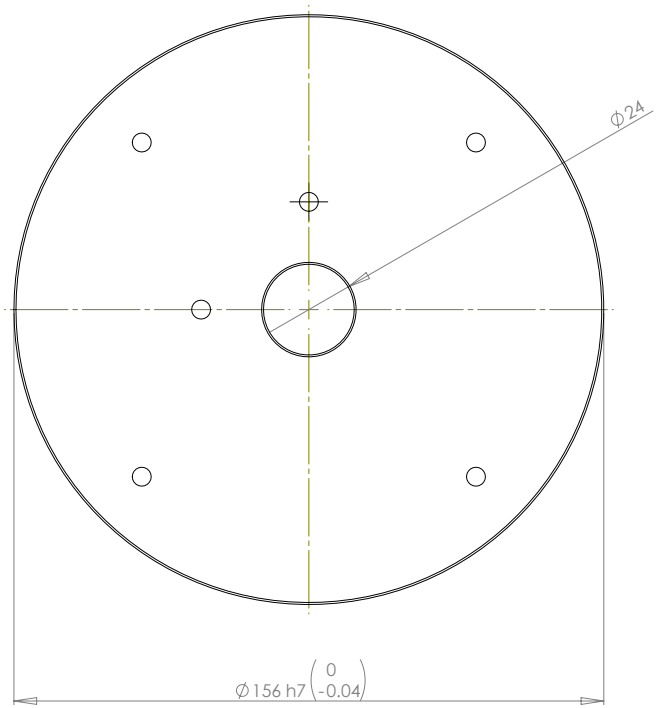

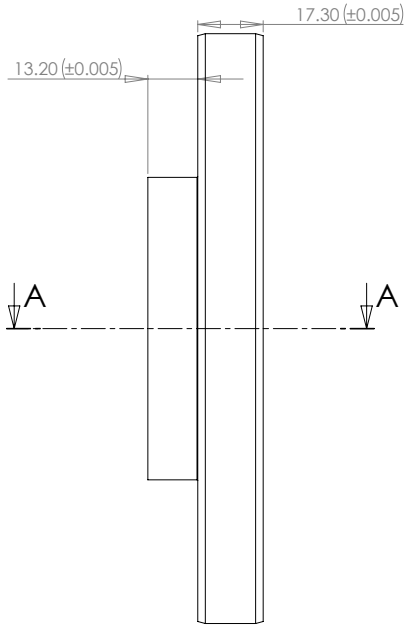

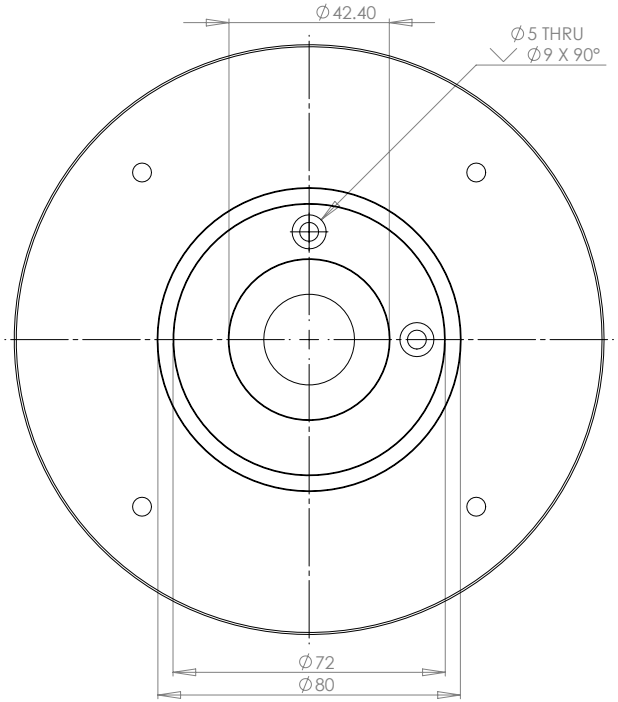

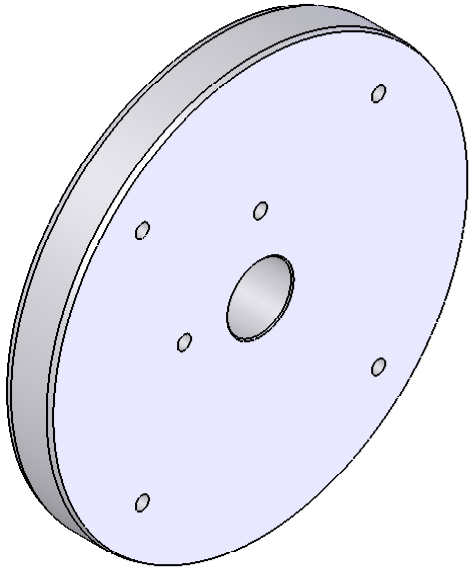

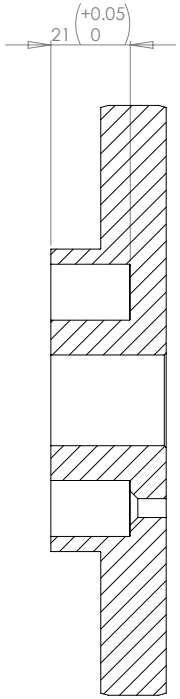

SECTION A-A
SCALE 1 : 1

UNLESS STATED OTHERWISE: REMOVE ALL BURRS AND SHARP EDGES								
SCREW THREAD: ISO 6H 6g								
GEOMETRIC TOL. TO BS 308 1972				MATERIAL:			MILD STEEL	
WELDING SYMBOLS TO BS 499/2							**CAD FILENAME:**	**SCALE:**
MACHINING TOLERANCES							AAMB-SC-001-A	1:2
OVER - TO	**±**	**±**	**±**				**COPYRIGHT NOTICE:**	
0 - 6	0.1	0.2	0.5				UNAUTHORISED USE, MANUFACTURE OR REPRODUCTION IN WHOLE OR IN PART IS PROHIBITED. DRAWING, DESIGN AND OTHER DISCLOSURES IS THE INTELLECTUAL PROPERTY OF NORTH-WEST UNIVERSITY. ALL RIGHTS RESERVED.	
6 - 30	0.2	0.5	0.8					
30 - 100	0.3	0.8	1.5					
100 - 300	0.5	1.2	2.0					
300 - 1000	0.8	2.0	3.0				SCHOOL OF MECHANICAL ENGINEERING POTCHEFSTROOM CAMPUS OF NW-U 11 HOFFMAN STREET POTCHEFSTROOM 2530	
1000 - 3000	1.2	3.0	5.0				SHEET 1 OF 1	AAMB 1
3000 PLUS:	2.0	4.0	8.0					
ANGLES:	1°	1°	1°		JJJVR	2007/10/30	C	**DWG. No.** AAMB-SC-001-C	C
SURFACE FIN:	1.6	6.3	12.5	**APPR.**	**DRAWN**	**DATE**	**REV.**	

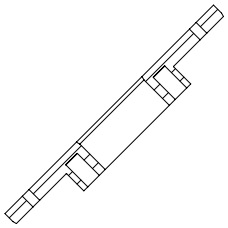

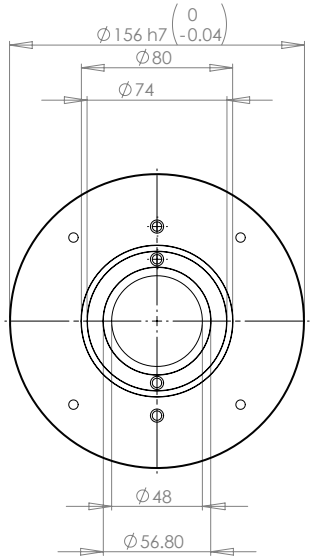

SECTION C-C

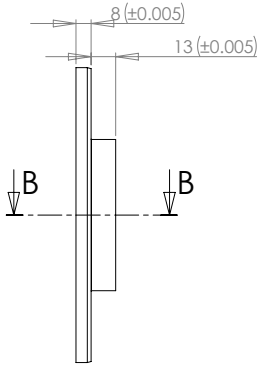

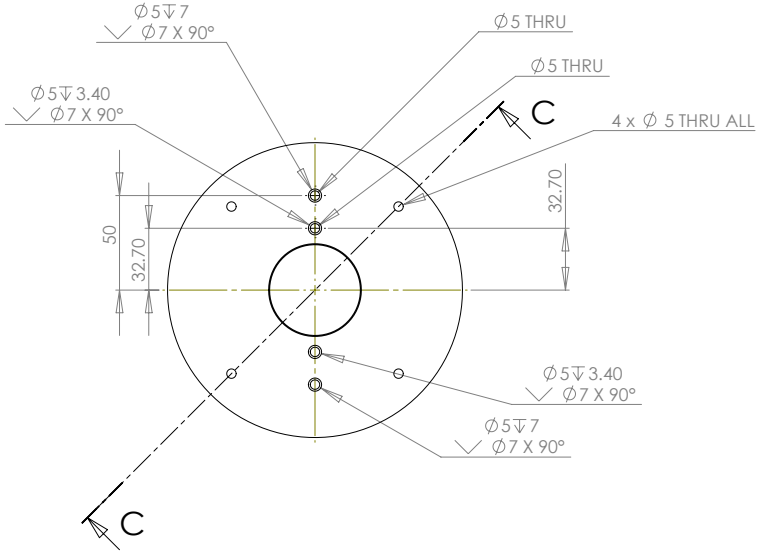

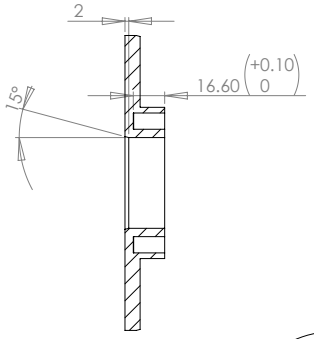

SECTION B-B

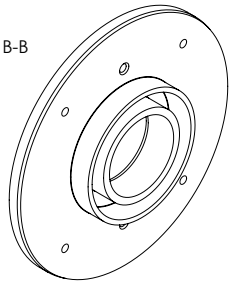

UNLESS STATED OTHERWISE: REMOVE ALL BURRS AND SHARP EDGES								
SCREW THREAD: ISO 6H 6g								
GEOMETRIC TOL. TO BS 308 1972								
WELDING SYMBOLS TO BS 499/2								
MACHINING TOLERANCES								
OVER - TO	**±**	**±**	**±**					
0 - 6	0.1	0.2	0.5					
6 - 30	0.2	0.5	0.8					
30 - 100	0.3	0.8	1.5					
100 - 300	0.5	1.2	2.0					
300 - 1000	0.8	2.0	3.0					
1000 - 3000	1.2	3.0	5.0					
3000 PLUS:	2.0	4.0	8.0					
ANGLES:	1°	1°	1°		JJJVR	2007/10/30	G	
SURFACE FIN:	1.6	6.3	12.5	**APPR.**	**DRAWN**	**DATE**	**REV.**	

CAD FILENAME: AAMB-SC-002-A | **SCALE:** 1:2

COPYRIGHT NOTICE:

UNAUTHORISED USE, MANUFACTURE OR REPRODUCTION IN WHOLE OR IN PART IS PROHIBITED. DRAWING, DESIGN AND OTHER DISCLOSURES IS THE INTELLECTUAL PROPERTY OF NORTH-WEST UNIVERSITY. ALL RIGHTS RESERVED.

SCHOOL OF MECHANICAL ENGINEERING
POTCHEFSTROOM CAMPUS OF NW-U
11 HOFFMAN STREET
POTCHEFSTROOM 2530

SHEET 1 OF 1

PMSM ENCLOSURE

DWG. No. AAMB-SC-002-G | G

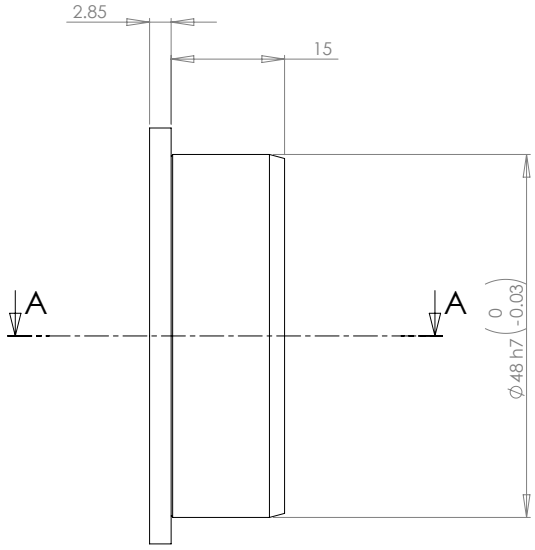

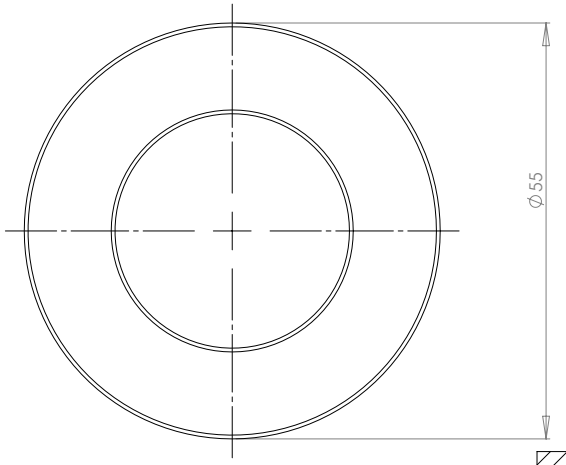

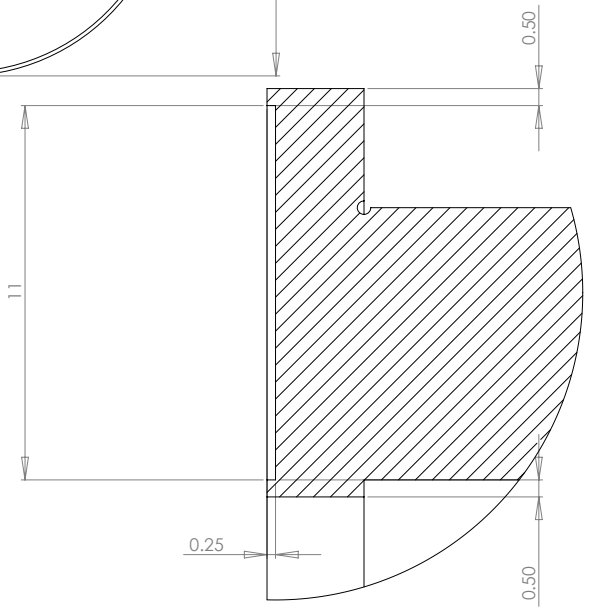

DETAIL B
SCALE 9 : 1

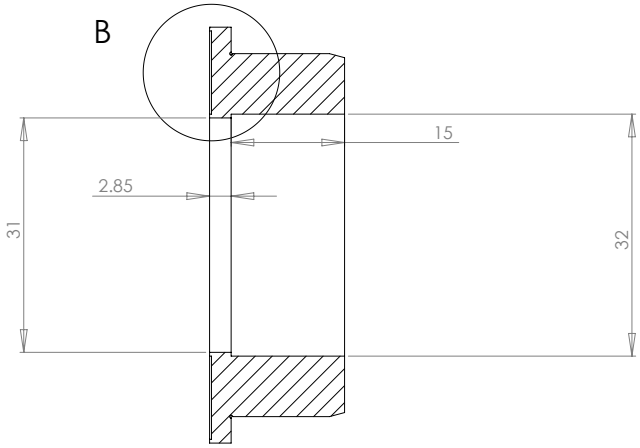

SECTION A-A

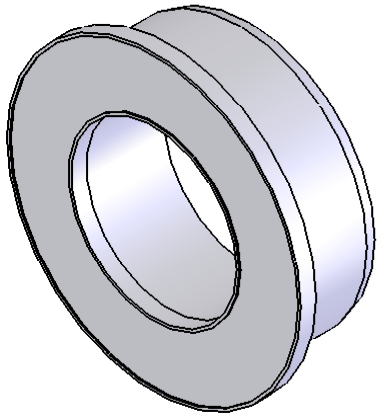

UNLESS STATED OTHERWISE: REMOVE ALL BURRS AND SHARP EDGES								
SCREW THREAD: ISO 6H 6g								
GEOMETRIC TOL. TO BS 308 1972					MATERIAL:			ALUMINIUM
WELDING SYMBOLS TO BS 499/2								**CAD FILENAME:** AAMB-SC-005-A — **SCALE:** 2:1
MACHINING TOLERANCES								
OVER - TO	**±**	**±**	**±**					**COPYRIGHT NOTICE:**
0 - 6	0.1	0.2	0.5					UNAUTHORISED USE, MANUFACTURE OR REPRODUCTION IN WHOLE OR IN PART IS PROHIBITED. DRAWING, DESIGN AND OTHER DISCLOSURES IS THE INTELLECTUAL PROPERTY OF NORTH-WEST UNIVERSITY. ALL RIGHTS RESERVED.
6 - 30	0.2	0.5	0.8					
30 - 100	0.3	0.8	1.5					
100 - 300	0.5	1.2	2.0					
300 - 1000	0.8	2.0	3.0					SCHOOL OF MECHANICAL ENGINEERING POTCHEFSTROOM CAMPUS OF NW-U 11 HOFFMAN STREET POTCHEFSTROOM 2530
1000 - 3000	1.2	3.0	5.0					SHEET 1 OF 1 — B-BEARING HOUSING
3000 PLUS:	2.0	4.0	8.0					
ANGLES:	1°	1°	1°		JJJVR	2007/10/30	C	**DWG. No.** AAMB-SC-005-C — C
SURFACE FIN:	1.6	6.3	12.5	**APPR.**	**DRAWN**	**DATE**	**REV.**	

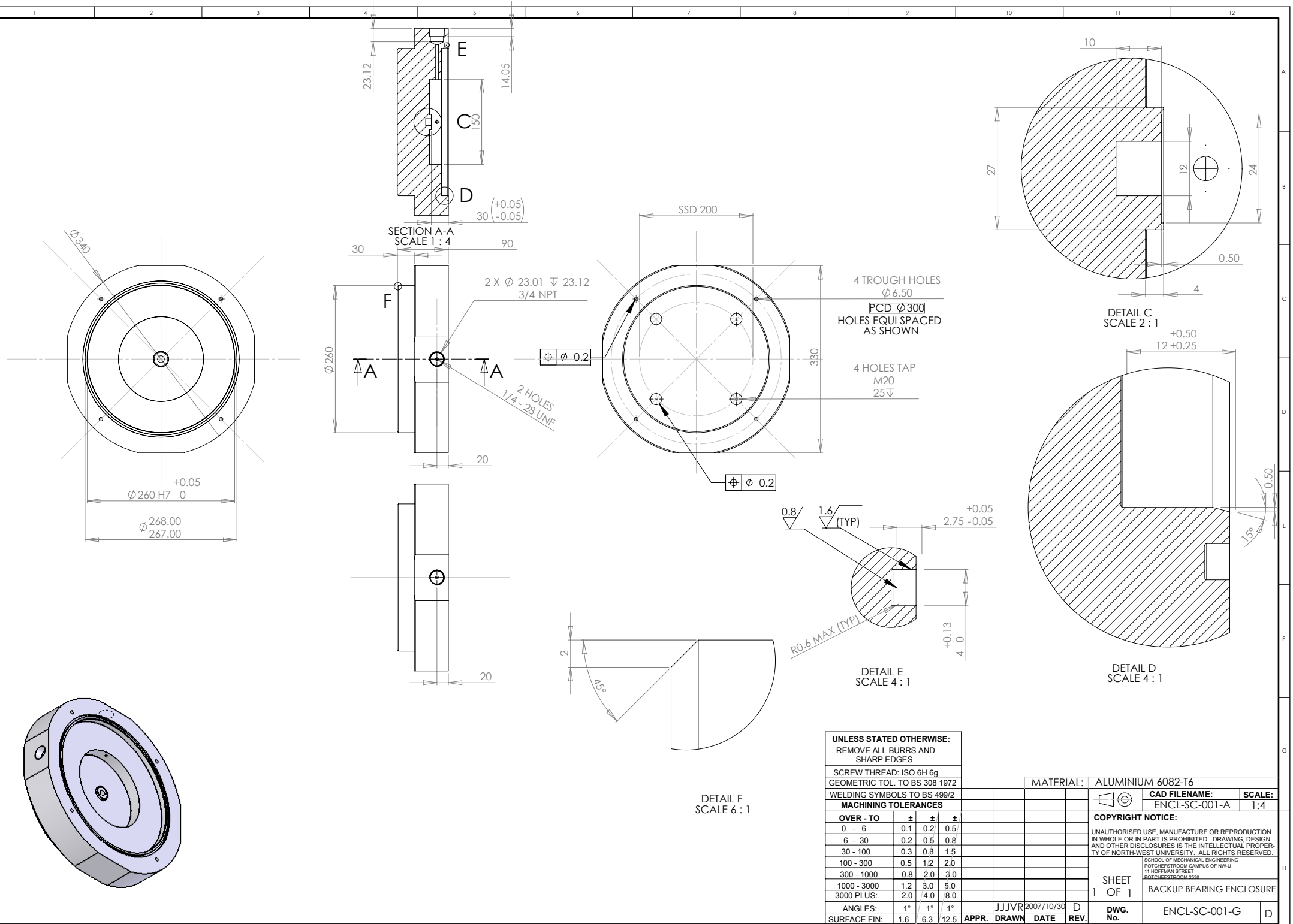

UNLESS STATED OTHERWISE: REMOVE ALL BURRS AND SHARP EDGES								
SCREW THREAD: ISO 6H 6g								
GEOMETRIC TOL. TO BS 308 1972								
WELDING SYMBOLS TO BS 499/2								
MACHINING TOLERANCES								
OVER - TO	**±**	**±**	**±**					
0 - 6	0.1	0.2	0.5					
6 - 30	0.2	0.5	0.8					
30 - 100	0.3	0.8	1.5					
100 - 300	0.5	1.2	2.0					
300 - 1000	0.8	2.0	3.0					
1000 - 3000	1.2	3.0	5.0					
3000 PLUS:	2.0	4.0	8.0					
ANGLES:	1°	1°	1°		JJJVR	2007/10/30	D	
SURFACE FIN:	1.6	6.3	12.5	**APPR.**	**DRAWN**	**DATE**	**REV.**	

MATERIAL: ALUMINIUM 6082-T6

CAD FILENAME: ENCL-SC-001-A **SCALE:** 1:4

COPYRIGHT NOTICE:
UNAUTHORISED USE, MANUFACTURE OR REPRODUCTION IN WHOLE OR IN PART IS PROHIBITED. DRAWING, DESIGN AND OTHER DISCLOSURES IS THE INTELLECTUAL PROPERTY OF NORTH-WEST UNIVERSITY. ALL RIGHTS RESERVED.

SCHOOL OF MECHANICAL ENGINEERING
POTCHEFSTROOM CAMPUS OF NW-U
11 HOFFMAN STREET
POTCHEFSTROOM 2530

SHEET 1 OF 1

BACKUP BEARING ENCLOSURE

DWG. No. ENCL-SC-001-G D

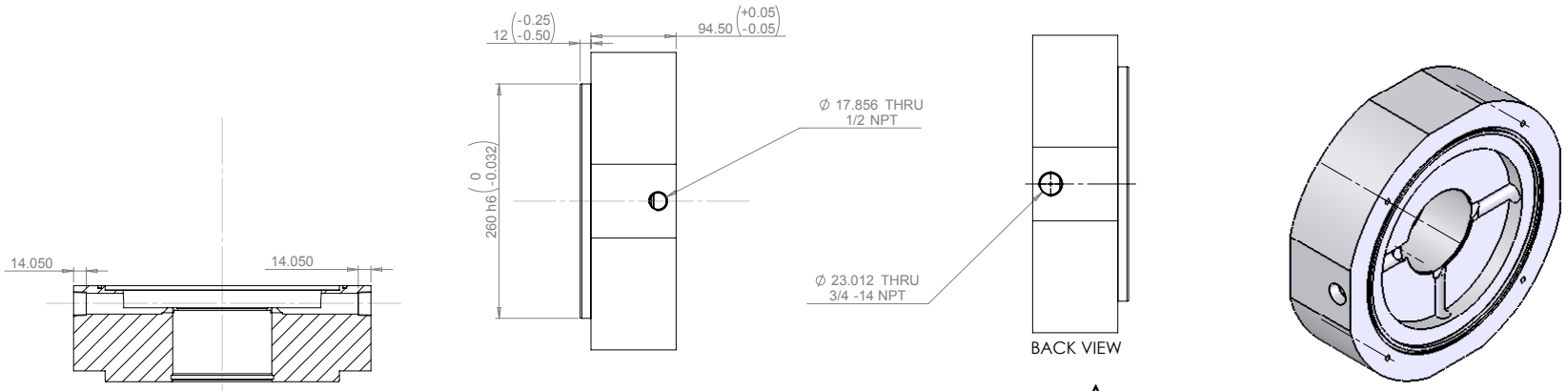

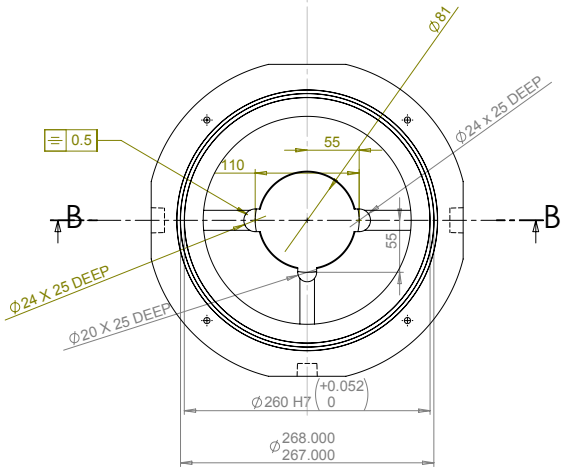

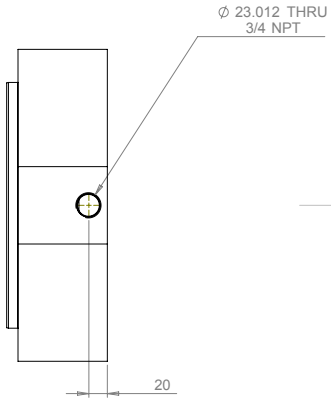

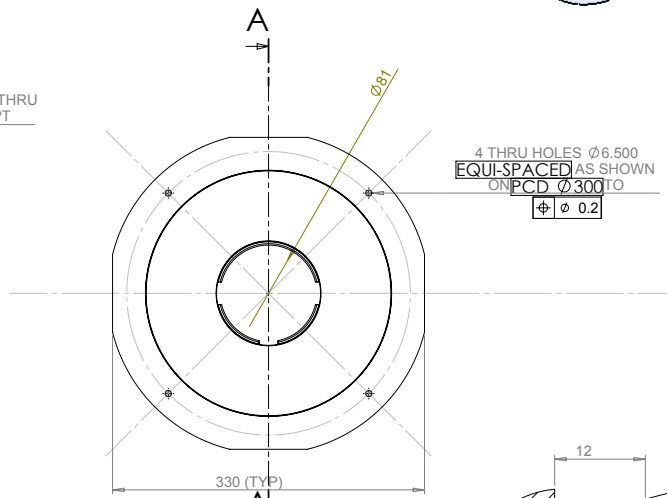

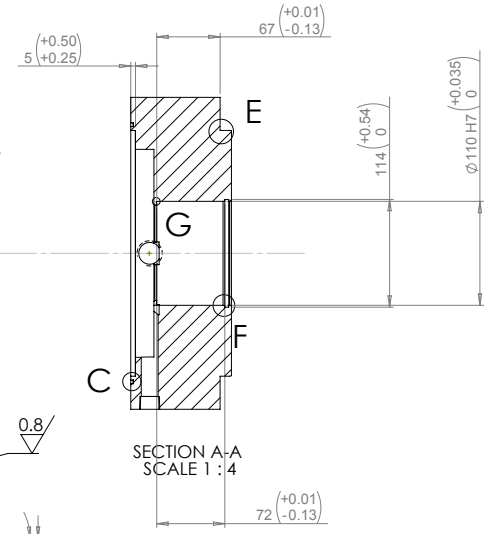

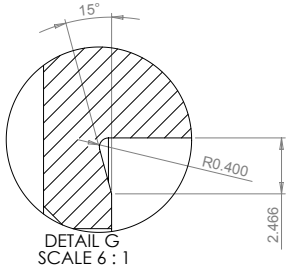

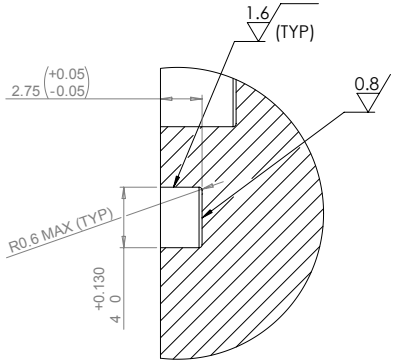

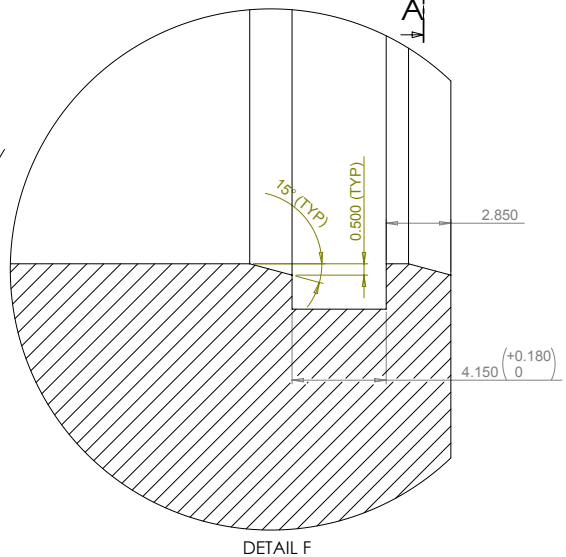

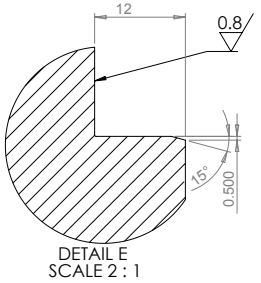

UNLESS STATED OTHERWISE: REMOVE ALL BURRS AND SHARP EDGES								
SCREW THREAD: ISO 6H 6g								
GEOMETRIC TOL. TO BS 308 1972								
WELDING SYMBOLS TO BS 499/2								
MACHINING TOLERANCES								
OVER - TO	**±**	**±**	**±**					
0 - 6	0.1	0.2	0.5					
6 - 30	0.2	0.5	0.8					
30 - 100	0.3	0.8	1.5					
100 - 300	0.5	1.2	2.0					
300 - 1000	0.8	2.0	3.0					
1000 - 3000	1.2	3.0	5.0					
3000 PLUS:	2.0	4.0	8.0					
ANGLES:	1°	1°	1°		JJJVR	2007/10/30	G	
SURFACE FIN:	1.6	6.3	12.5	**APPR.**	**DRAWN**	**DATE**	**REV.**	

MATERIAL:	ALUMINIUM 6082-t6	
	CAD FILENAME: ENCL-SC-003-A	**SCALE:** 1:4

COPYRIGHT NOTICE:
UNAUTHORISED USE, MANUFACTURE OR REPRODUCTION IN WHOLE OR IN PART IS PROHIBITED. DRAWING, DESIGN AND OTHER DISCLOSURES IS THE INTELLECTUAL PROPERTY OF NORTH-WEST UNIVERSITY. ALL RIGHTS RESERVED.

SCHOOL OF MECHANICAL ENGINEERING
POTCHEFSTROOM CAMPUS OF NW-U
11 HOFFMAN STREET
POTCHEFSTROOM 2530

SHEET 1 OF 1	PMSM ENCLOSURE	
DWG. No.	ENCL-SC-003-G	G

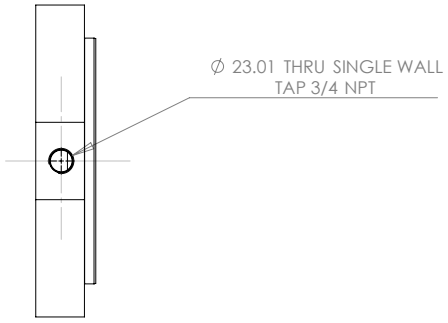

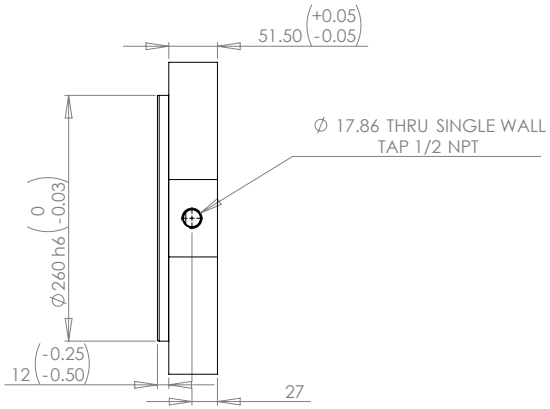

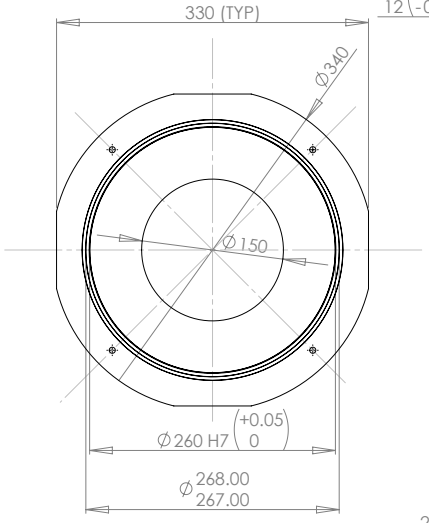

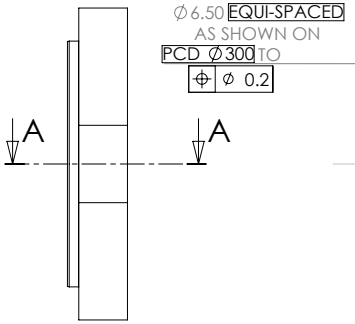

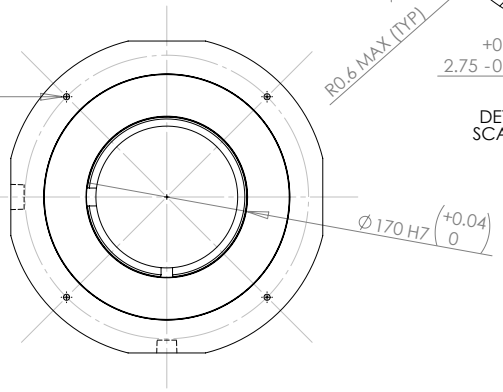

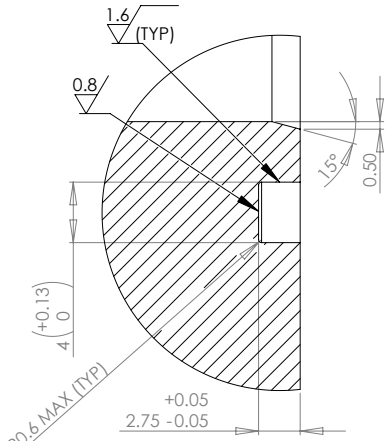

DETAIL C
SCALE 4 : 1

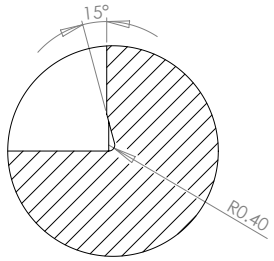

DETAIL B
SCALE 4 : 1

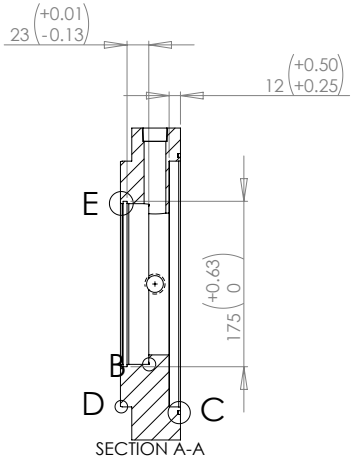

SECTION A-A

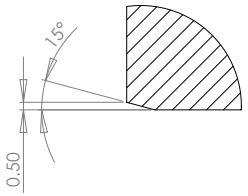

DETAIL D
SCALE 4 : 1

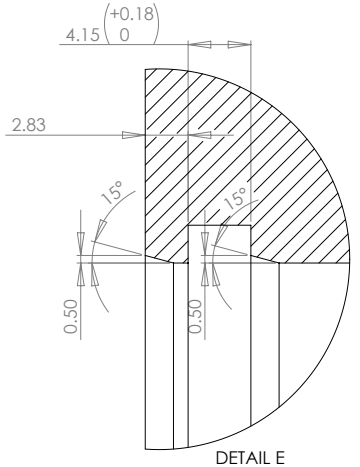

DETAIL E
SCALE 4 : 1

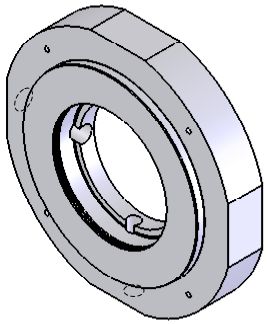

UNLESS STATED OTHERWISE: REMOVE ALL BURRS AND SHARP EDGES								
SCREW THREAD: ISO 6H 6g								
GEOMETRIC TOL. TO BS 308 1972								
WELDING SYMBOLS TO BS 499/2								
MACHINING TOLERANCES								
OVER - TO	**±**	**±**	**±**					
0 - 6	0.1	0.2	0.5					
6 - 30	0.2	0.5	0.8					
30 - 100	0.3	0.8	1.5					
100 - 300	0.5	1.2	2.0					
300 - 1000	0.8	2.0	3.0					
1000 - 3000	1.2	3.0	5.0					
3000 PLUS:	2.0	4.0	8.0					
ANGLES:	1°	1°	1°		JJJVR	2007/10/30	G	
SURFACE FIN:	1.6	6.3	12.5	**APPR.**	**DRAWN**	**DATE**	**REV.**	

MATERIAL: ALUMINIUM 6082-T6

CAD FILENAME: ENCL-SC-002-A **SCALE:** 1:4

COPYRIGHT NOTICE:
UNAUTHORISED USE, MANUFACTURE OR REPRODUCTION IN WHOLE OR IN PART IS PROHIBITED. DRAWING, DESIGN AND OTHER DISCLOSURES IS THE INTELLECTUAL PROPERTY OF NORTH-WEST UNIVERSITY. ALL RIGHTS RESERVED.

SCHOOL OF MECHANICAL ENGINEERING
POTCHEFSTROOM CAMPUS OF NW-U
11 HOFFMAN STREET
POTCHEFSTROOM 2530

SHEET 1 OF 1

LOWER AMB ENCLOSURE

DWG. No. ENCL-SC-002-G G

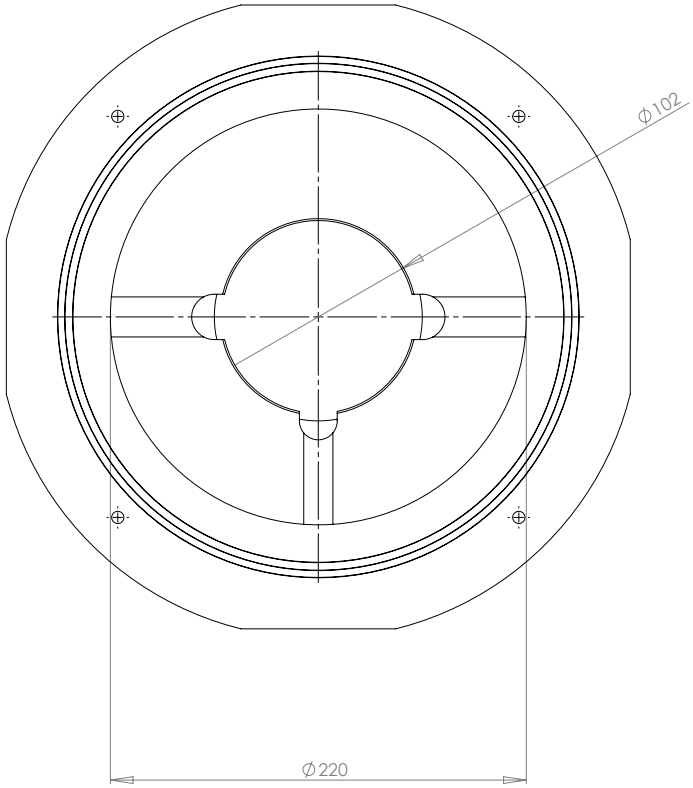

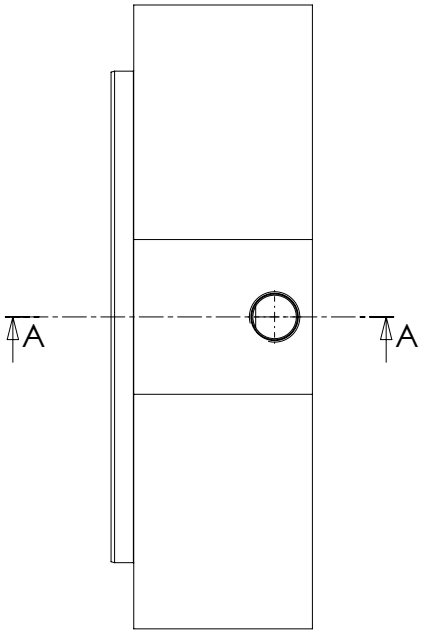

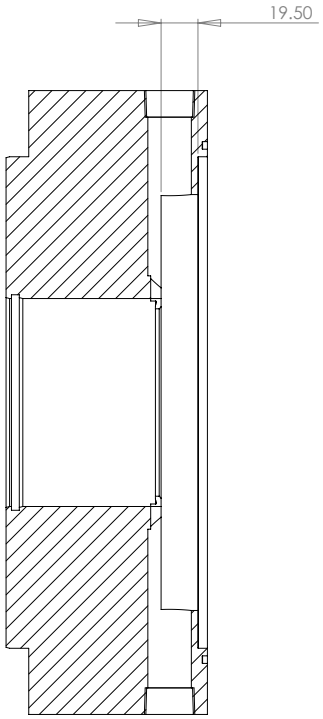

SECTION A-A
SCALE 1 : 2

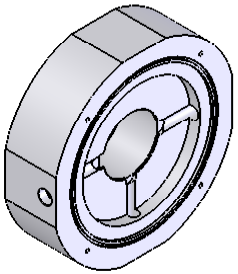

UNLESS STATED OTHERWISE: REMOVE ALL BURRS AND SHARP EDGES								
SCREW THREAD: ISO 6H 6g								
GEOMETRIC TOL. TO BS 308 1972								
WELDING SYMBOLS TO BS 499/2								
MACHINING TOLERANCES								
OVER - TO	**±**	**±**	**±**					
0 - 6	0.1	0.2	0.5					
6 - 30	0.2	0.5	0.8					
30 - 100	0.3	0.8	1.5					
100 - 300	0.5	1.2	2.0					
300 - 1000	0.8	2.0	3.0					
1000 - 3000	1.2	3.0	5.0					
3000 PLUS:	2.0	4.0	8.0					
ANGLES:	1°	1°	1°		JJJVR	2007/10/30	A	
SURFACE FIN:	1.6	6.3	12.5	**APPR.**	**DRAWN**	**DATE**	**REV.**	

CAD FILENAME:	**SCALE:**
ENCL-SC-003-A	1:5

COPYRIGHT NOTICE:

UNAUTHORISED USE, MANUFACTURE OR REPRODUCTION IN WHOLE OR IN PART IS PROHIBITED. DRAWING, DESIGN AND OTHER DISCLOSURES IS THE INTELLECTUAL PROPERTY OF NORTH-WEST UNIVERSITY. ALL RIGHTS RESERVED.

SCHOOL OF MECHANICAL ENGINEERING
POTCHEFSTROOM CAMPUS OF NW-U
11 HOFFMAN STREET
POTCHEFSTROOM 2530

SHEET 1 OF 1

PMSM ENCLOSURE

DWG. No. ENCL-SC-003-PM-A | A

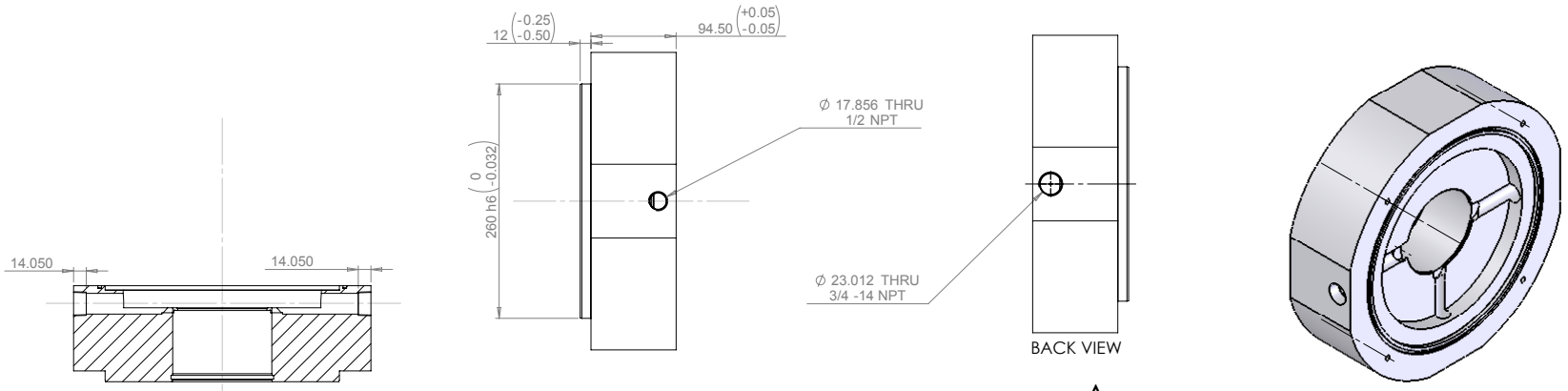

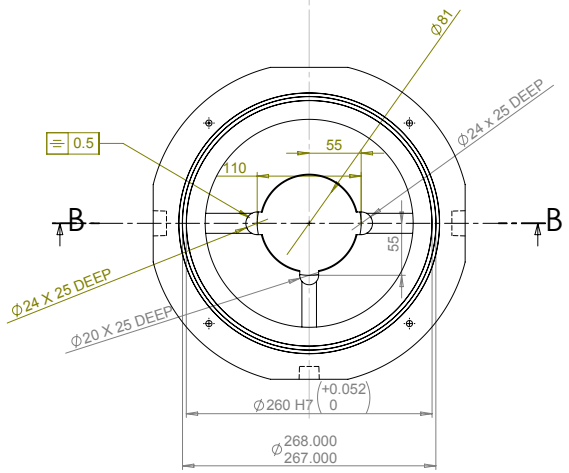

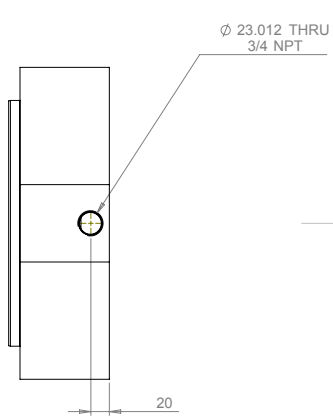

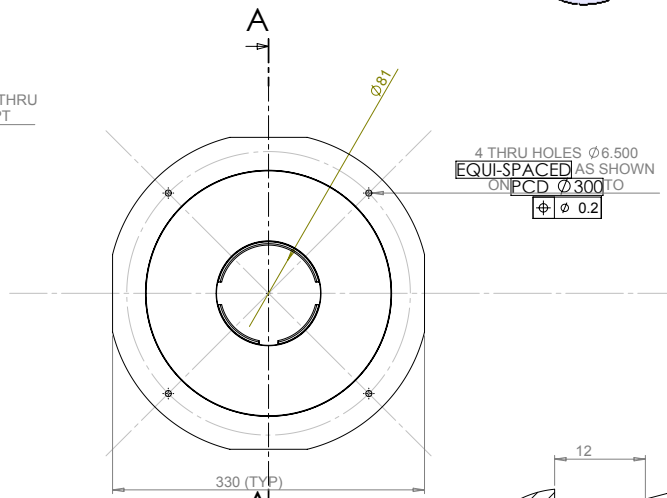

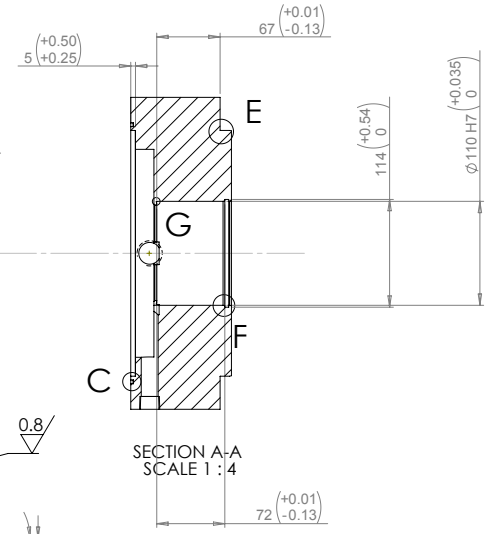

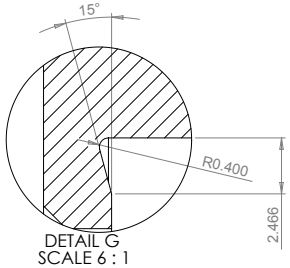

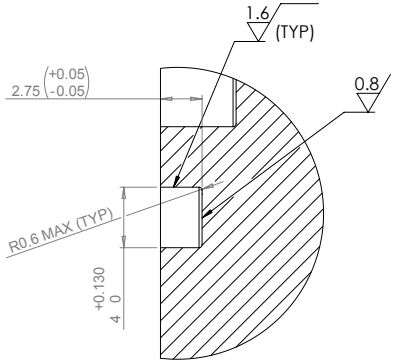

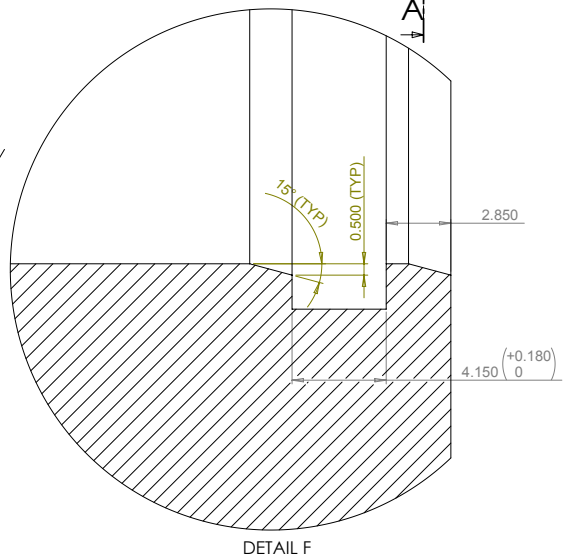

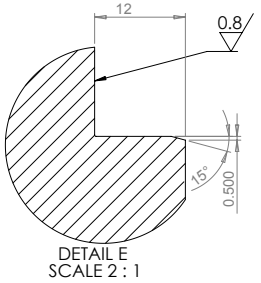

UNLESS STATED OTHERWISE:								
REMOVE ALL BURRS AND SHARP EDGES								
SCREW THREAD: ISO 6H 6g								
GEOMETRIC TOL. TO BS 308 1972								
WELDING SYMBOLS TO BS 499/2								
MACHINING TOLERANCES								
OVER - TO	**±**	**±**	**±**					
0 - 6	0.1	0.2	0.5					
6 - 30	0.2	0.5	0.8					
30 - 100	0.3	0.8	1.5					
100 - 300	0.5	1.2	2.0					
300 - 1000	0.8	2.0	3.0					
1000 - 3000	1.2	3.0	5.0					
3000 PLUS:	2.0	4.0	8.0					
ANGLES:	1°	1°	1°		JJJVR	2007/10/30	I	
SURFACE FIN:	1.6	6.3	12.5	**APPR.**	**DRAWN**	**DATE**	**REV.**	

MATERIAL:	ALUMINIUM 6082-t6	
	CAD FILENAME: ENCL-SC-003-A	**SCALE:** 1:4

COPYRIGHT NOTICE:
UNAUTHORISED USE, MANUFACTURE OR REPRODUCTION IN WHOLE OR IN PART IS PROHIBITED. DRAWING, DESIGN AND OTHER DISCLOSURES IS THE INTELLECTUAL PROPERTY OF NORTH-WEST UNIVERSITY. ALL RIGHTS RESERVED.

SCHOOL OF MECHANICAL ENGINEERING
POTCHEFSTROOM CAMPUS OF NW-U
11 HOFFMAN STREET
POTCHEFSTROOM 2530

SHEET 1 OF 1	PMSM ENCLOSURE
DWG. No.	ENCL-SC-003-RM-I | I

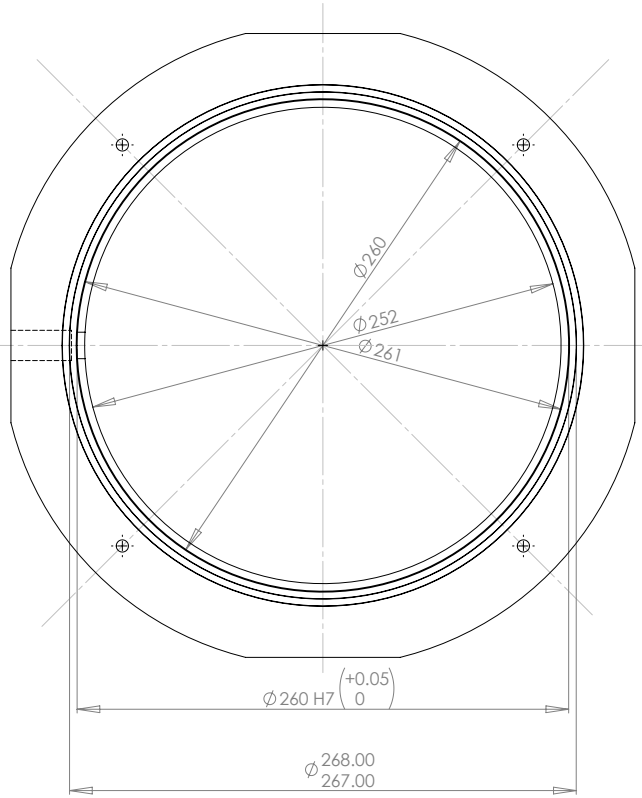

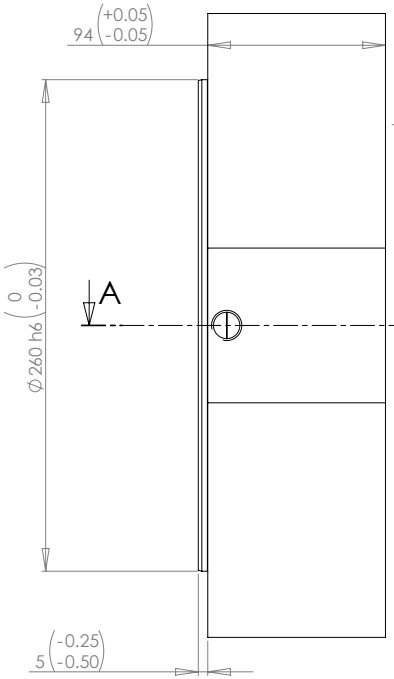

4 THRU HOLES Ø6.50
EQUI-SPACED AS SHOWN
ON PCD 300 TO
⌖ Ø 0.2

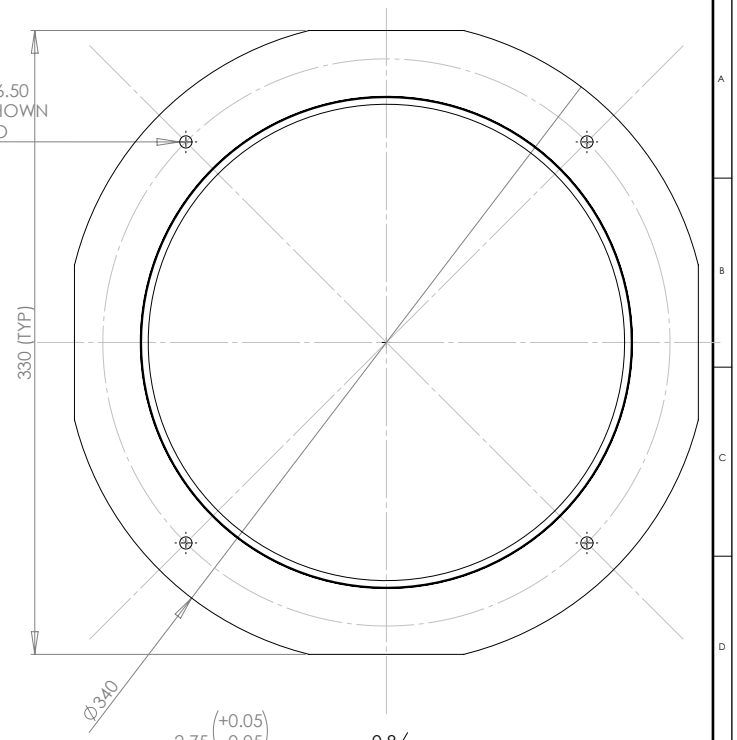

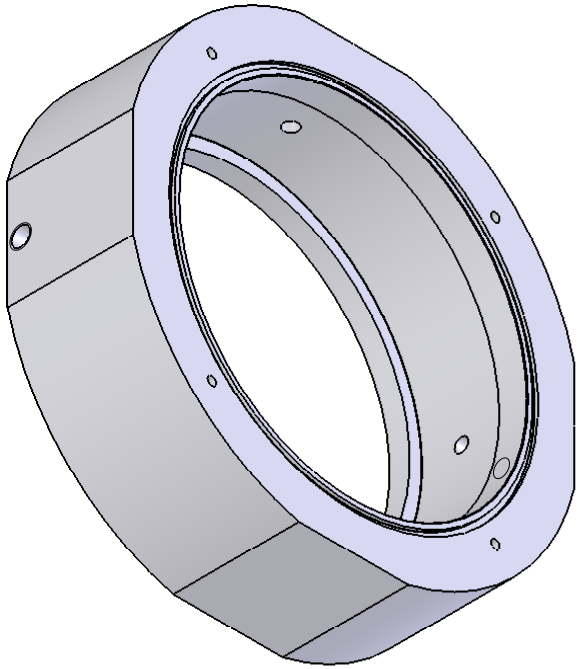

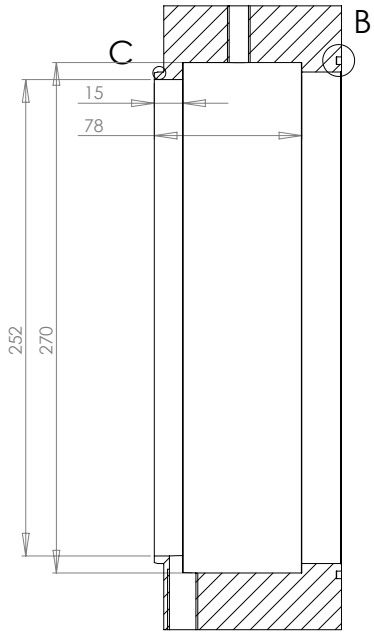

SECTION A-A

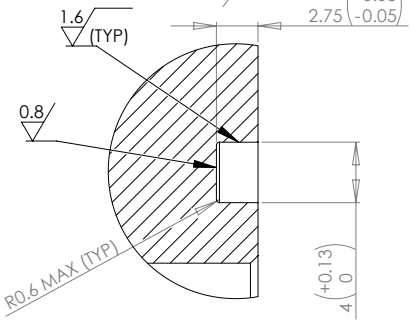

DETAIL B
SCALE 4 : 1

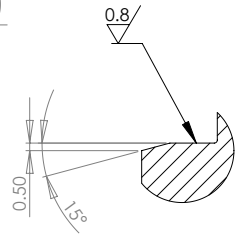

DETAIL C
SCALE 4 : 1

UNLESS STATED OTHERWISE: REMOVE ALL BURRS AND SHARP EDGES								
SCREW THREAD: ISO 6H 6g								
GEOMETRIC TOL. TO BS 308 1972								
WELDING SYMBOLS TO BS 499/2								
MACHINING TOLERANCES								
OVER - TO	**±**	**±**	**±**					
0 - 6	0.1	0.2	0.5					
6 - 30	0.2	0.5	0.8					
30 - 100	0.3	0.8	1.5					
100 - 300	0.5	1.2	2.0					
300 - 1000	0.8	2.0	3.0					
1000 - 3000	1.2	3.0	5.0					
3000 PLUS:	2.0	4.0	8.0					
ANGLES:	1°	1°	1°		JJJVR	2007/10/30	H	
SURFACE FIN:	1.6	6.3	12.5	**APPR.**	**DRAWN**	**DATE**	**REV.**	

MATERIAL: ALUMINIUM 6082-T6

CAD FILENAME: ENCL-SC-004-A | **SCALE:** 1:2

COPYRIGHT NOTICE:
UNAUTHORISED USE, MANUFACTURE OR REPRODUCTION IN WHOLE OR IN PART IS PROHIBITED. DRAWING, DESIGN AND OTHER DISCLOSURES IS THE INTELLECTUAL PROPERTY OF NORTH-WEST UNIVERSITY. ALL RIGHTS RESERVED.

SCHOOL OF MECHANICAL ENGINEERING
POTCHEFSTROOM CAMPUS OF NW-U
11 HOFFMAN STREET
POTCHEFSTROOM 2530

SHEET 1 OF 1

FLYWHEEL ENCLOSURE

DWG. No. ENCL-SC-004-H | H

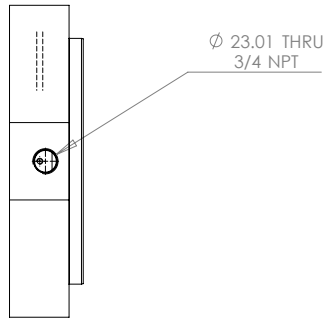

BACK VEIW

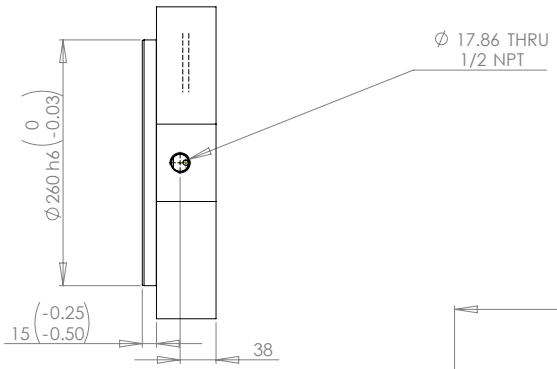

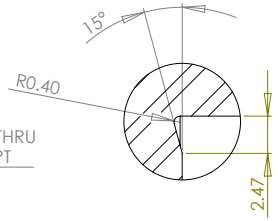

DETAIL D
SCALE 4 : 1

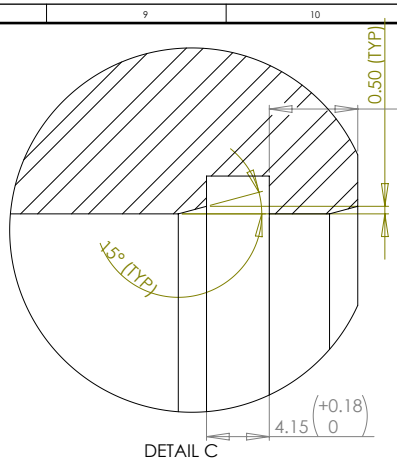

DETAIL C
SCALE 4 : 1

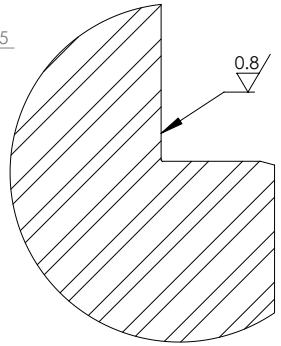

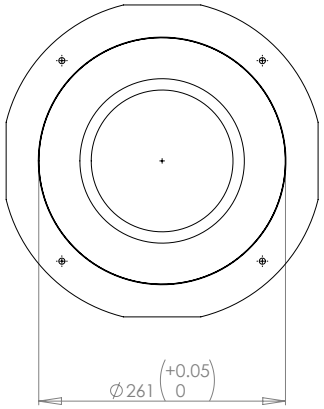

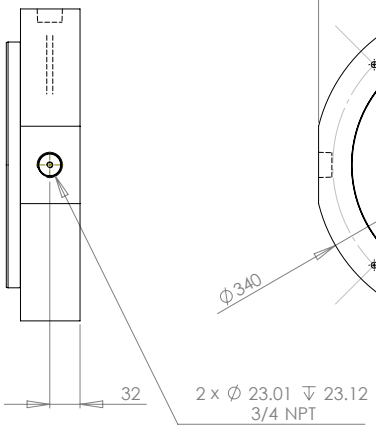

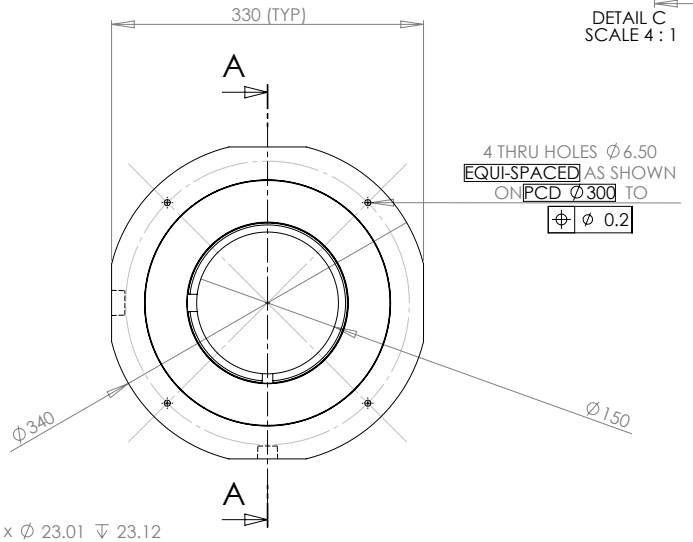

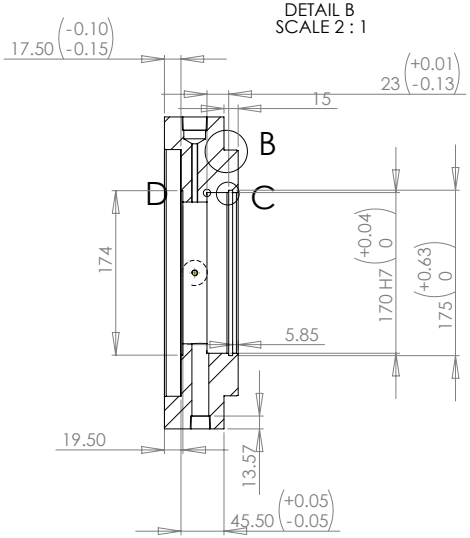

SECTION A-A

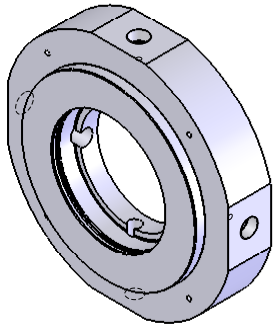

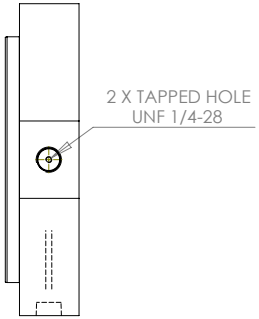

UNLESS STATED OTHERWISE: REMOVE ALL BURRS AND SHARP EDGES								
SCREW THREAD: ISO 6H 6g								
GEOMETRIC TOL. TO BS 308 1972								
WELDING SYMBOLS TO BS 499/2								
MACHINING TOLERANCES								
OVER - TO	**±**	**±**	**±**					
0 - 6	0.1	0.2	0.5					
6 - 30	0.2	0.5	0.8					
30 - 100	0.3	0.8	1.5					
100 - 300	0.5	1.2	2.0					
300 - 1000	0.8	2.0	3.0					
1000 - 3000	1.2	3.0	5.0					
3000 PLUS:	2.0	4.0	8.0					
ANGLES:	1°	1°	1°		JJJVR	2007/10/30	G	
SURFACE FIN:	1.6	6.3	12.5	**APPR.**	**DRAWN**	**DATE**	**REV.**	

MATERIAL: ALUMINIUM 6082-T6

CAD FILENAME: ENCL-SC-005-A **SCALE:** 1:4

COPYRIGHT NOTICE:
UNAUTHORISED USE, MANUFACTURE OR REPRODUCTION IN WHOLE OR IN PART IS PROHIBITED. DRAWING, DESIGN AND OTHER DISCLOSURES IS THE INTELLECTUAL PROPERTY OF NORTH-WEST UNIVERSITY. ALL RIGHTS RESERVED.

SCHOOL OF MECHANICAL ENGINEERING
POTCHEFSTROOM CAMPUS OF NW-U
11 HOFFMAN STREET
POTCHEFSTROOM 2530

SHEET 1 OF 1

UPPER AMB ENCLOSURE

DWG. No. ENCL-SC-005-G G

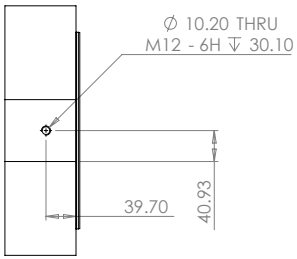

VIEW B

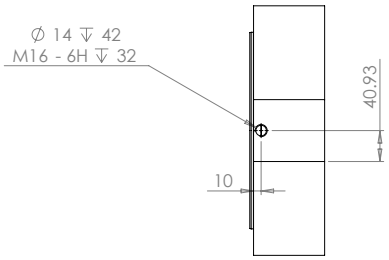

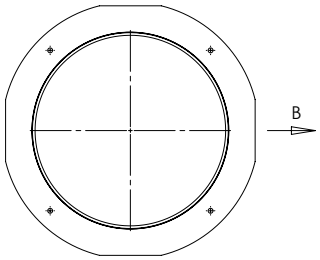

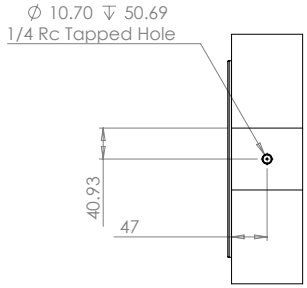

UNLESS OTHERWISE SPECIFIED: DIMENSIONS ARE IN MILLIMETERS SURFACE FINISH: TOLERANCES: LINEAR: ANGULAR:	FINISH:				DEBUR AND BREAK SHARP EDGES	DO NOT SCALE DRAWING / REVISION
	NAME	SIGNATURE	DATE			TITLE:
DRAWN						
CHK'D						
APP'V'D						
MFG						
Q.A				MATERIAL:		DWG NO. ENCL-SC-004-gate A3
				WEIGHT:	SCALE:1:5	SHEET 1 OF 1

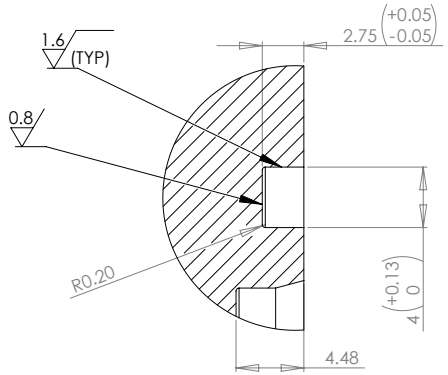

DETAIL B
SCALE 4 : 1

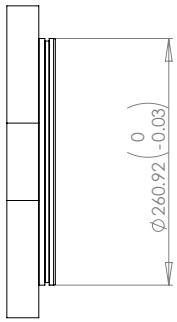

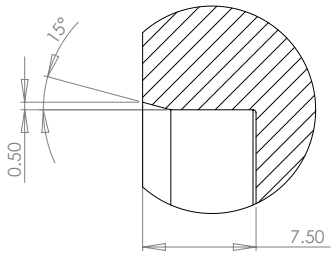

DETAIL E
SCALE 4 : 1

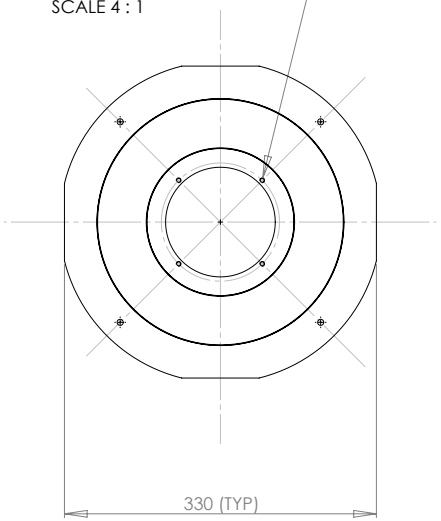

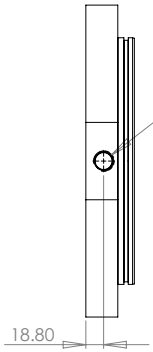

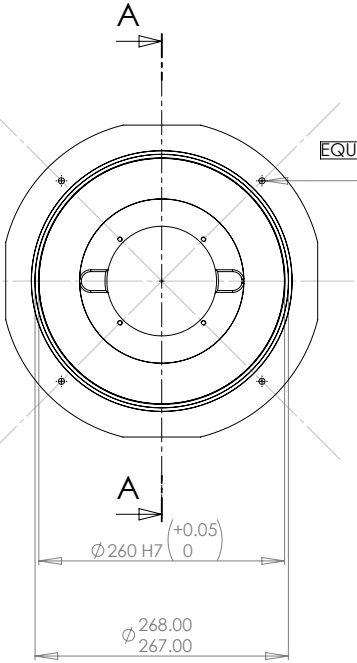

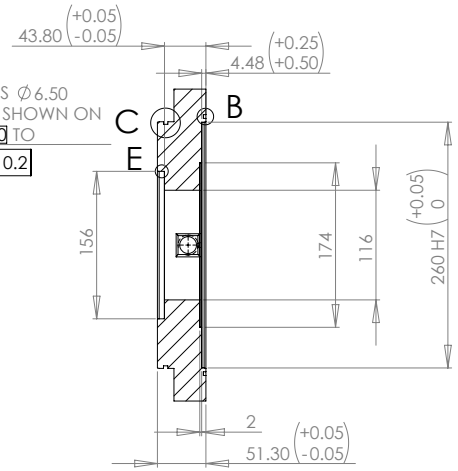

SECTION A-A

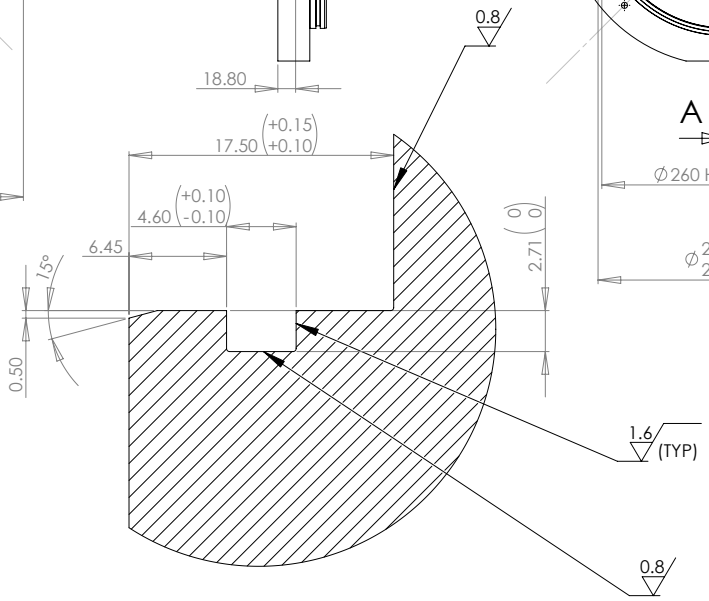

DETAIL C
SCALE 4 : 1

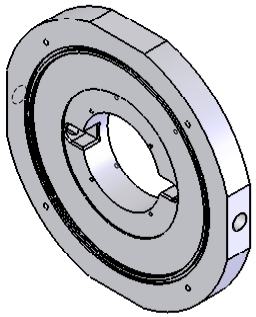

UNLESS STATED OTHERWISE: REMOVE ALL BURRS AND SHARP EDGES								
SCREW THREAD: ISO 6H 6g								
GEOMETRIC TOL. TO BS 308 1972								
WELDING SYMBOLS TO BS 499/2								
MACHINING TOLERANCES								
OVER - TO	**±**	**±**	**±**					
0 - 6	0.1	0.2	0.5					
6 - 30	0.2	0.5	0.8					
30 - 100	0.3	0.8	1.5					
100 - 300	0.5	1.2	2.0					
300 - 1000	0.8	2.0	3.0					
1000 - 3000	1.2	3.0	5.0					
3000 PLUS:	2.0	4.0	8.0					
ANGLES:	1°	1°	1°		JJJVR	2007/10/30	D	
SURFACE FIN:	1.6	6.3	12.5	**APPR.**	**DRAWN**	**DATE**	**REV.**	

MATERIAL: ALUMINIUM 6082-T6

CAD FILENAME: ENCL-SC-006-A | **SCALE:** 1:4

COPYRIGHT NOTICE:
UNAUTHORISED USE, MANUFACTURE OR REPRODUCTION IN WHOLE OR IN PART IS PROHIBITED. DRAWING, DESIGN AND OTHER DISCLOSURES IS THE INTELLECTUAL PROPERTY OF NORTH-WEST UNIVERSITY. ALL RIGHTS RESERVED.

SCHOOL OF MECHANICAL ENGINEERING
POTCHEFSTROOM CAMPUS OF NW-U
11 HOFFMAN STREET
POTCHEFSTROOM 2530

SHEET 1 OF 1

LOWER AXIAL AMB ENCLOSURE

DWG. No. ENCL-SC-006-G | D

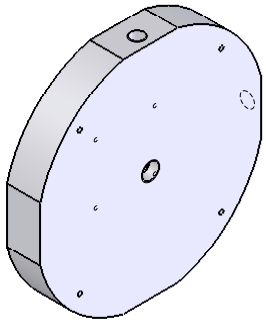

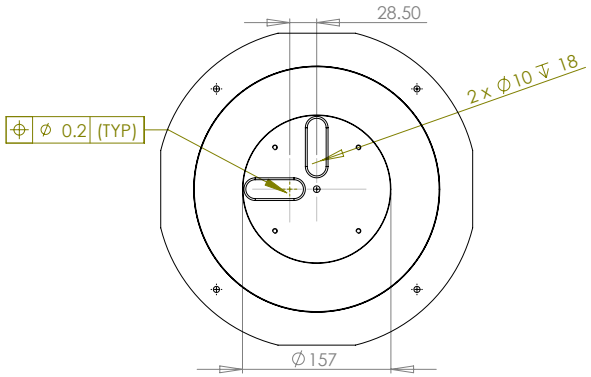

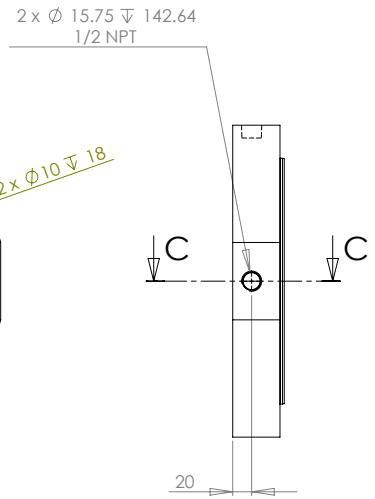

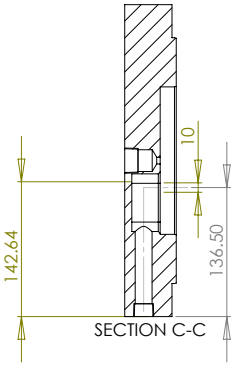

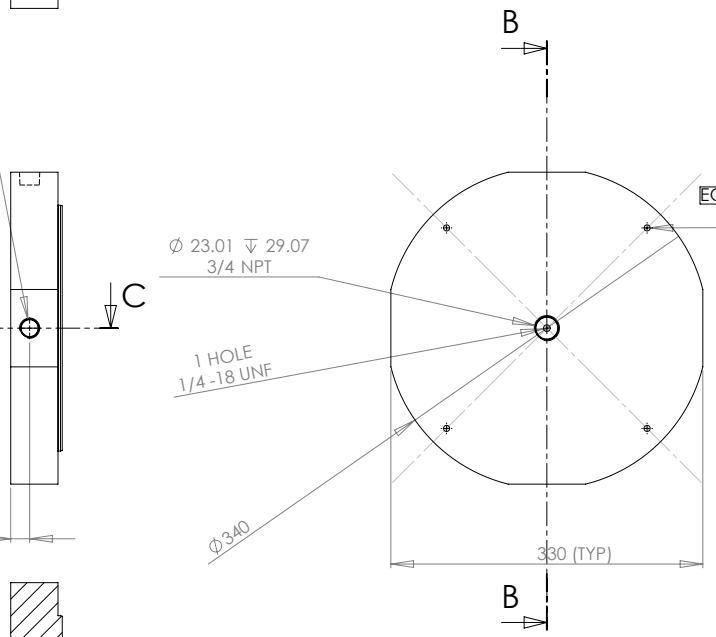

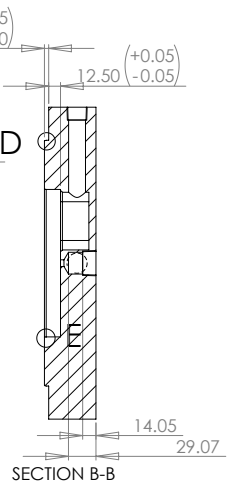

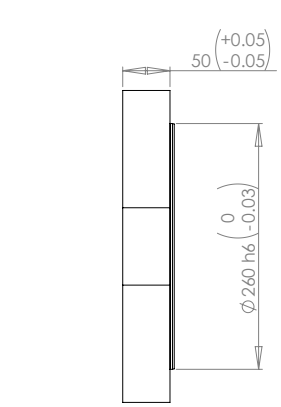

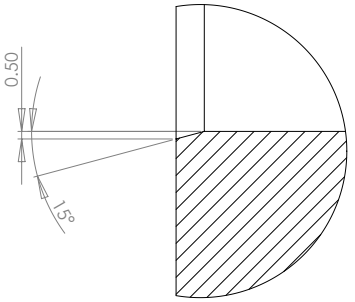

DETAIL E
SCALE 4 : 1

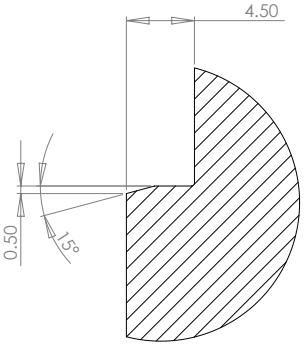

DETAIL D
SCALE 4 : 1

UNLESS STATED OTHERWISE:								
REMOVE ALL BURRS AND SHARP EDGES								
SCREW THREAD: ISO 6H 6g								
GEOMETRIC TOL. TO BS 308 1972								
WELDING SYMBOLS TO BS 499/2								
MACHINING TOLERANCES								
OVER - TO	**±**	**±**	**±**					
0 - 6	0.1	0.2	0.5					
6 - 30	0.2	0.5	0.8					
30 - 100	0.3	0.8	1.5					
100 - 300	0.5	1.2	2.0					
300 - 1000	0.8	2.0	3.0					
1000 - 3000	1.2	3.0	5.0					
3000 PLUS:	2.0	4.0	8.0					
ANGLES:	1°	1°	1°		JJJVR	2007/10/30	H	
SURFACE FIN:	1.6	6.3	12.5	**APPR.**	**DRAWN**	**DATE**	**REV.**	

MATERIAL: ALUMINIUM 6082-T6

CAD FILENAME: ENCL-SC-007-A | **SCALE:** 1:4

COPYRIGHT NOTICE:

UNAUTHORISED USE, MANUFACTURE OR REPRODUCTION IN WHOLE OR IN PART IS PROHIBITED. DRAWING, DESIGN AND OTHER DISCLOSURES IS THE INTELLECTUAL PROPERTY OF NORTH-WEST UNIVERSITY. ALL RIGHTS RESERVED.

SCHOOL OF MECHANICAL ENGINEERING
POTCHEFSTROOM CAMPUS OF NW-U
11 HOFFMAN STREET
POTCHEFSTROOM 2530

SHEET 1 OF 1

UPPER AXIAL AMB ENCLOSURE

DWG. No. ENCL-SC-007-H | H

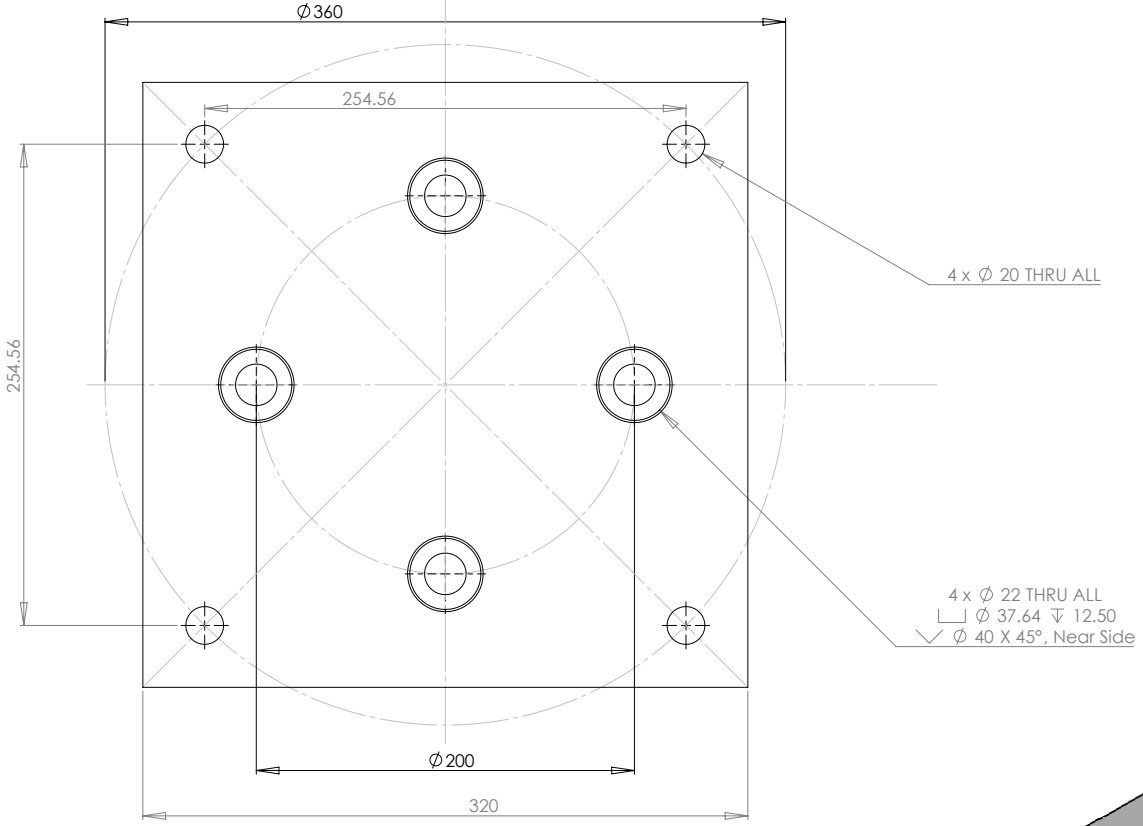

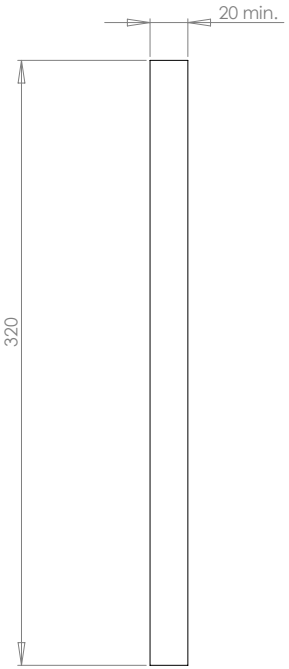

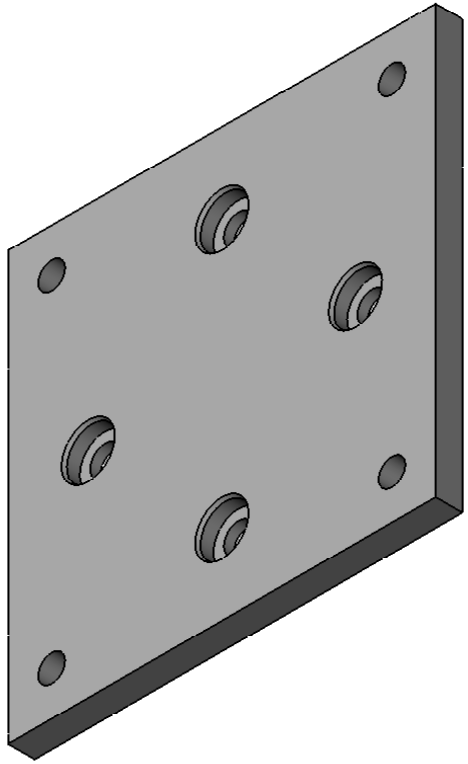

UNLESS STATED OTHERWISE: REMOVE ALL BURRS AND SHARP EDGES								
SCREW THREAD: ISO 6H 6g								
GEOMETRIC TOL. TO BS 308 1972					MATERIAL:			MILD STEEL
WELDING SYMBOLS TO BS 499/2								**CAD FILENAME:** ENCL-SC-022-A **SCALE:** 1:5
MACHINING TOLERANCES								
OVER - TO	**±**	**±**	**±**					**COPYRIGHT NOTICE:**
0 - 6	0.1	0.2	0.5					UNAUTHORISED USE, MANUFACTURE OR REPRODUCTION IN WHOLE OR IN PART IS PROHIBITED. DRAWING, DESIGN AND OTHER DISCLOSURES IS THE INTELLECTUAL PROPERTY OF NORTH-WEST UNIVERSITY. ALL RIGHTS RESERVED.
6 - 30	0.2	0.5	0.8					
30 - 100	0.3	0.8	1.5					
100 - 300	0.5	1.2	2.0					
300 - 1000	0.8	2.0	3.0					SCHOOL OF MECHANICAL ENGINEERING POTCHEFSTROOM CAMPUS OF NW-U 11 HOFFMAN STREET POTCHEFSTROOM 2530
1000 - 3000	1.2	3.0	5.0					SHEET 1 OF 1
3000 PLUS:	2.0	4.0	8.0					PMSM ENCLOSURE
ANGLES:	1°	1°	1°		JJJVR	2007/10/30	C	**DWG. No.** ENCL-SC-022-C C
SURFACE FIN:	1.6	6.3	12.5	**APPR.**	**DRAWN**	**DATE**	**REV.**	

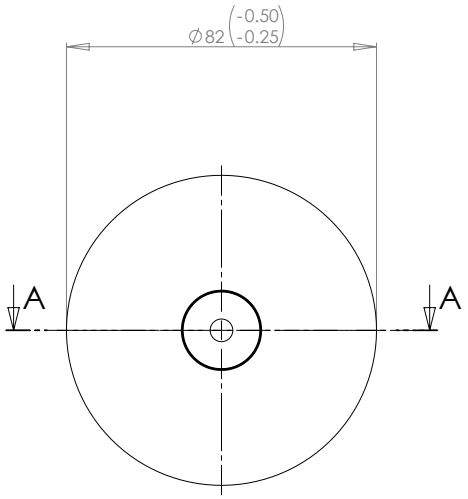

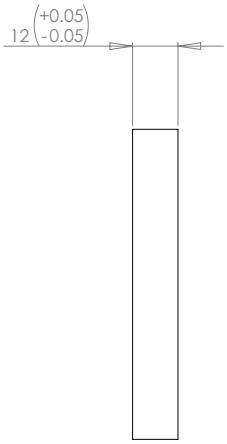

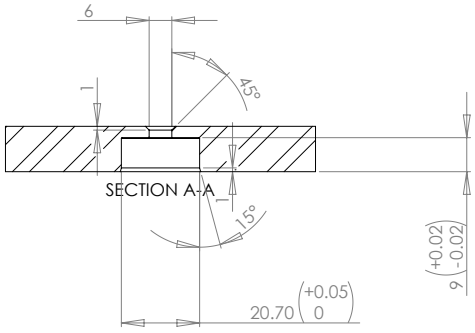

UNLESS STATED OTHERWISE: REMOVE ALL BURRS AND SHARP EDGES								
SCREW THREAD: ISO 6H 6g								
GEOMETRIC TOL. TO BS 308 1972								
WELDING SYMBOLS TO BS 499/2								
MACHINING TOLERANCES								
OVER - TO	**±**	**±**	**±**					
0 - 6	0.1	0.2	0.5					
6 - 30	0.2	0.5	0.8					
30 - 100	0.3	0.8	1.5					
100 - 300	0.5	1.2	2.0					
300 - 1000	0.8	2.0	3.0					
1000 - 3000	1.2	3.0	5.0					
3000 PLUS:	2.0	4.0	8.0					
ANGLES:	1°	1°	1°		JJJVR	2007/10/30	C	
SURFACE FIN:	1.6	6.3	12.5	**APPR.**	**DRAWN**	**DATE**	**REV.**	

CAD FILENAME: RF-SC-001-A | **SCALE:** 1:1

COPYRIGHT NOTICE:

UNAUTHORISED USE, MANUFACTURE OR REPRODUCTION IN WHOLE OR IN PART IS PROHIBITED. DRAWING, DESIGN AND OTHER DISCLOSURES IS THE INTELLECTUAL PROPERTY OF NORTH-WEST UNIVERSITY. ALL RIGHTS RESERVED.

SCHOOL OF MECHANICAL ENGINEERING
POTCHEFSTROOM CAMPUS OF NW-U
11 HOFFMAN STREET
POTCHEFSTROOM 2530

SHEET 1 OF 1

AXIAL DISC

DWG. No. RF-SC-001-C | C

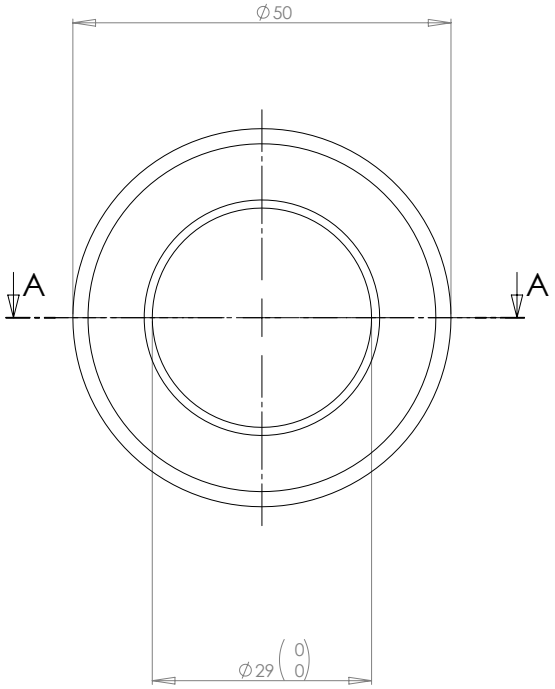

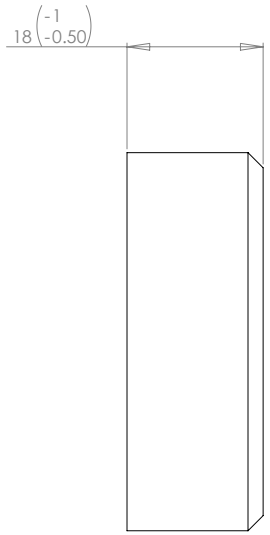

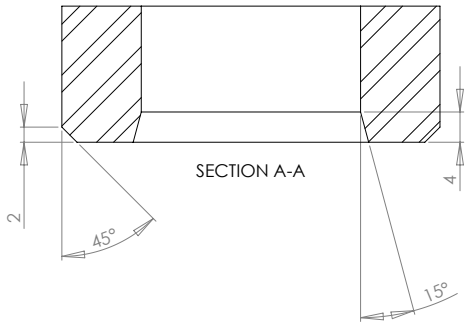

UNLESS STATED OTHERWISE: REMOVE ALL BURRS AND SHARP EDGES								
SCREW THREAD: ISO 6H 6g								
GEOMETRIC TOL. TO BS 308 1972								
WELDING SYMBOLS TO BS 499/2								
MACHINING TOLERANCES								
OVER - TO	**±**	**±**	**±**					
0 - 6	0.1	0.2	0.5					
6 - 30	0.2	0.5	0.8					
30 - 100	0.3	0.8	1.5					
100 - 300	0.5	1.2	2.0					
300 - 1000	0.8	2.0	3.0					
1000 - 3000	1.2	3.0	5.0					
3000 PLUS:	2.0	4.0	8.0					
ANGLES:	1°	1°	1°		JJJVR	2007/10/30	B	
SURFACE FIN:	1.6	6.3	12.5	**APPR.**	**DRAWN**	**DATE**	**REV.**	

CAD FILENAME: RF-SC-003-A | **SCALE:** 2:1

COPYRIGHT NOTICE:

UNAUTHORISED USE, MANUFACTURE OR REPRODUCTION IN WHOLE OR IN PART IS PROHIBITED. DRAWING, DESIGN AND OTHER DISCLOSURES IS THE INTELLECTUAL PROPERTY OF NORTH-WEST UNIVERSITY. ALL RIGHTS RESERVED.

SCHOOL OF MECHANICAL ENGINEERING
POTCHEFSTROOM CAMPUS OF NW-U
11 HOFFMAN STREET
POTCHEFSTROOM 2530

SHEET 1 OF 1

ENDSTOP 2

DWG. No. RF-SC-003-B | B

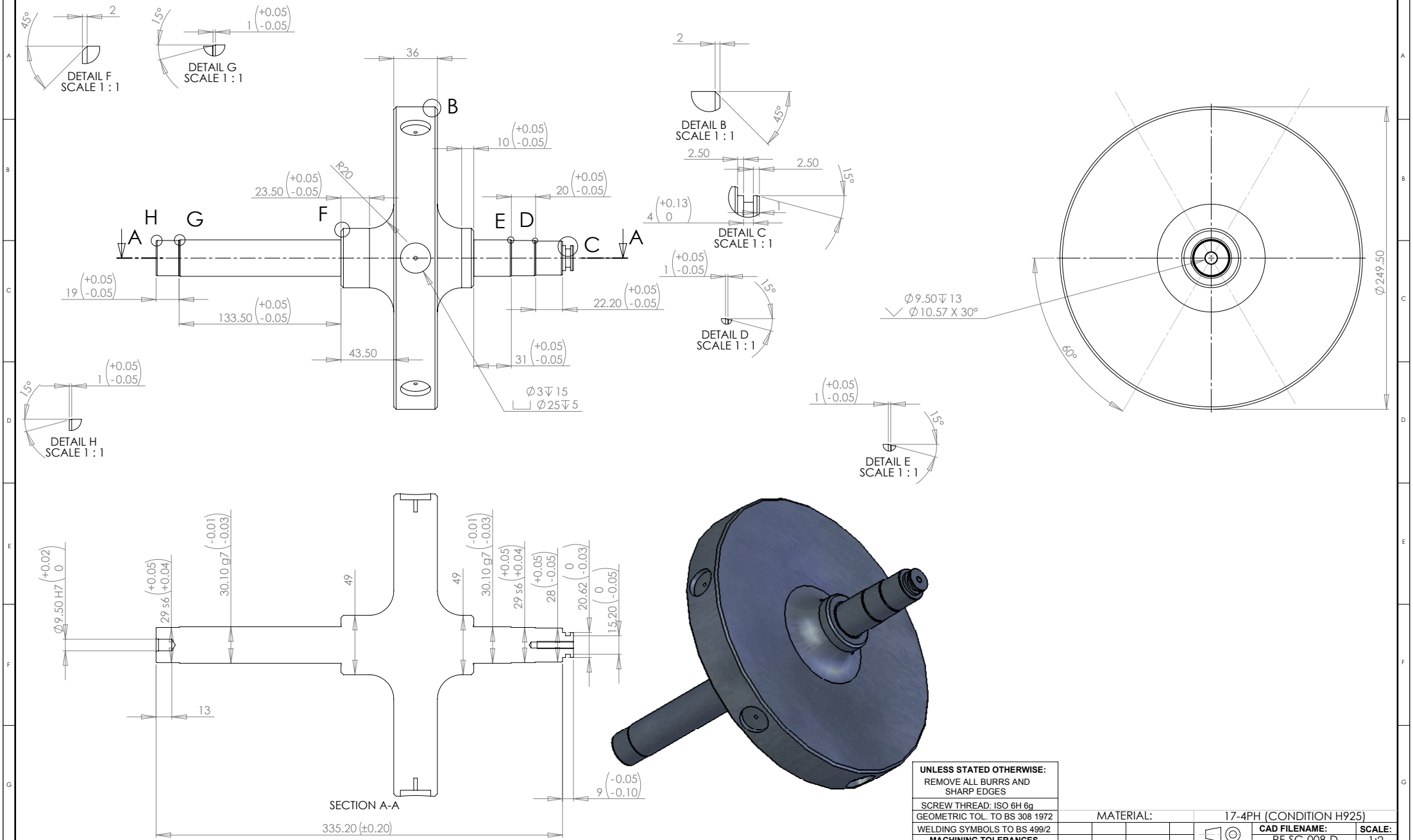

UNLESS STATED OTHERWISE: REMOVE ALL BURRS AND SHARP EDGES								
SCREW THREAD: ISO 6H 6g								
GEOMETRIC TOL. TO BS 308 1972					MATERIAL:			17-4PH (CONDITION H925)
WELDING SYMBOLS TO BS 499/2								**CAD FILENAME:** RF-SC-008-D / **SCALE:** 1:2
MACHINING TOLERANCES								
OVER - TO	**±**	**±**	**±**					**COPYRIGHT NOTICE:**
0 - 6	0.1	0.2	0.5					UNAUTHORISED USE, MANUFACTURE OR REPRODUCTION IN WHOLE OR IN PART IS PROHIBITED. DRAWING, DESIGN AND OTHER DISCLOSURES IS THE INTELLECTUAL PROPERTY OF NORTH-WEST UNIVERSITY. ALL RIGHTS RESERVED.
6 - 30	0.2	0.5	0.8					
30 - 100	0.3	0.8	1.5					
100 - 300	0.5	1.2	2.0					SCHOOL OF MECHANICAL ENGINEERING POTCHEFSTROOM CAMPUS OF NW-U 11 HOFFMAN STREET POTCHEFSTROOM 2530
300 - 1000	0.8	2.0	3.0					
1000 - 3000	1.2	3.0	5.0					SHEET 1 OF 1 — FLYWHEEL FINAL
3000 PLUS:	2.0	4.0	8.0					
ANGLES:	1°	1°	1°		JJJVR	2007/10/30	H	**DWG. No.** RF-SC-008-H H
SURFACE FIN:	1.6	6.3	12.5	**APPR.**	**DRAWN**	**DATE**	**REV.**	

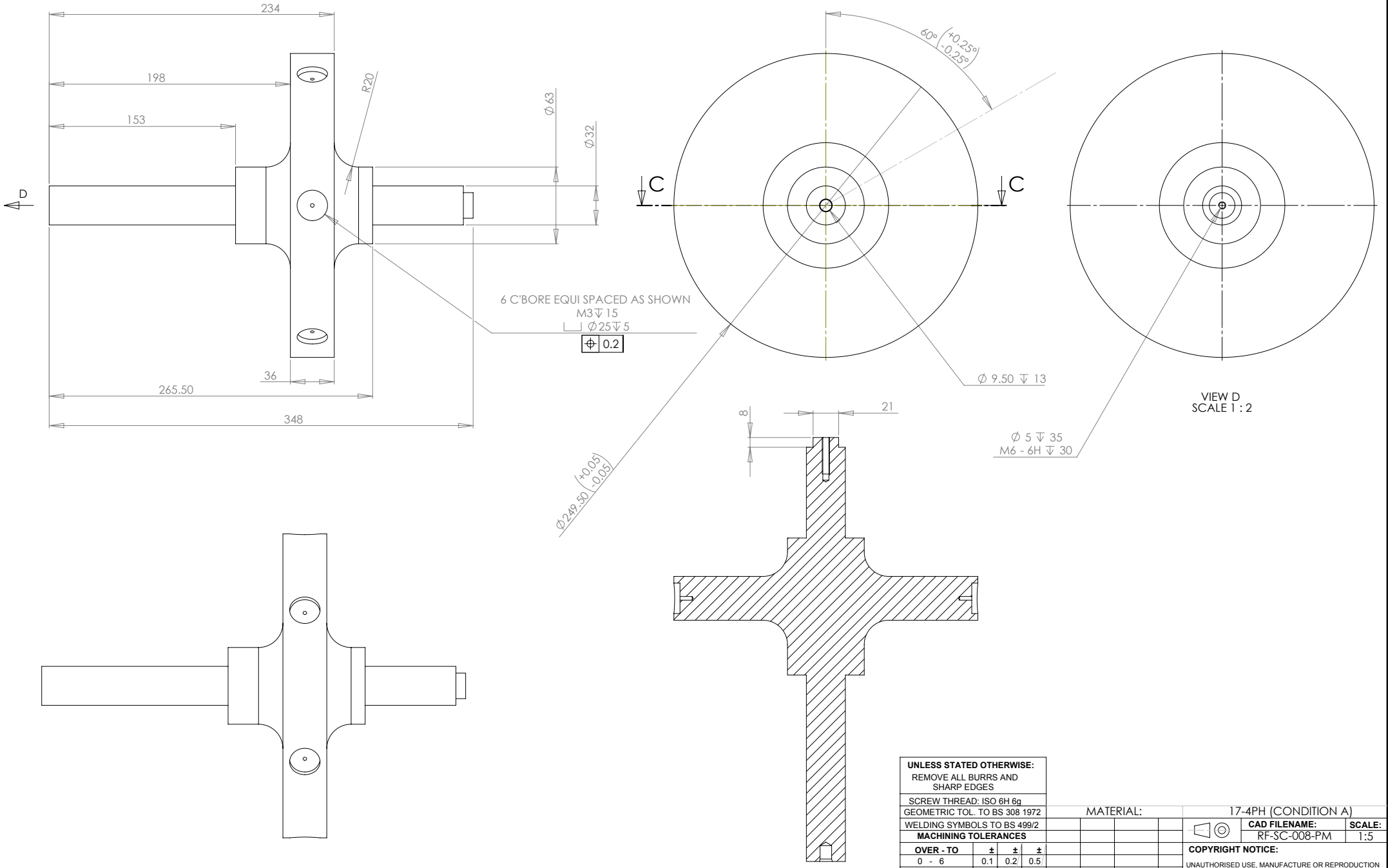

UNLESS STATED OTHERWISE: REMOVE ALL BURRS AND SHARP EDGES								
SCREW THREAD: ISO 6H 6g								
GEOMETRIC TOL. TO BS 308 1972					MATERIAL:			17-4PH (CONDITION A)
WELDING SYMBOLS TO BS 499/2								CAD FILENAME: RF-SC-008-PM / SCALE: 1:5
MACHINING TOLERANCES								
OVER - TO	**±**	**±**	**±**					**COPYRIGHT NOTICE:**
0 - 6	0.1	0.2	0.5					UNAUTHORISED USE, MANUFACTURE OR REPRODUCTION IN WHOLE OR IN PART IS PROHIBITED. DRAWING, DESIGN AND OTHER DISCLOSURES IS THE INTELLECTUAL PROPERTY OF NORTH-WEST UNIVERSITY. ALL RIGHTS RESERVED.
6 - 30	0.2	0.5	0.8					
30 - 100	0.3	0.8	1.5					
100 - 300	0.5	1.2	2.0					
300 - 1000	0.8	2.0	3.0					SCHOOL OF MECHANICAL ENGINEERING POTCHEFSTROOM CAMPUS OF NW-U 11 HOFFMAN STREET POTCHEFSTROOM 2530
1000 - 3000	1.2	3.0	5.0					SHEET 1 OF 1
3000 PLUS:	2.0	4.0	8.0					PRE HEAT TRETMENT
ANGLES:	1°	1°	1°		JJJVR	2007/10/30	G	DWG. No. RF-SC-008-PM-G G
SURFACE FIN:	1.6	6.3	12.5	APPR.	DRAWN	DATE	REV.	

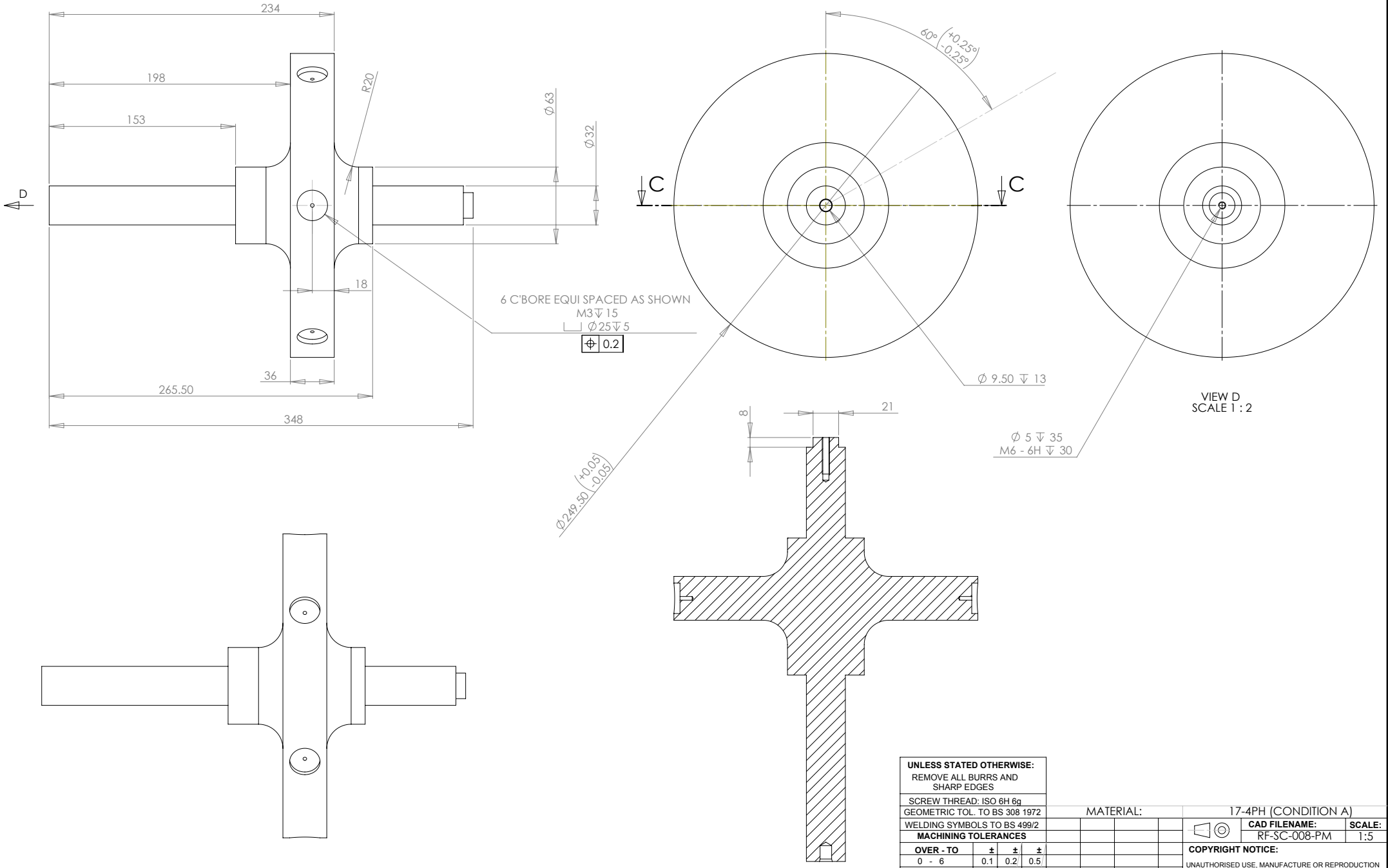

UNLESS STATED OTHERWISE: REMOVE ALL BURRS AND SHARP EDGES								
SCREW THREAD: ISO 6H 6g								
GEOMETRIC TOL. TO BS 308 1972					MATERIAL:			17-4PH (CONDITION A)
WELDING SYMBOLS TO BS 499/2								**CAD FILENAME:** RF-SC-008-PM / **SCALE:** 1:5
MACHINING TOLERANCES								
OVER - TO	**±**	**±**	**±**					**COPYRIGHT NOTICE:**
0 - 6	0.1	0.2	0.5					UNAUTHORISED USE, MANUFACTURE OR REPRODUCTION IN WHOLE OR IN PART IS PROHIBITED. DRAWING, DESIGN AND OTHER DISCLOSURES IS THE INTELLECTUAL PROPERTY OF NORTH-WEST UNIVERSITY. ALL RIGHTS RESERVED.
6 - 30	0.2	0.5	0.8					
30 - 100	0.3	0.8	1.5					
100 - 300	0.5	1.2	2.0					
300 - 1000	0.8	2.0	3.0					SCHOOL OF MECHANICAL ENGINEERING POTCHEFSTROOM CAMPUS OF NW-U 11 HOFFMAN STREET POTCHEFSTROOM 2530
1000 - 3000	1.2	3.0	5.0					SHEET 1 OF 1
3000 PLUS:	2.0	4.0	8.0					PRE HEAT TRETMENT
ANGLES:	1°	1°	1°		JJJVR	2007/10/30	H	**DWG. No.** RF-SC-008-PM-H / H
SURFACE FIN:	1.6	6.3	12.5	**APPR.**	**DRAWN**	**DATE**	**REV.**	

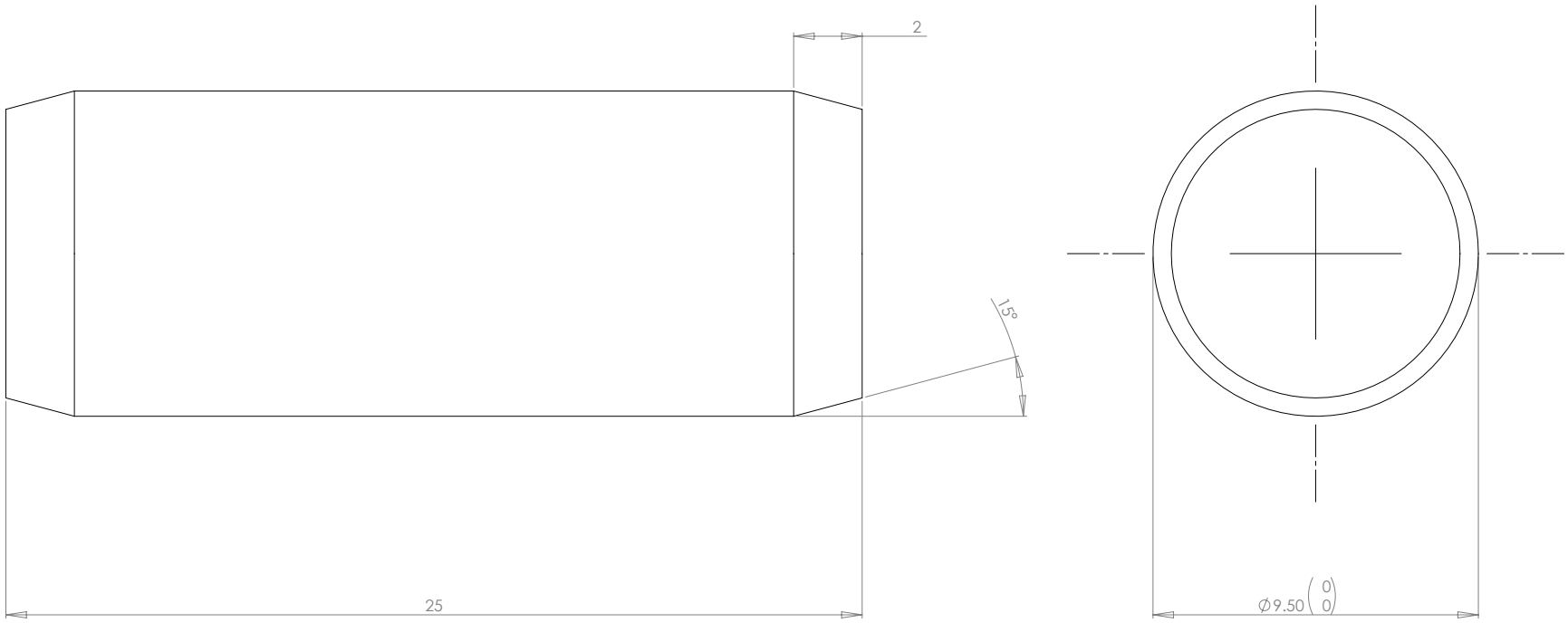

UNLESS STATED OTHERWISE: REMOVE ALL BURRS AND SHARP EDGES								
SCREW THREAD: ISO 6H 6g								
GEOMETRIC TOL. TO BS 308 1972								
WELDING SYMBOLS TO BS 499/2								
MACHINING TOLERANCES								
OVER - TO	**±**	**±**	**±**					
0 - 6	0.1	0.2	0.5					
6 - 30	0.2	0.5	0.8					
30 - 100	0.3	0.8	1.5					
100 - 300	0.5	1.2	2.0					
300 - 1000	0.8	2.0	3.0					
1000 - 3000	1.2	3.0	5.0					
3000 PLUS:	2.0	4.0	8.0					
ANGLES:	1°	1°	1°		JJJVR	2007/10/30	A	
SURFACE FIN:	1.6	6.3	12.5	**APPR.**	**DRAWN**	**DATE**	**REV.**	

	CAD FILENAME: RF-SC-011-A	**SCALE:** 10:1

COPYRIGHT NOTICE:

UNAUTHORISED USE, MANUFACTURE OR REPRODUCTION IN WHOLE OR IN PART IS PROHIBITED. DRAWING, DESIGN AND OTHER DISCLOSURES IS THE INTELLECTUAL PROPERTY OF NORTH-WEST UNIVERSITY. ALL RIGHTS RESERVED.

SCHOOL OF MECHANICAL ENGINEERING
POTCHEFSTROOM CAMPUS OF NW-U
11 HOFFMAN STREET
POTCHEFSTROOM 2530

SHEET 1 OF 1

BACKUP BEARING PIN

DWG. No. RF-SC-011-A A

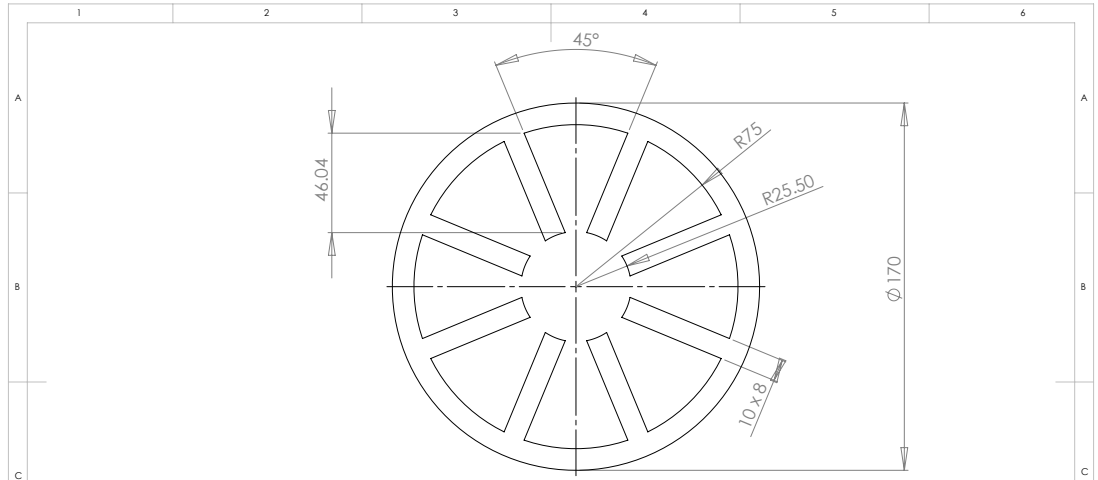

The laminations will be made of M270-35A silicon steel. The thickness of each lamination will be 0.35mm.

A total of 180 lamination sheets will be needed.

A minimum accuracy of +/- 0.1mm will be required.

UNLESS OTHERWISE SPECIFIED: DIMENSIONS ARE IN MILLIMETERS SURFACE FINISH: TOLERANCES: LINEAR: ANGULAR:	FINISH:		DEBUR AND BREAK SHARP EDGES	DO NOT SCALE DRAWING	REVISION A
	NAME	SIGNATURE	DATE	TITLE: RADIAL AMB LAMINATIONS	
DRAWN	STEFAN MYBURGH		29/08/06		
CHK'D					
APPV'D					
MFG					
Q.A				MATERIAL: M270-35A SILICON STEEL	DWG NO. RAMB-SC-001-A A4
				WEIGHT:	SCALE:1:1 SHEET 1 OF 1

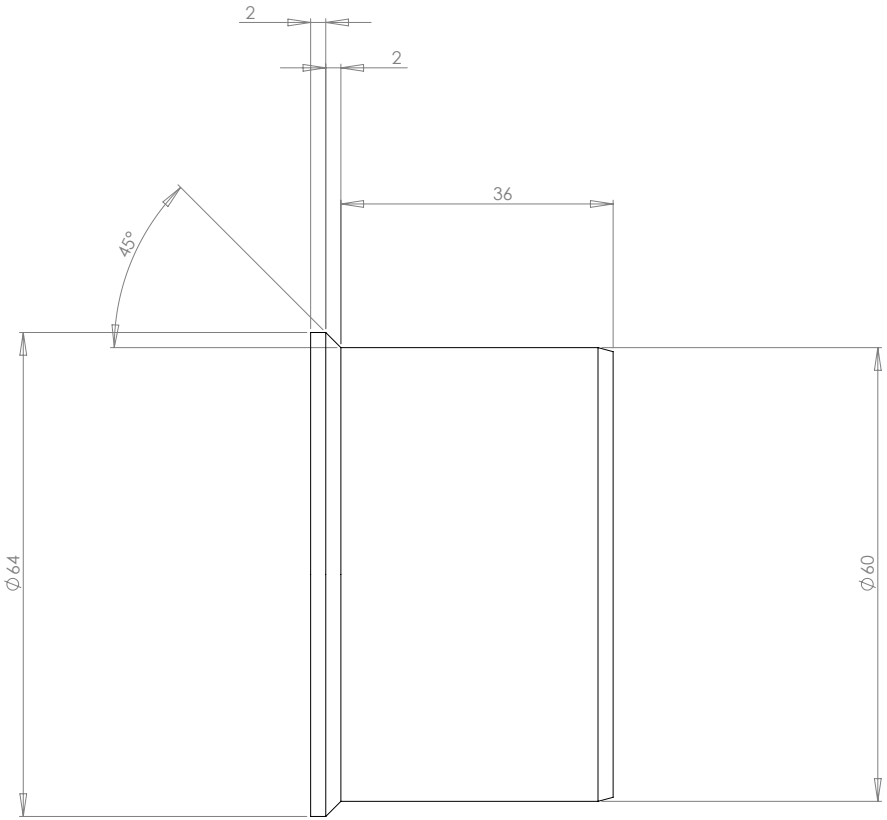

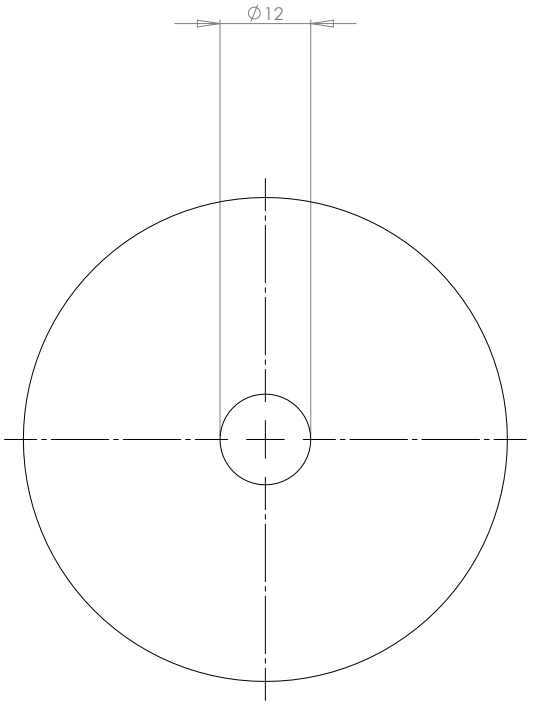

UNLESS STATED OTHERWISE: REMOVE ALL BURRS AND SHARP EDGES								
SCREW THREAD: ISO 6H 6g								
GEOMETRIC TOL. TO BS 308 1972								
WELDING SYMBOLS TO BS 499/2								
MACHINING TOLERANCES								
OVER - TO	**±**	**±**	**±**					
0 - 6	0.1	0.2	0.5					
6 - 30	0.2	0.5	0.8					
30 - 100	0.3	0.8	1.5					
100 - 300	0.5	1.2	2.0					
300 - 1000	0.8	2.0	3.0					
1000 - 3000	1.2	3.0	5.0					
3000 PLUS:	2.0	4.0	8.0					
ANGLES:	1°	1°	1°		JJJVR	2007/10/30	C	
SURFACE FIN:	1.6	6.3	12.5	**APPR.**	**DRAWN**	**DATE**	**REV.**	

CAD FILENAME: PJ-SC-001-A | **SCALE:** 2:1

COPYRIGHT NOTICE:

UNAUTHORISED USE, MANUFACTURE OR REPRODUCTION IN WHOLE OR IN PART IS PROHIBITED. DRAWING, DESIGN AND OTHER DISCLOSURES IS THE INTELLECTUAL PROPERTY OF NORTH-WEST UNIVERSITY. ALL RIGHTS RESERVED.

SCHOOL OF MECHANICAL ENGINEERING
POTCHEFSTROOM CAMPUS OF NW-U
11 HOFFMAN STREET
POTCHEFSTROOM 2530

SHEET 1 OF 1

PMSM ENCLOSURE

DWG. No. PJ-SC-001-A | C

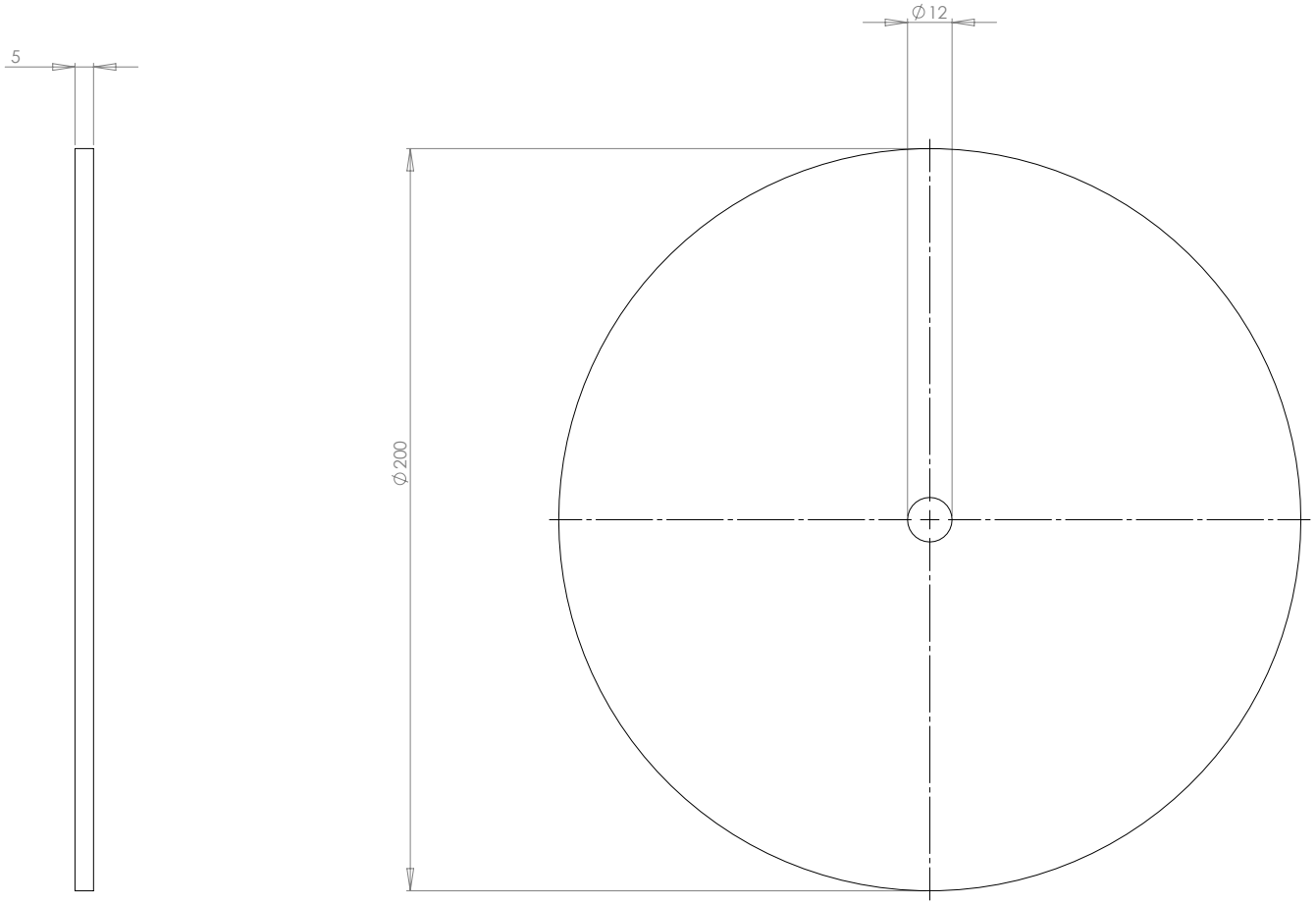

UNLESS STATED OTHERWISE:
REMOVE ALL BURRS AND SHARP EDGES

SCREW THREAD: ISO 6H 6g

GEOMETRIC TOL. TO BS 308 1972

WELDING SYMBOLS TO BS 499/2

MACHINING TOLERANCES

OVER - TO	±	±	±
0 - 6	0.1	0.2	0.5
6 - 30	0.2	0.5	0.8
30 - 100	0.3	0.8	1.5
100 - 300	0.5	1.2	2.0
300 - 1000	0.8	2.0	3.0
1000 - 3000	1.2	3.0	5.0
3000 PLUS:	2.0	4.0	8.0
ANGLES:	1°	1°	1°
SURFACE FIN:	1.6	6.3	12.5

APPR.	DRAWN	DATE	REV.
	JJJVR	2007/10/30	C

CAD FILENAME: PJ-SC-002-A

SCALE: 1:2

COPYRIGHT NOTICE:

UNAUTHORISED USE, MANUFACTURE OR REPRODUCTION IN WHOLE OR IN PART IS PROHIBITED. DRAWING, DESIGN AND OTHER DISCLOSURES IS THE INTELLECTUAL PROPERTY OF NORTH-WEST UNIVERSITY. ALL RIGHTS RESERVED.

SCHOOL OF MECHANICAL ENGINEERING
POTCHEFSTROOM CAMPUS OF NW-U
11 HOFFMAN STREET
POTCHEFSTROOM 2530

SHEET 1 OF 1

PMSM ENCLOSURE

DWG. No. PJ-SC-002-A C

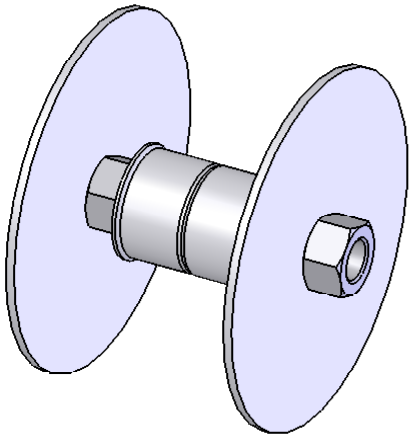

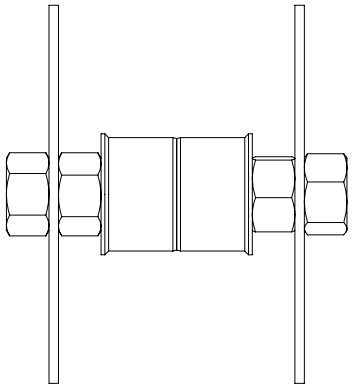

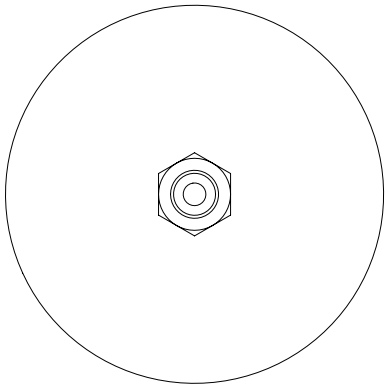

UNLESS STATED OTHERWISE:
REMOVE ALL BURRS AND SHARP EDGES
SCREW THREAD: ISO 6H 6g
GEOMETRIC TOL. TO BS 308 1972
WELDING SYMBOLS TO BS 499/2

MACHINING TOLERANCES			
OVER - TO	±	±	±
0 - 6	0.1	0.2	0.5
6 - 30	0.2	0.5	0.8
30 - 100	0.3	0.8	1.5
100 - 300	0.5	1.2	2.0
300 - 1000	0.8	2.0	3.0
1000 - 3000	1.2	3.0	5.0
3000 PLUS:	2.0	4.0	8.0
ANGLES:	1°	1°	1°
SURFACE FIN:	1.6	6.3	12.5

APPR.	DRAWN	DATE	REV.
	JJJVR	2007/10/30	C

CAD FILENAME:	SCALE:
PJ-FA-001	1:2

COPYRIGHT NOTICE:

UNAUTHORISED USE, MANUFACTURE OR REPRODUCTION IN WHOLE OR IN PART IS PROHIBITED. DRAWING, DESIGN AND OTHER DISCLOSURES IS THE INTELLECTUAL PROPERTY OF NORTH-WEST UNIVERSITY. ALL RIGHTS RESERVED.

SCHOOL OF MECHANICAL ENGINEERING
POTCHEFSTROOM CAMPUS OF NW-U
11 HOFFMAN STREET
POTCHEFSTROOM 2530

SHEET 1 OF 1

PMSM ENCLOSURE

DWG. No.	
PJ-FA-001	C

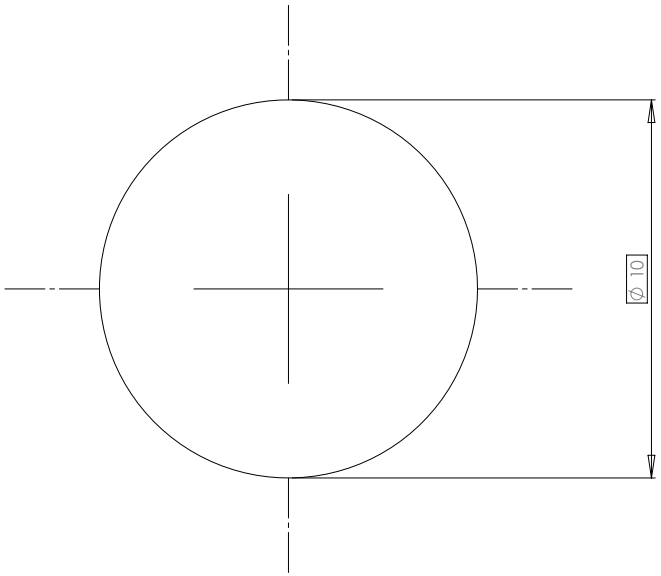

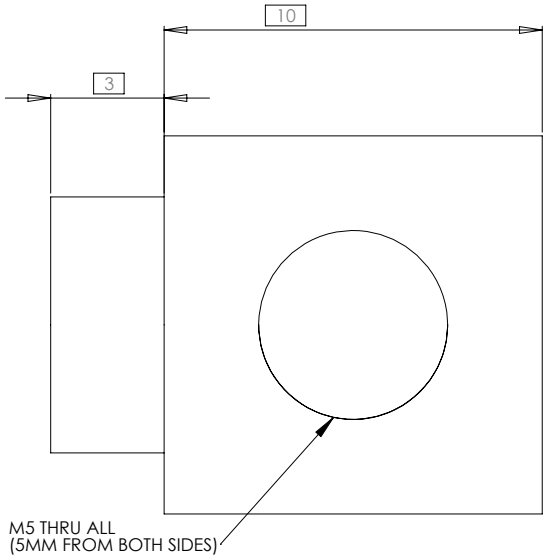

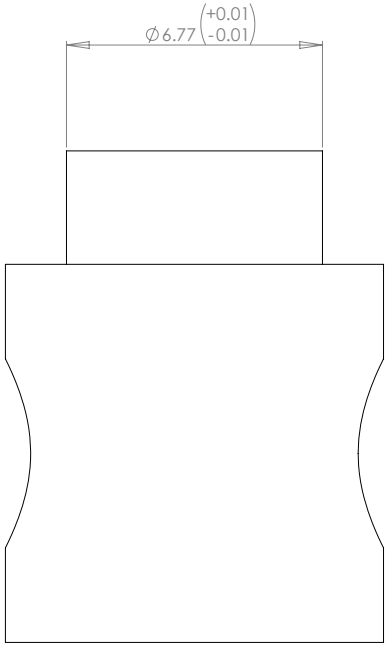

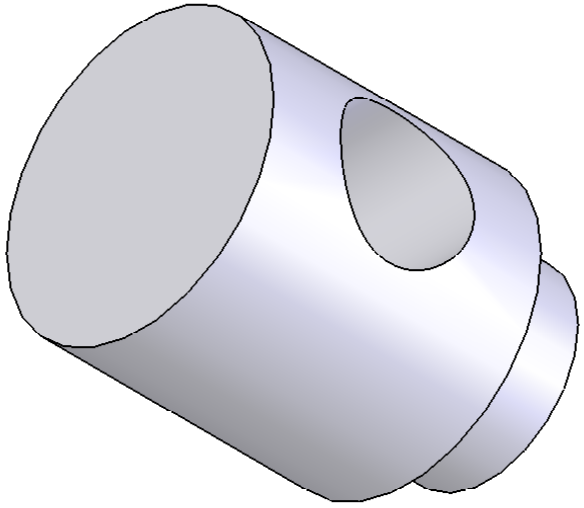

UNLESS STATED OTHERWISE: REMOVE ALL BURRS AND SHARP EDGES								
SCREW THREAD: ISO 6H 6g								
GEOMETRIC TOL. TO BS 308 1972								
WELDING SYMBOLS TO BS 499/2								
MACHINING TOLERANCES								
OVER - TO	**±**	**±**	**±**					
0 - 6	0.1	0.2	0.5					
6 - 30	0.2	0.5	0.8					
30 - 100	0.3	0.8	1.5					
100 - 300	0.5	1.2	2.0					
300 - 1000	0.8	2.0	3.0					
1000 - 3000	1.2	3.0	5.0					
3000 PLUS:	2.0	4.0	8.0					
ANGLES:	1°	1°	1°		JJJVR	2007/10/30	A	
SURFACE FIN:	1.6	6.3	12.5	APPR.	DRAWN	DATE	REV.	

CAD FILENAME:	**SCALE:**
PMM-SC-098-A	10:1

COPYRIGHT NOTICE:

UNAUTHORISED USE, MANUFACTURE OR REPRODUCTION IN WHOLE OR IN PART IS PROHIBITED. DRAWING, DESIGN AND OTHER DISCLOSURES IS THE INTELLECTUAL PROPERTY OF NORTH-WEST UNIVERSITY. ALL RIGHTS RESERVED.

SCHOOL OF MECHANICAL ENGINEERING
POTCHEFSTROOM CAMPUS OF NW-U
11 HOFFMAN STREET
POTCHEFSTROOM 2530

SHEET 1 OF 1

GLUE TEST-PIECE

DWG. No.	PMM-SC-098-A	A

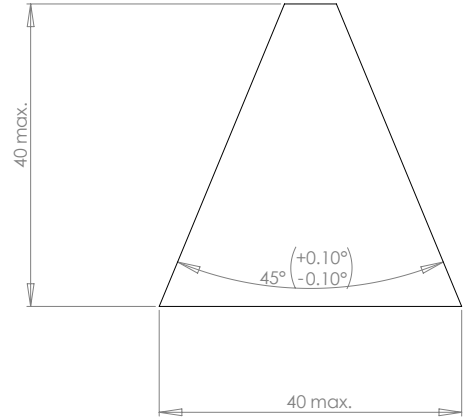

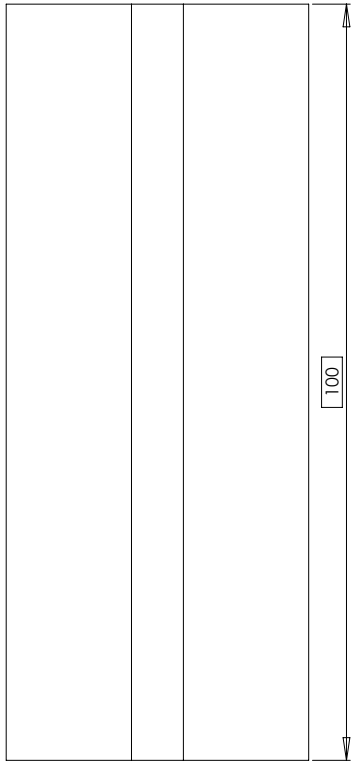

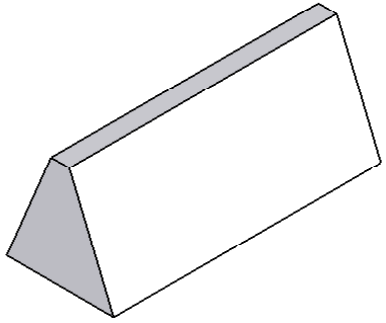

UNLESS STATED OTHERWISE:								
REMOVE ALL BURRS AND SHARP EDGES								
SCREW THREAD: ISO 6H 6g								
GEOMETRIC TOL. TO BS 308 1972				MATERIAL:				MILD STEEL
WELDING SYMBOLS TO BS 499/2								CAD FILENAME: jig-001 / SCALE: 2:1
MACHINING TOLERANCES								
OVER - TO	**±**	**±**	**±**					**COPYRIGHT NOTICE:**
0 - 6	0.1	0.2	0.5					UNAUTHORISED USE, MANUFACTURE OR REPRODUCTION IN WHOLE OR IN PART IS PROHIBITED. DRAWING, DESIGN AND OTHER DISCLOSURES IS THE INTELLECTUAL PROPERTY OF NORTH-WEST UNIVERSITY. ALL RIGHTS RESERVED.
6 - 30	0.2	0.5	0.8					
30 - 100	0.3	0.8	1.5					
100 - 300	0.5	1.2	2.0					
300 - 1000	0.8	2.0	3.0					SCHOOL OF MECHANICAL ENGINEERING POTCHEFSTROOM CAMPUS OF NW-U 11 HOFFMAN STREET POTCHEFSTROOM 2530
1000 - 3000	1.2	3.0	5.0					SHEET 1 OF 1 / RAMB PLACEMENT JIG
3000 PLUS:	2.0	4.0	8.0					
ANGLES:	1°	1°	1°		JJJVR	2007/10/30	A	DWG. No. jig-001 / A
SURFACE FIN:	1.6	6.3	12.5	APPR.	DRAWN	DATE	REV.	

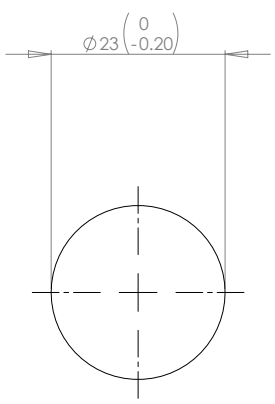

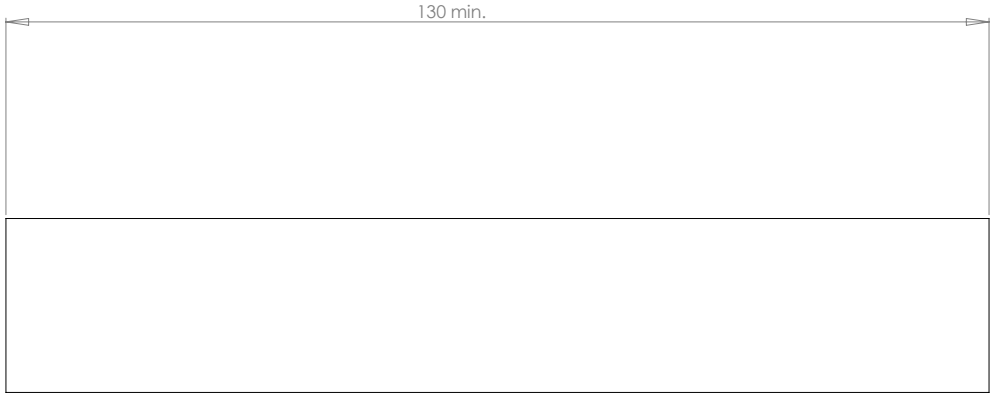

UNLESS STATED OTHERWISE: REMOVE ALL BURRS AND SHARP EDGES								
SCREW THREAD: ISO 6H 6g								
GEOMETRIC TOL. TO BS 308 1972				MATERIAL:			MILD STEEL	
WELDING SYMBOLS TO BS 499/2							**CAD FILENAME:** jig-002	**SCALE:** 5:1
MACHINING TOLERANCES								
OVER - TO	**±**	**±**	**±**				**COPYRIGHT NOTICE:**	
0 - 6	0.1	0.2	0.5				UNAUTHORISED USE, MANUFACTURE OR REPRODUCTION IN WHOLE OR IN PART IS PROHIBITED. DRAWING, DESIGN AND OTHER DISCLOSURES IS THE INTELLECTUAL PROPERTY OF NORTH-WEST UNIVERSITY. ALL RIGHTS RESERVED.	
6 - 30	0.2	0.5	0.8					
30 - 100	0.3	0.8	1.5					
100 - 300	0.5	1.2	2.0				SCHOOL OF MECHANICAL ENGINEERING POTCHEFSTROOM CAMPUS OF NW-U 11 HOFFMAN STREET POTCHEFSTROOM 2530	
300 - 1000	0.8	2.0	3.0					
1000 - 3000	1.2	3.0	5.0				SHEET 1 OF 1	RAMB PLACEMENT JIG 2
3000 PLUS:	2.0	4.0	8.0					
ANGLES:	1°	1°	1°		JJJVR	2007/10/30	A	**DWG. No.** jig-002 A
SURFACE FIN:	1.6	6.3	12.5	**APPR.**	**DRAWN**	**DATE**	**REV.**	

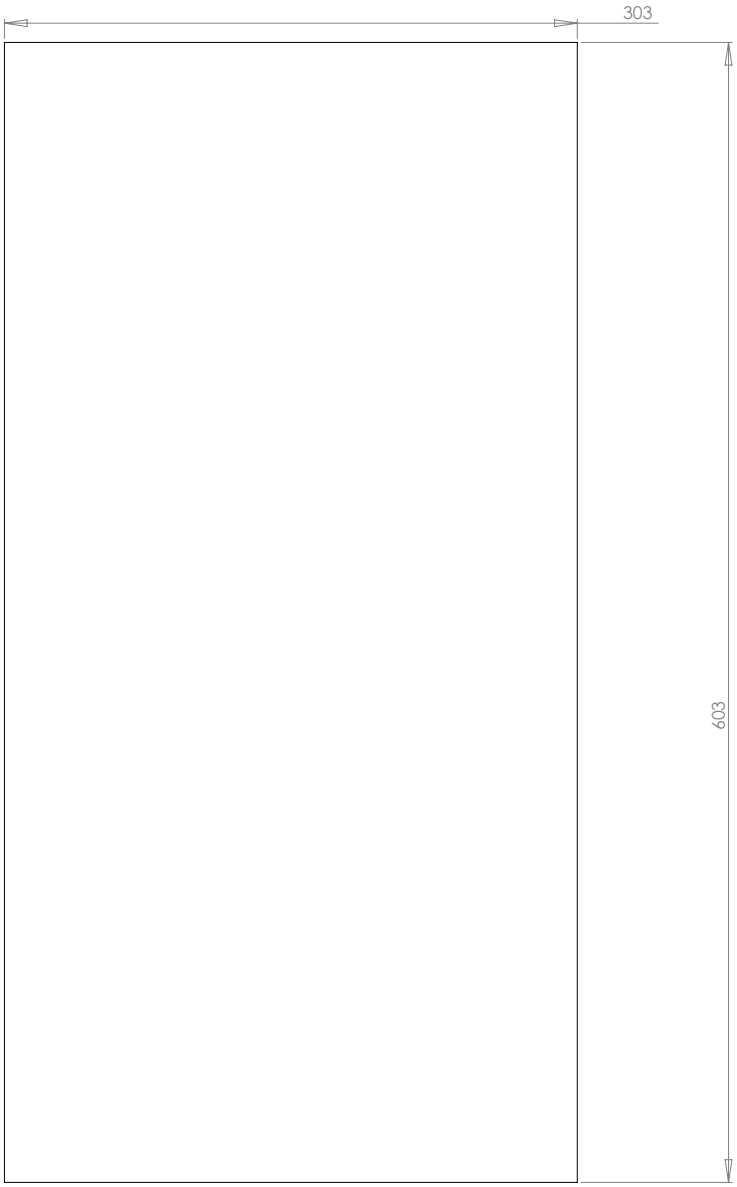

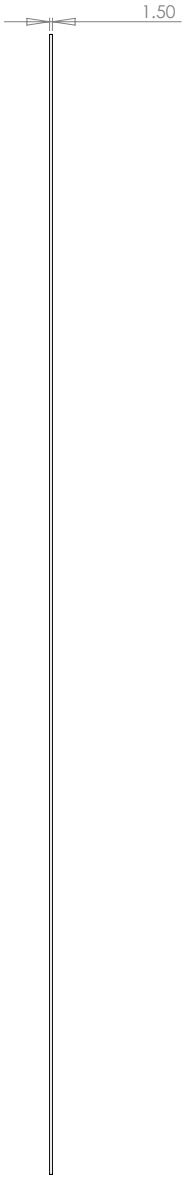

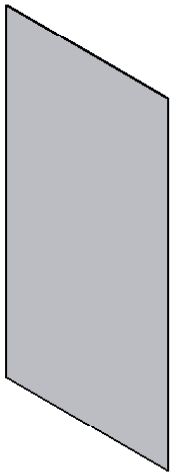

UNLESS STATED OTHERWISE:
REMOVE ALL BURRS AND SHARP EDGES
SCREW THREAD: ISO 6H 6g
GEOMETRIC TOL. TO BS 308 1972
WELDING SYMBOLS TO BS 499/2

MACHINING TOLERANCES			
OVER - TO	±	±	±
0 - 6	0.1	0.2	0.5
6 - 30	0.2	0.5	0.8
30 - 100	0.3	0.8	1.5
100 - 300	0.5	1.2	2.0
300 - 1000	0.8	2.0	3.0
1000 - 3000	1.2	3.0	5.0
3000 PLUS:	2.0	4.0	8.0
ANGLES:	1°	1°	1°
SURFACE FIN:	1.6	6.3	12.5

APPR.	DRAWN	DATE	REV.
	JJJVR	2007/10/30	A

CAD FILENAME:	SCALE:
DEKSEL	1:5

COPYRIGHT NOTICE:

UNAUTHORISED USE, MANUFACTURE OR REPRODUCTION IN WHOLE OR IN PART IS PROHIBITED. DRAWING, DESIGN AND OTHER DISCLOSURES IS THE INTELLECTUAL PROPERTY OF NORTH-WEST UNIVERSITY. ALL RIGHTS RESERVED.

SCHOOL OF MECHANICAL ENGINEERING
POTCHEFSTROOM CAMPUS OF NW-U
11 HOFFMAN STREET
POTCHEFSTROOM 2530

SHEET 1 OF 1

WEERSTANBANK DEKSEL

DWG. No.	DEKSEL	A

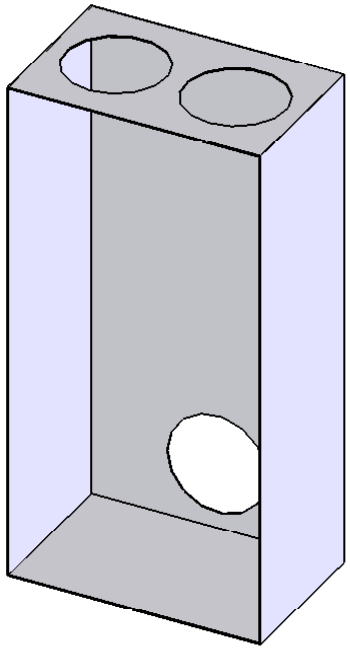

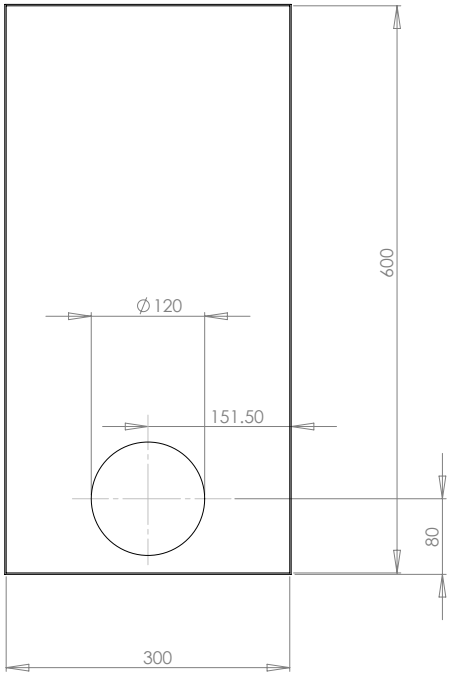

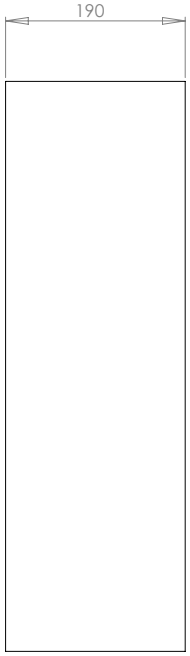

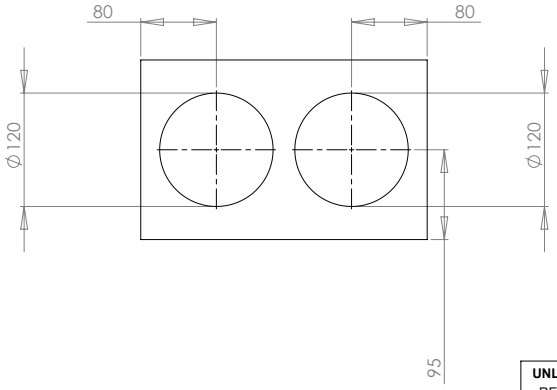

UNLESS STATED OTHERWISE: REMOVE ALL BURRS AND SHARP EDGES								
SCREW THREAD: ISO 6H 6g								
GEOMETRIC TOL. TO BS 308 1972								
WELDING SYMBOLS TO BS 499/2								
MACHINING TOLERANCES								
OVER - TO	**±**	**±**	**±**					
0 - 6	0.1	0.2	0.5					
6 - 30	0.2	0.5	0.8					
30 - 100	0.3	0.8	1.5					
100 - 300	0.5	1.2	2.0					
300 - 1000	0.8	2.0	3.0					
1000 - 3000	1.2	3.0	5.0					
3000 PLUS:	2.0	4.0	8.0					
ANGLES:	1°	1°	1°		JJJVR	2007/10/30	A	
SURFACE FIN:	1.6	6.3	12.5	**APPR.**	**DRAWN**	**DATE**	**REV.**	

CAD FILENAME:	**SCALE:**
DOP	1:5

COPYRIGHT NOTICE:

UNAUTHORISED USE, MANUFACTURE OR REPRODUCTION IN WHOLE OR IN PART IS PROHIBITED. DRAWING, DESIGN AND OTHER DISCLOSURES IS THE INTELLECTUAL PROPERTY OF NORTH-WEST UNIVERSITY. ALL RIGHTS RESERVED.

SCHOOL OF MECHANICAL ENGINEERING
POTCHEFSTROOM CAMPUS OF NW-U
11 HOFFMAN STREET
POTCHEFSTROOM 2530

SHEET 1 OF 1

WEERSTANDBANK HOUER

DWG. No. DOP A

D.10 Photos

LOCTITE
7063
CLEANER
LOCTITE
1075
LOCTITE
324
LOCTITE
7388
330

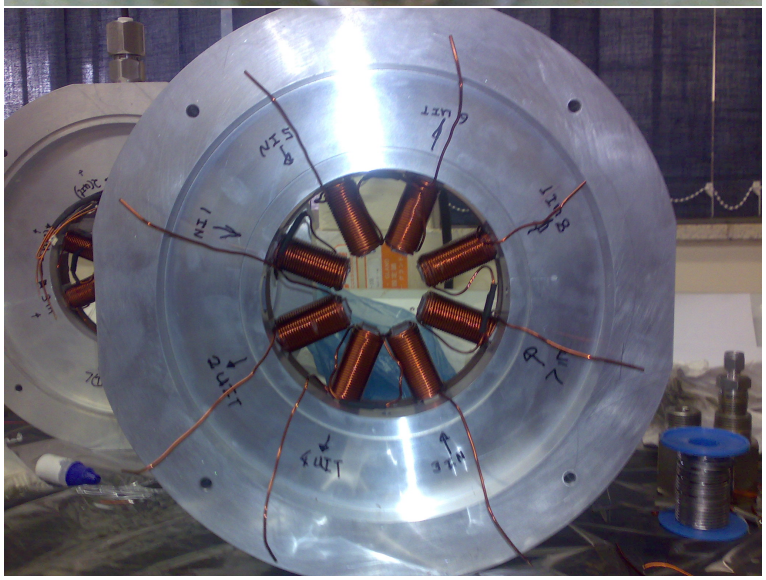

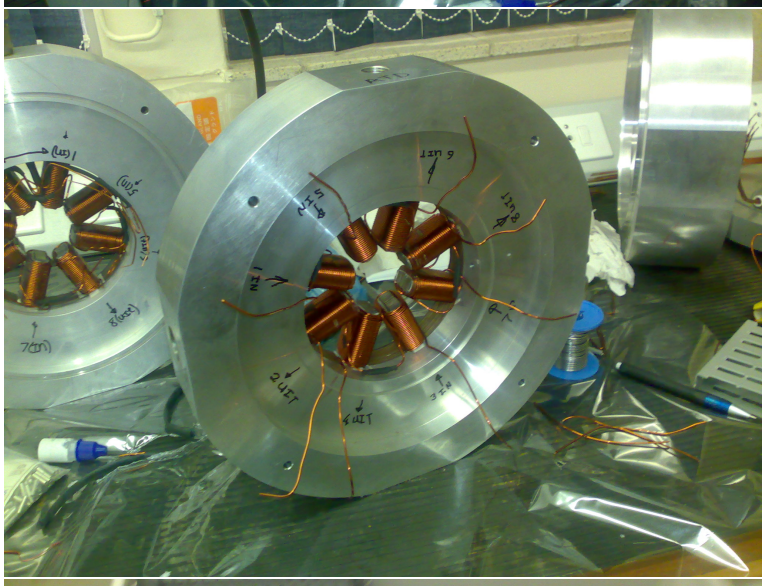

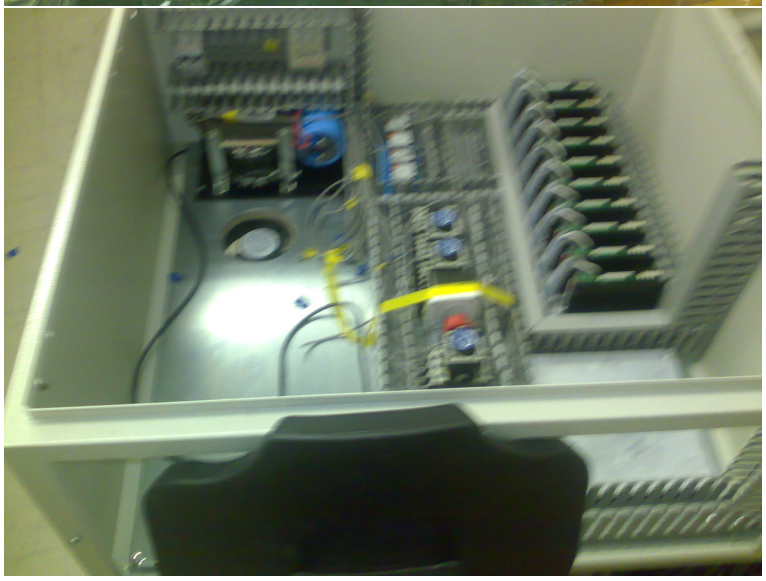

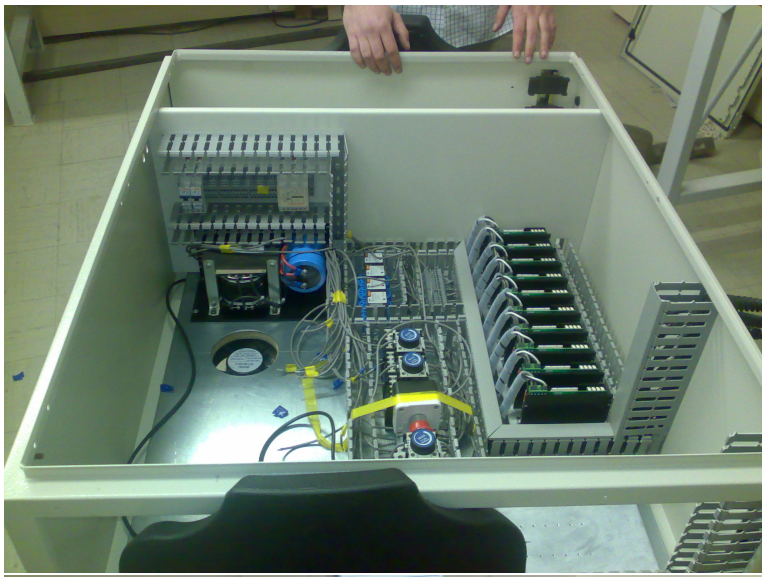

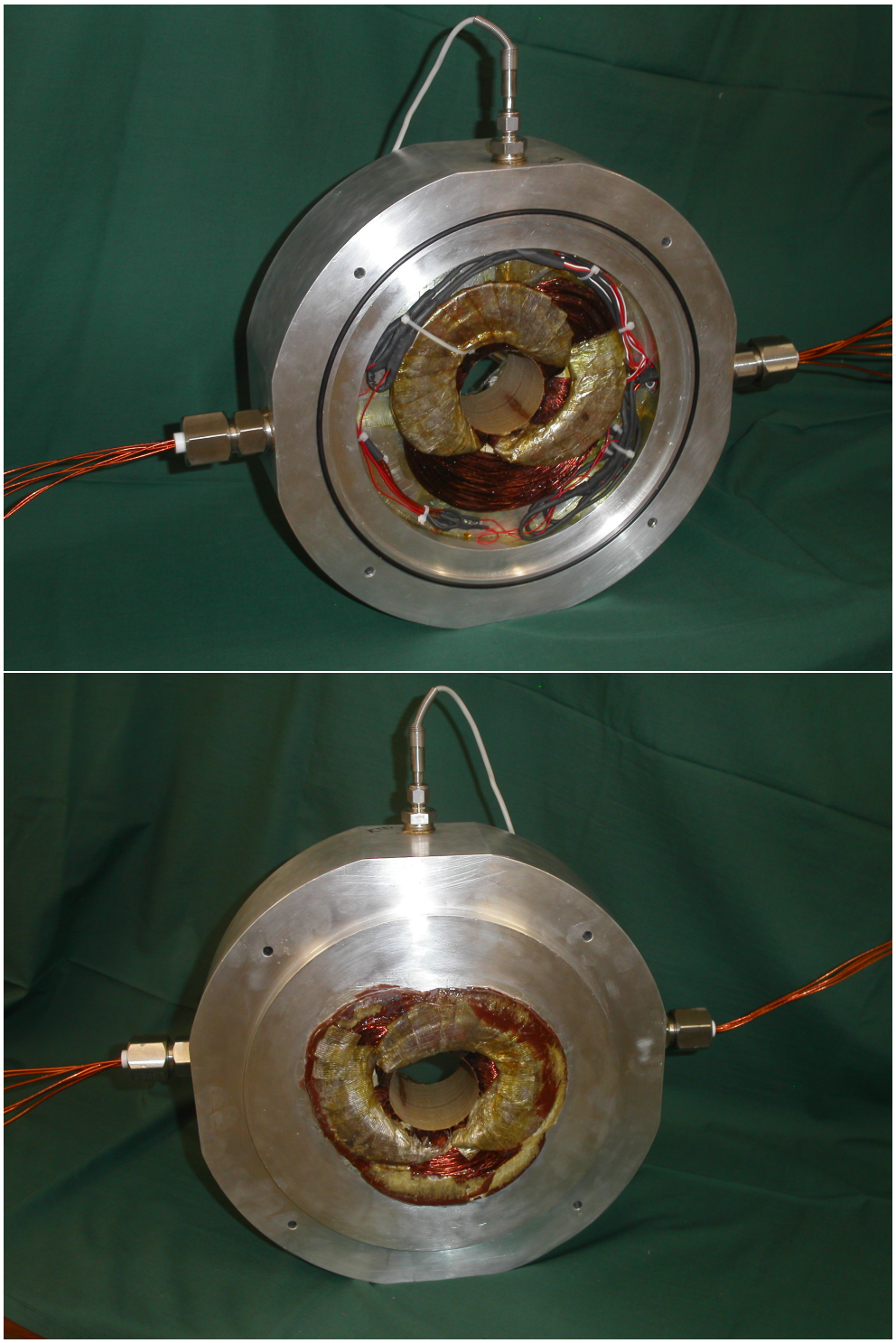

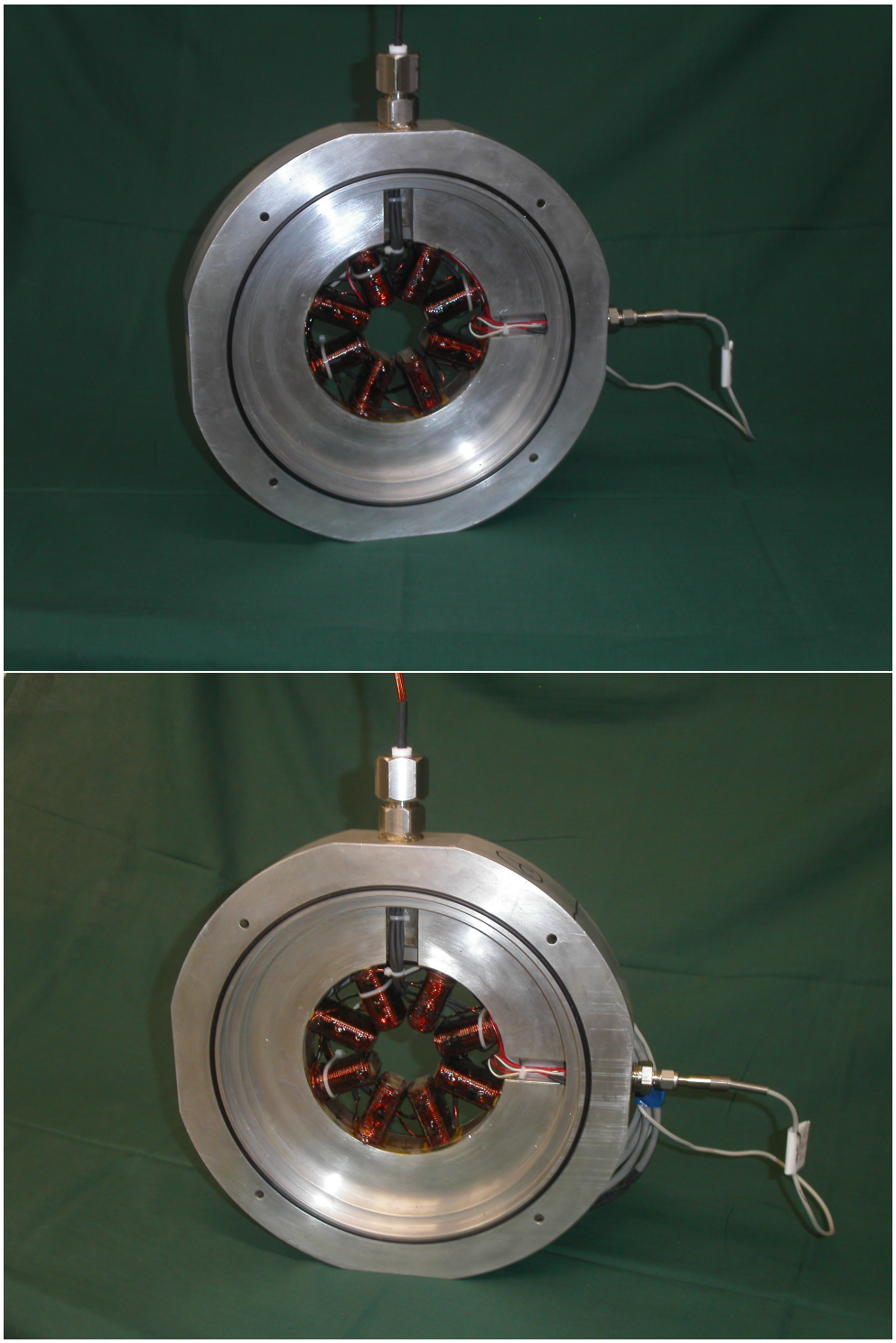

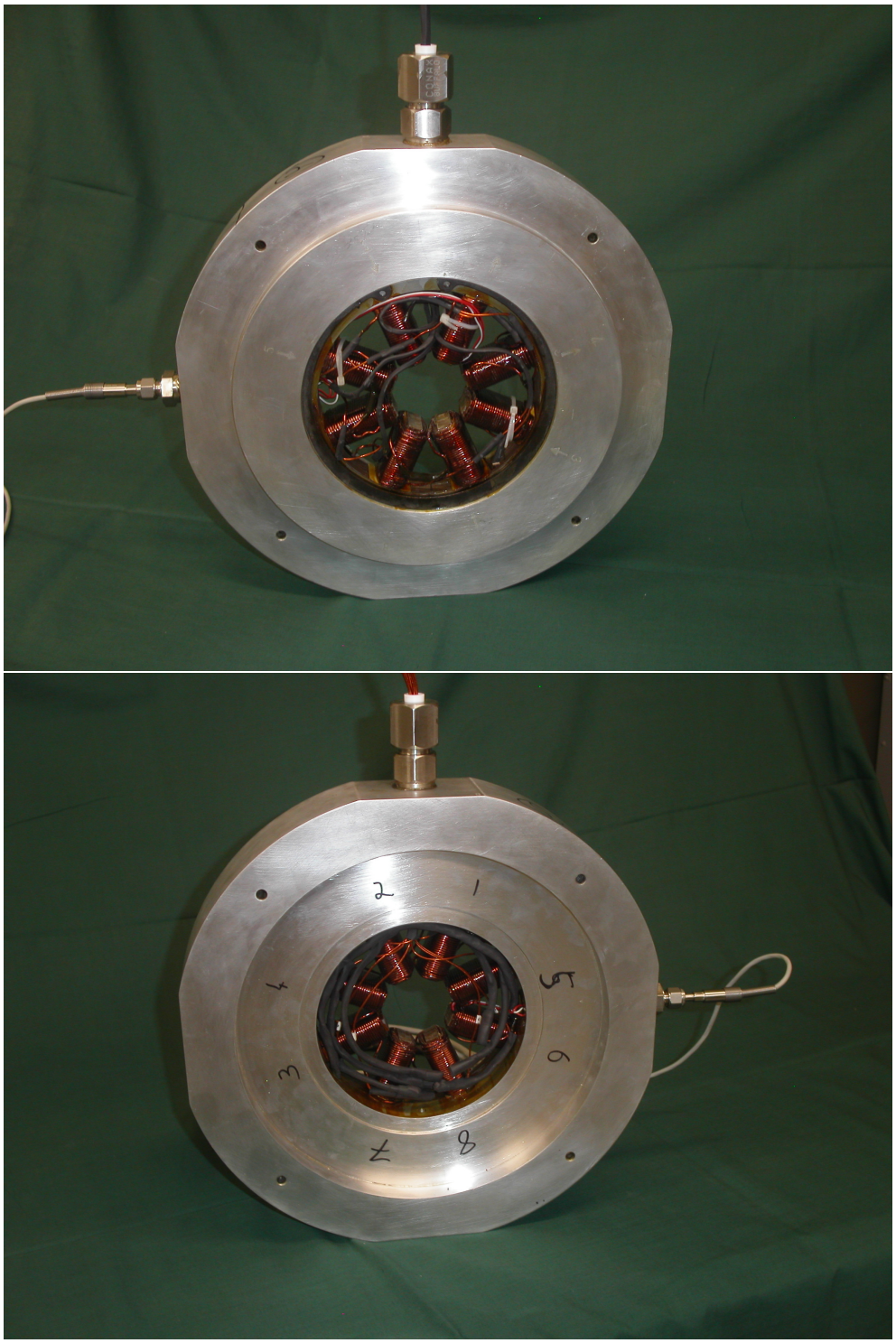
2
1
4
5
3
6
7
8

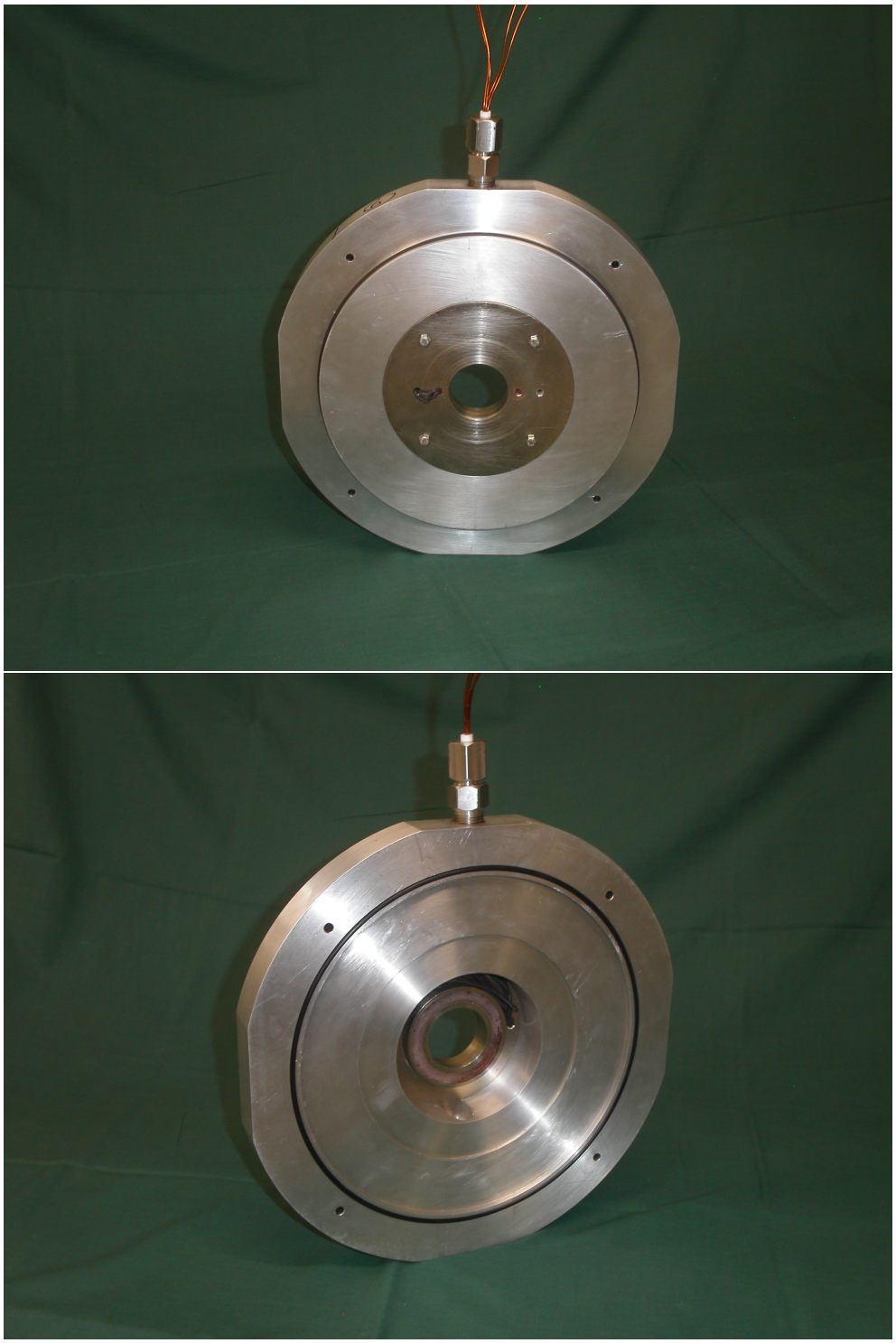

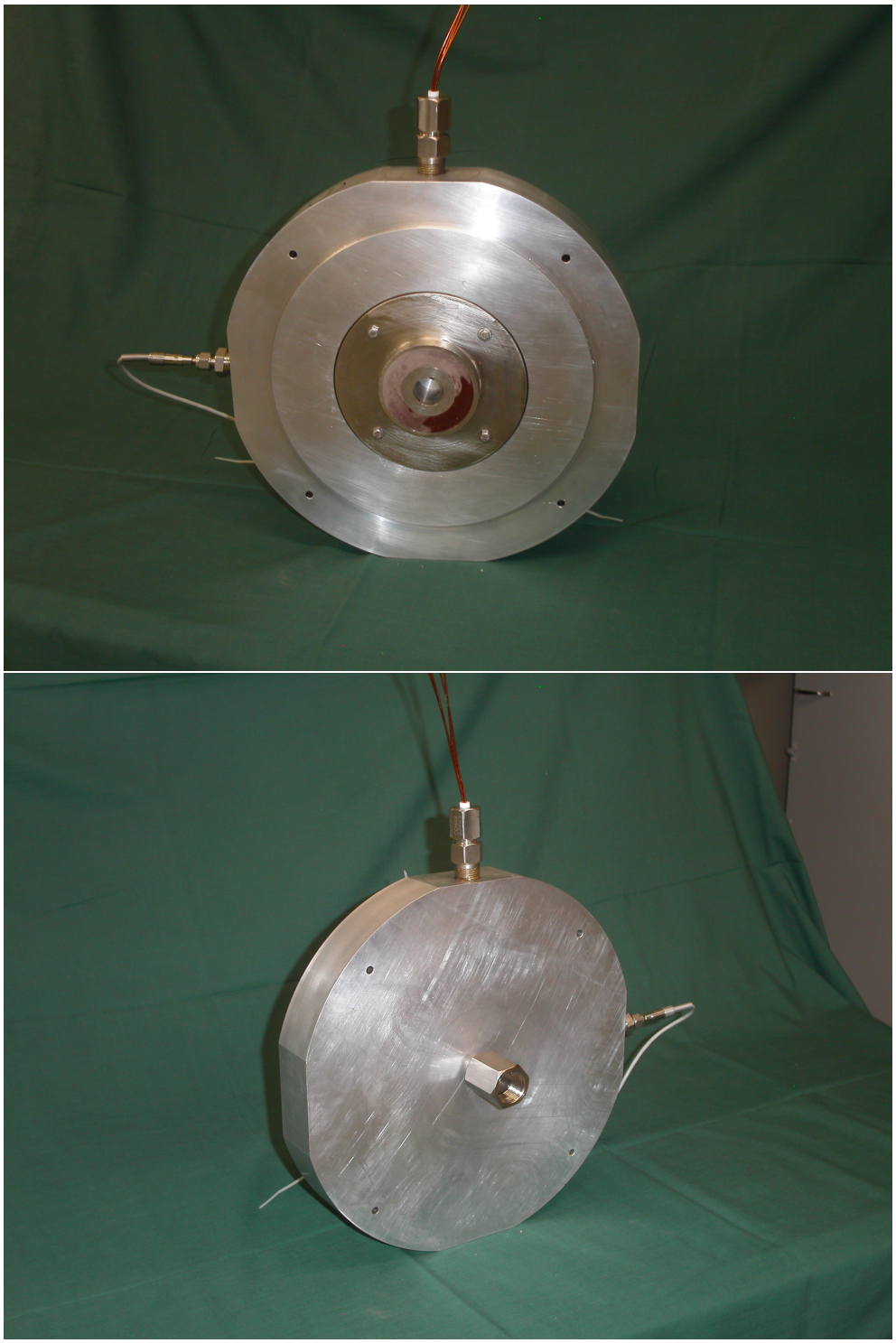

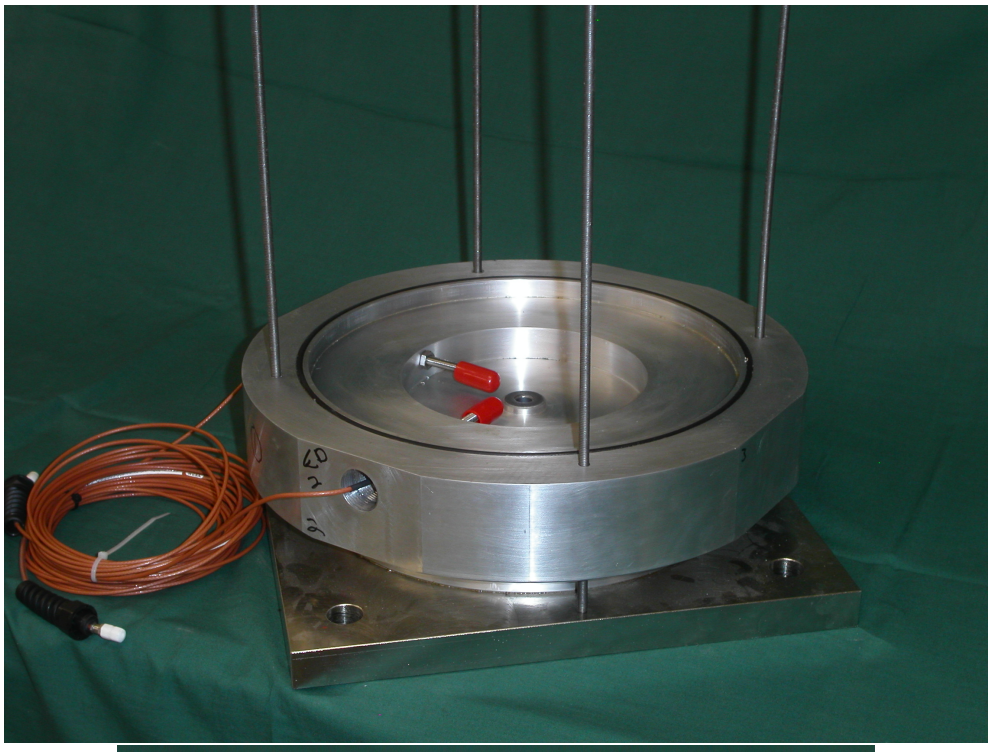

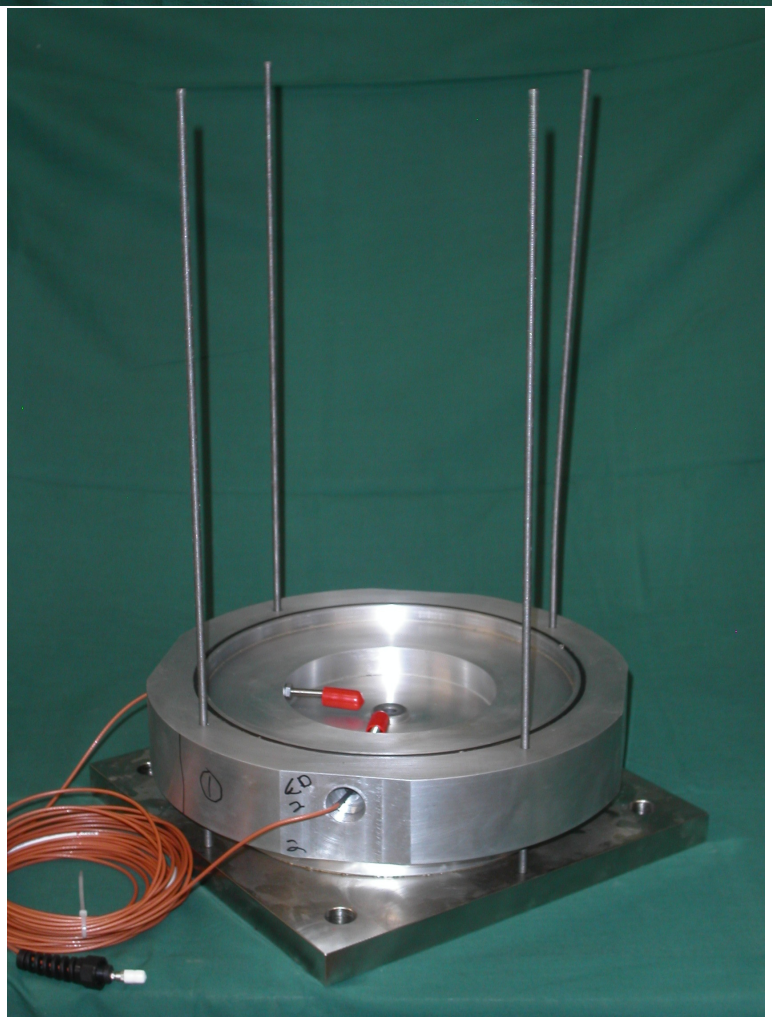

D.11 Data sheets

D.11.1 Adhesive

LOCTITE® 324™

February 2005

PRODUCT DESCRIPTION

LOCTITE® 324™ provides the following product characteristics:

Technology	Acrylic
Chemical Type	Urethane methacrylate ester
Appearance (uncured)	Transparent light amber liquid[LMS]
Components	One component - requires no mixing
Viscosity	Medium
Cure	Anaerobic with activator
Cure Benefit	Room temperature cure
Application	Bonding

LOCTITE® 324™ is used to bond flat parts together. Especially suitable for joining dissimilar materials, e.g. ferrite to plated materials in electric motors, loudspeakers, etc. This product is specifically formulated for toughness and impact strength. LOCTITE® 324™ cures when confined between close fitting parts with the aid of an activator.

TYPICAL PROPERTIES OF UNCURED MATERIAL

Specific Gravity @ 25 °C	1.06
Flash Point - See MSDS	
Viscosity, Brookfield - RVT, 25 °C, mPa·s (cP):	
Spindle 6, speed 20 rpm	10,000 to 24,000[LMS]

TYPICAL CURING PERFORMANCE

Cure Speed vs. Substrate

The rate of cure will depend on the substrate used. The graph below shows the shear strength developed with time on grit blasted steel lap shears compared to different materials and tested according to ISO 4587. (Activator 7075™ applied to one surface)

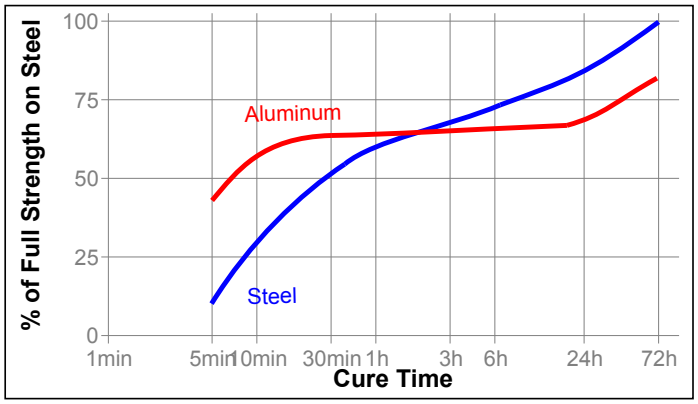

Cure Speed vs. Bond Gap

The rate of cure will depend on the bondline gap. The following graph shows the shear strength developed with time on grit blasted steel lap shears at different controlled gaps and tested according to ISO 4587. (Activator 7075™ applied to one surface)

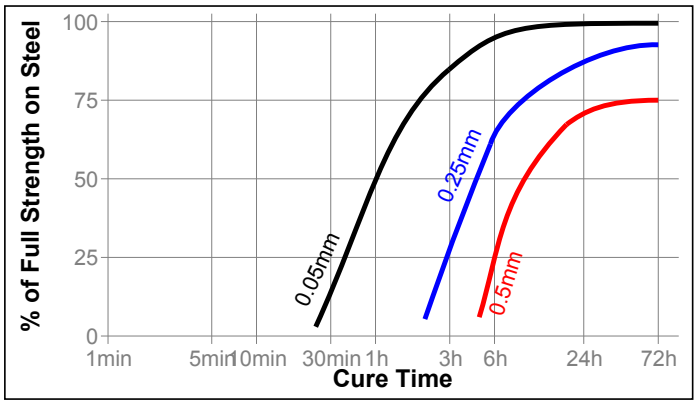

TYPICAL PROPERTIES OF CURED MATERIAL

Physical Properties:

Coefficient of Thermal Expansion, ASTM D 696, K^{-1}		80×10^{-6}
Coefficient of Thermal Conductivity, ASTM C 177, W/(m·K)		0.1
Specific Heat, kJ/(kg·K)		0.3
Elongation, at break, ISO 37, %		170
Tensile Strength, ISO 37	N/mm² (psi)	34 (4,900)
Tensile Modulus, ASTM D 638	N/mm² (psi)	614 (89,000)

Electrical Properties:

Dielectric Constant / Dissipation Factor, IEC 60250:	
100 Hz	5.5 / 0.033
1 kHz	5.2 / 0.031
1 MHz	4.5 / 0.004
Volume Resistivity, IEC 60093, Ω·cm	8×10^{12}
Surface Resistivity, IEC 60093, Ω	2×10^{17}
Dielectric Breakdown Strength, IEC 60243-1, kV/mm	73

TYPICAL PERFORMANCE OF CURED MATERIAL

Adhesive Properties

After 24 hours @ 22 °C, Activator 7075™ on 1 side

Lap Shear Strength, ISO 4587:

Steel (grit blasted):

0 gap	N/mm² (psi)	17 to 21 (2,500 to 3,000)
0.5 mm gap	N/mm² (psi)	21 to 25 (3,000 to 3,600)

"T" Peel Strength, ISO 11339:

Steel (grit blasted)	N/mm (lb/in)	2.2 (13)

After 24 hours @ 22 °C, Activator 7075™ on 2 sides

Lap Shear Strength, ISO 4587:

Steel (grit blasted):

0.5 mm gap	N/mm² (psi)	≥14[LMS] (≥2,030)

TYPICAL ENVIRONMENTAL RESISTANCE

Cured for 1 week @ 22 °C, Activator 7075™ on 1 side
Lap Shear Strength, ISO 4587:
Steel (grit blasted)

Hot Strength

Tested at temperature

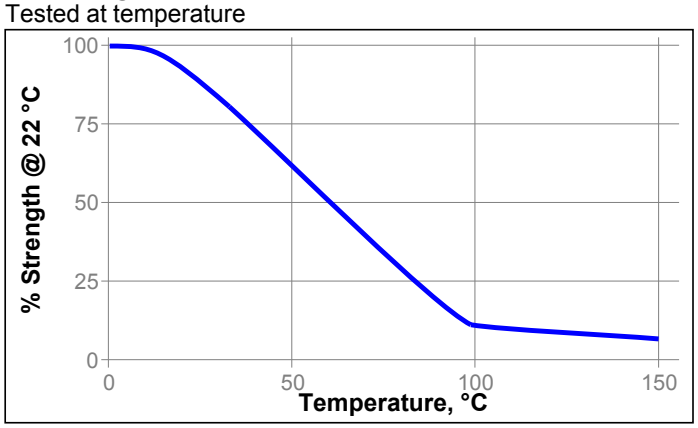

Heat Aging

Aged at temperature indicated and tested @ 22 °C

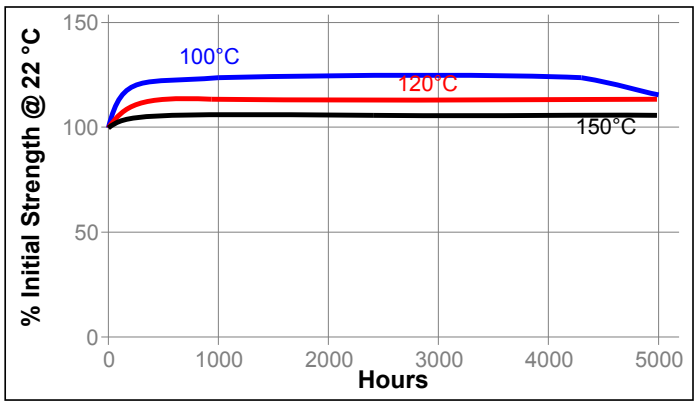

Chemical/Solvent Resistance

Aged under conditions indicated and tested @ 22 °C.

		% of initial strength
Environment	**°C**	**720 h**
Gasoline	87	50
Motor oil	87	100
Auto trans. fluid	87	100
Phosphate ester	87	100
Water/glycol 50/50	150	50
Humidity, 100% RH	50	55

GENERAL INFORMATION

This product is not recommended for use in pure oxygen and/or oxygen rich systems and should not be selected as a sealant for chlorine or other strong oxidizing materials.

For safe handling information on this product, consult the Material Safety Data Sheet (MSDS).

Where aqueous washing systems are used to clean the surfaces before bonding, it is important to check for compatibility of the washing solution with the adhesive. In some cases these aqueous washes can affect the cure and performance of the adhesive.

This product is not normally recommended for use on plastics (particularly thermoplastic materials where stress cracking of the plastic could result). Users are recommended to confirm compatibility of the product with such substrates.

Directions for use

1. For best performance bond surfaces should be clean and free from grease.
2. To ensure a fast and reliable cure, Activator 7075™ should be applied to one of the bond surfaces and the adhesive to the other surface. Parts should be assembled within 15 minutes.
3. The recommended bondline gap is 0.1mm. Where bond gaps are large (up to a maximum of 0.5 mm), or faster cure speed is required, Activator 7075™ should be applied to both surfaces. Parts should be assembled immediately (within 1 minute).
4. Excess adhesive can be wiped away with organic solvent.
5. Bond should be held clamped until adhesive has fixtured.
6. Product should be allowed to develop full strength before subjecting to any service loads (typically 24 to 72 hours after assembly, depending on bond gap, materials and ambient conditions).

Loctite Material Specification[LMS]

LMS dated September 1, 1995. Test reports for each batch are available for the indicated properties. LMS test reports include selected QC test parameters considered appropriate to specifications for customer use. Additionally, comprehensive controls are in place to assure product quality and consistency. Special customer specification requirements may be coordinated through Henkel Quality.

Storage

Store product in the unopened container in a dry location. Storage information may be indicated on the product container labeling.
Optimal Storage: 8 °C to 21 °C. Storage below 8 °C or greater than 28 °C can adversely affect product properties. Material removed from containers may be contaminated during use. Do not return product to the original container. Henkel Corporation cannot assume responsibility for product which has been contaminated or stored under conditions other than those previously indicated. If additional information is required, please contact your local Technical Service Center or Customer Service Representative.

Conversions
(°C x 1.8) + 32 = °F
kV/mm x 25.4 = V/mil
mm / 25.4 = inches
N x 0.225 = lb
N/mm x 5.71 = lb/in
N/mm² x 145 = psi
MPa x 145 = psi
N·m x 8.851 = lb·in
N·m x 0.738 = lb·ft
N·mm x 0.142 = oz·in
mPa·s = cP

Note
The data contained herein are furnished for information only and are believed to be reliable. We cannot assume responsibility for the results obtained by others over whose methods we have no control. It is the user's responsibility to determine suitability for the user's purpose of any production methods mentioned herein and to adopt such precautions as may be advisable for the protection of property and of persons against any hazards that may be involved in the handling and use thereof. In light of the foregoing, **Henkel Corporation specifically disclaims all warranties expressed or implied, including warranties of merchantability or fitness for a particular purpose, arising from sale or use of Henkel Corporation's products. Henkel Corporation specifically disclaims any liability for consequential or incidental damages of any kind, including lost profits.** The discussion herein of various processes or compositions is not to be interpreted as representation that they are free from domination of patents owned by others or as a license under any Henkel Corporation patents that may cover such processes or compositions. We recommend that each prospective user test his proposed application before repetitive use, using this data as a guide. This product may be covered by one or more United States or foreign patents or patent applications.

Trademark usage
Except as otherwise noted, all trademarks in this document are trademarks of Henkel Corporation in the U.S. and elsewhere. ® denotes a trademark registered in the U.S. Patent and Trademark Office.

Reference 3

LOCTITE® 330

July 2004

PRODUCT DESCRIPTION

LOCTITE® 330 provides the following product characteristics:

Technology	Acrylic
Chemical Type	Urethane methacrylate ester
Appearance (uncured)	Slightly cloudy, colorless to pale yellow liquid[LMS]
Components	One component - requires no mixing
Viscosity	High
Cure	Anaerobic with activator
Application	Bonding

LOCTITE® 330 is a general purpose adhesive is used to bond metal, wood, ferrite, ceramic and plastic materials. Applications include tool handles, appliances, sporting goods and decorative trim.

TYPICAL PROPERTIES OF UNCURED MATERIAL

Specific Gravity @ 25 °C	1.05
Flash Point - See MSDS	
Viscosity, Brookfield - RVT, 25 °C, mPa·s (cP):	
Spindle 7, speed 20 rpm	45,000 to 90,000[LMS]
Viscosity, EN 12092 - SV, 25 °C, after 180 s, mPa·s (cP):	
Shear rate 20 s^{-1}	30,000 to 70,000

TYPICAL CURING PERFORMANCE

Cure Speed vs. Substrate

The rate of cure will depend on the substrate used. The graph below shows the shear strength developed with time on grit blasted steel lap shears and tested according to ISO 4587. (Activator 7387 applied to one surface)

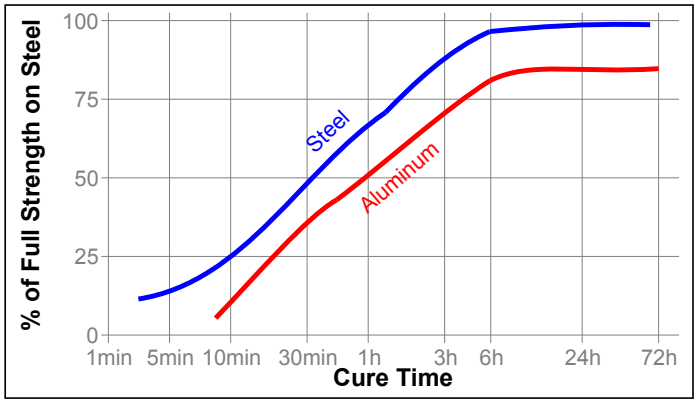

Cure Speed vs. Bond Gap

The rate of cure will depend on the bondline gap. The following graph shows shear strength developed with time on grit blasted steel lap shears at different controlled gaps and tested according to ISO 4587. (Activator 7387 applied to one surface.)

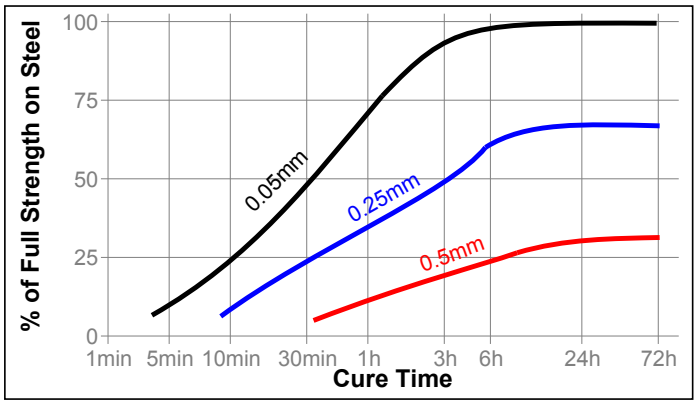

TYPICAL PROPERTIES OF CURED MATERIAL

Physical Properties:

Coefficient of Thermal Expansion, ASTM D 696, K^{-1}	8×10^{-6}
Coefficient of Thermal Conductivity, ASTM C 177, W/(m·K)	0.10
Specific Heat, kJ/(kg·K)	0.30

TYPICAL PERFORMANCE OF CURED MATERIAL

Adhesive Properties

After 24 hours @ 22 °C, Activator 7387 on 1 side

Lap Shear Strength, ISO 4587:

Mild steel (grit blasted)	N/mm²	15 to 30
	(psi)	(2,175 to 4,350)

Tensile Strength, ISO 6922:

Mild steel (grit blasted)	N/mm²	12 to 22
	(psi)	(1,740 to 3,190)

After 24 hours @ 22 °C, Activator 7387 or 7386 on 2 sides

Tensile Strength, ISO 6922:

Mild steel (grit blasted)	N/mm²	≥16.50[LMS]
	(psi)	(≥2,390)

TYPICAL ENVIRONMENTAL RESISTANCE

Cured for 1 week @ 22 °C, Activator 7387 on 1 side

Lap Shear Strength, ISO 4587:

Mild steel (grit blasted):

0.25 mm gap

Hot Strength

Tested at temperature

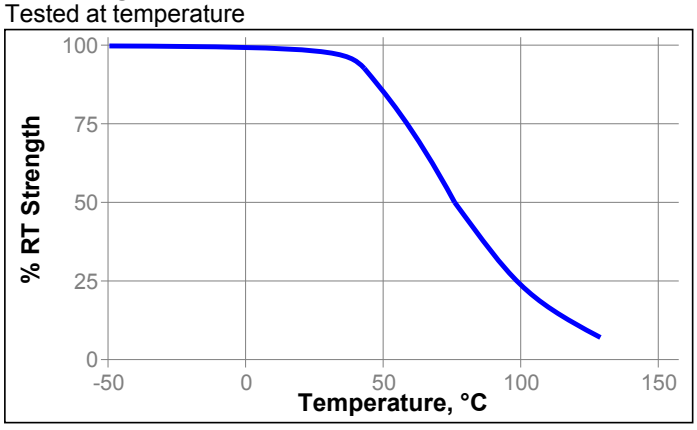

Heat Aging
Aged at temperature indicated and tested @ 22 °C

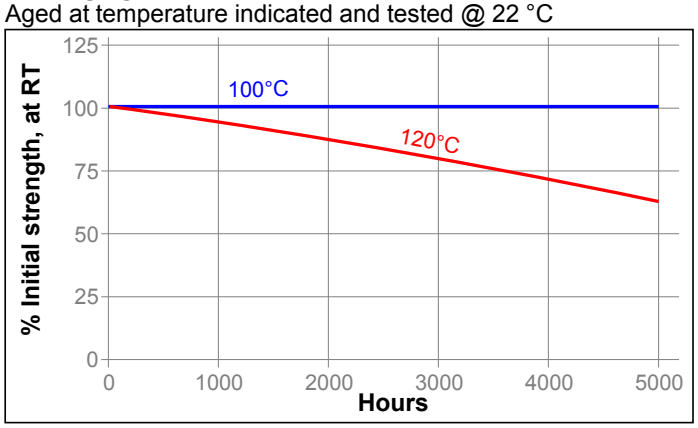

Chemical/Solvent Resistance
Aged under conditions indicated and tested @ 22 °C.

		% of initial strength	
Environment	**°C**	**350 hr**	**720 hr**
Acetone	22	10	10
Motor Oil	87	90	66
Unleaded Gasoline	22	20	20
Phosphate ester	87	93	75
Water Glycol 50/50	87	60	60

GENERAL INFORMATION

This product is not recommended for use in pure oxygen and/or oxygen rich systems and should not be selected as a sealant for chlorine or other strong oxidizing materials.

For safe handling information on this product, consult the Material Safety Data Sheet (MSDS).

Where aqueous washing systems are used to clean the surfaces before bonding, it is important to check for compatibility of the washing solution with the adhesive. In some cases these aqueous washes can affect the cure and performance of the adhesive.

Directions for use

1. For best performance bond surfaces should be clean and free from grease.
2. To ensure a fast and reliable cure, Activator 7387 or 7386 should be applied to one of the bond surfaces and the adhesive to the other surface. Parts should be assembled within 15 minutes.
3. The recommended bondline gap is 0.1mm. Where bond gaps are large (up to a maximum of 0.5 mm), or faster cure speed is required, Activator 7387 or 7386 should be applied to both surfaces. Parts should be assembled immediately (within 1 minute).
4. Excess adhesive can be wiped away with organic solvent.
5. Bond should be held clamped until adhesive has fixtured.
6. Product should be allowed to develop full strength before subjecting to any service loads (typically 24 to 72 hours after assembly, depending on bond gap, materials and ambient conditions).

Loctite Material Specification[LMS]
LMS dated March 11, 1996. Test reports for each batch are available for the indicated properties. LMS test reports include selected QC test parameters considered appropriate to specifications for customer use. Additionally, comprehensive controls are in place to assure product quality and consistency. Special customer specification requirements may be coordinated through Henkel Loctite Quality.

Storage
Store product in the unopened container in a dry location. Storage information may be indicated on the product container labeling.
Optimal Storage: 8 °C to 21 °C. Storage below 8 °C or greater than 28 °C can adversely affect product properties
Material removed from containers may be contaminated during use. Do not return product to the original container. Henkel Corporation cannot assume responsibility for product which has been contaminated or stored under conditions other than those previously indicated. If additional information is required, please contact your local Technical Service Center or Customer Service Representative.

Conversions
(°C x 1.8) + 32 = °F
kV/mm x 25.4 = V/mil
mm / 25.4 = inches
N x 0.225 = lb
N/mm x 5.71 = lb/in
N/mm² x 145 = psi
MPa x 145 = psi
N·m x 8.851 = lb·in
N·mm x 0.142 = oz·in
mPa·s = cP

Note
The data contained herein are furnished for information only and are believed to be reliable. We cannot assume responsibility for the results obtained by others over whose methods we have no control. It is the user's responsibility to determine suitability for the user's purpose of any production methods mentioned herein and to adopt such precautions as may be advisable for the protection of property and of persons against any hazards that may be involved in the handling and use thereof. In light of the foregoing, **Henkel Corporation specifically disclaims all warranties expressed or implied, including warranties of merchantability or fitness for a particular purpose, arising from sale or use of Henkel Corporation's products. Henkel Corporation specifically disclaims any liability for consequential or incidental damages of any kind, including lost profits.** The discussion herein of various processes or compositions is not to be interpreted as representation that they are free from domination of patents owned by others or as a license under any Henkel Corporation patents that may cover such processes or compositions. We recommend that each prospective user test his proposed application before repetitive use, using this data as a guide. This product may be covered by one or more United States or foreign patents or patent applications.

Trademark usage
LOCTITE is a trademark of Henkel Corporation

Reference 1

D.11.2 Rotational speed sensor and display

SELET M12 SERIES

INDUCTIVE PROXIMITY SWITCHES

Operating principle:

Inductive proximity switches are electronic sensors that are able to detect the presence of metallic objects in the vicinity of their sensing face.
Basically, they consist of an inductive oscillatory circuit. The coil in the circuit generates a high-frequency magnetic field (sensing face of sensor).
The presence of a metal object in this field modifies its energy. This situation is converted by a special circuit element into a switching of the output.

SENSOR MODEL
CYLINDRICAL, METAL

Distance	TYPE	Distance
2 mm	M12X1	4mm

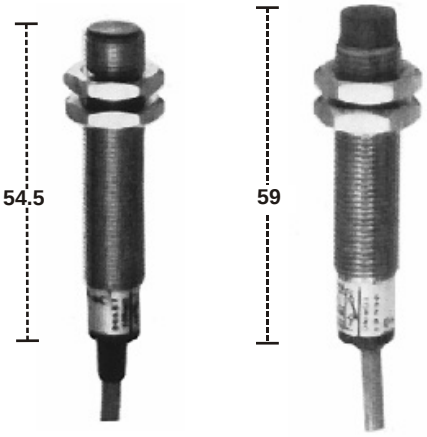

SPECIFICATIONS:

NAMUR TYPE		
Supply Voltage (V)	*3 ÷ 24 Vdc*	*7 ÷ 9 Vdc NAMUR*
Ripple %	*10%*	
Power absorbed (mA)		
In presence of Metal	*<1mA*	
In absence of Metal	*>4mA*	
Hysteresis (%Sn)	*£ 10%*	
Operating Frequency (HZ)	*2000HZ*	*1500 HZ*

D.C. TYPE		
Supply Voltage (V)	*10÷30 Vdc*	
Ripple %	*10%*	
Maximum current (mA)	*200* mA	
Minimum current (mA)	-	
Power absorbed (mA)	*≤10mA*	
Voltage drop (V)	*≤1,8V*	
Hysteresis (% Sn)	*≤10%*	
Operating frequency (HZ)	*1000HZ*	*1000HZ*

REFERENCE CODES		
NAMUR TYPE	*A12/2*	*AE12/4*

REF.CODES 3-WIRE,D.C. TYPE	*2mm*	*4mm*
No Output	*BG12/2PFAM*	*BEG12/4PFAM*
NC Output	*BG12/2PFCM*	*BEG12/4PFCM*
CO Output	*BG12/2PFSCM*	*BEG12/4PFSCM*

CONNECTION

PIN	***COLOUR***	***FUNCTION***
1	*Brown*	*Supply*
2	*White*	*N.C. Output (Option)*
3	*Blue*	*N.O. Output*
4	*Black.*	*0V*

selet

INSTROTECH
INSTRUMENTATION AND PROCESS CONTROL

P O Box 418, Honeydew 2040 South Africa
21 Precision Street, Kyasand Randburg.
Telephone: +27 11 462-1920
Telefax: +27 11 462-1958
email: info@instrotech.co.za
web: www.instrotech.co.za

Model 5012

PROGRAMMABLE COUNTER / SPEED / FREQUENCY / TIMER / TOTALISER / PERIOD / CLOCK / POSITION INDICATOR

INSTROTECH
INSTRUMENTATION AND PROCESS CONTROL

Processing your future

CERTIFICATION DEKRA DIN ISO 9001

TECHNOLOGY TOP · 100

CE

The Model 5012 is a 6 digit (-199999 to 999999) low-cost universal programmable indicator for use in all types of frequency & counting applications. The indicator has uni-polar & bi-polar pulse / frequency inputs for counting, frequency / speed (dual channel), period, flow, timing, totalising & positioning applications. It can be used in conjunction with most standard pulse / frequency generating sensors. Sensor excitation is standard & the output voltage is link selectable.

Options include analog output, alarm setpoints up to 4 alarms, BCD output, RS232 or RS485 communications & many more. The display & analog output is rangeable from the front pushbuttons. The instrument meets the European Community EMC directive 89/336/EEC & Low Voltage Directive 73/23/EEC.

Selected options now feature 'Plug & Play' technology, allowing option boards to be ordered separately & field fitted when required.

MODELS

Three variations of this instrument are available, depending on the required functionality :

Model 5012	6 digit (-199999 to 999999)	Freq, Period, Count, Rate, Totaliser, Event timer
Model 5012-C	6 digit (-199999 to 999999)	Real time clock + all Model 5012 features
Model 5012-Q	6 digit (-199999 to 999999)	Quadrature input + all Model 5012 features

All Models offer up & down counter (with reset/preset), dual channel frequency input, which can be added, subtracted, or ratioed. Period indication is also available as standard.

Time tagging feature is available onthe Model 5012-C as an option.

FEATURES

- ❑ DIN 48 x 96 enclosure, 147mm depth
- ❑ 6 digit (-199999 to 999999), 14.2mm bright red LED display
- ❑ 24VDC supply for encoders & proximity switches
- ❑ Low cost - high performance design
- ❑ Touch button ranging and setpoints
- ❑ Counting, frequency, speed, period, timing, totalising & positioning functions
- ❑ Dual channel frequency inputs (can be added, subtracted or ratioed)
- ❑ Analog output option with programmable zero & span
- ❑ RS232 & RS485 communication option.
- ❑ 'Plug & play' feature available with selected options.
- ❑ Keypad lockout available at no extra charge

SPECIFICATIONS

OPTIONS

3001-P	Two setpoints (solid state relays)	3010	95-265V AC/DC power supply
3001-M	Two setpoints (electro-mechanical)	3012	Peak / valley hold
3002	RS 485 communications	3013	RS 232 communications
3003	0 - 20mA / 4 - 20 mA analog output	3017-P	3 setpoints (solid state relays)
3004-P	One setpoint (solid state relays)	3017-M	3 setpoints (electro-mechanical)
3004-M	One setpoint (electro-mechanical)	3018-P	4 setpoints (solid state relays)
3006	Isolated outputs (order with 3002/3/7/13)	3018-M	4 setpoints (electro-mechanical)
3007	0 - 10V analog output	3020	Ultra bright Red LED display
3008	12 / 24V galvanic isolated DC supply	3023	Pulse output
3009	Parallel BCD output	3025	Keypad lockout

NOTE : Most of the above options are factory fitted. Customer / field fitted options are available as 'plug-&-play' boards and software activated options. Contact factory for more information.

NOTE : Option 3009 cannot be ordered together any alarm options.

FREQUENCY / SPEED

Input frequency range : 0.15Hz - 15000Hz. Up to 0.01Hz resolution.
Pulse amplitude : 50mV up to 24V maximum, uni-polar or bi-polar.
Frequency averaging : None, 0.5, 1.1 and 4.5 seconds programmable.
Selectable for most standard sensors by jumper links and differing connections.
Jumper links for hysteresis selection.

UP/DOWN COUNTER

Maximum pulse rate of 10000 pulses per second.
Pulse amplitude from 5V to 24V maximum, uni-polar or bi-polar.
Counter reset via 'Enter' key (press for 3 seconds) or via external reset (instantaneous).
Selectable for most standard sensors by jumper links and differing connections.
Jumper links for hysteresis selection.

SENSOR EXCITATION

(FOR ENCODERS, PROXIMITY SWITCHES ETC)

Link selectable for
24 VDC (17-26V), current limited to 25mA. Optional 50mA.
12VDC (10-13V), maximum 50mA.
5VDC ± 1%, maximum 50mA.

Optional : 24 VDC (17-26V), increased current capacity 100mA with Option 3010.

POWER SUPPLY

STANDARD
115 / 230 VAC ± 10% (standard), link selectable, 50/60Hz, 5VA typical
24VDC non-isolated on request, 5VA typical

OPTIONAL
12VDC isolated switch mode power supply option (Option 3008-12), 5VA typical
24VDC isolated switch mode power supply option (Option 3008-24), 5VA typical
95V-265V AC/DC switch mode power supply option (Option 3010), 5VA typical

ELECTRICAL SPECIFICATIONS

Accuracy	: 0.01% (scaling = 1), or 1 count
Internal oscillator	: 11.059 Mhz precision
Frequency calculation time	: 5 milliseconds (no averaging)
Operating temp. range	: -10°C to +50°C
Storage temperature range	: -40°C to +80°C
Humidity	: <85% non-condensing
Warm up time	: 10 minutes
Relays, electro-mechanical	: 250V AC, 30V DC, 2A, PF=1
Relays, solid state	: 400 V AC/DC, 0.5A, PF=1
Analog output accuracy	: 0.1% of full scale
Current analog output load	: 500 Ω maximum
Voltage analog output load	: 1 kΩ minimum
Memory retention (excl clock)	: Full non-volatile operation
Real time clock backup	: 2 years typically
Option 3006 isolation rating	: 1500 V
EC EMC & Low Volt directives	: 89/336/EEC & 73/23/EEC

NOTE : Digital inputs are available as standard for reset, preset, start, stop and other functions. A potential free contact is required to operate these digital inputs (active is low). Digital input functions differ depending on mode of operation.

PROGRAMMABLE SETTINGS (SHOWN FOR MODEL 5012 ONLY)

Frequency / counting factor	: 10.000, 1.000, 0.100, 0.010, 0.001
Frequency / counting scaler	: 000.001 to 999.999
Decimal point	: Selectable on any digit
Frequency resolution	: Up to 0.01Hz resolution
Frequency averaging	: None, 0.5, 1.1, 4.5 seconds selectable
Counter features	: Reset (count up) or Preset (count down)
*Analog output zero	: -199999 to 999999 (for 0 - 20mA / 4 - 20mA or 0 - 10V out)
*Analog output span	: -199999 to 999999
*Alarm values	: -199999 to 999999
*Alarm hysteresis	: 0 to 255 (default 1)
*Alarm delay	: 0 to 255 seconds (default 0)
*Alarm relay settings	: Selectable HIGH or LOW alarm
*Alarm relay state	: Selectable normally open or normally closed
*RS485 address	: 1 to 127 available (0 is for factory use)
*RS232 / RS485 baud rate	: 2400, 4800, 9600, 19200
*Protocol options	: DPM's DIGIbus or ASCIIbus

* indicates option

ORDERING EXAMPLE

Option modules (see page 2)

MODEL 5012-Q - 3001P - 3003

Model type :	Quadrature input
Auxiliary supply :	230 VAC
Analog output :	4 - 20 mA
Alarm setpoints :	2 setpoints with solid state relays

FRONT PANEL DIMENSIONS & CUTOUT

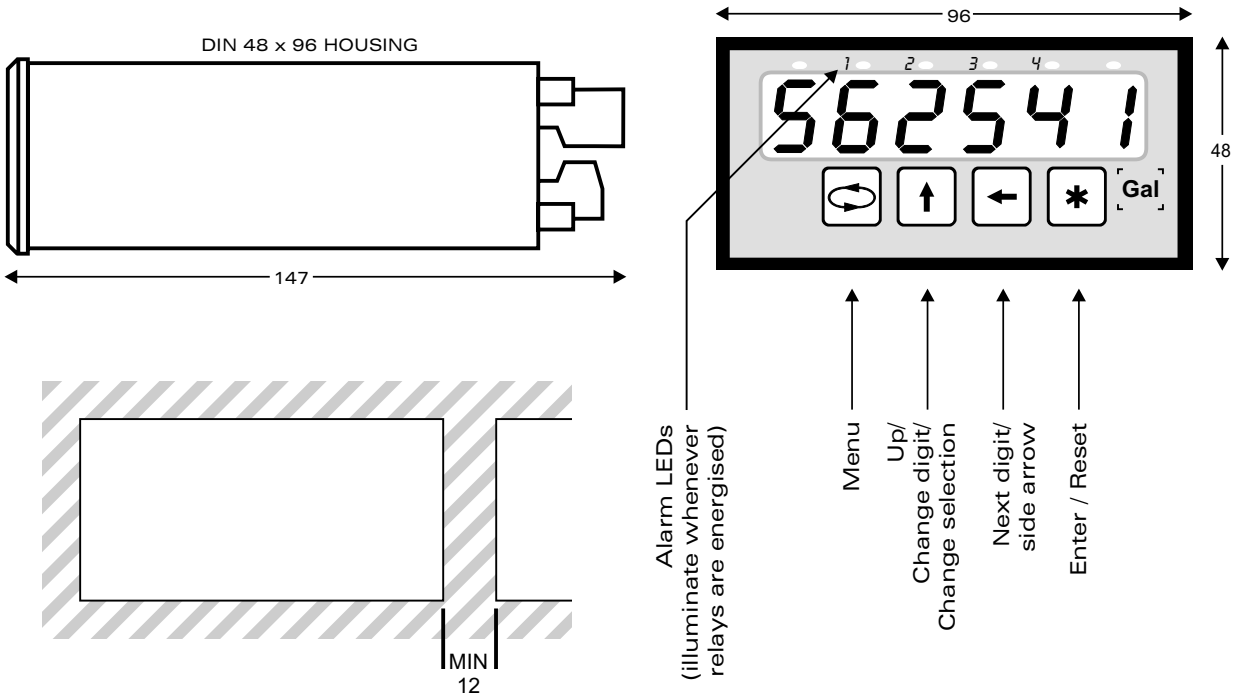

DIN 48 x 96 industrial strength single piece housing
Flame retardant ABS plastic, meets UL 94 V-0 flamability rating
IP53 rating (front panel)
IP65 (with optional panel seal added)

Dimension in mm

PINOUT

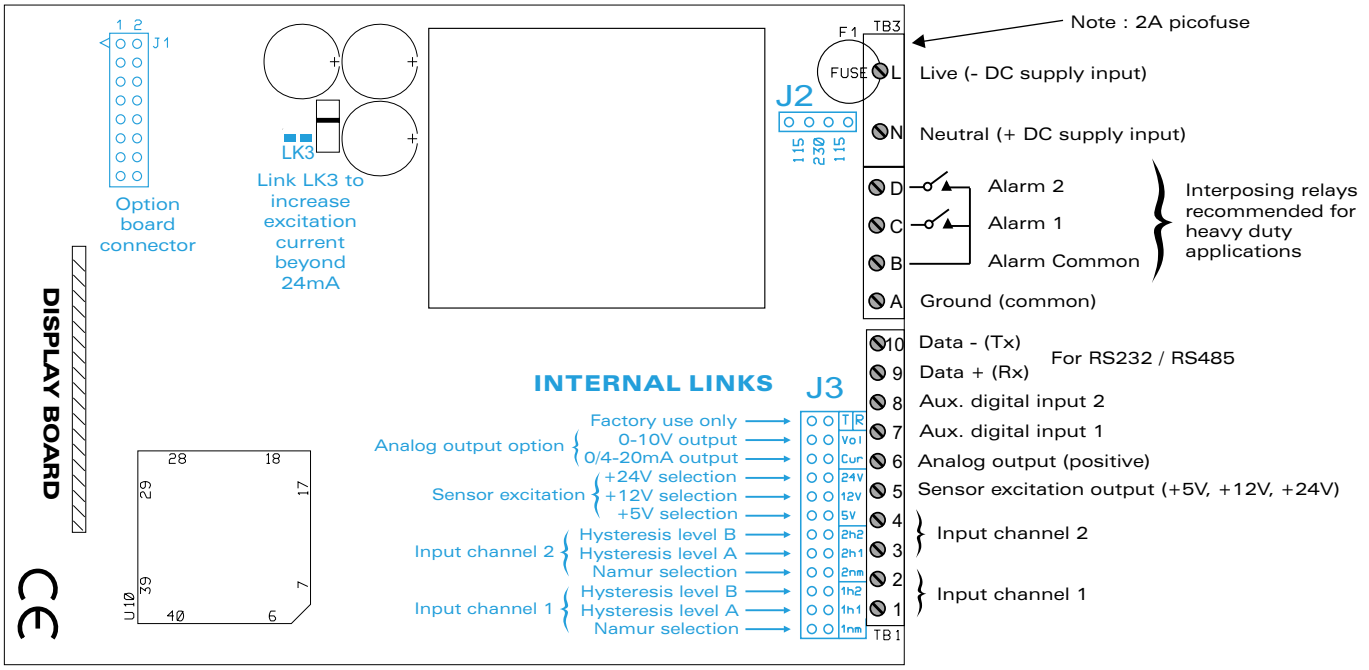

APPLICATION EXAMPLES

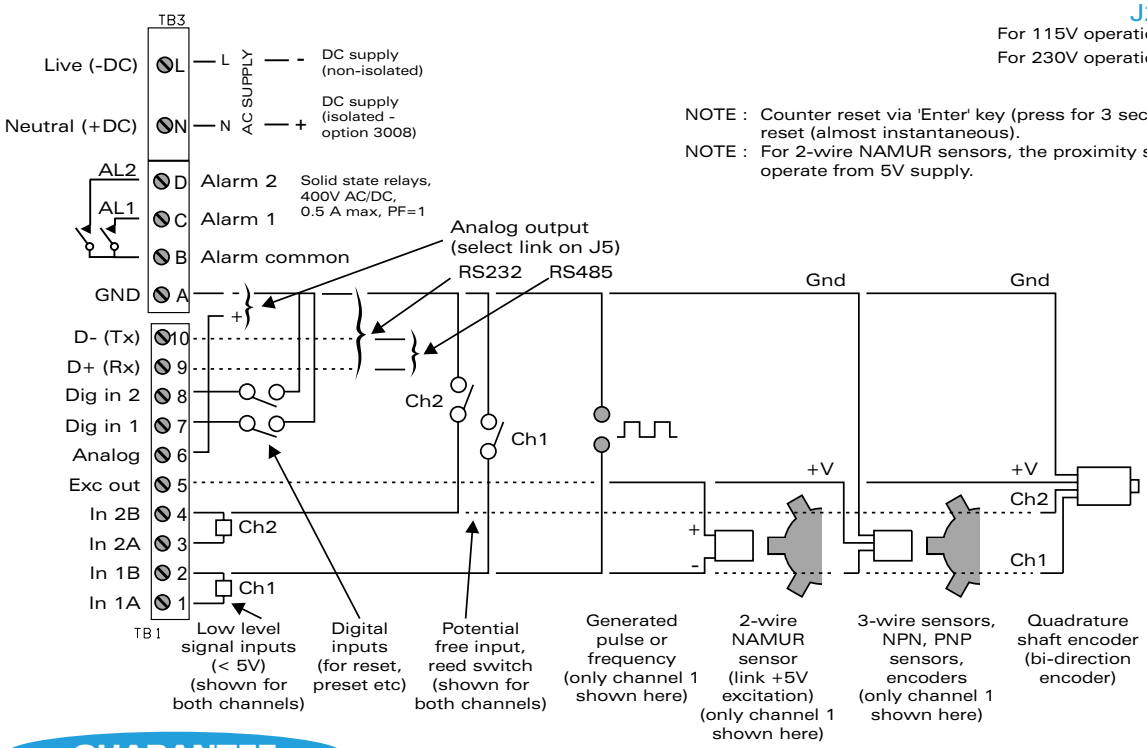

POWER SUPPLY LINKS

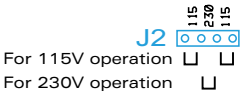

NOTE : Counter reset via 'Enter' key (press for 3 seconds) or via external reset (almost instantaneous).
NOTE : For 2-wire NAMUR sensors, the proximity switch must be able to operate from 5V supply.

GUARANTEE

This product is guaranteed against faulty workmanship or defective material, for a period of 3 (three) years from date of delivery by Instrotech.

Instrotech undertakes to replace without charge all defective equipment which is returned to it (transportation costs prepaid) during the period of guarantee, provided there is no evidence that the equipment has been abused or mishandled in any way.

Instrotech reserves the right to alter any specification without notice.

DISTRIBUTED BY:

CE

CERTIFICATION DEKRA DIN ISO 9001

Rev 1.1 - 22/09/99 - 4012b+

D.11.3 Vacuum pump

DIAPHRAGM PUMPS
ME 2 AND ME 2C

ME 2 one stage

1.9 m³/h
1.3 cfm
37 l/min

< 80 mbar
< 60 Torr

ME 2C one stage

1.7 m³/h
1.2 cfm
33 l/min

< 80 mbar
< 60 Torr

ME 2

The one stage diaphragm pumps ME 2 and ME 2C are totally oil free, mechanical vacuum pumps. The precise geometry of displacement and head space provides a low ultimate vacuum around 80 mbar and a high pumping speed of approx. 2 m³/h. Optimised kinetics for minimum work and wear of the diaphragm result in high reliability, low scuffing, long life and low noise level of the diaphragm. In a wide range of applications they are the modern alternative for evacuation and pumping of gases in chemical and physical laboratories e. g. alternative to water jet and rotary vane pumps.

ME 2C

SPECIAL ADVANTAGES

- continuous oil free pumping of gases and vapours
- selected chemically resistant materials (ME 2C)
- no water consumption, no drained water
- long lifetime, easy to change diaphragms and valves
- low noise level
- compact design

The choice between the two versions depends on the application:

Aluminium Version ME 2:
Gas contacting parts in aluminium, FPM (e. g. Viton®) and PE are designed for a multitude of applications of vacuum generation in laboratories and process plants, such as gas transfer for non-aggressive solvents, vacuum filtration, vacuum degassing and vacuum impregnation.

Chemistry Version ME 2C:
All parts of the chemistry version coming into contact with gases and vapours are made of chemically resistant fluorinated plastic materials. Typical applications are vacuum drying chambers, distillation, gel drying and transfer of aggressive gases and vapours.

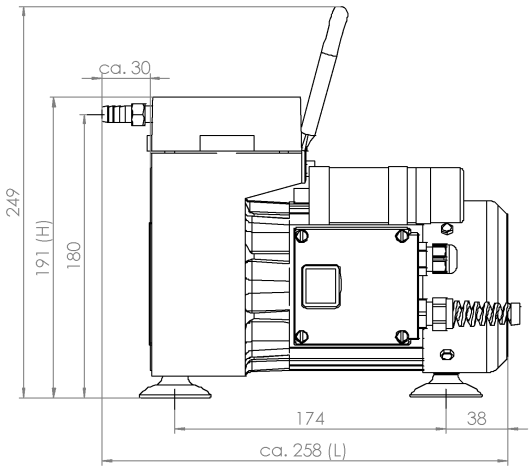

ME 2C

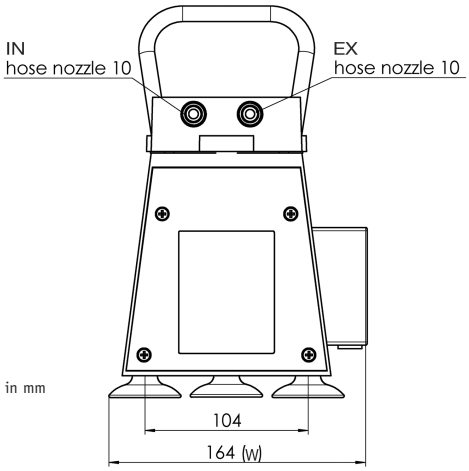

Dimensions in mm

DIAPHRAGM PUMPS
ME 2 AND ME 2C

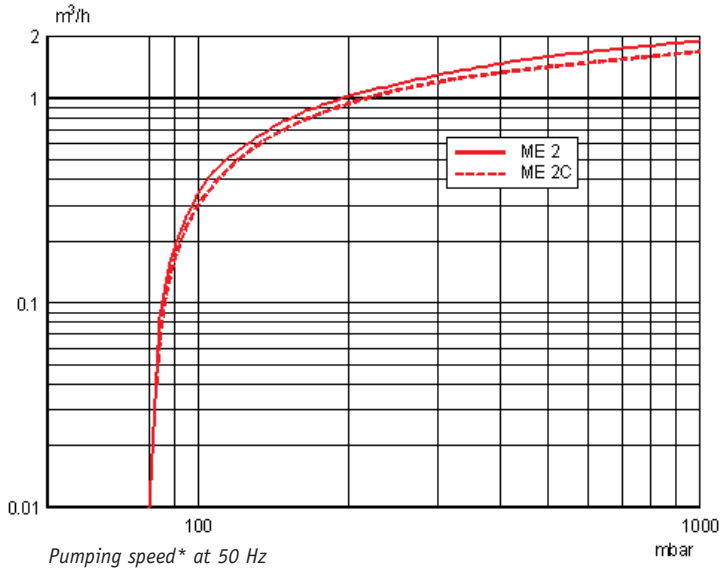

Pumping speed at 50 Hz*

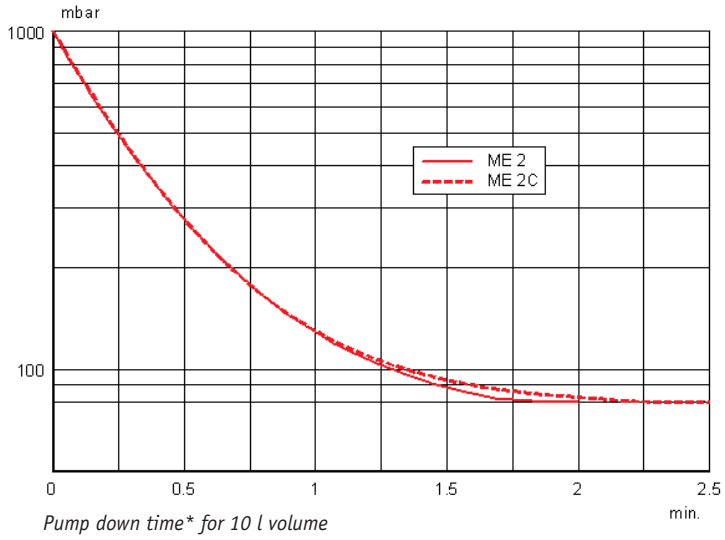

Pump down time for 10 l volume*

ME 2 one stage

.....1.9 m³/h
.....1.3 cfm
.....37 l/min

.....< 80 mbar
.....< 60 Torr

ME 2C one stage

.....1.7 m³/h
.....1.2 cfm
.....33 l/min

.....< 80 mbar
.....< 60 Torr

TECHNICAL DATA		ME 2	ME 2C
Number of stages		1	1
Max. pumping speed (DIN 28432) 50/60 Hz	m³/h//cfm	1.9/2.2//1.3	1.7/2.0//1.2
No. of cylinders		1	1
Ultimate vacuum (total)	mbar//Torr	< 80//< 60	< 80//< 60
Max. pressure outlet (total)	bar	2	2
Inlet connection (IN) Outlet connection (EX)		hose nozzle NW 10 silencer	hose nozzle NW 10 hose nozzle NW 10
Motor power A. C.	kW	0.12	0.12
Motor rpm. (nominal) 50/60 Hz	min⁻¹	1500/1800	1500/1800
Degree of protection		IP 54	IP 54
Dimensions (L x W x H)	mm	275 x 164 x 188	258 x 164 x 191
Mass	kg	6.8	7.1

Items supplied: Diaphragm pump with on/off switch, cable, plug and instructions for use.

ORDERING INFORMATION		ME 2	ME 2C
230 V ~ 50-60 Hz	plug CEE	69 61 20	69 61 21
230 V ~ 50-60 Hz	plug UK	69 61 26	69 61 32
120 V ~ 60 Hz	plug US	69 61 23	69 61 24

*Pumping speed and pump down time only for information. Ultimate pressure specification: see "Technical Data"

D.11.4 Pressure transducer

2200 Series / 2600 Series – General Purpose Industrial Pressure Transducers

- Gauge, Absolute, Vacuum and Compound Pressure Models Available
- Submersible, General Purpose and Wash Down Enclosures
- High Stability Achieved by CVD Sensing Element
- Millivolt, Voltage and Current Output Models

The 2200 series features stability and accuracy in a variety of enclosure options. The 2600 series extends the packaging options via an all welded stainless steel back end for demanding submersible and industrial applications. The 2200 and the 2600 feature proven CVD sensing technology, an ASIC (amplified units), and modular packaging to provide a sensor line that can easily accommodate specials while not sacrificing high performance.

Series 2200

Series 2600

Specifications

Input	
Pressure Range	Vacuum to 400 bar (6000 psi)
Proof Pressure	2 x Full Scale (FS) (1.5 x Fs for 400 bar, >= 5000 psi)
Burst Pressure	>35 x FS <= 6 bar (100 psi); >20 x FS >=60 bar (1000 psi); >5 x FS <= 400 bar (6000 psi)
Fatigue Life	Designed for more than 100 million FS cycles
Performance	
Long Term Drift	0.2% FS/year (non-cumulative)
Accuracy	0.25 % FS typical (optional 0.15% FS)
Thermal Error	1.5% FS typical (optional 1% FS)
Compensated Temperatures	-20°C to 80°C (-5°F to 180°F)
Operating Temperatures	-40°C to 125°C (-40°F to 260°F) for elec. codes A, B, C, 1 -20°C to 80°C (-5°F to 180°F) for elec. codes 2, D, G, 3 -20°C to 50°C (-5°F to 125°F) for elec. codes F,M, P Amplified units >100°C maximum 24 VDC supply
Zero Tolerance	1% of span
Span Tolerance	1% of span
Response Time	0.5 ms
Mechanical Configuration	
Pressure Port	See ordering chart
Wetted Parts	17-4 PH Stainless Steel
Electrical Connection	See ordering chart
Enclosure	316 ss, 17-4 PH ss IP65 NEMA 4 for elec. codes A, B, C, D, G,1, 2, 3 IP67 for elec. code "F" IP68 for elec. codes M, (max depth 200 meters H_2O) IP30 for elec. code "3" with flying leads
Vibration	70g, peak to peak sinusoidal, 5 to 2000 Hz (Random Vibration: 20 to 2000 Hz @ ≈20g Peak per MIL-STD.-810E Method 514.4)
Acceleration	100g steady acceleration in any direction 0.032% FS/g for 1 bar (15 psi) range decreasing logarithmically to 0.0007% FS/g for 400 bar (6000 psi) range.
Shock	20g, 11 ms, per MIL-STD.-810E Method 516.4 Procedure I
Approvals	CE, UR (22ET, 26ET Intrinsically Safe)
Weight	Approx. 100 grams (additional cable; 75 g/m)

Individual Specifications

Millivolt Output units	
Output	100 mV (10 mv/v)
Supply Voltage (Vs)	10 VDC (15 VDC max.) Regulated
Bridge resistance	2600-6000 ohms
Voltage Output units	
Output	see ordering chart
Supply Voltage (Vs)	1.5 VDC above span to 35 VDC @ 6 mA
Supply Voltage Sensitivity	0.01% FS/Volt
Min. Load Resistance	(FS output / 2) Kohms
Current Consumption	approx 6 mA at 7.5V output
Current Output units	
Output	4-20 mA (2 wire)
Supply Voltage (Vs)	24 VDC, (7-35 VDC)
Supply Voltage Sensitivity	0.01% FS/Volt
Max. Loop Resistance	(Vs-7) x 50 ohms

Electromagnetic Capability

Meets the requirement for CE marking of EN50081-2 for emissions and EN50082-2 for susceptibility.

Test Data:

- EN61000-4-2 Electrostatic Discharge. 8kV air discharge, 4kV contact discharge. Unit survived.
- ENV50140 Radiated RF Susceptibility. 10V/m, 80MHz-1GHz, 1kHz mod. Maximum recorded output error was <±1%
- ENV50204 Radiated RF Susceptibility to Mobile Telephones. 10V/m, 900MHz. Maximum recorded output error was <±1%.
- EN61000-4-4 Fast Burst Transient. 2kV, 5/50ns, 5kHz for 1 minute. Unit survived.
- ENV50141 Conducted RF Susceptibility. 10Vms, 1kHz mod, 150kHz - 80MHz. Maximum recorded output error was <±1%

Connection Code			**mV units**				**Voltage units**				**Current units** (4-20mA)		
			IN+	OUT+	OUT-	IN-	IN+	COM	OUT+	EARTH	(+)	(–)	EARTH
A, B, G	"DIN"	PIN	1	2	3	E	1	2	3	4	1	2	4
C	"10-6 Bayonet"	PIN	A	B	C	D	A	C	B	E	A	B	E
D	"cable"		R	Y	BL	G	R	BK	W	DRAIN	R	BK	DRAIN
F	"IP 67 cable"		R	W	G	BK	R	BK	W	DRAIN	R	BK	DRAIN
M	"Immersible"		R	Y	BL	W	R	W	Y	DRAIN	R	BL	DRAIN
1	"8-4 Bayonet"	PIN	A	B	C	D	A	C	B	D	A	B	D
2	"cable"		R	W	G	BK	R	BK	W	DRAIN	R	BK	DRAIN
3	"conduit & cable"		R	W	G	BK	R	BK	W	DRAIN	R	BK	DRAIN

Cable Legend:
R = Red
BL = Blue
BK = Black
W = White
Y = Yellow

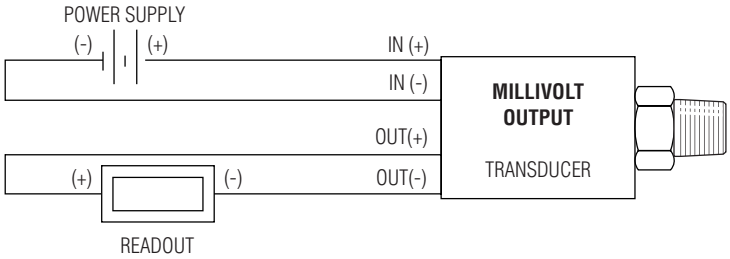

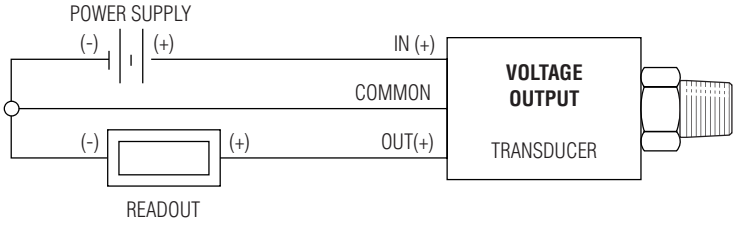

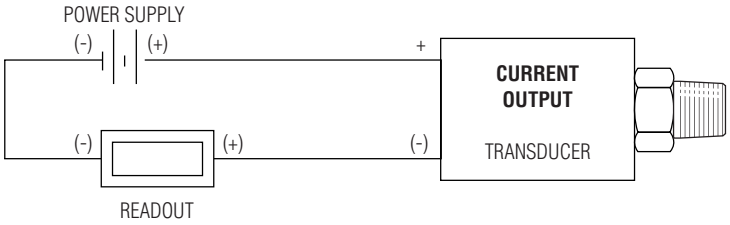

Dimensions

2200 Series

Mini 4 Pin - No Connector

Code B

Mini 4 Pin - With Connector

Code A

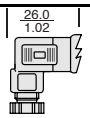

IP67 Cable (Waterproof)

Code F

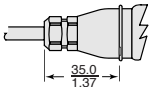

24 AWG Shielded PVC

IP65 or NEMA4 Cable

Code D or 2

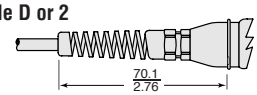

24 AWG Shielded PVC

mV Gauge/Absolute Amplified Gauge

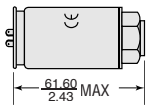

Amplified Absolute

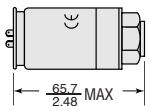

Maximum diameter 27.3 mm (1.07")

2600 Series

10-6 or 8-4 Mil-C Connector

10-6 Code C

8-4 Code 1

Large DIN 43650 Plug

Code G

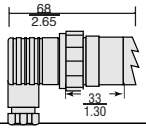

Conduit Connector with Cable

Code 3

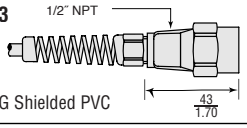

24 AWG Shielded PVC

Conduit Connector with Flying Leads

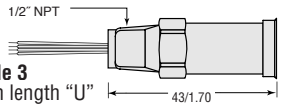

Code 3
with length "U"

Moulded, Immersible Cable

Code M

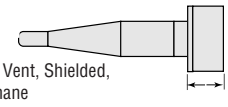

24 AWG, Vent, Shielded, Polyurethane

mV Gauge/Absolute Amplified Gauge

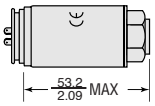

Amplified Absolute

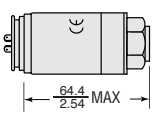

Maximum diameter 27.3 mm (1.07")

1/8-27 NPT

Code 08

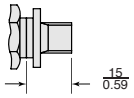

1/4 - 18 NPT

Code 02 with snubber

Code 0J with snubber

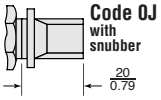

1/4-18 NPT Internal

Code 0E

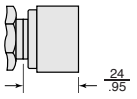

1/2-14 NPT

Code 0H

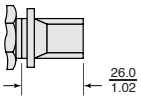

7/16-20 UNF-2A

Code 04

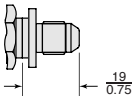

9/16-18 UNF-2A

Code 1P

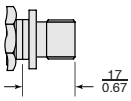

G 1/8 Internal

Code 09

G 1/4 External

Code 01

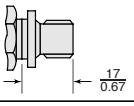

R 1/4

Code 0A

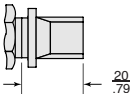

Nose Cone - Black Acetal

Code 19

Nose Cone Sink Weight

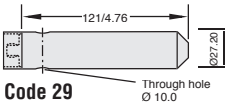

Code 29

mm
inch

How to Order

Use the **bold** characters from the chart below to construct a product code

2200 B G A60 01 A 3 U A

Series
2200 **2600** **22 ET**[4] **26 ET**[4]

Output
A - 100 mV **C** - 1-6V **J** - 0.5-5.5V **G** - 0.2-10.2V
B - 4-20mA **D** - 1-11V **R** - 0-5V **F** - 0.1-5.1V
H - 1-5V **S** - 0-10V

Pressure Datum
A* - Absolute **G** - Gauge
*Max absolute range is 25 bar. (≤ 300 psi)

Pressure Range[3] – psi

F15 - 0-15	**G60** - 0-600	**Vac** = -15 psi
F30 - 0-30	**H10** - 0-1,000	**1F5** - Vac-0
F60 - 0-60	**H15** - 0-1,500	**3F0** - Vac-15
G10 - 0-100	**H20** - 0-2,000	**6F0** - Vac-45
G15 - 0-150	**H30** - 0-3,000	**1G0** - Vac-85
G20 - 0-200	**H40** - 0-4,000	**1G5** - Vac-135
G30 - 0-300	**H50** - 0-5,000	**2G0** - Vac-185
G50 - 0-500	**H60** - 0-6,000	**3G0** - Vac-285

Pressure Range - bar

A10 - 0-1	**B25** - 0-25	**Vac** = -1 bar
A16 - 0-1.6	**B40** - 0-40	**1A0** - Vac-0
A25 - 0-2.5	**B60** - 0-60	**1A6** - Vac-0.6
A40 - 0-4	**C10** - 0-100	**2A5** - Vac-1.5
A60 - 0-6	**C16** - 0-160	**4A0** - Vac-3
B10 - 0-10	**C25** - 0-250	**6A0** - Vac-5
B16 - 0-16	**C40** - 0-400	**1B0** - Vac-9
		1B6 - Vac-15
		2B5 - Vac-24
		4B0 - Vac-39

Pressure Port
08 - 1/8-27 NPT External
02 - 1/4-18 NPT External
0J - 1/4 NPT External w/snubber
0E - 1/4 NPT Internal
0H - 1/2-14 NPT External
04 - 7/16-20 External (SAE #4, J514)
1P - 9/16-18 External (SAE #6, J1926-2)
IJ - 7/16-20 External (SAE #4, J1926-2)

European Threads
09 - G1/8 Internal
01 - G1/4 External
0A - R1/4 External
Submersible (2600 only)
19 - Plastic Nose Cone
29 - Sink Weight Nose Cone

Performance Code
Accuracy/Thermal
A - .25%/1.5%
B - .15%/1.0%

Cable Length[1]
U - No Cable Fitted[1 2]
D - 1 Metre (3 feet)
E - 3 Metres (9 feet)
F - 5 Metres (16 feet)
G - 10 Metres (32 feet)

Apparatus Protection
2 - mV Only Transient Protection CE Mark, UR
3 - Amplified Only RFI Protected CE Mark, UR
E - Amplified only IS mark (Div. 1 only)[4]
T - Amplified only IS mark (Div. 1 and 2)[4 5]

Electrical Connection (See Notes)
2200 Series
A - 4 PIN DIN (Micro) Mating Connector Supplied
B - 4 PIN DIN (Micro) Mating Connector Not Supplied
2 - Cable Nema 4 USA
D - Cable European Color Code
F - Cable Gland Metal IP67

2600 Series
C - Fixed Plug Size 10-6 Mating Plug Not Supplied
G - Fixed Plug To DIN 43650 Mating Plug Supplied
M - Moulded Cable Immersible
1 - Fixed Plug Size 8-4 Mating Plug Not Supplied
3 - Conduit Connector 1/2NPT Ext. 1M Cable[2]

Notes:
1. When electrical connection is cable please select a cable length from Table 1 below. When electrical connection is DIN or plug style "U" must be specified.
2. Where electrical connection **-3** and cable length **-U** occur in part number, the unit will be supplied with flying leads (4-1/2˝ IP30).
3. Additional Pressure Ranges are available. Please consult factory.
4. Intrinsically safe transducers are available with amplified outputs only. (ETL, entity approved for Class I, Division 1, Groups C & D, hazardous areas; Class I, Divisions 1 and 2, Groups C & D for Electrical Connection Codes **-A**, **-B**, **-G** or **-3** only.
5. Apparatus Protection Code **-T** is available for Electrical Connection Codes **-A**, **-B**, **-G** or **-3** only.

3-Day
Delivery
on Most Transducers

Table 1 - Cable Length

(2600 Series) (2200 Series select "U" through "G")

Code	Length (M)	Code	Length (M)
U	No Cable Fitted	M	40
D	1	N	50
E	3	P	75
F	5	Q	100
G	10	R	125
H	15	S	150
J	20	4	170
K	25	5	200
L	30	6	225

D.11.5 Wire gauge

AWG
SIZE TO INCHES

American Wire Gauge (AWG)	Size O.D. inches
6/0	0.5800
5/0	0.5165
4/0	0.4600
3/0	0.4096
2/0	0.3648
1/0	0.3249
1	0.2893
2	0.2576
3	0.2294
4	0.2043
5	0.1819
6	0.1620
7	0.1443
8	0.1285
9	0.1144
10	0.1019
11	0.0907
12	0.0808
13	0.0720
14	0.0641
15	0.0571
16	0.0508
17	0.0453
18	0.0403
19	0.0359
20	0.0320
21	0.0285
22	0.0253
23	0.0226
24	0.0201
25	0.0179
26	0.0159
27	0.0142
28	0.0126
29	0.0113
30	0.0100
31	0.00893
32	0.00795
33	0.00708
34	0.00630
35	0.00561
36	0.00500
37	0.00445
38	0.00396
39	0.00353
40	0.00314
41	0.00280
42	0.00249
43	0.00222
44	0.00198
45	0.00176
46	0.00157
47	0.00140
48	0.00124
49	0.00111
50	0.00099

2300 Walden Avenue • Buffalo, New York 14225
FAX: 716-684-7433 • Phone: 716-684-4500 • 1-800-223-2389
www.conaxbuffalo.com
e-mail: conaxbuf@conaxbuffalo.com

European Office
PO Box 91 • BOGNOR REGIS PO22 7JB, England
FAX: +44 (0)1243 587799 • Phone: +44 (0)1243 587878
e-mail: cbteurope@compuserve.com

D.11.6 SKF eddy current sensors

CMSS 958 Extension Cable

Temperature ranges, connectors, cable same as CMSS 65 Eddy Current Probe.

CMSS 665 and CMSS 665P Drivers

Operating Temperature Range: 0°C to +65°C (+32°F to +149°F)

Connections: Power, Signal, GND

Five terminal removable and reversible compression terminal block accepting up to 2 mm^2 (14 AWG) wire. Three connections necessary per block (-24 VDC; GND; Signal). The CMSS 665P has a permanent fixed connector with same connection characteristics.

Mounting: C-DIN Rail Mount which bolts onto Driver enclosure, or the standard four number 10 clearance holes in a square on 63.5 mm (2.5") centers.

SYSTEM PERFORMANCE

The following performance characteristics apply for the CMSS 65 Eddy Current Probe System in addition to quoted nominal specifications:

Extended Temperatures: With 1m probe and 4m extension cable operating in a range of -34°C to +120°C (-29°F to +248°F), and driver in the range of 0°C to +65°C (+32°F to +149°F):

Sensitivity: ± 10% of 7.87 mV/micron (200 mV/mil)

Linearity: ± 25.4 microns (1 mil) of best straight line over 2 mm (80 mil) range.

Minimum Target Size: ***Flat Surface:*** 10 mm (0.39")

Shaft Diameter: 15 mm (0.59")

Hazardous Area Approvals

NORTH AMERICA

Approvals granted by Factory Mutual (FM) and Canadian Standards Association (CSA).

Class 1 Division 1 Groups A, B, C, D when used with intrinsically safe zener barriers, or galvanic isolators. Contact representative for details.

Class 1 Division 2 Groups A, B, C, D when connected with National Electric Code (NEC) without Zener barriers or galvanic isolator. Contact representative for details.

EUROPE

Certification to ATEX Directive.

Drivers: Ex II 1 G EEx ia IIC T4
(-20°C ≤ Ta ≤ +75°C)
Certificate Number: BAS02ATEX1168X

Probes: Ex II 1 G EEx ia IIC T4 or T2
Certificate Number: BAS02ATEX1169

System: EEx ia IIC T4 or T2 (as per schedule)
Certificate Number: Ex 02E2170

Intrinsic Safety requires use of zener barriers. Contact representative for details.

See ordering details for probe and driver designations for hazardous area approved models.

Ordering Information

DIMENSIONS IN INCHES, EXCEPT AS NOTED

STANDARD MOUNT CASE

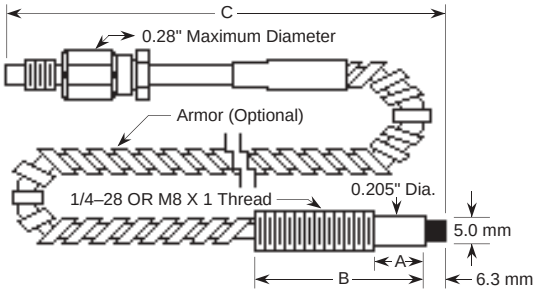

REVERSE MOUNT CASE

CMSS 65 — □□ — 0 — RM — 12 — □□

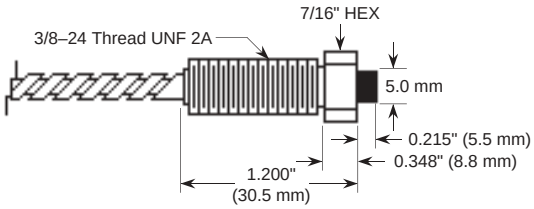

BUTTON (DISK) PROBE

CMSS 65 — □□ — E — 00 — 00 — □□

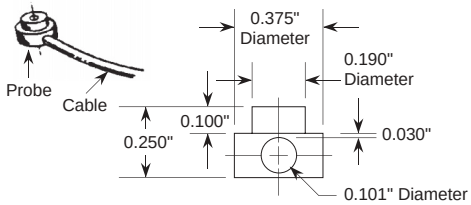

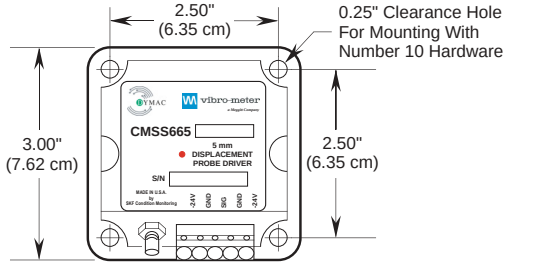

CONNECTOR: Stainless Steel Jack-Type Mates With CMSS 958 Extension Cable

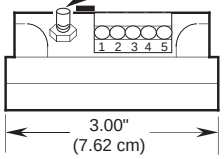

REMOVABLE OR PERMANENT FIXED CONNECTOR: Terminal Strip Type Rated For 250 V, 10 AMPS 14 AWG. Maximum Wire Size

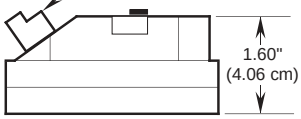

Ordering Information

Part 1: Eddy Current Probe (SKF Standard: CMSS 65-002-00-12-10)

CMSS 65 [ ][ ][ ] — [ ][ ] [ ][ ] [ ][ ]

CABLE	
Standard	00
Armored	01
Fiberglass Sleeved	02
CSA/FM/SIRA (ATEX) (Intrinsically Safe) Certified	07
CSA/FM/SIRA (ATEX) (Intrinsically Safe) Certified and Armored	08
FM (non-incendive)	09
FM (non-incendive) Armored	0B

CASE	
2	1/4–28 Threads (Standard)
3	M8 X 1 Threads
0	3/8–24 Threads
1	M10 X 1 Threads
4	No Case
E	Button Probe (Fiberglass)

"A" UNTHREADED CASE LENGTH	
Fully Threaded	00
0.1 Inches To 5.0 Inches Unthreaded	01 To 50
5.1 Inches To 9.9 Inches	51 To 99
Reverse Mount, 3/8–24 Thread	RM

"B" CASE LENGTH	
Standards:	
No Case	00
0.8 Inches	08
1.2 Inches	12
1.5 Inches	15
2.0 Inches	20
2.5 Inches	25
3.0 Inches	30
4.0 Inches	40
4.7 Inches	47
6.0 Inches	60
9.0 Inches	90
SPECIALS	
0.9 To 5.9 Inches	09 To 59
9.1 To 9.9 Inches	91 To 99

"C" OVERALL LENGTH +1	
05	0.5 Meter
10	1.0 Meter (Standard)
5A	5.0 Meter

+1: Length is **Nominal Electrical:** physical length may vary.

Compatible Systems:

0.5 m Probe
5.0 m System
CMSS 958 - XX - 045/CMSS 665
1.0 m Probe
5.0 m System:
CMSS 958 - XX - 040/CMSS 665
5.0 m Probe
5.0 m System: CMSS 665
The 5A units have integral cable and mate directly to the Driver.

Part 2: Extension Cable (SKF Standard: CMSS 958-00-040)

CMSS 958 [ ][ ] — [ ][ ][ ]

CABLE	
Standard	00
Armored	01
Fiberglass Sleeved	02
CSA/FM/SIRA (ATEX) (Intrinsically Safe) Certified	09
CSA/FM/SIRA (ATEX) (Intrinsically Safe) Certified and Armored	0A
FM (non-incendive)	0H
FM (non-incendive) Armored	0J

LENGTH (Compatible System Listed)	
CMSS 665, 2.0 m CMSS 65	030
CMSS 665, 1.0 m CMSS 65	040
CMSS 665, 0.5 m CMSS 65	045

Part 3: Driver (SKF Standard: CMSS 665)

Drivers containing the "P" in the model number, denote those models with permanent fixed connector.

Driver (5 metre system)

CMSS 665/CMSS 665P

7.87 mV/ micron (200 mV/mil). Use with:

- 1 m Probe and 4 m Extension Cable
- 0.5 m Probe and 4.5 m Extension Cable
- or 5 m Probe

Driver (10 metre system)

CMSS 665-1/CMSS 665P-1

Use with:

- 1 m Probe and 9 m Extension Cable
- or 10 m Probe

Usable Range: 2 mm (0.25 mm to 2.3 mm)
80 mils (10 mils to 90 mils)

Sensitivity: 7.87 mV/ micron (200 mV/mil) ± 10% of 200 mV/mil

Linearity: ± 38 microns (1.5 mil) from best straight line

Enhanced Environmental Protection

CMSS 665-8/CMSS 665P-8

Specifications same as standard driver, however is also filled with potting material to provide additional measure of protection when operated in adverse environmental conditions. Sensitivity 7.87 mV/micron (200 mV/mil).

Part 3: Driver (SKF Standard: CMSS 665) (continued)

Drivers containing the "P" in the model number, denote those models with permanent fixed connector.

HAZARDOUS AREA APPROVAL (INTRINSIC SAFETY) WITH 4140 STAINLESS STEEL TARGET

CMSS 665-16-9/CMSS 665P-16-9

CSA/FM/SIRA (Intrinsically Safe) Certified Driver for 5 m System. Use with CSA/FM/SIRA (Intrinsically Safe) Certified 1 m CMSS 65 Probe and 4 m CMSS 958 Extension Cable. For intrinsic safety installations, drivers must be installed with intrinsic safety (I-S) barriers.

Barriers: For FM Approval

Power: Stahl 8901/30-280/085/00

Signal: Stahl 8901/30-199/038/00

For CSA and SIRA Approval

Power/Signal: MTL 7096 Dual (neg)

Contact representative for more details.

Usable Range: 1.15 mm (0.25 mm to 1.4 mm)
45 mils (10 mils to 55 mils)

Sensitivity: 7.87 mV/ micron (200 mV/mil)

Linearity: ± 25.4 microns (1 mil) from best straight line over 1.15 mm (45 mil) range.

CMSS 665-16-xx (*see note)/CMSS 665P-16-xx (*see note)

CSA/FM/SIRA (Intrinsically Safe) Certified Driver for 5 m System calibrated for shaft materials other than standard 4140 stainless steel. Use with CSA/FM/SIRA (Intrinsically Safe) Certified 1 m CMSS 65 Probe and 4 m CMSS 958 Extension Cable. For intrinsic safety installations, drivers must be installed with intrinsic safety (I-S) barriers (see CMSS 665-16-9).

Usable Range: Best attainable for specific shaft material provided. Customer to provide identification of shaft material and sample (approximately 2.0" diameter disk, 0.5" thick). Range not expected to exceed the 45 mils of standard unit.

Sensitivity: 200 mV/mil, ± to be determined (TBD) percentage of 200 mV/mil dependent on the shaft sample material (-24 VDC supply).

Linearity: ± the minimum deviation (in microns or mils) from the best straight line attainable for the sample shaft material provided.

**** NOTE ****

xx = System calibrated for shaft materials other than standard 4140 stainless steel. For custom configurations, please contact an SKF Reliability Systems Representative.

HAZARDOUS AREA APPROVAL (NON-INCENDIVE) WITH 4140 STAINLESS STEEL TARGET

CMSS 665-20-00/CMSS 665P-20-00

FM (non-incendive) Certified Driver for the 5 m System. Use with FM (non-incendive) Certified 1 m CMSS 65 Probe and CMSS 958 Extension Cable.

Usable Range: 2 mm (0.25 mm to 2.25 mm)
80 mils (10 mils to 90 mils)

Sensitivity: 7.87 mV/ micron (200 mV/mil)

Linearity: ± 25.4 microns (1 mil) of best straight line over 2 mm (80 mil) range.

– NOTE –

All circuit boards used in SKF CMSS 665 Series Drivers are conformal coated as standard procedure.

D.11.7 Feedthroughs and glands

Insulated Leadwire (Power Lead) Sealing

PL Series

Conax Buffalo Model PL (Power Lead) Glands seal on insulated leadwire for use in transformers, motors, conduit boxes and pressure/vacuum chambers and as power or instrument feedthroughs. The soft sealant technology seals against gases or liquids and resists element movement under pressure. Immersion length adjustments and easy replacement of elements can be accomplished in the field.

PL glands may be purchased with or without wire. If supplied with wire, solid copper wire with Kapton® insulation is standard. This is provided as 24" total with the gland centered at mid-point. Standard sealants are Grafoil or Teflon. Other materials for wire and sealants can be provided for special applications. Consult your Conax Buffalo sales engineer for more information on available options.

Terminals can be furnished on all wire ends if specified, at additional cost. Bulk wire is available from Conax Buffalo for field assembly of PL glands. (See the Accessories Section, page 152.)

PL gland bodies with NPT threads and SAE threads are constructed from 303SST standard. Weld-neck style gland bodies are constructed from 316LSST standard. Caps and followers for all styles are constructed from 303SST standard. Many optional materials are also available, including 316LSST, Monel 405, Hastelloy C276, Inconel and more. For information on alternative materials, see page 7. Cap Style A offers a mounting thread only. Cap Style B provides threading on both ends for attachment to conduit or terminal heads. Alternative sealant materials are available. Please consult a Conax Buffalo sales engineer for custom needs.

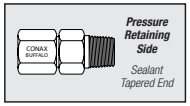

Type A has mounting thread only.

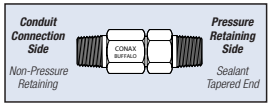

Type B has cap end threaded. B Cap NPT matches the standard mounting NPT.

- Temperature Range: -300˚ F to +450˚ F (-185˚ C to +232˚ C)
- Pressure Range: Vacuum to 10,000 PSIG (690 bar) – see Pressure Ratings in Specifications Chart.
- 600 Volts to 55 amps
- Seals 1-18 Wires
- Easy installation – no "potting"
- Wire Identification Markers applied
- Thermocouple Material conductors available, 18 gauge standard, other wire gauges optional

Accessories

The replaceable sealant permits repeated use of the same fitting. Assembly is simple and may be done in the field. Simply insert the elements and torque the cap. To replace the sealant or elements, simply loosen the cap, replace the necessary items, relubricate and retorque the cap.

Glands are supplied factory lubricated. When reused, the glands should be relubricated to maintain the published torque and pressure ratings. If glands are cleaned prior to assembly, they should be relubricated. On weld mount models, the heat from the welding process will destroy the lubricant. These models must be relubricated prior to use. See page 153 for information on our lubrication kit.

Replacement Packing Sets are available. These consist of a sealant and two insulators. Replacement sealants may also be ordered separately.

To order a Replacement Packing Set, order
RPS – (Gland) – (Wire Gauge) – (Number of Holes) – (Sealant)

Example: *RPS-PL-12-3-T*

To order a Replacement Sealant only, order
RS – (Gland) – (Wire Gauge) – (Number of Holes) – (Sealant)

Example: *RS-PL-12-3-T*

Catalog Numbering System

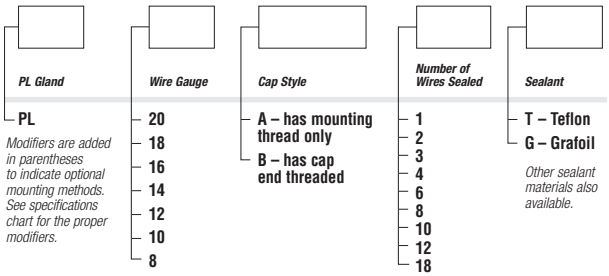

Example: ***PL-12-A3-T, 24/36***
(With Non-Standard Wire Length)

Example: ***PL-12-A3-T***
(With Standard Wire Length)

Example: ***PL-18(J)-A2-T, 24/36***
(With Thermocouple Material Conductors)

Example: ***PL-12-A3-T-XX***
(Without Conductors)

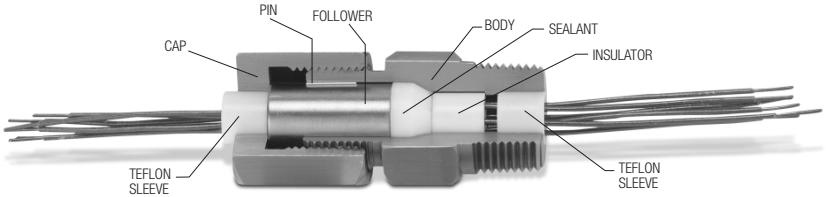

PL Selection Guide

Wire Gauge	Standard Number of Wires Offered								
	1	2	3	4	6	8	10	12	18
20		X	X	X	X	X			X
18	X	X	X	X	X	X	X	X	
16		X	X	X	X	X	X	X	
14	X	X	X	X	X	X	X	X	
12		X	X	X	X				
10		X	X	X					
8		X	X						

The number of wires offered is dependent on the mounting port size. See the Specifications charts on the subsequent pages for details.

Torque (ft-lbs)

	Number of Holes	Grafoil	Teflon
PL-20	2,3,4	90-100	60-70
PL-20	6,8	150-165	90-100
PL-20	18	250-265	125-140
PL-18	1	20-30	12-15
PL-18	2,3,4	90-100	60-70
PL-18	6,8	150-165	90-100
PL-18	10,12	250-265	125-140
PL-16	2,3,4	90-100	60-70
PL-16	6,8	150-165	90-100
PL-16	10,12	250-265	125-140
PL-14	1	25-30	12-15
PL-14	2	90-100	60-70
PL-14	3,4,6,8	150-165	90-100
PL-14	10,12	250-265	125-140
PL-12	2,3,4,6	150-165	90-100
PL-10	2,3,4	150-165	80-90
PL-8	2	150-165	75-85
PL-8	3	250-265	125-140

All pressure and torque ratings were determined at 68˚ F (20˚ C) using solid Kapton-insulated copper conductors as the element.

For proper assembly of these sealing glands, see the Assembly Instructions provided on page 156.

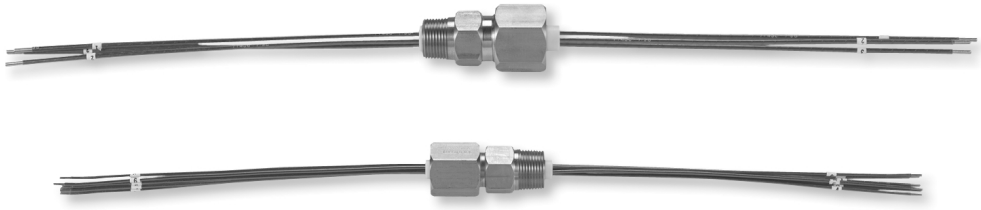

For more information call: **1-800-223-2389** • e-mail: **info@conaxbuffalo.com** • visit our website: **www.conaxbuffalo.com**

Specifications

PL Series

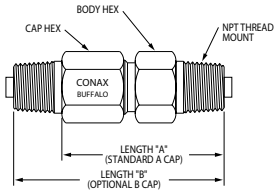

Standard NPT

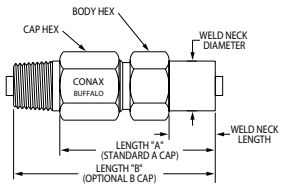

Weld Neck Mount

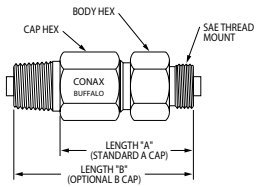

SAE Thread Mount

Catalog Number	Wire Gauge	Number of Wires	Amperage Rating Per Wire	Length A	Length B	Hex Size Body (Cap)*	Pressure Ratings (PSIG) Grafoil	Teflon
Standard 1/8 NPT								
PL-18-1	18	1	13	1-15/32"	1-27/32"	1/2 (9/16)"	10,000	1600
PL-14-1	14	1	24	1-15/32"	1-27/32"	1/2 (9/16)"	10,000	800
Weld Neck (Weld Neck Length 0.39", Diameter 0.405")**								
PL(SWM1/S316L)-18-1	18	1	13	1-15/32"	1-27/32"	1/2 (9/16)"	10,000	1600
PL(SWM1/S316L)-14-1	14	1	24	1-15/32"	1-27/32"	1/2 (9/16)"	10,000	800
SAE 3/8-24 Thread Mount (formerly MS)								
PL(MSE3/)-18-1	18	1	13	1-7/8"	2-1/4"	1/2 (9/16)"	10,000	1600
PL(MSE3/)-14-1	14	1	24	1-7/8"	2-1/4"	1/2 (9/16)"	10,000	800
Standard 1/2 NPT								
PL-20-2	20	2	9	2-5/8"	3-3/8"	1"	10,000	5000
PL-20-3	20	3	9	2-5/8"	3-3/8"	1"	10,000	5000
PL-20-4	20	4	9	2-5/8"	3-3/8"	1"	10,000	5000
PL-18-2	18	2	13	2-5/8"	3-3/8"	1"	10,000	4000
PL-18-3	18	3	13	2-5/8"	3-3/8"	1"	10,000	4000
PL-18-4	18	4	13	2-5/8"	3-3/8"	1"	10,000	4000
PL-16-2	16	2	17	2-5/8"	3-3/8"	1"	10,000	3000
PL-16-3	16	3	17	2-5/8"	3-3/8"	1"	10,000	3000
PL-16-4	16	4	17	2-5/8"	3-3/8"	1"	10,000	3000
PL-14-2	14	2	24	2-5/8"	3-3/8"	1"	10,000	1500
PL-14-3	14	3	24	2-7/8"	3-5/8"	1-1/8 (1-1/4)"	10,000	2000
PL-14-4	14	4	24	2-7/8"	3-5/8"	1-1/8 (1-1/4)"	10,000	1600
Optional 1/4 NPT								
PL(PTM2/)-20-2	20	2	9	2-5/8"	3-3/8"	1"	10,000	5000
PL(PTM2/)-20-3	20	3	9	2-5/8"	3-3/8"	1"	10,000	5000
PL(PTM2/)-20-4	20	4	9	2-5/8"	3-3/8"	1"	10,000	5000
PL(PTM2/)-18-2	18	2	13	2-5/8"	3-3/8"	1"	10,000	4000
PL(PTM2/)-18-3	18	3	13	2-5/8"	3-3/8"	1"	10,000	4000
PL(PTM2/)-18-4	18	4	13	2-5/8"	3-3/8"	1"	10,000	4000
PL(PTM2/)-16-2	16	2	17	2-5/8"	3-3/8"	1"	10,000	3000
PL(PTM2/)-16-3	16	3	17	2-5/8"	3-3/8"	1"	10,000	3000
PL(PTM2/)-16-4	16	4	17	2-5/8"	3-3/8"	1"	10,000	3000
PL(PTM2/)-14-2	14	2	24	2-5/8"	3-3/8"	1"	10,000	1500
PL(PTM2/)-14-3	14	3	24	2-7/8"	3-5/8"	1-1/8 (1-1/4)"	10,000	2000
PL(PTM2/)-14-4	14	4	24	2-7/8"	3-5/8"	1-1/8 (1-1/4)"	10,000	1600

Note: the pressure and torque ratings provided in this catalog apply only when bores are drilled by Conax Buffalo Technologies.
** Hex size for the body and cap are the same unless a cap size is provided in parentheses.*
*** Weld neck models require lubrication prior to use.*

Catalog Number	Wire Gauge	Number of Wires	Amperage Rating Per Wire	Length A	Length B	Hex Size Body (Cap)*	Pressure Ratings (PSIG) Grafoil	Teflon
Weld Neck (Weld Neck Length 0.78", Diameter 0.840")**								
PL(SWM4/S316L)-20-2	20	2	9	2-5/8"	3-3/8"	1"	10,000	5000
PL(SWM4/S316L)-20-3	20	3	9	2-5/8"	3-3/8"	1"	10,000	5000
PL(SWM4/S316L)-20-4	20	4	9	2-5/8"	3-3/8"	1"	10,000	5000
PL(SWM4/S316L)-18-2	18	2	13	2-5/8"	3-3/8"	1"	10,000	4000
PL(SWM4/S316L)-18-3	18	3	13	2-5/8"	3-3/8"	1"	10,000	4000
PL(SWM4/S316L)-18-4	18	4	13	2-5/8"	3-3/8"	1"	10,000	4000
PL(SWM4/S316L)-16-2	16	2	17	2-5/8"	3-3/8"	1"	10,000	3000
PL(SWM4/S316L)-16-3	16	3	17	2-5/8"	3-3/8"	1"	10,000	3000
PL(SWM4/S316L)-16-4	16	4	17	2-5/8"	3-3/8"	1"	10,000	3000
PL(SWM4/S316L)-14-2	14	2	24	2-5/8"	3-3/8"	1"	10,000	1500
PL(SWM4/S316L)-14-3	14	3	24	2-7/8"	3-5/8"	1-1/8 (1-1/4)"	10,000	2000
PL(SWM4/S316L)-14-4	14	4	24	2-7/8"	3-5/8"	1-1/8 (1-1/4)"	10,000	1600
SAE 3/4-16 Thread Mount (formerly MS)								
PL(MSE8/)-20-2	20	2	9	2-3/4"	3-1/2"	1"	10,000	5000
PL(MSE8/)-20-3	20	3	9	2-3/4"	3-1/2"	1"	10,000	5000
PL(MSE8/)-20-4	20	4	9	2-3/4"	3-1/2"	1"	10,000	5000
PL(MSE8/)-18-2	18	2	13	2-3/4"	3-1/2"	1"	10,000	4000
PL(MSE8/)-18-3	18	3	13	2-3/4"	3-1/2"	1"	10,000	4000
PL(MSE8/)-18-4	18	4	13	2-3/4"	3-1/2"	1"	10,000	4000
PL(MSE8/)-16-2	16	2	17	2-3/4"	3-1/2"	1"	10,000	3000
PL(MSE8/)-16-3	16	3	17	2-3/4"	3-1/2"	1"	10,000	3000
PL(MSE8/)-16-4	16	4	17	2-3/4"	3-1/2"	1"	10,000	3000
PL(MSE8/)-14-2	14	2	24	2-3/4"	3-1/2"	1"	10,000	1500
SAE 7/8-14 Thread Mount (formerly MS)								
PL(MSE10/)-14-3	14	3	24	3"	3-1/4"	1-1/8 (1-1/4)"	10,000	2000
PL(MSE10/)-14-4	14	4	24	3"	3-1/4"	1-1/8 (1-1/4)"	10,000	1600
Standard 3/4 NPT								
PL-20-6	20	6	9	2-7/8"	3-5/8"	1-1/8 (1-1/4)"	10,000	3200
PL-20-8	20	8	9	2-7/8"	3-5/8"	1-1/8 (1-1/4)"	10,000	3200
PL-20-18	20	18	9	3-1/8"	3-7/8"	1-1/4 (1-1/2)"	10,000	2400
PL-18-6	18	6	13	2-7/8"	3-5/8"	1-1/8 (1-1/4)"	10,000	2700
PL-18-8	18	8	13	2-7/8"	3-5/8"	1-1/8 (1-1/4)"	10,000	2700
PL-18-10	18	10	13	2-7/8"	3-5/8"	1-1/4 (1-1/2)"	10,000	2100
PL-18-12	18	12	13	2-7/8"	3-5/8"	1-1/4 (1-1/2)"	10,000	2100
PL-16-6	16	6	17	2-7/8"	3-5/8"	1-1/8 (1-1/4)"	10,000	2700
PL-16-8	16	8	17	2-7/8"	3-5/8"	1-1/8 (1-1/4)"	10,000	2700
PL-16-10	16	10	17	2-7/8"	3-5/8"	1-1/4 (1-1/2)"	10,000	1700
PL-16-12	16	12	17	2-7/8"	3-5/8"	1-1/4 (1-1/2)"	10,000	1700
PL-14-6	14	6	24	2-7/8"	3-5/8"	1-1/8 (1-1/4)"	10,000	1600
PL-14-8	14	8	24	2-7/8"	3-5/8"	1-1/8 (1-1/4)"	10,000	1600
PL-14-10	14	10	24	2-7/8"	3-5/8"	1-1/4 (1-1/2)"	10,000	1400
PL-14-12	14	12	24	2-7/8"	3-5/8"	1-1/4 (1-1/2)"	10,000	1400
PL-12-2	12	2	30	2-7/8"	3-5/8"	1-1/8 (1-1/4)"	8800	1200
PL-12-3	12	3	30	2-7/8"	3-5/8"	1-1/8 (1-1/4)"	8800	1200
PL-12-4	12	4	30	2-7/8"	3-5/8"	1-1/8 (1-1/4)"	8800	1200
PL-12-6	12	6	30	2-7/8"	3-5/8"	1-1/8 (1-1/4)"	8800	1200
PL-10-2	10	2	40	2-7/8"	3-5/8"	1-1/8 (1-1/4)"	8000	1200
PL-10-3	10	3	40	2-7/8"	3-5/8"	1-1/8 (1-1/4)"	8000	1200
PL-10-4	10	4	40	2-7/8"	3-5/8"	1-1/8 (1-1/4)"	8000	1200
PL-8-2	8	2	55	2-7/8"	3-5/8"	1-1/8 (1-1/4)"	8000	800
PL-8-3	8	3	55	2-7/8"	3-5/8"	1-1/4 (1-1/2)"	8000	800

All pressure and torque ratings were determined at 68˚ F (20˚ C) using solid Kapton-insulated copper conductors as the element. Pressure ratings may degrade at higher temperatures. Pressure rating guide values are provided for glands with elements restrained by the compressed sealant. Higher pressure may be attained with additional element restraints. Tolerance of tube or probe diameter is ±0.005. Deviation from the nominal may affect pressure ratings.

For more information call: **1-800-223-2389** • e-mail: **info@conaxbuffalo.com** • visit our website: **www.conaxbuffalo.com**

Specifications

PL Series

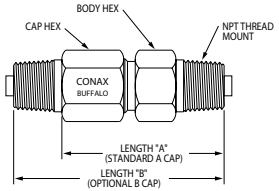

Standard NPT

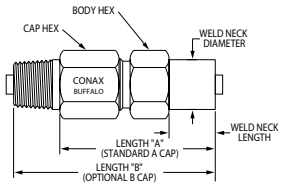

Weld Neck Mount

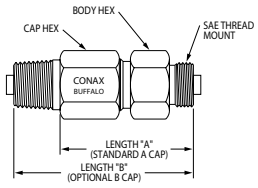

SAE Thread Mount

Catalog Number	Wire Gauge	Number of Wires	Amperage Rating Per Wire	Length A	Length B	Hex Size Body (Cap)*	Pressure Ratings (PSIG) Grafoil	Teflon
Optional 1/2 NPT								
PL(PTM4/)-20-6	20	6	9	2-7/8"	3-5/8"	1-1/8 (1-1/4)"	10,000	3200
PL(PTM4/)-20-8	20	8	9	2-7/8"	3-5/8"	1-1/8 (1-1/4)"	10,000	3200
PL(PTM4/)-18-6	18	6	13	2-7/8"	3-5/8"	1-1/8 (1-1/4)"	10,000	2700
PL(PTM4/)-18-8	18	8	13	2-7/8"	3-5/8"	1-1/8 (1-1/4)"	10,000	2700
PL(PTM4/)-16-6	16	6	17	2-7/8"	3-5/8"	1-1/8 (1-1/4)"	10,000	2700
PL(PTM4/)-16-8	16	8	17	2-7/8"	3-5/8"	1-1/8 (1-1/4)"	10,000	2700
PL(PTM4/)-14-6	14	6	24	2-7/8"	3-5/8"	1-1/8 (1-1/4)"	10,000	1600
PL(PTM4/)-14-8	14	8	24	2-7/8"	3-5/8"	1-1/8 (1-1/4)"	10,000	1600
PL(PTM4/)-12-2	12	2	30	2-7/8"	3-5/8"	1-1/8 (1-1/4)"	8800	1200
PL(PTM4/)-12-3	12	3	30	2-7/8"	3-5/8"	1-1/8 (1-1/4)"	8800	1200
PL(PTM4/)-12-4	12	4	30	2-7/8"	3-5/8"	1-1/8 (1-1/4)"	8800	1200
PL(PTM4/)-12-6	12	6	30	2-7/8"	3-5/8"	1-1/8 (1-1/4)"	8800	1200
PL(PTM4/)-10-2	10	2	40	2-7/8"	3-5/8"	1-1/8 (1-1/4)"	8000	1200
PL(PTM4/)-10-3	10	3	40	2-7/8"	3-5/8"	1-1/8 (1-1/4)"	8000	1200
PL(PTM4/)-10-4	10	4	40	2-7/8"	3-5/8"	1-1/8 (1-1/4)"	8000	1200
PL(PTM4/)-8-2	8	2	55	2-7/8"	3-5/8"	1-1/8 (1-1/4)"	8000	800
Weld Neck (Weld Neck Length 0.79", Diameter 1.050")**								
PL(SWM5/S316L)-20-6	20	6	9	2-7/8"	3-5/8"	1-1/8 (1-1/4)"	10,000	3200
PL(SWM5/S316L)-20-8	20	8	9	2-7/8"	3-5/8"	1-1/8 (1-1/4)"	10,000	3200
PL(SWM5/S316L)-20-18	20	18	9	3-1/8"	3-7/8"	1-1/4 (1-1/2)"	10,000	2400
PL(SWM5/S316L)-18-6	18	6	13	2-7/8"	3-5/8"	1-1/8 (1-1/4)"	10,000	2700
PL(SWM5/S316L)-18-8	18	8	13	2-7/8"	3-5/8"	1-1/8 (1-1/4)"	10,000	2700
PL(SWM5/S316L)-18-10	18	10	13	2-7/8"	3-5/8"	1-1/4 (1-1/2)"	10,000	2100
PL(SWM5/S316L)-18-12	18	12	13	2-7/8"	3-5/8"	1-1/4 (1-1/2)"	10,000	2100
PL(SWM5/S316L)-16-6	16	6	17	2-7/8"	3-5/8"	1-1/8 (1-1/4)"	10,000	2700
PL(SWM5/S316L)-16-8	16	8	17	2-7/8"	3-5/8"	1-1/8 (1-1/4)"	10,000	2700
PL(SWM5/S316L)-16-10	16	10	17	2-7/8"	3-5/8"	1-1/4 (1-1/2)"	10,000	1700
PL(SWM5/S316L)-16-12	16	12	17	2-7/8"	3-5/8"	1-1/4 (1-1/2)"	10,000	1700
PL(SWM5/S316L)-14-6	14	6	24	2-7/8"	3-5/8"	1-1/8 (1-1/4)"	10,000	1600
PL(SWM5/S316L)-14-8	14	8	24	2-7/8"	3-5/8"	1-1/8 (1-1/4)"	10,000	1600
PL(SWM5/S316L)-14-10	14	10	24	2-7/8"	3-5/8"	1-1/4 (1-1/2)"	10,000	1400
PL(SWM5/S316L)-14-12	14	12	24	2-7/8"	3-5/8"	1-1/4 (1-1/2)"	10,000	1400
PL(SWM5/S316L)-12-2	12	2	30	2-7/8"	3-5/8"	1-1/8 (1-1/4)"	8800	1200
PL(SWM5/S316L)-12-3	12	3	30	2-7/8"	3-5/8"	1-1/8 (1-1/4)"	8800	1200
PL(SWM5/S316L)-12-4	12	4	30	2-7/8"	3-5/8"	1-1/8 (1-1/4)"	8800	1200
PL(SWM5/S316L)-12-6	12	6	30	2-7/8"	3-5/8"	1-1/8 (1-1/4)"	8800	1200
PL(SWM5/S316L)-10-2	10	2	40	2-7/8"	3-5/8"	1-1/8 (1-1/4)"	8000	1200
PL(SWM5/S316L)-10-3	10	3	40	2-7/8"	3-5/8"	1-1/8 (1-1/4)"	8000	1200
PL(SWM5/S316L)-10-4	10	4	40	2-7/8"	3-5/8"	1-1/8 (1-1/4)"	8000	1200
PL(SWM5/S316L)-8-2	8	2	55	2-7/8"	3-5/8"	1-1/8 (1-1/4)"	8000	800
PL(SWM5/S316L)-8-3	8	3	55	3-1/8"	3-7/8"	1-1/4 (1-1/2)"	8000	800

Catalog Number	Wire Gauge	Number of Wires	Amperage Rating Per Wire	Length A	Length B	Hex Size Body (Cap)*	Pressure Ratings (PSIG) Grafoil	Teflon
SAE 7/8-14 Thread Mount (formerly MS)								
PL(MSE10/)-20-6	20	6	9	3"	3-3/4"	1-1/8 (1-1/4)"	10,000	3200
PL(MSE10/)-20-8	20	8	9	3"	3-3/4"	1-1/8 (1-1/4)"	10,000	3200
PL(MSE10/)-20-18	20	18	9	3-1/4"	4"	1-1/4 (1-1/2)"	10,000	2400
PL(MSE10/)-18-6	18	6	13	3"	3-3/4"	1-1/8 (1-1/4)"	10,000	2700
PL(MSE10/)-18-8	18	8	13	3"	3-3/4"	1-1/8 (1-1/4)"	10,000	2700
PL(MSE10/)-18-10	18	10	13	3"	3-3/4"	1-1/8 (1-1/4)"	10,000	2100
PL(MSE10/)-18-12	18	12	13	3"	3-3/4"	1-1/8 (1-1/4)"	10,000	2100
PL(MSE10/)-16-6	16	6	17	3"	3-3/4"	1-1/8 (1-1/4)"	10,000	2700
PL(MSE10/)-16-8	16	8	17	3"	3-3/4"	1-1/8 (1-1/4)"	10,000	2700
PL(MSE10/)-16-10	16	10	17	3"	3-3/4"	1-1/8 (1-1/4)"	10,000	1700
PL(MSE10/)-16-12	16	12	17	3"	3-3/4"	1-1/8 (1-1/4)"	10,000	1700
PL(MSE10/)-14-6	14	6	24	3"	3-3/4"	1-1/8 (1-1/4)"	10,000	1600
PL(MSE10/)-14-8	14	8	24	3"	3-3/4"	1-1/8 (1-1/4)"	10,000	1600
PL(MSE10/)-14-10	14	10	24	3"	3-3/4"	1-1/8 (1-1/4)"	10,000	1400
PL(MSE10/)-14-12	14	12	24	3"	3-3/4"	1-1/8 (1-1/4)"	10,000	1400
PL(MSE10/)-12-2	12	2	30	3"	3-3/4"	1-1/8 (1-1/4)"	8800	1200
PL(MSE10/)-12-3	12	3	30	3"	3-3/4"	1-1/8 (1-1/4)"	8800	1200
PL(MSE10/)-12-4	12	4	30	3"	3-3/4"	1-1/8 (1-1/4)"	8800	1200
PL(MSE10/)-12-6	12	6	30	3"	3-3/4"	1-1/8 (1-1/4)"	8800	1200
PL(MSE10/)-10-2	10	2	40	3"	3-3/4"	1-1/8 (1-1/4)"	8000	1200
PL(MSE10/)-10-3	10	3	40	3"	3-3/4"	1-1/8 (1-1/4)"	8000	1200
PL(MSE10/)-10-4	10	4	40	3"	3-3/4"	1-1/8 (1-1/4)"	8000	1200
PL(MSE10/)-8-2	8	2	55	3"	3-3/4"	1-1/8 (1-1/4)"	8000	800
PL(MSE10/)-8-3	8	3	55	3-1/4"	4"	1-1/4 (1-1/2)"	8000	800

** Hex size for the body and cap are the same unless a cap size is provided in parentheses.*

*** Weld neck models require lubrication prior to use.*

All pressure and torque ratings were determined at 68˚ F (20˚ C) using solid Kapton-insulated copper conductors as the element. Pressure ratings may degrade at higher temperatures. Pressure rating guide values are provided for glands with elements restrained by the compressed sealant. Higher pressure may be attained with additional element restraints. Tolerance of tube or probe diameter is ±0.005. Deviation from the nominal may affect pressure ratings.

For more information call: **1-800-223-2389** • e-mail: **info@conaxbuffalo.com** • visit our website: **www.conaxbuffalo.com**

PL Glands with KF (ISO) Vacuum Flange Mount

PL Series

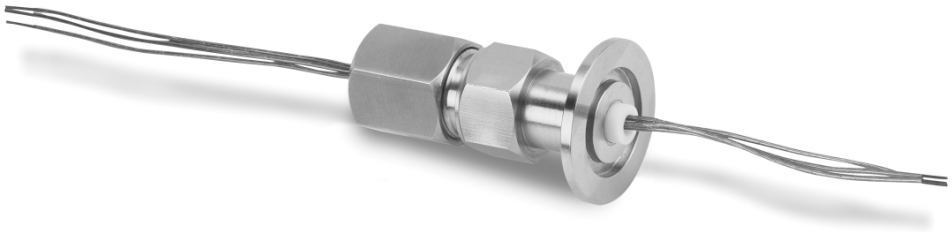

KF Vacuum Flange Mounts offer fast assembly and disassembly. They mate to Varian Klamp-Flange®, MDC Kwik-Flange® and similar vacuum flanges. This mounting style is ideal for roughing and high vacuum applications requiring frequent changeover, including sintering furnaces, vacuum furnaces, and semiconductor and powder metal fabrication processes.

Conax Buffalo KF flanges are constructed from 304SST. The PL glands use 316LSST bodies with 303SST caps and followers. Grafoil sealants are standard. Teflon sealants are also offered.

For those who would prefer a non-welded assembly, a threaded female adapter is available for mating to a male NPT PL gland.

Alternative sealant materials are available. Please consult a Conax Buffalo sales engineer for custom needs.

Available accessories include hinged aluminum clamps, replacement Viton O-rings, centering rings (with Viton O-rings), and replacement sealants for the packing gland.

For accessories, see page 152.

- Vacuum Rating at 68˚ F (20˚ C): 5 x 10^{-6} Torr
- Operating Temperature Range: -10˚ F to +300˚ F (-23˚ C to +150˚ C)
- Helium Leak Rate at 68˚ F (20˚ C): 1 x 10^{-6} scc/sec typical

Catalog Numbering System

( ) / S316L

PL Gland	Flange Style	Gland Body Material of Construction	Wire Gauge	Cap Style	Number of Wires Sealed	Sealant
PL	KF6W KF8W KF9W	S316L	20 18 16 14 12 10 8	A – has mounting thread only B – has cap end threaded	1 2 3 4 6 8 10 12 18	T – Teflon G – Grafoil *Other sealant materials also available.*

PL Gland / Flange Style / Gland Body Material of Construction / Wire Gauge / Cap Style / Number of Wires Sealed / Sealant

Example: ***PL(KF8W/S316L)-10-B4-T***

Accessories

To order a Replacement Packing Set, order RPS – (Gland) – (Wire Gauge) – (Number of Holes) – (Sealant)

Example: ***RPS-PL-12-3-T***

To order a Replacement Sealant only, order RS – (Gland) – (Diameter) – (Number of Holes) – (Sealant)

Example: ***RS-PL-12-3-T***

For centering ring and replacement O-ring, see Accessories section, page 154.

Flange Selection Guide

	Number of Holes	Conax Flange Style/ISO Equivalent KF6W/NW25	KF8W/NW40	KF9W/NW50
PL-20	2-18		X	X
PL-18	1	X	X	X
PL-18	2-12		X	X
PL-16	2-12		X	X
PL-14	1	X	X	X
PL-14	2-12		X	X
PL-12	2-6		X	X
PL-10	2-4		X	X
PL-8	2,3		X	X

Gland Torque (ft-lbs)

	# of Holes	Grafoil	Teflon
PL-20	2,3,4	90-100	60-70
PL-20	6,8	150-165	90-100
PL-20	18	250-265	125-140
PL-18	1	20-30	12-15
PL-18	2,3,4	90-100	60-70
PL-18	6,8	150-165	90-100
PL-18	10-12	250-265	125-140
PL-16	2,3,4	90-100	60-70
PL-16	6,8	150-165	90-100

	# of Holes	Grafoil	Teflon
PL-16	10,12	250-265	125-140
PL-14	1	25-30	12-15
PL-14	2	90-100	60-70
PL-14	3,4,6,8	150-165	90-100
PL-14	10,12	250-265	125-140
PL-12	2,3,4,6	150-165	90-100
PL-10	2,3,4	150-165	80-90
PL-8	2	150-165	75-85
PL-8	3	250-265	125-140

All pressure and torque ratings were determined at 68˚ F (20˚ C) using solid Kapton-insulated copper conductors as the element.

For proper assembly of these sealing glands, see the Assembly Instructions provided on page 156.

Female Pipe Adapter (Thermometer Cap)

For use with male NPT thread mount PL glands (PL gland sold separately, not assembled.)

Part Number	NPT	Accepts Gland Type	Number of Holes	D Diameter	A Length	Wrench Flats
KF6T-125	1/8	PL-18	1	1.58 (40.1)	1.04 (26.4)	0.75 (19.1)
		PL-14	1	1.58 (40.1)	1.04 (26.4)	0.75 (19.1)
KF8T-125	1/8	PL-18	1	2.17 (55.1)	1.04 (26.4)	0.75 (19.1)
		PL-14	1	2.17 (55.1)	1.04 (26.4)	0.75 (19.1)
KF8T-500	1/2	PL-20	2,3,4	2.17 (55.1)	1.65 (41.9)	1.13 (28.7)
		PL-18	2,3,4	2.17 (55.1)	1.65 (41.9)	1.13 (28.7)
		PL-16	2,3,4	2.17 (55.1)	1.65 (41.9)	1.13 (28.7)
		PL-14	2,3,4	2.17 (55.1)	1.65 (41.9)	1.13 (28.7)
KF8T-750	3/4	PL-20	6,8,18	2.17 (55.1)	1.65 (41.9)	1.25 (31.8)
		PL-18	6,8,10,12	2.17 (55.1)	1.65 (41.9)	1.25 (31.8)
		PL-16	6,8,10,12	2.17 (55.1)	1.65 (41.9)	1.25 (31.8)
		PL-14	6,8,10,12	2.17 (55.1)	1.65 (41.9)	1.25 (31.8)
		PL-12	2,3,4,6	2.17 (55.1)	1.65 (41.9)	1.25 (31.8)
		PL-10	2,3,4	2.17 (55.1)	1.65 (41.9)	1.25 (31.8)
		PL-8	2,3	2.17 (55.1)	1.65 (41.9)	1.25 (31.8)
KF9T-125	1/8	PL-18	1	2.95 (74.9)	1.04 (26.4)	0.75 (19.1)
		PL-14	1	2.95 (74.9)	1.04 (26.4)	0.75 (19.1)
KF9T-500	1/2	PL-20	2,3,4	2.95 (74.9)	1.65 (41.9)	1.13 (28.7)
		PL-18	2,3,4	2.95 (74.9)	1.65 (41.9)	1.13 (28.7)
		PL-16	2,3,4	2.95 (74.9)	1.65 (41.9)	1.13 (28.7)
		PL-14	2,3,4	2.95 (74.9)	1.65 (41.9)	1.13 (28.7)
KF9T-750	3/4	PL-20	6,8,18	2.95 (74.9)	1.65 (41.9)	1.25 (31.8)
		PL-18	6,8,10,12	2.95 (74.9)	1.65 (41.9)	1.25 (31.8)
		PL-16	6,8,10,12	2.95 (74.9)	1.65 (41.9)	1.25 (31.8)
		PL-14	6,8,10,12	2.95 (74.9)	1.65 (41.9)	1.25 (31.8)
		PL-12	2,3,4,6	2.95 (74.9)	1.65 (41.9)	1.25 (31.8)
		PL-10	2,3,4	2.95 (74.9)	1.65 (41.9)	1.25 (31.8)
		PL-8	2,3	2.95 (74.9)	1.65 (41.9)	1.25 (31.8)

Conax Buffalo recommends the use of Teflon tape as a thread sealant during assembly. If you wish to purchase the glands pre-assembled, please contact the factory.

Dimensions – Inches (mm)

Flange	Gland Type	Number of Holes	D Diameter	Overall Length A-Cap	Overall Length B-Cap	B-Cap NPT Thread Size	Hex Size Body (Cap)*
KF6W	PL-18	1	1.58 (40.1)	1.47 (37.3)	1.84 (46.7)	1/8	1/2 (9/16)"
	PL-14	1	1.58 (40.1)	1.47 (37.3)	1.84 (46.7)	1/8	1/2 (9/16)"
KF8W	PL-18	1	2.17 (55.1)	1.47 (37.3)	1.84 (46.7)	1/8	1/2 (9/16)"
	PL-14	1	2.17 (55.1)	1.47 (37.3)	1.84 (46.7)	1/8	1/2 (9/16)"
	PL-20	2,3,4	2.17 (55.1)	2.63 (66.8)	3.38 (85.9)	1/2	1"
	PL-18	2,3,4	2.17 (55.1)	2.63 (66.8)	3.38 (85.9)	1/2	1"
	PL-16	2,3,4	2.17 (55.1)	2.63 (66.8)	3.38 (85.9)	1/2	1"
	PL-14	2	2.17 (55.1)	2.63 (66.8)	3.38 (85.9)	1/2	1"
	PL-14	3,4	2.17 (55.1)	2.88 (73.2)	3.63 (92.2)	1/2	1-1/8 (1-1/4)"
	PL-20	6,8	2.17 (55.1)	2.88 (73.2)	3.63 (92.2)	3/4	1-1/8 (1-1/4)"
	PL-20	18	2.17 (55.1)	3.13 (79.5)	3.88 (98.6)	3/4	1-1/4 (1-1/2)"
	PL-18	6,8	2.17 (55.1)	2.88 (73.2)	3.63 (92.2)	3/4	1-1/8 (1-1/4)"
	PL-18	10,12	2.17 (55.1)	2.88 (73.2)	3.63 (92.2)	3/4	1-1/4 (1-1/2)"
	PL-16	6,8	2.17 (55.1)	2.88 (73.2)	3.63 (92.2)	3/4	1-1/8 (1-1/4)"
	PL-16	10,12	2.17 (55.1)	2.88 (73.2)	3.63 (92.2)	3/4	1-1/4 (1-1/2)"
	PL-14	6,8	2.17 (55.1)	2.88 (73.2)	3.63 (92.2)	3/4	1-1/8 (1-1/4)"
	PL-14	10,12	2.17 (55.1)	2.88 (73.2)	3.63 (92.2)	3/4	1-1/4 (1-1/2)"
	PL-12	2,3,4,6	2.17 (55.1)	2.88 (73.2)	3.63 (92.2)	3/4	1-1/8 (1-1/4)"
	PL-10	2,3,4	2.17 (55.1)	2.88 (73.2)	3.63 (92.2)	3/4	1-1/8 (1-1/4)"
	PL-8	2	2.17 (55.1)	2.88 (73.2)	3.63 (92.2)	3/4	1-1/8 (1-1/4)"
	PL-8	3	2.17 (55.1)	3.13 (79.5)	3.88 (98.6)	3/4	1-1/4 (1-1/2)"
KF9W	PL-18	1	2.95 (74.9)	1.47 (37.3)	1.84 (46.7)	1/8	1/2 (9/16)"
	PL-14	1	2.95 (74.9)	1.47 (37.3)	1.84 (46.7)	1/8	1/2 (9/16)"
	PL-20	2,3,4	2.17 (55.1)	2.63 (66.8)	3.38 (85.9)	1/2	1"
	PL-18	2,3,4	2.95 (74.9)	2.63 (66.8)	3.38 (85.9)	1/2	1"
	PL-16	2,3,4	2.95 (74.9)	2.63 (66.8)	3.38 (85.9)	1/2	1"
	PL-14	2	2.95 (74.9)	2.63 (66.8)	3.38 (85.9)	1/2	1"
	PL-14	3,4	2.95 (74.9)	2.88 (73.2)	3.63 (92.2)	1/2	1-1/8 (1-1/4)"
	PL-20	6,8	2.95 (74.9)	2.88 (73.2)	3.63 (92.2)	3/4	1-1/8 (1-1/4)"
	PL-20	18	2.95 (74.9)	3.13 (79.5)	3.88 (98.6)	3/4	1-1/4 (1-1/2)"
	PL-18	6,8	2.95 (74.9)	2.88 (73.2)	3.63 (92.2)	3/4	1-1/8 (1-1/4)"
	PL-18	10,12	2.95 (74.9)	2.88 (73.2)	3.63 (92.2)	3/4	1-1/4 (1-1/2)"
	PL-16	6,8	2.95 (74.9)	2.88 (73.2)	3.63 (92.2)	3/4	1-1/8 (1-1/4)"
	PL-16	10,12	2.95 (74.9)	2.88 (73.2)	3.63 (92.2)	3/4	1-1/4 (1-1/2)"
	PL-14	6,8	2.95 (74.9)	2.88 (73.2)	3.63 (92.2)	3/4	1-1/8 (1-1/4)"
	PL-14	10,12	2.95 (74.9)	2.88 (73.2)	3.63 (92.2)	3/4	1-1/4 (1-1/2)"
	PL-12	2,3,4,6	2.95 (74.9)	2.88 (73.2)	3.63 (92.2)	3/4	1-1/8 (1-1/4)"
	PL-10	2,3,4	2.95 (74.9)	2.88 (73.2)	3.63 (92.2)	3/4	1-1/8 (1-1/4)"
	PL-8	2	2.95 (74.9)	2.88 (73.2)	3.63 (92.2)	3/4	1-1/8 (1-1/4)"
	PL-8	3	2.95 (74.9)	3.13 (79.5)	3.88 (98.6)	3/4	1-1/4 (1-1/2)"

** Hex size for the body and cap are the same unless a cap size is provided in parentheses.*

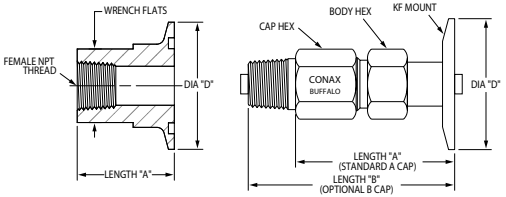

For more information call: **1-800-223-2389** • e-mail: **info@conaxbuffalo.com** • visit our website: **www.conaxbuffalo.com**

PL Glands with CF (NW) Vacuum Flange Mount

PL Series

Designed to mate with Varian Con-Flat®, MDC Del-Seal® or similar vacuum flanges, the Conax Buffalo PL Gland with CF Vacuum Flange Mount provides high performance and reliable sealing in all types of vacuum applications.

A non-rotatable 304LSST flange with non-tapped throughholes is welded to a 316LSST PL gland body. Caps and followers are 303SST. The flange is available with an oxygen-free copper gasket or a Viton gasket for unbaked applications. The PL gland is available with a Grafoil or Teflon sealant.

Alternative sealant materials are available. Please consult a Conax Buffalo sales engineer for custom needs.

- Vacuum Rating at 68˚ F (20˚ C): 5 x 10^{-6} Torr
- Temperature Range: -328˚ F to +842˚ F (-200˚ C to +450˚ C) with metal gasket and Grafoil sealant
- Temperature Range: -4˚ F to +300˚ F (-20˚ C to +150˚ C) with Viton gasket
- Helium Leak Rate at 68˚ F (20˚ C): 1 x 10^{-6} scc/sec typical

Catalog Numbering System

PL Gland	Flange Style	Gland Body Material of Construction	Wire Gauge	Cap Style	Number of Wires Sealed	Sealant
PL	CFNC1W CFNC2W CFNC3W CFNC4W CFNC5W	S316L (standard)	20 18 16 14 12 10 8	A – has mounting thread only B – has cap end threaded	1 2 3 4 6 8 10 12 18	T – Teflon G – Grafoil *Other sealant materials also available.*

PL (Flange Style / S316L) Wire Gauge Cap Style Number of Wires Sealed Sealant

PL Gland — Flange Style — Gland Body Material of Construction — Wire Gauge — Cap Style — Number of Wires Sealed — Sealant

Example: ***PL(CFNC3W/S316L)-10-B4-T***

Accessories

To order a Replacement Packing Set, order RPS – (Gland) – (Wire Gauge) – (Number of Holes) – (Sealant)

Example: ***RPS-PL-12-3-T***

To order a Replacement Sealant only, order RS – (Gland) – (Diameter) – (Number of Holes) – (Sealant)

Example: ***RS-PL-12-3-T***

For replacement gaskets, see Accessories section, page 154.

Flange Selection Guide

	Number of Holes	Conax Flange Style/Comparable To CFNC1/NW16CF	CFNC2/NW25CF	CFNC3/NW35CF	CFNC4/NW50CF
PL-18	1	X	X	X	X
PL-14	1	X	X	X	X
PL-20	2,3,4		X	X	X
PL-18	2,3,4		X	X	X
PL-16	2,3,4		X	X	X
PL-14	2		X	X	X
PL-14	3,4			X	X
PL-20	6-18			X	X
PL-18	6-12			X	X
PL-16	6-12			X	X
PL-14	6-12			X	X
PL-12	2,3,4,6			X	X
PL-10	2,3,4			X	X
PL-8	2,3			X	X

Gland Torque (ft-lbs)

	Number of Holes	Grafoil	Teflon
PL-20	2,3,4	90-100	60-70
PL-20	6,8	150-165	90-100
PL-20	18	250-265	125-140
PL-18	1	20-30	12-15
PL-18	2,3,4	90-100	60-70
PL-18	6,8	150-165	90-100
PL-18	10-12	250-265	125-140
PL-16	2,3,4	90-100	60-70
PL-16	6,8	150-165	90-100
PL-16	10,12	250-265	125-140
PL-14	1	25-30	12-15
PL-14	2	90-100	60-70
PL-14	3,4,6,8	150-165	90-100
PL-14	10,12	250-265	125-140
PL-12	2,3,4,6	150-165	90-100
PL-10	2,3,4	150-165	80-90
PL-8	2	150-165	75-85
PL-8	3	250-265	125-140

All pressure and torque ratings were determined at 68˚ F (20˚ C) using solid Kapton-insulated copper conductors as the element.

For proper assembly of these sealing glands, see the Assembly Instructions provided on page 156.

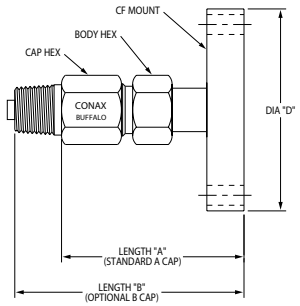

Dimensions – Inches (mm)

Flange	Gland Type	Number of Holes	D Diameter	Overall Length A-Cap	Overall Length B-Cap	B-Cap NPT Thread Size	Hex Size Body (Cap)*
CFNC1	PL-18	1	1.33 (33.8)	1.55 (39.4)	1.92 (48.8)	1/8	1/2 (9/16)"
	PL-14	1	1.33 (33.8)	1.55 (39.4)	1.92 (48.8)	1/8	1/2 (9/16)"
CFNC2	PL-18	1	2.13 (56.3)	1.68 (42.7)	2.05 (52.1)	1/8	1/2 (9/16)"
	PL-14	1	2.13 (56.3)	1.68 (42.7)	2.05 (52.1)	1/8	1/2 (9/16)"
	PL-20	2,3,4	2.13 (56.3)	2.84 (72.1)	3.59 (91.2)	1/2	1"
	PL-18	2,3,4	2.13 (56.3)	2.84 (72.1)	3.59 (91.2)	1/2	1"
	PL-16	2,3,4	2.13 (56.3)	2.84 (72.1)	3.59 (91.2)	1/2	1"
	PL-14	2	2.13 (56.3)	2.84 (72.1)	3.59 (91.2)	1/2	1"
CFNC3	PL-18	1	2.75 (69.9)	1.68 (42.7)	2.05 (52.1)	1/8	1/2 (9/16)"
	PL-14	1	2.75 (69.9)	1.68 (42.7)	2.05 (52.1)	1/8	1/2 (9/16)"
	PL-20	2,3,4	2.75 (69.9)	2.84 (72.1)	3.59 (91.2)	1/2	1"
	PL-18	2,3,4	2.75 (69.9)	2.84 (72.1)	3.59 (91.2)	1/2	1"
	PL-16	2,3,4	2.75 (69.9)	2.84 (72.1)	3.59 (91.2)	1/2	1"
	PL-14	2	2.75 (69.9)	2.84 (72.1)	3.59 (91.2)	1/2	1"
	PL-14	3,4	2.75 (69.9)	3.14 (79.8)	3.89 (98.8)	1/2	1-1/8 (1-1/4)"
	PL-20	6,8	2.75 (69.9)	3.09 (78.5)	3.84 (97.5)	3/4	1-1/8 (1-1/4)"
	PL-20	18	2.75 (69.9)	3.29 (83.6)	4.04 (103.0)	3/4	1-1/4 (1-1/2)"
	PL-18	6,8	2.75 (69.9)	3.09 (78.5)	3.84 (97.5)	3/4	1-1/8 (1-1/4)"
	PL-18	10,12	2.75 (69.9)	3.09 (78.5)	3.84 (97.5)	3/4	1-1/4 (1-1/2)"
	PL-16	6,8	2.75 (69.9)	3.09 (78.5)	3.84 (97.5)	3/4	1-1/8 (1-1/4)"
	PL-16	10,12	2.75 (69.9)	3.09 (78.5)	3.84 (97.5)	3/4	1-1/4 (1-1/2)"
	PL-14	6,8	2.75 (69.9)	3.09 (78.5)	3.84 (97.5)	3/4	1-1/8 (1-1/4)"
	PL-14	10,12	2.75 (69.9)	3.09 (78.5)	3.84 (97.5)	3/4	1-1/4 (1-1/2)"
	PL-12	2,3,4,6	2.75 (69.9)	3.09 (78.5)	3.84 (97.5)	3/4	1-1/8 (1-1/4)"
	PL-10	2,3,4	2.75 (69.9)	3.09 (78.5)	3.84 (97.5)	3/4	1-1/8 (1-1/4)"
	PL-8	2	2.75 (69.9)	3.09 (78.5)	3.84 (97.5)	3/4	1-1/8 (1-1/4)"
	PL-8	3	2.75 (69.9)	3.09 (78.5)	3.84 (97.5)	3/4	1-1/4 (1-1/2)"
CFNC4	PL-18	1	3.38 (85.7)	1.80 (45.7)	2.17 (55.1)	1/8	1/2 (9/16)"
	PL-14	1	3.38 (85.7)	1.80 (45.7)	2.17 (55.1)	1/8	1/2 (9/16)"
	PL-20	2,3,4	3.38 (85.7)	2.89 (73.4)	3.64 (92.5)	1/2	1"
	PL-18	2,3,4	3.38 (85.7)	2.89 (73.4)	3.64 (92.5)	1/2	1"
	PL-16	2,3,4	3.38 (85.7)	2.89 (73.4)	3.64 (92.5)	1/2	1"
	PL-14	2	3.38 (85.7)	2.89 (73.4)	3.64 (92.5)	1/2	1"
	PL-14	3,4	3.38 (85.7)	3.14 (79.8)	3.89 (98.8)	1/2	1-1/8 (1-1/4)"
	PL-20	6,8	3.38 (85.7)	3.14 (79.8)	3.89 (98.8)	3/4	1-1/8 (1-1/4)"
	PL-20	18	3.38 (85.7)	3.34 (84.8)	4.09 (104.0)	3/4	1-1/4 (1-1/2)"
	PL-18	6,8	3.38 (85.7)	3.14 (79.8)	3.89 (98.8)	3/4	1-1/8 (1-1/4)"
	PL-18	10,12	3.38 (85.7)	3.14 (79.8)	3.89 (98.8)	3/4	1-1/4 (1-1/2)"
	PL-16	6,8	3.38 (85.7)	3.14 (79.8)	3.89 (98.8)	3/4	1-1/8 (1-1/4)"
	PL-16	10,12	3.38 (85.7)	3.14 (79.8)	3.89 (98.8)	3/4	1-1/4 (1-1/2)"
	PL-14	6,8	3.38 (85.7)	3.14 (79.8)	3.89 (98.8)	3/4	1-1/8 (1-1/4)"
	PL-14	10,12	3.38 (85.7)	3.14 (79.8)	3.89 (98.8)	3/4	1-1/4 (1-1/2)"
	PL-12	2,3,4,6	3.38 (85.7)	3.14 (79.8)	3.89 (98.8)	3/4	1-1/8 (1-1/4)"
	PL-10	2,3,4	3.38 (85.7)	3.14 (79.8)	3.89 (98.8)	3/4	1-1/8 (1-1/4)"
	PL-8	2	3.38 (85.7)	3.14 (79.8)	3.89 (98.8)	3/4	1-1/8 (1-1/4)"
	PL-8	3	3.38 (85.7)	3.14 (79.8)	3.89 (98.8)	3/4	1-1/4 (1-1/2)"

** Hex size for the body and cap are the same unless a cap size is provided in parentheses.*

For more information call: **1-800-223-2389** • e-mail: **info@conaxbuffalo.com** • visit our website: **www.conaxbuffalo.com**

PL Glands with SFA Sanitary Flange Mount

PL Series

SFA Flange Mounts are designed to mount to Tri-Clover® 16 AMP sanitary flanges and equivalent. These mounts provide pressure/vacuum sealing against gases and liquids in pharmaceutical, food and dairy processing.

Conax Buffalo SFA flanges are constructed from 316LSST. The PL glands use 316LSST bodies with 303SST caps and followers. Standard finish on the flange face is 32 Ra. Optional 16 Ra finish is also available. Teflon sealants are standard.

For those who would prefer a non-welded assembly, a threaded female adapter is available for mating to a male NPT PL gland. Teflon tape is standard as the thread sealant.

Alternative sealant materials and custom bore sizes are available. Please consult a Conax Buffalo sales engineer for custom needs.

- Vacuum Rating at 68˚ F (20˚ C): 5 x 10⁻⁶ Torr
- Assembly Pressure Rating is determined by the lowest of the following: clamp rating, gland rating or 500 psig
- Operating Temperature Range is determined by the gasket used.
- Helium Leak Rate at 68˚ F (20˚ C): 1 x 10⁻⁶ scc/sec typical

Catalog Numbering System

( ) / S316L

PL Gland
- PL

Flange Style
- SFA10W
  - 1" & 1-1/2" tube O.D.
- SFA20W
  - 2" tube O.D.
- SFA25W
  - 2-1/2" tube O.D.
- SFA30W
  - 3" tube O.D.
- SFA40W
  - 4" tube O.D.

Gland Body Material of Construction
- S316L (standard)

Wire Gauge
- 20
- 18
- 16
- 14
- 12
- 10
- 8

Cap Style
- A – has mounting thread only
- B – has cap end threaded

Number of Wires Sealed
- 1
- 2
- 3
- 4
- 6
- 8
- 10
- 12
- 18

Sealant
- T – Teflon

Other sealant materials also available.

PL Gland / Flange Style / Gland Body Material of Construction / Wire Gauge / Cap Style / Number of Wires Sealed / Sealant

Example: ***PL(SFA10W/S316L)-14-B4-T***

Flange Selection Guide

Conax Flange Style: Tube O.D.:	Number of Wires	SFA05 1/2 & 3/4	SFA10 1 & 1-1/2	SFA20 2	SFA25 2-1/2	SFA30 3	SFA40 4
PL-20	2-18		X	X	X	X	X
PL-18	1	X	X	X	X	X	X
PL-18	2-12		X	X	X	X	X
PL-16	2-12		X	X	X	X	X
PL-14	1	X	X	X	X	X	X
PL-14	2-12		X	X	X	X	X
PL-12	2-6		X	X	X	X	X
PL-10	2-4		X	X	X	X	X
PL-8	2,3		X	X	X	X	X

Female Pipe Adapter

For use with male NPT thread mount packing glands (Packing gland sold separately, not assembled.)

Part Number	Size Tube O.D.	Accepts Gland Type	Number of Holes	Thickness	D Diameter	Female NPT
318820-006	1	PL-20	2,3,4	0.63 (16.0)	1.98 (50.3)	1/2
		PL-18	2,3,4	0.63 (16.0)	1.98 (50.3)	1/2
		PL-16	2,3,4	0.63 (16.0)	1.98 (50.3)	1/2
		PL-14	2	0.63 (16.0)	1.98 (50.3)	1/2
		PL-14	3,4	0.63 (16.0)	1.98 (50.3)	1/2
318820-001	1-1/2	PL-20	6,8,18	0.63 (16.0)	1.98 (50.3)	3/4
		PL-18	6,8,10,12	0.63 (16.0)	1.98 (50.3)	3/4
		PL-16	6,8,10,12	0.63 (16.0)	1.98 (50.3)	3/4
		PL-14	6,8,10,12	0.63 (16.0)	1.98 (50.3)	3/4
		PL-12	2,3,4,6	0.63 (16.0)	1.98 (50.3)	3/4
		PL-10	2,3,4	0.63 (16.0)	1.98 (50.3)	3/4
		PL-8	2,3	0.63 (16.0)	1.98 (50.3)	3/4
318820-002	2	PL-20	6,8,18	0.63 (16.0)	2.52 (64.0)	3/4
		PL-18	6,8,10,12	0.63 (16.0)	2.52 (64.0)	3/4
		PL-16	6,8,10,12	0.63 (16.0)	2.52 (64.0)	3/4
		PL-14	6,8,10,12	0.63 (16.0)	2.52 (64.0)	3/4
		PL-12	2,3,4,6	0.63 (16.0)	2.52 (64.0)	3/4
		PL-10	2,3,4	0.63 (16.0)	2.52 (64.0)	3/4
		PL-8	2,3	0.63 (16.0)	2.52 (64.0)	3/4
318820-003	2-1/2	PL-20	6,8,18	0.63 (16.0)	3.05 (77.5)	3/4
		PL-18	6,8,10,12	0.63 (16.0)	3.05 (77.5)	3/4
		PL-16	6,8,10,12	0.63 (16.0)	3.05 (77.5)	3/4
		PL-14	6,8,10,12	0.63 (16.0)	3.05 (77.5)	3/4
		PL-12	2,3,4,6	0.63 (16.0)	3.05 (77.5)	3/4
		PL-10	2,3,4	0.63 (16.0)	3.05 (77.5)	3/4
		PL-8	2,3	0.63 (16.0)	3.05 (77.5)	3/4
318820-004	3	PL-20	6,8,18	0.63 (16.0)	3.58 (90.0)	3/4
		PL-18	6,8,10,12	0.63 (16.0)	3.58 (90.0)	3/4
		PL-16	6,8,10,12	0.63 (16.0)	3.58 (90.0)	3/4
		PL-14	6,8,10,12	0.63 (16.0)	3.58 (90.0)	3/4
		PL-12	2,3,4,6	0.63 (16.0)	3.58 (90.0)	3/4
		PL-10	2,3,4	0.63 (16.0)	3.58 (90.0)	3/4
		PL-8	2,3	0.63 (16.0)	3.58 (90.0)	3/4
318820-004	4	PL-20	6,8,18	0.63 (16.0)	4.68 (119.0)	3/4
		PL-18	6,8,10,12	0.63 (16.0)	4.68 (119.0)	3/4
		PL-16	6,8,10,12	0.63 (16.0)	4.68 (119.0)	3/4
		PL-14	6,8,10,12	0.63 (16.0)	4.68 (119.0)	3/4
		PL-12	2,3,4,6	0.63 (16.0)	4.68 (119.0)	3/4
		PL-10	2,3,4	0.63 (16.0)	4.68 (119.0)	3/4
		PL-8	2,3	0.63 (16.0)	4.68 (119.0)	3/4

Conax Buffalo recommends the use of Teflon tape as a thread sealant during assembly. If you wish to purchase the glands pre-assembled, please contact the factory.

Gland Torque (ft-lbs)

	Number of Holes	Teflon
PL-20	2,3,4	60-70
PL-20	6,8	90-100
PL-20	18	125-140
PL-18	1	12-15
PL-18	2,3,4	60-70
PL-18	6,8	90-100
PL-18	10,12	125-140
PL-16	2,3,4	60-70
PL-16	6,8	90-100
PL-16	10,12	125-140
PL-14	1	12-15
PL-14	2	60-70
PL-14	3,4,6,8	90-100
PL-14	10,12	125-140
PL-12	2,3,4,6	90-100
PL-10	2,3,4	80-90
PL-8	2	75-85
PL-8	3	125-140

All pressure and torque ratings were determined at 68˚ F (20˚ C) using solid Kapton-insulated copper conductors as the element.

For proper assembly of these sealing glands, see the Assembly Instructions provided on page 156.

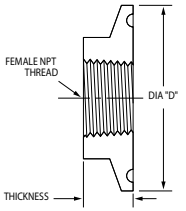

Accessories

To order a Replacement Packing Set, order RPS – (Gland) – (Diameter) – (Number of Holes) – (Sealant)

Example: ***RPS-PL-12-3-T***

To order a Replacement Sealant only, order RS – (Gland) – (Diameter) – (Number of Holes) – (Sealant)

Example: ***RS-PL-12-3-T***

For more information call: **1-800-223-2389** • e-mail: **info@conaxbuffalo.com** • visit our website: **www.conaxbuffalo.com**

PL Glands with SFA Sanitary Flange Mount

PL Series

Dimensions – Inches (mm)

Flange	Gland Type	Number of Holes	Size Tube O.D.	D Diameter	Overall Length A-Cap	Overall Length B-Cap	Hex Size Body (Cap)*
SFA05	PL-18	1	1/2 & 3/4	1.00 (25.4)	1.47 (37.3)	1.84 (46.7)	1/2 (9/16)"
	PL-14	1	1/2 & 3/4	1.00 (25.4)	1.47 (37.3)	1.84 (46.7)	1/2 (9/16)"
SFA10	PL-18	1	1 & 1-1/2	1.98 (50.3)	1.47 (37.3)	1.84 (46.7)	1/2 (9/16)"
	PL-14	1	1 & 1-1/2	1.98 (50.3)	1.47 (37.3)	1.84 (46.7)	1/2 (9/16)"
	PL-20	2,3,4	1 & 1-1/2	1.98 (50.3)	2.63 (66.8)	3.38 (85.9)	1"
	PL-18	2,3,4	1 & 1-1/2	1.98 (50.3)	2.63 (66.8)	3.38 (85.9)	1"
	PL-16	2,3,4	1 & 1-1/2	1.98 (50.3)	2.63 (66.8)	3.38 (85.9)	1"
	PL-14	2	1 & 1-1/2	1.98 (50.3)	2.63 (66.8)	3.38 (85.9)	1"
	PL-14	3,4	1 & 1-1/2	1.98 (50.3)	2.88 (73.2)	3.63 (92.2)	1-1/8 (1-1/4)"
	PL-20	6,8	1 & 1-1/2	1.98 (50.3)	2.88 (73.2)	3.63 (92.2)	1-1/8 (1-1/4)"
	PL-20	18	1 & 1-1/2	1.98 (50.3)	3.13 (79.5)	3.88 (98.6)	1-1/4 (1-1/2)"
	PL-18	6,8	1 & 1-1/2	1.98 (50.3)	2.88 (73.2)	3.63 (92.2)	1-1/8 (1-1/4)"
	PL-18	10,12	1 & 1-1/2	1.98 (50.3)	2.88 (73.2)	3.63 (92.2)	1-1/4 (1-1/2)"
	PL-16	6,8	1 & 1-1/2	1.98 (50.3)	2.88 (73.2)	3.63 (92.2)	1-1/8 (1-1/4)"
	PL-16	10,12	1 & 1-1/2	1.98 (50.3)	2.88 (73.2)	3.63 (92.2)	1-1/4 (1-1/2)"
	PL-14	6,8	1 & 1-1/2	1.98 (50.3)	2.88 (73.2)	3.63 (92.2)	1-1/8 (1-1/4)"
	PL-14	10,12	1 & 1-1/2	1.98 (50.3)	2.88 (73.2)	3.63 (92.2)	1-1/4 (1-1/2)"
	PL-12	2,3,4,6	1 & 1-1/2	1.98 (50.3)	2.88 (73.2)	3.63 (92.2)	1-1/8 (1-1/4)"
	PL-10	2,3,4	1 & 1-1/2	1.98 (50.3)	2.88 (73.2)	3.63 (92.2)	1-1/8 (1-1/4)"
	PL-8	2	1 & 1-1/2	1.98 (50.3)	2.88 (73.2)	3.63 (92.2)	1-1/8 (1-1/4)"
	PL-8	3	1 & 1-1/2	1.98 (50.3)	3.13 (79.5)	3.88 (98.6)	1-1/4 (1-1/2)"
SFA20	PL-18	1	2	2.52 (64.0)	1.47 (37.3)	1.84 (46.7)	1/2 (9/16)"
	PL-14	1	2	2.52 (64.0)	1.47 (37.3)	1.84 (46.7)	1/2 (9/16)"
	PL-20	2,3,4	2	2.52 (64.0)	2.63 (66.8)	3.38 (85.9)	1"
	PL-18	2,3,4	2	2.52 (64.0)	2.63 (66.8)	3.38 (85.9)	1"
	PL-16	2,3,4	2	2.52 (64.0)	2.63 (66.8)	3.38 (85.9)	1"
	PL-14	2	2	2.52 (64.0)	2.63 (66.8)	3.38 (85.9)	1"
	PL-14	3,4	2	2.52 (64.0)	2.88 (73.2)	3.63 (92.2)	1-1/8 (1-1/4)"
	PL-20	6,8	2	2.52 (64.0)	2.88 (73.2)	3.63 (92.2)	1-1/8 (1-1/4)"
	PL-20	18	2	2.52 (64.0)	3.13 (79.5)	3.88 (98.6)	1-1/4 (1-1/2)"
	PL-18	6,8	2	2.52 (64.0)	2.88 (73.2)	3.63 (92.2)	1-1/8 (1-1/4)"
	PL-18	10,12	2	2.52 (64.0)	2.88 (73.2)	3.63 (92.2)	1-1/4 (1-1/2)"
	PL-16	6,8	2	2.52 (64.0)	2.88 (73.2)	3.63 (92.2)	1-1/8 (1-1/4)"
	PL-16	10,12	2	2.52 (64.0)	2.88 (73.2)	3.63 (92.2)	1-1/4 (1-1/2)"
	PL-14	6,8	2	2.52 (64.0)	2.88 (73.2)	3.63 (92.2)	1-1/8 (1-1/4)"
	PL-14	10,12	2	2.52 (64.0)	2.88 (73.2)	3.63 (92.2)	1-1/4 (1-1/2)"
	PL-12	2,3,4,6	2	2.52 (64.0)	2.88 (73.2)	3.63 (92.2)	1-1/8 (1-1/4)"
	PL-10	2,3,4	2	2.52 (64.0)	2.88 (73.2)	3.63 (92.2)	1-1/8 (1-1/4)"
	PL-8	2	2	2.52 (64.0)	2.88 (73.2)	3.63 (92.2)	1-1/8 (1-1/4)"
	PL-8	3	2	2.52 (64.0)	2.88 (73.2)	3.63 (92.2)	1-1/4 (1-1/2)"
SFA25	PL-18	1	2-1/2	3.05 (77.5)	1.47 (37.3)	1.84 (46.7)	1/2 (9/16)"
	PL-14	1	2-1/2	3.05 (77.5)	1.47 (37.3)	1.84 (46.7)	1/2 (9/16)"
	PL-20	2,3,4	2-1/2	3.05 (77.5)	2.63 (66.8)	3.38 (85.9)	1"
	PL-18	2,3,4	2-1/2	3.05 (77.5)	2.63 (66.8)	3.38 (85.9)	1"
	PL-16	2,3,4	2-1/2	3.05 (77.5)	2.63 (66.8)	3.38 (85.9)	1"
	PL-14	2	2-1/2	3.05 (77.5)	2.63 (66.8)	3.38 (85.9)	1"
	PL-14	3,4	2-1/2	3.05 (77.5)	2.88 (73.2)	3.63 (92.2)	1-1/8 (1-1/4)"
	PL-20	6,8	2-1/2	3.05 (77.5)	2.88 (73.2)	3.63 (92.2)	1-1/8 (1-1/4)"
	PL-20	18	2-1/2	3.05 (77.5)	3.13 (79.5)	3.88 (98.6)	1-1/4 (1-1/2)"
	PL-18	6,8	2-1/2	3.05 (77.5)	2.88 (73.2)	3.63 (92.2)	1-1/8 (1-1/4)"
	PL-18	10,12	2-1/2	3.05 (77.5)	2.88 (73.2)	3.63 (92.2)	1-1/4 (1-1/2)"
	PL-16	6,8	2-1/2	3.05 (77.5)	2.88 (73.2)	3.63 (92.2)	1-1/8 (1-1/4)"
	PL-16	10,12	2-1/2	3.05 (77.5)	2.88 (73.2)	3.63 (92.2)	1-1/4 (1-1/2)"
	PL-14	6,8	2-1/2	3.05 (77.5)	2.88 (73.2)	3.63 (92.2)	1-1/8 (1-1/4)"

Dimensions – Inches (mm)

Flange	Gland Type	Number of Holes	Size Tube O.D.	D Diameter	Overall Length A-Cap	Overall Length B-Cap	Hex Size Body (Cap)*
	PL-14	10,12	2-1/2	3.05 (77.5)	2.88 (73.2)	3.63 (92.2)	1-1/4 (1-1/2)"
	PL-12	2,3,4,6	2-1/2	3.05 (77.5)	2.88 (73.2)	3.63 (92.2)	1-1/8 (1-1/4)"
	PL-10	2,3,4	2-1/2	3.05 (77.5)	2.88 (73.2)	3.63 (92.2)	1-1/8 (1-1/4)"
	PL-8	2	2-1/2	3.05 (77.5)	2.88 (73.2)	3.63 (92.2)	1-1/8 (1-1/4)"
	PL-8	3	2-1/2	3.05 (77.5)	2.88 (73.2)	3.63 (92.2)	1-1/4 (1-1/2)"
SFA30	PL-18	1	3	3.58 (90.9)	1.47 (37.3)	1.84 (46.7)	1/2 (9/16)"
	PL-14	1	3	3.58 (90.9)	1.47 (37.3)	1.84 (46.7)	1/2 (9/16)"
	PL-20	2,3,4	3	3.58 (90.9)	2.63 (66.8)	3.38 (85.9)	1"
	PL-18	2,3,4	3	3.58 (90.9)	2.63 (66.8)	3.38 (85.9)	1"
	PL-16	2,3,4	3	3.58 (90.9)	2.63 (66.8)	3.38 (85.9)	1"
	PL-14	2	3	3.58 (90.9)	2.63 (66.8)	3.38 (85.9)	1"
	PL-14	3,4	3	3.58 (90.9)	2.88 (73.2)	3.63 (92.2)	1-1/8 (1-1/4)"
	PL-20	6,8	3	3.58 (90.9)	2.88 (73.2)	3.63 (92.2)	1-1/8 (1-1/4)"
	PL-20	18	3	3.58 (90.9)	3.13 (79.5)	3.88 (98.6)	1-1/4 (1-1/2)"
	PL-18	6,8	3	3.58 (90.9)	2.88 (73.2)	3.63 (92.2)	1-1/8 (1-1/4)"
	PL-18	10,12	3	3.58 (90.9)	2.88 (73.2)	3.63 (92.2)	1-1/4 (1-1/2)"
	PL-16	6,8	3	3.58 (90.9)	2.88 (73.2)	3.63 (92.2)	1-1/8 (1-1/4)"
	PL-16	10,12	3	3.58 (90.9)	2.88 (73.2)	3.63 (92.2)	1-1/4 (1-1/2)"
	PL-14	6,8	3	3.58 (90.9)	2.88 (73.2)	3.63 (92.2)	1-1/8 (1-1/4)"
	PL-14	10,12	3	3.58 (90.9)	2.88 (73.2)	3.63 (92.2)	1-1/4 (1-1/2)"
	PL-12	2,3,4,6	3	3.58 (90.9)	2.88 (73.2)	3.63 (92.2)	1-1/8 (1-1/4)"
	PL-10	2,3,4	3	3.58 (90.9)	2.88 (73.2)	3.63 (92.2)	1-1/8 (1-1/4)"
	PL-8	2	3	3.58 (90.9)	2.88 (73.2)	3.63 (92.2)	1-1/8 (1-1/4)"
	PL-8	3	3	3.58 (90.9)	2.88 (73.2)	3.63 (92.2)	1-1/4 (1-1/2)"
SFA40	PL-18	1	4	4.68 (119.0)	1.47 (37.3)	1.84 (46.7)	1/2 (9/16)"
	PL-14	1	4	4.68 (119.0)	1.47 (37.3)	1.84 (46.7)	1/2 (9/16)"
	PL-20	2,3,4	4	4.68 (119.0)	2.63 (66.8)	3.38 (85.9)	1"
	PL-18	2,3,4	4	4.68 (119.0)	2.63 (66.8)	3.38 (85.9)	1"
	PL-16	2,3,4	4	4.68 (119.0)	2.63 (66.8)	3.38 (85.9)	1"
	PL-14	2	4	4.68 (119.0)	2.63 (66.8)	3.38 (85.9)	1"
	PL-14	3,4	4	4.68 (119.0)	2.88 (73.2)	3.63 (92.2)	1-1/8 (1-1/4)"
	PL-20	6,8	4	4.68 (119.0)	2.88 (73.2)	3.63 (92.2)	1-1/8 (1-1/4)"
	PL-20	18	4	4.68 (119.0)	3.13 (79.5)	3.88 (98.6)	1-1/4 (1-1/2)"
	PL-18	6,8	4	4.68 (119.0)	2.88 (73.2)	3.63 (92.2)	1-1/8 (1-1/4)"
	PL-18	10,12	4	4.68 (119.0)	2.88 (73.2)	3.63 (92.2)	1-1/4 (1-1/2)"
	PL-16	6,8	4	4.68 (119.0)	2.88 (73.2)	3.63 (92.2)	1-1/8 (1-1/4)"
	PL-16	10,12	4	4.68 (119.0)	2.88 (73.2)	3.63 (92.2)	1-1/4 (1-1/2)"
	PL-14	6,8	4	4.68 (119.0)	2.88 (73.2)	3.63 (92.2)	1-1/8 (1-1/4)"
	PL-14	10,12	4	4.68 (119.0)	2.88 (73.2)	3.63 (92.2)	1-1/4 (1-1/2)"
	PL-12	2,3,4,6	4	4.68 (119.0)	2.88 (73.2)	3.63 (92.2)	1-1/8 (1-1/4)"
	PL-10	2,3,4	4	4.68 (119.0)	2.88 (73.2)	3.63 (92.2)	1-1/8 (1-1/4)"
	PL-8	2	4	4.68 (119.0)	2.88 (73.2)	3.63 (92.2)	1-1/8 (1-1/4)"
	PL-8	3	4	4.68 (119.0)	2.88 (73.2)	3.63 (92.2)	1-1/4 (1-1/2)"

** Hex size for the body and cap are the same unless a cap size is provided in parentheses.*

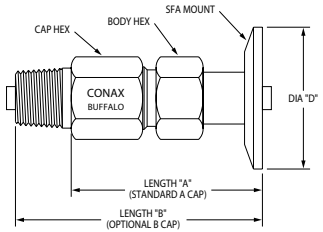

PL Glands with ASME/ANSI Raised Face (RF) Flanges

PL Series

Conax Buffalo sealing glands can be welded or threaded to ASME B16.5 flanges to create a rugged mounting for environmental sealing and/or securing the position of instrumentation sensor probes. Use of flanges eliminates the need to weld mounting adapters to the pipe or vessel. Common applications include petrochemical processing and distribution, industrial furnaces, bulk cargo carriers, gas sampling coupons and gas storage silos.

Conax Buffalo ASME/ANSI flanges are constructed from 304SST, 316SST or carbon steel. PL bodies are constructed from 316LSST standard for welded assemblies or 303SST standard for threaded glands (316LSST is available as an option on threaded assemblies). Caps and followers are constructed from 303SST standard. Optional materials are available. See page 7 for details.

Single or multiple glands may be attached to the flange. Multiple glands may consist of multiple glands of the same type or a combination of various Conax Buffalo sealing gland types.

- Specifications are shown here for Class 150 and Class 300 flanges. Class 600 – Class 2500 flanges are also available. Please consult factory.
- Pressure ratings for flange/gland combinations are determined by the lowest-rated element in the assembly (flange or gland). Flange pressure ratings may decrease when assembled with multiple sealing assemblies.
- Flat faced flanges are also available. Please consult factory.

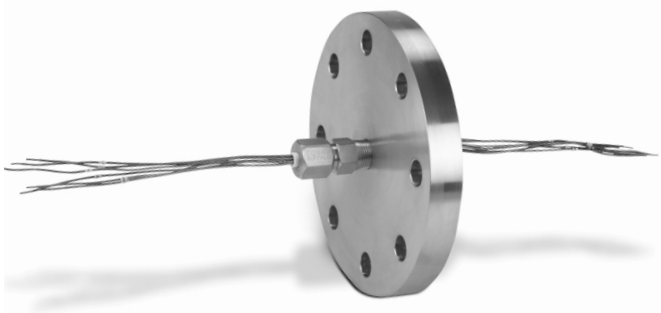

Catalog Numbering System

PL Gland	(RF	Flange Desig.	Flange Class	Flange Pipe Size	Attachment Style	Flange Material of Construction	/	Gland Material of Construction	)	Wire Gauge	Cap Style	# Wires Sealed	Sealant
PL			1 = 150 lb. 2 = 300 lb.	4 = 0.50" 5 = 0.75" 6 = 1.00" 8 = 1.50" 9 = 2.00" 11 = 3.00" 13 = 4.00" 14 = 5.00" 15 = 6.00"	T – Threaded W – Welded	S304 – Stainless Steel S316 – Stainless Steel CS – Carbon Steel		S303 – Threaded Assy. Only S316L – Standard for Welded Assemblies, Optional for Threaded Assemblies		20 18 16 14 12 10 8	A – has mounting thread only B – has cap end threaded	1 2 3 4 6 8 10 12 18	T – Teflon G – Grafoil *Other sealant materials also available.*

PL Gland · Flange Designator · Flange Class · Flange Pipe Size · Attachment Style · Flange Material of Construction · Gland Material of Construction · Wire Gauge · Cap Style · Number of Wires Sealed · Sealant

Example: ***PL(RF211WS304/S316L)-16-A4-G***

Flange Selection Guide

Part Number	Flange Size	PL-18 1 Hole	PL-14 1 Hole	PL-18 2-12 Hole	PL-16 2-12 Hole	PL-14 2-12 Hole	PL-12 2-6 Hole	PL-10 2-4 Hole	PL-8 2 & 3 Hole
RF14	1/2 - 150#	X	X						
RF15	3/4 - 150#	X	X						
RF16	1 - 150#	X	X						
RF18	1-1/2 - 150#	X	X						
RF19	2 - 150#	X	X	X	X	X	X	X	X
RF111	3 - 150#	X	X	X	X	X	X	X	X
RF113	4 - 150#	X	X	X	X	X	X	X	X
RF114	5 - 150#	X	X	X	X	X	X	X	X
RF115	6 - 150#	X	X	X	X	X	X	X	X
RF24	1/2 - 300#	X	X						
RF25	3/4 - 300#	X	X						
RF26	1 - 300#	X	X	X	X	X	X	X	X
RF28	1-1/2 - 300#	X	X	X	X	X	X	X	X
RF29	2 - 300#	X	X	X	X	X	X	X	X
RF211	3 - 300#	X	X	X	X	X	X	X	X
RF213	4 - 300#	X	X	X	X	X	X	X	X
RF214	5 - 300#	X	X	X	X	X	X	X	X
RF215	6 - 300#	X	X	X	X	X	X	X	X

Gland Torque (ft-lbs)

	Number of Holes	Grafoil	Teflon
PL-20	2,3,4	90-100	60-70
PL-20	6,8	150-165	90-100
PL-20	18	250-265	125-140
PL-18	1	20-30	12-15
PL-18	2,3,4	90-100	60-70
PL-18	6,8	150-165	90-100
PL-18	10-12	250-265	125-140
PL-16	2,3,4	90-100	60-70
PL-16	6,8	150-165	90-100
PL-16	10,12	250-265	125-140
PL-14	1	25-30	12-15
PL-14	2	90-100	60-70
PL-14	3,4,6,8	150-165	90-100
PL-14	10,12	250-265	125-140
PL-12	2,3,4,6	150-165	90-100
PL-10	2,3,4	150-165	80-90
PL-8	2	150-165	75-85
PL-8	3	250-265	125-140

All pressure and torque ratings were determined at 68° F (20° C) using solid Kapton-insulated copper conductors as the element.

For proper assembly of these sealing glands, see the Assembly Instructions provided on page 156.

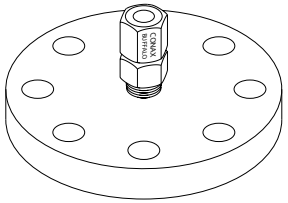

ASME/ANSI Flange with Single Gland

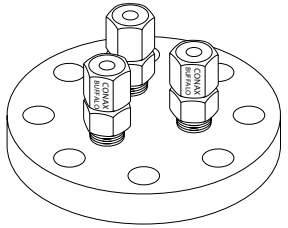

ASME/ANSI Flange with Multiple Glands (Same Size)

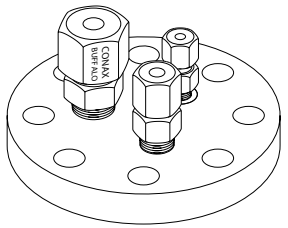

ASME/ANSI Flange with Multiple Glands (Different Sizes)

Note: Flange pressure ratings may decrease when assembled with multiple sealing assemblies.

Conax Buffalo Technologies

For more information call: ***1-800-223-2389*** *• e-mail:* ***info@conaxbuffalo.com*** *• visit our website:* ***www.conaxbuffalo.com***

PL Glands with ASME/ANSI Raised Face (RF) Flanges

PL Series

Dimensions – Inches

Part Number	Gland Type	Number of Holes	Flange Size	Flange Thickness	Flange Diameter	Overall Length A-Cap	Overall Length B-Cap	Hex Size Body (Cap)*
150# FLANGE MOUNTS								
RF14	PL-18	1	1/2	0.438	3.500	1.64	2.02	1/2 (9/16)"
	PL-14	1	1/2	0.438	3.500	1.64	2.02	1/2 (9/16)"
RF15	PL-18	1	3/4	0.500	3.875	1.71	2.08	1/2 (9/16)"
	PL-14	1	3/4	0.500	3.875	1.71	2.08	1/2 (9/16)"
RF16	PL-18	1	1	0.563	4.250	1.77	2.15	1/2 (9/16)"
	PL-14	1	1	0.563	4.250	1.77	2.15	1/2 (9/16)"
RF18	PL-18	1	1-1/2	0.688	5.000	1.90	2.27	1/2 (9/16)"
	PL-14	1	1-1/2	0.688	5.000	1.90	2.27	1/2 (9/16)"
RF19	PL-18	1	2	0.750	6.000	1.96	2.33	1/2 (9/16)"
	PL-14	1	2	0.750	6.000	1.96	2.33	1/2 (9/16)"
	PL-18	2,3,4	2	0.750	6.000	2.88	3.63	1"
	PL-16	2,3,4	2	0.750	6.000	2.88	3.63	1"
	PL-14	2	2	0.750	6.000	2.88	3.63	1"
	PL-14	3,4	2	0.750	6.000	3.13	3.88	1-1/8 (1-1/4)"
	PL-18	6,8	2	0.750	6.000	3.09	3.84	1-1/8 (1-1/4)"
	PL-18	10,12	2	0.750	6.000	3.09	3.84	1-1/4 (1-1/2)"
	PL-16	6,8	2	0.750	6.000	3.09	3.84	1-1/8 (1-1/4)"
	PL-16	10,12	2	0.750	6.000	3.09	3.84	1-1/4 (1-1/2)"
	PL-14	6,8	2	0.750	6.000	3.09	3.84	1-1/8 (1-1/4)"
	PL-14	10,12	2	0.750	6.000	3.09	3.84	1-1/4 (1-1/2)"
	PL-12	2,3,4,6	2	0.750	6.000	3.09	3.84	1-1/8 (1-1/4)"
	PL-10	2,3,4	2	0.750	6.000	3.09	3.84	1-1/8 (1-1/4)"
	PL-8	2	2	0.750	6.000	3.09	3.84	1-1/8 (1-1/4)"
	PL-8	3	2	0.750	6.000	3.09	3.84	1-1/4 (1-1/2)"
RF111	PL-18	1	3	0.938	7.500	2.15	2.52	1/2 (9/16)"
	PL-14	1	3	0.938	7.500	2.15	2.52	1/2 (9/16)"
	PL-18	2,3,4	3	0.938	7.500	3.06	3.81	1"
	PL-16	2,3,4	3	0.938	7.500	3.06	3.81	1"
	PL-14	2	3	0.938	7.500	3.06	3.81	1"
	PL-14	3,4	3	0.938	7.500	3.31	4.06	1-1/8 (1-1/4)"
	PL-18	6,8	3	0.938	7.500	3.27	4.02	1-1/8 (1-1/4)"
	PL-18	10,12	3	0.938	7.500	3.27	4.02	1-1/4 (1-1/2)"
	PL-16	6,8	3	0.938	7.500	3.27	4.02	1-1/8 (1-1/4)"
	PL-16	10,12	3	0.938	7.500	3.27	4.02	1-1/4 (1-1/2)"
	PL-14	6,8	3	0.938	7.500	3.27	4.02	1-1/8 (1-1/4)"
	PL-14	10,12	3	0.938	7.500	3.27	4.02	1-1/4 (1-1/2)"
	PL-12	2,3,4,6	3	0.938	7.500	3.27	4.02	1-1/8 (1-1/4)"
	PL-10	2,3,4	3	0.938	7.500	3.27	4.02	1-1/8 (1-1/4)"
	PL-8	2	3	0.938	7.500	3.27	4.02	1-1/8 (1-1/4)"
	PL-8	3	3	0.938	7.500	3.27	4.02	1-1/4 (1-1/2)"
RF113	PL-18	1	4	0.938	9.000	2.15	2.52	1/2 (9/16)"
	PL-14	1	4	0.938	9.000	2.15	2.52	1/2 (9/16)"
	PL-18	2,3,4	4	0.938	9.000	3.06	3.81	1"
	PL-16	2,3,4	4	0.938	9.000	3.06	3.81	1"
	PL-14	2	4	0.938	9.000	3.06	3.81	1"
	PL-14	3,4	4	0.938	9.000	3.31	4.06	1-1/8 (1-1/4)"
	PL-18	6,8	4	0.938	9.000	3.27	4.02	1-1/8 (1-1/4)"
	PL-18	10,12	4	0.938	9.000	3.27	4.02	1-1/4 (1-1/2)"
	PL-16	6,8	4	0.938	9.000	3.27	4.02	1-1/8 (1-1/4)"
	PL-16	10,12	4	0.938	9.000	3.27	4.02	1-1/4 (1-1/2)"

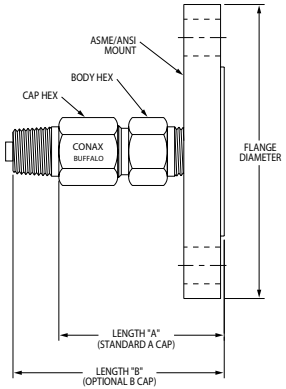

Accessories

To order a Replacement Packing Set, order RPS – (Gland) – (Diameter) – (Number of Holes) – (Sealant)

Example: ***RPS-PL-12-3-T***

To order a Replacement Sealant, order RS – (Gland) – (Diameter) – (Number of Holes) – (Sealant)

Example: ***RS-PL-12-3-T***

Dimensions – Inches

Part Number	Gland Type	Number of Holes	Flange Size	Flange Thickness	Flange Diameter	Overall Length A-Cap	Overall Length B-Cap	Hex Size Body (Cap)*
RF113	PL-14	6,8	4	0.938	9.000	3.27	4.02	1-1/8 (1-1/4)"
	PL-14	10,12	4	0.938	9.000	3.27	4.02	1-1/4 (1-1/2)"
	PL-12	2,3,4,6	4	0.938	9.000	3.27	4.02	1-1/8 (1-1/4)"
	PL-10	2,3,4	4	0.938	9.000	3.27	4.02	1-1/8 (1-1/4)"
	PL-8	2	4	0.938	9.000	3.27	4.02	1-1/8 (1-1/4)"
	PL-8	3	4	0.938	9.000	3.27	4.02	1-1/4 (1-1/2)"
RF114	PL-18	1	5	0.938	10.000	2.15	2.52	1/2 (9/16)"
	PL-14	1	5	0.938	10.000	2.15	2.52	1/2 (9/16)"
	PL-18	2,3,4	5	0.938	10.000	3.06	3.81	1"
	PL-16	2,3,4	5	0.938	10.000	3.06	3.81	1"
	PL-14	2	5	0.938	10.000	3.06	3.81	1"
	PL-14	3,4	5	0.938	10.000	3.31	4.06	1-1/8 (1-1/4)"
	PL-18	6,8	5	0.938	10.000	3.27	4.02	1-1/8 (1-1/4)"
	PL-18	10,12	5	0.938	10.000	3.27	4.02	1-1/4 (1-1/2)"
	PL-16	6,8	5	0.938	10.000	3.27	4.02	1-1/8 (1-1/4)"
	PL-16	10,12	5	0.938	10.000	3.27	4.02	1-1/4 (1-1/2)"
	PL-14	6,8	5	0.938	10.000	3.27	4.02	1-1/8 (1-1/4)"
	PL-14	10,12	5	0.938	10.000	3.27	4.02	1-1/4 (1-1/2)"
	PL-12	2,3,4,6	5	0.938	10.000	3.27	4.02	1-1/8 (1-1/4)"
	PL-10	2,3,4	5	0.938	10.000	3.27	4.02	1-1/8 (1-1/4)"
	PL-8	2	5	0.938	10.000	3.27	4.02	1-1/8 (1-1/4)"
	PL-8	3	5	0.938	10.000	3.27	4.02	1-1/4 (1-1/2)"
RF115	PL-18	1	6	1.000	11.000	2.21	2.58	1/2 (9/16)"
	PL-14	1	6	1.000	11.000	2.21	2.58	1/2 (9/16)"
	PL-18	2,3,4	6	1.000	11.000	3.13	3.88	1"
	PL-16	2,3,4	6	1.000	11.000	3.13	3.88	1"
	PL-14	2	6	1.000	11.000	3.13	3.88	1"
	PL-14	3,4	6	1.000	11.000	3.38	4.13	1-1/8 (1-1/4)"
	PL-18	6,8	6	1.000	11.000	3.34	4.09	1-1/8 (1-1/4)"
	PL-18	10,12	6	1.000	11.000	3.34	4.09	1-1/4 (1-1/2)"
	PL-16	6,8	6	1.000	11.000	3.34	4.09	1-1/8 (1-1/4)"
	PL-16	10,12	6	1.000	11.000	3.34	4.09	1-1/4 (1-1/2)"
	PL-14	6,8	6	1.000	11.000	3.34	4.09	1-1/8 (1-1/4)"
	PL-14	10,12	6	1.000	11.000	3.34	4.09	1-1/4 (1-1/2)"
	PL-12	2,3,4,6	6	1.000	11.000	3.34	4.09	1-1/8 (1-1/4)"
	PL-10	2,3,4	6	1.000	11.000	3.34	4.09	1-1/8 (1-1/4)"
	PL-8	2	6	1.000	11.000	3.34	4.09	1-1/8 (1-1/4)"
	PL-8	3	6	1.000	11.000	3.34	4.09	1-1/4 (1-1/2)"
300# FLANGE MOUNTS								
RF24	PL-18	1	1/2	0.563	3.750	1.77	2.15	1/2 (9/16)"
	PL-14	1	1/2	0.563	3.750	1.77	2.15	1/2 (9/16)"
RF25	PL-18	1	3/4	0.625	4.625	1.83	2.21	1/2 (9/16)"
	PL-14	1	3/4	0.625	4.625	1.83	2.21	1/2 (9/16)"
RF26	PL-18	1	1	0.688	4.875	1.90	2.27	1/2 (9/16)"
	PL-14	1	1	0.688	4.875	1.90	2.27	1/2 (9/16)"
	PL-18	2,3,4	1	0.688	4.875	2.81	3.56	1"
	PL-16	2,3,4	1	0.688	4.875	2.81	3.56	1"
	PL-14	2	1	0.688	4.875	2.81	3.56	1"
	PL-14	3,4	1	0.688	4.875	3.02	3.77	1-1/8 (1-1/4)"
	PL-18	6,8	1	0.688	4.875	3.02	3.77	1-1/8 (1-1/4)"
	PL-18	10,12	1	0.688	4.875	3.02	3.77	1-1/4 (1-1/2)"
	PL-16	6,8	1	0.688	4.875	3.02	3.77	1-1/8 (1-1/4)"
	PL-16	10,12	1	0.688	4.875	3.02	3.77	1-1/4 (1-1/2)"

** Hex size for the body and cap are the same unless a cap size is provided in parentheses.*

For more information call: **1-800-223-2389** • e-mail: **info@conaxbuffalo.com** • visit our website: **www.conaxbuffalo.com**

PL Glands with ASME/ANSI Raised Face (RF) Flanges

PL Series

Dimensions – Inches

Part Number	Gland Type	Number of Holes	Flange Size	Flange Thickness	Flange Diameter	Overall Length A-Cap	Overall Length B-Cap	Hex Size Body (Cap)*
300# FLANGE MOUNTS								
RF26	PL-14	6,8	1	0.688	4.875	3.02	3.77	1-1/8 (1-1/4)"
	PL-14	10,12	1	0.688	4.875	3.02	3.77	1-1/4 (1-1/2)"
	PL-12	2,3,4,6	1	0.688	4.875	3.02	3.77	1-1/8 (1-1/4)"
	PL-10	2,3,4	1	0.688	4.875	3.02	3.77	1-1/8 (1-1/4)"
	PL-8	2	1	0.688	4.875	3.02	3.77	1-1/8 (1-1/4)"
	PL-8	3	1	0.688	4.875	3.02	3.77	1-1/4 (1-1/2)"
RF28	PL-18	1	1-1/2	0.813	6.125	2.02	2.40	1/2 (9/16)"
	PL-14	1	1-1/2	0.813	6.125	2.02	2.40	1/2 (9/16)"
	PL-18	2,3,4	1-1/2	0.813	6.125	2.94	3.69	1"
	PL-16	2,3,4	1-1/2	0.813	6.125	2.94	3.69	1"
	PL-14	2	1-1/2	0.813	6.125	2.94	3.69	1"
	PL-14	3,4	1-1/2	0.813	6.125	3.19	3.94	1-1/8 (1-1/4)"
	PL-18	6,8	1-1/2	0.813	6.125	3.15	3.90	1-1/8 (1-1/4)"
	PL-18	10,12	1-1/2	0.813	6.125	3.15	3.90	1-1/4 (1-1/2)"
	PL-16	6,8	1-1/2	0.813	6.125	3.15	3.90	1-1/8 (1-1/4)"
	PL-16	10,12	1-1/2	0.813	6.125	3.15	3.90	1-1/4 (1-1/2)"
	PL-14	6,8	1-1/2	0.813	6.125	3.15	3.90	1-1/8 (1-1/4)"
	PL-14	10,12	1-1/2	0.813	6.125	3.15	3.90	1-1/4 (1-1/2)"
	PL-12	2,3,4,6	1-1/2	0.813	6.125	3.15	3.90	1-1/8 (1-1/4)"
	PL-10	2,3,4	1-1/2	0.813	6.125	3.15	3.90	1-1/8 (1-1/4)"
	PL-8	2	1-1/2	0.813	6.125	3.15	3.90	1-1/8 (1-1/4)"
	PL-8	3	1-1/2	0.813	6.125	3.15	3.90	1-1/4 (1-1/2)"
RF29	PL-18	1	2	0.875	6.500	2.08	2.46	1/2 (9/16)"
	PL-14	1	2	0.875	6.500	2.08	2.46	1/2 (9/16)"
	PL-18	2,3,4	2	0.875	6.500	3.00	3.75	1"
	PL-16	2,3,4	2	0.875	6.500	3.00	3.75	1"
	PL-14	2	2	0.875	6.500	3.00	3.75	1"
	PL-14	3,4	2	0.875	6.500	3.25	4.00	1-1/8 (1-1/4)"
	PL-18	6,8	2	0.875	6.500	3.21	3.96	1-1/8 (1-1/4)"
	PL-18	10,12	2	0.875	6.500	3.21	3.96	1-1/4 (1-1/2)"
	PL-16	6,8	2	0.875	6.500	3.21	3.96	1-1/8 (1-1/4)"
	PL-16	10,12	2	0.875	6.500	3.21	3.96	1-1/4 (1-1/2)"
	PL-14	6,8	2	0.875	6.500	3.21	3.96	1-1/8 (1-1/4)"
	PL-14	10,12	2	0.875	6.500	3.21	3.96	1-1/4 (1-1/2)"
	PL-12	2,3,4,6	2	0.875	6.500	3.21	3.96	1-1/8 (1-1/4)"
	PL-10	2,3,4	2	0.875	6.500	3.21	3.96	1-1/8 (1-1/4)"
	PL-8	2	2	0.875	6.500	3.21	3.96	1-1/8 (1-1/4)"
	PL-8	3	2	0.875	6.500	3.21	3.96	1-1/4 (1-1/2)"
RF211	PL-18	1	3	1.125	8.250	2.33	2.71	1/2 (9/16)"
	PL-14	1	3	1.125	8.250	2.33	2.71	1/2 (9/16)"
	PL-18	2,3,4	3	1.125	8.250	3.25	4.00	1"
	PL-16	2,3,4	3	1.125	8.250	3.25	4.00	1"
	PL-14	2	3	1.125	8.250	3.25	4.00	1"
	PL-14	3,4	3	1.125	8.250	3.50	4.25	1-1/8 (1-1/4)"
	PL-18	6,8	3	1.125	8.250	3.46	4.21	1-1/8 (1-1/4)"
	PL-18	10,12	3	1.125	8.250	3.46	4.21	1-1/4 (1-1/2)"
	PL-16	6,8	3	1.125	8.250	3.46	4.21	1-1/8 (1-1/4)"
	PL-16	10,12	3	1.125	8.250	3.46	4.21	1-1/4 (1-1/2)"
	PL-14	6,8	3	1.125	8.250	3.46	4.21	1-1/8 (1-1/4)"
	PL-14	10,12	3	1.125	8.250	3.46	4.21	1-1/4 (1-1/2)"
	PL-12	2,3,4,6	3	1.125	8.250	3.46	4.21	1-1/8 (1-1/4)"
	PL-10	2,3,4	3	1.125	8.250	3.46	4.21	1-1/8 (1-1/4)"
	PL-8	2	3	1.125	8.250	3.46	4.21	1-1/8 (1-1/4)"
	PL-8	3	3	1.125	8.250	3.46	4.21	1-1/4 (1-1/2)"

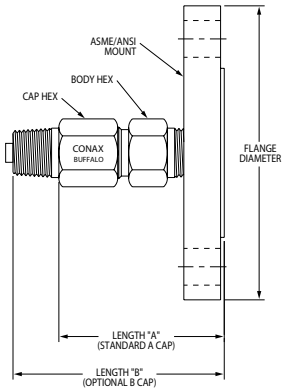

Dimensions – Inches

Part Number	Gland Type	Number of Holes	Flange Size	Flange Thickness	Flange Diameter	Overall Length A-Cap	Overall Length B-Cap	Hex Size Body (Cap)*
RF213	PL-18	1	4	1.250	10.000	2.46	2.84	1/2 (9/16)"
	PL-14	1	4	1.250	10.000	2.46	2.84	1/2 (9/16)"
	PL-18	2,3,4	4	1.250	10.000	3.38	4.13	1"
	PL-16	2,3,4	4	1.250	10.000	3.38	4.13	1"
	PL-14	2	4	1.250	10.000	3.38	4.13	1"
	PL-14	3,4	4	1.250	10.000	3.63	4.38	1-1/8 (1-1/4)"
	PL-18	6,8	4	1.250	10.000	3.59	4.34	1-1/8 (1-1/4)"
	PL-18	10,12	4	1.250	10.000	3.59	4.34	1-1/4 (1-1/2)"
	PL-16	6,8	4	1.250	10.000	3.59	4.34	1-1/8 (1-1/4)"
	PL-16	10,12	4	1.250	10.000	3.59	4.34	1-1/4 (1-1/2)"
	PL-14	6,8	4	1.250	10.000	3.59	4.34	1-1/8 (1-1/4)"
	PL-14	10,12	4	1.250	10.000	3.59	4.34	1-1/4 (1-1/2)"
	PL-12	2,3,4,6	4	1.250	10.000	3.59	4.34	1-1/8 (1-1/4)"
	PL-10	2,3,4	4	1.250	10.000	3.59	4.34	1-1/8 (1-1/4)"
	PL-8	2	4	1.250	10.000	3.59	4.34	1-1/8 (1-1/4)"
	PL-8	3	4	1.250	10.000	3.59	4.34	1-1/4 (1-1/2)"
RF214	PL-18	1	5	1.375	11.000	2.58	2.96	1/2 (9/16)"
	PL-14	1	5	1.375	11.000	2.58	2.96	1/2 (9/16)"
	PL-18	2,3,4	5	1.375	11.000	3.50	4.25	1"
	PL-16	2,3,4	5	1.375	11.000	3.50	4.25	1"
	PL-14	2	5	1.375	11.000	3.50	4.25	1"
	PL-14	3,4	5	1.375	11.000	3.75	4.50	1-1/8 (1-1/4)"
	PL-18	6,8	5	1.375	11.000	3.71	4.46	1-1/8 (1-1/4)"
	PL-18	10,12	5	1.375	11.000	3.71	4.46	1-1/4 (1-1/2)"
	PL-16	6,8	5	1.375	11.000	3.71	4.46	1-1/8 (1-1/4)"
	PL-16	10,12	5	1.375	11.000	3.71	4.46	1-1/4 (1-1/2)"
	PL-14	6,8	5	1.375	11.000	3.71	4.46	1-1/8 (1-1/4)"
	PL-14	10,12	5	1.375	11.000	3.71	4.46	1-1/4 (1-1/2)"
	PL-12	2,3,4,6	5	1.375	11.000	3.71	4.46	1-1/8 (1-1/4)"
	PL-10	2,3,4	5	1.375	11.000	3.71	4.46	1-1/8 (1-1/4)"
	PL-8	2	5	1.375	11.000	3.71	4.46	1-1/8 (1-1/4)"
	PL-8	3	5	1.375	11.000	3.71	4.46	1-1/4 (1-1/2)"
RF215	PL-18	1	6	1.438	12.500	2.65	3.02	1/2 (9/16)"
	PL-14	1	6	1.438	12.500	2.65	3.02	1/2 (9/16)"
	PL-18	2,3,4	6	1.438	12.500	3.56	4.31	1"
	PL-16	2,3,4	6	1.438	12.500	3.56	4.31	1"
	PL-14	2	6	1.438	12.500	3.56	4.31	1"
	PL-14	3,4	6	1.438	12.500	3.81	4.56	1-1/8 (1-1/4)"
	PL-18	6,8	6	1.438	12.500	3.77	4.52	1-1/8 (1-1/4)"
	PL-18	10,12	6	1.438	12.500	3.77	4.52	1-1/4 (1-1/2)"
	PL-16	6,8	6	1.438	12.500	3.77	4.52	1-1/8 (1-1/4)"
	PL-16	10,12	6	1.438	12.500	3.77	4.52	1-1/4 (1-1/2)"
	PL-14	6,8	6	1.438	12.500	3.77	4.52	1-1/8 (1-1/4)"
	PL-14	10,12	6	1.438	12.500	3.77	4.52	1-1/4 (1-1/2)"
	PL-12	2,3,4,6	6	1.438	12.500	3.77	4.52	1-1/8 (1-1/4)"
	PL-10	2,3,4	6	1.438	12.500	3.77	4.52	1-1/8 (1-1/4)"
	PL-8	2	6	1.438	12.500	3.77	4.52	1-1/8 (1-1/4)"
	PL-8	3	6	1.438	12.500	3.77	4.52	1-1/4 (1-1/2)"

** Hex size for the body and cap are the same unless a cap size is provided in parentheses.*

For more information call: **1-800-223-2389** • e-mail: **info@conaxbuffalo.com** • visit our website: **www.conaxbuffalo.com**

Cable Packing Gland Assembly for *Single Cable Exit Only*

CMSS 301120xx*

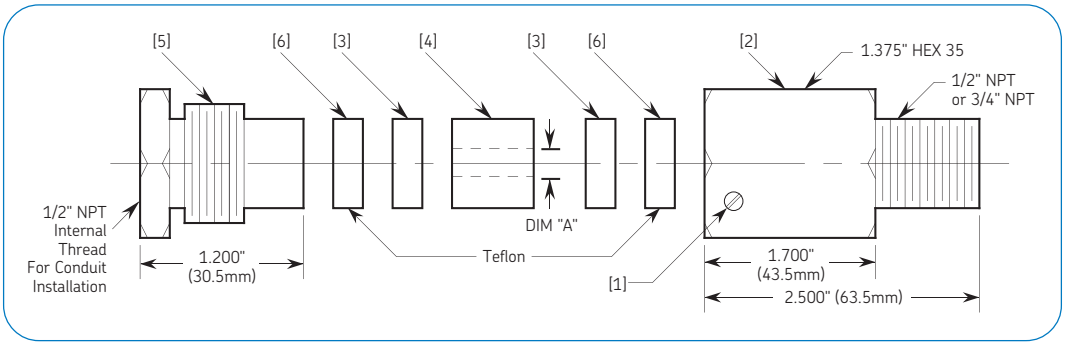

The Cable Packing Gland (CPG) Assembly offers a splash-proof cable exit from the machine case. It is an ideal accessory for use with both the standard and radiation resistant versions of Eddy Probe and Extension Cables when the need arises. It is an effective and easily installed low pressure (60 PSI/4 bars) seal. The internal oil resistant neoprene packing as well as washers are split to allow cable installation without connector removal.

Functional Descriptions

[1] Set Screw – 10-32 UNF-2B hole.

[2] Body – Threads into 1/2" NPT or 3/4" NPT tapped hole in machine casing depending on model number.

[3] Split Washers – Depending on model number, various combinations of split washers are provided. Those washers with the 0.125" slots are used with standard Eddy Probe System Cable and those washers with 0.257" slots for the radiation resistant Eddy Probe System Cable.

[4] Gland – Neoprene rubber disk with slit for cable. Has 0.12" diameter hole (DIM "A"). Must drill to 0.156" for radiation resistant cable.

[5] Compression Nut – Threads into body **[2]**. Screws down to compress gland **[4]** between teflon washers **[6]** and split washers **[3]**. Held by set screw **[1].**

[6] Teflon Washers – Used to preclude metal-to-metal binding between split washers, body and compression nut while tightening.

Cable Packing Gland Assembly for Single Cable Exit Only

CMSS
301120xx*

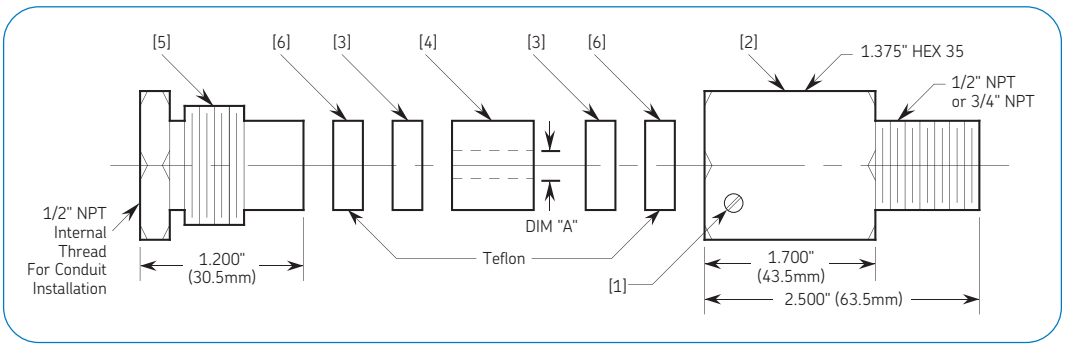

Installation Procedure

a. If installation requires radiation resistant cable, first assemble the Cable Packing Gland Assembly without the cable. Torque items **[2]** and **[5]** to approximately pressure-tight fit, and tighten set screw **[1]**. Then drill through neoprene gland to enlarge to 0.156" as appropriate.

b. Drill hole in machine casing for 1/2" NPT or 3/4" NPT as appropriate.

c. Thread cable through hole in casing and through CPG Assembly body **[2]**.

d. Coat male threaded portion of CPG Assembly body with pipe joint compound, and screw into 1/2" NPT or 3/4" NPT tapped hole in the machine casing.

e. Install first washer(s) **[6]** then **[3]**, gland **[4]** second washer(s) **[3]** then **[6]** in CPG Assembly body. (It may be necessary to wet the neoprene gland **[4]** or spray it with silicone compound for lubrication in order to insert it fully into the body.)

f. Thread cable through compression nut **[5]** and screw nut onto body **[2]**. Torque the compression nut down until gland is pressure tight, approximately 30 ft. lbs. (40 newton/meters). Then tighten set screw **[1]** firmly enough to hold compression nut in position.

g. Half inch conduit for the cable can be attached to the compression nut by the 1/2" NPT internal female threads provided.

Single-Cable Exit Only!

**** xx – Number will vary depending on configuration ordered.***

SKF Reliability Systems
5271 Viewridge Court • San Diego, California 92123 USA
Telephone: +1 858-496-3400 • FAX: +1 858-496-3531

Web Site: www.skf.com/reliability

Although care has been taken to assure the accuracy of the data compiled in this publication, SKF does not assume any liability for errors or omissions. SKF reserves the right to alter any part of this publication without prior notice.

- *SKF is a registered trademark of SKF.*
- *All other trademarks are the property of their respective owners.*

CM2090 (Revised 10-04) • Copyright © 2004 by SKF Reliability Systems. ALL RIGHTS RESERVED.

D.11.8 NPT pipe

NPT Pipe Thread Sizes

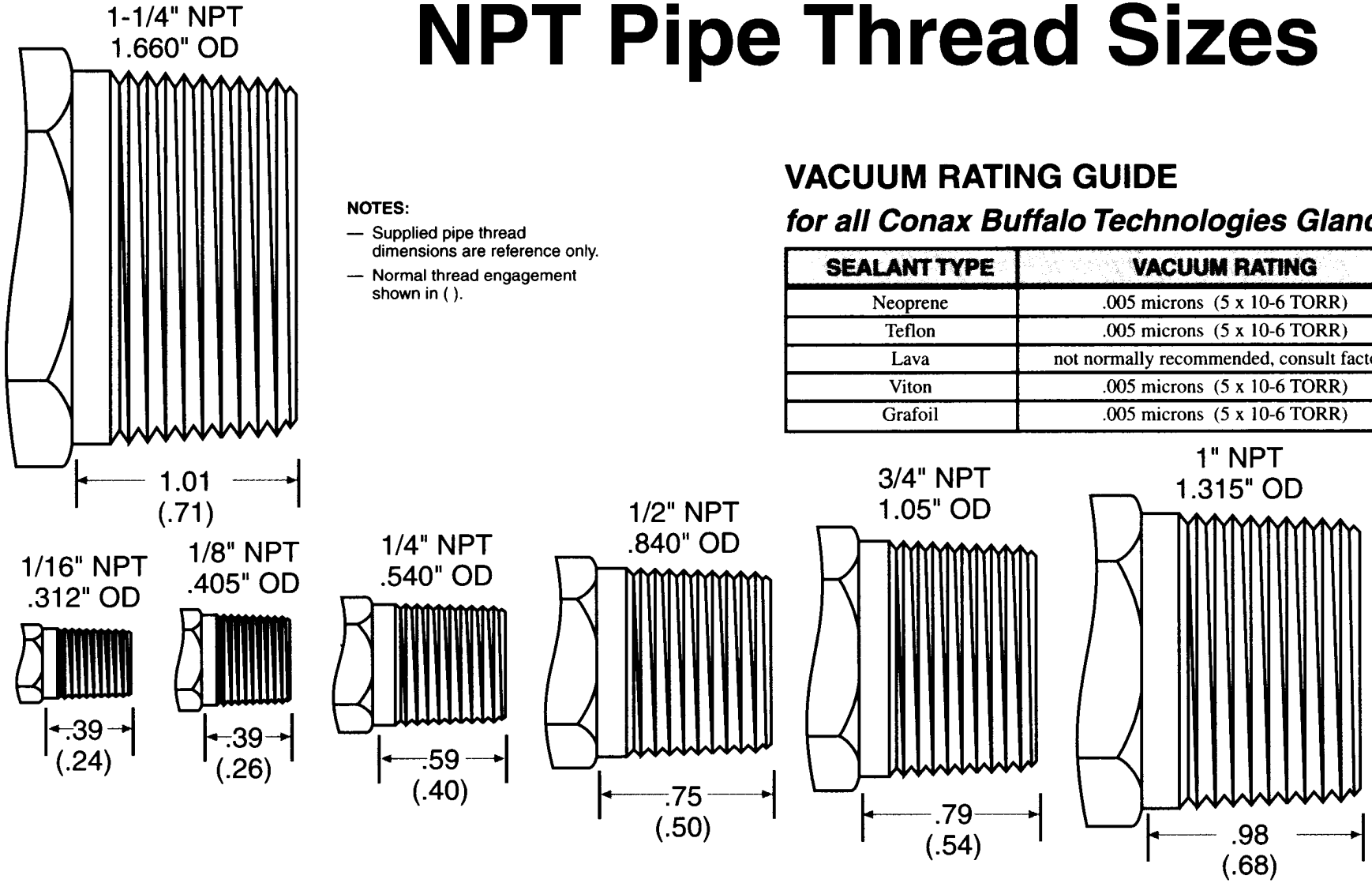

NOTES:

— Supplied pipe thread dimensions are reference only.

— Normal thread engagement shown in ( ).

VACUUM RATING GUIDE

for all Conax Buffalo Technologies Glands:

SEALANT TYPE	VACUUM RATING
Neoprene	.005 microns (5 x 10-6 TORR)
Teflon	.005 microns (5 x 10-6 TORR)
Lava	not normally recommended, consult factory
Viton	.005 microns (5 x 10-6 TORR)
Grafoil	.005 microns (5 x 10-6 TORR)

Conax™ Buffalo Technologies

2300 Walden Avenue • Buffalo, New York 14225
FAX: 716-684-7433 • Phone: 716-684-4500 • 1-800-223-2389
www.conaxbuffalo.com
e-mail: conaxbuf@conaxbuffalo.com

European Office
PO Box 91 • BOGNOR REGIS PO22 7JB, England
FAX: +44 (0)1243 587799 • Phone: +44 (0)1243 587878
e-mail: cbteurope@compuserve.com

D.11.9 PT100 resistive table

PT100 Resistance Table

°C	0	1	2	3	4	5	6	7	8	9	°C
-200.00	18.52										-200.00
-190.00	22.83	22.40	21.97	21.54	21.11	20.68	20.25	19.82	19.38	18.95	-190.00
-180.00	27.10	26.67	26.24	25.82	25.39	24.97	24.54	24.11	23.68	23.25	-180.00
-170.00	31.34	30.91	30.49	30.07	29.64	29.22	28.80	28.37	27.95	27.52	-170.00
-160.00	35.54	35.12	34.70	34.28	33.86	33.44	33.02	32.60	32.18	31.76	-160.00
-150.00	39.72	39.31	38.89	38.47	38.05	37.64	37.22	36.80	36.38	35.96	-150.00
-140.00	43.88	43.46	43.05	42.63	42.22	41.80	41.39	40.97	40.56	40.14	-140.00
-130.00	48.00	47.59	47.18	46.77	46.36	45.94	45.53	45.12	44.70	44.29	-130.00
-120.00	52.11	51.70	51.29	50.88	50.47	50.06	49.65	49.24	48.83	48.42	-120.00
-110.00	56.19	55.79	55.38	54.97	54.56	54.15	53.75	53.34	52.93	52.52	-110.00
-100.00	60.26	59.85	59.44	59.04	58.63	58.23	57.82	57.41	57.01	56.60	-100.00
-90.00	64.30	63.90	63.49	63.09	62.68	62.28	61.88	61.47	61.07	60.66	-90.00
-80.00	68.33	67.92	67.52	67.12	66.72	66.31	65.91	65.51	65.11	64.70	-80.00
-70.00	72.33	71.93	71.53	71.13	70.73	70.33	69.93	69.53	69.13	68.73	-70.00
-60.00	76.33	75.93	75.53	75.13	74.73	74.33	73.93	73.53	73.13	72.73	-60.00
-50.00	80.31	79.91	79.51	79.11	78.72	78.32	77.92	77.52	77.12	76.73	-50.00
-40.00	84.27	83.87	83.48	83.08	82.69	82.29	81.89	81.50	81.10	80.70	-40.00
-30.00	88.22	87.83	87.43	87.04	86.64	86.25	85.85	85.46	85.06	84.67	-30.00
-20.00	92.16	91.77	91.37	90.98	90.59	90.19	89.80	89.40	89.01	88.62	-20.00
-10.00	96.09	95.69	95.30	94.91	94.52	94.12	93.73	93.34	92.95	92.55	-10.00
0.00	100.00	99.61	99.22	98.83	98.44	98.04	97.65	97.26	96.87	96.48	0.00
0.00	100.00	100.39	100.78	101.17	101.56	101.95	102.34	102.73	103.12	103.51	0.00
10.00	103.90	104.29	104.68	105.07	105.46	105.85	106.24	106.63	107.02	107.40	10.00
20.00	107.79	108.18	108.57	108.96	109.35	109.73	110.12	110.51	110.90	111.29	20.00
30.00	111.67	112.06	112.45	112.83	113.22	113.61	114.00	114.38	114.77	115.15	30.00
40.00	115.54	115.93	116.31	116.70	117.08	117.47	117.86	118.24	118.63	119.01	40.00
50.00	119.40	119.78	120.17	120.55	120.94	121.32	121.71	122.09	122.47	122.86	50.00
60.00	123.24	123.63	124.01	124.39	124.78	125.16	125.54	125.93	126.31	126.69	60.00
70.00	127.08	127.46	127.84	128.22	128.61	128.99	129.37	129.75	130.13	130.52	70.00
80.00	130.90	131.28	131.66	132.04	132.42	132.80	133.18	133.57	133.95	134.33	80.00
90.00	134.71	135.09	135.47	135.85	136.23	136.61	136.99	137.37	137.75	138.13	90.00
100.00	138.51	138.88	139.26	139.64	140.02	140.40	140.78	141.16	141.54	141.91	100.00
110.00	142.29	142.67	143.05	143.43	143.80	144.18	144.56	144.94	145.31	145.69	110.00
120.00	146.07	146.44	146.82	147.20	147.57	147.95	148.33	148.70	149.08	149.46	120.00
130.00	149.83	150.21	150.58	150.96	151.33	151.71	152.08	152.46	152.83	153.21	130.00
140.00	153.58	153.96	154.33	154.71	155.08	155.46	155.83	156.20	156.58	156.95	140.00
150.00	157.33	157.70	158.07	158.45	158.82	159.19	159.56	159.94	160.31	160.68	150.00
160.00	161.05	161.43	161.80	162.17	162.54	162.91	163.29	163.66	164.03	164.40	160.00
170.00	164.77	165.14	165.51	165.89	166.26	166.63	167.00	167.37	167.74	168.11	170.00
180.00	168.48	168.85	169.22	169.59	169.96	170.33	170.70	171.07	171.43	171.80	180.00
190.00	172.17	172.54	172.91	173.28	173.65	174.02	174.38	174.75	175.12	175.49	190.00
200.00	175.86	176.22	176.59	176.96	177.33	177.69	178.06	178.43	178.79	179.16	200.00
210.00	179.53	179.89	180.26	180.63	180.99	181.36	181.72	182.09	182.46	182.82	210.00
220.00	183.19	183.55	183.92	184.28	184.65	185.01	185.38	185.74	186.11	186.47	220.00
230.00	186.84	187.20	187.56	187.93	188.29	188.66	189.02	189.38	189.75	190.11	230.00
240.00	190.47	190.84	191.20	191.56	191.92	192.29	192.65	193.01	193.37	193.74	240.00
250.00	194.10	194.46	194.82	195.18	195.55	195.91	196.27	196.63	196.99	197.35	250.00
260.00	197.71	198.07	198.43	198.79	199.15	199.51	199.87	200.23	200.59	200.95	260.00
270.00	201.31	201.67	202.03	202.39	202.75	203.11	203.47	203.83	204.19	204.55	270.00
280.00	204.90	205.26	205.62	205.98	206.34	206.70	207.05	207.41	207.77	208.13	280.00
290.00	208.48	208.84	209.20	209.56	209.91	210.27	210.63	210.98	211.34	211.70	290.00
300.00	212.05	212.41	212.76	213.12	213.48	213.83	214.19	214.54	214.90	215.25	300.00
310.00	215.61	215.96	216.32	216.67	217.03	217.38	217.74	218.09	218.44	218.80	310.00
320.00	219.15	219.51	219.86	220.21	220.57	220.92	221.27	221.63	221.98	222.33	320.00

ºC	0	1	2	3	4	5	6	7	8	9	ºC
330.00	222.68	223.04	223.39	223.74	224.09	224.45	224.80	225.15	225.50	225.85	**330.00**
340.00	226.21	226.56	226.91	227.26	227.61	227.96	228.31	228.66	229.02	229.37	**340.00**
350.00	229.72	230.07	230.42	230.77	231.12	231.47	231.82	232.17	232.52	232.87	**350.00**
360.00	233.21	233.56	233.91	234.26	234.61	234.96	235.31	235.66	236.00	236.35	**360.00**
370.00	236.70	237.05	237.40	237.74	238.09	238.44	238.79	239.13	239.48	239.83	**370.00**
380.00	240.18	240.52	240.87	241.22	241.56	241.91	242.26	242.60	242.95	243.29	**380.00**
390.00	243.64	243.99	244.33	244.68	245.02	245.37	245.71	246.06	246.40	246.75	**390.00**
400.00	247.09	247.44	247.78	248.13	248.47	248.81	249.16	249.50	249.85	250.19	**400.00**
410.00	250.53	250.88	251.22	251.56	251.91	252.25	252.59	252.93	253.28	253.62	**410.00**
420.00	253.96	254.30	254.65	254.99	255.33	255.67	256.01	256.35	256.70	257.04	**420.00**
430.00	257.38	257.72	258.06	258.40	258.74	259.08	259.42	259.76	260.10	260.44	**430.00**
440.00	260.78	261.12	261.46	261.80	262.14	262.48	262.82	263.16	263.50	263.84	**440.00**
450.00	264.18	264.52	264.86	265.20	265.53	265.87	266.21	266.55	266.89	267.22	**450.00**
460.00	267.56	267.90	268.24	268.57	268.91	269.25	269.59	269.92	270.26	270.60	**460.00**
470.00	270.93	271.27	271.61	271.94	272.28	272.61	272.95	273.29	273.62	273.96	**470.00**
480.00	274.29	274.63	274.96	275.30	275.63	275.97	276.30	276.64	276.97	277.31	**480.00**
490.00	277.64	277.98	278.31	278.64	278.98	279.31	279.64	279.98	280.31	280.64	**490.00**
500.00	280.98	281.31	281.64	281.98	282.31	282.64	282.97	283.31	283.64	283.97	**500.00**
510.00	284.30	284.63	284.97	285.30	285.63	285.96	286.29	286.62	286.95	287.29	**510.00**
520.00	287.62	287.95	288.28	288.61	288.94	289.27	289.60	289.93	290.26	290.59	**520.00**
530.00	290.92	291.25	291.58	291.91	292.24	292.56	292.89	293.22	293.55	293.88	**530.00**
540.00	294.21	294.54	294.86	295.19	295.52	295.85	296.18	296.50	296.83	297.16	**540.00**
550.00	297.49	297.81	298.14	298.47	298.80	299.12	299.45	299.78	300.10	300.43	**550.00**
560.00	300.75	301.08	301.41	301.73	302.06	302.38	302.71	303.03	303.36	303.69	**560.00**
570.00	304.01	304.34	304.66	304.98	305.31	305.63	305.96	306.28	306.61	306.93	**570.00**
580.00	307.25	307.58	307.90	308.23	308.55	308.87	309.20	309.52	309.84	310.16	**580.00**
590.00	310.49	310.81	311.13	311.45	311.78	312.10	312.42	312.74	313.06	313.39	**590.00**
600.00	313.71	314.03	314.35	314.67	314.99	315.31	315.64	315.96	316.28	316.60	**600.00**
610.00	316.92	317.24	317.56	317.88	318.20	318.52	318.84	319.16	319.48	319.80	**610.00**
620.00	320.12	320.43	320.75	321.07	321.39	321.71	322.03	322.35	322.67	322.98	**620.00**
630.00	323.30	323.62	323.94	324.26	324.57	324.89	325.21	325.53	325.84	326.16	**630.00**
640.00	326.48	326.79	327.11	327.43	327.74	328.06	328.38	328.69	329.01	329.32	**640.00**
650.00	329.64	329.96	330.27	330.59	330.90	331.22	331.53	331.85	332.16	332.48	**650.00**
660.00	332.79	333.11	333.42	333.74	334.05	334.36	334.68	334.99	335.31	335.62	**660.00**
670.00	335.93	336.25	336.56	336.87	337.18	337.50	337.81	338.12	338.44	338.75	**670.00**
680.00	339.06	339.37	339.69	340.00	340.31	340.62	340.93	341.24	341.56	341.87	**680.00**
690.00	342.18	342.49	342.80	343.11	343.42	343.73	344.04	344.35	344.66	344.97	**690.00**
700.00	345.28	345.59	345.90	346.21	346.52	346.83	347.14	347.45	347.76	348.07	**700.00**
710.00	348.38	348.69	348.99	349.30	349.61	349.92	350.23	350.54	350.84	351.15	**710.00**
720.00	351.46	351.77	352.08	352.38	352.69	353.00	353.30	353.61	353.92	354.22	**720.00**
730.00	354.53	354.84	355.14	355.45	355.76	356.06	356.37	356.67	356.98	357.28	**730.00**
740.00	357.59	357.90	358.20	358.51	358.81	359.12	359.42	359.72	360.03	360.33	**740.00**
750.00	360.64	360.94	361.25	361.55	361.85	362.16	362.46	362.76	363.07	363.37	**750.00**
760.00	363.67	363.98	364.28	364.58	364.89	365.19	365.49	365.79	366.10	366.40	**760.00**
770.00	366.70	367.00	367.30	367.60	367.91	368.21	368.51	368.81	369.11	369.41	**770.00**
780.00	369.71	370.01	370.31	370.61	370.91	371.21	371.51	371.81	372.11	372.41	**780.00**
790.00	372.71	373.01	373.31	373.61	373.91	374.21	374.51	374.81	375.11	375.41	**790.00**
800.00	375.70	376.00	376.30	376.60	376.90	377.19	377.49	377.79	378.09	378.39	**800.00**
810.00	378.68	378.98	379.28	379.57	379.87	380.17	380.46	380.76	381.06	381.35	**810.00**
820.00	381.65	381.95	382.24	382.54	382.83	383.13	383.42	383.72	384.01	384.31	**820.00**
830.00	384.60	384.90	385.19	385.49	385.78	386.08	386.37	386.67	386.96	387.25	**830.00**
840.00	387.55	387.84	388.14	388.43	388.72	389.02	389.31	389.60	389.90	390.19	**840.00**
850.00	390.48										**850.00**

Thermocouple Instruments Limited
Pontygwindy Road, Caerphilly, CF83 2WJ, UK
Tel: (+44) 029 20807400 Fax: (+44) 029 20807410
Internet: http://www.thermocouple.co.uk
E-mail: enquiries@thermocouple.co.uk

All Rights Reserved. © Copyright 1999 Thermocouple Instruments Ltd.
Iss. 01

D.11.10 17-4PH stainless

P R O D U C T D A T A S H E E T

17-4 PH STAINLESS STEEL

UNS S17400

AK Steel

AK Steel 17-4 PH® is a martensitic precipitation-hardening stainless steel that provides an outstanding combination of high strength, good corrosion resistance, good mechanical properties at temperatures up to 600°F (316°C), good toughness in both base metal and welds, and short-time, low-temperature heat treatments that minimize warpage and scaling. This versatile material is widely used in the aerospace, chemical, petrochemical, food processing, paper and general metalworking industries.

COMPOSITION

	%
Carbon	0.07 max.
Manganese	1.00 max.
Phosphorus	0.040 max.
Sulfur	0.030 max.
Silicon	1.00 max.
Chromium	15.00 - 17.50
Nickel	3.00 - 5.00
Copper	3.00 - 5.00
Columbium plus Tantalum	0.15 - 0.45

AVAILABLE FORMS

AK Steel produces 17-4 PH Stainless Steel sheet and strip in thicknesses from 0.015" to 0.125" (0.38 to 3.18 mm) in Condition A.

STANDARD HEAT TREATMENTS

As supplied from the mill in Condition A, AK Steel 17-4 PH Stainless Steel can be heat treated at a variety of temperatures to develop a wide range of properties. Eight standard heat treatments have been developed.

	Condition	Heat To ± 15°F (8.4°C)	Time at Temperature, hour	Type of Cooling
Condition A Solution Treated 1900°F ± 25°F (1038°C ± 14°C) Air cool below 90°F (32°C)	H 900	900°F (482°C)	1	Air
	H 925	925°F (496°C)	4	Air
	H 1025	1025°F (551°C)	4	Air
	H 1075	1075°F (580°C)	4	Air
	H 1100	1100°F (593°C)	4	Air
	H 1150	1150°F (621°C)	4	Air
	H 1150+1150	1150°F (621°C)	4 *followed by*	Air
		1150°F (621°C)	4	Air
	H 1150-M	1400°F (760°C)	2 *followed by*	Air
		1150°F (621°C)	4	Air

FORMABILITY

Because this alloy in Condition A is hard, forming normally should be limited to mild operations. However, formability can be greatly improved by heat treating before cold working or by use of hot-forming methods.

CORROSION RESISTANCE

AK Steel 17-4 PH Stainless Steel withstands corrosive attack better than any of the standard hardenable stainless steels and is comparable to Type 304 in most media.

AK STEEL 17-4 PH STAINLESS STEEL DATA SHEET

MECHANICAL PROPERTIES

Typical Mechanical Properties*

Property	A	H 900	H 925	Condition H 1025	H 1075	H 1150	H 1150-M
UTS, ksi (MPa)	160 (1103)	210 (1448)	200 (1379)	185 (1276)	175 (1207)	160 (1103)	150 (1034)
0.2% YS, ksi (MPa)	145 (1000)	200 (1379)	195 (1345)	170 (1172)	165 (1148)	150 (1034)	130 (896)
Elongation, % in 2" (50.8 mm)	5.0	7.0	8.0	8.0	8.0	11.0	12.0
Hardness, Rockwell	C35	C45	C43	C38	C37	C35	C33

*Cold-flattened sheets and strip.

PHYSICAL PROPERTIES

	Condition A (Magnetic)	Condition H 900 (Magnetic)	Condition H 1075 (Magnetic)	Condition H 1150 (Magnetic)
Density, lbs/in^3 (g/cm^3)	0.28 (7.78)	0.282 (7.80)	0.283 (7.81)	0.284 (7.82)
Electrical Resistivity, microhm-cm	98	77	–	–
Specific Heat BTU/lb/°F (32 - 212°F) kJ/kg•K (0 - 100°C)	0.11 (0.46)	0.11 (0.46)		
Thermal Conductivity BTU/hr/ft^2/in/°F (W/m•K)				
300°F (149°C)		124 (17.9)		
500°F (260°C)		135 (19.5)		
900°F (482°C)		157 (22.6)		
Mean Coefficient of Thermal Expansion in/in/°F (µm/m•K)				
–100 - 70°F (-73 - 21°C)	–	5.8 x 10^{-6} (10.4)	–	6.1 x 10^{-6} (11.0)
70 - 200°F (21 - 93°C)	6.0 x 10^{-6} (10.8)	6.0 x 10^{-6} (10.8)	6.3 x 10^{-6} (11.3)	6.6 x 10^{-6} (11.9)
70 - 600°F (21 - 316°C)	6.2 x 10^{-6} (11.2)	6.3 x 10^{-6} (11.3)	6.6 x 10^{-6} (11.9)	7.1 x 10^{-6} (12.8)
70 - 800°F (21 - 427°C)	6.3 x 10^{-6} (11.3)	6.5 x 10^{-6} (11.7)	6.8 x 10^{-6} (12.2)	7.2 x 10^{-6} (13.0)

WELDABILITY

The precipitation hardening class of stainless steels is generally considered to be weldable by the common fusion and resistance techniques. Special consideration is required to achieve optimum mechanical properties by considering the best heat-treated conditions in which to weld and which heat treatments should follow welding. This particular alloy is the most common member of the class and is generally considered to have the best weldability. When a weld filler is needed, AWS E/ER 630 is most often specified. AK Steel 17-4 PH Stainless Steel is well known in reference literature and more information can be obtained in this way.

SPECIFICATIONS

Specifications are listed without revision indications. Contact ASTM Headquarters for latest ASTM revision. For AMS revision, contact AMS Division of SAE.

AMS 5604 Sheet, Strip and Plate

ASTM A 693 Plate, Sheet and Strip (Listed as Grade 630-UNS S17400)

METRIC CONVERSION

Data in this publication are presented in U.S. customary units. Approximate metric equivalents may be obtained by performing the following calculations:

Length (inches to millimeters) – Multiply by 25.4

Strength (ksi to megapascals or meganewtons per square meter) – Multiply by 6.8948

Temperature (Fahrenheit to Celsius) – (°Fahrenheit - 32) – Multiply by 0.5556

Density (pounds per cubic inch to kilograms per cubic meter) – Multiply by 27,670

The information and data in this product data sheet are accurate to the best of our knowledge and belief, but are intended for general information only. Applications suggested for the materials are described only to help readers make their own evaluations and decisions, and are neither guarantees nor to be construed as express or implied warranties of suitability for these or other applications.

Data referring to mechanical properties and chemical analyses are the result of tests performed on specimens obtained from specific locations with prescribed sampling procedures; any warranty thereof is limited to the values obtained at such locations and by such procedures. There is no warranty with respect to values of the materials at other locations.

AK Steel and the AK Steel logo, 17-4 PH, 17-7 PH and PH 15-7 Mo are registered trademarks of AK Steel Corporation.

SPECIALTY AND STAINLESS STEEL FIELD SALES OFFICES

AK Steel Corporation
703 Curtis Street
Middletown, OH 45043-0001
Customer Service 800-331-5050

Butler Works
P.O. Box 1609
Butler, PA 16003-1609
Customer Service 800-381-5663

Coshocton Works
17400 State Route 16
Coshocton, OH 43812
Customer Service 800-422-4422

AK Steel Sales Offices
Atlanta, GA-Southeast Region 770-514-0023
Baltimore, MD 410-612-1338
Charlotte, NC 704-662-0786
Chicago, IL-West Central Region 630-368-0001
Cincinnati, OH- Mideast Region 513-683-5300
Detroit, MI-North Central Region 248-641-7595
Grand Rapids, MI 616-949-5278
Nashville, TN-Southwest Region 615-771-3134
New England 401-658-3468
Pittsburgh, PA 412-635-9835
Tulsa, OK 918-298-2272
International Sales-Houston, TX ... 281-872-8741
Specialty Stainless and Electrical Commercial-Butler, PA 800-381-5663

© 2000 AK Steel Corporation

Specification Sheet: 17-4PH (UNS S17400)

A 17Cr-4Ni-3Cu Precipitation Hardening Martensitic Stainless Steel

Alloy 17-4PH is a precipitation hardening martensitic stainless steel with Cu and Nb/Cb additions. The grade combines high strength, hardness (up to 572°F / 300°C), and corrosion resistance.

Mechanical properties can be optimized with heat treatment. Very high yield strength up to 1100-1300 MPa (160-190 ksi) can be achieved.

The grade should not be used at temperatures above 572°F (300°C) or at very low temperatures. It has adequate resistance to atmospheric corrosion or in diluted acids or salts where its corrosion resistance is equivalent to grade 304 or 430.

Applications

- Offshore (foils, helicopter deck platforms, etc.)
- Food industry
- Pulp and paper industry
- Aerospace (turbine blades, etc.)
- Mechanical components
- Nuclear waste casks

Standards

ASTM .....A693 grade 630 (AMS 5604B) UNS S17400

EURONORM ...1.4542 X5CrNiCuNb 16-4

AFNOR.....Z5 CNU 17-4PH

DIN 1.4542

Corrosion Resistance

Alloy 17-4PH withstands corrosive attacks better than any of the standard hardenable stainless steels and is comparable to type 304 in most media.

If there are potential risks of stress corrosion cracking, the higher aging temperatures then must be selected over 1022°F (550°C), preferably 1094°F (590°C).

1022°F-550°C is the optimum tempering temperature in chloride media.

1094°F-590°C is the optimum tempering temperature in H2S media.

The alloy is subject to crevice or pitting attack if exposed to stagnant seawater for any length of time.

It is corrosion resistant in some chemical, petroleum, paper, dairy, and food processing industries (equivalent to 304L grade).

Chemical Analysis

Typical values (Weight %)

C	Cr	Ni	Cu	Nb/Cb	Mn
0.04	16.5	4.5	3.3	0.3	0.7
PREN (%cr+3.3%Mo+16%N)≥ 17					

Mechanical Properties

Room temperature properties (longitudinal direction)

Guaranteed values (ASTM A693 hot rolled plates); thickness from 3/16” up to 3”.

Heat treatment	YS 0.2% N/mm		UTS N/mm		YS 0.2% ksi		UTS ksi		El%	
	Min.	Typ.	Min.	Typ.	Min.	Typ.	Min.	Typ.	Min.	Typ.
A	1070	1207	1170	1310	155	175	170	190	8	14
B	790	931	965	1034	115	135	140	150	10	17

A: hardening 925°F (496°C) - 4 hours - air cooling
B: hardening 1100°F (593°C) - 4 hours - air cooling
2 examples of heat treatments that may be applied.
For specific requests, please contact us.

Elevated temperature properties

Minimum guaranteed values following EN 10088 hot rolled plates.
The EN guaranteed values are valid for a thickness from 3/16" up to 3".

Temperature °F / Temperature °C		212 100	302 150	392 200	482 250	572 300
YS 0.2%	N/mm_	730	710	690	670	650
	ksi	106	103	100	97	95

Heat treatment : hardening 1094°F (590°C) - 4 hours - air cooling
1 example of heat treatments that may be applied.
For specific requests, please consult us.

Minimum guaranteed room temperature impact values

Minimum guaranteed values following ASTM A693 hot rolled plates.
The ASTM guaranteed values are valid for a thickness from 3/16" up to 3".

Heat treatment	KV transverse	
	J	ft.lbf
Hardening 1100° F (593° C) - 4 hours - air cooling	20	15

Minimum guaranteed room temperature hardness values

Minimum guaranteed values following ASTM A693 hot rolled plates.
The ASTM guaranteed values are valid for a thickness from 3/16" up to 3".

Heat treatment	Hardness	
	Rockwell	Brinell
Hardening 925° F (496° C) - 4 hours - air cooling	C38	375
Hardening 1100° F (593° C) - 4 hours - air cooling	C29	293

For specific requests, please consult us.

SANDMEYER STEEL COMPANY
ONE SANDMEYER LANE • PHILADELPHIA, PA 19116-3598
800-523-3663 • FAX 215-677-1430 • www.SandmeyerSteel.com

Physical Properties

Density: 7800 kg/m3 (.28 lbs/in3)
The following physical properties have been obtained after hardening 896°F (480°C) – 1 hour - air cooling

Interval Temperature °C	Thermal expansion $\alpha x10^{-6}°C^{-1}$	°F	°C	Thermal conductivity $(w.m^{-1}.K^{-1})$	Young modulus (GPa)
0-100	10.8	68	20	14	197
0-200	11	212	100	16	193
0-300	11.3	392	200	18.5	186
0-400	11.6	572	300	20	180
0-500	12	752	400	22	175
		932	500	23	170

Room temperature properties:
Resistivity : 80 µ*.cm
Specific heat : 460 $J.kg^{-1}.K^{-1}$
Tension modulus : 77 GPa
The alloy is magnetic.

Heat Treatment

Martensitic transformation
Indicative values
Ms : 266°F (130°C)
Mf : 86°F (30°C)

Solution annealing
1925°F+ /-50°F (1050°C +/-25°C) – 30 min up to 1 hour
Air cooling / oil quenching below 76°F (25°C)

Aging / Tempering
The highest mechanical properties are obtained with the following heat treatment: 896°F (480°C) – 1 hour – air cooling.
Higher ductilities are obtained when using higher aging temperatures up to 1148°F (620°C).

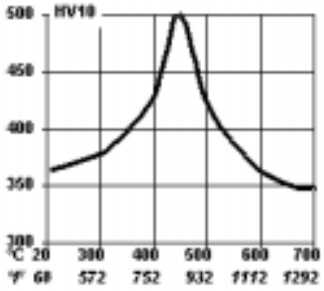

Hardness/Temperature tempered for 4 hours after austenitizing at 1904°F (1040°C) for 30 min quenched 100°C/sec (212°F/sec)

Processing

Hot forming
Hot forming should be carried out in a temperature range of 1742°-2192°F (950°-1200°C). A full heat treatment including solution annealing, cooling lower than 76°F (25°C) and aging at the required temperature must be made after hot forming (function of the requested mechanical properties).

Cold forming
Cold forming can be performed only to a limited extent and only on plates in the fully softened condition. Stress corrosion resistance is improved by re-aging at the precipitation hardening temperature after cold working.
The following processes may be performed: rolling, bending, hydroforming, etc. (fully softened conditions).

Cutting
Thermal cutting (plasma, thermal sawing, etc.). Due to the HAZ, the grade requires a suited cutting process. After cutting, grinding is necessary to eliminate the oxide formed layer.
Mechanical cutting (shearing, stamping, cold sawing, etc.).

Welding

Alloy 17-4PH can be welded by the following welding processes: SMAW, GTAW, PAW, and GMAW. SAW should not be used without preliminary testing (to check freedom of cracks and toughness of the weld metal).
Due to a ferrite delta primary type of solidification, the hot cracking risk of the weld metal or the HAZ is reduced.
Generally, no preheating must be done, and interpass temperature must be limited to 248°F (120°C). The better toughness is obtained in the weld after a complete heat treatment (solution annealing + precipitation hardening).
Due to the martensitic microstructure, a low oxygen content in the weld metal is preferable to increase ductility and toughness. To avoid cold cracking, the introduction of hydrogen in the weld must be limited.
Alloy 17-4PH can be welded with homogeneous filler metals such as E 630 (AWS A5.4) electrodes and ER 630 (AWS A5.9) wires.
Austenitic filler material can be used when the mechanical properties of 17-4PH steel are not required in the weld and, in this case, no post-weld heat treatment must be applied.

Machining

Alloy 17-4PH can be machined in both solution treated and precipitation hardened conditions. Machining condition may vary according to the hardness of the material. High speed steel tools or, preferably, carbide tools with standard lubrication are normally used. If very stringent tolerances are required, it is necessary to take into account the dimensional changes during heat treatment.

SANDMEYER
STEEL COMPANY

D.11.11 Valves

SOLENOID VALVE
2/2 - NC (Normally closed)
Pilot operated
G 3/8 ÷ G1

L180

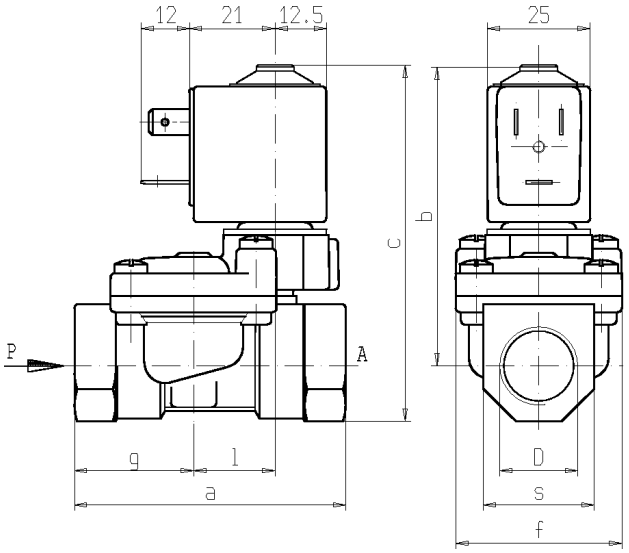

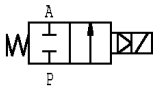

D	a	b	c	e	f	g	m	n	l	s
G 3/8	60	71	82	25	40	25,5	21	12,5	20	22
G 1/2	66	73,5	87	25	40	29	21	12,5	20	27
G 3/4	79	79,5	96	25	50	35,5	21	12,5	24,5	33
G 1	105	93	114	25	71	46	21	12,5	28	42

► GENERAL FEATURES

Diaphragm valve, pilot operated, having full orifice.
Suitable to shut off liquid and gaseous fluids (verify the compatibility of fluid with materials in contact).

► TECHNICAL FEATURES

Maximum allowable pressure (PS)	20 bar
Opening time	from ~300ms to ~1500ms
Closing time	from ~1000ms to ~2000m
Fluid temperature	-10°C +90°C (NBR) 0°C +130°C (FPM)
Max viscosity	5°E (~37 cStokes or mm^2/s)

► MATERIALS IN CONTACT WITH FLUID

Body	Brass
Sealing	NBR or FPM
Internal components	Brass and stainless steel
Seat	Brass
Guide assembly	Stainless steel
Shading ring	Copper

► COIL

Continuous duty		ED 100%
Encapsulation material		PET (polyethylene terephtalate) fiberglass reinforced.
Coil insulation class		F (155 °C) on request class H (180°C) - UL
Ambient temperature		-10 C° +60 °C
Electric connenctions		DIN 46340 - 3 poles connector
Protection degree		IP 65 (EN 60529) with plug connector
Voltages	*DC*	12-24V (+10% -5%)
	AC	24V/50-60Hz - 110V/50-60Hz (120V/60Hz) - 230V/50-60Hz (+10% -15%)
		(Other voltages and frequencies on request).

Port size ISO 228	Orifice size (mm)	Differential pressure (bar)					Kv (m^3/h)	Series and type			Power absorption			Sealings	Notes	Weight (kg)
		Δp min	Δp max					Valve	Valve with manual override	Coil	AC (VA)		DC (W)			
			Gases		Liquids						Inrush	Holding				
			AC	DC	AC	DC										
3/8	11,5	0,35	12 (10)	12 (10)	12 (10)	12 (10)	1,7	L180(*)17	L180(*)18	Z610A	16	10	6	(*) = B (NBR) (*) = V (FPM) (*) = Q (NBR)	1 – 2	0,370
1/2	13,5		16 (12)	16 (12)	16 (12)	16 (12)	3,8	L180(*)31	L180(*)32							0,440
3/4	18		12 (10)	12 (10)	12 (10)	12 (10)	5	L180(*)17	L180(*)18							0,575
1	24						11									1,140

► NOTES

- Sealings: B(NBR)=Nitrile-butylene elastomer V(FPM)=Fluoro-carbon elastomer Q(NBR)= WRAS approved nitrile-butylene elastomer.
- Operation with gazeous media , at high pressure without any outlet restriction, can reduce the diaphragm life.

1 - The bracketed values of Δp max are related to valves with V(FPM) seals.
2 - L180Q17 - L180Q18 - L180Q31 - L180Q32 WRAS homologated solenoid valves.

0402/0502

SIRAI ELETTROMECCANICA S.r.l. - BUSSERO (MI) – Italy - Tel. (+39) 02950371 - Fax (+39) 0295037555 – E-mail: info@sirai.com - www.sirai.com

► SPARE PARTS

L180 B-V-Q 17-31

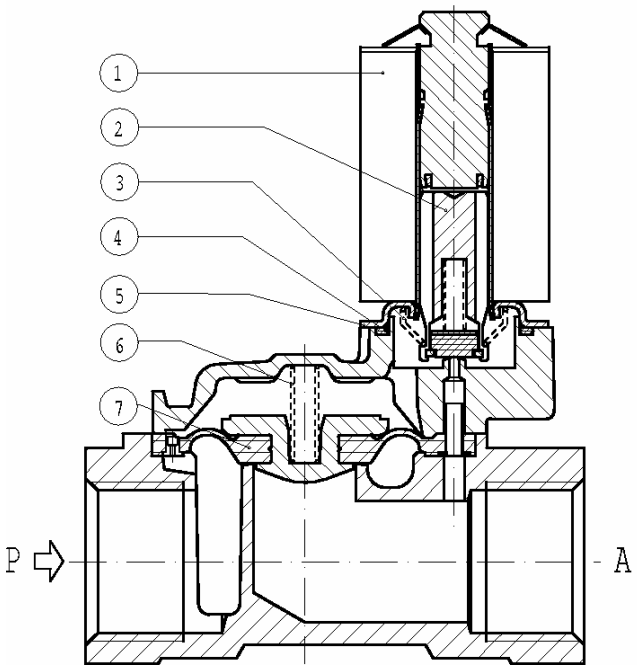

L180 B-V-Q 18-32

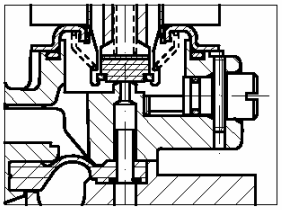

Kit description		Kit P.N.	Consisting of:
Core kit	L180B.. L180V.. L180Q..	G2937301 G2937303 G2937304	Core pos. 2 Core return spring pos. 3 OR guide assembly pos. 4
Core return spring kit		G2927101	N. 10 core return springs pos.3
Spring on diapragm kit	G 3/8 G 1/2 G3/4 G1	G2424101 G2831901 G1844501 G2380201	N. 10 springs on diaphragm pos. 6
OR guide assembly kit	L180B.. L180V.. L180Q..	GU2421000017 GU2424000017 GU2436000017	N. 10 OR guide assembly pos. 4
Diaphragm assembly	G 3/8 B17-B18 G 1/2 B31-B32 G3/4 B17-B18 G1 B17-B18 G 3/8 V17-V18 G 1/2 V31-V32 G3/4 V17-V18 G1 V17-V18 G 3/8 Q17-Q18 G 1/2 Q31-Q32 G3/4 Q17-Q18 G1 Q17-Q18	2782501R 2844302R 2299701R 2380101R 2782502R 2844303R 2299702R 2380102R 2782507R 2844301R 2299707R 2380104R	Diaphragm assembly pos. 7
Guide assembly		2593201R	Guide assembly pos. 5
Coil		Z610A	Coil pos. 1

► MOUNTING

- Solenoid valve can be mounted in any position; vertical with coil upwards preferred.

THE VALIDITY OF REPORTED DATA IS REFERRED TO THE DATE OF ISSUE. POSSIBLE UPDATING ARE AVAILABLE ON REQUEST.

D.11.12 Auxiliary bearings

GGB
BEARING TECHNOLOGY

DS™

Characteristics

- Marginally lubricated and dry bearing material developed for oscillating conditions
- DS does not cause fretting corrosion damage to the shaft under low amplitude oscillating movements
- Performance is similar to DX, but with lower friction

Applications

Automotive

- Steering gear
- power steering
- pedal bushes
- seat slides
- king-pin bushes
- tailgate pivots
- brake caliper bushes, etc.

Industrial

- Mechanical handling and lifting equipment
- machine slides
- hydraulic cylinders
- hydraulic motors
- ski-lifts
- pneumatic equipment
- medical equipmen
- textile machinery
- agricultural equipment
- scientific equipment, etc.

DS™

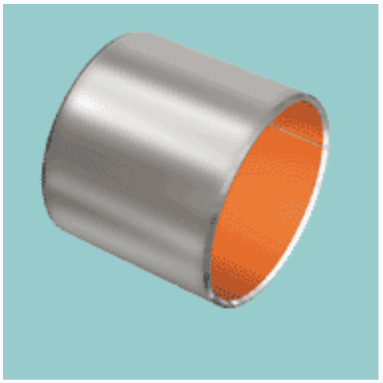

Composition & Structure

Steel + porous bronze sinter + acetal + filler

Operating Conditions

dry	good
oiled	very good
greased	very good
water	fair
process fluid	fair

Availability

Ex Stock

- N/A

To order

- Cylindrical bushes
- thrust washers
- strip and special parts (all forms also available with lubrication indents)

Bearing Properties

Bearing Properties	Unit	Value
Dry		
Maximum sliding speed U	m/s	1.5
Maximum PU factor	N/mm² * m/s = W/mm²	1.4
Coefficient of friction f	–	0.15-0.30
Grease lubrication		
Maximum sliding speed U	m/s	2.5
Maximum PU factor	N/mm² * m/s = W/mm²	2.8
Coefficient of friction f	–	0.05-0.10
General		
Maximum temperature T_{max}	°C	+130
Minimum temperature T_{min}	°C	-60
Maximum load P static	N/mm²	110
Maximum load P dynamic	N/mm²	45
Shaft surface finish Ra	µm	0.4
Shaft hardness	HB	>200
Shaft hardness for longer service life	HB	>350

Microsection

POM + additives

Sinter bronze

Steel

DS™ is a trademark of GGB.
©2006 GGB. All rights reserved

D.12 Adhesive technologies

The selection of a adhesive is a important part of the detail design of the rotor now that the performance requirements on the adhesive is known the need to investigate the different types of adhesive technologies available arises. The adhesive technologies that will be investigated further are listed below. [28]

- Acrylics, Two-Step
- Acrylics, Two-Part
- Anaerobics
- Cyanoacrylates
- Epoxies
- Hot Melts
- Light Cure
- Polyurethanes
- Silicones

The typical applications, advantages, disadvantages and a general description are described for each of the technologies listed above:

D.12.1 Acrylics, Two-Step

D.12.1.1 Typical Applications:

- Magnets to rotors or housings
- Stators to housings
- Mounting brackets to housings
- Commutator to shaft

D.12.1.2 Advantages:

- Fast fixture speed
- Room temperature cure
- No mixing required
- High peel and impact strength
- Good environmental resistance
- Bonds to lightly contaminated surfaces
- Cure can be accelerated with heat

D.12.1.3 Disadvantages:

- Limited cure through depth (0.040″)
- Activator may contain solvents
- Activator requires controlled dispensing process
- Adhesive may have strong odour

D.12.1.4 General Description

Two-step acrylic adhesives consist of a resin and an activator. The resin component is a solvent-free, high viscosity liquid. The activator is a low viscosity liquid catalyst.[28]

When the resin and activator contact each other, the resin begins to cure very rapidly fixturing in 15 seconds to several minutes depending on the specific adhesive used and joint gap. The resin can also be cured with light or heat. Light curing can be used to fully cure resin that light can reach. While the cure time depends on many factors, 15 to 30 seconds is typical. A typical heat cure cycle is 10 to 20 minutes at 300F (149C). Heat curing normally offers higher bond strengths, improved thermal resistance, better chemical resistance and achieves complete cure faster than using an activator. Heat cure is sometimes also used to eliminate any residual odour of the acrylic adhesive from the cured assembly and minimize outgassing.[28]

D.12.2 Acrylics, Two-Part

D.12.2.1 Typical Applications:

- Magnet bonding
- Brackets to housings
- Support frame assembly
- Repairing broken cooling fins
- Bonding or reinforcing brush holders
- Fans to shafts or rotors
- Name plate assembly

D.12.2.2 Advantages:

- High cure through depth
- Room temperature cure
- High peel and impact strength
- Good environmental resistance
- Bonds to moderately contaminated surfaces
- Cure can be accelerated with heat

D.12.2.3 Disadvantages:

- Slow fixture times (5 to 30 min)
- Waste associated with static mix process
- May have strong odour

D.12.2.4 General Description

Two-part acrylic adhesives consist of a resin and an activator both of which are normally high viscosity liquids typically in the range of 5,000 to 100,000 cP.While the activator is chemically similar to that of a two-step acrylic, it is delivered as a high viscosity liquid that is normally similar in viscosity to the resin. The two components are mixed just prior to dispensing at

mix ratios ranging from 1:1 and 10:1 by volume. By mixing the activator and resin, two-part acrylics have much larger cure through depths than two-step acrylics that only have the activator applied to the surface.[28]

To maintain the ratio of the resin and activator, equipment is required. For small to moderate volume applications, the adhesive is packaged in a dual cartridge that sets the ratio. For high volume applications, metre mix dispense equipment is used. The resin and activator are mixed by passing them through a static mix tip this allows the material to be dispensed as a homogenous one-part material. Since the mixed adhesive is curing in the mix tip, there will be trade-off between the open time and the fixture time. Faster curing products will require that mix tips be changed after shorter idle times.[28]

D.12.3 Anaerobics

D.12.3.1 Typical Applications:

Gasketing:

- Gear box covers
- End plates

Retaining:

- Bearings to shafts or housings
- Rotors to shafts
- Speed controls to shafts
- Commutators to shafts
- Keys in slots
- Unitising lamination stacks

Threadlocking:

- Through bolts
- Assembly screws
- Thread Sealing

Grease Fittings:

- Plugs for junction boxes

D.12.3.2 Advantages:

- One-part, solvent-free
- Room temperature cure
- Controlled strengths
- Superior chemical and thermal resistance
- Long shelf life / room temperature storage

D.12.3.3 Disadvantages:

- Limited cure through depth (0.020")
- Low peel and impact strength
- Generally not compatible with plastics

D.12.3.4 General Description

Anaerobics are one-part, solvent-free liquids that typically range in viscosity from 10 cP to thixotropic pastes. Anaerobics cure in the absence of air and the presence of metal. A typical fixture time on steel generally ranges from 5 minutes to 1 hour. Using a primer or heating the assembly can accelerate the cure speed. When using a primer, such as Loctite 7090TM, 7649TM or 7471TM, fixture times can be less than 10 seconds.[28]

The presence of metal acts as a catalyst to initiate the polymeric reaction. The more "active" the metal, the faster the adhesive will cure. Active metals are metals that rust or oxidise easily such as steel, aluminium, brass, and copper. Inactive metals are those that do not easily rust including stainless steel, zinc dichromate, or nickel. Since anaerobics do not cure unless confined between two metal surfaces, excess adhesive outside the joint will not cure and can be easily wiped off.[28]

Anaerobics are generally not compatible with plastics or elastomers. The absence of metal prevents them from curing and uncured anaerobic can stress crack some plastics. Anaerobics have been successfully used to join an active metal to a plastic that is not prone to stress cracking, such as when a nylon bearing is retained onto a steel shaft. While all anaerobics

cure similarly, their viscosity, bond strength and cured properties vary widely depending on their intended use:

Retaining compounds are the strongest and are intended for bonding close-fitting cylindrical metal assemblies. Generally, they are the fastest curing anaerobic formulations.[28]

Threadlockers have strengths that vary widely to make them suitable for a wide range of threaded fastener sizes.[28]

Thread sealants are designed to create a chemically resistant seal on threaded fittings and also to maintain low strength to facilitate maintenance.[28]

Gasketing materials are thixotropic gels designed to replace or augment gaskets for sealing flanges.[28]

D.12.4 Cyanoacrylates

D.12.4.1 Typical Applications:

- Insulation to stators, rotors, and wires
- Magnets to plastic rotors
- Tacking lead wires
- Bonding brush holders

D.12.4.2 Advantages:

- One-part, solvent-free
- Rapid room temperature cure
- Excellent adhesion to most substrates
- Wide range of viscosities available
- Primers available for polyolefins and difficult-to-bond plastics
- Light cure versions available

D.12.4.3 Disadvantages:

- Poor solvent resistance
- Low temperature resistance
- Bonds skin rapidly
- May stress crack some plastics
- Poor peel strength
- Limited gap cure
- Poor durability on glass

D.12.4.4 General Description

Cyanoacrylates are one-part, room-temperature-curing adhesives that are available in viscosities ranging from water-thin liquids to thixotropic gels. When pressed into a thin film between two surfaces, the moisture present on the bonding surfaces causes the cyanoacrylate to cure rapidly to form rigid thermoplastics with excellent adhesion to most substrates. Typical fixture times are 5 to 30 seconds. In addition to standard cyanoacrylates, there are many specialty formulations with enhanced performance properties:

Rubber toughened grades offer high peel strength and impact resistance.[28]

Thermally resistant cyanoacrylates are available which offer excellent bond strength retention after exposure to temperatures as high as 250F for thousands of hours.[28]

Surface insensitive cyanoacrylates offer rapid fixture times and cure speeds on acidic surfaces, such as wood or dichromated metals, which could slow the cure of a standard cyanoacrylate.[28]

Low odour/low bloom grades minimize the potential for a white haze to occur around the bond line.[28]

Light curing cyanoacrylates utilize proprietary photoinitiators to cure cyanoacrylates in seconds when exposed to light of the appropriate wavelength.[28]

Accelerators, such as Loctite 712TM, 7109TM, 7113TM, 7452TM and 7453TM, can be used to speed the cure of cyanoacrylate adhesives and are primarily used to reduce fixture times and to cure excess adhesive.[28]

Primers, such as Loctite 770TM and 793TM, dramatically increase the strength achieved on difficult-to-bond plastics such as polypropylene, polyethylene and Delrin (Acetal).[28]

D.12.5 Epoxies

D.12.5.1 Typical Applications

- Magnet bonding
- Reinforcing wires
- Potting wire connectors
- Tacking lead wires
- Bonding or reinforcing brush holders
- Bonding fans to shafts or rotors
- Potting printed circuit boards
- Bonding stators to housings or frames

D.12.5.2 Advantages

- Wide variety of formulations available
- High adhesion to many substrates
- Good toughness
- Cure can be accelerated with heat
- Excellent depth of cure
- Superior environmental resistance

D.12.5.3 Disadvantages

- Two-part systems require mixing
- One-part systems require heat cure
- Long cure and fixture times

D.12.5.4 General Description

Epoxy adhesives are supplied as one and two-part systems with viscosities that range from a few thousand centipoise to thixotropic pastes. Upon cure epoxies typically form tough, rigid, thermoset polymers with high adhesion to a wide variety of substrates and superior environmental resistance. A major advantage of epoxies is there are a wide variety of commercially available resins, hardeners and fillers that allow the performance characteristics of epoxies to be tailored to the needs of almost any application.[28]

When using a one-part, heat cure system, the resin and a latent hardener are supplied already mixed and typically need to be stored refrigerated or frozen. By heating the system, the latent hardener is activated causing cure to initiate. The epoxy will normally start to cure rapidly at temperatures of 100 to 125C (212 to 257F) and cure times of 30 to 60 minutes are typical. Heat curing also generally improves bond strengths, thermal resistance, and chemical resistance.[28]

When using a two-part system, the resin and hardener are packaged separately and are mixed just prior to use. This allows more active hardeners to be used so that the two-part epoxies will rapidly cure at ambient conditions.[28]

Two-part system are normally mixed by passing them through a static mix tip. This allows the two-part material to be dispensed as a single homogenous liquid when it exits the mix tip.[28]

Since the mixed adhesive is curing in the mix tip, the adhesive's viscosity and performance changes during idle times and the mix tip must be changed after the idle time exceeds the adhesive's open time. This creates a trade-off between fixture time and open time. Faster curing products will require that mix tips be changed after shorter idle times.[28]

To maintain the ratio of the resin and hardener, equipment is required. For small to moderate volume applications, the adhesive is normally packaged in a dual cartridge that sets the ratio. For high volume applications, metre mix dispense equipment is recommended.[28]

D.12.6 Hot Melts

D.12.6.1 Typical Applications

- Tacking insulation to stators, rotors, or wires

D.12.6.2 Advantages

- One-part, solvent-free

- Fast fixturing
- High adhesion to plastics
- Wide variety of formulations available
- Low volumetric cost

D.12.6.3 Disadvantages

- Hot dispense point
- Poor adhesion on metals
- Cools quickly
- Equipment is required
- Thermoplastic parts may deform
- Charring in reservoir
- Moisture sensitivity

D.12.6.4 General Description

The performance of the hot melt varies widely based on their chemistry:

Ethylene vinyl acetate (EVA) hot melts are the "original" hot melt. They have good adhesion to many substrates, the lowest cost and a wide range of open times, but typically have the poorest temperature resistance.[28]

Polyamide hot melts are a higher cost, higher performing adhesive with excellent high temperature resistance (up to 300F). Specialty formulations are available that carry a UL-94 V-0 flammability rating.[28]

Polyolefin hot melts are specially formulated for adhesion to polyolefins such as polypropylene and polyethylene plastics. Compared to other chemistries, they have longer open times and they have excellent resistance against polar solvents.[28]

Reactive polyurethanes (PUR) are supplied as an urethane prepolymer, behaving much like a standard hot melt until it cools. Once the PUR cools, it reacts with moisture over time (a few days) to crosslink into a tough thermoset polyurethane. They offer lower dispense temperatures, higher adhesion to metals and improved thermal resistance.[28]

D.12.7 Light Cure

D.12.7.1 Typical Applications

- Stators to housings
- Tacking lead wires
- Insulation to rotors, stators or wires
- Wire reinforcement
- Bonding or unitising laminates

D.12.7.2 Advantages

- One-part, solvent-free
- Fast cure time (seconds)
- High cure through depths (¿0.5″)
- Wide range of viscosities available
- Wide range of physical properties

D.12.7.3 Disadvantages

- Light must be able to reach the joint line
- Oxygen can inhibit cure at the surface
- Equipment expense for light source
- If a high intensity light source is used, ozone must be vented

D.12.7.4 General Description

Light cure adhesives ″cure on demand″ eliminating the normal trade-off between open time and cure speed. At ambient conditions, all but the fastest light curing adhesives remain unaffected by ambient light for hours allowing for almost infinite part adjustment time. Upon exposure to light of the proper intensity and spectral output, the photoinitiator in the adhesive initiates cure rapidly yielding a cured polymer. While cure times depend on many factors, 10 to 30 second exposure times to achieve full cure are typical and cure depths in excess of 0.5″ (13 mm) are possible. Light curing adhesives are available with physical properties ranging from soft, flexible elastomers to very rigid glass-like materials.[28]

While light cure acrylic adhesives are the most well known and commonly used type of light curing adhesive, the four other chemistries that can be cured with light are anaerobics, cyanoacrylates, epoxies and silicones. Significant development has occurred on these light curing adhesives in the last five years and they may offer improved performance when compared to light cure acrylics in many motor applications as shown below.[28]

D.12.8 Polyurethanes

D.12.8.1 Typical Applications

- Potting wire connectors
- Potting printed circuit boards

D.12.8.2 Advantages

- Extremely tough
- Good resistance to solvents
- High cohesive strength
- Good impact resistance
- Good abrasion resistance

D.12.8.3 Disadvantages

- Mixing required for two-part polyurethanes
- Limited depth of cure for one-part polyurethanes
- Primer may be needed for adhesion to some substrates
- Limited high temperature use

D.12.8.4 General Description

Polyurethane adhesives are supplied as one and two-part systems which range in viscosity from self-levelling liquids to non-slumping pastes. They cure to form thermoset polymers with good solvent and chemical resistance. They are extremely versatile and can range in cured form from extremely soft elastomers to rigid, extremely hard plastics.[28]

Polyurethanes offer a good blend of cohesive strength and flexibility that makes them very tough, durable adhesives. They bond well to most unconditioned substrates, but may require the use of solvent-based primers to achieve high bond strengths. They offer good toughness at low temperatures, but typically degrade in strength after long-term exposure over 302F (150C).[28]

Since the cure of one-part, moisture-curing polyurethanes is dependent on moisture diffusing through the polymer, the maximum depth of cure that can be achieved in a reasonable time is limited at approximately 0.375" (9.5 mm). Two-part systems, on the other hand, offer unlimited depth of cure.[28]

Two-part system are normally mixed by passing them through a static mix tip. This allows the two-part material to be dispensed as a single homogenous liquid when it exits the mix tip. Since the mixed adhesive is curing in the mix tip, the adhesive's viscosity and performance changes during idle times and the mix tip must be changed after the idle time exceeds the adhesive's open time. This creates a trade-off between fixture time and open time. Faster curing products will require that mix tips be changed after shorter idle times.[28]

To maintain the ratio of the resin and hardener, equipment is required. For small to moderate volume applications, the adhesive is packaged in a dual cartridge that sets the ratio. For high volume applications, metre mix dispense equipment is used.[28]

D.12.9 Silicones

D.12.9.1 Typical Applications

- Potting printed circuit boards
- Potting / sealing wire connectors
- Sealing end plates
- Sealing gear boxes

D.12.9.2 Advantages

- One-part, solvent-free
- Room temperature cure
- Excellent adhesion to many substrates
- Extremely flexible
- Superior thermal resistance
- Light curing formulations available

D.12.9.3 Disadvantages

- Poor cohesive strength
- Moisture cure systems have limited depth of cure
- May be swelled by non-polar solvents

D.12.9.4 General Description

Silicone adhesives are typically supplied as one-part systems that range in viscosity from self-levelling liquids to non-slumping pastes. They cure to soft thermoset elastomers with excellent property retention over a wide temperature range. Silicones have good adhesion to many substrates, but are limited in their utility as structural adhesives by their low cohesive strength. Silicone adhesives are typically cured via reaction with ambient humidity, although formulations are also available which can be cured by heat, mixing of two components, or exposure to light.[28]

Since the cure of moisture-curing silicones is dependent on moisture diffusing through the silicone matrix, the cure rate is strongly affected by the ambient relative humidity and the maximum depth of cure is limited to 0.375 to 0.500". At 50% relative humidity, moisture cure silicones will generally cure to a tack-free surface in 5 to 60 minutes. Complete cure through thick sections of silicone can take up to 72 hours. It should be noted that adhesive strength may continue to develop for 1 to 2 weeks after the silicone has been applied. This occurs because the reaction between the reactive groups on the silicone polymer and the reactive groups on the substrate surface is slower than the crosslinking reaction of the silicone groups with themselves.[28]

Moisture curing silicones are categorized by the by product they give off as they react with water:

Acetoxy silicones are general-purpose silicones. Their largest limitation is the potential for the by-product, acetic acid, to promote corrosion.[28]

Alkoxy silicones have alcohol by-products so they are non-corrosive. This makes them well suited for electronic and medical applications where acetic acid could be a problem. They have lower adhesion and take longer to cure than acetoxy silicones.[28]

Oxime silicones are non-corrosive, fast curing, and have excellent adhesion. There are also grades available with improved chemical resistance.[28]

Light curing silicones in general, also have a secondary moisture cure mechanism to ensure that any silicone that is not irradiated with ultraviolet light will still cure. Upon exposure to ultraviolet light of the proper wavelength and intensity, they will form a tack-free surface and cure to a polymer with up to 80% of its ultimate physical strength in less than a minute. Initial adhesion can be good, but because ultimate bond strength is dependent on the moisture cure mechanism of the silicone, full bond strength can take up to a week to develop. Silicones with a secondary acetoxy cure show good bond strength while those with a secondary alkoxy cure will show lower bond strength.[28]